University of Belgrade
Technical Faculty in Bor

Chamber of Commerce
and Industry of Serbia

XV International Mineral Processing & Recycling Conference

IMPRC
INTERNATIONAL MINERAL PROCESSING & RECYCLING CONFERENCE

Proceedings

Editors:
Jovica Sokolović
Milan Trumić

17-19 May 2023 | Belgrade SERBIA

University of Belgrade,
Technical faculty in Bor

Chamber of Commerce
and Industry of Serbia

XV International Mineral Processing & Recycling Conference

IMPRC
INTERNATIONAL MINERAL PROCESSING & RECYCLING CONFERENCE

Proceedings

Editors:
Jovica Sokolović
Milan Trumić

17 – 19 May 2023, Belgrade, Serbia

XV International Mineral Processing & Recycling Conference

PUBLISHER:
University of Belgrade, Technical Faculty in Bor

FOR THE PUBLISHER:
Dean: Prof. Dr Dejan Tanikić

EDITORS:
Prof. Dr Jovica Sokolović
Prof. Dr Milan Trumić

PROCEEDINGS COVER DESIGN:
Vojislav Jotović

PRINTED BY:
Grafomed - Trade Bor d.o.o., Bor, Serbia
Printed: 200 copies

PUBLICATION YEAR:
2023

==========

CIP - Каталогизација у публикацији
Народна библиотека Србије, Београд

622.7(082)
502.131.1:628.477.6(082)
628.477.6(082)

INTERNATIONAL Mineral Processing and Recycling Conference (15 ; 2023 ; Belgrade)
Proceedings / XV International Mineral Processing and Recycling Conference, IMPRC, 17-19 May 2023, Belgrade, Serbia ; editors Jovica Sokolović, Milan Trumić. - Belgrade : University, Technical Faculty in Bor, 2023 (Bor : Grafomed Trade). - XII, 634 str. : ilustr. ; 25 cm

Na vrhu nasl. str.: Chamber of Commerce and Industry of Serbia. - Tiraž 200. - Bibliografija uz većinu radova.

ISBN 978-86-6305-133-1

а) Руде -- Припрема -- Зборници б) Отпадне материје -- Одрживи развој -- Зборници в) Отпадне материје -- Рециклажа -- Зборници

COBISS.SR-ID 114566153

==========

Conference is financially supported by Republic of Serbia, Ministry of Science, Technological Development and Innovation

COMMITTEES

Scientific Committee

Prof. Dr Milan Trumić, Serbia, President;
Prof. Dr Grozdanka Bogdanović, Serbia, Vice President;
Prof. Dr Jovica Sokolović, Serbia, Vice President;
Prof. Dr Zhiyong Gao, China;
Prof. Dr Lijie Guo, China;
Prof. Dr Mauricio Torem, Brazil;
Prof. Dr Pablo Brito-Parada, United Kingdom;
Prof. Dr Przemyslaw Kowalczuk, Norway;
Prof. Dr Erin Bobicki, Canada;
Prof. Dr Kazutoshi Haga, Japan;
Dr Maoming Fan, USA;
Dr Aleksandar Janković, Australia;
Prof. Dr Rraghupatruni Bhima Rao, India;
Prof. Dr Junbeum Kim, France;
Prof. Dr Srećko Stopić, Germany;
Prof. Dr Magdalena Regel-Rosocka, Poland;
Prof. Dr Alejandro Rodriguez Pascual, Spain;
Prof. Dr Georgios Anastassakis, Greece;
Prof. Dr Mehmet Polat, Turkey;
Prof. Dr Valery Morozov, Russian Federation;
Prof. Dr Silvie Heviánková, Czech Republic;
Dr Slavomir Hredzak, Slovakia;
Prof. Dr Gabor Musci, Hungary;
Prof. Dr Francisc Popescu, Romania;
Prof. Dr Irena Grigorova, Bulgaria;
Prof. Dr Jakob Lamut, Slovenia;
Prof. Dr Aleksandra Anić Vučinić, Croatia;
Prof. Dr Ilhan Bušatlić, Bosnia & Herzegovina;
Prof. Dr Svjetlana Sredić, Bosnia & Herzegovina;
Prof. Dr Mirjana Golomeova, North Macedonia;
Prof. Dr Aleksandar Jovović, Serbia;
Prof. Dr Milena Kostović, Serbia;
Prof. Dr Željko Kamberović, Serbia;
Prof. Dr Vlada Veljković, Serbia;
Prof. Dr Goran Vujić, Serbia;
Prof. Dr Srđan Rončević, Novi Sad, Serbia;
Prof. Dr Bogdana Vujić, Serbia;

Prof. Dr Marina Stamenović, Serbia;
Prof. Dr Nada Štrbac, Serbia;
Prof. Dr Milan Antonijević, Serbia;
Prof. Dr Zoran Stević, Serbia;
Prof. Dr Dejan Tanikić, Serbia;
Prof. Dr Snežana Šerbula, Serbia;
Prof. Dr Snežana Milić, Serbia;
Prof. Dr Mira Cocić, Serbia;
Prof. Dr Zoran Štirbanović, Serbia;
Prof. Dr Maja Trumić, Serbia;
Prof. Dr Ljubiša Andrić, Serbia;
Asst. Prof. Dr Vladan Milošević, Serbia;
Dr Ivana Smičklas, Serbia;
Dr Miroslav Sokić, Serbia;
Dr Dragan Radulović, Serbia;
Dr Sonja Milićević, Serbia;
Dr Milinko Radosavljević, Serbia;
Dr Mile Bugarin, Serbia;
Dr Zoran Stevanović, Serbia;
Dr Radmila Marković, Serbia;
Dr Miroslav Ignjatović, Serbia.

Organizing Committee

Prof. Dr Jovica Sokolović, President, Serbia;
Prof. Dr Milan Trumić, Serbia;
Prof. Dr Grozdanka Bogdanović, Serbia;
Prof. Dr Zoran Stević, Serbia;
Prof. Dr Zoran Štirbanović, Serbia;
Prof. Dr Maja Trumić, Serbia;
Dr Miroslav Ignjatović, Serbia;
Dr Vladimir Nikolić, Serbia;
MSc Dragana Marilović, Serbia;
MSc Predrag Stolić, Serbia;
MSc Katarina Balanović, Serbia;
MSc Ivana Ilić, Serbia;
MSc Oliver Marković, Serbia;
BSc Vera Ražnatović, Serbia;
BSc Sandra Vasković, Serbia;
Dobrinka Trujić, Serbia.

TABLE OF CONTENTS

PLENARY LECTURES

XV International Mineral Processing and Recycling Conference
17-19 May 2023, Belgrade, Serbia

RESEARCH PROGRESS, TRENDS, AND INNOVATIONS OF DEVELOPMENT ON MINING BACKFILL TECHNOLOGY OF UNDERGROUND METALLIFEROUS MINE

L. Guo[1,2], Y. Zhao[1,2,#], Q. Ma[1,2], G. Tang[1,2], C. Jia[1,2], C. Li[1,2]

[1] Beijing General Research Institute of Mining and Metallurgy, Beijing, China

[2] National Centre for International Research on Green Metal Mining, Beijing, China

ABSTRACT – Backfill mining technology used extensively in underground metal mines is critical for conducting green and low-carbon mining operations. Also, backfill mining can achieve the maximum recovery of underground mineral resources and environmentally friendly disposal of mining wastes. This paper systematically reviews the development of backfill mining methods. The latest technology application progresses from three aspects: high-efficiency and large-scale backfill mining, continuous backfill mining, and how to reduce backfill mining costs. Then the backfill mining technology used in metal mines evolved and developed. The application and development trend of the whole process of backfill technology covering the preparation and transportation of tailings backfill slurry, barricades design, and the drainage of backfill slurry in the stope are analyzed. The mechanism of heterogeneous characteristics and self-weight consolidation behavior of tailings backfill slurry are analyzed, and the comparison of the traditional method used for strength requirement analysis of the backfill structure with the improved strength calculation-design method is made. Also, the field monitoring method of the backfill slurry is introduced. Based on the above research, it is proposed that innovation of backfill mining technology is the core element to achieve low-cost backfill mining, the development of a whole-process backfill mining system is the key to the stable preparation of high-quality underground tailings backfill slurry, and the stability of the underground backfill structure is the base to ensure the safe, efficient, and economical application of backfill mining technology. Also, the improvement of the standard system is the guarantee for accelerating the promotion of the application of backfill mining technology. At the same time, the research direction that should be focused on in the future is clarified. Accelerating the development of new technologies, materials, and equipment for green and low-carbon filling is the driving force to promote the transformation and development of backfill mining.

Keywords: Metal Mine, Backfill Mining, Green Mining, Mine Backfill, Backfill Mechanics.

INTRODUCTION

For a long time, the world will still be in the middle and late stages of industrialization and rapid urbanization, and the rigid demand for metal mineral resources and the contradiction between supply and demand will still exist for a long time. With the depletion of the mining of shallow mineral resources in the world, the development of mineral resources in the future will fully enter the deep deposits within the second depth space (1000-2000m), and deep mining of metal mines will become the norm. Deep mining faces a complex environment of 'three highs and one disturbance'. Filling mining can effectively control ground pressure and movement of overlying strata and will be

corresponding author: zhaoyue@bgrimm.com

widely used in deep metal deposit mining. The recovery rate of filling mining resources is high, and the solid waste accumulated on the surface can be backfilled into the goaf underground, which can not only improve the safety of mining operations but also prevent the occurrence of surface disasters and can fully absorb the surface solid waste. The application of cemented filling technology can enable the filling mining method to control the movement of rock strata and surface subsidence effectively, making it possible to mine under water bodies and structures and to preferentially mine high-grade ore bodies in deep parts or footwalls, providing an excellent opportunity for the effective use of resources and the improvement of enterprise competitiveness.

In recent years, with the integration of advanced cross-technology, advanced experimental methods, and filling mining technology, metal ore filling mining technology and technology has also developed rapidly, and many new theories, new methods, and new technologies have emerged in the basic theory and application technology of mine filling technology. Therefore, the author systematically sorts out and summarizes the research progress of metal ore filling mining technology to inspire future technological innovation work.

APPLICATION PROGRESS OF BACKFILL MINING IN UNDERGROUND METAL MINE

The evolution of backfill mining

Backfill mining is an ancient mining method. Backfill technology was first used in mining in the 16th century, mainly by Spanish colonists at some mines in Mexico, using wood and waste rock as supports to create a safe mining environment [1]. Tailings and other types of solid wastes were introduced into underground metal mining in the 19th century, but a dedicated backfill mining method was not yet been formed.

The hydraulic backfill mining method appeared in the 1950s and was popularized in metal mines in Canada and South Africa. The overhand cut-and-fill mining and open stoping with subsequent backfill mining using the high-density cemented tailings backfill appeared in Canada in the 1960s.

In the early 1970s, large-diameter long-hole backfill mining was first applied in the Copper Cliff North Mine. In 1975, the vertical crater retreat (VCR) mining method with a hole depth of 40 m and large diameter (165 mm) was applied in the Levack Mine successfully. In 1982, the VCR mining method was first used in China at underground mines, and Professor Sun Zhongming [2] at the Beijing General Research Institute of Mining and Metallurgy (BGRIMM) led a team to start the field test and application at Fankou Lead-Zinc Mine. After its successful application, it was gradually used in Jinchangyu Gold Mine, Shizishan Copper Mine, and Fenghuangshan Copper Mine in China. At the beginning of the 21st century, the team led by Professor Sun Zhongming [3] further developed the massive ore-dropping technology based on the spherical charge funnel blasting, which allowed the establishment of an underground super-mining ore factory. After 2000, with the development of advanced mining equipment, the panel mechanized cut-and-fill method has been successively applied in Jinchuan No. 2 mining area and the Fankou lead-zinc mine in China.

At present, most of the large-scale metal mines are developed on thick-inclined or steeply inclined deposits. The methods adopted for such deposits are mainly the

pillarless caving method and the open stopping with subsequent backfill mining. The latter, with large-diameter deep holes, has been paid more attention due to its high production efficiency, high recovery intensity, and the ability to prevent surface subsidence.

The vertical staggered continuous mining with high stopes for thick and large ore bodies was proposed by Professor Yang Xiaocong at BGRIMM [4]. As shown in Figure 1, this mining method allows a safe and efficient recovery under the backfill roof without leaving a horizontal ore pillar using the high stopes.

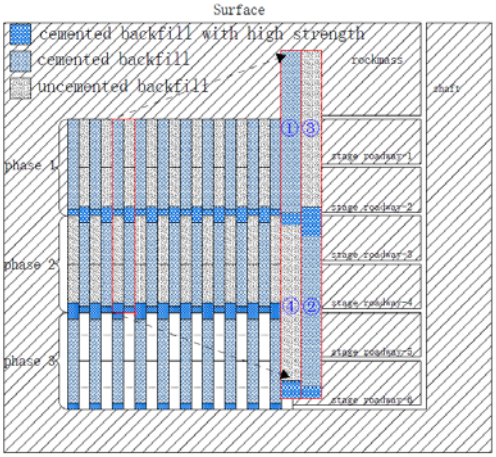

Figure 1 The vertical staggered continuous mining with high stopes

High-efficiency and large-scale backfill mining

High-efficiency and large-scale mining is the eternal pursuit of mines because efficiently recovering ore from the ore body means more significant economic benefits. The caving method using large-scale blasting and high-efficiency mining equipment is widely applied in underground metal mines in China, especially iron mines. In recent years, with the country's emphasis on environmental protection and solving the problem of underground voids and tailings disposal, more and more mines adopt open stoping with subsequent backfill mining.

As shown in **Figure 2**, the ore body is generally divided into a series of primary and secondary stops using the open stoping with subsequent backfill mining [5]. The typical mining sequence is mining the primary stope first and filled with cemented backfill, and then the secondary stope is mined with the support of the adjacent cured backfill.

The length of the primary or secondary stope is generally controlled below 60 m, the width is usually 6~30 m, and the height is generally 40~60 m in mines using the open stoping with subsequent backfill mining in China. The large-diameter and deep-hole rock drilling equipment is often used to match the large-size stope. The commonly used Simba364 drilling jumbo at Anqing Copper Mine in China can achieve a drilling depth of 51 m a day with a drilling diameter of 90~178 mm [7]. The Dongguashan Copper Mine in China, which adopts the open stoping with subsequent backfill mining, has a comprehensive panel production capacity of 2400 t/d.

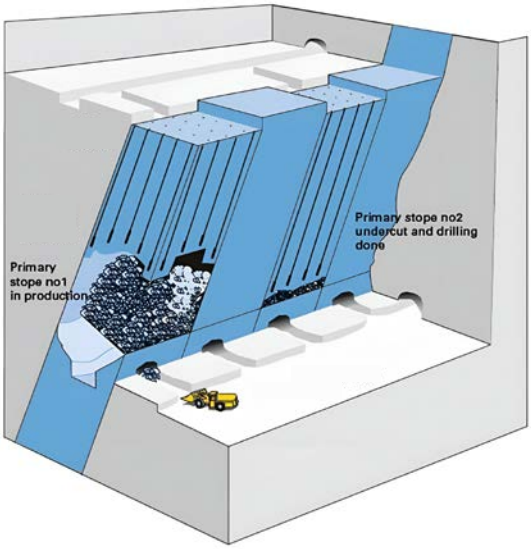

Figure 2 Open stoping with subsequent backfill mining [6]

Continuous backfill mining

The underground void with an exposed area that reaches a critical value is prone to collapse, so different mining methods take various measures to limit the exposed area. For example, the open stoping with subsequent backfill mining methods limits the exposed area by dividing the ore body into primary and secondary stopes. The overhand/underhand cut-and-fill mining methods limit the exposed area by dividing the ore body into a series of aligned drifts. The common feature of these two mining methods is that in each mining cycle, the filling process is delayed after the mining process. Therefore, the waiting time between mining and backfill processes increases the difficulty of production management and reduces mining efficiency. For this reason, some scholars have proposed the continuous mining and backfill method. The basic concept is to use some mined areas within the partially mined stope as temporary working spaces and backfill the mined voids before the completion of mining [8].

The continuous dry filling long room method (Avoca, **Figure 3**) addresses the efficient continuous mining of steeply inclined and medium thick orebody [9]. The mining is carried out from one end to the other end of the stope, and the LHD is used for continuous ore extraction, followed by continuous dry filling of the formed voids. Because the void is filled in time and the exposed area is small, the stope length is not limited, which has significant safety management advantages compared with the large exposed area and long exposure time of the void in the open stoping with subsequent mining. For medium-thick ore bodies, this continuous method can achieve considerable production capacity [10]. The modified Avoca mining method used in the Qinglonggou gold mine in China, as shown in **Figure 4**, allows ultimately continuous mining and filling, and its production capacity can reach 307 t/d with a 9.6% ore loss rate and 7.5% ore dilution rate.

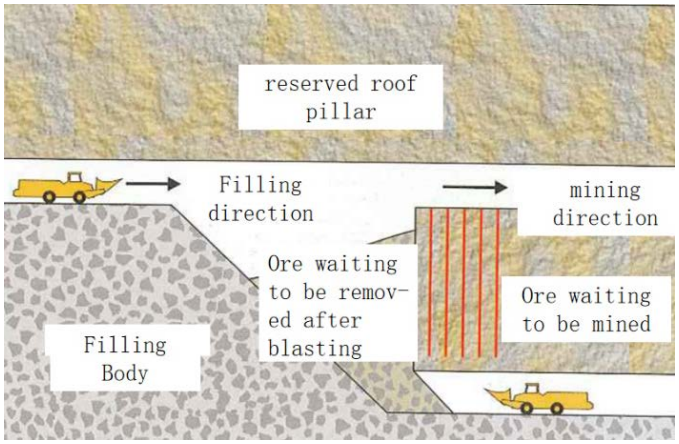

Figure 3 Diagram of Avoca mining method

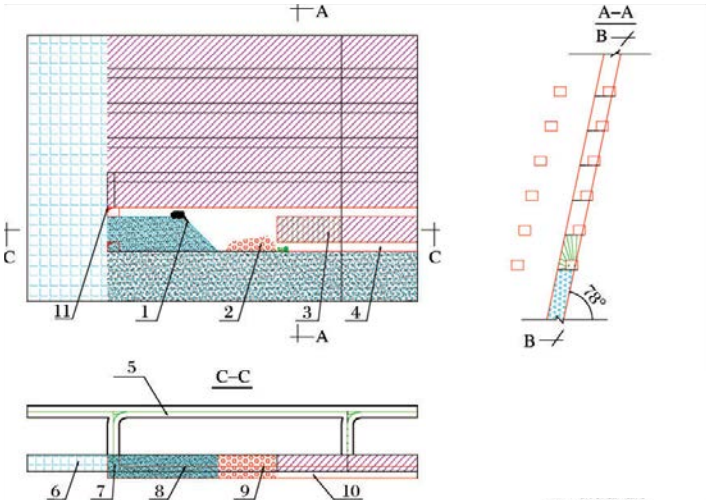

Figure 4 Avoca mining method applied in Qinglonggou gold mine (1- cemented rock fill, 2- ore, 3- fan-shaped drilling pattern, 4- drilling roadway, 5- sublevel roadway, 6- surrounding rock, 7- cutting roadway, 8- cemented rock fill, 9- ore, 10- drilling roadway, 11- cutting shaft)

Underhand cut-and-fill mining is suitable for broken ore bodies surrounded by cracked rock mass, which has low mining efficiency, high backfill costs, and complex safety management. By changing the existing mining process, the underhand sublevel continuous backfill mining with the medium-deep hole was proposed by BGRIMM. This method can reduce the preparatory work, improve the individual stope's production efficiency and reduce the mining operations' cost. **Figure 5** shows the underhand high-sublevel continuous mining method of the Karatunk copper-nickel mine. After successful application, the production capacity of the panel increased from 164.27t/d to 423.21t/d, and the production cost was reduced from RMB 108/t to RMB 50/t, with significant economic benefits.

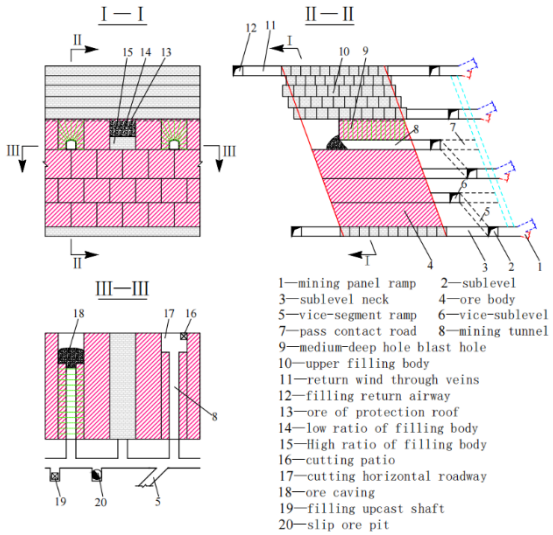

Figure 5 Downward high-segmented continuous mining method

Reduce the backfill costs

Backfill mining mainly relies on the support provided by the backfill structure to perform safe and efficient mining processes, which requires a specific strength of the backfill to play the functions of man and machine walking, self-standing, and high-strength roof protection [11].In order to meet the strength requirements of the backfill, cement and other cementitious materials are commonly added to the backfill slurry, resulting in a considerable consumption of cementitious materials and making the cost of cementitious materials account for 70-80% of the total cost of backfill operations [4].On the one hand, this is due to the unreasonable design of the required backfill strength, leading to a conservative backfill design. In addition, the high price of cement and other cementitious materials and the inappropriate mining methods used by mines also lead to a large proportion of the cost of cementitious materials. Therefore, the scientific optimization of the backfill design, the development and application of low-cost cementitious materials, and the reasonable use of efficient mining methods are the main ways to reduce the cost of backfill mining.

Scientifically optimize the required strength of the backfill to reduce the cement consumption reasonably. Canada, Australia, and other foreign-developed mining countries attach great importance to the fundamental theories and methods of backfill mechanics. Starting from the stress analysis within the backfilled stope, they have established the backfill mechanics analysis and backfill strength requirements calculation methods represented by the classical Mitchell method using model tests, analytical analysis, or numerical calculations, forming the theoretical basis for the backfill mechanics. Liu Guangsheng [5] of BGRIMM proposed a three-dimensional analytical model and calculation method for the required backfill strength with front wall exposure and back wall pressure. In addition, rationally optimizing the design of the spatial distribution of the strength of the cemented backfill is also the key to reducing cement

consumption. For example, the required strength of the plug pour and the final pour should be optimized to reduce backfill costs [12].

Develop new cementitious materials to replace cement. It reduces cemented backfill costs by developing and applying cheaper cementitious materials to replace cement partially. Fly ash and non-ferrous metallurgical slag (copper slag, nickel slag, lead-zinc slag) contain mineral components such as silicate, aluminate, and iron-aluminate shown in Figure 6. Under the excitation of activation excitation and phase reconstruction, it can be activated to form C-S-H gel, so it has the potential and feasibility of making cheap cementitious materials used for backfill [12]. Existing studies have shown that [13] adding fly ash and non-ferrous metallurgical slag to ordinary Portland cement can increase the long-term strength of the backfill containing sulfide.

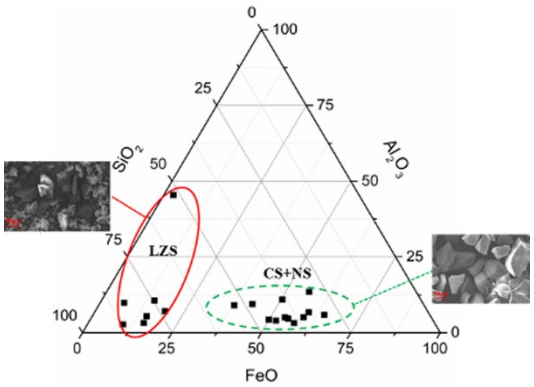

Figure 6 Chemical composition distribution of typical non-ferrous metallurgical slag

RESEARCH PROGRESS OF METAL ORE SOLID WASTE BACKFILL TECHNOLOGY

Evolution and development of mine backfill technology

Mine backfilling technology is the core element of metal ore-filling mining technology. It has always troubled or restricted early backfill mining methods' development, application, and promotion. Until 1957, the cemented filling of graded tailings and Portland cement was established in the Canadian Eagle Bridge Company. Hardy Nickel Mine was successfully applied, and the cemented filling process was applied to the production stage for the first time. This prompted the rapid development of the filling mining method during this period.

In 1977, Australia's Mount Isa Mine and the University of New South Wales jointly developed a low-cost cemented filling process using slag as an auxiliary gelling agent; since the 1980s, China began to develop high-concentration mortar filling and block stone cement slurry cemented filling At the same time, Canada is developing high-concentration tailings cemented filling based on vertical sand bins, and Australia is developing low-cost waste rock tailings cemented filling technology [14]. In the late 1980s, Germany built the world's first paste backfill mine in the Bad Grund lead-zinc mine; in 1994, China built the first paste-filling process system in Jinchuan No. The Tonglushan Copper Mine and the Huize Lead-Zinc Mine built an unclassified tailings paste

filling system [15], as shown in **Figure 7**; after 2000, two technological modes of tailings high-concentration cemented filling and paste cemented filling dominated The filling of metal mines has also evolved a new filling technology on this basis.

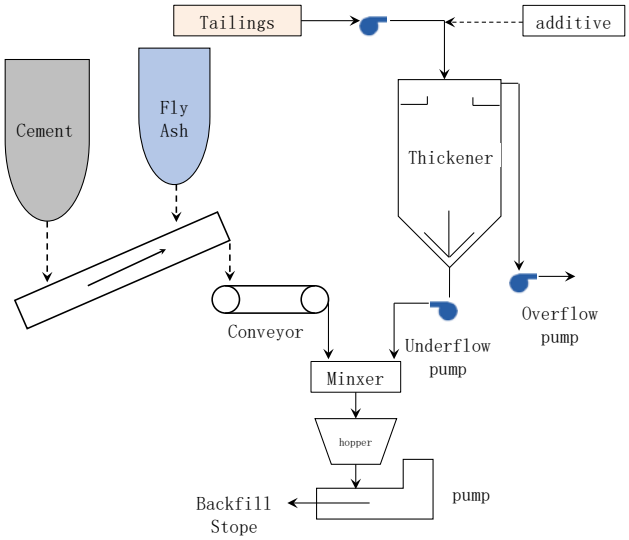

Figure 7 Backfill technology applied in metal mine

Backfill slurry preparation technology

The metal mine backfill process is still dominated by tailings filling, mainly divided into tailings high-concentration backfill, tailings paste backfill, and waste rock tailings paste backfill.

Classified tailings filling is still one of the most widely used filling technologies at present, and it is mainly gravity conveying. The graded tailings filling adopts the technology of swirl classification and vertical sand bin hydraulic joint slurry making, and the mass concentration of the filling slurry prepared by it is generally 65% to 72%. The vertical sand bin preparation system is generally used for the high-concentration slurry of graded tailings. The traditional process has the problems of tailings compacting in the bin, significant fluctuations in sand concentration, and reduced tailings mortar. In 2012, Professor Guo Lijie of the Beijing General Research Institute of Mining and Metallurgy proposed a vertical sand silo tailings wind and water two-stage time-sharing slurry-making technology around the wall (**Figure 8**), which realized the stable preparation of graded tailings high-concentration filling slurry. In 2014, the Beijing General Research Institute of Mining and Metallurgy [16] developed a high-concentration filling technology for an optimized combination of tailings based on the beneficiation process (**Figure 9**), using classified coarse tailings and overflowed fine sand to concentrate separately and then optimize the combination in proportion, transformed into a high-concentration filling with good gradation and stable filling quality. This technology effectively improves the filling quality and solves the problem of insufficient classified tailings for backfill purposes.

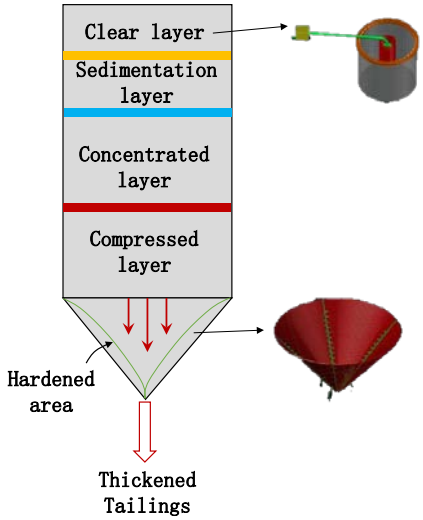

Figure 8 A new slurry preparation technology used in the vertical sand tank

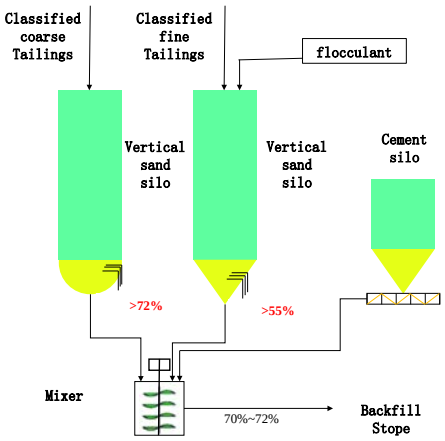

Figure 9 High concentration backfill technology based on mineral process

Paste slurry is a backfill slurry that does not segregate and has excellent and stable plasticity and fluidity. Due to the wide range of filling aggregate sources, the material properties vary greatly. Quantifying the paste with a single index, such as mass concentration, is difficult. The yield stress is mainly used to evaluate the paste in the world quantitatively. It is believed that when the yield stress of the slurry is greater than 200±25Pa, it can be regarded as a paste [14, 17]. Paste tailings slurry is generally prepared by dehydration equipment such as a deep cone thickener (**Figure 10**) and filter press/filter. Tailings gradation is the decisive factor affecting filling quality. With the advancement of mineral processing technology, the particle size of metal ore dressing tailings is getting finer and finer, resulting in poor tailings settlement concentration. It is not easy to prepare a stable paste. Chris Lee from Canada's Gundam Consulting Co., Ltd. proposed a combination of different gradation tailings, first cyclone classification, and

then using different high-efficiency concentration and dehydration methods to prepare the paste (**Figure 11**). This method realizes the stable and efficient preparation of fine tailings paste.

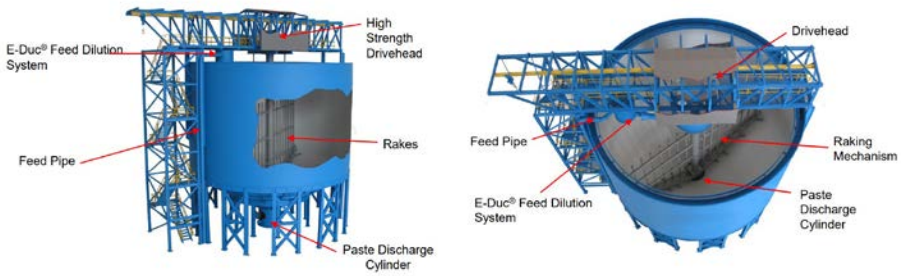

Figure 10 Deep cone thickener for tailings paste

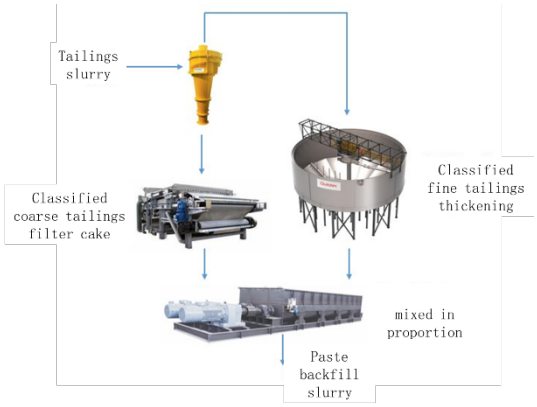

Figure 11 Combined-process preparation for cemented paste backfill

Backfill retaining wall technologies

The filling retaining wall appeared as an essential safety support structure for the closure of the filling stop. At first, it was mainly supported by simple wooden structures [18]. With the development and perfection of mining technology and scale, the structure and form of the filling retaining wall in underground metal mines have experienced various forms, such as wooden structures, reinforced concrete structures, brick structures, and steel structures [19, 20]. Currently, the filling retaining walls of underground metal mines domestically and overseas can be divided into reinforced concrete retaining walls, concrete block retaining walls, and flexible retaining walls supported by steel and wood structures. The structure and form of the retaining wall are closely related to the filling mining process. The reinforced concrete retaining wall has a large bearing capacity and strong universality. It is used in various filling process conditions, but its engineering cost is relatively high [21], as shown in **Figure 12a** shown; Concrete blocks (such as concrete prefabricated bricks, **Figure 12b**) and flexible closed retaining walls are suitable for drift backfill mining method with low load-bearing

requirements [22]; In addition to the traditional concrete retaining wall, brick retaining wall and flexible retaining wall, in recent years, with the gradual deepening of people's understanding of the mechanical characteristics of filling stopes, some green and low-cost filling stope sealing technologies have emerged, such as adopting detachable and recyclable assembled retaining wall with metal components. The primary force-bearing member of this retaining wall is a curved steel beam, which adopts assembled parts and can be disassembled and recycled, which significantly reduces the cost of filling stope closure. In China, Anqing Copper Mine, Axi Gold Mine, and other mining are applicating this retaining wall, as shown in **Figure 12c**.

(a) Concrete rigid retaining wall

(b) Brick retaining wall [18]

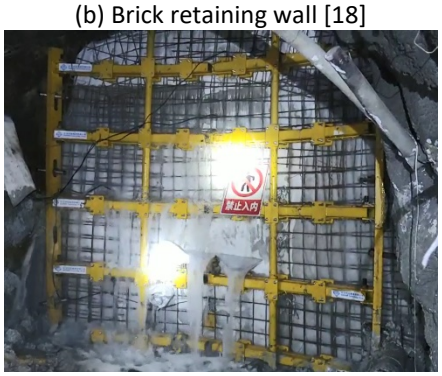

(c) Assembled retaining wall with metal components

Figure 12 Types of retaining wall

The selection of the closed structure form of the filling stope needs to consider various factors such as filling quality, filling mechanics, manufacturing process, and cost, among which the stress characteristics of the retaining wall and stope dehydration are the key points. Hughes' research shows that [23, 24] the load characteristics on the filling retaining wall have a great relationship with the shape of the slurry, and the wall pressure calculated using the limit equilibrium theory has a great relationship with the selection of the limit slip surface. If the load on the wall achieves rapid consolidation and hardening under good drainage conditions or a better technological level, the measured stress on the wall is much smaller than the theoretical value. The mechanical model is proposed to deepen people's understanding of the bakcfill body. If considering the arch effect, the force on the retaining wall will no longer be a linear relationship of height. Yang [25] thought that the mechanical effect of the traditional arching effect was not apparent at the initial stage of filling and only appeared in the later stage of filling slurry curing and forming, so a mechanical model of shear yielding-induced arching effect was proposed to describe short-term loads on retaining walls. From the traditional simplified model to the progressive mechanical thinking proposed according to the characteristics of working conditions, the research results have enriched people's understanding of filling retaining walls. For example, Lu [21] introduced a new type of lightweight retaining wall, which has significant advantages in terms of bearing capacity and engineering slurry; Berndt [22] introduced a retaining wall of permeable brick walls, which play an essential role in achieving stope dehydration and ensuring the bearing capacity of the filling stope.

With the continuous expansion of the filling mining scale of underground mines, new and higher requirements have been put forward for safe, efficient, green, and low-cost stope closure technology, which is mainly reflected in the precise matching between the structural design of the filling retaining wall and the filling process, high efficiency, low-cost new construction methods, accurate measurement and safety monitoring about retaining wall loads. In the future, safer, low-cost, and monitorable methods will inevitably become the main development method for the technology of filling stope closure in the underground mine.

ADVANCES IN MINE BACKFILL MECHANICS RESEARCH

The traditional analytical method to determine the strength of backfill in stopes

The open stoping with subsequent backfill mining method represents the development direction of large-scale, high efficiency, green and clean mining. However, the cemented backfilling cost of the backfill in primary stopes accounts for more than 70% of the total backfilling cost. How to ensure the stability of the cemented backfill when it is laterally exposed during the mining process while optimally controlling the cemented backfilling cost is a bottleneck for safe, economical, and efficient backfill mining.

In Canada, Australia, and other foreign countries with the developed mining industry, starting from the stress analysis of the backfill in stopes, the theory and method of mechanical analysis and strength design of the backfill in open stoping with subsequent backfill mining represented by Mitchell's method have been established and widely

adopted in foreign mines, which has extensively promoted the development of backfill mechanics and backfill mining technology abroad.

In the 1980s, foreign backfill mining researchers mainly drew on the self-weight stress of the overburden ($\sigma c \geqslant \gamma H$) or the laterally exposed slope model ($\sigma c \geqslant \gamma H/2$) in soil mechanics for the design of the stress and strength requirement of the backfill in stopes (where σc is the strength requirement of the backfill, γ is the bulk unit weight of the backfill and H is the height of the laterally exposed face of the backfill) [26]. However, both of these methods do not consider factors such as the confinement of the backfill by the surrounding rock and its three-dimensional stress state, resulting in an overly conservative backfill design strength and high backfilling costs. On this basis, Mitchell et al. carried out a series of indoor physical model tests of the backfill with unilateral exposure, researched and proposed a three-dimensional wedge sliding analytical model and method for calculating the strength requirement of the lateral exposure backfill [27], which took into account the three-dimensional failure mode and mechanical behavior of the backfill in stopes, reasonably reduced the backfill strength design index, and was successfully applied in many Canadian mines using backfill mining methods, which is of historical importance.

Figure 13 shows the analytical model of three-dimensional limit equilibrium constructed by Mitchell et al. based on the sliding failure of unilaterally exposed cemented backfill with different sizes and strengths in indoor physical model tests, **Figure 13** shows the analytical model of three-dimensional limit equilibrium constructed by Mitchell et al. based on the sliding failure of unilaterally exposed cemented backfill with different sizes and strengths in indoor physical model tests, in which the sliding failure of the backfill is assumed to occur along the potential plane through to the back wall of the backfill, and only the cohesion of the contact surfaces between the backfill and the surrounding rock of both sidewalls is considered, ignoring the angle of internal friction on the contact surfaces of the sidewalls, and both the cohesion and angle of internal friction on the contact surface between the backfill and the surrounding rock of the back wall of the stope are assumed to be zero, resulting in an analytical equation for the strength requirement of the cemented backfill with lateral exposure and its safety factor (as in equation (1)).

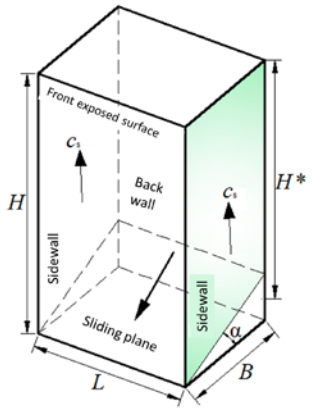

Figure 13 Illustrations of required strength model of cemented backfill with lateral exposure (Mitchell's method)

$$\sigma_c = \frac{1}{2 \cdot M} \cdot \frac{\gamma L \cdot (FS \tan\alpha - \tan\phi) \cdot \left[H - \frac{B \tan\alpha}{2}\right] \cdot \sin\alpha}{L \tan\alpha + r_s \cdot (FS \tan\alpha - \tan\phi) \cdot \left[H - \frac{B \tan\alpha}{2}\right] \cdot \sin\alpha} \quad (1)$$

Where: σ_c is the uniaxial compressive strength (kPa) required for a laterally exposed cemented backfill to be self-supporting; FS is the safety factor for a laterally exposed backfill; L is the length of the exposed face of the backfill (m); B is the width of the backfill (m); H is the overall height of the exposed face of the backfill (m); H^* is the equivalent height of the potential sliding wedge of the backfill (m), $H^* = H - (B \tan\alpha)/2$; γ is the bulk unit weight of the cemented backfill (kN/m³); M is the ratio of the cohesion c of the backfill to the uniaxial compressive strength σ_c of the backfill ($M = c/\sigma_c$); ϕ is the angle of internal friction of the backfill (°); α is the angle between the potential sliding plane and the horizontal plane (°), $\alpha = 45 + \phi/2$; r_s is the ratio of the cohesion cs on the contact surface between the surrounding rock and the backfill to the cohesion c of the backfill ($r_s = \mathrm{cs/c}$), Mitchell's method assumes r_s=1.

Mitchell et al. further assumed that the angle of internal friction of the backfill ϕ=0, M = 0.5 (i.e., σ_c=2c), r_s=1 (i.e., $cs = c$), and that H>>B makes $H^* \approx H$, based on the analysis of the backfill in the physical model. A simplified classical Mitchell's method was obtained for the limit equilibrium state with the safety factor $FS = 1$, as in equation (2).

$$\sigma_c = \frac{\gamma H}{1 + \frac{H}{L}} \quad (2)$$

This simplified classical Mitchell's method has been widely used in industry and academia worldwide in backfill mining and provides the basis for calculating the strength requirement of laterally exposed backfill. However, Mitchell's method has many assumptions, and although the method agrees well with the physical model test results, some of the assumptions do not match the actual situation, e.g., Mitchell's method assumes that the angle of internal friction of the backfill is 0. Although Mitchell's method has certain limitations, the model provides a solid basis for later developing lateral exposure backfill strength calculation methods [28].

An improved method for calculating and designing the strength requirement of backfill in stopes

The stress distribution of the backfill is the mechanical basis for calculating the strength requirement of the backfill and its stability analysis under lateral exposure conditions in the open stoping with subsequent backfill mining methods. International and domestic scholars have conducted exploratory studies on the arching stress effect of the backfill in stopes [29-33]. Due to the ease of analysis of backfill stress and strength requirement, researchers have continued to improve and develop analytical models of backfill stress and strength requirement in stopes, allowing them to be quickly applied to guide the design of backfill strength in mines.

Based on Mitchell's original model, Zou, and Nadarajah [34] considered the top load of the backfill in stopes, and Dirige et al. [35] considered the effect of the angle of

inclination of the backfill and improved the analytical calculation method of the backfill strength requirement respectively. However, they still followed all the assumptions of Mitchell's original model. In Canada, Li and Aubertin et al. systematically combined the research basis of the stress distribution characteristics and anisotropic mechanical boundaries of the backfill, gradually overcame the limitations of the assumed conditions in Mitchell's original model, and extended the theory and method of calculating the strength requirement of the backfill by considering the delamination phenomenon of the actual backfill in stopes, the frictional effect between the backfill and the surrounding rock of the stope sidewalls. [36]

However, the previous analytical model for the correction of the strength of the backfill mainly focuses on the lateral exposure of the cemented backfill in a single isolated stope and does not take into account the influence of the backfill in adjacent stope and its mechanical contact with the surrounding rock of the stope during the actual mining and backfilling process (e.g., **Figure 14a**), and the theoretical approach for the design of the strength requirement of the backfill is still not mature and perfect.

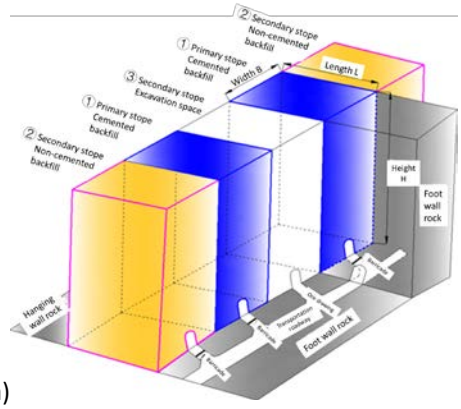

(a)

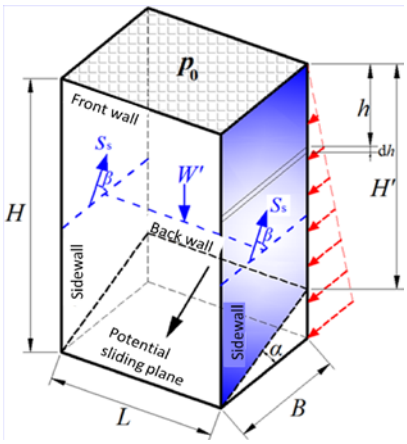

(b)

Figure 14 Spatial relationships between the backfill and rock mass and illustrations of required strength model of the backfill of two-stage open stoping with the subsequent backfill mining method

In this regard, Liu Guangsheng et al. [37] proposed a three-dimensional analytical model and calculation method for the strength requirement of the cemented backfill with the front wall exposed and the back wall compressed, based on the actual excavating-backfilling sequences of the two-step open stoping with subsequent backfill mining method, focusing on the lateral pressure effect of the non-cemented backfill in the secondary stopes on the adjacent cemented backfill in the primary stopes. By comparing the numerical simulation solution of the strength requirement of the backfill in the limit equilibrium state with its analytical results, it was determined that the numerical simulation and analytical calculation results of the strength requirement of cemented backfill in primary stopes agree best when the potential sliding plane angle of the backfill α=45°+ϕ/2 and the angle of internal friction between the backfill and the sidewall surrounding rock β=45°-ϕ/2 [38]. This backfill strength calculation method has been successfully applied to the backfill strength design of mines such as Sanshandao Gold Mine, CaoLou Iron Mine, and Karatunk Copper-Nickel Mine.

On this basis, how to reasonably transform the theoretical value of strength requirement into the actual strength requirement and ration parameters matching the technical level of the mine backfilling according to the quality control effect of the stopes backfilling in different periods of different mines is a crucial link to improve the design of the backfill strength of underground metal mines. For this, a statistical calculation method for the floating safety factor FS was proposed by combining the statistical analysis of backfill specimens' strength and in-situ core specimens' strength, as in equation (3).

$$FS = \frac{UCS_p}{\bar{x} - 2\varpi} \tag{3}$$

Where: UCS_p is the standard reference value of uniaxial compressive strength of a backfill specimen measured by indoor proportioning tests under a particular backfill ratio parameter, MPa; $\bar{x}$ is the average of the specimen set of uniaxial compressive strength data from core specimens drilled in the in-situ backfill after the slurry prepared by the mine backfill station has cured in the stope for at least 28 days using the same backfill proportioning parameters, MPa; $\bar{\omega}$ is the standard deviation of the strength of the same in-situ backfill core specimens. This equation recommends a range of 2 times the standard deviation of the sample mean of the core sample strength, which can cover 95.45% of the sample data area and is an empirical equation in line with the engineering application significance of mine backfill mining.

By combining the theoretical, analytical solution for the strength requirement of the backfill in different stopes with the floating safety factor for different periods in different mines, the actual strength requirement of the backfill in the current period of the mine can be derived, thus determining the values of the proportioning parameters of the mine backfill system.

By incorporating in-situ backfill coring and core specimen strength testing into the daily production tasks of the mine, the sample database of mine backfill quality control effects can be continuously supplemented with feedback to derive floating safety factors for different periods of the mine and achieve floating optimization of mine backfill

strength requirement. When the stability of the mine backfill system and the quality control of the backfill are significantly improved, it will increase the average strength and decrease the dispersion of the core samples of the mine backfill. The floating safety factor calculated by core testing and mathematical statistics will be reduced accordingly. The actual strength requirement of the mine backfill will then be reduced. Conversely, if the stability of the backfill system is reduced, this will eventually feed through to an increase in the design index of the actual strength requirement.

CONCLUSION

This paper systematically reviews the development of backfill mining methods. The latest technology application progresses are introduced from three aspects: backfill mining methods used in metal mines, backfill technology, and backfill mechanics. The research progress and development trend of backfill mining are analyzed.

(1) Backfill mining is an important carrier to realize the green mining of metal mines. Advanced backfill mining theory and technological innovation is the key to the efficient recovery of mineral resources, minimizing environmental impact and reducing mining and backfill costs.

(2) Large-scale and high-efficiency continuous backfill mining is a significant development direction of underground mining technology for metal mines in the future. The open stopping with subsequent backfill mining is critical to realize large-scale and efficient mining of thick ore bodies. Continuous backfill mining is a revolutionary development of achieving highly efficient mining of broken ore bodies.

(3) Backfill technology is the core element of backfill mining. The stable density of the backfill slurry in the pipeline is more important than the level of the slurry concentration itself. A stable, reliable, and simple transport process of the backfill slurry is more effective than the complex automatic control.

(4) The innovation in the low-cost backfill material is critical to promoting the development of backfill technology. The green and low-carbon backfill technologies, new materials, and new equipment should be paid more attention, such as developing the cemented paste backfill systems with a capacity of more than 250 m3/h, promoting the application of slag cementitious materials instead of ordinary Portland cement, and using the dismountable barricades instead of a traditional concrete retaining wall.

(5) The test methods and standards for cemented backfill's basic physical and mechanical parameters are not uniform, and the correlation model between laboratory and in-situ backfill strength has not yet been established. Emphasis should be placed on developing scientific and unified backfill mechanics testing methods and constructing the required backfill strength model that matches the in-situ stress state within the stope.

ACKNOWLEDGEMENT

Financial support from the National Key Research and Development Program of China (Grant No. 2022YFE0135100), National Nature Fund Project (No.: 52104131), and the Exploration fund of BGRIMM（02-2229）is gratefully acknowledged.

REFERENCES

1. Landriault, D. (2001) Backfill in underground mining. Underground mining methods: engineering fundamentals and international case studies, 601-614.
2. Lang, L. C., SUN, Z. (1980) Funnel blasting methods devel-oped into new underground mining techniques. Mining Engineering, 6 (7), 43-50.
3. Sun, Z. M., Chen, H., Wang, H. X. (2006) Huge ore caving technology with spherical explosive cartridges and cluster drilling holes. In A collection of papers of forum on new advances in mining science and technology of metal mines, 4-6.
4. Xiao-Cong, Y. A. N. G., Zhi-Qiang, Y. A. N. G., Lian-Ku, J. I. E., Ming, W. E. I. (2013) Experimental Research on the New Non-pillar Continuous Mining Method for Underground Metal Mines. Metal Mine, 42 (07), 35.
5. Liu, G. S. (2017) Required Strength Model of Cemented Backfill with Research on Arching Mechanism Considering Backfill-Rock Interaction (Doctoral dissertation, Dissertation]. Beijing: University of Science and Technology Beijing.
6. Tommila, E. (2014) Mining method evaluation and dilution control in Kittilä mine (Master's thesis).
7. Wang, X., Xu, Z., Xu. H. (2017) Discussion on mining technologies for open stoping with subsequent filling. China Mining Magazine, 26 (8), 99-103.
8. Chen, Q., Zhou, K., Gu, D. (2012) Cavity synergetic utilization mechanism. Journal of Central South University (Science and Technology), 43 (3), 1080-1086.
9. Zhang, T., Zhao, X., Li, H. (2019) Continuous dry filling of long room method for steeply inclined and medium thick orebody. Gold Science and Technology, 27 (5), 704-711.
10. Potvin, Y., Thomas, E., Fourie, A. (2005) Handbook on mine fill. In Not available (p. 179). Australian Centre for Geomechanics.
11. Hai-yong, C. H. E. N. G., Ai-xiang, W. U., Shun-chuan, W. U., Jia-qi, Z. H. U., Hong, L. I., Jin, L. I. U., Yong-hui, N. I. U. (2022) Research status and development trend of solid waste backfill in metal mines. Chinese Journal of Engineering, 44 (1), 11-25.
12. Grabinsky, M., Bawden, W., Thompson, B. (2021) Required Plug Strength for Continuously Poured Cemented Paste Backfill in Longhole Stopes. Mining, 1 (1), 80-99.
13. Guo, L., Zhang, L., Li, W. (2020) Progress and pro-spects of the preparation of cementitious materials based on nonferrous metallurgical slags. Gold Science and Technology, 28 (5), 321-636.
14. Ai-Xiang, W. U., Ying, Y. A. N. G., Hai-yong, C. H. E. N. G., Shun-man, C. H. E. N., Yue, H. A. N. (2018) Status and prospects of paste technology in China. Chinese Journal of Engineering, 40 (5), 517-525.
15. Ai-Xiang, W. U., Yong, W. A. N. G., Hong-Jiang, W. A. N. G. (2016) Status and prospects of the paste backfill technology. Metal Mine, 45 (07), 1.
16. Guo, L., Peng, X., Yang, X., Shi, C., Yu, B., Xu, W., Jia, Q. (2017) Industrial practice on optimizing tailings composition combined with ore concentration processes. In 12th International Conference on Mining with Backfill 2017, Minefill 2017, Denver, United States 19-22 February 2017, 69-79. Society for Mining, Metallurgy and Exploration.
17. Jewell, R. J., Fourie, A. B. (Eds.). (2006) Paste and thickened tailings: a guide. Australian Centre for Geomechanics, The University of Western Australia.

18. Mitchell, R. J., Roettger, J. J. (1984) Bulkhead pressure measurements in model fill pours. CIM Bull. (Canada), 77 (868).
19. Zheng, J., Li, L. (2020) Experimental study of the "short-term" pressures of uncemented paste backfill with different solid contents for barricade design. Journal of Cleaner Production, 275, 123068.
20. Cui, L., Fall, M. (2017) Modeling of pressure on retaining structures for underground fill mass. Tunnelling and Underground Space Technology, 69, 94-107.
21. Lu, H., Qi, C., Li, C., Gan, D., Du, Y., Li, S. (2020) A light barricade for tailings recycling as cemented paste backfill. Journal of Cleaner Production, 247, 119388.
22. Berndt, C. C., Rankine, K. J., Sivakugan, N. (2007) Materials properties of barricade bricks for mining applications. Geotechnical and Geological Engineering, 25, 449-471.
23. Li, L., Aubertin, M. (2009) Horizontal pressure on barricades for backfilled stopes. Part II: Submerged conditions. Canadian Geotechnical Journal, 46 (1), 47-56.
24. Hughes, P. B., Pakalnis, R., Hitch, M., Corey, G. (2010) Composite paste barricade performance at Goldcorp Inc. Red Lake Mine, Ontario, Canada. International Journal of Mining, Reclamation and Environment, 24 (2), 138-150.
25. Pengyu, Y., & Li, L. (2015) Investigation of the short-term stress distribution in stopes and drifts backfilled with cemented paste backfill. International Journal of Mining Science and Technology, 25 (5), 721-728.
26. Duncan, J. M., Wright, S. G., Brandon, T. L. (2014) Soil strength and slope stability. John Wiley & Sons.
27. Mitchell, R. J., Olsen, R. S., Smith, J. D. (1982) Model studies on cemented tailings used in mine backfill. Canadian Geotechnical Journal, 19 (1), 14-28.
28. Liu, G., Li, L., Yang, X., Guo, L. (2016) Stability analyses of vertically exposed cemented backfill: A revisit to Mitchell's physical model tests. International Journal of Mining Science and Technology, 26 (6), 1135-1144.
29. Li, L., Aubertin, M., Belem, T. (2005) Formulation of a three dimensional analytical solution to evaluate stresses in backfilled vertical narrow openings. Canadian Geotechnical Journal, 42 (6), 1705-1717.
30. Pirapakaran, K., Sivakugan, N. (2007) Arching within hydraulic fill stopes. Geotechnical and Geological Engineering, 25 (1), 25-35.
31. Ting, C. H., Shukla, S. K., Sivakugan, N. (2011) Arching in soils applied to inclined mine stopes. International Journal of Geomechanics, 11 (1), 29-35.
32. Liu, G., Li, L., Yang, X., Guo, L. (2016) A numerical analysis of the stress distribution in backfilled stopes considering nonplanar interfaces between the backfill and rock walls. International Journal of Geotechnical Engineering, 10 (3), 271-282.
33. Hassani, F. P., Mortazavi, A., Shabani, M. (2008) An investigation of mechanisms involved in backfill-rock mass behaviour in narrow vein mining. Journal of the Southern African Institute of Mining and Metallurgy, 108 (8), 463-472.
34. Zou, S., Nadarajah, N. (2006, June). Optimizing backfill design for ground support and cost saving. In Golden Rocks 2006, The 41st US Symposium on Rock Mechanics (USRMS). OnePetro.
35. Dirige, A. P. E., McNearny, R. L., Thompson, D. S. (2009, May) The effect of stope inclination and wall rock roughness on back-fill free face stability. In Rock Engineering

in Difficult Conditions: Proceedings of the 3rd Canada-US Rock Mechanics Symposium 9-15.

36. Li, L. (2014) Analytical solution for determining the required strength of a side-exposed mine backfill containing a plug. Canadian Geotechnical Journal, 51 (5), 508-519.
37. Liu, G., Li, L., Yang, X., Guo, L. (2018) Required strength estimation of a cemented backfill with the front wall exposed and back wall pressured. International Journal of Mining and Mineral Engineering, 9 (1), 1-20.
38. Liu, G. S., Yang, X. C., Guo, L. J. (2019) Models of three-dimensional arching stress and strength requirement for the backfill in open stoping with subsequent backfill mining. Journal of China Coal Society, 44 (5), 1391-1403.

XV International Mineral Processing and Recycling Conference
17-19 May 2023, Belgrade, Serbia

INNOVATIVE TECHNIQUE FOR ANOMALOUSLY FLUORESCENT DIAMONDS RECOVERY BASED ON LUMINOPHORE-CONTAINING MODIFIERS

V.A. Chanturia, V.V. Morozov[#], G.P. Dvoichenkova, E.L. Chanturia, Yu.A. Podkamenny
Institute of Complex Exploitation of Mineral Resources of the Russian Academy of Sciences, Moscow, Russia

ABSTRACT – The mechanism of X-ray luminescence signal formation from a diamond with a luminophore-containing composition fixed on its surface has been experimentally studied. Applying zinc sulfide-based inorganic luminophores or zinc orthosilicate and anthracene mixture-based luminophores in the compositions has been justified. The use of medium molecular weight oil fractions with high adhesive ability to diamonds and inorganic luminophores as a collector for the luminophore-containing composition was proposed. It was shown that the selected composition (FL-530, anthracene, diesel fuel fraction, catalytic cracking heavy gaso) provided the modification of diamond spectral characteristics. The tests demonstrated the possibility of increasing diamond recovery by 5% due to the detection of diamond crystals with initially weak or anomalous fluorescence, modified using the proposed composition.

Keywords: Diamonds, X-Ray Fluorescence Separation, Luminophores, Organic Collector, Characteristics.

INTRODUCTION

Analysis of the causes of diamond losses shows that more than 5% of diamond crystals have an anomalously low or high amplitude of fast and slow X-ray luminescence signal components, which, as well as their ratio, prove outside the permitted intervals of criteria in the separator settings. This leads to the crystal losses in the X-ray luminescent process. A promising way to decrease losses of weak and anomalously luminescent diamonds in X-ray luminescent separation process is to modify their spectral characteristics by special luminophore compositions. The luminophore modifiers used include inorganic and organic luminophores, which provide the desirable change in the kinetic characteristics of the X-ray luminescence signal of a diamond, as well as an organic collector, which ensures the fixation of the composition on the surface of diamonds.

MATERIAL AND METHODS OF WORK

The experimental procedure included the preparation of a luminophore emulsion, consisting of luminophores, a collector (organic liquid), and an aqueous phase, then the emulsion treatment of a mixture of diamonds and kimberlite minerals, the emulsion removal, and the analysis of the spectral and kinetic characteristics of the treated minerals.

[#] corresponding author: dchmggu@mail.ru

To assess the efficiency of luminophore fixation on the surface of diamonds, a visiometric method was used, which included obtaining and analyzing images of diamond crystals or kimberlite mineral grains with the fixed luminophores in UV light [1]. In the tests, the collections of diamonds and kimberlite minerals with grain sizes from 2 to 5 mm, selected from gravity concentrate, were used.

The spectral and kinetic characteristics of diamond crystals and kimberlite mineral grains were measured at a "Polus-M" manufactured by CJSC "Burevestnik" [2]. The X-ray luminescence signal of diamonds and kimberlite minerals was detected by the following parameters: amplitudes of slow and fast signal components (A_{SC}, A_{FC}), a signal attenuation time constant (τ_a), a normalized correlation function, a signal convolution (*Sv*), and the ratio of the signal amplitude components (K_A) [3].

An industrial X-ray luminescent separator LS-D-4-03H was used in commercial tests.

THE PRINCIPLE OF SELECTING THE COMPOSITION OF LUMINOPHORE-CONTAINING MODIFIERS

The selected principle implies a simultaneous increasing A_{SC} и A_{FC} in such a ratio that the spectral characteristics of diamonds are shifted to the area of their detection (identification as diamonds) in the ranges of the separator settings. This requires shifting other characteristics (*Sv* and τ_a) of weakly and anomalously luminescent diamond crystals to the zone of positive detection.

The analysis of the changes in the amplitudes of the fluorescence signal from diamonds and kimberlite minerals under the action of luminophore-containing emulsion showed that the diamonds showed the increase in the amplitudes of 500-1600 mV. For the accompanying kimberlite minerals, due to less adsorption of the luminophore-containing composition, the increase in the components amplitudes proved lesser, 63-245 mV.

When using the compositions containing FL-530 and anthracene, a 490 mV increase in A_{SC} and a 450 mV increase in A_{FC} were achieved for diamonds (Fig. 1). The component gain ratio is close to 1, and this allows to steadily detect anomalous and weakly luminescent diamonds after their corresponding treatment. Such an increase in the components causes a shift in the component ratio K_A from 14.7 to 10.3, which ensures the detection of anomalously luminescent diamonds by this criterion.

When treated with the emulsion with the selected composition and concentrations of luminophores, anomalously and weakly fluorescent diamonds demonstrate increasing A_{SC} and A_{FC} and are detected as diamonds with common spectral characteristics (Fig. 1, vectors *4*, *5*). Most of kimberlite minerals characterized by low A_{SC} and A_{FC} does not reach the identification area. Magnesian ilmenite and phlogopite (vectors *6* and *9*) are the closest to this area.

At the same time, the values of these components of minerals with high A_{FC} (pyrope) change to a small extent and do not reach the identification area (Fig. 1, vector *10*). The characteristics of kimberlite minerals with high A_{SC} and low A_{FC} (zircon) also do not reach the positive identification zone (Fig. 1, vector *8*).

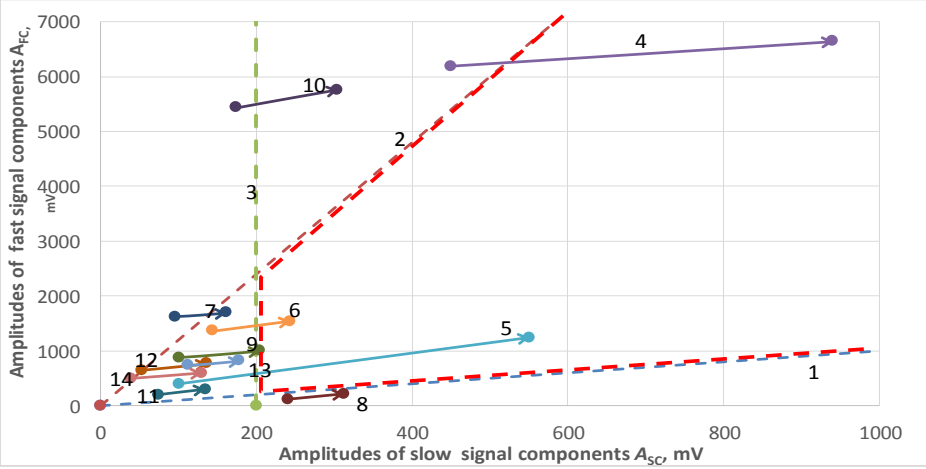

Figure 1 Changes in the spectral characteristics A_{SC} and A_{FC} of diamonds and associated kimberlite minerals after treatment with luminophore emulsion: *1*, *2* - lower and upper limits of the diamond identification area based on K_A; *3* - boundary of the diamond identification area based on A_{SC}, where *4*, *5* - anomalous and weakly fluorescent diamonds; *6* – magnesian ilmenite; *7* - phlogopite; *8* - zircon; *9* - olivine; *10* - pyrope; *11* - leucocratic rock; *12* - melanocratic rock; *13* - chalcopyrite; *14* - pyrite; ⬚ - area of positive identification (detection)

RESULTS AND DISCUSSION: STUDY OF INTERACTIONS IN A DIAMOND – LUMINOPHORE - ORGANIC LIQUID SYSTEM

Obtaining a stable heterophase system diamond - luminophore - organic liquid is ensured due to the efficient extraction of the inorganic luminophore by the organic liquid and the adhesion of the luminophore-containing composition on diamonds. The formation of diamond aggregates in which individual crystals are bound together by the luminophore-containing liquid was confirmed by the findings of luminescence microscopy study (Fig. 2a). After drying, the luminophores contained in the organic liquid are stably fixed on the surface of diamond crystals (Fig. 2b).

Calculation of the X-ray luminescent signal from a diamond with the organic phase and luminophore drops fixed on its surface involves adding the signals of all components of the luminophore-containing composition to the diamond's own signal. When determining the resulting characteristics, it is necessary to take into account the attenuation of a diamond's own signal due to shielding of the light flux by the luminophore composition with luminophore particles and the attenuation of the signal from the luminophores due to the absorption and scattering of the light flux by diamond crystals, as well as shielding the light flux by other luminophore grains and the organic collector.

To determine the degree of shielding of the diamond surface by luminophores, the distribution of luminophore on the surface of diamonds treated with the luminophore emulsion was measured using the technique of visiometric analysis in ultraviolet light using a Micromed 3 LUM microscope (Fig.3) [4].

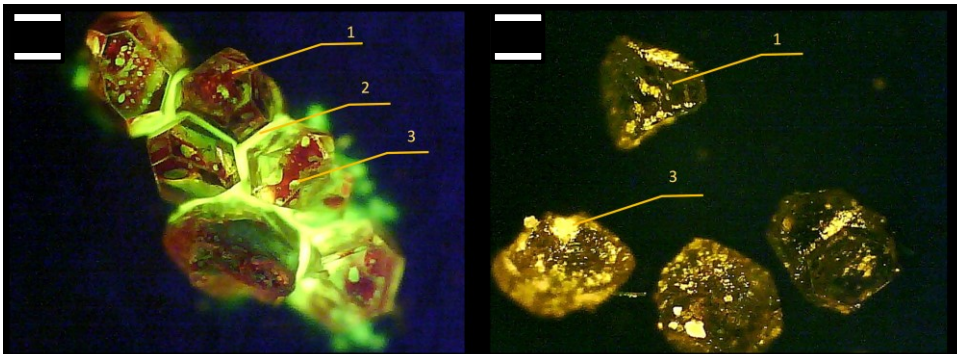

Figure 2 Diamond aggregate in organic liquid containing soluble luminophores (a) and individual diamond crystals after removal of excess luminophore-containing liquid and drying (b): 1 - diamond; 2 - luminophore-containing organic liquid; 3 - organic luminophore coating on the diamond surface

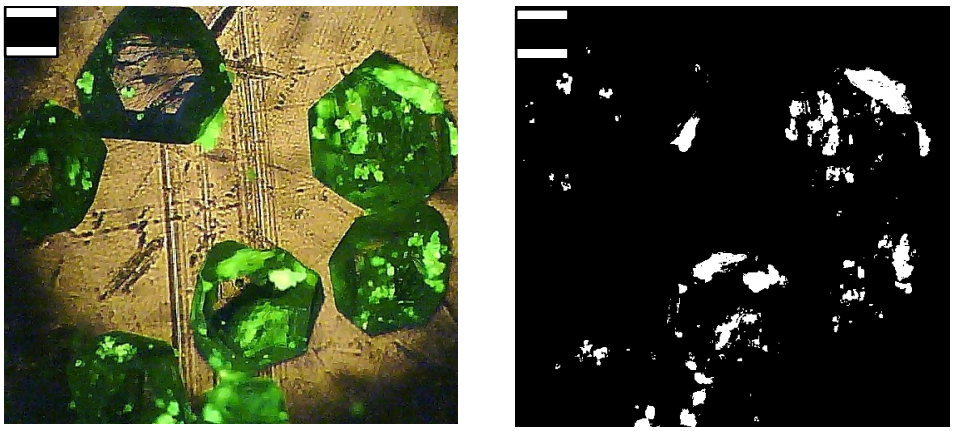

Figure 3 Image of a diamond crystal with fixed luminophore FL-530 in ultraviolet light (a) and the findings of visiometric analysis with detection of areas with fixed luminophore (ν=525 nm)

The findings of the analysis of the obtained images showed that the degree of spreading luminophores over the surface of diamonds was variable, ranging 5 to 50%, while for kimberlite minerals, the degree ranged 1 to 15%. The comparison of the signals of the diamond with luminophore and those of the luminophore individually showed that the attenuation of the signal from the diamonds due to scattering and shielding of light flux was 5-15%, while that from the kimberlite minerals was 20-40%.

RESULTS AND DISCUSSION: SELECTION OF LUMINOPHORE SYSTEM COMPOSITION

The form of the X-ray luminescent signal from treated diamonds when using the composition based on FL-530 luminophore and anthracene is closest to the form of the X-ray fluorescence signal of natural diamond [5]. Other promising luminophores are zinc sulfides activated by copper ions. The advantage of the latter group of luminophores is

the closest X-ray luminescent signal wavelength to that of natural diamonds and the presence of phosphorescence effect, leading to the appearance of the so-called slow attenuation component. The selected luminophores of the group of zinc and cadmium sulfides and zinc orthosilicate are characterized by high fluorescence brightness and acceptable spectral characteristics (Table 1).

Table 1 Spectral characteristics of the investigated luminophores)

No.	Brand name	Composition	Wavelength of spectral characteristics maximum, nm	Wavelength perceivable by photo-electronic multiplier, nm*	Fluorescence intensity, $\mu W/cm^2/nm$
Zinc and cadmium sulfides and selenides group					
1	EL 570M	ZnS, ZnSe : Cu, Ag	563	555	0.077
2	FC-110	ZnS : Cu	465, 510, 545	465	0.122
3	P-530	ZnS, CdS : Ag	534	525	0.308
4	FS-4	ZnS : Ag	474	465	0.204
5	PC-424	ZnS : Ag	563	443	0.058
6	FK-1	ZnS : Ag	484	466	0.152
7	FK-2	ZnS : Ag	527	498	0.200
8	E-455-115	ZnS ; Cu	515	468	0.194
9	E-515-115	ZnS : Cu	515	510	0.118
Zinc orthosilicate					
10	FL-530	$ZnSiO_4$: Mn	530, 544, 575	520	0.109

The selected luminophores are in the middle operating range of the detectors (photo-electronic multipliers) used in separators. This confirms the possibility of signal detection in the separators and substantiates the possibility of shifting the signal wavelength of diamonds with the original emission in the yellow and red region into the detection area by the application of luminophores.

The main requirement for selecting reagent-hydrophobisers for luminophores and determining their operating concentrations is creating conditions for irreversible chemisorption reactions of heteropolar ion directly on the surface of the luminophores.

For sulfide minerals, the use of potassium xanthate as a surface hydrophobizator is known [6]. To facilitate the interaction with xanthate ions, the surface of zinc sulfide is activated by copper ions. In this case, the concentration of xanthate ions required for the hydrophobization of zinc sulfide decreases by several tens of times.

Maximum oleophilicity is achieved by the hydrophobization of E-515-125 luminophore with butyl xanthate in the concentration of more than 10^{-4} mol/L, when the fraction of the luminophore passing into the aqueous phase decreases by 25 times. The similar results were obtained for the other studied luminophors [7].

As organic collectors (the basis of the luminophore-containing composition), a compound of diesel fuel fraction (DFF) and catalytic cracking heavy gasoil (CCHG) belonging to the viscous light fractions of fuel oil recycling was proposed. The comparison of the spectral and kinetic characteristics of the dry samples of luminophores FL-530 and E-515-115 and the same luminophores moistened with CCHG showed almost complete retention of the properties of the original luminophores.

The performance of the selected compositions of luminophore-containing emulsions was confirmed by the findings of the visiometric analysis, which confirmed the selective fixation of the luminophore compositions on diamonds (Fig. 4).

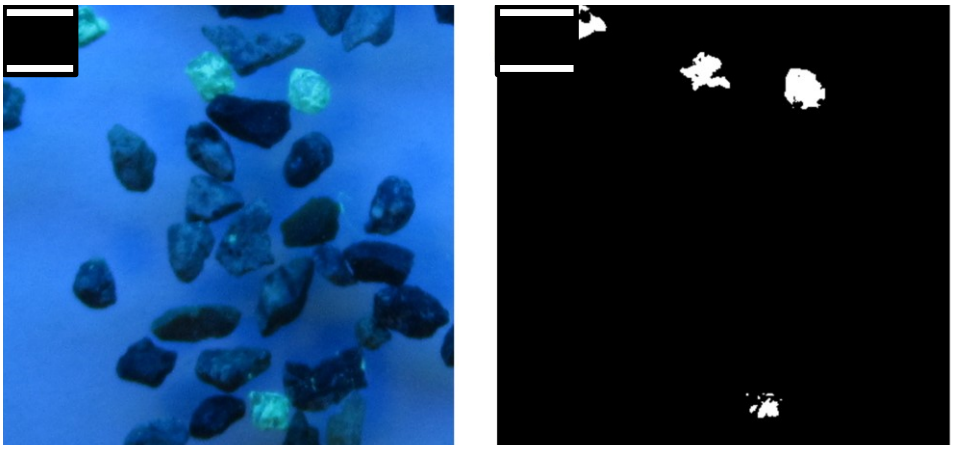

Figure 4 Image of diamond crystals and kimberlite mineral grains after treatment with E-515-115-based luminophore composition: (a) in UV light; (b) at visiometric analysis (ν=510 nm)

The analysis of the findings of the studies presented in Table 2 showed that after the treatment, a significant increase in the amplitudes of the fast and slow components (by 30-40%) was observed for diamonds without the deterioration of other spectral and kinetic characteristics. The treatment of diamonds with the luminophore-containing composition provides increasing their recovery from 40 to 75%. When using the composition based on luminophores E-515-115 and FL-530 treated in a hydrophobizator, the extraction of weakly luminescent diamonds into concentrate increased to 85-90% (test 3).

RESULTS AND DISCUSSION: APPRAISAL OF THE TECHNIQUE FOR MODIFYING DIAMOND CHARACTERISTICS BY LUMINOPHORE COMPOSITIONS

The tests of the selected mode of diamond-containing material preparation using luminophore emulsions were carried out at a LS-D-4-03H separator [8] with the use of natural diamonds and kimberlite product of the main XRF separation operation (Fig. 5).

During the tests, the diamond and kimberlite samples were treated with an aqueous-organic emulsion containing a mixture of luminophores FL-530 and anthracene with an organic collector. After processing the initial feed, the excess of the luminophore-containing emulsion was removed, and the diamonds and kimberlite were fed into the

X-ray luminescent separator. The separator settings used and the recorded parameters (the values of the main spectral and kinetic characteristics) corresponded to those used in the operating X-ray luminescent separators.

Table 2 Results of testing modifiers with hydrophobic luminophores for treatment of weakly (w) and anomalously (a) luminescent diamonds

No.	Collector composition	Mineral	Sv	τ_a, ms	A_{FC}, mV	A_{FC} - A_{Fa}, mV	K_A	Recovery, %
1	Without luminophors	Diamond (w)	0.15	4.3	120	564	5.7	40
		Diamond (a)	-	0.1	No changes	1022	≥50	20
		Kimberlite	-	-	No changes	<50	-	0.5
2	E-515-115 + DFF	Diamond (w)	0.25	2.4	231	1345	7.7	75
		Diamond (a)	0.11	0.4	59	1332	13.8	60
		Kimberlite	-	-	No changes	156	-	0.6
3	E-515-115-G5 + CCHG + DFF	Diamond (w)	0.25	2.4	275	1122	5.1	90
		Diamond (a)	0.17	0.6	167	1,499	10.0	85
		Kimberlite	-	-	No changes	<50	-	0.7
4	FL-530-G3 + anthracene + DFF	Diamond (w)	0.22	1.6	296	1336	5.5	60
		Diamond (a)	0.11	0.4	209	1332	7.4	85
		Kimberlite	-	-	No changes	<50	-	0.7
5	FL-530-G3 + CCHG + DFF	Diamond (w)	0.22	1.6	329	1216	4.7	80
		Diamond (a)	0.17	0.6	275	1469	6.3	90
		Kimberlite	-	-	No changes	<50	-	0.9

A_F is the amplitude of the fast component of the air X-ray luminescent signal (background)

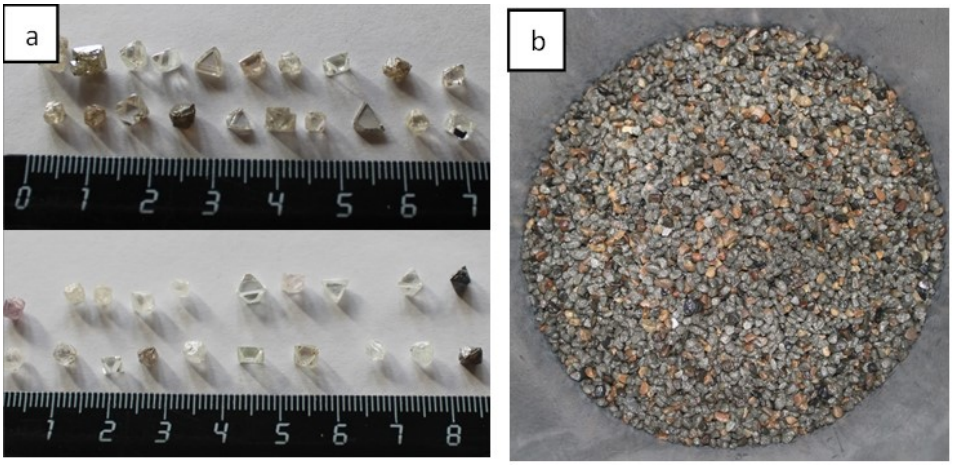

Figure 5 Photographs of diamonds (a) and concentrate samples (b) used in the tests on X-ray luminescent separator

Counting of diamond crystals in the concentrate showed that after the treatment with the luminophor-containing emulsion, all diamonds were extracted from the sample, including the crystals previously not detected by the X-ray luminescent LS-D-4-03H separator detecting system when processing the same sample in the check test. The increase in the diamond recovery was 5% in the first series and 4.7% in the second series. This increase corresponds well to the fraction of weakly and anomalously fluorescent diamonds in the initial feed; thus, these diamonds were successfully extracted. One more important finding is the fact of the complete extraction of normally fluorescent diamond crystals, i.e., the absence of negative impact of the treatment on natural diamonds with normal fluorescence was confirmed. Thus, the study findings confirmed the effectiveness of the developed technique as a whole and the selected compositions and proposed methods for improving and intensifying luminophore fixation on the surface of diamonds.

CONCLUSION

The principles of modifying the spectral-kinetic characteristics of weakly and abnormally luminescent diamonds with luminophore-containing compositions are proposed. The efficient compositions of reagent-modifiers of spectral-kinetic characteristics of diamonds have been developed. It was shown that the condition for increasing diamond recovery process performance was to obtain a stable heterophase diamond - organic liquid - luminophore system. The study findings showed that the treatment of weakly and anomalously fluorescent diamonds with luminophore-containing reagents based on zinc sulfides (E-515-115) and zinc orthosilicate (FL-530) improved their spectral characteristics and thus enabled their extraction into concentrate in X-ray luminescent separation with ensuring high selectivity of the process.

ACKNOWLEDGEMENT

The research was carried out with the financial support of the Russian Science Foundation under the project No. 21–17-00020 (https://rscf.ru/project/21-17-00020).

REFERENCES

1. Gonzalez, R., Woods, R., Eddins, S. (2006) Digital Image Processing in the Matlab Environment, (Publ. Technosphere, Moscow), 616, (in Russian).
2. https://www.bourevestnik.ru/products/sorters/portable-sorters/polyus-m/
3. Martynovich, E.F., Mironov, V.P. (2009) X-ray luminescence of diamonds and its use in the diamond-mining industry. *Izv. vuzov. Fizika* [Proceedings of Higher Education Institutions. Physics], 52 (12/3), 202-210 (in Russian).
4. Vinogradova, G.N., Zakharov, V.V. (2020) *Osnovy mikroskopii, chast' 2* [Fundamentals of microscopy, part 2]: (Publ. ITMO University, St. Petersburg,), 248, (in Russian).
5. Chanturia, V.A., Dvoichenkova, G.P., Morozov, V.V., Yakovlev, V.N., Koval'chuk, O.E., Podkamennyi, Yu.A. (2019) Experimental Substantiation of Luminophore-Containing Compositions for Extraction of Nonluminescent Diamonds, Journal of Mining Science, 55 (1), 116-123.

6. Abramov, A.A. (2008) *Flotatsionnye metody obogashcheniya* [Flotation beneficiation techniques]. Textbook (Gornaya Kniga Publ., Moscow), 710. (in Russian).
7. Morozov, V.V., Chanturia, V.A., Dvoichenkova, G.P., Chanturia, E.L. (2021) Stimulating modification of spectral and kinetic characteristics of diamonds by hydrophobization of luminophores. Journal of Mining Science. 57 (5), 821-833.
8. https://ued-lab.ru/catalog/analiticheskoe-oborudovanie/oborudovanie-dlya-almazodobyvayushchey-promyshlennosti/rentgenolyuminestsentnyy-separator-ls-d-4-03n/

XV International Mineral Processing and Recycling Conference
17-19 May 2023, Belgrade, Serbia

WTE AS INTEGRATED PART OF CIRCULAR ECONOMY

G. Vujić, N. Maoduš, M. Živančev
University of Novi Sad, Faculty of Technical Sciences, Novi Sad, Serbia

ABSTRACT – More serious development of waste management in Serbia began after the democratic changes and passing of the first waste management strategy in 2010. Waste management experts, as well as a large share of the public view this development as very slow or, at least, not fast enough. We are witnesses of a large number of illegal dump sites, low level of recycling, as well as various other indicators (plastic waste in rivers and landscape, landfill fires, etc.) which indicate inadequate, or in some cases, uncivilized waste management methods. This paper traces the path of waste management development in Serbia, i.e. achieving the principles of a circular economy with the analysis of social and economic indicators, with the aim of finding the cause of a current state of waste management, i.e. defining whether that path has really slowed down or maybe it is completely appropriate for the overall state of a developing country like Serbia.

Keywords: Waste, Management, Circular, Economy, Serbia.

INTRODUCTION

Improvement of waste management system in the Republic of Serbia began in 2002 when the first sanitary landfill was built in Vranje, however, that landfill never became a regional landfill. Next, the private Austrian company ASA, the current FCC group, started the operation of a sanitary landfill in Kikinda, which even to this day does not have a regional character, due to the fact that the municipalities belonging to the region do not bring waste to that landfill. After that, the private company Porr Werner Weber built sanitary landfills in Jagodina and Leskovac, which were supported by other municipalities in the region, and since 2009, these landfills have been functioning as regional landfills. In 2011, a public regional landfill was built in Užice for 7 municipalities, and then in 2015 in a similar way, the landfill for the cities of Sr. Mitrovica and Šabac in Sremska Mitrovica, as well as the landfill in Pancevo were built. In the Subotica region, sanitary landfill in Bikovo started operating in 2019, and finally, the largest project in the field of waste management in Serbia is the construction of sanitary landfill project in Belgrade, which is based on a PPP (public private partnership) with the French company SUEZ, now Veolia, where a waste incinerator was also built on the site next to the sanitary landfill as a key segment of waste management.

The increase in the number of sanitary landfills in the Republic of Serbia over the past 20 years is shown on Fig. 1.

According to the data of the Republic of Serbia Environmental Protection Agency [1], when looking at the amount of waste, it can be noted that the percentage of reused waste increases during this period, mostly due to the EPR (extended producer

corresponding author: goranvujic@uns.ac.rs

responsibility) system for packaging waste, but also due to increased reuse capacity of other waste streams related to treatment, such as electronic waste, waste tires, vehicles etc.

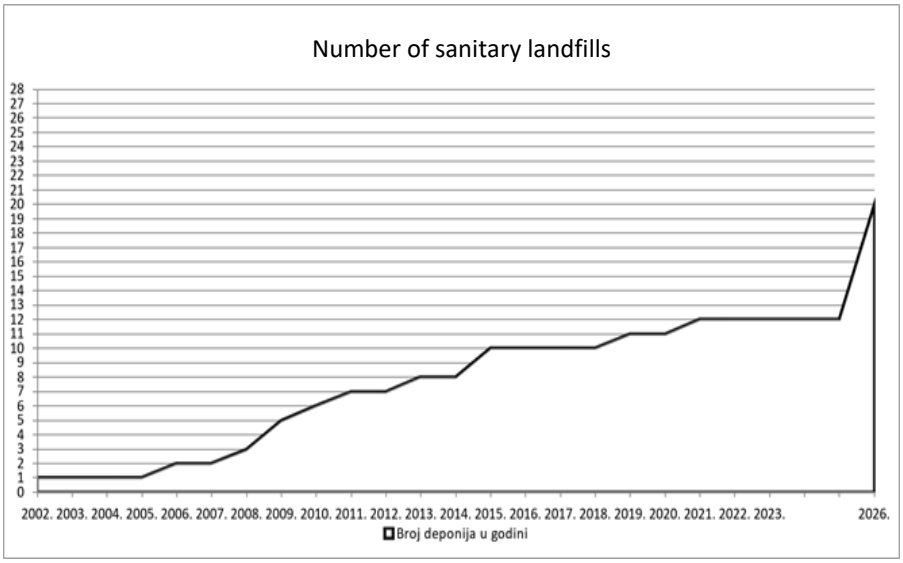

Figure 1 Development of sanitary landfills from 2002 to 2023

A big increase in the amount of collected and treated waste occurs with the start of operation of the sanitary landfill in Vinča, which, according to the city of Belgrade, accepts about 630,000 tons of waste annually. The waste incinerator, the only one at the moment in Serbia, has a capacity of about 310,000 tons of waste starting in 2023.

If we look at the ongoing projects, we can say that in the next 3 to 4 years, several more regional centers should be completed in Serbia.

Novi Sad is about to announce a tender for a sanitary landfill and an MBT (mechanical biological treatment) plant with a total value of around 95 million Euros.

Sombor and Valjevo are in the EBRD (European Bank for Reconstruction and Development) loan, as part of this loan, the existing landfills in Užice and Pirot will be upgraded, while a transfer station will be built in Nova Varoš, from where the waste will be taken to the landfill in Užice. The entire arrangement with the EBRD is over 110 million Euros worth.

The municipalities of Kruševac and Vranje are building regional landfills with a KfW loan, with a value of around 30 million euros. As the funds have been secured and the projects are mostly completed, it can be expected that the treatment of waste in Serbia will increase significantly in the next 3 to 4 years.

According to the data of the Ministry of Environmental Protection, the Environmental Protection Agency, the amount of disposed waste at sanitary landfills was around 385,228 t/year in 2015 and in 2021 that amount increased to 850,115 t/year.

The amount of reused/treated waste in the period from 2011 to 2021 is shown in the table below.

Table 1 Amount of recycled waste [1]

Year	Total treated (t)	Treated with process R1 – R10 (t)	Treated with process R11 – R13 (t)
in 2011	1,453,772	1,422,017	31,775
in 2012	1,119,482	940.662	178,820
in 2013	1,787,664	1,493,388	294.275
in 2014	2,005,387	1,660,068	345.319
in 2015	1,639,486	1,279,231	360,255
in 2016	1,679,340	1,418,226	261.122
in 2017	1,740,131	1,479,522	260.609
in 2018	2,033,149	1,700,470	332,679
in 2019	2,270,398	1,971,395	299,003*
in 2020	2,143,134	2,050,048	93,086*
in 2021	2,288,832	2.203.126	85,706*

* The amount entered in the column treated with procedure R11 - R13 for the period 2019–2021 refers only to procedure R11.

The amounts of secondary raw materials that are subjected to utilization in one of the R operations are shown in the table below.

Table 2 Types and quantities of recycled waste representing secondary raw materials [1]

Type of waste	Amount of waste subjected to waste recovery operation (t)
Metals	816.013
Plastic	58,804
Glass	2.172
Wood waste	85,445
Paper and cardboard	246.193
Batteries and accumulators	21,298
Textiles	1.052

The table below shows the amount of packaging that was put into the market and the amount of collected and reused packaging waste on the territory of the Republic of Serbia in the period from 2010 to 2021.

Table 3 The amount of packaging put into circulation and the amount of collected and reused packaging waste in the period from 2010 to 2021 [1]

	in 2010	in 2011	in 2012	in 2013	in 2014	in 2015	in 2016	in 2017	in 2018	in 2019	in 2020	in 2021
Packaging put into market (t)	303.337	343,657	344.246	321,585	333.016	344,074	348,872	357,919	358,955	370.607	362.237	389,956
Recycled packaging (t)	15,465	49,988	67,916	87,950	102,673	134,970	155,573	182.393	200,857	228,547	226.021	247,634
Utilization (%)	5.1	14.5	19.7	27.3	30.8	39.2	44.6	51.0	56.0	61.7	62.4	63.5

In Tab. 4 general and specific goals of waste management defined by EU Directives are shown, Council Directive 2008/98/EC on waste [2], which replaces and supplements Framework Directive 75/442/EEC, 2006/12/EC, Council Directive 99/31/EC on landfills [3], EU Directive 2018/850 on amendments [4] to the directive on landfills, Council Directive 94/62/EC on packaging and packaging waste [5] amended by Directive 2005/20/EC, 2004/12/EC, 1882/2003/EC and EU Directive 2018/852 [6].

Table 4 General and specific waste management goals defined by EU directives

Type of waste	Year	MIN Reuses	MIN recycling	Collection coverage
Packaging waste	in 2008	60%	55%	
	in 2025	Separate collection for paper, metal, plastic, glass and textiles		
	2030	70% recycling (55% plastic, 30% wood, 80% ferrous metals, 75% glass, 85% paper and cardboard)		
Biodegradable waste removed from landfills	in 2006	A reduction to 75% of the 1995 level.		
	in 2009	A reduction to 50% of the 1995 level.		
	in 2016	A reduction to 35% of the 1995 level.		
It was waste	in 2023	Separate and recycle at source, or collect separately and do not mix with other types of waste		
Municipal waste	in 2020	50% recycling of municipal waste		
	in 2035	65% reuse and recycling		
Municipal hazardous waste	in 2024	Separate collection		
Shot	in 2020	70% recycling, reuse of shot		
Vehicles	in 2015	95	85	100
Electro	in 2006	70%	50%	min 4 kg per nhabitant per yea
Batteries	in 2011	50-75 efficiency		
	in 2012			25%
	in 2016			45%
Tires		0% deposit		

However, the situation that is now and will be in 2026 is especially and quite satisfactory in comparison with the situation during the period at the beginning of this century up to 2010, when only a few percent of waste in Serbia was deposited in sanitary landfills. In fact, we should look at the reasons for the transition from the system of wild or illegal disposal to the sanitary system of disposal, incineration and partly recycling. The EU waste targets are unattainable for most of the countries that are already members of the EU, and for Serbia they are even more unattainable in this period. The transition from unsanitary disposal to sanitary and then to advanced waste treatment methods such as recycling and WTE (waste to energy) is adequate [7]. No country has switched directly from wild dumping to recycling or illusory 0 waste, or waste prevention methods. All

countries must firstly enable the basics of waste management, which is sanitary landfilling, and then introduce advanced methods [8].

Analyzing waste management in other countries, the most widespread argument that tells when environmental issues begin to be resolved is the Kuznets curve, which is a curve that compares the growth of GDP/capita (gross domestic product/capita) and environmental load. The analysis of the curve shows that the environmental load, which is reflected in the amount of pollution, depends on the influence of public opinion, because public opinion does not care about environmental pollution if it is burdened with existential problems. These questions stop when the GDP reaches a certain peak, at that moment public opinion also wants a healthy environment and the GDP is at a level where it is possible to allocate funds for environmental protection, which until then went to the development of the economy and infrastructure.

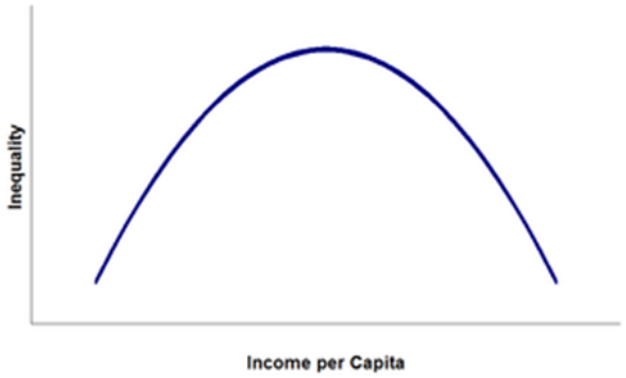

Figure 2 Kuznetsov's curve

The growth of GDP in Serbia is evident; data from the World Bank are shown in Fig. 3. The increase in GDP per capita from 2002 to 2022 increased from some 2.5 kEuro to almost 9 kEuro in 2022.

Figure 3 Growth in the Republic of Serbia, GDP/capp [9]

Looking at the growth of GDP/capp in Serbia, it cannot be concluded that growth of GDP increased so much that it caused environmental protection, and with it the question of waste management, to be placed at the top of the priorities of politicians in Serbia. Comparing GDP/capp in 2002 and 2022 is an obvious difference, however it must be clearly said that in all countries GDP/capp is increasing due to inflation.

It is necessary to look at other parameters of the society in order to determine what caused the slow or normal speed of the way of solving the waste management issues:

- Political stability
- Average salary
- Employment
- Raising standards
- Development of consciousness
- Legal regulations

Looking at waste management in the Republic of the Netherlands, which, like in world football, is one of the world champions. In this case, Argentina and Brazil are certainly not there, but the Netherlands, Japan, Austria and Germany are the countries that are leaders in the advanced treatment of waste management. By analyzing the changes in the Netherlands, it was shown that it was mostly caused by legislation, which was shown in Fig. 4.

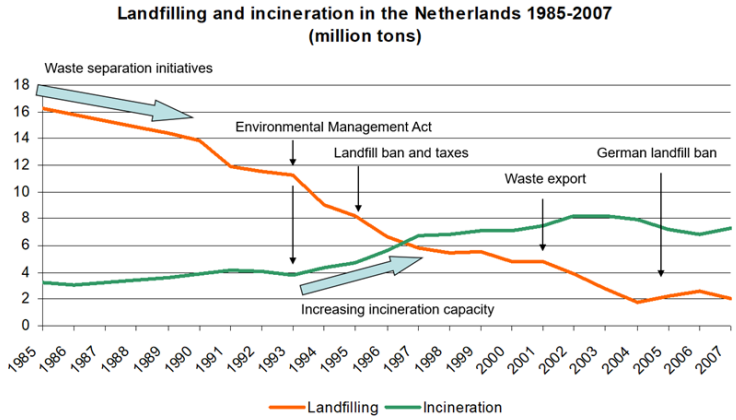

Figure 4 The shift from escrow to advanced technologies in the Netherlands

Looking at the general situation in waste management in the Republic of Serbia, it can be noted that the most significant leap in advanced waste treatment in Serbia is the beginning of WTE in Belgrade. 310,000 tons of waste is burned, energy is produced from waste, where part is converted into electricity and part into heat, which is used as a sanitary technique in the Belgrade heating system. Instead of using natural gas, waste is used. According to the EU, this is not a circular economy and the goals in recycling have not been achieved. According to the authors of the paper, WTE is a successful project in terms of all environmental, economic, sustainable development, civilizational, and circular economy parameters.

REFERENCES

1. Đorđević, Lj. Redžić, N., Radovanović, N., Jovanović, G., Embeli, E. (2022) Upravljanje otpadom u Republici Srbiji u periodu 2011. - 2021. godine. Beograd : Ministarstvo zaštite životne sredine, Agencija za zaštitu životne sredine, str. 43.
2. The European parliament and the Council of the European Union (2008) Directive 2008/98/EC of the European Parliament and of the Council of 19 November 2008 on waste and repealing certain Directives. Official Journal of the European union.
3. The Council of European Union (1999) Council Directive of 26 April 1999 on the landfill of waste. Official Journal of the European Communities.
4. The European Parliamanet nad the Council of the European Union (2018) Directive (EU) 2018/850 of the European parliament and of the Council of 30 May 2018 amending Directive 1999/31/EC on the landfill of waste. Official journal of the European Union.
5. The European Parlaiment and the Council of the European Union (1994) European Parliament and Council Directive 94/62/EC of 20 December 1994 on packaging and packaging waste. Official Journal of the European Communities.
6. The European Parliament and the Council of the European Union (2018) Dierctive (EU) 2018/852 of the European Parliament and of the Council of 30 May 2018 amending Directive 94/62/EC on packaging and packaging waste. Official Journal of the European Union.
7. Mihajlović, V., et al. (2016) Financial implications of compliance with EU waste management goals: Feasibility and consequences in a transition country. Waste Management & Research, 34, 923-932. DOI: 10.1177/0734242X16652962.
8. Ragossnig, A.M., Vujić, G. (2015) Challenges in technology transfer from developed to developing countries. Waste Management & Research, 33, 93-95. DOI: 10.1177/0734242X15569403.
9. World bank. The World Bank GDP per capita (current US$) - Serbia. The World Bank. [Online] [Cited: 04 13, 2023.] https://data.worldbank.org/indicator/NY.GDP.PCAP.CD?end=2021&locations=RS&start=2002.

XV International Mineral Processing and Recycling Conference
17-19 May 2023, Belgrade, Serbia

CRITICAL METALS RECOVERY FROM E-WASTE: FROM MICROFLUIDICS HYDROMETALLURGY TO ECONOMICALLY VIABLE PROCESSES

JC. P. Gabriel[1,2#], H. Bo[2], N. M. Charpentier[1,2], S. M. Chevrier[1], Y. Deng[1,3], F. L. Olivier[1,2], X. Dong[2]

[1] Université Paris-Saclay,LICSEN, NIMBE, CNRS, CEA, Gif-sur-Yvette, France
[2] Nanyang Technological University, SCARCE Laboratory, Energy Research Institute @ NTU (ERI@N), Singapore
[3] Ecologic France, Guyancourt, France

ABSTRACT – Conventional recovery and recycling of metals from wasted Printed Circuit Boards (WPCBs) require first a labour intensive process for their isolation, followed by mostly manual retrieval of high value electronic components (ECs), prior for the reminder to be crushed for further processing by pyrometallurgy and electrorefining processes. This allows for the recovery of the main elements (by weight or value), but all other elements are oxidized, mixed, diluted and therefore lost in post-processing wastes or ashes. To retrieve these elements, we are studying a change of paradigm: the disassembly of WPCBs combined with the sorting of ECs, followed by the fast development of physical and chemical treatments specific to each sorting bin [1, 2]. This enables ECs to be separated by composition and to significantly increase the bin's chemical elements concentrations while simplifying its composition, thus rendering minority metal's recovery economically viable. In this presentation, we will rapidly present current state-of-the-art processes for PCBs. We will then identify research and business opportunities in the case of some elements such as refractory metals (Ta, Nb, W, Mo), gallium, or lanthanides as well as present our laboratory's results beyond the state of the art regarding: (i) new physical recycling treatment of wasted PCBs [1]; (ii) the fast process development using an instrumented microfluidic platform [2]; (iii) Example of new processes for the recovery of strategic metals[3]; and (iv) their upcycling into nanomaterials/catalysts [4].*
* This abstract is adapted from the abstract published in reference [1a].

Keywords: Electronic Waste, Hydrometallurgy, Sorting, Microfluidics, Critical Metals.

Figure 1 Wasted Printed Circuit Boards as collected in industrial settings

corresponding author: jean.gabriel@cea.fr

ACKNOWLEDGEMENT

J.C.G., H.B., N.M.C., S.M.C., F.L.O., D.X. acknowledge financial support from the SCARCE project, which is supported by the National Research Foundation, Singapore, and National Environment Agency, Singapore under its Closing the Waste Loop Funding Initiative (Award No. USS-IF-2018-4 & SCARCE Phase2 Award No.CTRL-2023-1D-01).

REFERENCES

1. (a) Maurice, A., Dinh, K.N., Charpentier, N., Brambilla, A., Gabriel, J.C.P. (2021) Dismantling of Printed Circuit Boards Enabling Electronic Components Sorting and Their Subsequent Treatment Open Improved Elemental Sustainability Opportunities., Sustainability 13(18), 10357. https://doi.org/10.3390/su131810357. (b) Charpentier, N.M., Maurice, A.A., Xia, D., Li, W.J., Chua, C.S., Brambilla, A., Gabriel, J.C.P. (2023) Urban Mining of Unexploited Spent Critical Metals from E-waste Made Possible Using Advanced Sorting. Submitted.
2. (a) Maurice, A., Theisen, Gabriel, J.C.P. (2020) Microfluidic lab-on-chip advances for liquid-liquid extraction process studies. Current Opinion In Colloid & Interface Science 46, 20-35. https://doi.org/10.1016/j.cocis.2020.03.001 ; (b) Maurice, A., Theisen, J., J., Rai, V., Olivier, F., El Maangar, A., Duhamet, J., Zemb, T., Gabriel, J.C.P. (2021) First online X-ray fluorescence characterization of liquid-liquid extraction in microfluidics. Nano Select 2021, 1-12. https://doi.org/10.1002/nano.202100133; (c) Olivier, F., Maurice, A., Meyer, D., Gabriel, J.C.P. « Liquid-liquid extraction: thermodynamics-kinetics driven processes explored by microfluidics. (2022) Comptes Rendus Chim. 25, 137-148. https://doi.org/10.5802/crchim.172 ; (d) Olivier, F., Chevrier, S.M., Keller, B., Gabriel, J.C.P. (2023) On-line Quantification of Solid-Phase Metal Extraction Efficiencies Using Instrumented Millifluidics Platform. Chemical Engineering Journal 454(3) 140306. https://doi.org/10.1016/j.cej.2022.140306 .
3. (a) Xia, D., Charpentier, N.M., Maurice, A.A., Brambilla, A., Yan, Q., Gabriel, J.C.P. Sustainable Route for Nd Recycling from Waste Electronic Components Featured with Unique Element-Specific Sorting Enabling Simplified Hydrometallurgy. (2022) Chem. Eng. J. 441, 135886. https://doi.org/10.1016/j.cej.2022.135886; (b) Bo, H., Chevrier, S.M., Gabriel, J.C.P. (2023) Tailorable metal-organic framework based thin film nanocomposite membrane for lithium recovery from wasted batteries. Submitted
4. Xu, J., Liu, D., Lee, C., Feydi, P., Chapuis, M., Yu, J., Billy, E., Yan, Q., Gabriel, J.C.P. (2022) Efficient Electrocatalyst Nanoparticles from Upcycled Class II Capacitors» Nanomaterials 12(15) 2697. https://doi.org/10.3390/nano12152697

SESSION LECTURES

XV International Mineral Processing and Recycling Conference
17-19 May 2023, Belgrade, Serbia

3D IMAGING AND APPLICATIONS IN MINERAL PROCESSING

F. Nakhaei[1#], I. Jovanović[2]
[1] School of Chemical and Minerals Engineering, North West University, Potchefstroom 2531, South Africa
[2] Mining and Metallurgy Institute Bor, Serbia

ABSTRACT – Optical sensors are essential for monitoring the status and condition of mineral processing processes by characterizing the internal and external structures of particles such as size, shape, density and composition. The goal of this review paper is to consider the state of the art of 3-D imaging systems in mineral processing on the basis of the recent growth in 3-D sensors. The structure of this manuscript comprises an overview of the two 3-D imaging systems such as RhoVol and computed X-ray tomography, based on the basic principles. Afterwards, their applications in mineral processing are explained. The depth dimension taken by 3-D sensors provides key data that significantly facilitates the execution of automation and control in mineral processing processes.

Keywords: 3-D sensors, Mineral processing, RhoVol, Computed X-ray tomography, Automation

INTRODUCTION

New advances in digital technology and their application in mining industries, particularly in the mineral processing plants, have resulted in the emergence of machines or tools that may be used to improve efficiency and control of separation processes. Digital image processing is a fast, non-invasive and low-cost technology for achieving process-related information, and it is well accepted in mineral processing processes [1, 2].

With development of new computer technology, three-dimensional (3D) imaging systems became popular and successfully implemented in mineral processing [3, 4]. 3D measurement methods become more and more important, because they enable the precise analysis of complex particle morphologies and 3D spatial distribution, simultaneously. Recent advances in the field of 3D imaging systems not only open a new windows to replace new identification methods, but also have the potential to mitigate some common errors in traditional methods. From mining to grinding operations, the 3D characterization of particles ranging in size from meters to micrometers is now possible. Spatial particle features, such as size, shape and composition, are fundamental characteristics that can determine the efficiency of the plant operations in the mining industries.

This brief review presents the application of 3D imaging techniques which includes Rhovol and X-ray tomography along with their information in mineral processing processes. A review is given with recent advances considered, such as high-speed

corresponding author: 36598704@nwu.ac.za

scanning and image analysis techniques to describe significant particle characteristics, including size, shape, volume, density and composition.

The application of 3D imaging techniques is summarized as follows (Table 1):

Table 1 Application of 3D imaging techniques

No.	Feature	Reference
1.	Morphological characterization and quantification (size and shape)	[5, 6]
2.	Determination of microstructural features such as: - crack density, rock characteristics; - intergranular fracture and crack surface area during multiphase particle breakage in comminution operations	 [7, 8] [9,10]
3.	Quantitative characterization of pore size and structural features	[11]
4.	- Mineral liberation and grade grade-recovery curves - Exposed grain surface area	[3, 12-14] [15, 16]

RHOVOL

Latest progresses in the imaging systems can generate external geometry of particles into 3D models that can be used to measure the main particle morphology descriptors such as the values of length, diameter, perimeter and volume.

The RhoVol machine, commercially developed by De Beers Group Technology, measures and records the mass of each particle, followed by a 3D reconstruction of its silhouette [17]. This machine was originally designed for using in a diamond application, but later upgraded for other uses, such as coal. It uses seven cameras at various angles to capture seven silhouettes of a particle at a time (Figure 1) [18]. Three types of RhoVol machines are commercially available for fine (-3+1 mm), medium (8+3 mm) and coarse (-8+25 mm) particles.

RhoVol's software creates a 3D model of a sample by merging integrated data, so that any physical dimensions or ratios can be extracted such as density (ratio of the mass to volume), size, elongation, flatness, compactness and volume of a given particle. It is also equipped with a sorting functionality (twelve discrete bins) that enables us to separate the samples into bins that are based on any of the selected particle features.

Figure 2 shows the RhoVol system. Figure 3 and Table 2 shows the multiple simultaneous views and the results of geometry calculations of a particle using seven cameras, respectively.

Botlhoko et al. [18] compared the particle size distributions (PSD) of coal samples obtained by the RhoVol and sieving tests. There were only small differences between the particle size distributions based on sieving and RhoVol results. Therefore, the RhoVol

system provides a practical reference to establish the applicability of the 3D image-based method to measure particle size

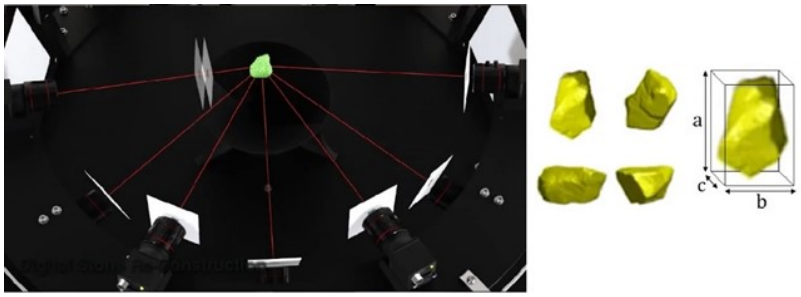

Figure 1 A generated 3D model of a particle using seven cameras [18]

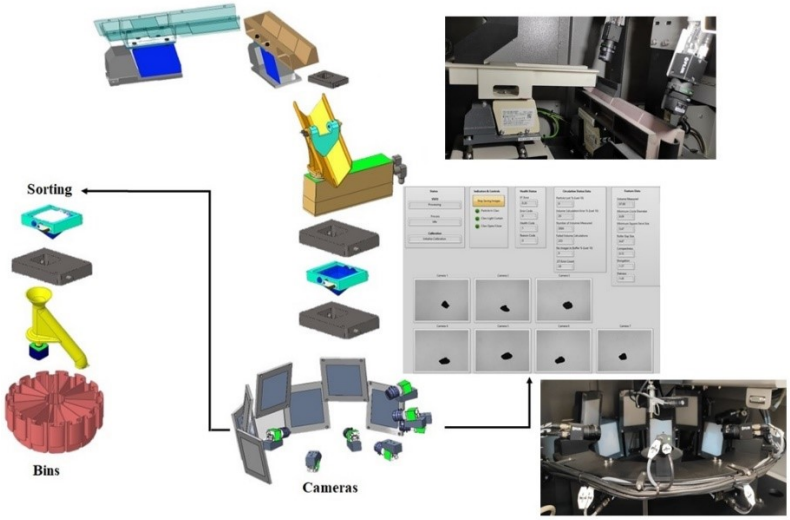

Figure 2 The RhoVol machine [19]

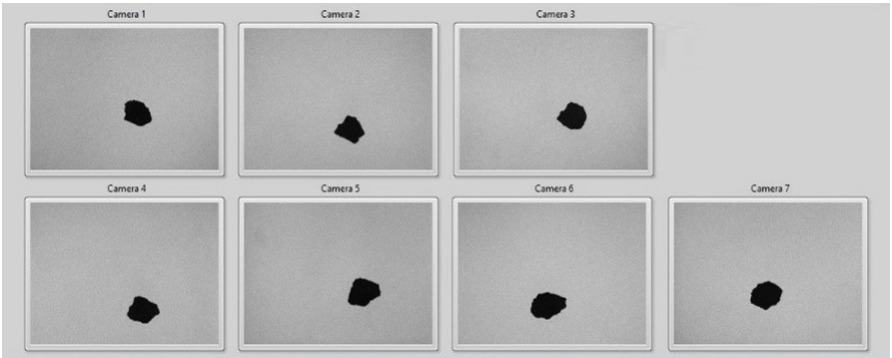

Figure 3 The multiple simultaneous views of a particle using RhoVol.

Table 2: Particle geometry results of a coal particle shown in Figure 3

Particle	Volume	Minimum circle diameter	Elongation	Flatness	Compactness	Minimum square sieve size	Roller gap size
	(mm^3)	(mm)	a/b*	b/c*	$(bc/a^2)^{1/3*}$	(mm^2)**	(mm)
1	96.6	6.23	1.27	1.09	0.83	5.47	5.04

*The length (a), width (b) and thickness (c) are the longest, intermediate and smallest dimension of the minimum bounding box, respectively.
**Minimum square sieve size is described as the limiting size at which a particle can pass through a square aperture with side dimension.

Washability analyses is used to specify the yield and quality of clean coal produced in coal processing plants. Traditional coal washability data are commonly achieved by tedious sink-float test. Reliable density measurements are critical for characterizing raw coal and estimating the coal washing plant's performance [20]. The comparison of the float-sink test and RhoVol for determination of coal washability curves was studied by Botlohoko et al. [18]. The RhoVol and float-sink results for two samples are given in Figure 4.

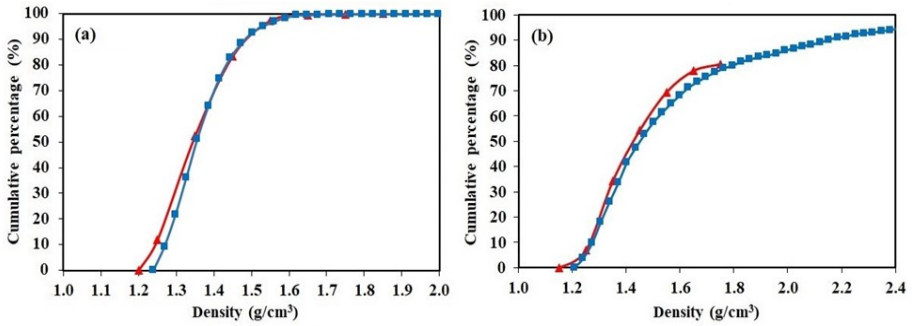

Figure 4 The comparison of the cumulative density distribution obtained by float-sink (red curve) and RhoVol (blue curve) for two samples [18]

The curves achieved by the RhoVol are in agreement with the float–sink test. However, the amount of required sample is much smaller in RhoVol compared to float-sink test. The accuracy of 3D imaging technique was evaluated by comparing the yield-cumulative ash content results created by the RhoVol and float-sink test (Figure 5).

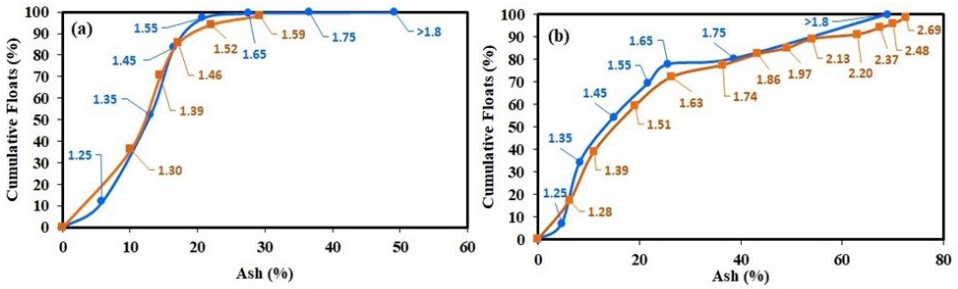

Figure 5 Washability curves achieved by RhoVol (orange curve) and sink–float (blue curve) tests [18]

From the similarity between the RhoVol and float-sink test outcomes, it is obvious that 3D imaging system is able to specify washability of any kinds of coals.

The obtained results by the RhoVol can be used to determine the coal washability curves without doing float-sink tests. It leads to save time and reduce the consumption of heavy liquid media. Unlike the float–sink tests that are often implemented at a restricted ranges of density, RhoVol can sort coal particles in a wide range of densities. Therefore, RhoVol is an important practical alternative to the sink–float method.

X-RAY TOMOGRAPHY

Over the last few decades, advancements in computer instrumentation and software tools have reached an extraordinary level, so that 3D characterization of multiphase particles is now possible using X-ray tomography. This technology is broadly used at the airports for luggage inspection and the basic principles have been implemented as a sorting method [21, 22]. This non-destructive quantitative method is essential for sustainable development and the more effective utilization of valuable mineral resources. The main benefit of X-ray computed tomography (XCT) is its ability to record the 3D internal structure of the ore at resolutions as low as a few microns, hence mitigating stereological inaccuracy obtained via 2D projections [4].

Figure 6 shows a schematic of a typical XCT system. The particles are exposed to the incoming X-ray beam rotated 180° during data acquisition to make a series of projections (usually between 600 - 3600 projections). After reconstruction, these projections form 2D slices of the measured volume. The pixels in the 2D slices maintain spatial information about the original volume elements (voxels), allowing for stacking and rendering of the slices to see the sample's 3D volume [23].

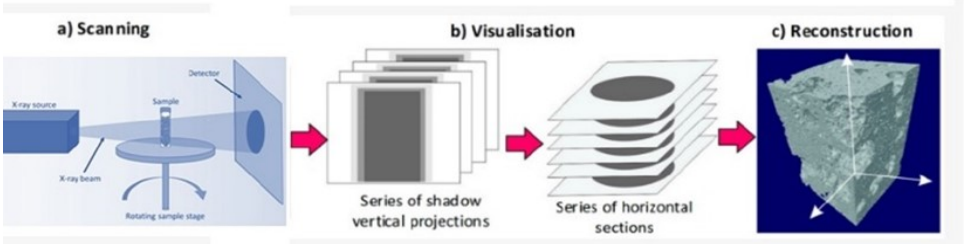

Figure 6 A schematic of a typical XCT system. (a) scanning of the sample in X-ray beam, (b) mathematical transformation of the shadow vertical projections into a series of horizontal sections of the sample, (c) produce 3D images of the sample [24]

XCT has been used for quantitative analysis of the main parameters, such as particle size, shape and composition [25]. Recent progresses in XCT have provided the high-speed scanning and image analysis procedures to account for characteristic features of multiphase particles within minutes [26]. Opportunities for plant-site 3D coarse particle characterization with automated high-speed XCT are now possible.

Guntoro et al. [23] provided a comprehensive review paper on the available useful data analysis approaches for processing 3D datasets obtained by laboratory μCT system as a mineral characterization tool. Liu et al. [27] extensively reviewed the application of

XCT on coal characterization. Furthermore, the imaging principle of CT and the recognition method of microstructure were exxplained, and they summarized the research development of CT in the quantitative characterization of coal microstructures and the qualitative evaluation of macroscopic properties.

Several studies have investigated the application of X-ray tomography in mineral processing processes for using in laboratory analysis, containing (1) multiphase particle characterization [14, 28]; (2) particle crack and breakage as a result of blasting/comminution [7, 9]; (3) liberation characterization and exposed grain surface area analysis to clarify the locked particles [15, 29, 30]; and (4) floc size, shape and water content. For example, HRXMT with about 5 µm resolution has been used for the mineral liberation analysis of feed to copper ore flotation (+150 µm). Volume rendered images for this sample are shown in Figure 7.

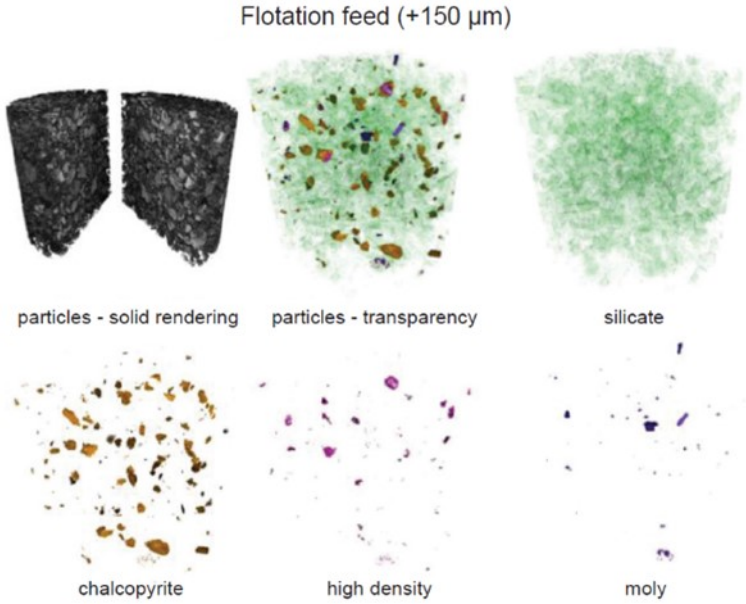

Figure 7 3D images of copper flotation feed (+150 µm) including chalcopyrite; high-density minerals such as covellite, chalcocite and bornite; molybdenum; and gangue minerals obtained by HRXMT (voxel resolution = 5 µm) [31]

Ore sorting is a pre-concentration method that is applied before the main processing line to decrease the amount of gangue from ores before the grinding circuit. The copper sulfide particles inside of the ore were imaged in 3D by micro XCT [32]. If the gangue particles can be recognized and removed from the processing line, the remained particles will have a higher feed grade, and thus, the energy cost for following grinding can be considerably decreased. Zhang et al. [33] used dual-Energy X-ray Transmission (DE-XRT) to sort the sulphides from the non-sulphide minerals. Density measurements using DE-XRT were emplyed to determine average atomic density by measuring the X-ray attenuation for each sample. In their experiments, COMEX's MSX-400-VL-XR machine installed at the University of British Columbia was employed (Figure 8).

Figure 8 COMEX's MSX-400-VL-XR System in UBC's Coal and Mineral Processing Laboratory [33]

It was found from Figure 9 that DE-XRT sorting method can recover 90% of the sulphides with a 55% mass yield. The DE-XRT is an efficient sensor that can be used to separate sulphides from gangue minerals.

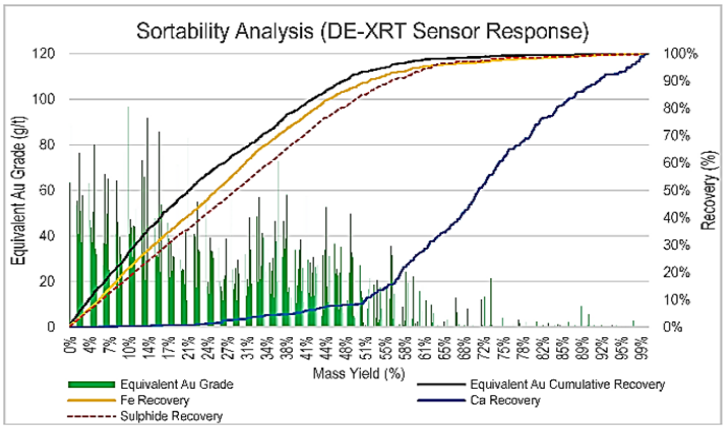

Figure 9 Scatter plot of equivalent gold assay versus average relative density [33]

In another study, Zhang et al. [34] explained the fundamentals of the DE-XRT analysis and its data processing techniques to specify the relative densities and how to determine washability curves and density of separation for coal sorting. They showed that similar to float-sink tests, the DE-XRT can estimate a relative density by quantifying the attenuation of x-rays from two different energy levels. The coal washability curve derived from DE-XRT results was able to model washability using sink-and-float test.

Miller et al. [35] used high resolution X-ray microtomography (HRXMT) to compare the degree of exposed grain surface area needed to recover very coarse (850×500 μm) particles using the HydroFloat and the mechanical flotation cell. Figure 10 displays the volume-rendered view of the original 3D reconstructed image set (992×1013×790 voxels)

achieved from HRXMT for designated particles from the HydroFloat concentrate and tailing. These 3D images perfectly show that little or no exposed grain surfaces of sulfide minerals are present in the HydroFloatTM tailing samples.

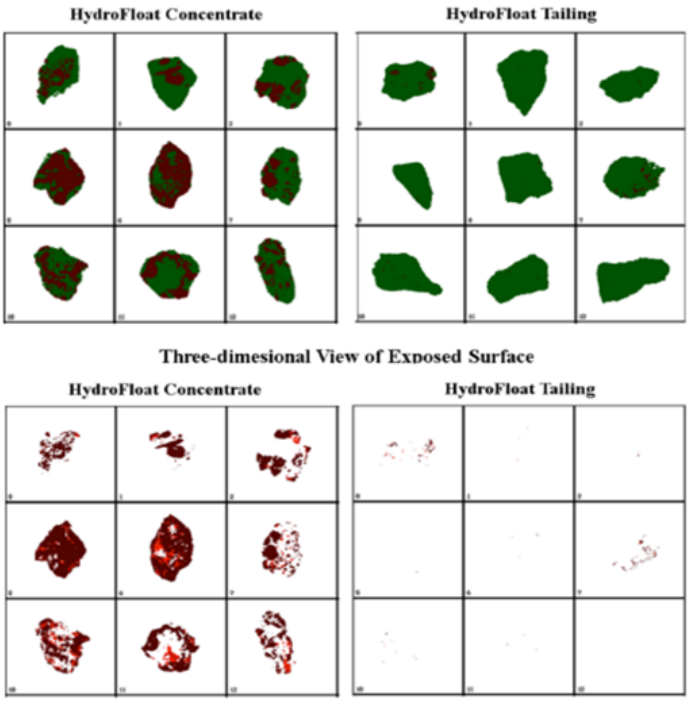

Figure 10 3D images of 9 particles and exposed surface of 850×500 μm particles of HydroFloat concentrate and tailing (gangue surface = green, exposed valuable mineral surface = red) [35]

CONCLUSION

3D imaging sensors are technologically advanced to a great extent, so a breakthrough is already possible if enough research projects are implemented. This review paper indicates that there is a rapid development of new techniques and algorithms capable of processing XCT datasets, but application of such techniques is often sample-specific. Since mineral processing processes are substantially complicated, 3-D imaging systems can play a remarkable role in increasing the efficiency that could be suitable in a number of applications in every separation scenario. The applications include the determination of microstructure such as particle size, shape, breakage and crack, porosity and pore structure, permeability, mineral composition, coal washability, mineral liberation, and exposed grain surface area. Reasons like increasing the quality of final products, scarcity of high-grade mineral resources, and discarding dangerous separation methods are driving the need for automation in mineral industries. Since 3-D vision is a key technology for automation, more implementations are yet to come.

ACKNOWLEDGEMENT

Authors are thankful to De Beers Group company and Prof. Quentin Peter Campbell for their support and valuable suggestions during this research work. This paper is financially supported by the Ministry of Education, Science and Technological Development of the Republic of Serbia, Grant No. 451-03-47/2023-01/200052.

REFERENCES

1. Nakhaei, F., Irannajad, M., Mohammadnejad, S. (2018) Evaluation of column flotation froth behavior by image analysis: effects of operational factors in desulfurization of iron ore concentrate. Energy Sources, Part A: Recovery, Utilization, and Environmental Effects 40 (19): 2286-2306
2. Nakhaei, F., Irannajad, M., Mohammadnejad, S. (2019) A comprehensive review of froth surface monitoring as an aid for grade and recovery prediction of flotation process. Part A: structural features, Energy Sources, Part A: Recovery, Utilization, and Environmental Effects, DOI: 10.1080/15567036.2019.1663313
3. Wang, Y., Miller, J.D. (2020) Current developments and applications of micro-CT for the 3D analysis of multiphase mineral systems in geometallurgy. Earth-Science Reviews, Volume 211, December 2020, 103406
4. Guntoro, P.I., Ghorbani, Y., Rosenkranz, J. (2021) 3D Ore Characterization as a Paradigm Shift for Process Design and Simulation in Mineral Processing. Berg Huettenmaenn Monatsh 166, 384–389
5. Lin, C.L., Miller, J.D. (2005) 3D characterization and analysis of particle shape using X-ray microtomography (XMT), Powder Technology, Volume 154, Issue 1, 2005, Pages 61-69
6. Bagheri, G.H., Bonadonna C., Manzella I., Vonlanthen, P. (2015) On the characterization of size and shape of irregular particles, Powder Technology Volume 270, Part A, January 2015, Pages 141-153
7. Ghorbani, Y., Becker, M., Petersen, J., Morar, S.H., Mainza, A., Franzidis, J.-P. (2011) Use of X-ray computed tomography to investigate crack distribution and mineral dissemination in sphalerite ore particles. Miner. Eng. 2011, 24, 1249–1257
8. Johnson, J.C., Puvvada, S., Lu, Y., Lin, C.L., Miller, J.D. (2019) Energy dissipation and fragmentation of granite core during high velocity impact. Mining. Metall. Explor. 36, 839–849
9. Garcia, D., Lin, C.L., Miller, J.D. (2009) Quantitative analysis of grain boundary fracture in the breakage of single multiphase particles using X-ray microtomography procedures. Miner. Eng. 22 (3), 236–243
10. Xu, W., Dhawan, N., Lin, C.L., Miller, J.D. (2013) Further study of grain boundary fracture in the breakage of single multiphase particles using X-ray microtomography procedures. Miner. Eng. 46–47, 89–94
11. Moreno-Atanasio, R., Williams, R.A., Jia, X. (2010) Combining X-ray microtomography with computer simulation for analysis of granular and porous materials. Particuology 8 (2), 81–99

12. Miller, J.D., Lin, C.L., Hupka, L., Al-Wakeel, M.I., (2009) Liberation-limited grade/ recovery curves from X-ray micro CT analysis of feed material for the evaluation of separation efficiency. Int. J. Miner. Process. 93 (1), 48–53
13. Cnudde, V., Boone, M.N., (2013) High-resolution X-ray computed tomography in geosciences: a review of the current technology and applications. Earth-Science Rev. 123, 1–17
14. Guntoro, P.I., Ghorbani, Y., Butcher, A.R., Kuva, J., Rosenkranz, J. (2020) Textural Quantification and Classification of Drill Cores for Geometallurgy: Moving Toward 3D with X ray Microcomputed Tomography (µCT), Natural Resources Research 29, 3547–3565
15. Wang, Y., Lin, C.L., Miller, J.D. (2017) Quantitative analysis of exposed grain surface area for multiphase particles using X-ray microtomography. Powder Technol. 308, 368–377
16. Wang, Y., McClung, C., Lin, C.L., Miller, J.D. (2018) Stereological correction of perimeter based estimates of exposed grain surface area. Miner. Eng. 126, 64–73
17. Fofana, M., Steyn, T. (2019) Monitoring the performance of DMS circuits using RhoVol technology by Journal of the Southern African Institute of Mining and Metallurgy, vol.119, n.2, pp.133-138
18. Botlhoko, S., Campbell, Q.P., Le Roux, M., Nakhaei, F. (2023) Washability Analysis of Coal Using RhoVol: A Novel 3D Image-based Method, Mineral Processing and Extractive Metallurgy Review, 44:2, 125-137
19. Nakhaei, F., Campbell, Q.P., Le Roux, M., Botlhoko, S. (2022) Estimation of coal density using a 3D imaging system: RhoVol. Journal of the Southern African Institute of Mining and Metallurgy, vol. 122, no. 8, pp. 443–450
20. Sushobhan, P. Satyabrata, M. (2020) A method to perform float-and-sink test for separation of coal samples of various densities and determination of 'Probable Error' and 'Imperfection', IOP SciNotes 1: 024403
21. Khan S.U., Khan I.U., Ullah I., Saif N., Ullah I. (2020) A Review of Airport Dual Energy X-ray Baggage Inspection Techniques: Image Enhancement and Noise Reduction. J. X-ray Sci. Technol. 2020;28:481–505
22. Von Ketelhodt, L. (2010) Dual energy X-ray transmission sorting of coal. J. S. Afr. Inst. Min. Metall. 2010, 110, 371–378
23. Guntoro, P.I., Ghorbani, Y., Koch, P.-H., Rosenkranz, J. (2019) X-ray Microcomputed Tomography (µCT) for Mineral Characterization: A Review of Data Analysis Methods. Minerals 2019, 9, 183
24. Popov, O., Talovina, I., Lieberwirth, H., Duriagina, A. (2020) Quantitative Microstructural Analysis and X-ray Computed Tomography of Ores and Rocks—Comparison of Results. Minerals 2020, 10, 129
25. Behnsen, J.G., Black, K., Houghton, J.E., Worden, R.H. (2023) A Review of Particle Size Analysis with X-ray CT. Materials 2023, 16, 1259
26. Ulusoy, U. (2023) A Review of Particle Shape Effects on Material Properties for Various Engineering Applications: From Macro to Nanoscale. Minerals 2023, 13, 91
27. Liu, D.M., Zhao, Z., Cai, Y.D., Sun, F.R., Zhou, Y.F. (2022) Review on applications of X-Ray computed tomography for coal characterization: Recent progress and perspectives. Energy Fuels 2022, 36 (13), 6659– 6674

28. Miller, J.D., Lin, C.L., Cortes, A.B. (1990) A review of X ray computed tomography and its applications in mineral processing, Mineral Procesing and Extractive Metallurgy Review, 7 (1990), pp. 1–18
29. Miller, J.D., Lin, C.-L., Hupka, L., Al-Wakeel, M.I. (2009) Liberation-limited grade/recovery curves from X-ray micro CT analysis of feed material for the evaluation of separation efficiency. Int. J. Miner. Process. 2009, 93, 48–53
30. Reyes, F., Lin, Q.; Cilliers, J.J., Neethling, S.J. (2018) Quantifying mineral liberation by particle grade and surface exposure using X-ray microCT. Miner. Eng. 2018, 125, 75–82
31. Miller, J.D., Lin, C.L. (2018) X-ray tomography for mineral processing technology - 3D particle characterization from mine to mill, Minerals & Metallurgical Processing volume 35, pages 1–12
32. Jin, J., Lin, CL., Miller, J.D. Zhao, C., Li, T. (2022) X-ray Computed Tomography Evaluation of Crushed Copper Sulfide Ore for Pre-concentration by Ore Sorting. Mining, Metallurgy & Exploration 39, 13–21
33. Zhang, Y.; Yoon, N.; Holuszko, M.E. (2021) Assessment of Sortability Using a Dual-Energy X-ray Transmission System for Studied Sulphide Ore. Minerals 2021, 11, 490
34. Zhang, Y.R., Yoon, N. Holuszko, M.E. (2022) Assessment of coal sortability and washability using dual energy X-ray transmission system, International Journal of Coal Preparation and Utilization, 42:10, 2895-2907
35. Miller, J.D., Lin, C., Wang, Y., Mankosa, M., Kohmuench J., Luttrell G. (2016) Significance of Exposed Grain Surface Area in Coarse Particle Flotation of Low-Grade Gold Ore with the Hydrofloat ™ Technology, IMPC 2016: XXVIII International Mineral Processing Congress Proceedings, September 11-15, Quebec City, Canada

XV International Mineral Processing and Recycling Conference
17-19 May 2023, Belgrade, Serbia

NOVEL APPROACHES TO RECOVER TOTAL HEAVY MINERALS FROM DIFFERENT GRADE BEACH SAND DEPOSITS USING GRAVITY CONCENTRATORS

D. Singh[1], S. Basu[2], B. Mishra[1], R. Bhima Rao[1#]
[1] Indian Rare Earths Limited, Dept of Atomic Energy, India
[2] CSIR IMMT, Bhubaneswar, India

ABSTRACT – In the present investigation, an attempt is made to synergizing the effects of textural, physical and chemical characteristic of new placer deposits which are associated with lean and of grade placer heavy minerals having typically different in total heavy minerals, textural variations and compositions and occur all along the costal stretch of Bay of Bengal, from Chatrapur to Puri Dists, Odisha, India, are chosen for recovery of total heavy minerals using different models of gravity concentrates.

Keywords: Beach Sand, Placer Heavy Minerals, Mineral Separator, Spiral Concentrators.

INTRODUCTION

Since the very dawn of civilization, i.c. Paleolithic (500000 BC) age, man made use of natural –gravity- sorted stones, pebbles, and rocs as hunting instruments. As knowledge increased so did man's needs better tools and ornamentation. The native metal gold was first recognised during Neolic (8000BC) age and concentrated deposits was started [1]. In due course of time, because of its scarcity, the crude forms of industrial gravity concentration techniques took birth in Chalcolithic age (4200 BC) in the field of gold collection. Since then, gravity concentration remained as a dominant concept in mineral processing. The concentration of heavy minerals can occur if the minerals possess the three properties: a. high specific gravity, b. chemical resistance and c. hardness. Mechanical concentration [Nature's process] and gravity concentration [man made design process] not only depend on the above three factors it also depends on size and shape of particles. More over the difference in specific gravity is accentuated in water as compare to air. Panning is one of the oldest techniques employed first in recovery of gold from placer minerals. Gold panning is simple processes which can clearly be seen from Fig. 1.

Once a suitable placer deposit is located, some alluvial deposits are scooped into a pan, where they are then wetted and loosed from attached soils by soaking, fingering, and aggressive agitation in water. This is called stratification; which helps dense materials, like gold, sink to the bottom of the pan. Materials with low specific gravity will rise upward, allowing these to be washed out of the pan, whereas materials with higher specific gravity, sinking to the bottom of the sediment during stratification,

corresponding author: dr.r.bhimarao@gmail.com

will remain in the pan allowing examination and collection by the prospector. More recently gravity concentration has been reassessed due to the relative simplicity of gravity processes and the fact that they create significantly less environmental pollution. Gravity separation does not require the use of chemicals in beneficiation of minerals. So, the technique offers significant advantages over many other methods of mineral concentration in meeting environmental requirements. In many situations a large portion of the valuable mineral can at least be pre-concentrated effectively by economical and environmentally acceptable gravity systems. Gravity separation of minerals at coarser sizes, as soon as liberation is achieved, can boast significant advantages for downstream treatment stages due to decreased surface area, more efficient dewatering and the absence of chemical coatings that can interfere with further processing.

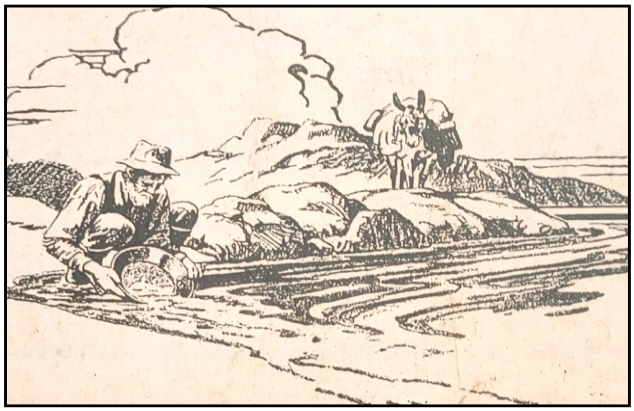

Figure 1 Gold panning along the streams [1]

It is widely accepted from a home maker to industrialist that gravity concentration is one of the oldest mineral beneficiation processes which has evolved over the decades and continues to play an important role in modern mineral processing operations. Gravity concentration has been used throughout the ages to separate minerals, with many of the historic methods still used to the current day. Pre-concentration of placer heavy minerals using gravity concentrators specially spiral concentrators is the primary stage of beneficiation in mineral processing plants. The spiral concentrator first appeared as production unit in 1943 in the form of Humphrey Spiral, invented by I B Humphreys for the separation chromite from beach sands in Oregon. By 1950's spirals were the standard primary wet gravity concentrators in the Australian mineral sand industry. In India, wet spiral concentrator is the primary unit operation to recover total heavy minerals which has industrial applications. The intermediate products such as zircon, sillimanite etc are again separated by using gravity tables. In the present investigation, an attempt is made to investigate the synergising the effects of textural and physical properties on different types of and models of spiral concentrators and other gravity units and separation media such as water and sea water on recovery of total heavy minerals.

MATERIALS AND METHODS

Bulk placer sands of five different grades in Total Heavy Minerals [THM] composition (4.72, 5.6, 9.5, 15.7 and 19.5 THM) were collected all along the costal line from Sipasurubil to Bramhagiri, Puri Dist, Odisha, India. Size analysis of all five samples were carried out using IS standard sieves. THM, VHM (Very Heavy Minerals between 2.8 sp. gr. and 3.3 sp. gr. and LHM (light heavy mineral <3.3 sp. gr.) of all the samples were carried out using organic liquids as media. Total Magnetic Minerals (TMM) was determined by using high intensity magnetic separator. Initially different types of gravity units (Fig. 3) were used on a single grade (4.72 THM) sample for recovery of total heavy minerals. Effect of HG8 spiral units on different grades of samples for recovery of total heavy minerals was studied. The effect of water media and sea water media was studied on the Humphreys spiral concentrator using a single grade (4.72 THM) sample. A recommendation was made to advocate for use mobile spiral concentrator all along the coast using sea water for recovery of total heavy minerals and supply to mineral sand industries after dewatering of saline water from the total heavy minerals.

Figure 2 Sample location map

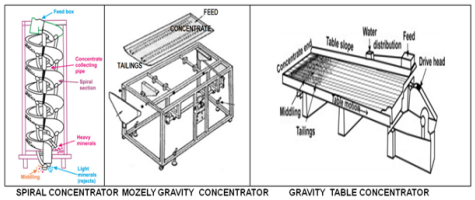

Figure 3 Different types of gravity units

Figure 4 Different models of spirals

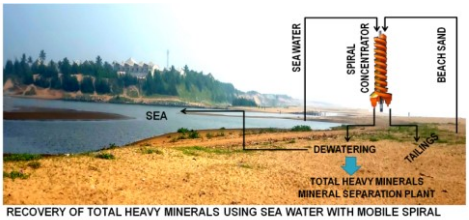

Figure 5 Advocating using seawater mobile spirals

RESULTS AND DISCUSSIONS

Physical properties, THM, TMM and size analysis of all five grades of samples are given in Table 1 and size analysis data shown in Fig. 6. The data given in Table 1 indicate that all samples exhibit the colour black with metallic shine and all are free grains with more less same specific gravity. Further an interesting fact observed from the data Table 1 that with increasing the THM content the d80 passing sizes of samples is decreasing where sample contain 4.72% THM has d80 passing size 400 microns and sample 5 contain 19.5% THM has d80 passing size 140 microns. The trend is similar in TMM

(Total Magnetic Minerals) content. TMM content is increasing from 2.97 for sample THM 4.74% to 4.5% for sample 3 (THM 9.5%). But the higher THM samples 5 and 6 have almost constant TMM content (12.6% and 11.81% respectively). The trend of VHM 3.19% (Very Heavy Minerals) for sample 1 (4.72% THM) is to gradually increasing to VHM 12.70% for sample 5 (19.5% THM). Similar way the trend for LHM (Light Heavy Minerals) 1.53% for sample 1 (4.72% THM) is to gradually increasing to 6.8% LHM for sample 5 (19.5% THM).

Table 1 Physical properties of different grades [THM] of beach placer deposit

Details	Sample 1	Sample 2	Sample 3	Sample 4	Sample 5
Colour	Black	Black	Black	Black	Black
Nature	Free grains	Free grains	Free grains	Free grains	Free grains
Bulk sp. gr.	2.89	2.91	2.93	2.96	2.96
d80 passing size µm	400	380	360	340	140
THM %	4.72	5.6	9.5	15.7	19.5
TMM %	2.97	3.01	4.5	12.6	11.81
VHM %	3.19	3.82	2.30	11.40	12.70
LHM%	1.53	1.78	2.2	4.3	6.8

Particle size analysis of all different five samples shown in Fig. 6 a, b, c, d, e and f indicate that sample A to Sample E the weight percent is decreasing from 600 microns to below 5 microns. Whereas, the total heavy minerals are increasing from 600 microns to below 75 microns for samples A to sample E. It indicates that the coarser fraction contains very less amount of total heavy minerals and the finer fraction contains more total heavy minerals.

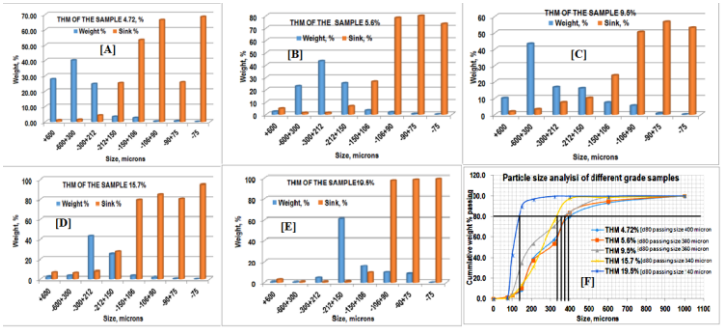

Figure 6 Particle size analysis of all five grades (THM) of samples

It is concluded that the chosen five different samples have difference in textural and other physical properties. As per the industrial practice it is expected that the nature of possessing total heavy minerals in fines is a challenging problem in the present mineral processing units for recovery total heavy minerals. In view of this sample 1 which contains the lowest THM 4.72% content has chosen to select the gravity separation unit. Experiments carried with Mozley gravy separator using V tray, gravity

wet table and Humphreys' spiral concentrator. The results of the Mozely separator on sample-1 which contain 4.72% THM using V tray is shown in Fig. 7. Beneficiation studies carried out on low grade beach sand sample using Mozley separator shown in Fig. 7 indicate that one rougher unit and cleaner units are required to achieve 93.15% grade with 4.2% overall yield and 82.8% recovery. The results would have been much better if the sample classified at 100 microns size and subjected +100 micron sample to V tray and -100 micron sample subjected to flat tray as per the design aspects. However, Mozley separator indicated that above 90% THM grade can be recovered.

The results of the gravity wet table separator on sample-1 which contain 4.72% THM using sand table tray is shown in Fig. 8. The test results obtained from gravity table indicate that one rougher table and one cleaner table is sufficient to achieve the 92.2% THM grade with 3.9% yield and 59% recovery. The gravity sand table is also indicated that there is a possibility to recover high grade THM using sand and slime table on classified feed at 100 microns. Since these Mozley and gravity tables have limitations in all aspects of size of particles and capacity of the units, the other alternative unit is spiral concentrator.

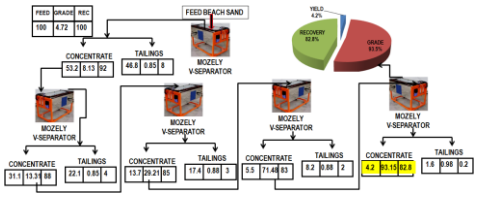

Figure 7 Flowsheet with mass balance achieved on sample-1 (4.72%THM) by using Mozely gravity separator

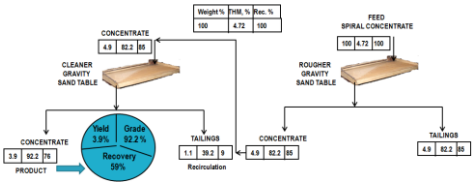

Figure 8 Flowsheet with mass balance achieved on sample-1 (4.72%THM) by using wet gravity sand table

Beneficiation studies carried out on low grade beach sand sample-1 (4.72% THM) using HG8 spiral separator shown in Fig. 9 indicate that one rougher unit and two cleaner units and two scavenging cleaner units are required to achieve 92.9% grade with 3% overall yield and 59% recovery. Similarly, the beneficiation studies carried out with Humphreys spiral concentrator on the sample-1 (Fig. 10) reveals that one rougher spiral and three clear spirals are required to achieve the grade 98.2% with overall 3.3% yield and 69% Recovery. The results indicate that by using CT spirals a grade containing 93.6% with overall 3.9% yield and 77% Recovery is achieved (Fig. 11). This data is supporting the laboratory modal gravity table data (Fig. 8) which normally mineral processing manufacturers claim. Summary of results obtained from different gravity units with mono feed grade [THM 4.72%] of beach placer deposit is shown in Table 2. The data reveal a fact that lower capacity unit operations such as Mozley and gravity tables produced similar grade 92.2 -93.2% THM with same recovery. HG 8 spiral also produced same grade but the recovery has fallen to a level of 52%. Among all the unit operations, Humphreys spiral concentrator produced higher grade 98.2% THM and CT spiral produced higher recovery 77%. The grade achieved contain 98.2% grade with 69% recovery from a feed contain 4.72% THM.

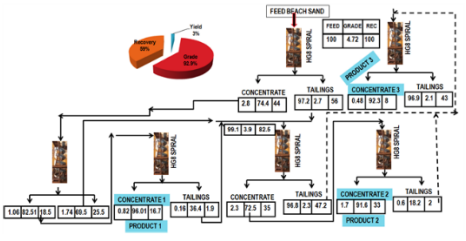

Figure 9 Flowsheet with mass balance achieved on sample-1 (4.72%THM) by using HG 8 spirals

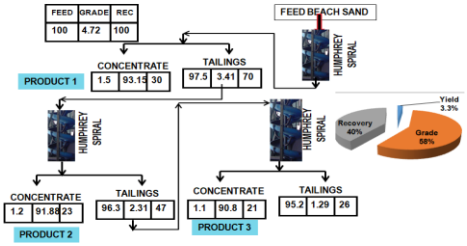

Figure 10 Flowsheet with mass balance achieved on sample-1 (4.72%THM) by using Humphreys spirals

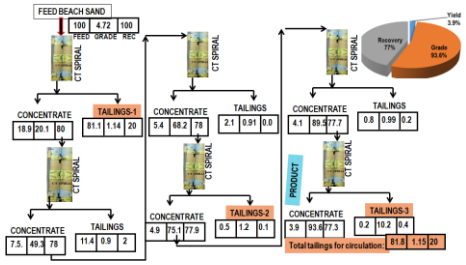

Figure 11 Flowsheet with mass balance achieved on sample-1 (4.72%THM) by using CT spirals

Table 2 Summary of results of different gravity units with feed mono grade [THM 4.72%] of beach placer deposit

Details	MOZELY TABLE	GRAVITY TABLE	HG8 SPIRAL	CT SPIRAL	HUMPHERY SPIRAL
Yield %	4.2	3.9	3	3.9	3.3
Grade %	93.2	92.2	92.9	93.6	98.2
Recovery %	83	76	59	77.3	69
Rougher	1	1	1	1	1
No. of cleanings	4	1	2	5	3
No. of scavengings	-	-	3	-	-

It can be concluded from the data presented in Figs. 9 to 11 and Table 2 that the lower capacity gravity units are restricted for low tonnage samples where as spiral is designed for high tonnage samples. It may be noted here that the designed spirals are not suited for low grade samples with finer heavy particles. In view of this it is essential to understand the relation between the textural characteristic of the samples and design aspects of the gravity unit operations. The concentration of heavy minerals can occur if the minerals possess the three properties: a. high specific gravity, b. chemical resistance and c. hardness. Mechanical concentration [Nature's process] and gravity concentration [man made design process] not only depend on the above three factors it also depends on size and shape of particles. More over the difference in specific gravity is accentuated in water as compare to air. For example, the concentration criterion/the ratio of gold (sp. gr. 19) to quartz (sp. gr. 2.6) is as follows:

Gold in air, 19/Quartz in air 2.6 = 7.3/1.6,
Gold in water, 19/Quartz in water 2.6 = 11.2/1.6.

The effect of concentration criterion [4] on gravity concentration is shown in Table 3.

Table 3 Effect of concentration criterion on gravity concentration

Concentration Criterion	**Net results**
1.25	Separation is possible at gravel size
1.50	Separation is difficult but can be applied commercially up to 2 mm size
1.75	Commercial Separation is possible down to 150 microns
2.00	Reasonable separation is possible
2.50	Clean concentrate can be obtained with large tonnage of midlings but difficult to get low grade tailings
3.00	Gravity Separation is possible at all sizes down to fine sand

If this concentration criterion value is less than 1.25 practical separation is subsequently impossible and direct separation under turbulent conditions is usually uneconomical. Thus, it is essential to know concentration criterion for the beach sand samples containing different specific gravity heavy minerals used with different spiral units. Gravity concentration criterion of heavy minerals with reference to quartz (2.6 sp. gr.) and ground water and sea water as media for separation of minerals given in Table 4.

Table 4 Gravity concentration criterion of heavy minerals with reference to quartz (2.6 sp. gr.)

Minerals	**Specific gravity**	**Concentration Criterion [air]**	**Concentration Criterion [ground water]**	**Concentration Criterion [sea water]**
Ilmenite	4.75	1.8	2.34	3.2
Rutile	4.21	1.6	2.00	2.8
Garnet	4.25	1.6	2.03	2.8
Sillimanite	3.23	1.2	1.39	2.2
Zircon	4.69	1.8	2.31	3.1
Monazite	5.10	2.0	2.56	3.4

The data given in Table 4 indicate that all heavy minerals are more than the quartz specific gravity. The highest specific gravity mineral is monazite 5.10 sp.gr. and the lowest specific gravity mineral is sillimanite 3.23 sp.gr. Accordingly the concentration criterion for monazite is 2.56 where as for Silliminite is 1.39. According to the data presented in Table 3 that the gravity concentration criterion 2.00 is possible for reasonable separation. Hence there is every possibility the silliminite which is major mineral in the THM to join along with lighter minerals quartz. Moreover silliminate is flaky/needle shape mineral and other minerals are sub rounded to round in shape. This is resulting to exhibit poor grade and recovery in the process of spiral operation. Hence an attempt is made further to understand the minimum grade required to a specific designed spiral, different grades of THM samples are subjected to relatively low efficiency model HG8 spiral chosen and the data are given in Table 5 and shown in Figs. 12 to 15.

Table 5 Summary of results of HG8 Spiral with different feed grades [THM] of beach placer deposits

Details	4.72 THM	5.6 THM	9.5 THM	15.7 THM	19.5 THM
Yield %	3	4.9	8.5	15.3	19.0
Grade %	92.9	82.8	90.7	98.2	98.1
Recovery %	59	72	81	95	95
No. of cleanings	3	4	3	1	1
No. of scavengings	3	-	-	1	-

Data shown in Table 5 indicate that with increasing the grade (THM) of the feed sample, the achieved the output of the product grade and recoveries are higher. It may noted here that when sample 4.72% THM feed used in the HG8 spiral the product grade achieved is 92.9% with 59% recoveries, where as when the sample containing 19.5%THM, the feed used in the HG8 spiral the product grade achieved is 98.1 with 95% recoveries. Data shown in Figs. 12-15 indicate that at lower concentration of feed containing below 6% needs six stages of spirals where as for higher grade 19.5% THM the 2 stage spirals are required to achieve desired grade.

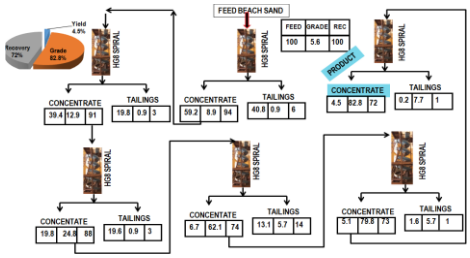

Figure 12 Flowsheet with mass balance achieved on sample-2 (5.6%THM) by using HG8 spirals

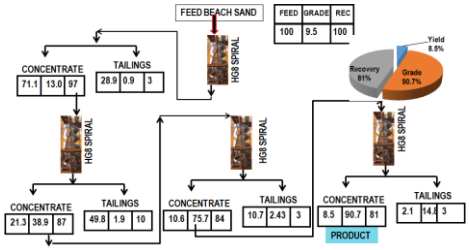

Figure 13 Flowsheet with mass balance achieved on sample-3 (9.5%THM) by using HG8 spirals

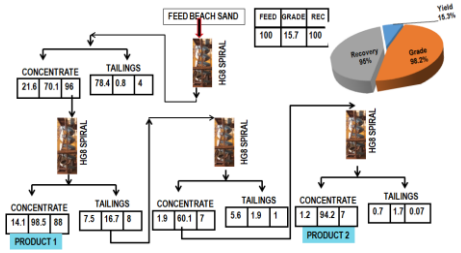

Figure 14 Flowsheet with mass balance achieved on sample-4 (15.7%THM) by using HG8 spirals

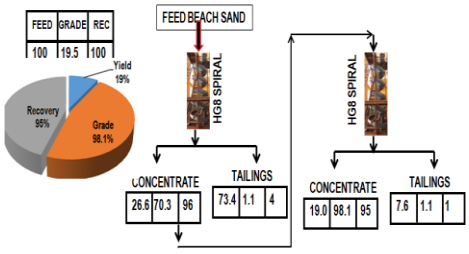

Figure 15 Flowsheet with mass balance achieved on sample-5 (19.5%THM) by using HG8 spirals

Humphreys' spiral used to see the effect of sea water on preparation bulk concentration from beach sand. Prior to assess the effect of sea water on recovery of total heavy minerals, an attempt is made to recovery the THM by clear spiral set and scavenging spiral set. Here cleaner spiral means, tailings should be free from the values,

where as scavenging spirals means THM is free from gangue. The study reveals that cleaner spirals gave better grade 98.2% THM and scavenging spiral route gave better recovery 74% with a grade of 92.1% THM. The results achieved with sea water using cleaner spiral route and scavenging spiral route indicate that cleaner spiral for the same grade 98.2% THM gave much better recovery 85% where as for scavenging route for the same grade 93% THM the recovery achieved is 89%. This can clearly be seen from Figs 16-17 and Table 6.

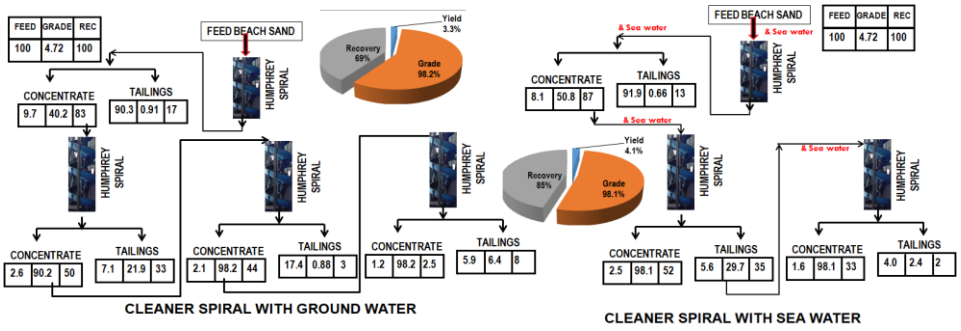

Figure 16 Flowsheet with mass balance achieved on sample-1 (4.72%THM) by using Humphrey cleaner spirals using ground water and sea water media of separation

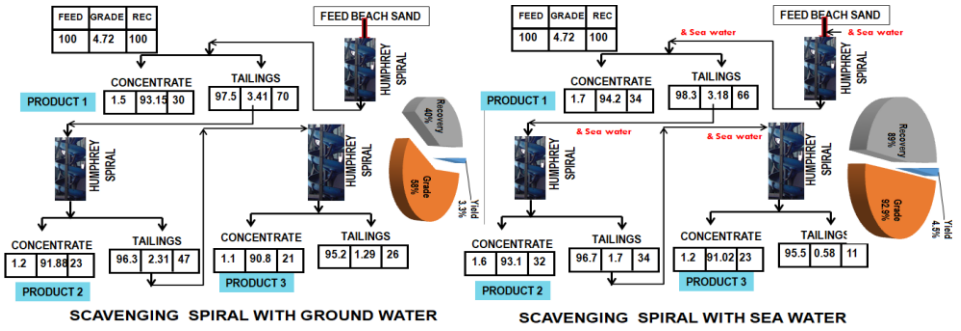

Figure 17 Flowsheet with mass balance achieved on sample-1 (4.72%THM) by using Humphrey scavenging spirals and ground water media of separation

Table 6 Summary of results on the effect of sea water in clear and scavenging Humphrey spirals with feed mono grade [THM 4.72%] of beach placer deposit

Details	CLEANER SPIRAL WITH GROUND WATER	CLEANER SPIRAL WITH SEA WATER	SCAVENGING SPIRAL WITH GROUND WATER	SCAVENGING SPIRAL WITH SEA WATER
Yield %	3.3	4.1	3.8	4.5
Grade %	98.2	98.1	92.1	93
Recovery %	69	85	74	89
No. of cleanings	1	1	-	-
No. of scavenging	1	1	3	2

CONCLUSIONS

The conclusions drawn from the study of synergizing placer heavy minerals up gradation with physical and textural characters of minerals from lean grade beach sand deposits using different gravity concentrators that the performance of spirals are much significant at higher grade and coarse size of feed. Use of sea water has shown significant effect on grade and recovery of THM. The study reveals that 98.1% THM with 85% grade can be achieved from a feed sample contain 4.72% THM. Hence it is recommended to use mobile spirals along coast and use sea water. The THM recovered by using sea water may be washed with ground water and drained the water before sending to mineral separation plant.

REFERENCES

1. Wolfe, J.A. Mineral Resources- a world review.
2. Batman, A.M. (1962) Economic mineral deposits, Asia publishing house, Bombay, 227-44.
3. Thnbury, W.D. Principles of geomorphology.
4. Bhima Rao, R. (1994) Gravity Concentration. Proceedings, National Seminar on gravity concentration, 1-150.
5. Mineral Technologies. Cost Estimation Hand Book, Sponsor by Mineral Technologies, Chapter 12, Beneficiation – Concentration, 273-274.
6. Gucbilmez, D., Ergun, S.L. (2012) A Comparison of Performances of Spiral Concentrators Having Different Geometries. In: XXVI International Mineral Processing Congress (IMPC), Proceedings, New Delhi, India, 24 - 28 September 2012, Paper No. 654, 01733-01739.
7. Khoza, I. (2016) Minerals Processing Practical 4: Gravity Concentration – Spiral, School of Engineering Department of Materials Science and Metallurgical Engineering NMP 310, 1-17.
8. Sunil Kumar Tripathy, Rama Murthy, Y. (2012) Multiobjective optimisation of spiral concentrator for separation of ultrafine chromite, Int. J. Mining and Mineral Engineering, Vol. 4, No. 2, 151-162.
9. Mahran, G.M.A., Doheim, M.A., Abdel Gawad, A.F., Abu-Ali, M.H., Rizk, A.M. (2015) Numerical simulation of particulate flow in spiral separators (15% solids), Afinidad LXXII, 571, Julio - Septiembre 2015, 223-229.
10. Gulsoy, O.Y., Kademli, M. (2006) Effects of operational parameters of spiral concentrator on mica–feldspar separation, Mineral Processing and Extractive Metallurgy (Trans. Inst. Min. Metall. C), Vol 115, No 2, 80-84.

XV International Mineral Processing and Recycling Conference
17-19 May 2023, Belgrade, Serbia

ROLE OF PARTICLE SHAPE IN THE FLOATABILITY OF TONER PARTICLE

M.S. Trumić#, K.S. Balanović
University of Belgrade, Technical Faculty in Bor, Bor, Serbia

ABSTRACT – This paper aims to research the influence of the particle shape of the iron oxide-containing toner on flotation efficiency and to test first-order and second-order kinetics models to determine the model which better describes the flotation of the coarse plate-like particles.
Hallimond tube flotation were carried out on two toner samples (regular round plate-like and irregular plate-like particles), with no collector in use. Contact angle measurements were conducted by sessile drop method. The results show that both samples have the same high value of contact angle which indicates that the toner samples are hydrophobic. High toner flotation recovery is achieved with round plate-shaped toners after prolonged time and flotation kinetics of toner was described by classical first order flotation model. The toner with the irregular plate-shape has reduced flotation recovery even after a long time of flotation and flotation kinetics of toner was described by modified first order flotation model.
It should be emphasized that no significant differences were observed when measuring the contact angle of samples, and that the lower recovery obtained for sample with irregular plate-like particles can be attributed to the different shape of the particles.

Keywords: Flotation, Hydrophobicity, Contact Angle, Flotation Kinetics, Toner, Particle Shape.

INTRODUCTION

Particle shape plays an important role in flotation, and that role is difficult to define for few reasons. First, the method of obtaining particles of different shapes leads to a change in the roughness of the surface and thus to a change in hydrophobicity. Second, flotation depends on reagent concentration and type, particle surface hydrophobicity, particle size, and other factors such as the speed of agitating, solid content in the suspension, etc. [1-6].

The mechanism of particle shape affecting particle floatability is discussed by several authors [1,3,7]. Namely, they all pointed out that by grinding, the surface roughness changes and thus the hydrophobicity of the particles, and that changes in flotation efficiency cannot be attributed only to changes in particle shape, that often occur due to comminution. That is why these studies were carried out on synthetic toner samples, of different shape but with the same hydrophobicity.

Flotation kinetics for small spherical particles has been described by the second-order flotation model [5], and the aim here will be to define order of the flotation model which better describes flotation of coarse plate-like particles.

corresponding author: majatrumic@tfbor.bg.ac.rs

EXPERIMENTAL

Materials and methods

A Laser Jet 1018 printer was used to prepare realistic synthetic sample (free toner particles). Toner particles produced from laser toner are usually plate, regular round or irregular shaped in deinking suspension [3]. According to the material safety data sheet (MSDS, 2022), the toner inside the cartridge is mainly composed of a styrene/acrylate copolymer (<55 wt %), iron oxide (<50 wt %) and amorphous silica (<3 wt %). Its solubility in water is negligible, and it is partially soluble in toluene and xylene. The material should soften between 100°C and 150°C, and decomposition temperature is > 200 °C. The density of the toner is 1.4 g/cm^3.

On the foil thickness 100 μm previously coated with (PVA) polyvinyl alcohol [8], circles with a diameter of 1 mm were printed, and after agitation in a mechanical stirrer, plate-shaped particles were obtained. After wet sieving, two samples were formed for microflotation experiments (Table 1 and Figure 1).

Table 1 Characteristics of toner particles

Sample 1			
size (diameter) of screens d (μm)	W (%)	average size (diameter) of particles, d_{sr} (μm)	Shape
-1000+600	100	800	regular round plate-like
-600+150	0		
Sample 2			
-1000+600	48	500	regular round plate-like, irregular plate-like
-600+150	52		

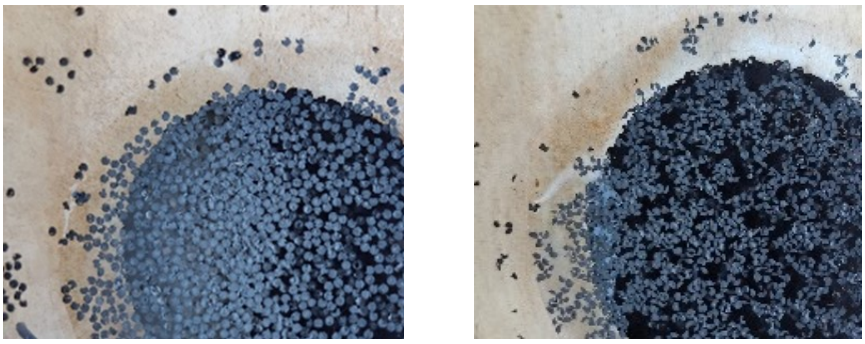

a) b)

Figure 1 Shape of samples: a) regular round plate-like, b) irregular plate-like

Based on contact angle measurements, the surface properties of the toner sample were characterized. Measurements were made with a sessile drop method [9] using an optical goniometer (Advex Instrument) with appropriate software SeeSystem. The liquid used was distilled water and a 0.1 μL droplet formed using a micropipette (VITRUM/VVR) that was captured after dropping onto the toner surface. After manually

selecting the three points on the droplet's perimeter, the software automatically calculates the value of the contact angle.

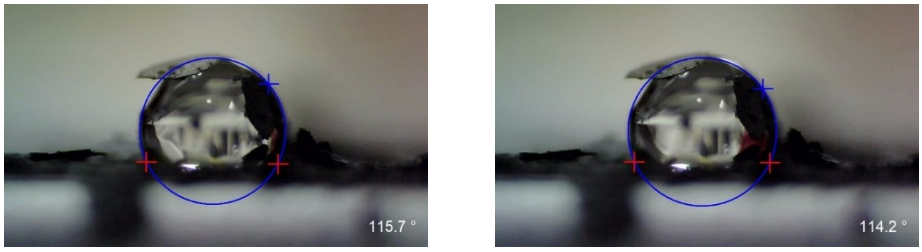

a) b)

Figure 2 Images of a water drop onto surface of toner before microflotation a) after 30 s and b) after 60 s

Liquid (water) surface wetting and liquid (water) spreading are very important aspects of practical surface chemistry, which is the basis of the microflotation process. Microflotation experiments were performed in a modified Hallimond flotation cell (Figure 3) which is often called a monobubble Hallimond tube in the literature [10].

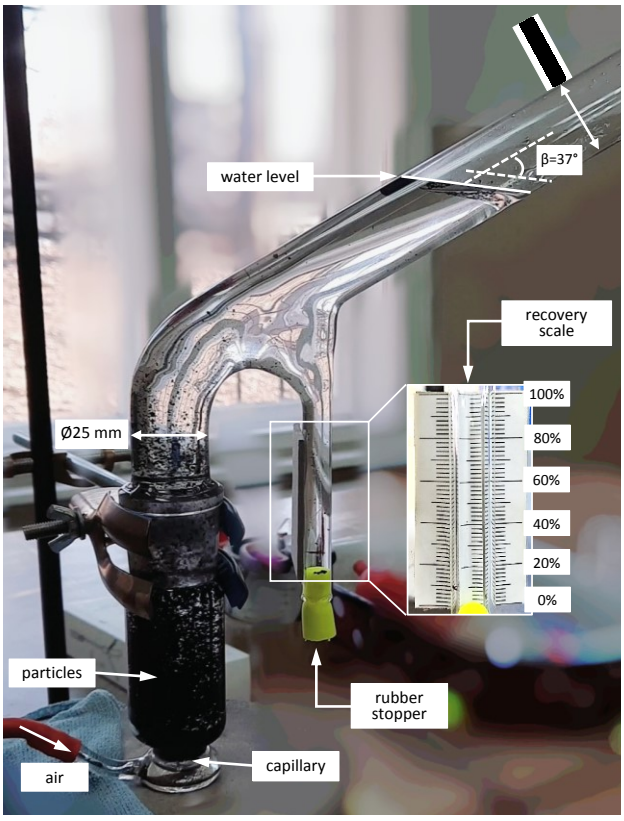

Figure 3 Monobubble Hallimond tube with recovery scale

The experimental apparatus consists of a glass tube placed on a magnetic stirrer, a capillary for creating air bubbles and a digital camera. A sample of toner particles, with a solids concentration of 2.5 g/L, was placed in a 120 ml glass tube and diluted with constant volume of distilled water to create the toner suspension. The suspension was mixed at 400 rpm for fixed period of time, and then a constant air flow of 40 L/h through the capillary of the Hallimond tube generated bubbles, and the process of particle flotation was recorded with a digital camera in a time interval of 60 min. Toner recovery was read directly from the recovery scale. After drying, the contact angle was determined on floatable and non-floatable particles.

The results are presented in the form of recovery of floatable particles (I), as a function of flotation time (t), in order to represent the flotation kinetics of the toner particles through a suitable flotation model. All microflotation experiments were performed in distilled water at a temperature of 20 °C without a collector.

RESULTS AND DISCUSSION

Figure 4 shows flotation recovery of floatable toner particles as a function of time. In general, increasing the flotation time resulted in an increase in the flotation recovery of floatable toner, and higher recovery was achieved at longer flotation times.

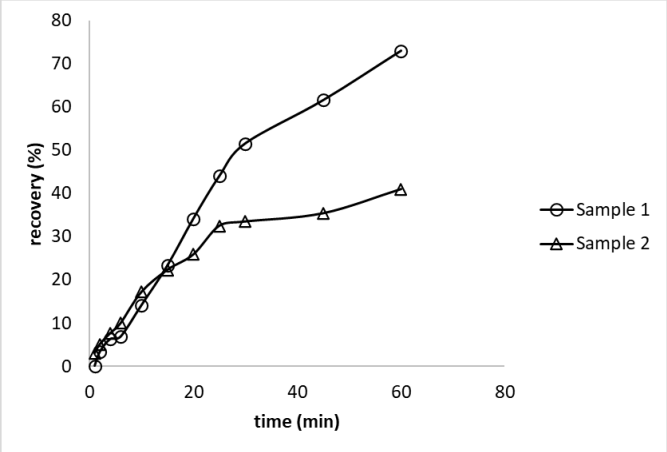

Figure 4 Microflotation kinetics of toner

At the 15 minutes of microflotation, the recovery of both toner samples was 22%. After the 25 minutes of microflotation, toner recovery on sample 1 (d_{sr}=800 µm, regular round plate-like particles) initially increases with the time, and max achieved recovery value was 72% after 60 minutes. For the same time interval (after 25 minutes of microflotation), toner recovery on sample 2 (d_{sr}=500 µm, regular round plate-like particles and irregular plate-like particles), levels off at a maximum constant value (around 36%). Drzymala emphasized in his research [10] that the mentioned (for sample 2) generally occurs between 10 and 15 minutes of flotation, depending on the size of the particles (10 minutes for calcite d_{sr}=180 µm, 15 minutes for calcite d_{sr}=112.5 µm). From Figure 4, it can be seen that in these studies it takes a longer time

(25 minutes) to achieve a constant toner recovery value with a larger d_{sr}=500 µm, which indicates that in addition to the particle size, the shape of the particles also has a great influence (calcite has a cubic shape and toner has a regular round plate and an irregular plate shape).

Many authors in their research [1-3], have shown that the influence of the shape of particles on the floatability is of great importance. It was emphasized that irregular, elongated and plate-shaped particles have a higher recovery compared to round and spherical particles during the flotation of minerals that have a higher density [3]. Schmidt and Berg [11] based their research on small round plate-like toner particles, which have a significantly lower density than minerals, and concluded that these particles are less likely to adhere to an air bubble.

From Figure 4, it can be seen that the recovery of toner with round flat particles is significantly higher (by 32%), compared to toner with irregular plate shaped particles, which may indicate that mechanical carryover occurred. This assumption should be verified in subsequent studies by monitoring the dependence of the toner flotation kinetics and the pH value of the solution, and which would confirm the observations of the authors Drzymala and Lekki [12].

The toner particles exhibited a high floatability without the addition of a collector. This can be understood by considering the measured value of the contact angle (114.2°), which indicates that the toner samples are hydrophobic.

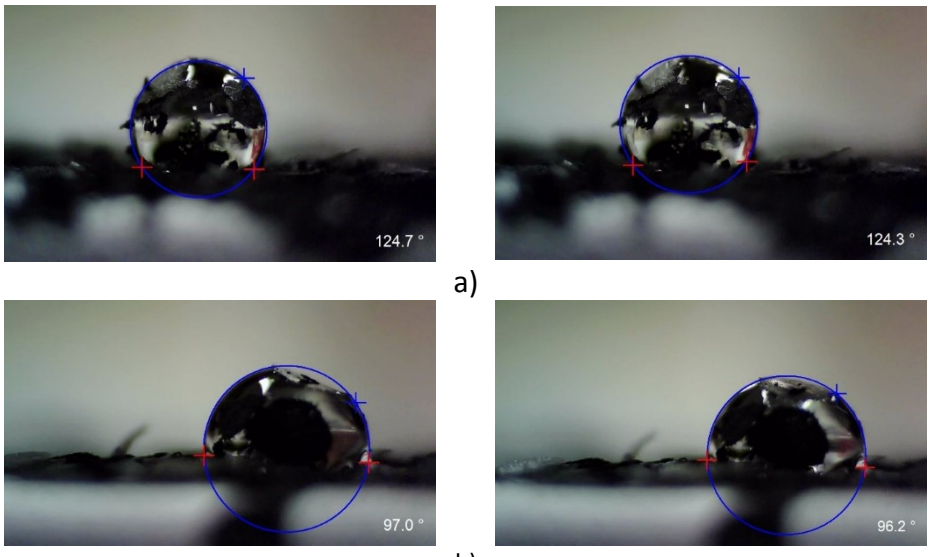

Figure 5 Images of water droplets onto surface of sample 1 after flotation
a) floatable particles after 30 s (left), after 60 s (right) and b) non-floatable particles after 30 s (left), after 60 s (right)

It should be emphasized that no significant differences were observed when measuring the contact angle of sample 1 and sample 2, and that the lower recovery obtained for sample 2 can be attributed to the different shape and size of the particles.

Given that the assessment of flotation kinetics requires the analysis of the flotation rate, first- and second-order flotation models were used in the paper for the assessment of toner flotation kinetics [5,13-15].

Pan et al. [13] in his research described the flotation kinetics of ink particles under laboratory conditions by the classical model of the first order kinetics using the expression (1), and conclusion was that the value of kinetic constant of flotation, k, can be determined from the expression (1) as long as the flotation time is short and the diameter of the ink particles is constant.

$$ln(1/(1-I)) = kt \quad (1)$$

where: I- flotation recovery of ink particles in froth product, t- flotation time, k- kinetic constant of flotation.

Trumic and Antonijevic [15] in their research on the flotation of cube-shaped toners made the observation that only for a short flotation time, up to 4 min, the particle flotation process follows first-order kinetics with a good correlation, which also Nikolaev [5] confirmed in the case of toner flotation of spherical shape for a total flotation time of 2 min.

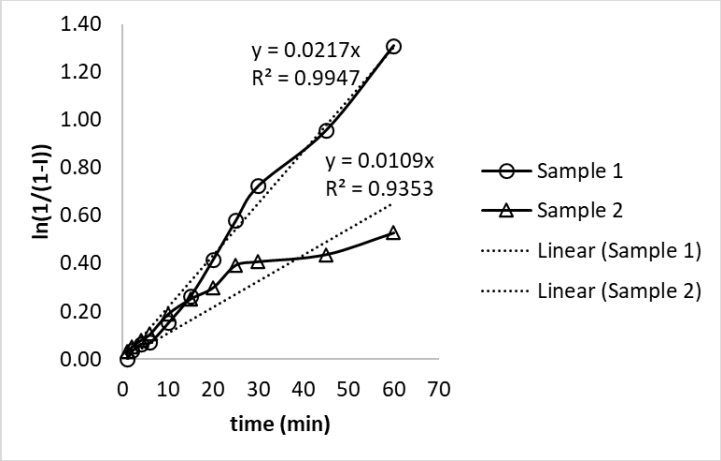

Figure 6 The classical first order fitting of flotation responses, fitting for the total flotation time 60 min

In Figure 6, it can be clearly seen that for sample 2 (d_{sr}=500 µm, regular round plate particles and irregular plate particles), the break between the two linear parts of each curve implies that two flotation mechanisms are operating: one is a short time mechanism and the other longer time mechanism. That is why Pan [13] implied that no single value of the constant k is sufficient to express the data even if the minimum value R^2 Volk [16], for a correlation is reached (R_{min}^2=0.447). For sample 1 (d_{sr}=800 µm, regular round plate-like particles), for the total tested time of 60 min, the model is valid, which indicates that the uniformity of the particles and the shape of the particles have a significant impact on the application of this model.

The second model (Figure 7) that was tested is the first-order model modified by Trumic and Magdalinovic, expression (2) [15].

$$I/(1-I) = kt \tag{2}$$

where I- flotation recovery of ink particles in froth product, t- flotation time, k- kinetic constant of flotation.

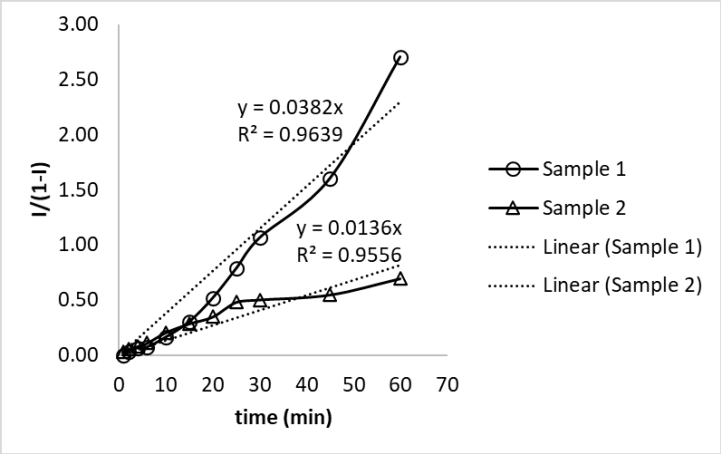

Figure 7 The modified first order by Trumic and Magdalinovic fitting of flotation responses, fitting for the total flotation time 60 min

The correlation coefficient R^2, for sample 2, has a higher value and the points on the curve better follow the dependence of the straight line, that is, only, the mechanism for a long time of flotation is present which can be represented by single value of the constant k.

Several authors [5,17] obtained the linearity of experimental toner flotation data via second-order flotation kinetics, using expression (3).

$$t/I = (t/I_\infty) + (1/I_\infty^2 k) \tag{3}$$

where I_∞- maximum flotation recovery, I- flotation recovery of ink particles in froth product, t- flotation time, k- kinetic constant of flotation.

For both samples (Figure 8), it can be said that there is a break between the two linear parts of each curve, implying that two flotation mechanisms are functioning: one is a short time mechanism of up to 6 min and the other is a longer time mechanism. The correlation coefficients, R^2, have a significantly higher value, but linearity was not achieved for the total flotation time of 60 min. Nikolaev [5] showed that the flotation kinetics of the toner, spherical in shape, for a short flotation time of 2 min, is described by second order flotation model.

There are several studies [5,14,15] in the literature showing first-order and second-order kinetics for the flotation of toners with the smallest particle sizes, spherical and cubic, in short flotation times. Therefore, in this work there are no experimental data

that could be compared with the results obtained for coarse particles, regular and irregular in shape, in a long time of flotation.

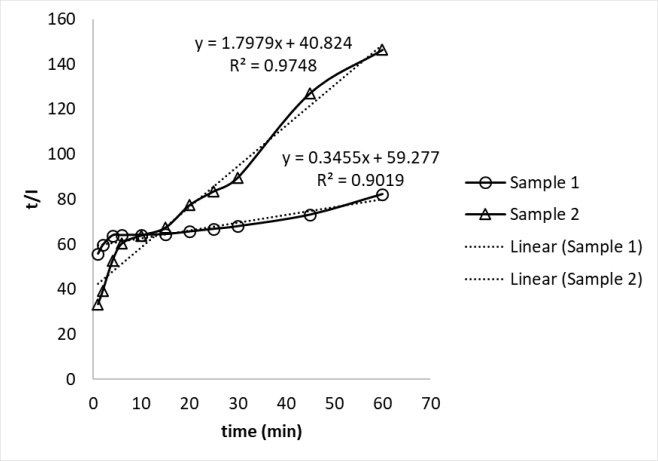

Figure 8 The second order fitting of flotation responses, fitting for the total flotation time 60 min

CONCLUSION

Coarse toner particles, consist of iron oxide, regular round and irregular plate-like shape have high degree of hydrophobicity. High toner flotation recovery is achieved in pure water with round plate-shaped toners after prolonged time. The toner, which contains 50% of the irregular plate-shaped toner, did not float effectively even after a long time of flotation, (toner flotation recovery reduced by approximately 50%), due to the influence of particles of irregular plate shape. Generally, flotation kinetics of the toner (coarse plate particles), is described by first order flotation model. The flotation rate constant k, was slightly lower in the flotation of toners containing regular and irregular plate-shaped particles.

A flotation test using a Hallimond tube of known hydrodynamic pattern can enable the distinction between mechanical transfer, non-contact and collector flotation. In order to confirm the assumption that under the given conditions mechanical carryover of round plate particles took place, further research is necessary.

ACKNOWLEDGEMENT

"The research presented in this paper was done with the financial support of the Ministry of Education, Science and Technological Development of the Republic of Serbia, within the funding of the scientific research work at the University of Belgrade, Technical Faculty in Bor, according to the contract with registration number 451-03-47/2023-01/200131".

REFERENCES

1. Schmidt, D.C. (1996) Flotation deinking of toner-printed papers. Dissertation, University of Washington, USA.

2. Chau, T.T., Bruckard, W.J., Koh, P.T.L., Nguyen, A.V. (2009) A review of factors that affect contact angle and implications for flotation practice. Advances in colloid and interface science, 150(2), 106-115.
3. Xia, W. (2017) Role of particle shape in the floatability of mineral particle: An overview of recent advances. Powder technology, 317, 104-116.
4. Tsatsis, D.E., Valta, K.A., Vlyssides, A.G., Economides, D.G. (2019) Assessment of the impact of toner composition, printing processes and pulping conditions on the deinking of office waste paper. Journal of Environmental Chemical Engineering, 7(4), 103258.
5. Nikolaev, A.A. (2019) Flotation recovery of toner containing iron oxide from water suspension. Minerals Engineering, 144, 106027.
6. Ulusoy, U. (2023) A Review of Particle Shape Effects on Material Properties for Various Engineering Applications: From Macro to Nanoscale. Minerals, 13(1), 91.
7. Ahmed, M.M. (2010) Effect of comminution on particle shape and surface roughness and their relation to flotation process. International Journal of Mineral Processing, 94(3-4), 180-191.
8. Lin, D., Kuang, Y., Chen, G., Kuang, Q., Wang, C., Zhu, P., Peng, C., Fang, Z. (2017). Enhancing moisture resistance of starch-coated paper by improving the film forming capability of starch film. Industrial Crops and Products, 100, 12-18.
9. Liber-Kneć, A., Łagan, S. (2021) Surface testing of dental biomaterials—determination of contact angle and surface free energy. Materials, 14(11), 2716.
10. Drzymala, J. (1994) Characterization of materials by Hallimond tube flotation. Part 1: maximum size of entrained particles. International Journal of Mineral Processing, 42(3-4), 139-152.
11. Schmidt, D.C., Berg, J.C. (1997) Selective removal of toner particles from repulped slurries by flotation. Pulp And Paper Canada, 98(2), 21-24.
12. Drzymala, J., Lekki, J. (1989) Mechanical, contactless, and collector flotation in the Hallimond tube. Journal of colloid and interface science, 130(1), 197-204.
13. Pan, R., Paulsen, F.G., Johnson, D.A., Bousfield, D.W., Thompson, E.V. (1996) A global model for predicting flotation efficiency. Part I: model results and experimental studies. Tappi journal, 79(4), 177-185.
14. Pelach Serra, M.A. (1998) Proces de destintatge del paper per flotacio. Avaluacio de l'eficacia d'eliminacio de tinta. Dissertation, Universitat deGirona, Girona, pp. 278.
15. Trumic, M.S., Antonijevic, M. (2016) Toner recovery from suspensions with fiber and comparative analysis of two kinetic models. Physicochemical Problems of Mineral Processing 52, 5-17.
16. Volk, W. (1965) Statystyka stosowana dla inżynierów, Wydawnictwa Naukowo – Techniczne, Warszawa.
17. Yalcin, R.H., Luttrell, S. (2011) Flotation kinetics of a pyritic gold ore. International Journal of Mineral Processing, 98, 48-54.

XV International Mineral Processing and Recycling Conference
17-19 May 2023, Belgrade, Serbia

COPPER SORPTION CAPACITY OF THE SOIL TREATED WITH UNCONVENTIONAL ALKALIZING AGENTS

I. Smičiklas[#], M. Egerić, M. Jović
University of Belgrade, "VINČA" Institute of Nuclear Sciences - National Institute of the Republic of Serbia, Belgrade, Serbia

ABSTRACT – The influence of unconventional alkaline additives (ground seashells and bauxite residue) on the copper (Cu) sorption and retention capacity of acidic soil was investigated. The soil collected near the mining and metallurgical complex in Bor (Serbia) was treated with different doses of additives, and the Cu sorption and desorption were assessed in batch conditions. The waste-derived materials proved to be efficient and sustainable alternatives to conventional alkalizers, increasing the maximum sorption capacity for Cu in correspondence with the soil pH increase. Nevertheless, added Cu was largely mobilized by weak acid extraction, demonstrating the importance of maintaining optimal soil pH for Cu leaching prevention.

Keywords: Soil Management, Seashell Waste, Red Mud, Copper Sorption Capacity.

INTRODUCTION

Copper mining and metallurgy are important activities that cause significant damage to the environment and biota through the emission of waste gases and the inadequate disposal of waste enriched with metals [1]. The deposition of metals in soil is a long-term process that leads to the accumulation, but also to the transport and biotoxicity of their mobile and bioavailable chemical forms. In addition to heavy metals with no known biological significance, essential metals such as copper (Cu) can be found in the surrounding soils in concentrations with high toxic potential [2]. The quality of soil is further compromised by acidification from acid precipitation and leaching, which causes nutrient imbalance, reduced microbial community activity, and reduced soil's natural ability to retain heavy metals to which they are continuously exposed [3]. Agricultural land located close to industrial plants is a significant element of risk due to the bioaccumulation of elements in the food chain.

Treating soil with alkaline additives is one of the leading methods for improving pH to bring it into the optimal range, reducing the mobility and availability of toxic metals and mitigating environmental risks [4]. Due to the incentive policy of the circular economy, many alkaline waste materials and by-products are currently being considered for possible application in the soil to achieve multiple benefits [5,6].

As a producer of copper and precious metals with a tradition of more than a hundred years, the mining and metallurgical complex in Bor causes the greatest heavy

[#] corresponding author: ivanat@vin.bg.ac.rs

metal pollution in Serbia, especially high concentrations of Cu in the surrounding soils and plant species [7].

In this study, the Cu sorption properties of acid soil sampled near the complex and soil samples treated with unconventional additives were investigated in batch sorption and desorption experiments. The objective was to determine and compare the influence of two waste materials (ground seashells and bauxite residue) and their dosage on the sorption and retention of Cu in the soil.

EXPERIMENTAL

The control soil (S) from Slatina village (Serbia) and the samples of soils treated with different doses of grounded seashell waste (SW: 0.15%, 0.3%, 2%, and 5%) and red mud (RM: 0.3%, 2%, and 5%) were prepared as previously described [8]. The sorption of Cu was examined by equilibrating the soil samples and $Cu(NO_3)_2$ solutions with increasing Cu concentrations (10^{-4} – $5 \cdot 10^{-3}$ mol/L). Working solutions were prepared in a background electrolyte ($NaNO_3$) with a concentration of 10^{-2} mol/L, and their initial pH was adjusted to 5.0. Suspensions with a soil/liquid ratio of 1g/10mL were agitated on an overhead laboratory shaker (10 rpm) at room temperature (21±1°C) for 48 h to attain equilibrium. After phase separation by centrifugation and filtration, residual Cu concentrations and the concentrations of displaced Ca ions were measured (Inductively Coupled Plasma Optical Emission Spectroscopy, ICP-OES, Perkin Elmer Avio 200). The equilibrium solution pH values were measured by a WTW InoLab pH meter.

The dry solid residues from sorption experiments were exposed to the extraction with 0.11 mol/L acetic acid. The solid/solution ratio was 1g/40mL, and the extraction was performed during 16 h of agitation at room temperature to isolate the most mobile metal fraction (F1) of the sequential extraction scheme recommended by the European Community Bureau of Reference (BCR) [9]. The extracted Cu concentrations were measured in filtrates by ICP-OES.

RESULTS AND DISCUSSION

The pH of SW and RM samples (9.30 and 10.0, respectively) was markedly higher than the soil pH (4.93) [8]. Accordingly, the addition of SW and RM led to the soil pH increase and influenced other essential soil properties. The descriptive statistics of soil properties are presented in Table 1.

Table 1 Descriptive statistics of soil properties (n=8) [8]

Variable	Unit	Mean	Minimum	Maximum	StDev
pH	/	6.44	4.93	7.65	1.05
$CaCO_3$	%	1.181	0.000	6.090	2.159
Cation exchange capacity (CEC)	$cmol_c/kg$	11.82	11.40	12.20	0.34
N	%	0.171	0.164	0.177	0.005
C	%	1.669	1.460	2.280	0.273
Available P	mg P_2O_5/100g	6.21	2.88	15.60	4.04
Available K	mg K_2O/100g	42.46	41.10	43.40	0.70
Electrical conductivity (EC)	dS/m	0.724	0.378	1.214	0.324

The sorption of Cu by tested soil samples is given in the form of isotherms (Figure 1) representing the relationships between equilibrium Cu concentrations in the liquid (C_e, mmol/L) and solid (Q_e, mmol/g) phase. The linear relationships almost parallel to the y-axis, obtained for soil samples SW2, SW5, and RM5, reflect their high affinity for Cu in the entire investigated concentration range, while the isotherms characteristic for samples S, RM0.3, RM2, SW0.15, and SW0.3 exhibit an "L" type shape, indicating gradual saturation of the soil. Compared to the control soil, all treatments stimulated increased Cu sorption. Experimentally obtained maximum sorption capacities ($Q_{max,sor}$) ranged from 0.040 mmol/g (control soil, S) to 0.053 mmol/g (SW2 and SW5) and followed the order: SW2=SW5>RM5>RM2>SW0.3>SW0.15>RM0.3>S.

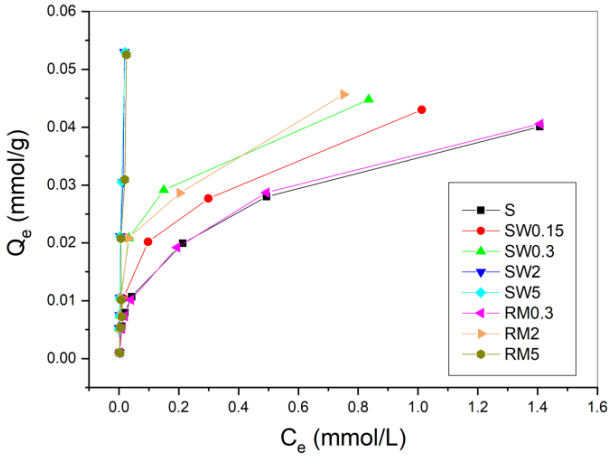

Figure 1 Cu sorption isotherms on the control and treated soil samples

As shown in Figure 2a, the pH values of the Cu solutions in equilibrium with treated soil samples were commonly higher compared to the control soil. The pH was influenced by both the type and quantity of additive so that the lowest values were obtained for the lowest doses of both additives, while at the same dose, higher values were obtained using SW compared to RM. Furthermore, with the increased amounts of Cu ions sorbed, the pH decreased in all investigated systems demonstrating that the specific Cu sorption takes place on protonated surface groups accompanied by the release of H^+ ions.

Figure 2b further discloses the linear relationships between the amounts of Cu ions sorbed and Ca ions released into the solution. After adding SW, the amount of displaced Ca is higher compared to the control soil and increases with the increase in the dose of SW, which is a consequence of its high calcium carbonate content (95.8%) [8]. On the other hand, even though the RM's high alkalinity and complex oxide composition [8] resulted in increased Cu sorption with the increase in RM dose, the amount of released Ca decreased and turned out to be lower compared to the amount displaced from the untreated soil. The results overall indicate different contributions of Cu-binding mechanisms, such as specific Cu sorption, ion exchange, and, possibly, precipitation, in soils treated with SW and RM.

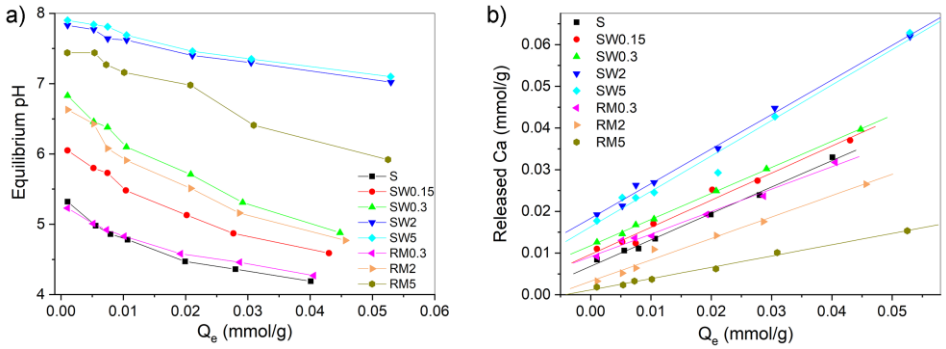

Figure 2 Relationships between the sorbed amounts of Cu and a) final pH values, b) displaced amounts of Ca

The isotherm sorption data (Figure 1) were fitted with the Freundlich linear equation:

$$log\ Q_e = log\ K_F + 1/n\ log\ C_e \quad (1)$$

The calculated empirical constants K_F ((mmol/g)/(mmol/L)$^{1/n}$) and *1/n,* related to the capacity and affinity of the sorbent, are given in Table 2.

Table 2 Cu sorption parameters by soil samples calculated using the Freundlich model

Soil sample	K_F	$1/n$	R^2
S	0.036	0.393	1.00
SW0.15	0.044	0.351	0.99
SW0.3	0.053	0.323	0.98
SW2	0.233	0.471	0.82
SW5	1.828	0.872	0.96
RM0.3	0.037	0.414	1.00
RM2	0.055	0.362	0.96
RM5	1.803	0.892	0.88

Considering the coefficients of determination (R^2), good fitting with the Freundlich model ($0.96<R^2<1.00$) was obtained for all Cu sorption isotherms except for samples SW2 and RM5 where more significant deviations (R^2 = 0.82 and 0.88, respectively) result from almost complete Cu sorption in the entire tested range of concentrations. The K_F values increased with the application of SW and RM and reached the highest values when 5% of additives were applied.

Linear correlation analysis (Table 3) was used to examine the dependency of the Cu sorption parameters on essential properties of the soil, and the statistical importance of the correlation coefficients (r) was evaluated by calculating the Pearson correlation coefficients (p). The $Q_{max,sor}$ was significantly and positively correlated with soil pH, EC, and the Freundlich constant K_F. The pH values >6 specifically promote the increase in pH-dependent surface charge on Fe, Al, and Mn oxides, as well as the metal chelation

by organic matter, and metal-hydroxide precipitation, thus, stimulating several mechanisms of Cu binding [10].

Table 3 Coefficients of correlation (*r*) between Cu sorption/desorption parameters and soil properties

	$CaCO_3$	CEC	N	C	Available P	Available K	pH	EC	$Q_{max,sor}$	K_F
$Q_{max,sor}$	0.649	-0.040	0.124	0.589	0.486	0.454	0.980**	0.932**		
K_F	0.568	0.108	-0.464	0.482	0.653	0.419	0.712*	0.710*	0.728*	
$Q_{max,des}$	0.569	-0.085	-0.213	0.455	0.576	0.128	0.813*	0.838**	0.856**	0.849**

*Statistically significant at confidence levels of *95% (p<0.05) and **99% (p<0.01).*

The relationships between the Cu quantities sorbed by the control and treated soil samples and the quantities extracted within the BCR1 fraction are displayed in Figure 3. In contrast to the Cu distribution pattern characteristic for the original soil [8], added Cu ions were present mainly in the weak acid soluble fraction.

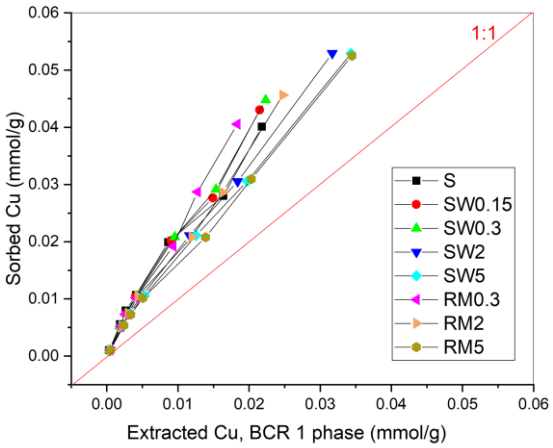

Figure 3 Relationships between sorbed and extracted Cu amounts

The experimentally obtained maximum desorbed quantities ($Q_{max,des}$) were significantly and positively correlated with soil pH and with the Cu sorption parameters $Q_{max,sor}$ and K_F (Table 3). These results confirm the association of recently added Cu with soil inorganic and organic constituents by cation exchange and specific sorption mechanism. Therefore, increasing migration risk through runoff and leaching arises under lower pH conditions.

CONCLUSION

The treatments with variable doses of SW and RM altered the Cu sorption and retention in the soil under the leading influence of soil pH. From both environmental and economic points of view, soil treatment with SW should be a more practical option due to the higher purity of the material and smaller doses for achieving the positive effects on soil pH and Cu sorption capacity. The soil amended with investigated

alternative alkalizers can prevent Cu migration; nevertheless, the long-term retention performance should be ensured by preventing re-acidification of the soil. Continuous monitoring of soil conditions is thus required for the assessment of risks and the necessity of periodic repetition of the treatment.

ACKNOWLEDGEMENT

This work was supported by the Ministry of Science, Technological Development, and Innovation of the Republic of Serbia (Contract No. 451-03-47/2023-01/200017).

REFERENCES

1. Izydorczyk, G., Mikula, K., Skrzypczak, D., Moustakas, K., Witek-Krowiak, A., Chojnacka, K. (2021) Potential environmental pollution from copper metallurgy and methods of management. Environmental Research, 197, Article 111050.
2. Adrees, M., Ali, S., Rizwan, M., Ibrahim, M., Abbas, F., Farid, M., Zia-Ur-Rehman, M., Irshad, M.K., Bharwana, S.A. (2015) The effect of excess copper on growth and physiology of important food crops: a review. Environmental Science and Pollution Research, 22 (11), 8148–8162.
3. Kicińska, A., Pomykała, R., Izquierdo-Diaz, M. (2022) Changes in soil pH and mobility of heavy metals in contaminated soils. European Journal of Soil Science, 73 (1), e13203.
4. Bolan, N.S., Adriano, D.C., Curtin, D. (2003) Soil acidification and liming interactions with nutrient and heavy metal transformation and bioavailability. Advances in Agronomy, 78, 215-272.
5. Ramírez-Pérez, A.M., Paradelo, M., Nóvoa-Muñoz, J.C., Arias-Estévez, M., Fernández-Sanjurjo, M.J., Álvarez-Rodríguez, E., Núñez-Delgado, A. (2013) Heavy metal retention in copper mine soil treated with mussel shells: batch and column experiments. Journal of Hazardous Materials, 248–249, 122-130.
6. Hua, Y., Heal, K.V., Friesl-Hanl, W. (2017) The use of red mud as an immobiliser for metal/metalloid-contaminated soil: a review. Journal of Hazardous Materials, 325, 17-30.
7. Nujkić, M., Dimitrijević, M., Alagić S.Č., Tošić, S.B., Petrović, J.V. (2016) Impact of metallurgical activities on the content of trace elements in the spatial soil and plant parts of *Rubus fruticosus* L. Environmental Science: Processes & Impacts, 18, 350-360.
8. Egerić, M., Smičiklas, I., Dojčinović, B., Sikirić, B., Jović, M., Šljivić-Ivanović, M., Čakmak, D. (2019) Interactions of acidic soil near copper mining and smelting complex and waste-derived alkaline additives. Geoderma, 352, 241–250.
9. Ure, A.M., Quevauviller, P., Muntau, H., Griepink, B. (1993) Speciation of heavy metals in soils and sediments. An account of the improvement and harmonization of extraction techniques undertaken under the auspices of the BCR of the Commission of the European Communities. International Journal of Environmental Analytical Chemistry, 51 (1–4), 135–151.
10. Adriano, D.C., Wenzel, W.W. Vangronsveld, J., Bolan, N.S. (2004) Role of assisted natural remediation in environmental cleanup. Geoderma, 122 (2–4), 121-142.

XV International Mineral Processing and Recycling Conference
17-19 May 2023, Belgrade, Serbia

COPPER ORE BIOLEACHING FROM ECOLOGICAL POINT OF VIEW

V. Conić#, I. Jovanović

Mining and Metallurgy Institute Bor, Bor, Serbia

ABSTRACT – Microorganisms in bioleaching processes are characterized by their oxidative effect on iron ions and forms of reduced sulfur species in acidic environments. To oxidize metal sulfides found in copper ores and concentrates using microorganisms, copper leachate is oxidized as copper sulfate. The bioleach solution is extracted through extraction technologies, after which the technology of electrodeposition of copper, obtaining the final product a copper cathode of high purity.

Keywords: Bioleaching, Eco Friendly Technology, Base Metal, Sulfide Ore, Concentrate.

INTRODUCTION

The mineral industry has suffered in recent year's two significant impacts: The raise on energy cost and more strict environmental regulations were in place for the metallurgical processing of sulfide ores and concentrates, mainly those containing arsenic. These impacts moved the mineral industry to develop alternative processes to roasting and smelting and searching for alternative processes to avoid the high energy consumption, grinding operation and flotation of sulphide minerals. Bioleaching must compete with alternative approaches for extracting metals from ores and concentrates. The main obstacle is the time required for metal extraction, which ranges from days, in the case of bioreactor leaching, to one or more years in the case of bio-piles and waste rock dumps. On the other hand, bioleaching is generally a much more ecological ("green") approach, requiring operation at much lower temperatures, thus energy costs are lower. Microorganisms in oxidation processes are autotrophs, i.e. they consume carbon dioxide like plants. Large amounts of CO_2 are emitted during melting. Bioprocessing also works at atmospheric pressure and at relatively low temperatures (20–80 °C). An external heat source is usually not needed because, like the oxidation of sulphide minerals, it is an exothermic process. Indeed, excess heat is generated where oxidation rates are intense (eg stirred tank operation) and systems need to be cooled to maintain the appropriate temperature. Bioprocessing also has advantages where, first of all, the ore or concentrate contains significant amounts of arsenic (which is released in gaseous emissions during smelting but remains in the liquid and solid phase in (bio)hydrometallurgical processing) and secondly, for the processing of low-quality and complex polymetallic ore.

In the Mining and Metallurgy Institute Bor (MMI Bor) Serbia Figure 1., two continuous facilities for the treatment of bioleaching raw materials were installed in

corresponding author: vesna.conic@irmbor.co.rs

order to evaluate the techno-economic drivers that regulate the application of this technology. Topics covered include choosing between tank and pile bioleaching, microbiology and process operating temperature selection, influence of ore mineralogy on process options, environmental considerations, and metallurgical test design programs.

Bor lake MMI Bor Bor Serbia

City Bor

Figure 1 Conventional pyrometallurgical treatment of mineral raw materials in Bor

EXPERIMENTAL

Evolution of bioleaching technology

Microbes that play a very important role in the leaching processes of copper minerals are: *At. Thiooxidans*, which was isolated in 1922 by (Waksman and Joffre), then *At. Ferrooxidans* isolated in 1947 by (Colmer and Hinkler) and *Ferroobacilus Ferrooxidans* isolated in 1954 by (Leathen and Breley). Their ability is reflected in the ability to oxidize iron with the formation of ferric iron (the main oxidant of sulphide minerals) and the formation of sulfuric acid, which accelerates the dissolution of minerals.

The first forms of leaching in situ, dump leaching and heap leaching are replicated to the improved procedures of heap bioleaching arranged drained piles, for providing oxygen, carbon dioxide and microbes, universally adapted, such as plastic membranes covers, to capture heat and preventing water evaporation, drainage tubes to collect the solutions, network of drippers to irrigate the heap with solutions leaving behind the sprinklers, on/off irrigation system, and slowly adding more instrumentation to monitor the process [1].

In situ leaching

This process allows the extraction of metals from a porous ore body without the need for conventional mining involving drill and blast, open cut or underground mining.

Microorganisms may be induced to release the metals into solution without any mechanical mining of the metal-bearing rocks. If the ore is not porous, holes are drilled in the ore deposit. Explosives are also used for easier penetration of the solution. The leaching solution is pumped into the deposit where it comes into contact with the ore. The leach solution is then pumped to the surface and processed, Figure 2.

Figure 2 In situ leaching

Dump leaching

The leaching of landfills begins with the leaching of tailings from large surface mines, the leaching time of which is measured in years. The ore is crushed and piled, then subjected to a continuous spray of water containing biomining microbes. The leaching solution is collected from the bottom and after metal extraction is used again for washing, Figure 3.

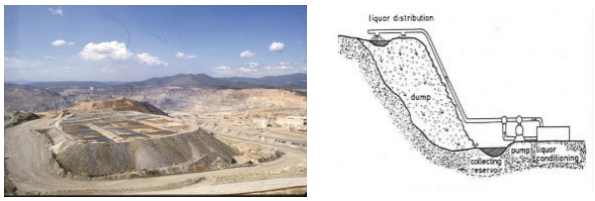

Figure 3 Dump leaching

Heap leaching

The ore is placed in orderly heaps on a water impermeable membrane. The leaching solution is pumped to the top of the pile and the leachate is collected and processed for metal recovery, Figure 4.

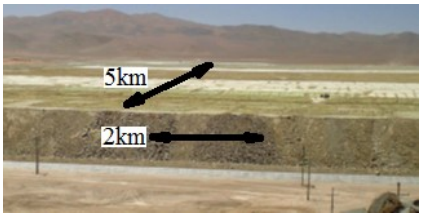

Figure 4 Heap leaching

Mechanism of bioleaching

Bioleaching of the ore body of copper ore is presented in Figure 5. Acidic iron-rich fluid is injected through the borehole into the fractured ore body, where it oxidizes the copper sulfide minerals. A liquid rich in copper and iron is pumped to the surface, the copper is extracted by the SX-EW process. The barren solution is regenerated in a bioreactor containing acidophilic cultures that oxidize iron Fe^{2+} to Fe^{3+}.

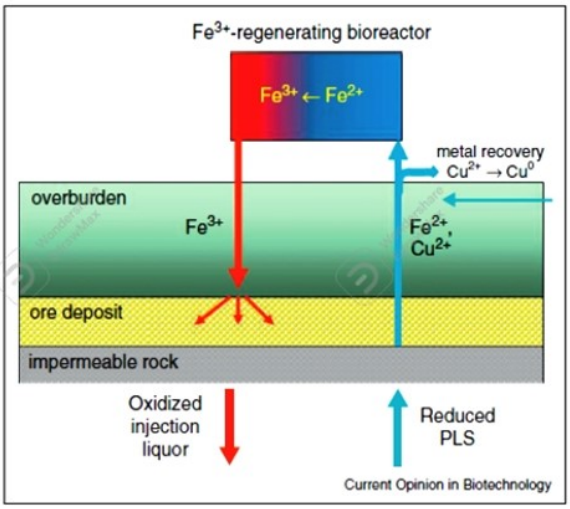

Figure 5 Indirect bioleaching mechanism ore body

Factors affecting the extraction of metals from minerals

Particle size

Ores and concentrates during the leaching process serve as substrates, so that the leaching activity is proportional to the available surface. Reducing the particle size means increasing the total surface area of the particles so that a higher metal yield can be achieved. This means that the surface area plays an important role. The particle size used in bioleaching processes of 20-75µm of about 42µm is considered optimal for bioreactor leaching, while the particle size is different from minerals in heap and landfill leaching in inches.

To carry out the bioleaching operation, it is necessary that the raw material be ground as finely as possible so that it does not destroy the microbes and that the microbes overcome it as easily as possible. On the other hand, research shows that 5% of the world's total energy production is spent on mining ore bodies and grinding ore.

Pulp density

An increase in mineral surface area can be accompanied by an increase in pulp density. Usually, the content of the solid phase in the pulp used in bioleaching

processes is up to 20% (w/v). An uncontrolled increase in pulp density has a negative effect on the diffusion of gases, mixing and therefore on the activity of the organism.

It can also lead to the dissolution of certain compounds that have an inhibitory or even toxic effect on the growth of bacteria.

Temperature

The optimal temperature growth and development mesophilic microorganisms *At. ferrooxidans* and *At. thiooxidans* is between 28-30 °C. The required temperature for the growth and development of moderate thermophiles such as *Sulfolobus, Acidiphilum, Thiobacillus caldus* is 45-55 °C. Extreme thermophiles have the greatest activity at temperature 60-90 °C.

pH

Necessary condition for the growth of acidophilic bacteria is the pH value, which ranges from pH 1.8 to 2.2. Adjusting the pH value in leaching processes is also one of the important factors for metal solubility.

Eh

The Eh-redox potential in bioleaching processes ranges from 350-700 mV. With the dissolution of iron and the increase in the concentration of Fe^{3+} ions, the redox potential increases. It is very important to maintain the redox potential to optimize metal dissolution and control iron deposition.

O_2 and CO_2

The concentration of carbon dioxide in the air is not sufficient for the growth of microbes, so it is necessary to add it. As bacteria are aerobic in nature, an adequate supply of oxygen is a prerequisite for a high degree of leaching.

Nutrients

Microbes need inorganic compounds for growth and development, which they otherwise acquire from nature, such as ammonium sulfate, dipotassium hydrogen phosphate, potassium chloride, magnesium sulfate, and calcium nitrate.

RESULTS AND DISCUSSION

Types of microbes and isolation

Mesophilic microorganisms *At. ferrooxidans* and *At. Thiooxidans*, Figure 6., can be isolated from open pit water presented in Figure 7., underground water that is collected in pits and from ore in Bor, Serbia and these are their natural habitats. Moderate thermophiles can be isolated from the warmer habitats of South Africa. Extremely thermophiles bacteria can be isolated example from hot springs [5].

The increase in the number of bacteria is achieved in a standard nutrient solution of mineral inorganic salts (KCl, $(NH_4)_2SO_4$, K_2HPO_4, $MgSO_4x7H_2O$) in an incubator at the required temperature for the growth of the selected bacterial culture, Figure 8.

After the development of microorganisms, it is very important that the microorganisms first adapt to the leaching conditions in the shaker, Figure 9., for the later successful management of the bioleaching process.

Mesophiles 28-32 °C | Moderate thermophiles 45-55 °C | Extreme thermophiles 60-90 °C

Figure 6 Spaces of microbes that participate in bioleaching processes

Figure 7 Inoculum isolation from open pit

Figure 8 Incubator

Figure 9 Shaker

With the help of adapted microbiological culture, bioleaching tests are performed in bioreactors with CO_2 gas and air supply. Monitoring of the bioleaching process is carried out by daily sampling, in order to control the pH value, redox potential and concentration of leached metals.

The intensity of the oxidation process during bioleaching increases due to the increase in the number of bacteria, the concentration of iron ions, the increase in the acidity of the solution and the redox potential of the solution Eh.

Intensive bioleaching occurs when the basic parameters of the process (pH, Eh, pulp density, concentration of metal ions in the solution, as well as the activity and number of microorganisms) are stabilized.

Bioleaching is a slow process, but by adapting microbes to mineral raw materials and establishing continuous bioleaching in a series of bioreactors after determining the residence time it is possible to continuously obtain leached pulp every day.

Small scale continuous bioleach reactors

Mintek believes that for tank bioleaching, much more value can be derived from continuous testing, as opposed to batch testing [3]. This is simply because batch tests do not provide the reliable kinetic data that can be obtained from continuous test work. The retention time in the continuous bioleaching process is usually six days. Taking into account the start-up time and residence time for the process to achieve stable operation, it takes about three weeks to complete the test. One of the biggest problems with this is that the amount of sample required to conduct such testing becomes very large.

In order to avoid this, at MMI Bor (Institute for Mining and Metallurgy in Bor) a set of reactors for continuous bioleaching of small scales, with a total process volume of up to 6 L per reactor, was designed and established, which enable continuous tests to be carried out without consumption of large quantities of (usually scarce) concentrate samples. This is particularly useful in the early stages of a metallurgical testing work program and increases the value of the data that can be provided to the client at scope study or pre-feasibility study level. The bioreactor continuous system is shown in Figure 10.

Figure 10 Small scale continuous bioleach reactors of ore with a capacity of 1L pulp/day

Integrated bioleach Pilot plant

For larger-scale piloting, usually conducted to provide data for a feasibility study, an integrated pilot plant incorporating several downstream process unit operations was developed with the help of Mintek Company from Johannesburg (South Africa) at the Institute of Mining and Metallurgy Bor, as shown in Figure 11. This plant can provide detailed design information for the bioleaching process, as well as solid-liquid separation, iron removal and solution purification, SX -EW, and metal hydroxide precipitation.

In South Africa is initially processed 14 tons concentrate/day, while now being produced 55 t/day. In Kazakhstan on Suzdal BIOX plant are produce 192 t gold concentrate/day in sub-zero temperatures, Figure 12.

Figure 11 Integrated bioleach Pilot plant facility, capacity 20L pulp/day

a) b)

Figure 12 Bioleaching tanks of refractory gold in a) South Africa, b) Kazakhstan

Solvent extraction

Extraction of copper by solvent extraction, Figure 13, is based on the interphase transfer of copper from the aqueous phase to the organic phase. The transfer takes place at the interphase boundary, where the kinetics of the process depends on the

intensity of agitation of the two phases (flow of phases through the agitator-precipitator). The process then continues with phase separation, whereby agitators-settlers are used in hydrometallurgy. During the interphase transfer, cupric ions move to the organic phase and hydrogen ions to the aqueous phase, and copper forms an organometallic complex with the extractant according to the reaction:

$$2RH + Cu^{2+} = CuR_2 + 2H^+ \quad (1)$$

in which two moles of oxime (active component) in the organic phase and one mole of copper release two moles of hydrogen ions in the pH range of 0.5 - 3.5.

Extractants based on 5-nonyl-salicylic-aldoxes are capable of reacting with the stoichiometric amount of copper from alkaline solutions up to 35 g/L Cu^{2+} and a minimum acidity of pH 1.4. The extractant itself forms a very strong organometallic complex from which copper is difficult to extract using the output electrolyte with a composition of 30 g/L Cu and 190 g/L H_2SO_4. This problem is solved by adding a suitable modifier to the extractant. Specific modifiers for certain extracts are nonyl phenol, tridecanol and ester modifier.

Figure 13 Laboratory plant for leaching, solvent extraction and electrowinning
A1 - reactor for leaching, B1 - feed tank for bioleach solution, C1 - tank for organic solution, D1 - mixer - settlers, E1 – electrowinning cell, F1 - control panel

For copper extraction, organic reagent M.5640 is used. Reagent M.5640 from Acorga is an ideal extractant for extracting copper from solution due to the high selectivity of copper extraction compared to iron. The laboratory solvent extraction system for copper extraction is composed of 5 identical mixer-settlers there of 3 in extraction and 2 in stripping. The process of solvent extraction is followed by the process of electrolytic extraction.

Electrolytic extraction of copper

Electrolytic extraction of copper using insoluble anodes can be described as the deposition of copper from a copper-bearing electrolyte due to the passage of a direct current. The overall reaction is represented as follows:

$$CuSO_4 + H_2O \rightarrow Cu^o + H_2SO_4 + 0.5O_2 \quad (2)$$

according to which copper is deposited on the cathode and oxygen is released on the anode. PVC electrolytic cell equipped with Ti cathodes and Pb/Sn/Ca anodes.

ACKNOWLEDGEMENT

This work was financially supported by the Ministry of Education, Science and Technological Development of the Republic of Serbia, Grant No. 451-03-47/2023-01/200052.

CONCLUSION

By applying biotechnology in the metal extraction process, energy consumption is reduced, almost any risk of air pollution is eliminated, and the extracted metals of interest as well as potential pollutants are translated into an aqueous solution that can be easily further treated. Compared to pyrometallurgical processes, biotechnology is better for the environment and human health.

New technologies and scada software that are installed in reactor systems enable all information about the operation of the instruments and the monitoring of the technological parameters of the process to be sent wirelessly to the operator. At the same time, precise correction of process parameters can lead to a reduction in process management costs and an increase in recovery.

REFERENCES

1. Sobral, L.G.S., de Oliveira, D.M., de Souza, C.E.G. (2010) Biohydrometallurgical processes: A practical approach. Rio de Janeiro CETEM/MCT, 360.
2. Johnson, D.B. (2014) Biomining - biotechnologies for extracting and recovering metals from ores and waste materials. Current Opinion in Biotechnology, 30, 24-31.
3. Neale, J., Gericke, M., Ramcharan, K. (2011) The application of bioleaching to base metal sulfides in southern Africa: prospects and opportunities. The Southern African Institute of Mining and Metallurgy, 6th Southern African Base Metals Conference, 18-20 July, Phalaborwa, 367-388
4. Gericke, M., Neale, J., Van Staden, P. (2009) A Mintek perspective of the past 25 years in minerals bioleaching. Journal of the Southern African Institute of Mining and Metallurgy, 109, 567-585.
5. Gericke, M., Pinches, A. (1999) Bioleaching of copper sulphide concentrate using extreme thermophilic bacteria. Minerals Engineering, 12 (8), 893-904.

XV International Mineral Processing and Recycling Conference
17-19 May 2023, Belgrade, Serbia

LIFE CYCLE ASSESSMENT AND USE OF NATURAL RESOURCES

S. Cvetković[#], M. Popović, J. Perendija
Institute of Chemistry, Technology, and Metallurgy (ICTM),
University of Belgrade, Belgrade, Serbia

ABSTRACT - In the modern era, human society consumes more natural resources than ever before. Increasing demands for energy, food, water, metals, and other natural resources have resulted in resource depletion, environmental pollution, and nature destruction. It is necessary to establish different sustainable approaches to define these effects on the environment. Life Cycle Assessment as an analytical approach can provide a determination of environmental impacts as a consequence of the use of natural resources. The aim of this study is to highlight the significance of life cycle assessment and reveal how it is connected to sustainable issues in the use of the natural resource.

Keywords: Natural Resources, Life Cycle Assessment, Environment, Sustainability

INTRODUCTION

Natural resources ensure input materials for the production of goods. Also, natural resources are related to climate regulation, flood control, and natural habitats that are necessary to human society. There are different ways to classify natural resources [1] including:

- The origin. Categorizes resources as biotic and abiotic. Biotic resources are obtained from living things while abiotic resources originate from non-organic materials (land, water, air, gold, iron, copper, silver, etc.).
- Stage of development: This approach categorizes natural resources as potential, actual, reserve, and stock resources.
- Renewability. This approach categorizes natural resources as renewable (wind, hydro, and solar energy) and non-renewable (minerals and fossil fuels). A natural resource is defined as non-renewable when its rate of utilization exceeds the rate of recovery.

The use of materials obtained from natural resources has many environmental, economic, and social consequences [2]. The environmental pressures are related to the extraction, processing, transport, use, and disposal of natural materials (pollution, waste, loss of habitat), as well as, and their effects on environmental quality (air, water, soil, biodiversity) and human health. A sustainable strategy for use of natural resources which combines environmental, economic, and social aspects is presented in Figure 1.

[#] corresponding author: slobodan.cvetkovic@ihtm.bg.ac.rs

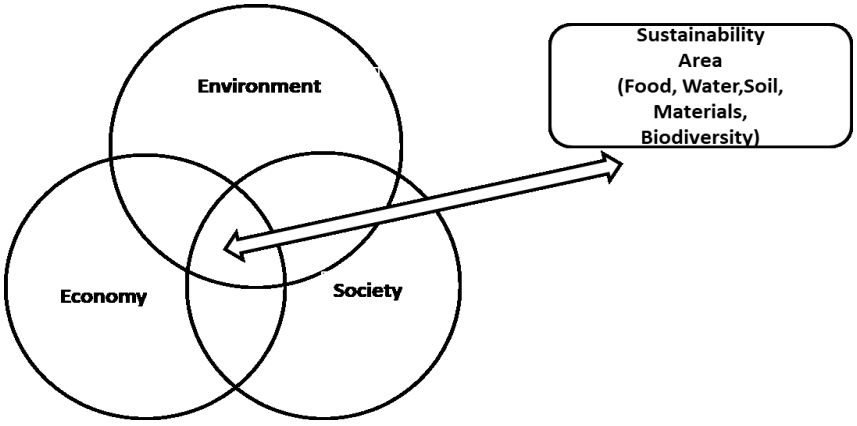

Figure 1 A sustainable strategy for use of natural resources

For sustainable use of natural resources [3], a life cycle assessment (LCA) approach is necessary. The stages of the LCA approach include: Natural resources extraction, then manufacture, use, and waste management to the Reuse, Disposal, or end-of-life cycle (Figure 2). After catastrophic chemical incidents during the 1960s in the USA, Coca-Cola company conducted the first well-known LCA study in 1969. Several analyses with a focus on energy were published during the energy crisis (1973-1979). The Society of Environmental Toxicology and Chemistry (SETAC) announced the "Code of Practice" in 1993[4], which presents a framework for the implementation of LCA. The final standardization of the methodological framework for LCA was defined in ISO 14040: 2006[5] and ISO 14044:2006 [6].

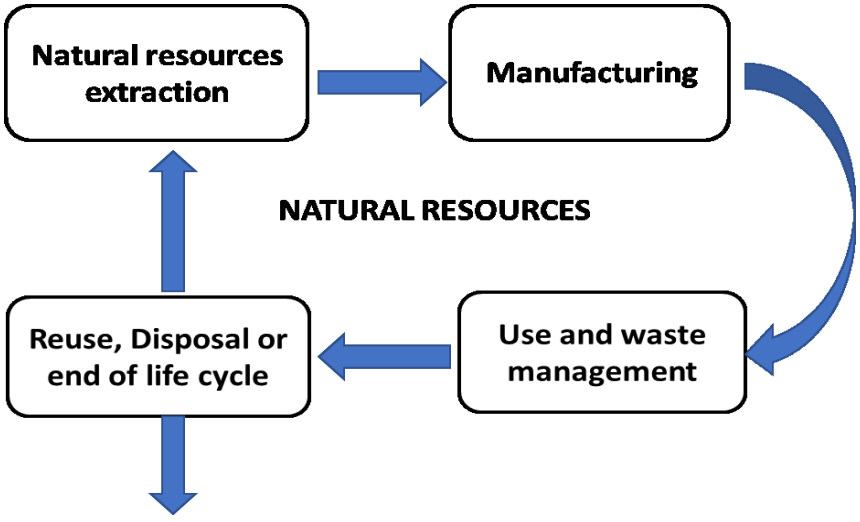

Figure 2 LCA stages for the use of natural resources

Life Cycle Assessment as an analytical method can determine environmental impacts joined with the use of natural resources. The aim of this research is to highlight the significance of life cycle assessment and reveal how it relates to sustainability issues in the use of natural resources.

LCA METHODOLOGY FOR THE USE OF NATURAL RESOURCES

LCA is a valuable tool that improves environmental management. According to the ISO 14040: 2006 and ISO 14044: 2006, phases of LCA are (Figure 3):

- Goal definition and scope
- Inventory analysis
- Impact assessment
- Data interpretation

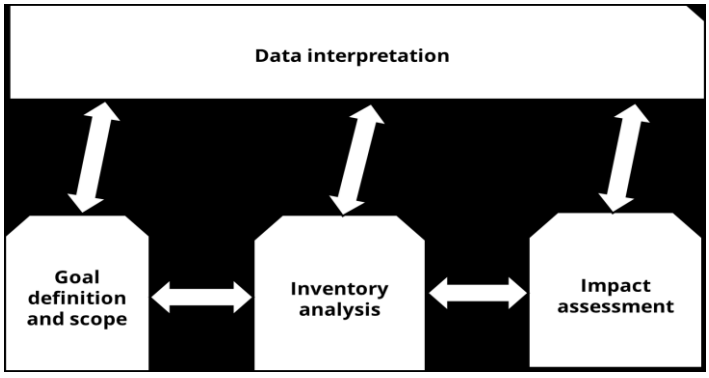

Figure 3 LCA methodology framework related to ISO 14044

These steps are connected and reflect on how the results are interpreted, which includes describing how they affect the environment and offering suggestions and actions for final users.

Goal definition and scope

In accordance with ISO 14040 standards, the purpose of the LCA study must identify the application and justification for conducting the study. A system's limitations and functionality can be determined with the help of the scope specification. The boundaries, function unit, and system (Figure 4.) under research are described in this step.

All material and energy flows, as well as any impacts those flows may have, are related to the functional unit. As a result, any comparisons between the sensitivity analysis and other items under investigation within the same functional unit use the functional unit as a foundation. In order to compare the findings of several investigations, all data must be related to a single functional unit. The ISO 14040 standards demand that functional units be clearly defined, measured, and pertinent to input.

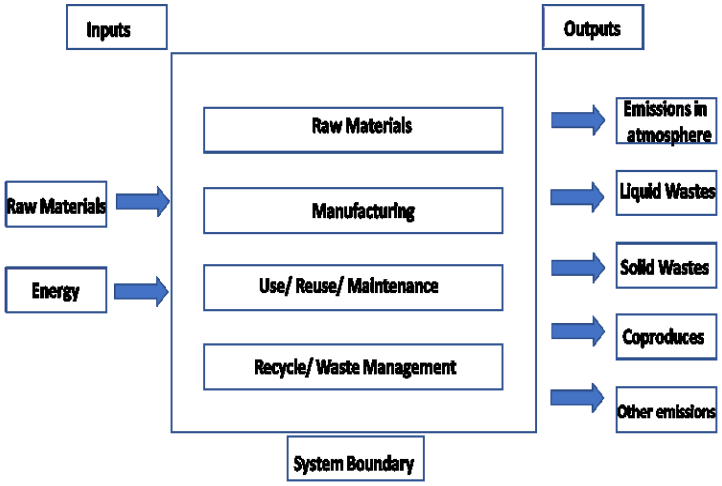

Figure 4. System boundary, material, and energy flows and emissions into the environment in LCA for utilization of natural resources

Inventory analysis

In this phase, the life cycle established and all energy and material requirements; emissions to air, water, and soil and other releases are quantified. Inventory analysis contents next steps:

- Development of Flow Diagrams (Materials and Energy)
- Data collection
- Multi-output processes
- Reporting

This stage is the most demanding in LCA, it requires a lot of data.

Impact assessment

In the impact assessment phase, an assessment of all potential impacts has been conducted on the environment and human health due to the use of energy, water, natural resources, and emissions that are identified in the inventory phase. This phase has further steps:

- Selecting the relevant impact categories
- Classification
- Characterization:
- Normalization
- Grouping
- The relative weighting of impact categories; and evaluation and reporting

The most examined environmental impact categories in LCA studies are given in Table 1.

Table 1 Commonly used environmental impact categories, adapted from [7]

Categories	LCI Data (classification)	Determination of Characterization Factor
Global Warming	Carbon Dioxide (CO2) Nitrogen Dioxide (NO2) Methane (CH4) Chlorofluorocarbons (CFCs) Hydrochlorofluorocarbons (HCFCs) Methyl Bromide (CH3Br)	Converts LCI data to carbon dioxide (CO2) equivalents
Ozone Depleting	Chlorofluorocarbons (CFCs) Hydrochlorofluorocarbons (HCFCs) Halons Methyl Bromide (CH3Br)	Converts LCI data to trichlorofluoromethane (CFC-11) equivalents
Acidification	Sulfur Oxides (SOx) Nitrogen Oxides (NOx) Hydrochloric Acid (HCL) Hydroflouric Acid (HF) Ammonia (NH4)	Converts LCI data to hydrogen (H+) ion equivalents.
Eutrophication	Phosphate (PO4) Nitrogen Oxide (NO) Nitrogen Dioxide (NO2) Nitrates Ammonia (NH4)	Converts LCI data to phosphate (PO4) equivalents.
Photochemical Oxident Creation	Non-methane hydrocarbon (NMHC)	Converts LCI data to ethane (C2H6) equivalents.
Other (Terrestrial Toxicity, Aquatic Toxicity, Human Health, Resource Depletion, Land and Water Use)	/	/

Interpretation

The interpretation phase uses sensitivity and uncertainty analysis to interpret the findings of the previous phases, considering the study's objectives. This phase covers:

- Identification of significant issues
- Evaluation of completeness, sensitivity, and consistency of the data
- Drawing conclusions and make recommendations

The interpretation may lead to a finding that serves as a suggestion to decision-makers who typically weigh environmental impacts with economic and social factors in a sustainable framework.

Nowadays, different software systems are used to implement a LCA study such as: SimaPro (PRé Consultant, Netherlands), Umberto (Institute for Environmental Informatics, Hamburg, and Institute for Energy and Environmental Research,

Heidelberg), GaBi (Department of Life Cycle Engineering, University of Stuttgart, with the company "PE International") and GEMIS (Institute for Applied Ecology, Öko-Institut, Berlin).

CONCLUSION

Natural resources extraction and consumption can harm the ecosystem. It is important to utilize natural resources in a sustainable manner in order to meet future societal demands. The life cycle assessment is a foundation for evaluating the inputs of natural resources and related emissions into the environment. This study is emphasized the importance of life cycle assessment and show how it links to concerns about the sustainable use of natural resources.

ACKNOWLEDGMENT:

This work was financially supported by the Ministry of Science, Technological Development, and Innovation the Republic of Serbia (Grant No. 451-03-68/2023-14/200026).

REFERENCES

1. Sonderegger, T., Dewulf, J., Fantke, P., de Souza, D. M., Pfister, S., Stoessel, F., Hellweg, S. (2017). Towards harmonizing natural resources as an area of protection in life cycle impact assessment. The International Journal of Life Cycle Assessment, *22*, 1912-1927.
2. Ragnarsdóttir, K. V., Sverdrup, H. U., Koca, D. (2012). Assessing long term sustainability of global supply of natural resources and materials. In Sustainable Development-Energy, Engineering and Technologies-Manufacturing and Environment. IntechOpen.
3. Dewulf, J., Benini, L., Mancini, L., Sala, S., Blengini, G.A., Ardente, F., Recchioni, M., Maes, J., Pant, R. and Pennington, D. (2015). Rethinking the area of protection “natural resources” in life cycle assessment. Environmental science & technology, 49 (9), 5310-5317.
4. Sonnemann, G., Castells, F., Schumacher, M. (2003). Integrated Life-Cycle and Risk Assessment for Industrial Processes. 1 ed. Lewis Publishers, London.
5. ISO 14044, 2006. Environmental management - Life cycle assessment - Requirements and guidelines. International Organization for Standardization.
6. ISO 14040, 2006. Environmental management - Life cycle assessment - Principles and framework. International Organization for Standardization.
7. Scientific Applications International Corporation (SAIC), Curran, M. A., National Risk Management Research Laboratory (US), & Office of Research and Development, Environmental Protection Agency, United States. (2006). Life-cycle assessment: principles and practice.

WORKSHOP PAPERS

Batterflai Workshop:
Sustainable and efficient recovery of battery minerals using lignin nanoparticles as flotation collectors

XV International Mineral Processing and Recycling Conference
17-19 May 2023, Belgrade, Serbia

COMBINED USE OF ORGANOSOLV LIGNIN AND XANTHATES ON SPHALERITE FLOTATION FROM MIXED SULPHIDES

P. M. Angelopoulos[#], G. Anastassakis, N. Kountouris, N. Koukoulis, M. Taxiarchou
National Technical University of Athens (NTUA), School of Mining and Metallurgical Engineering, Greece

ABSTRACT – The use of xanthates at the flotation of sphalerite raises questions about the sustainability of the process, due to the negative environmental impact. In addition, the development of local bio-collectors production is necessary to replace currently utilized flotation collectors and depressants, which are manufactured mostly in China. In this study we investigate the performance of lignin nanoparticles as sphalerite collectors in combination with xanthates. Among the parameters tested are replacement ratio, dilution temperature and lignin type. Interestingly, the partial replacement of xanthate collectors with bio collector lignin is viable. We tested a variety of attributes such as concentration, lignin types and sizes with a 3-stage flotation. After evaluation of the products is showed that a 50% replacement of collector with lignin does not affect the sphalerite grades and recovery, while decreasing the recovery of the gangue mineral (Au), thus leading to improved selectivity.

Keywords: Sphalerite, Flotation, Lignin, Collector, Selectivity.

INTRODUCTION

Froth flotation is the most widely applied technique for the recovery of sphalerite from mixed sulfides. Sphalerite's floatability is greatly enhanced by the exchange of Zn ions with metal ions of the pulp, acting as active sites to react with collector. Long-chain xanthate works effectively as a collector in sphalerite flotation [1]. The use of xanthates however possesses certain important drawbacks related to the followings; (i) serious environmental impact, (ii) the centralized production that is mainly in China, and (iii) the quality variation that affect the flotation performance.

Lignin nanoparticles and microparticles are sustainable and environmental friendly materials, possessing satisfactory performance in Cu flotation [2]. In this paper, we investigate the potentiality of the use of lignin as collector in sphalerite flotation. More specifically, we tested the use of lignin micro- and nanoparticles from different origins, in different proportions for the selective recovery of sphalerite, and evaluated the results in terms of zinc and gangue minerals grade and recovery.

MATERIAL AND METHODS

Lignin preparation

Birch and spruce wood chips were pretreated with organosolv to remove the lignin,

[#] corresponding author: pangelopoulos@metal.ntua.gr

which was then utilized to create lignin nanoparticles [3].The spruce woodchips were pretreated in a 60% v/v ethanol in water solution at 183 °C for 1 hour whereas the birch woodchips were pretreated at 183 °C in a 50% v/v ethanol in water solution. The ethanol/water solution's 5% w/v lignin was then homogenized at 750 bars using a pressure homogenizer. Deionized water was used to further dilute the homogenized liquid, which caused nanoparticles to develop. The material was freeze dried in order to produce nanoparticles as a dry powder.

Chemical and mineralogical analyses

In this study, a mixed sulphide ore containing Pyrite, Arsenopyrite, Galena, Sphalerite from Olympiada, Chalkidiki was obtained from the production line of HellasGold facility. The sample was obtained from the tailing of galena recovery circuit thus possessing minimum lead content. The ore d_{80} was 130 μm. **Table 1** presents the chemical analysis expressed in oxides. ZnO content is about 4.33%. In addition, as it is known that gold particles are distributed inside pyrite and arsenopyrite ores, and it is important to avoid its collection[3]. Moreover, the Loss On Ignition (LOI) of the sample was found to be relatively high at 12.86%, attributed to the decomposition of various sulphide minerals.

Table 1 Total Oxide X-Ray Analysis with X-Ray Fluorescence Spectrometer for ZnS feed

Element	Content (%)
PbO	0.69
ZnO	4.33
Fe_2O_3	17.81
As_2O_3	5.25
S	12.12
Sb	0.03
CuO	0.04
C	3.42
MgO	1.73
Al_2O_3	4.67
SiO_2	18.80
K_2O	0.97
CaO	13.83
MnO	0.98
Loss On Ignition	12.86
Other	2.46

A modal analysis was done by chemically balancing the elements to their corresponding minerals and presented in **Table 2**.

Table 2 Modal analysis of ZnS feed

Ore	Content (%)
Galena (PbS)	0.74
Sphalerite (ZnS)	5.18
Pyrite (FeS)	14.09
Arsenopyrite (FeAsS)	6.04

Experimental procedure

Seven different flotation experiments were carried out with a constant solid ratio of ~45% and stirring speed of 1500 rpm. The flotation experiments were divided into 2 main categories; on the first, the gradual replacement of xanthate by lignin was implemented, and on the second, 4 different types of lignin were utilized. **Table *3*** shows the quantity of reagents, as well as the conditioning and frothing times and the pH.

Table 3 Flotation reagents dosages, pH and duration

Stages	pH	Conditioning (min)	Frothing (min)	CuSO4 (g/t)	SIPX/Lignin (g/t)
Conditioning	10	5		270	48
Rougher	9.5-10		2		
Scavenger 1	9.5-10	1	2		12
Scavenger 2	9.5-10		1		

RESULTS AND DISCUSSION

Figure *1* presents Zn and Au grade and recovery in the concentrate, in terms of the xanthate replacement ratio. The 50% replacement of SIPX by lignin allowed the production of concentrate with similar properties of the one obtained using solely SIPX , in terms of Zn grade and recovery. Also, the addition of lignin in collector mixture increases selectivity, through decreasing of the Au grade and recovery. The use of chemical collector SIPX recovered 85% of the sphalerite inside the ore but also 45% of the gangue mineral (Au). By adding 50% SIPX and 50% lignin as collectors, an increase in selectivity is evident by reducing the recovery of gold by 33% (from 45.9% to 30.5%), in comparison with the SIPX collector, while maintaining the same Zn recovery. On the contrary, for 100% replacement of chemical collector, Zn recovery decreases significantly making it apparent that a full replacement of chemical collector is not possible. By using only lignin as a collector, a Zn recovery of 54% is possible.

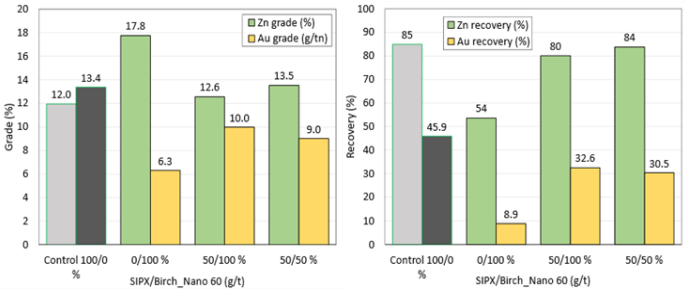

Figure 1 Chemical collector replacement with lignin

The selectivity index was developed by Gaudin as the practical approach to measure two-way separation [4].

$$SI = \sqrt{\frac{Rv \times Rg}{(100-Rv)\times(100-Rg)}} \quad (1)$$

where R_v % is the recovery of Zn in the flotation concentrate, and R_g % is the recovery of gangue (Au) in the tailing fraction. By definition, the selectivity index (SI) can be used to show the degree to which valuable minerals are separated from the gangue ones. The SI takes into account two parameters: the recovery of precious minerals in the concentrate and the recovery of gangue minerals in the tailing. Another, criterion for evaluating the results is the separation efficiency [5], which is use for evaluating the separation of the mineral, focusing on the recovery of valuable and gangue minerals in the concentrate. SE is given by the following equation:

$$SE = R_a - R_b \quad (2)$$

where R_a and R_b are the recoveries of valuable and gangue minerals in the concentrate respectively. **Table 4** presents SE and SI, together with Zn and Au recovery, in terms of the SIPX replacement ratio by lignin. As it shown, the SI of Control sample is 2.6 and the separation efficiency is 38.9. By 100% replacement with lignin, the SI increases to 3.5 and also the SE increases to 44.8, but with very low recovery grades as mentioned earlier. Though, the maximum SE value was obtained applying a 50%/50% SIPX/lignin collector mixture; the SE increased from 38.9 (control sample) to 53.3, a solid 27% increase, and at the same time the selectivity from 2.6 to 3.4.

Table 4 Selectivity Index and separation efficiency parameters

Collector 60 (g/t)	Zn recovery in concentrate, R_{vZn} (%)	Au recovery in tailing, R_{gAu} (%)	Au recovery in concentrate, R_{bAu} (%)	Separation Efficiency, SE	Selectivity Index, SI
SIPX 100 %	84.8	54.1	45.9	38.9	2.6
SIPX/BN 50/50 %	83.8	69.5	30.5	53.3	3.4
SIPX/BN 50/100 %	80	67.4	32.6	47.4	2.9
BN 100%	53.7	91.1	8.9	44.8	3.5

At last, a comparison between 4 different types of lignin was investigated regarding their particle sizes (µm and nm) and qualities (Birch and Spruce). The results are presented in **Figure *2***.

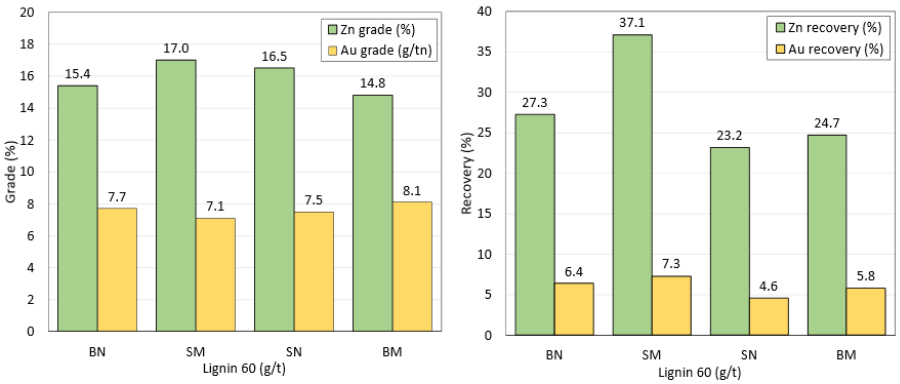

Figure 2 Lignin type replacement graph

Overall, no considerable difference in flotation performance is observed among the different types. The grades of sphalerite derived range between 14.8 - 17% and the recoveries between 27.3-37.1%, which are very low. A difference at the final recoveries of Zn with Spruce Micro as a collector is identified, however, it is not considered remarkable, in combination with the overall low recovery achieved.

CONCLUSIONS

Lignin micro- and nanoparticles have been as collectors in copper bearing minerals flotation with satisfactory results. Lignin is ecofriendly and produced from a practically abundant raw material. In this study we investigate the potentiality of the partial replacement of xanthates by lignin in the flotation of sphalerite from mixed sulfides. The effect of different SIPX/lignin collectors' proportions was investigated in terms of the Zn and Au grade and recovery in the concentrate.

At the control sample a 60 g/t SIPX was used as a collector, achieving Zn recovery and grade of 85% and 12%, respectively. Since Au is solely found in arsenopyrite and pyrite minerals, and knowing that both minerals should be depressed and recovered in a later flotation circuit, Au was also measured targeting minimum recovery at the existing concentrate and considered as a gangue. In the concentrate produced using SIPX, the Au recovery and grade was 45.9 % and 13.4%, respectively. With the use of 50/50% lignin/ SIPX collectors' mixture, Zn grade increased to 13.5%, without changing recovery. A sharp decrease of Au recovery in concentrate was observed from 45.9% to 30.5%, possessing beneficial impact to the process eliminating the gold bearing minerals losses. When using the 100% SIPX solution the SI was 2.6, and increased to 3.4 in case of using the 50/50% lignin/SIPX collectors' mixture. The same trend is observed for the concentrate separation efficiency, which for sole SIPX usage it was 38.9 and with the lignin addition increased to 53.3, a 27% performance increase. No significant differences in flotation performance were observed among different lignin grades (micro and nano sized, originated from spruce and birch). The obtained results show that a partial replacement of toxic xanthate by eco-friendly lignin as sphalerite collector is viable, possessing better selectivity, and improving the environmental footprint of the process.

ACKNOWLEDGEMENT

This research has received funding from the EIT RawMaterials research and innovation programme under Proposal Number n°19089, project BATTERFLAI. Supply of BATTERy minerals using lignin nanoparticles as FLotAtIon collectors.

REFERENCES

1. Han, G., Xu, L., Feng, Q. (2019) Activation mechanism of lead ions in the flotation of sphalerite depressed with zinc sulfate. Miner. Eng., 146, 106132.
2. Hrůzová, K.,. Matsakas, L, Sand, A., Rova, U., Christakopoulos, P. (2020) Organosolv lignin hydrophobic micro- and nanoparticles as a low-carbon footprint biodegradable flotation collector in mineral flotation. Bioresour. Technol., 306, 123235.
3. Adam, K., Prevosteau, J., Kontopoulos, A., Stefanakis, M., Errington, M. (1990) Applications of pyrite mineralogy on the treatment of Olympias Pyrite Concentrate.

In: Proceedings of the Gold ’90 Symposium, 341–351.
4. Gaudin, A.M. (1957) Flotation. 2nd ed. New York: McGraw-Hill.
5. Wills, B.A. (2013) Mineral processing technology: an introduction to the practical aspects of ore treatment and mineral recovery. Elsevier.

XV International Mineral Processing and Recycling Conference
17-19 May 2023, Belgrade, Serbia

PARTIAL REPLACEMENT OF XANTHATE BY ORGANOSOLV LIGNIN ON PYRITE/ARSENOPYRITE FLOTATION

P. M. Angelopoulos[#], N. Kountouris, G. Anastassakis, M. Taxiarchou
National Technical University of Athens (NTUA), School of Mining and Metallurgical Engineering, Athens, Greece

ABSTRACT – Since xanthates are toxic chemicals that are eventually disposed to the environment, the utilization of chemical collectors during the flotation of pyrite and arsenopyrite raises concerns about the sustainability of the process. The partial substitution of xanthate collectors with bio collector lignin turns out to be a viable option. In this study, we investigate the potentiality of lignin micro and nanoparticles to be used as collectors in the flotation process, focusing on the application of different collectors' mixtures (SIPX/lignin). It was found out that a 50% replacement of SIPX is viable, leading to improvement of pyrite/arsenopyrite grade and recovery in concentrate.

Keywords: Pyrite, Flotation, Lignin, Collector, Selectivity.

INTRODUCTION

The recovery of pyrite and arsenopyrite from mixed sulphide ore originated from Halkidiki, Greece is of interest due to its gold content. The use of traditional collectors such as xanthates to generate a bulk concentrate made up of pyrite and arsenopyrite have been achieved with relative ease and often the practice [1]. Both minerals are readily floatable with several type of collectors like xanthates, dithiophosphates and fatty acids [2]. Despite their efficiency, xanthates possess negative environmental impact. Also, their production is centralized in China, while the frequent quality deviations affect the efficiency of separation [3]. There is an increasing trend in the development and use of eco-friendly chemicals in the flotation process [4,5].

Lignin is an abundant and low-cost material obtained from forest residues and side streams of the pulp industry, and it has been shown that, lignin micro- and nanoparticles can be used as collectors in copper recovery by froth flotation process [6]. In the current study, we investigate the potentiality of the use of lignin nano and microparticles as collectors in pyrite and arsenopyrite flotation, aiming partial replacement of xanthates. In this frame, various xanthate/lignin proportion mixtures were prepared and used in the flotation of mixed sulphide ore aiming the recovery of pyrite and arsenopyrite.

MATERIAL AND METHODS

Lignin preparation

The lignin of wood chips from birch and spruce was first extracted with organosolv

[#] corresponding author: pangelopoulos@meya.ntua.gr

and then used to make lignin nanoparticles. The birch woodchips were prepared at 183 °C for 1 hour in a 50% v/v ethanol in water solution whereas the spruce woodchips were pretreated at the same temperature in a 60% v/v ethanol in water solution before allowing it to dissolve in a mixture of 75% ethanol and water, drying the separated lignin [7]. Using a pressure homogenizer, 5% w/v of the lignin in the ethanol/water solution was then homogenized at 750 bars. The homogenized liquid was further diluted with deionized water, which resulted in the formation of nanoparticles. To create dry powdered nanoparticles, the material was freeze dried.

Chemical and mineralogical analyses

The sample used in the experiments was obtained from the production line of HellasGold facility at Olympiada, Chalkidiki. It is the residue (tailing) after the implementation of two consecutive flotation stages targeting the selection of galena and sphalerite. Indeed, as shown in **Table 1**, the sample presents very low Pb and Zn content. As for the granulometry of the sample, it is size of d_{80}=193.

Table 1 Total Oxide X-Ray Analysis with X-Ray Fluorescence Spectrometer of Au feed

Oxide	Content (%)
PbO	0.50
ZnO	0.66
Fe_2O_3	16.67
As_2O_3	7.60
S	11.31
Sb	0.02
CuO	0.03
C	3.54
MgO	2.11
Al_2O_3	4.57
SiO_2	19.94
K2O	1.06
CaO	14.76
MnO	1.07
Loss On Ignition	13.80
Other	2.36
Total	100

According to modal analysis presented in **Table 2**, approx. 22 wt. % of the sample consists of pyrite and arsenopyrite.

Table 2 Modal mineralogical analysis

Mineral	Content (%)
Galena (PbS)	0.53
Sphalerite (ZnS)	0.79
Pyrite (FeS)	13.64
Arsenopyrite (FeAsS)	8.74

Flotation Experiments

$CuSO_4$ was utilized as activatior for the flotation of pyrite/arsenopyrite at a concentration of around 170 g/t. Additionally, sodium isopropyl xanthate (SIPX) and lignin were added as collectors in two phases; 80% of the collector was added at the conditioning stage and the remaining 20% right after the end of the rougher flotation stage. Dowfroth was used as a frother, while H_2SO_4 served as a pH regulator. **Table 3** demonstrates the pH and the duration of each processing stage. The trials were conducted with a stirring speed of 1500 rpm.

Table 3 Pyrite/arsenopyrite circuit pH and time schedule

Stages	pH	Conditioning min	Froth min
Conditioning	6.8-7.5	5	
Rougher	6.8-7.5		5
Scavenger 1	7.2-8.2	1	7
Scavenger 2	7.2-8.2		6

RESULTS AND DISCUSSION

Figure *1* depicts Au and Pb grade and recovery in the concentrate obtained by applying different collector composition. On the control trial, where solely SIPX was used as collector, Au recovery reached 90.7% while the recovery of gangue (Pb) was at 61.4%. In case were solely lignin was used as collector, Au recovery dropped drastically to 11.8% and Pb recovery was 40.5%. The results are much improved when SIPX/lignin mixture was sued as collector; when the 50/50 wt.% mixture of collectors was applied, Au recovery exceeded 96%, which is also the case for Pb which recovery reached 68.5%.

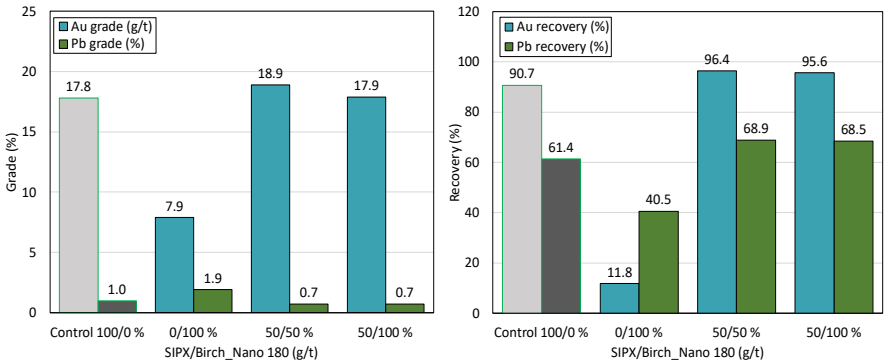

Figure 1 Xanthate partial replacement with lignin (180 g/t) graph

The selectivity index (SI) was developed by Gaudin as a valuable metric for the evaluation two-way separation and collectors' selectivity [8]. It is defined as:

$$SI = \sqrt{\frac{Rv \times Rg}{(100-Rv)\times(100-Rg)}} \quad (1)$$

where R_v % is the recovery of Au in the flotation concentrate, and R_g % is the recovery of gangue (Pb) in the tailing fraction. *SI* takes into account two parameters: the recovery of precious minerals in the concentrate and the recovery of gangue minerals in the tailing. Another, criterion for evaluating the results is also the separation efficiency (SE), which is use for assessing the separation process [9].

$$SE = R_a - R_b \quad (2)$$

where R_a and R_b are the recoveries of valuable and gangue minerals in the concentrate respectively.

Table 4 presents Au and Pb recovery in concentrates and SE and SI values. SI for the control sample is 3.9 and drops to 3.3 when lignin is added by 50% followed with minor difference in Pb recovery. Also, the SE falls from 29.6 to 27.1. For sole lignin, the calculated SE and SI factors inform about the poor separation thus informing that only partial replacement of SIPX is viable.

Table 4 Selectivity Index and Separation Efficiency parameters [Collector dos: 180 g/t]

Collector composition	Au recovery in concentrate, R_{vAu} (%)	Pb recovery in concentrate, R_{bPb} (%)	Separation Efficiency (*SE*)	Selectivity Index (*SI*)
SIPX 100 %	91	61.4	29.6	3.9
SIPX/BN 50/50 %	96	68.9	27.1	3.3
SIPX/BN 50/100 %	96	68.5	27.5	3.3
Birch Nano 100%	12	40.5	28.5	0.4

At the second series of experiments, the collector dosage was increased from 180 g/t to 200 g/t. **Figure *2*** presents Au and Pb grade and recovery for different collector composition. The results confirmed the findings of the previous series of separation experiments; 50% replacement of SIPX is viable, since Au grade and recovery are equal or higher compared to the control sample where solely xanthate is used.

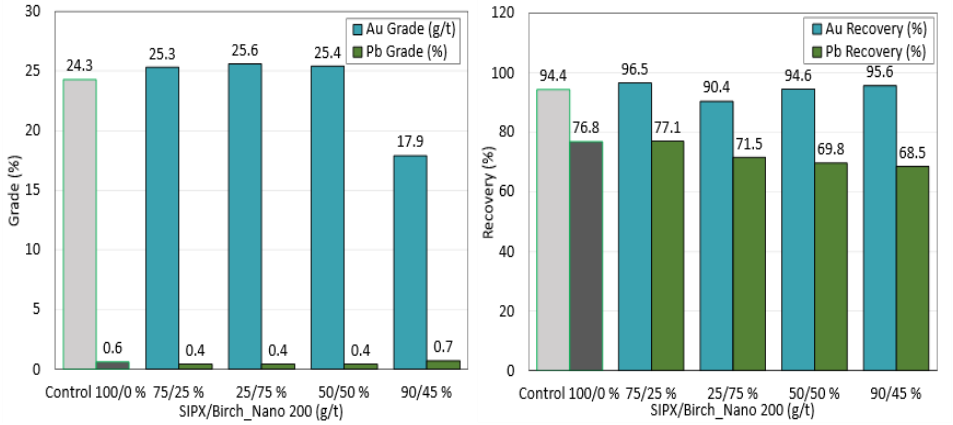

Figure 2 Xanthate partial replacement with lignin (200 g/t) graph

Comparing the data presented in **Figure *2*** and **Figure *1***, for 50/50 % collector composition, the results are in agreement; Au recoveries from the concentrate were 96.4 % to 94.6 %, and Pb recovery were 68.9% to 69.8% for collector dosage of 180 and 200 g/t, respectively.

Table *5* presents SE and SI values for the separation experiemnts presented in **Figure *2***.

Table 5 SI and SE parameters for Pyrite/Arsenopyrite separation using different collector compositions [Collector dosage: 200 g/t]

Collector composition	Au recovery in concentrate, R_{vAu} (%)	Pb recovery in tailing, R_{gPb} (%)	Pb recovery in concentrate, R_{bPb} (%)	Separation Efficiency (*SE*)	Selectivity Index (*SI*)
SIPX 100 %	94.4	23.2	76.8	17.6	2.3
SIPX/BN 75/25 %	96.5	22.9	77.1	19.4	2.9
SIPX/BN 50/50 %	94.6	30.2	69.8	24.8	2.8
SIPX/BN 25/75 %	90.4	28.5	71.5	18.9	1.9
SIPX/BN 90/45 %	95.6	31.5	68.5	27.1	3.2

Overall, the best performance is achieved for collector composition SIPX/BN 90/45 % (270 g/t collector) where SE and SI values were 27.1 and 3.2, respectively. However, those results are comparable to the results obtained by using SIPX/BN 50/50% collector composition.

CONCLUSIONS

This study was focused on the use of lignin as collector in the recovery of both pyrite and arsenopyrite from mixed sulfides through froth flotation process. The experiments were conducted to materials obtained from Olympias processing plant, Halkidiki, Greece and were previously treated for recovery of galena and sphalerite. In comparison to the case where solely SIPX was used, a 50% replacement of SIPX by lignin nanoparticles led to and increase of both Au grade and recovery from 17.8 to 18.9 g/t and from 90.7% to 96.4%, respectively. For the same replacement ratio, both SE and SI values were found as 27.1 and 3.3, respectively. From those preliminary results it can be shown that lignin can partially replace SIPX without affection of the separation efficiency. Moreover, it is expected that, the use of lignin can increase the Au recovery, provided that the separation will take place under the optimum application conditions.

ACKNOWLEDGEMENT

This research has received funding from the EIT RawMaterials research and innovation programme under Proposal Number n°19089, project BATTERFLAI. Supply of BATTERy minerals using lignin nanoparticles as FLotAtIon collectors.

REFERENCES

1. Forson, P., Zanin, M., Skinner, W., Asamoah, R. (2021) Differential flotation of pyrite and arsenopyrite: Effect of hydrogen peroxide and collector type. Miner. Eng., 163,

106808.
2. Wang, X.H., Eric Forssberg, K.S. (1991) Mechanisms of pyrite flotation with xanthates. Int. J. Miner. Process., 33 (1–4), 275–290.
3. Williams, C., Peng, Y., Dunne, R. (2013) Eucalyptus oils as green collectors in gold flotation. Miner. Eng., 42, 62–67.
4. Saim, A.K., Darteh, F.K. (2022) Eco-Friendly and Biodegradable Depressants in Chalcopyrite Flotation: A Review. Miner. Process. Extr. Metall. Rev., 00 (00), 1–19.
5. Slabov, V., Jain, G., Larsen, E., Kota, H.R., Chernyshova, I. (2023) Eco-Friendly Collectors for Flotation of Fine Hematite and Malachite Particles. Mining, Metall. Explor., 475–492.
6. Hrůzová, K., Matsakas, L., Sand, A., Rova, U., Christakopoulos, P. (2020) Organosolv lignin hydrophobic micro- and nanoparticles as a low-carbon footprint biodegradable flotation collector in mineral flotation. Bioresour. Technol., 306, 123235.
7. Kalogiannis, K.G., Matsakas, L., Aspden, J., Lappas, A.A., Rova, U., Christakopoulos, P. (2018) Acid assisted organosolv delignification of beechwood and pulp conversion towards high concentrated cellulosic ethanol via high gravity enzymatic hydrolysis and fermentation. Molecules, 23 (7), 1–18.
8. Gaudin, A. M. (1957) Flotation. 2nd ed. McGraw-Hill.
9. Wills, B.A. (2013) Mineral processing technology: an introduction to the practical aspects of ore treatment and mineral recovery. Elsevier.

XV International Mineral Processing and Recycling Conference
17-19 May 2023, Belgrade, Serbia

ORGANOSOLV LIGNIN PARTICLES: A NOVEL GREEN REAGENT THAT INCREASES THE FLOTATION EFFICIENCY OF SULFIDE ORES

K. Hrůzová[1#], J.A. Bazar[1], L. Matsakas[1], A. Sand[2], U. Rova[1], P. Christakopoulos[1]
[1] University of Technology, Biochemical Process Engineering, Division of Chemical Engineering, Department of Civil, Environmental and Natural Resources Engineering, SE-971 87 Luleå, Sweden
[2] Boliden Mineral AB, SE-936 81 Boliden, Sweden

ABSTRACT – Sustainable future requires a lot of metals that must be mined and processed. Common way of mineral recovery is a mineral froth flotation. Flotation reagents are necessary for selective recovery of target minerals. The main purpose of the study was to demonstrate a novel sustainable flotation process for selective extraction of chalcopyrite from sulphide ores, based on partial replacement of fossil-based xanthate flotation collectors with bio-based, biodegradable, and non-toxic organosolv lignin particles. The addition of organosolv lignin particles provided increased recovery of copper with high selectivity. The amounts of required reagents were also significantly lowered in the newly proposed process.

Keywords: Organosolv, Lignin, Reagent, Chalcopyrite, Flotation.

INTRODUCTION

Mineral froth flotation is a process facilitating separation of valuable target minerals from gangue minerals of ore. The separation of the mineral is based on their hydrophobicity and hydrophilicity, where the hydrophobic minerals are carried by bubbles into the froth and recovered from the process. Flotation reagents are compounds that modify the mineral surface to increase or decrease the hydrophobicity. The most common collector use for recovery of sulphide minerals is xanthate. However, xanthates are fossil-based, and their decomposition products are toxic. The production of xanthates is also limited in Europe and the reagent must be imported. There is an increasing interest in replacement of the xanthate reagent for more environmentally friendly alternative. All current alternatives are either not performing as well as xanthates or are significantly more expensive.

The main purpose of the study was to demonstrate a novel sustainable flotation process for selective extraction of target minerals from sulphide ores, based on partial replacement of xanthates with bio-based, biodegradable, and non-toxic organosolv lignin particles (OLPs). The rougher-cleaner flotation was performed to study the effect of OLP on the grade and recovery of target minerals.

corresponding author: katerina.hruzova@ltu.se

EXPERIMENTAL

OLPs were prepared by dissolving organosolv lignin (isolated from birch and spruce woodchips) in 75% v/v ethanol/water solution and homogenized at 750 bar by using a APV-2000 homogenizer (SPX FLOW, Charlotte, NC, USA). Subsequently, two methods of particle formation were used, and microparticles and nanoparticles were prepared. Finally, the particles were isolated in a powder by freeze-drying [1].

The copper sample had an average copper content of 1.2% w/w in the form of chalcopyrite The ore sample was grinded to below 3 mm and milled prior to the flotation trials. For the milling experiment, 600 g ore sample and 300 g process water (Boliden, Stockholm, Sweden) was added to the stainless-steel rod mill with 12.9 kg of rods of various diameter. After 15 min of milling, the slurry was transferred to a 2 L flotation cell (Outotec, Helsinki, Finland) with additional process water. The agitation was set at 1300 rpm. The rotor diameter was 45 mm, and the air flowrate was set at 2 L/min.

The rougher-cleaner flotation was performed as a 3-step rougher stage followed by 3-step cleaner stage. An optimal dosage of potassium amyl xanthate (PAX) and OLP was evaluated during the dosage studies. As a result, a general dosage of 3 g/ton (step 3), 2 g/ton (step 4), and 1 g/ton (step 5) were selected as a PAX baseline. Table 1 presents an overview of the chemicals added during the process. The PAX control was performed with pH adjustment by lime up to 10.5 in rougher and up to 11.1 in the cleaner stage, while the trials with PAX+OLP was performed with no pH adjustment.

The handheld XRF device (X-MET8000, Hitachi, Tokyo, Japan) was used for analyzing the samples obtained during the trials. The homogenized sample was placed in a plastic capsule, covered by a thin film, and measured in duplicates. The provided mining FP calibration was used.

Table 1 Dosage of chemicals for the rougher-cleaner flotation based on the flowsheet

Step	**Milling**	**Cond**	**R 1**	**R 2**	**R 3**	**C 1**	**C 2**	**C 3**
pH	7.5	10.5*				11.1*		
Conditioning time (min)	15	3	1	1	1			
Flotation time (min)			1	2	4	5	5	5
Lime		A				A		
PAX (g/ton)			3	2	1			
OLP (g/ton)			X	X	X			
Nasfroth 350 (drops)			1	1	1			

*Added only in the control measurement; A – the amount needed to reach the pH value;
X – a corresponding fraction of the PAX dosage, which was considered 100%.

Gaudin's selectivity index (SI) was also calculated to determine the separation efficiency of the flotation process in the absence and presence of OLP. Gaudin's selectivity index was determined by the following equation (1):

$$SI = \sqrt{\frac{Racc_{Cu}}{Racc_{Fe}} * \frac{(100 - Racc_{Fe})}{(100 - Racc_{Cu})}} \quad (1)$$

where $Raac_{Cu}$ and $Raac_{Fe}$ represent the cumulative recovery of copper and iron, respectively. The higher the value is, the higher selectivity toward copper is.

RESULTS AND DISCUSSION

The setup of the rougher-cleaner was selected based on extensive dosage study (Data not shown), where OLP was tested as a sole reagent and in a combination with the PAX. Sole OLP was not sufficient for the recovery of copper during flotation. However, it was observed that OLP in combination with PAX significantly improved the flotation performance. The recovery and selectivity of the process improved significantly while the grades remained similar. Thus, two mixtures of PAX and OLP were selected for the rougher-cleaner flotation trails.

The rougher flotation with PAX alone resulted in recovery of 71.2% with a grade of 7.07%, while the PAX+OLP1 and PAX+OLP2 mixtures resulted in the recoveries of 87.8% and 89.0% with grades of 12.21% and 12.29%, respectively. Thus, the PAX+OLP system performed significantly better in the rougher flotation. In the cleaner stages, there were significant loses in recovery when PAX was used alone. The recovery in the final concentrate was as low as 29.8%, which could be partially caused by the low amounts of solids in the flotation cell in the laboratory conditions that led to instability of the froth. The final grade was high and reached up to 23.3% as the chalcopyrite concentrate was very pure. The recovery of copper, when the PAX+OLP system was used, was 72.7% and 69.0%, respectively, with the grades of 19.3% and 20.9% for the PAX+OLP1 and PAX+OLP2. The froth instability was not observed in this case and the recovery was significantly better compared to the PAX alone.

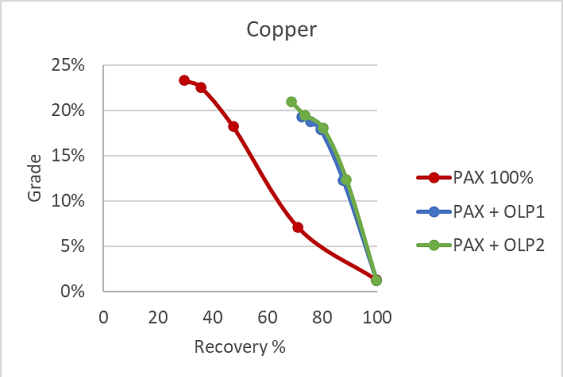

Figure 1 The grade-recovery curve of copper in rougher-cleaner flotation

Table 2 Overview of recoveries, grades, and selectivity index for the final concentrate of the rougher-cleaner flotation tests

Flotation test	Recovery in rougher	Recovery in concentrate	Grade in concentrate	Selectivity index Cu/Fe
Pax	71.2%	29.8%	23.3%	3.7
PAX+OLP1	87.8%	72.7%	19.3%	5.1
PAX+OLP2	89.0%	69.0%	20.9%	4.9

In the current industrial set up, the selectivity for pyrite and chalcopyrite is provided by addition of lime in the flotation process [2]. As a pH modifier and depressant, lime can depress pyrite with the formation of hydroxide moieties on the pyrite surface and when the pH value is above 10, with the oxidation of xanthate to dixanthogen which can be responsible for pyrite flotation does not occur. In the case of dissolution of metal ions such as Cu^{2+} that could activate pyrite, calcium and hydroxyl ions could create hydrophilic precipitates on the pyrite surface at higher pH. However, increasing concentration of lime leads to depression of other minerals such as chalcopyrite and the copper recovery would decrease as well [2,3]. It was observed during our trials that the selectivity can be improved by addition of OLP in the flotation system even in the absence of lime. Thus, the control flotation was performed with the addition of 3-2-1 g/ton of PAX in the respective step of the rougher flotation with pH adjustment to 10.5 by lime and further adjustment to 11.1 in the cleaner stage to set the baseline for industrial process. On the other hand, the PAX+OLP trials were performed without pH adjustment. Moreover, use of lime is a significant contributor of the process CO_2 footprint and a successful removal of lime from the process without affecting the selectivity would be economically and environmentally beneficial [4].

The selectivity between chalcopyrite and pyrite can be expressed as a selectivity between copper and iron in the flotation process. The Gaudin's selectivity index showed that the selectivity towards copper was significantly better when the PAX+OLP was used in the rougher flotation (Figure 2). While the value for PAX alone was below 4 for the whole flotation process, the PAX+OLP started with value of 6.6 and 6.9, respectively, for the OLP1 and OLP2. Although the selectivity decreased during the cleaner stages, the PAX+OLP outperformed the PAX alone.

The selectivity between copper and mass pull indicates how much gangue minerals was floated with the target mineral of chalcopyrite. Figure 2 shows that the PAX+OLP is producing concentrate with less gangue minerals. The PAX alone floated a significant amount of gangue especially during the rougher stages.

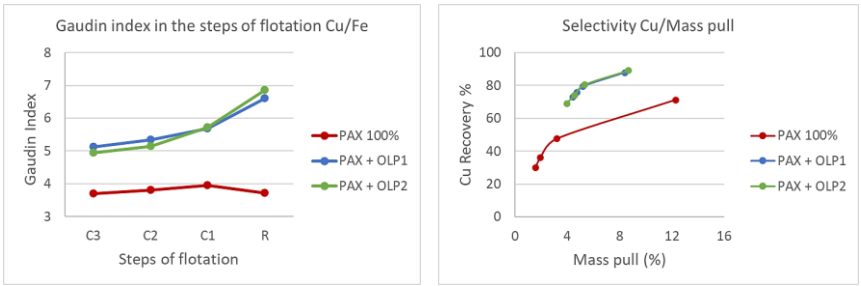

Figure 2 The selectivity curve of copper and total mass, and the selectivity index of copper and iron in different steps of the rougher-cleaner flotation test

Other elements were followed during the flotation trials. Those included other valuable element such as molybdenum and cobalt, and penalty elements that could cause problems in further processing of the concentrates.

The increased recoveries and grades of cobalt (Figure 3) and molybdenum in the flotation trial that were using the PAX and OLP mixture. However, due to the low

concentration of them, the results need to be cautiously interpreted due to possible measurement deviations.

For zinc, the penalty level is a grade of 3.5% and the highest obtained grade in concentrate was only 0.5% (Figure 3). For lead, the penalty level is 0.5% and the highest obtained with PAX+OLP was only 0.14%. The use of OLP led to a small increase in zinc and lead recovery. Despite the increase the grades are much lower than the allowed limit.

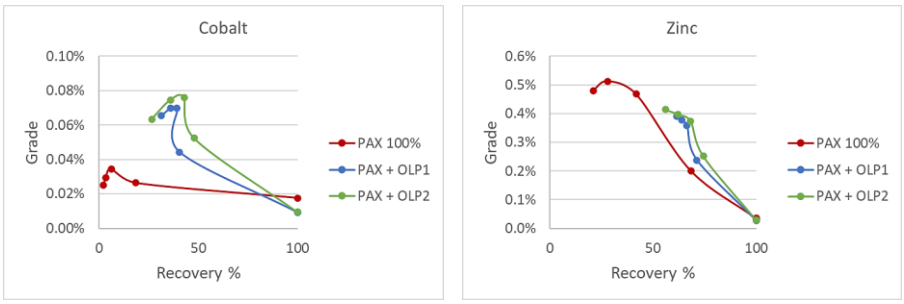

Figure 3 The grade-recovery curve of cobalt and zinc in rougher-cleaner flotation

High concentration of dissolved salts in the process water has a big impact on the flotation efficiency of the reagents as ions such as Ca^{2+} and SO_4^{2-} can form complexes in the mineral surface that could hinder xanthate adsorption [5]. Other studies also suggest that if the concentration of these dissolved salts go beyond a certain limit, it could increase entrainment as it over stabilizes the froth and thus, reduce the grade [6]. Also, the presence of residual xanthate in process water is known to be detrimental in the flotation where its oxidation products, specifically dixanthogen, can act as a nonselective collector [7]. In addition, the concentration of dissolved salts works as a buffer and the pH of the trials without pH adjustment was significantly lower in process water (7.5) than in the trials with tap water (8.6).

Finally, the mechanism of OLP action in the mineral flotation is unknown. Different suggestion can be found in literature for lignosulfonate-based reagent but very little in know about the organosolv lignin [2]. Mu et al. (2014, 2016) done extensive study on the interaction lignosulfonates with the pyrite and chalcopyrite mineral surfaces and its effect on the flotation of the minerals [2,8,9]. Multiple modes of action were observed when the interaction of lignosulfonate and pyrite was studies. Firstly, the lignosulfonates can passivate the pyrite surface and reduce the oxidation of mineral surface and xanthate, which inhibits the formation of dixanthogen and flotation. In addition, the attached lignosulfonate increases the hydrophilicity of the surface [8]. Secondly, lignosulfonates have a chelating ability and it seems that the complexing strength of lignosulfonates is sufficient to extract the copper ions from their xanthate complexes and from copper-activated pyrite surface, which again reduces the ability of pyrite to float and enables the xanthate to attach to other surfaces [9]. Lastly, Lui et al. studied adsorption of lignosulfonate calcium on mineral surface of chalcopyrite and pyrite mixture, and found that lignosulfonate interacted preferentially with pyrite surface, which led to pyrite depression in flotation trials [10]. Despite those potential mechanisms have been reported for lignosulfonates, those differ significantly from organosolv lignin.

Therefore, elucidating the mechanism of OLP during flotation is crucial towards further improving the process and consists of the next step in our study.

CONCLUSION

The general conclusion of our work it that the application of the OLP-PAX system as compared to PAX control led to improvement in the recovery and selectivity of Cu, while maintaining the grades at comparable levels. The total dose of PAX was lowered by 50% compared to the initial industrial control. An increased recovery of valuable element such as cobalt and molybdenum was also observed. Whereas minimal increase in penalty elements such as lead and zinc was shown. Additionally, it was observed that lime is not necessary for pH adjustment and depression of pyrite when the OLP-PAX system is applied, contributing to the reduction of the total amount of reagents needed, which has positive effect on both process economics and environmental performance.

ACKNOWLEDGEMENT

This research has received funding from the EIT Raw Materials research and innovation program under Proposal Number n°19089, project BATTERFLAI. Supply of BATTERy minerals using lignin nanoparticles as FLotAtIon collectors.

REFERENCES

1. Matsakas, L., Gerber, M., Yu, L., Rova, U., Christakopoulos, P. (2020) Preparation of low carbon impact lignin nanoparticles with controllable size by using different strategies for particles recovery. Ind. Crops Prod., 147, 112243.
2. Mu, Y., Peng, Y., Lauten, R.A. (2016) The depression of pyrite in selective flotation by different reagent systems – A Literature review. Miner. Eng., 96–97, 143–156.
3. Zanin, M., Lambert, H., du Plessis, C.A. (2019) Lime use and functionality in sulphide mineral flotation: A review. Miner. Eng., 143, 105922.
4. Shan, Y., Liu, Z., Guan, D. (2016) CO_2 emissions from China's lime industry. Appl. Energy, 166, 245–252.
5. Ikumapayi, F., Makitalo, M., Johansson, B., Rao, K.H. (2012) Recycling of process water in sulphide flotation: Effect of calcium and sulphate ions on flotation of galena. Miner. Eng., 39, 77–88.
6. Dzingai, M., Manono, M., Corin, K. (2020) Simulating the Effect of Water Recirculation on Flotation through Ion-Spiking: Effect of Ca^{2+} and Mg^{2+}. Miner.,10, 1033.
7. Rao, S.R., Finch, J.A. (1989) A review of water re-use in flotation. Miner. Eng., 2, 65–85.
8. Mu, Y., Peng, Y., Lauten, R.A. (2015) Electrochemistry aspects of pyrite in the presence of potassium amyl xanthate and a lignosulfonate-based biopolymer depressant. Electrochim. Acta, 174, 133–142.
9. Mu, Y., Peng, Y., Lauten, R.A. (2016) The depression of copper-activated pyrite in flotation by biopolymers with different compositions. Miner. Eng., 96–97, 113–122.
10. Liu, R.-Q., Sun, W., Hu, Y.-H., Wang, D.-Z. (2009) Effect of organic depressant lignosulfonate calcium on separation of chalcopyrite from pyrite. J. Cent. South Univ. Technol, 16, 753–0757.

XV International Mineral Processing and Recycling Conference
17-19 May 2023, Belgrade, Serbia

ENVIRONMENTAL BENEFITS OF LIGNIN BASED ECO-FRIENDLY SURFACTANTS FOR FLOTATION PROCESSES TOWARDS CURRENT PRACTICES

A. Peppas[#], D. Skenderas, C. Politi, P. M. Angelopoulos
National Technical University of Athens, School of Mining and Metallurgical Engineering, Athens, Greece

ABSTRACT – Froth flotation is known to be one of the keys enabling technologies allowing the selective separation of values from uneconomic mineral resources. Froth flotation utilizes the differences in the wettability of minerals in a three–phase system that consists of solids, gas, and water. Xanthates are currently the most used collectors in sulphide flotation, produced mainly in China. Nevertheless, the application of toxic reagents and the high amount of freshwater intake raises severe environmental concerns. In this frame, the study investigates the environmental benefits of replacing the flotation reagent of Xanthate with Lignin nanoparticles for the treatment of 1 tonne of mined ore, subjected to flotation.

Keywords: Flotation Reagents, Flotation Technology, Life Cycle Assessment, Xanthate, Lignin.

INTRODUCTION

Froth flotation is a concentration process that selectively separates minerals [1]. This process is a physicochemical separation technique that exploits the difference in the surface wettability of mineral particles [2]. The ore is ground to a sufficient size to liberate desired minerals. The hydrophobic particles of the heterogenous solid mixture are made to attach the gas bubbles, carried to the froth phase and recovered as a froth product [2]. For reaching the aimed selectivity, flotation method is dependent on the reagents. Reagents are used to regulate the conditions of the flotation and modify the surface of minerals. The xanthates salts are widely used as collectors for sulphides mineral flotation.

Xanthates have their share in rubber processing, agrochemicals, textile production, and other markets [3]. Thus, the mining sector remains a major share of the overall xanthates market [4]. The projected growth of the mining industry and the focus of mining companies on extracting ores from deep underground reserves entails the consumption of higher amounts of xanthates. Besides, xanthates are used as a catalyst in the production of polyvinyl chloride (PVC). These, will drive the xanthates market leading to its steady growth [5].

Asia Pacific (APAC) holds a prominent share of the global xanthates market for both the production and consumption of xanthates. China has the dominant stake in the APAC and the global xanthates market. China's xanthates market size is forecasted to reach US$130.5 Million by 2027, with a compound annual growth rate (CAGR) of 8.7% over the analysis period, 2020-2027 [4].

Xanthates are considered very valuable and are used for more than a century in

[#] corresponding author: peppas@metal.ntua.gr

mineral processing of sulphides ores. Xanthates are a group of synthesized toxic organic chemicals, most commonly obtained by the reaction of alcohol, hydroxide, and carbon disulphide (CS_2) [6]. Among the different types of xanthates, ethyl, isopropyl, isobutyl, amyl, and hexyl xanthates are usually preferred in the flotation process [7].

Xanthates have been characterised as hazardous, combustible, and toxic in nature. Their use involves additional costs and restrictions associated with storage, transportation and handling, among others. Their decomposition behaviour is arising concerns in terms of safety, health, and environmental impact. Decomposition has been reported to generate toxic substances such as carbon disulphide, carbonyl sulphide (COS), hydrogen sulphides, and hydrogen peroxide. The formation of toxic CS_2 comes as a result of xanthates' exposure to heat, moisture and acid leads. CS_2 can reach high vapor concentrations at room temperature resulting in a hazardous work environment. Human health can be significantly affected from being in contact with CS_2 [8]. Except for humans, xanthates and xanthates degradation pose a potential hazard for animals, soil and aquatic organisms, enzymatic system, etc. [3].

In the frame of green transition and sustainable development, there is observed the tendency for developing new, eco-friendlier solutions of similar functional standards. A novel approach, with the potential to offer a sustainable solution is the use of organosolv lignin (OL) for producing lignin micro- and nanoparticles, with the last being a promising alternative [9]. Lignin is found in abundant amounts in nature, resulting in growing interest in utilising lignin as a raw material for production of bio-products. Lignin is obtained after treatment of forest residues and side streams of the pulp industry [9]. There are three main types of lignin, sulphonated lignin, kraft lignin, and OL [10].

OL can be used in different applications as coatings, adhesives and sealants, personal care products, etc. The global OL market is projected to grow at a CAGR of 8.5% during the period 2022-2030. This is mainly due to the increased demand in pulp and paper products that will lead to higher generation OL; the favourable policies for biobased chemical production; the technological evolution regarding OL and other factors [11, 12].

Organosolv is a pulping approach that utilises organic solvents to solubilize lignin and hemicelluloses [13]. Among the different sources of lignin, OL has the advantage of being sulphur-free and of low ash content compared to other types of industrial lignin resulting in more pure lignin as a by-product [10]. In this framework, an OL-based reagent is developed for utilization in beneficiation process as a more environmentally friendly solution.

The scope of this study is to quantify the environmental impact of xanthates' use in the beneficiation process and evaluate the feasibility of partially replacing the xanthate reagent with organosolv lignin nanoparticles (OLN) reagent in the flotation process. The present work aims to compare the life cycle environmental impact of the established process of using only xanthates and the integration of OLN in the process. Life Cycle Assessment (LCA) as a well-established tool for evaluating the environmental impact and sustainable development, was implemented to fulfil this objective. The gate-to-gate model that was developed, considers the base case scenario of using 100% xanthates as collector reagents and the alternative proposed scenario of using 50% xanthates and 50% OLN reagent as collectors in the flotation process. The schemes outlined are based on a case study applied in the framework of the *BATTERFLAI* project. The partial Life Cycle

Impact Assessment (LCIA) was completed using the models. This study will serve for the quantification of the environmental impact of the two cases which will lead to their accurate and justified comparison.

MATERIALS AND METHODS

LCA Methodology

LCA is a standardized method for assessing the environmental aspects associated with a product, process or service over its life cycle measuring a list of impacts on local, regional and global levels [14]. To assess and compare the environmental impact of xanthates and OLN use in flotation process, an LCA was performed. The standardized procedures as described by ISO 14040:2006 and ISO 14044:2006, and the International Life Cycle Data (ILCD) Handbook [15-17].

The LCA is an interoperable process that consists of four stages: (i) Goal and Scope definition, (ii) Life Cycle Inventory (LCI), (iii) Life Cycle Impact Assessment (LCIA) and (iv) Interpretation of the results. The modelling of the different cases was performed with the commercial software Sphera LCA FE.

Goal, Scope and Functional Unit

In the framework of goal and scope definition the purpose of the assessment is established and decisions are made about the details of the studied product system including the selection of the functional unit (FU) [18]. The FU is a quantified description of the function of a product that serves as the reference basis for all calculations regarding impact assessment [19].

A gate-to-gate LCA was conducted to assess the environmental impact outcoming from the use of the xanthate reagent. The scope of the LCA was to investigate the environmental benefits of partially replacing xanthates with OLN reagent in flotation process. The FU selected was 1 kg of ore that will be processed.

Scenarios description and System boundaries

The analysis of the flotation process emphasises in the reagents used, to guarantee the comparison accuracy. Two different scenarios were developed. In the base case scenario (BCS) xanthate is used as the collector reagent in the flotation process. In the scenario 1 (S1) there is used 50% xanthate and 50% OLN reagent as collector. Into the system boundaries except for the flotation process where included the processes of reagents production as well.

Life Cycle Inventory

Life Cycle Inventory (LCI) involves the data compilation to quantify resource use (energy, water, chemicals use) and exiting products and emissions (product, wastes, emissions to soil, etc.) for each process defined in the system boundaries [20].

Life Cycle Impact Assessment

The LCIA quantifies the environmental impacts using the results of the LCI analysis and the impact factors. The mass of the environmental load is associated with the FU [20-22]. The impact categories selected, (i) Climate change, default, excl. biogenic carbon (kg CO_2 eq.), (ii) Freshwater ecotoxicity (FEP) (kg 1,4-Db eq.), (iii) Human toxicity, cancer (HTP) (kg 1,4-Db eq.), (iv) Photochemical Ozone Formation, Human Health (POFP) (kg NO_x eq.) and (v) Terrestrial ecotoxicity (TEP) (kg 1,4-Db eq.), are in accordance with Product Environmental Footprint Category Rules (PEFCR) Guidance, in line with the scope of the study and complying with ISO 14040 and ISO 14044 standards. As xanthates are considered toxic chemicals, the main focus is on the toxicological evaluation of its reaction and the impact on humans and environment. The evaluation method chosen for the impact assessment is ReCiPe 2016 (E) to be in line with literature review for comparison reasons.

RESULTS AND DISCUSSION

Results

In this section are presented the outcomes resulting from the comparison of the two evaluated scenarios. In the first scenario, which is the base case scenario, the flotation process is realised using xanthate reagent as collector. In the second scenario the xanthate reagent is replaced by OLN reagent at the rate of 50%. In all impact categories evaluated, the S1 shows to decrease the environmental impact of the flotation process. The Climate Change have a decreased impact of 0.03%, while the toxicity related impact categories, FWP, HTP, POFP and TEP have a decrease of 39.88%, 0.07%, 0.24% and 0.04% respectively. ***Table 1*** summaries the results of BCS and the S1 for each category.

Table 1 LCIA results for 1 kg of ore treated within the flotation process

Impact Category	BCS	S1
Climate change, default, excl. biogenic carbon (kg CO_2 eq.)	4.6630E-02	4.6615E-02
FEP (kg 1,4-Db eq.)	2.1817E-05	1.3116E-05
HTP (kg 1,4-Db eq.)	2.1754E-04	2.1738E-04
POFP (kg NO_x eq.)	6.5480E-05	6.5327E-05
TEP (kg 1,4-Db eq.)	1.7718E-02	1.7711E-02

Discussion

Xanthate reagents are a standardized reagent used in the mineral beneficiation process of sulphide ores. Its decomposition, and especially the release of CS_2 raises concerns regarding their impact in terms of safety, health, and environment. The replacement of a consolidated reagent as xanthates in the mining industry may be proven challenging.

Considering the huge amounts of minerals processed in the mining industry using xanthates, generates the necessity for the partially or entirely replacement of xanthates.

Thus, the development of more environmentally friendly reagents that will enable the same efficiency and will be more sustainable is a solution.

The use of lignin-based reagents is a promising option. Lignin is a low-cost organic material that occurs from side streams or from forest residues and can be found in great amounts. Taking advantage of such materials, leads towards the path of a more environmentally friendly and sustainable economy.

CONCLUSIONS

The results of this study highlight the concerns raised regarding the impact of xanthates' use. Xanthates decomposition affects environment and human health. The reduction of xanthates use can improve significantly the environmental and safety performance of beneficiation process of the sulphide ores.

The LCA implemented and presented in this study, shows that a there is an important improvement of flotation process impact by replacing the 50% of the xanthate reagent with an eco-friendlier reagent as is OLN. In all of the impact categories evaluated, the impact has been improved, with the greatest improvement of 39.88% to be observed in the case of FEP.

It is evident that the use of an alternative reagent, as OLN proposed in this study can efficiently replace xanthates, at the specific ratio analysed, resulting to important environmental improvement.

ACKNOWLEDGEMENT

This research has received funding from the EIT RawMaterials research and innovation programme under Proposal Number n°19089, project BATTERFLAI. Supply of BATTERy minerals using lignin nanoparticles as FLotAtIon collectors.

REFERENCES

1. Min, Q., et al. (2008) Froth Flotation of Mineral Particles: Mechanism. Drying Technology, 26 (8), 985-995.
2. Wang, D., Liu, Q. (2021) Hydrodynamics of froth flotation and its effects on fine and ultrafine mineral particle flotation: A literature review. Minerals Engineering, 173, 107220.
3. Prudence, B.P.C.M., Niyoyitungiye, L., Buhungu, S. (2022) Essentiality, Fate, Ecotoxicity, and Health Effects of Xanthates and Xanthates Based-Compounds-A Review. Journal of Geoscience and Environment Protection, 10 (12), 161-203.
4. Xanthates. Market Research.com, 2022.
5. Xanthates Market is expected to expand at a CAGR of 7% from 2022 to 2029
6. Milosavljević, M., et al. New Eco-Friendly Xanthate-Based Flotation Agents. Minerals, 2020. 10: p. 350.
7. Mokgethwa, M., et al., (2016) An Evaluation of Sodium Ethyl Xanthate for the Froth Flotation Upgrading of a Carbonatitic Copper Ore. Journal of Physical Science, 27, 13-21.

8. Shen, Y. (2016) Chemical Fate Studies of Mining Reagents: Understanding the Decomposition Behavior under Various Conditions. (Doctoral Theses), Columbia University, Graduate School of Arts of Sciences, New York, United States, 317.
9. Hrůzová, K., et al. (2020) Organosolv lignin hydrophobic micro- and nanoparticles as a low-carbon footprint biodegradable flotation collector in mineral flotation. Bioresource Technology, 306, 123235.
10. Yadav, P., et al. (2021) Environmental impact and cost assessment of a novel lignin production method. Journal of Cleaner Production, 279, 123515.
11. Global Organosolv Lignins Market by Type, Pulping with acetic acid, By Application And By Region, Forecast From 2022 To 2030. 2021; Available from: https://dataintelo.com/report/organosolv-lignins-market/.
12. Global Organosolv Lignins Market by Type (Ethanol/water pulping (Alcell process), Pulping with acetic acid (CIMV process), Other), By Application (Ink, Varnishes, Paints, Others) And By Region (North America, Latin America, Europe, Asia Pacific and Middle East & Africa), Forecast From 2022 To 2030. 2021; Available from: https://dataintelo.com/report/organosolv-lignins-market/.
13. Jarrell, T.M., et al. (2014) Characterization of organosolv switchgrass lignin by using high performance liquid chromatography/high resolution tandem mass spectrometry using hydroxide-doped negative-ion mode electrospray ionization. Green Chemistry, 16 (5), 2713-2727.
14. Muralikrishna, I.V. Manickam, V. (2017) Chapter Five - Life Cycle Assessment, in Environmental Management, I.V. Muralikrishna and V. Manickam, Editors. Butterworth-Heinemann. 57-75.
15. ISO 14044:2006 Environmental management — Life cycle assessment — Requirements and guidelines. 2022.
16. ISO 14040:2006 Environmental management — Life cycle assessment — Principles and framework. 2022.
17. Life Cycle Assessment (LCA). European Platform on Life Cycle Assessment.
18. Curran, M.A. (2017) Overview of Goal and Scope Definition in Life Cycle Assessment, in Goal and Scope Definition in Life Cycle Assessment, M.A. Curran, Editor. 2017, Springer Netherlands: Dordrecht. 1-62.
19. Arzoumanidis, I., et al. (2020) Functional Unit Definition Criteria in Life Cycle Assessment and Social Life Cycle Assessment: A Discussion, in Perspectives on Social LCA: Contributions from the 6th International Conference, M. Traverso, L. Petti, and A. Zamagni, Editors., Springer International Publishing: Cham. 1-10.
20. Fraval, S., et al. (2019) Life Cycle Assessment of Food Products, in Encyclopedia of Food Security and Sustainability, P. Ferranti, E.M. Berry, and J.R. Anderson, Editors., Elsevier: Oxford. 488-496.
21. Accorsi, R. (2019) Chapter 5 - A support-design procedure for sustainable food product-packaging systems, in Sustainable Food Supply Chains, R. Accorsi and R. Manzini, Editors., Academic Press. 61-81.
22. Kikuchi, Y., Kanematsu,Y. (2020) Chapter 27 - Life cycle assessment, in Plant Factory (Second Edition), T. Kozai, G. Niu, and M. Takagaki, Editors., Academic Press. 383-395.

XV International Mineral Processing and Recycling Conference
17-19 May 2023, Belgrade, Serbia

EVALUATION OF BATTERY MINERALS FLOTATION PROCESS ECO FRIENDLINESS UTILISING BIODEGRADABLE LIGNIN REAGENTS

A. Peppas[1], K. Hurzova[2], D. Skenderas[1#], C. Politi[1], L. Matsakas[2], P.M. Angelopoulos[1]

[1] National Technical University of Athens, School of Mining and Metallurgical Engineering, Athens, Greece

[2] Luleå University of Technology, Biochemical Process Engineering, Division of Chemical Engineering, Department of Civil, Environmental and Natural Resources Engineering, Luleå, Sweden

ABSTRACT – As copper (Cu), nickel (Ni) and cobalt (Co) are main components of the Li-ion batteries, rising demand from the battery sector will "have a disruptive impact" over the next 10 years. There is a high need for replacing existing flotation reagents with more-environmentally friendly products. An efficient, sustainable lignin-based flotation concept for the selective extraction of base metals, such as Cu, Ni, Co and Au is proposed in the framework of "Batterflai" EIT funded project. This work presents environmental impact of the life cycle of lignin reagents for the preparation and use. The results will prepare the ground for integrating the natural, biodegradable lignin to flotation processes.

Keywords: Life Cycle Assessment, Lignin, Eco-Friendly Reagents.

INTRODUCTION

Froth flotation is a mineral processing that selectively separates the valuable minerals from each other and the gangue. The flotation method takes advantage of mineral hydrophobicity. Different types of reagents contribute to achieving the desired separation. Xanthates are commonly used as collector reagents in this process; however, they are characterised by health and environmental risks due to their toxicity. The urge for a green and sustainable transition in industry generates the need for total or partial replacement of such reagents. The development of a lignin-based reagent serves in this direction.

Lignin is a low-cost material that can be found in abundant amounts as it occurs from natural terrestrial organic material, such as forest residues, side streams of the pulp industry, and secondary ethanol production. Wood pulping and other biorefinery industries extract more than 50 million tonnes of lignin annually, whereas the total worldwide production is approximately 100 million tonnes annually [1, 2]. Thus, only about 2% is recovered for utilisation in applications.

The two prevailing categories of lignin are lignosulphonate and kraft lignin. Organosolv lignin (OL), that account for about 2%, is a new category that gains ground due to its high quality and purity [3]. OL from the pre-treatment of birch and spruce wood

corresponding author: skenderasdoris@metal.ntua.gr

chips was used as the raw material for the preparation of micro- and nanoparticles to be used as lignin-based flotation reagents [4].

This study aims to quantify and evaluate the environmental impact of the newly-developed lignin-based flotation reagent. For reaching this, a Life Cycle Assessment (LCA) analysis, is implemented. LCA is a technique used to assess the environmental impact of a product or system through its life cycle. The cradle-to-gate model that was developed, considers the different processes applied from the phase of birch and spruce wood chips to the final phase of nanoparticle reagent production. The processing method applied is under the case study applied in the framework of "BATTERy minerals using lignin nanoparticles as FLotAtIon collectors – BATTERFLAI" project.

EXPERIMENTAL

Organosolv pre-treatment of lignocellulosic biomass and particle preparation

Two types of biomasses have been used for this study, Norway spruce (*Picea abies L.*) and silver birch (*Betula pendula L.*) in form of woodchips. The biomass was milled before the pre-treatment to pass a 1 mm screen. The organosolv pre-treatment is performed using biomass, ethanol, and water mixture of 50% (birch) or 60% v/v (spruce). The biomass slurry is heated and after the pre-treatment, the slurry is filtered to recover solid pre-treated biomass and the hemicellulose-rich liquid that contains dissolved lignin. Lignin is recovered by precipitation due to ethanol removal by evaporation. Three separate fractions, cellulose, hemicellulose, and lignin, are obtained as a result of the organosolv pre-treatment [5]. The purity of the lignin recovered exceeds 94% in both birch and spruce samples.

Table 1. Organosolv pre-treatment mixture and processes conditions

	Birch	**Spruce**
Biomass	110g	110g
Ethanol	1.1L	1.1L
Water mixture	50%	60%
Heat (autoclave reactors)	183°C – 1h	183°C – 1h

Table 2. Sample concentration and recovery

		Birch	**Spruce**
Untreated sample (concentration)	Cellulose	35.2%	39.3%
	Hemicellulose	28.0%	30.5%
	Lignin	26.1%	28.1%
Pre-treated sample recovery		61.0%	72.0%
Pre-treated sample (concentration)	Cellulose	62.2%	50.3%
	Hemicellulose	3.0%	13.2%
	Lignin	16.0%	23.7%
Lignin recovery (raw organosolv lignin)		44.7%	37.5%
Lignin purity		>95%	>94%

The nanoparticles were prepared from raw OL by solvent exchange method. The 5% w/v lignin was dissolved in 75% v/v ethanol solution and mixed for 8h. Subsequent homogenization was performed at 750 bars, by using an APV-2000 homogenizer (SPX FLOW, Charlotte, NC, USA). The homogenized lignin solution was diluted with distilled water in ration of 1:6, which caused the nanoparticle formation. OL nanoparticles were obtained as a dry powder after freeze-drying process [6].

In the same line, the microparticles were prepared from 1% w/v lignin in 75% v/v ethanol solution, which was mixed for 8h and homogenized. After homogenization, the ethanol was slowly removed by distillation. The decreasing concentration of ethanol triggered the formation of microparticles. OL microparticles were obtained as a dry powder after the freeze-drying process [6].

LCA Methodology

Goal and scope definition

The goal of this study was the quantification of the environmental impact of OL particles reagent production from birch and spruce bark. The pre-treatment of the biomass and the preparation of OL particles reagent were analysed.

Functional Unit

Functional unit (FU) provides the reference to which all inputs and outputs data in the assessment are normalised. In the study presented, the FU is 1kg of OL reagent produced.

System Boundary

A cradle-to-gate approach was adopted. The model was investigated in two phases, i) the pre-treatment of biomass and ii) the particles production. All inputs (biomass, electricity, water, chemicals, etc.), and outputs (pre-treated biomass, raw OL, recovered liquids, etc.) responding to each phase, were included within the system boundaries. The biomass used in the study was birch and spruce bark and the reagents generated were micro- and nanoparticle reagents.

As a result, four models were assessed. Both birch and spruce feedstock used for the lignin production were considered to be wastes of forest industry eliminating the harvesting emissions they might carry. Besides, was considered that the lignin production and reagent preparation facility are located near a sawmill. Thus, no transportation regarding the bark and the OL were required.

Table 3. Four scenarios assessed

Model	Scenario
Nano-Birch OLN	S1
Nano-Spruce OLN	S2
Micro-Birch OLN	S3
Micro-Spruce OLN	S4

Life Cycle Inventory (LCI)

In this section, LCI information regarding the processes followed for the production of the OL reagents. The LCI for implementation of this study is based on the data acquired form the laboratory process.

Life Cycle Impact Assessment (LCIA)

The LCIA quantifies the environmental impacts using the results of the LCI analysis and the impact factors. The mass of the environmental load is associated with the FU.

The impact categories selected to evaluate the four scenarios are: i) Climate change, default, excl. biogenic carbon (kg CO_2 eq.), ii) Freshwater ecotoxicity (FEP) (kg 1,4-Db eq.), iii) Human toxicity, cancer (kg 1,4-Db eq.) (HTP), iv) Photochemical Ozone Formation, Human Health (kg NO_x eq.) (POFP), v) Terrestrial ecotoxicity (kg 1,4-Db eq.) (TEP).

RESULTS AND DISCUSSION

Results

Spruce biomass and birch biomass are pre-treated for the reagents; production. Raw OL is the output of the biomass pre-treatment and it is followed by further treatment in order to create the nano- and micro- reagent. The outcomes resulting from the evaluation and modelling of the four scenarios for the production of the OL reagents are presented in Table 4.

Table 4. LCIA results per 1kg of OL reagent produced

Impact Category	**S1**	**S2**	**S3**	**S4**
Climate change, default, excl. biogenic carbon (kg CO_2 eq.)	164	174	133	187
FEP (kg 1,4-Db eq.)	0.097	0.102	0.059	0.071
HTP (kg 1,4-Db eq.)	1.630	1.760	2.220	3.660
POFP (kg NO_x eq.)	0.358	0.375	0.225	0.277
TEP (kg 1,4-Db eq.)	113	119	65.5	75.9

The greatest environmental impact of OLN reagent preparation comes from the grid electricity consumed mainly in the process of nano- or microparticles formation. The formation of nanoparticles requires more energy than microparticles formation affecting almost all the impact categories. On the other hand, spruce biomass pre-treatment requires more ethanol production, affecting the HTP.

Discussion

Lignin is a low-cost material that can be found in abundant amounts as forest residues or side product of other processes. OL, have the advantage to be sulphur-free in comparison with kraft lignin. That gives the opportunity to be explored as the basis for the production of reagents that can be utilized in flotation process.

The production of an environmentally friendly reagent that can efficiently enter in the mine industry and specifically in the beneficiation process replacing partially xanthates reagent can contribute to improve the impact of beneficiation process. Therefore, different methods are implemented to develop a novel, promising reagent.

CONCLUSION

The utilisation of lignin, for generating a product that may replace a harmful for both health and environment material, as xanthates complies with the targets to reach a more environmentally friendly and sustainable industry. In this framework, four scenarios have been implemented for the production of an OLN reagent.

The LCA presented in this paper examined the impact of each scenario to evaluate the environmental burden of each of the four proposed solutions and to detect the hot spots that requires improvement. As results, the electricity consumed for particles formation is responsible for the main part of reagents impact, especially in the case of nanoparticle reagent.

It is important to mention that this study is based on laboratory data. An LCA implemented based on laboratory data gives a limited indication of the industrial scale production environmental impact. However, it serves to give environmental guidance for the emerging product. The impact of the product in a large-scale production process can be significantly lower than in laboratory scale.

ACKNOWLEDGEMENT

This research has received funding from the EIT RawMaterials research and innovation program under Proposal Number n°19089, project BATTERFLAI. Supply of BATTERy minerals using lignin nanoparticles as FLotAtIon collectors.

REFERENCES

1. Bajwa, D.S., et al. (2019) A concise review of current lignin production, applications, products and their environmental impact. Industrial Crops and Products, 139, 111526.
2. The Global Market for Lignin 2023-2033. 2023, Available from: https://www.giiresearch.com/report/fmi1223534-global-market-lignin.html
3. Shrotri, A., Kobayashi, H., Fukuoka, A. (2017) Chapter Two - Catalytic Conversion of Structural Carbohydrates and Lignin to Chemicals, in Advances in Catalysis, C. Song, Editor., Academic Press. 59-123.
4. Hrůzová, K., et al. (2020) Organosolv lignin hydrophobic micro- and nanoparticles as a low-carbon footprint biodegradable flotation collector in mineral flotation. Bioresource Technology, 306, 123235.
5. Nitsos, C., et al. (2016) Isolation and Characterization of Organosolv and Alkaline Lignins from Hardwood and Softwood Biomass. ACS Sustainable Chemistry & Engineering, 4 (10), 5181-5193.
6. Matsakas, L., et al. (2020) Preparation of low carbon impact lignin nanoparticles with controllable size by using different strategies for particles recovery. Industrial Crops and Products, 147, 112243.

XV International Mineral Processing and Recycling Conference
17-19 May 2023, Belgrade, Serbia

ENVIRONMENTAL ASSESSMENT OF RARE EARTHS RECOVERY METHOD FROM BAUXITE RESIDUES

A. Peppas, C. Politi[#], D. Skenderas, P. M. Angelopoulos
National Technical University of Athens, School of Mining and Metallurgical Engineering, Athens, Greece

ABSTRACT – Bauxite residue is highly alkaline and very fine-grained by-product of the Bayer process with an increasing annual production of about 150 million tonnes. The management and safe disposal of bauxite residue are therefore a major issue for bauxite and alumina industries affecting the production cost. This study focuses on the environmental assessment of an innovative integrated process for the recovery of Rare Earth Elements and Scandium from bauxite residue in the framework of the European research project REEScue. The aim is to identify hot spots and provide a quantified assessment of the environmental impacts of the new technologies and final materials.

Keywords: Rare Earth Elements, Critical Metals, Bauxite Residues, Secondary Raw Material, Life Cycle Assessment.

INTRODUCTION

Aluminium is important in various sections of industry and the economy. Bauxite is the basic raw material processed and converted to alumina for aluminium and industrial alumina production [1]. The Bayer process is the method utilised for this transformation. One of the challenges facing the Bayer process is the need of treatment and disposal of bauxite residues (BR) commonly known as red mud (RM).

BR is the major waste material produced during alumina production following the Bayer process. It is derived from the process of caustic digestion of crushed bauxite at elevated temperatures. BR is characterized by tiny particle size and high alkaline value [2]. These properties make the disposal of RM a very challenging process as it leads to serious environmental issues and affects production cost.

Depending on the quality of the bauxite processed, 1.0 to 1.8 tons of bauxite residues are generated per tonne of alumina produced, on average [3, 4]. The annual production of BR is about 150 million tonnes. BR is rich in minerals and metals of high economical interest. Typically, BR material contains mainly CaO, Al_2O_3, Fe_2O_3, SiO_2, TiO_2, Na_2O, V_2O_5 and Rare Earth Oxides (REO). The exact composition is related to the bauxite ore sources and production processes [1]. The exploitation of BR as a low-cost secondary raw material and metal resource could be a solution for BR reduction and would enter the waste again in the economic cycle [5]. The content of the single elements is not very high; hence the total amount of resource is huge leading to considerable amounts of recovered elements.

[#] corresponding author: chrysapol@metal.ntua.gr

One approach is tapping BR as a source of scandium as it accounts for more than 90% of rare earth elements (REEs) with economic value present in BR [1], and other REEs. According to a policy brief of the EU-funded SCALE project, it is estimated that extracting the REE from the Aluminium of Greece's annual BR production can meet the needs of approximately 10% of the of Europe's demand [6]. Innovative extraction and separation technologies are suggested to tackle the weaknesses and risks resulting from the existing methods utilised.

In the framework of the REEScue project, two processes are developed; i) the direct acid leaching of BR with the addition of oxidative agents and, ii) the hydrothermal conversion of hematite to magnetite, magnetic separation of magnetite and the production of a non-magnetic fraction rich in basic metals and REEs, leaching of metals from the non-magnetic fraction.

The aim of this study is to assess the expected environmental impact and the sustainability of the developed processes, and to detect the hotspots that requires taking action, in terms of energy efficiency and environmental impacts. The implementation of the Life Cycle Assessment (LCA) is the main tool for reaching this objective.

EXPERIMENTAL

Bauxite Residues Treatment Processes

Two process options are evaluated for the extraction of scandium and REEs from BR. The two processes are the direct leaching of bauxite residues process and the hydrothermal transformation process.

Direct leaching of Bauxite Residues

Leaching is a primary process in hydrometallurgy for recovery of the desired elements, applied mainly when there is low concentration. It is a mass transfer operation in which constitutes of the solid material are released into a contacting water phase with the contribution of different solvents [7]. The selection of the solvent for operating the leaching process is of great importance. The solvent affects the extraction efficiency, the purity of desired elements recovery, and the concentration of REEs in the leachate.

In this case there is examined the direct acid leaching of the BR, i) using solution with higher acid concentrations, and ii) adding oxidative agents.

Hydrothermal transformation process

Hydrothermal transformation for the exploitation of BR is a novel approach. This process is a sequence of different sub-processes. At first the hematite is transformed magnetite implementing hydrothermal conversion. Hydrothermal treatment, is a treatment method which generates a reaction of material with high temperature and high-pressure steam, with the contribution of alkaline media. In this case, the red mud is processed with the hydrothermal treatment for hematite to be transformed into magnetite to enhance its magnetization character [8]. BR treatment takes place in autoclave combined with Fe source. To reduce hematite to magnetite high temperature, reaching 250°C and, alkaline conditions are required.

The magnetic separation follows and then the leaching process. Magnetic separation, follows. The magnetite and the non-magnetic materials are separated, taking advantage of their magnetic properties. The non-magnetic fraction is rich in basic metals and REEs. From this procedure an iron-rich concentrate and a residue are produced. Leaching of the metals from the non-magnetic fraction produced and collected as residues is the final step. The residues generated from the magnetic separation phase are processed with the use of acid agents, as hydrogen chloride (HCl), to dilute the REEs. Both direct leaching and hydrothermal transformation processes are followed by the recovery of REEs from the leaching solutions using ionic resins.

Life Cycle Assessment

Methodology

LCA is a well-established, internationally recognized and standardised methodology for assessing the environmental impacts and detecting the environmental hotspots of a production process that require taking action in order to optimise it. According to ISO14040 (ISO, 2006), an LCA consists of the following steps: i) definition of goal and scope, ii) life cycle inventory (LCI), iii) life cycle impact assessment (LCIA) and iv) interpretation of the results [9, 10].

Goal and Scope

The goal of this study is to assess and evaluate the expected environmental impacts and to identify the points with the highest environmental burden. The life cycle phases of the input and output material flows, the energy flows, the wastes and emissions generated are under consideration.

The functional unit (FU), is part of the scope definition and provides the reference for the normalisation of all the flows. In the present study the FU defined is 1kg of BR used.

System Boundary

Two different models are designed corresponding to the different cases examined. The first model concerns the direct leaching of the BR. All inputs (BR, electricity, water, solvents, acids, etc.), and outputs (recovered material, solid waste residues, recovered liquids, etc.), are included within the system boundaries.

The second model concerns the hydrothermal transformation. This model is investigated in three different phases; i) the hydrothermal transformation, ii) the magnetic separation and, iii) the leaching of the non-magnetic fraction. All inputs (BR, electricity, water, solvents, etc.), and outputs (recovered material, solid residues, recovered liquids, etc.) corresponding to each of phase, are included within the system boundaries.

Life Cycle Inventory

The LCI realised for the implementation of this environmental assessment is based on the data acquired from the use cases implemented and the literature review.

Information concerning the inputs and outputs entering and exiting the system boundaries, for the assessment of BR treatment will be collected and evaluated. The information acquired will be evaluated in terms of accuracy, coherence and consistency. The material treated (BR), the solvents used for the treatment, the energy required for processes' implementation and the water used are some of the inputs. In the other hand, the product produced or extracted, the solid and liquid wastes generated, the emissions ejected, etc. comprise the output flows.

Life Cycle Impact Assessment

LCIA uses the results of the LCI modelling analysis and the impact factors defined for the quantification of the environmental impacts of the processes. The mass of the environmental impact is connected with the FU.

RESULTS AND DISCUSSION

Results

BR results in the large amounts of waste produced in industrial level affecting the Aluminium production industries in terms of production cost and environmental impact. Every new method and technique suggested is assessed and evaluated to better understand their feasibility and environmental performance.

For the extraction of Scandium from BR the model 1 uses combination of processes, namely: i) leaching with mineral acid (LMA), ii) Purification with selective ion recovery and ion exchange, iii) Purification with solvent extraction, iv) antisolvent crystallization and v) calcination, the greenhouse gas (GHG) value totals at 0.1-0.12 kg CO_2-eq. per kg of BR treated [11]. The LMA counts for the largest share of the impact accounted, ~93% of the total impact, approximately 0.093-0.11 kg CO_2-eq per kg of BR treated. The elevated amount of acid required for the process and the energy consumption, accounts for more than 80% of the total impact resulting from the analysis. Besides, the theoretical maximum avoided burden for extracting scandium oxide from 1kg is estimated at 1.13 kg CO_2-eq when comparing with the landfilling of BR.

Model 2 includes: i) the hydrothermal treatment, ii) the magnetic separation and, iii) the leaching of the non-magnetic fraction. In both hydrothermal treatment and magnetic separation, the energy consumption is responsible for the environmental impact of the two processes. The GHG value of these processes is 3.44 kg CO_2-eq. per kg of BR treated. The non-magnetic fraction that will be leached to recover the RRE, is approximately 20% of the BR treated. The GHG value for leaching process is approximately 0.022-0.026 kg CO_2-eq. per kg of BR treated. The GHG value of for this model totals at 3.462-3.466 kg CO_2-eq. per kg of BR treated.

Discussion

The bauxite processing to Aluminium production results in BR after the Bayer plant processing. The BR is an important factor impacting on the function of an Aluminium industry and having significant environmental risks.

From the moment slurry bauxite exits the washers within the Bayer plant until the place of bauxite residues in the disposal area, transport, dewatering, disposal, recovery and discharge take place. Additionally, this combined with the huge amounts of BR generated from the industry and the space needed for their disposal rise the need for introducing new better methods for BR management.

Further treatment of BR and extraction of economically important elements is a solution for both industry viability and environmental sustainability. In this study, two new methods are presented and evaluated for their efficiency and sustainability, the direct leaching of BR and the hydrothermal transformation process. As occurring from other BR treatment methods for extracting RRE, numerous sub-processes are conducted. Each sub-process and the system as a whole must be evaluated to better understand their impact and make any necessary improvements implementing LCA.

CONCLUSION

In this study, it is described the methodology followed for the LCA implementation on two new methods for BR treatment and Scandium extraction. The acid leaching process is the one with the most environmental burden due to the amount of acid used and the energy consumption need. However, the extraction of Scandium from BR remains a better solution than disposing the BR combined with directly extracting Sc from ore mines.

ACKNOWLEDGEMENT

This research has received funding from the ERA-MIN2 research and innovation programme under ID: 82, project REEScue. Integrated process for the recovery of Rare Earth Elements and Scandium from Bauxite Residues.

REFERENCES

1. Wang, L., et al. (2019) A Review on Comprehensive Utilization of Red Mud and Prospect Analysis. Minerals, 9 (6), 362.
2. Khairul, M.A., Zanganeh, J., Moghtaderi, B. (2019) The composition, recycling and utilisation of Bayer red mud. Resources, Conservation and Recycling, 141, 483-498.
3. Hydrogen As the Reducing Agent in the REcovery of metals and minerals from metallurgical waste (HARARE). 2022.
4. Tang, W., Khavarian, M., Yousefi, A. (2022) 14 - Red Mud, in Sustainable Concrete Made with Ashes and Dust from Different Sources, R. Siddique and R. Belarbi, Editors., Woodhead Publishing, 577-606.
5. IAI Releases Updated Sustainable Bauxite Residue Management Guidance. International Aluminium 2022.
6. Production of Scandium compounds and Scandium Aluminum alloys from European metallurgical by- products. 2021.
7. Leaching Environmental Assessment Framework, Leaching Process. Vanderbilt University 2021; Available from: https://www.vanderbilt.edu/leaching/leaching-process/.

8. Pasechnik, L.A., et al. (2020) A promising process for transformation of hematite to magnetite with simultaneous dissolution of alumina from red mud in alkaline medium. Hydrometallurgy, 196, 105438.
9. ISO 14040:2006 Environmental management - Life cycle assessment - Principles and framework. Available from: https://www.iso.org/standard/37456.html.
10. ISO 14044:2006 Environmental management - Life cycle assessment - Requirements and guidelines.; Available from: https://www.iso.org/standard/38498.html.
11. Markus Lenz, D.H., Victor Misev, SCALE, Deliverable 5.2, LCA/LCC to estimate environmental impacts. 2021.

PAPERS

XV International Mineral Processing and Recycling Conference
17-19 May 2023, Belgrade, Serbia

MODIFIED BOND AND RITTINGER ENERGY-SIZE RELATIONSHIPS FOR LABORATORY FINE GRINDING

A. Jankovic[1#], W. Valery[1], M. Sederkenny[2], K. Duffy[1]
[1] Hatch, 61 Petrie Terrace, Brisbane Qld, 4000 Australia
[2] Queensland Alumina Limited, Gladstone, Qld, Australia

ABSTRACT – Laboratory-scale fine grinding tests remain the most practical method of assessing material grindability and predicting energy requirements for industrial scale fine grinding mills. This review describes several different fine grinding laboratory tests and analyses 88 test results. It was found that the original Bond and Rittinger energy-size models do not reproduce the experimental results with sufficient accuracy for fine grinding applications. Both the total average model error and standard deviation for individual laboratory data set results were high; mostly in the range of 15 - 20%. However, modified Bond and Rittinger energy-size models using a variable grindability coefficient were much more accurate. The total average model error and standard deviation reduced to mostly below 5%. This increased accuracy indicates potential to improve predictions of industrial scale energy requirements from fine grinding laboratory-scale tests using modified Bond and Rittinger energy-size models.

Keywords: Laboratory, Fine Grinding, Comminution, Energy, Size, Modelling.

INTRODUCTION

Fine grinding is becoming more common as unexploited deposits have increased complexity with reduced grain size and thus finer liberation size. The definition of fine and ultrafine grinding varies. However, grinding of material with an F80 (80% passing feed size) of less than 100 µm down to a P80 (80% passing product size) of 7 - 30 µm is generally considered fine grinding. While grinding of material with F80 of less than 20 µm down to P80 values with lower size limits of several µm is considered ultrafine grinding [1,2].

Ball mills have traditionally been used for fine grinding of minerals; however, efficiency decreases when grinding below 75 µm and ball mills are rarely economical below around 30 µm [4]. Fine grinding consumes higher specific energy than coarser grinds and is more efficiently achieved in alternative comminution devices with different dominant breakage mechanisms (attrition breakage rather than impact and abrasion). Stirred mills are typically used for fine grinding, including: tower mills, stirred media detritors and IsaMills™.

A tower mill is a low-speed vertical stirred mill where media motion is driven by the rotation of a helical impeller. It was invented in the 1950s by the Japan Tower Mill Company, and in the 1980s Metso introduced the Vertimill™, which is an adaptation of this technology. Almost exclusively steel grinding media is used with diameters typically at least 12 mm, up to several cm [5]. Sizing for industrial scale tower mills can be achieved using a pilot unit or Metso mostly uses a “jar test”, which

corresponding author: alex.jankovic@hatch.com

is a batch ball mill test, for sizing the Vertimill™ [7].

The Stirred Media Detritor (SMD) is a medium-speed vertical stirred mill, which uses multi-layer pin impeller to fluidise the media (with media diameters typically of several millimeters) [5]. In the 1960s English China Clay (now Imerys) developed the SMD which originally used sand as media, and in recent decades sand was replaced with small ceramic grinding media beads. SMDs have been used in kaolin and calcium carbonate grinding applications, producing particle sizes down to 1–2 µm and Metso manufacture them for use in ultrafine grinding of metalliferous ores.

The IsaMill™ is a high-speed horizontal disc mill, developed by Mount Isa Mines Ltd. and Netzsch and commercialised for ultrafine grinding of ore in 1999 [8]. It consists of a horizontal cylindrical chamber, with the agitator being a series of perforated discs attached to a central shaft. It can produce very fine product sizes, with P80 values as low as 7 µm being practical [1], enabled by the relatively fine ceramic grinding media, in the range 1–8 mm in diameter [6].

Laboratory-scale fine grinding tests remain the most practical method of assessing material grindability and predicting industrial energy requirements. The Bond test is used for standard ball milling applications and the Levin test is a batch grinding test in the Bond mill developed for samples that are not conforming with the standard Bond procedure requirements. Specific tests and laboratory equipment are also available for the different stirred mill technologies. Examples of the fine grinding laboratory equipment used for the tests considered in this study are shown in Figure 1. The Levin test [10] is conducted using the standard Bond ball mill test equipment.

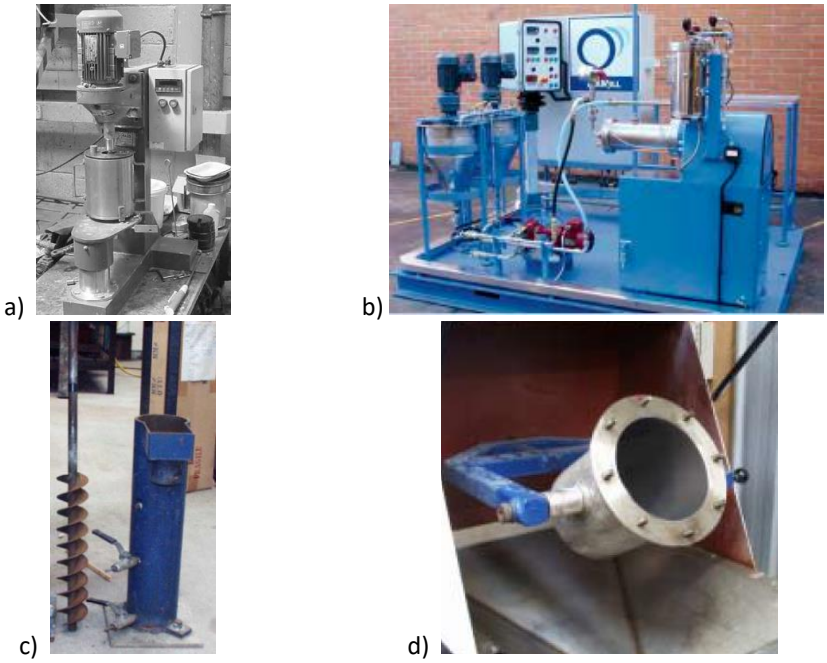

Figure 1 Laboratory fine grinding units a) Stirred Media Detritor (SMD), b) IsaMill™, c) tower mill, d) batch ball mill

EXPERIMENTAL

Test results from five different types of fine grinding laboratory tests from the authors data base were analyzed. The type of test, number of tests and data points from the test are summarized in Table 1. A total of 88 test results were analyzed with over 420 data points. IsaMill™, SMD and Levin tests are standardized tests and were conducted by commercial laboratories. The tower mill tests results are from the author's research work [9] and the batch ball mill test results were part of the authors consulting projects.

Table 1 Database of laboratory tests

Test type	Number of tests	Data points (energy-size pairs)
IsaMill Test	14	89
SMD Test	10	52
Tower Mill Test	40	187
Batch Ball Mill Test	14	48
Levin Test	10	47

For each grinding test the specific comminution energy (SE) was determined by measuring the power draw, or torque, or in the case of Levin test using the calibrated equations [10]. Most of the particle sizing was carried out using the laser sizing technology and only the Levin test used sieve sizing. Results for all tests are presented as product 80% passing size (P80) versus the specific energy (kWh/t) required to achieve this product size.

RESULTS AND DISCUSSION

To determine grinding energy requirements, well known Rittinger (1) and Bond (2) equations are commonly used to relate feed size, product size, and energy.

$$E_{1-2} = 10 * R\left(\frac{1}{x_2} - \frac{1}{x_1}\right) \quad \text{Von Rittinger} \quad (1)$$

$$E_{1-2} = 10 * B\left(\frac{1}{\sqrt{x_2}} - \frac{1}{\sqrt{x_1}}\right) \quad \text{Bond} \quad (2)$$

Where:

$E_{1\text{-}2}$ = Specific grinding net energy to grind from particle size x_1 to x_2, kWh/t;

B, R = Constant of the respective equation (i.e., Bond and Rittinger constants are considered to be related to material properties and grinding conditions);

x_1, x_2 are the feed and product particle size respectively, that describes size distribution (80% passing size), microns.

Rittinger and Bond equations were applied to the energy-size data from all the tests listed in Table 1 and the constants were back-calculated for each energy-size pair. Factor 10 is used to conform with standard form of Bond equation.

Theoretically, for a set of grinding tests (same test type and ore type), the constant determined for each of the energy-size pairs should be the same; i.e., one constant should cover the whole test range. This was not the case for the test data analyzed in this study. The model constant for each test set was determined using a solver function to minimize the model error between the model energy output and the energy measured in the testwork. The constant determined for each test set was generally close to the mean of the back-calculated individual energy-size constants for that set of tests.

It was found that, for all the types of laboratory tests, the Bond and Rittinger energy-size models with fixed value constants R and B poorly predicted the experimental results. This was concluded based on the average error (Equation 3) and standard deviation (Equation 4) for each laboratory test set, as reported in the first two columns of Table 2.

$$\text{Average error} \qquad \mu = {\sum yi}/{n} \tag{3}$$

$$\text{Standard deviation} \qquad \delta = \sqrt{{\sum (yi - \mu)^2}/{n}} \tag{4}$$

Where yi are individual errors and n is the total number of data points for the laboratory test type.

It can be observed from Table 2 (first two columns), that the total average model error and standard deviation for individual laboratory data set results were high, mostly 15 - 20% for both Bond and Rittinger models with fixed value constants. Models with such high errors are not useful and the slightly lower errors from the Rittinger model are not worth further discussion.

Table 2 Average error and standard deviation of different forms of the Bond and Rittinger models

Average model errors/Standard Deviation of Model Errors (%)						
Model version	Fixed value Constant		Variable coefficient Linear		Variable coefficient Polynomial/Power	
Lab Test	Rittinger	Bond	Rittinger	Bond	Rittinger	Bond
Isamill	15.3/20.3	16.9/20.1	7.5/9.0	7.5/7.4	3.7/3.7	4.2/3.4
SMD	15.9/16.8	20.2/18.3	7.1/6.9	10.6/6.9	4.1/3.3	5.6/4.2
Batch Ball mill	17.2/18.2	22.0/20.4	10.6/14.8	13.5/13.5	8.5/3.8	8.6/4.6
Tower mill	9.6/11.2	11.0/12.1	4.8/5.9	4.4/4.2	2.7/2.9	2.6/2.9
Levin	14.2/17.4	13.4/15.2	6.0/5.6	6.4/5.5	3.1/4.2	3.4/4.0

Hukki [3] evaluated different energy-size grinding models (including Bond and Rittinger) and suggested that all models were valid, but each within a certain size range, as shown in Figure 2. Hukki observed that the energy requirements for breakage increase as particle size decreases and concluded that the exponent of the size terms in the energy-size relationship (or slope of the relationship) varies with size and material. Based

on this, it is not unexpected that the Rittinger model had lower errors for these fine grinding tests; however, the error is still too large for the model to be useful.

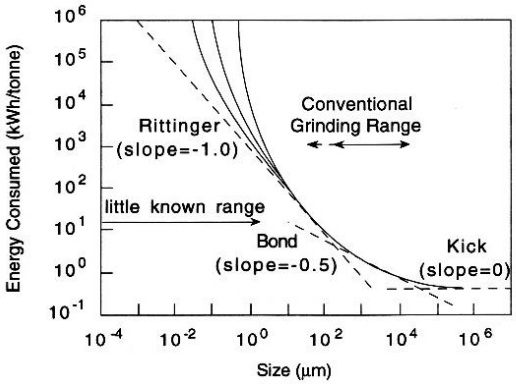

Figure 2 Relationship between energy input and particle size in comminution [3]

Considering the relationship between comminution energy and particle size, and to investigate reasons for poor predictions and how model error could be improved, the back-calculated set of constants were plotted against the product size (P80). Various "best fit" trends were found for each of the data sets, including linearly increasing and decreasing, polynomial and power trends. A small fraction of data had no trend. Some examples where the back calculated "constants" were strongly related to P80 are shown in Figure 3.

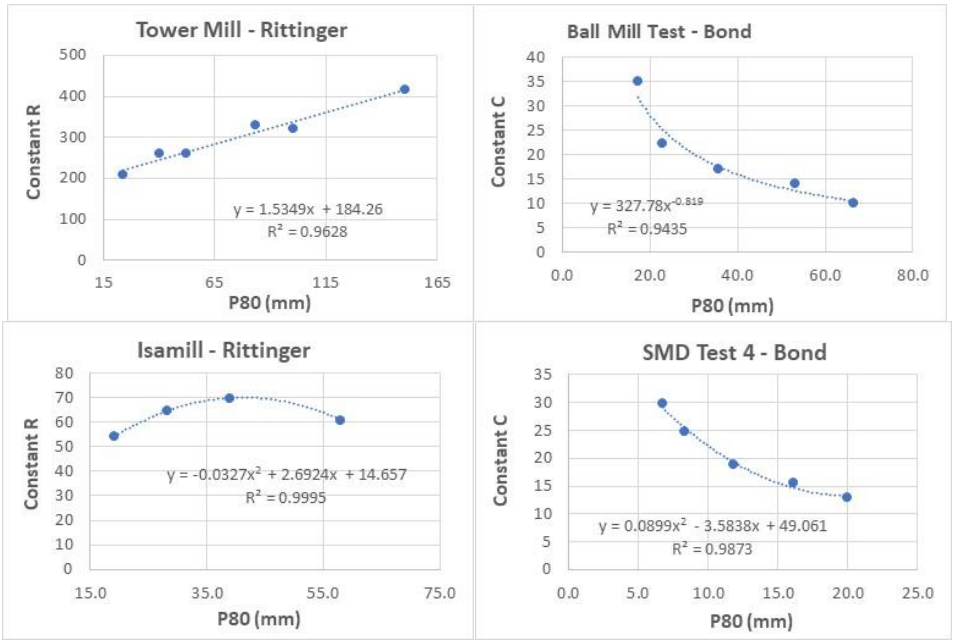

Figure 3 Examples of Bond and Rittinger constants dependance on product size P80

Based on the above analysis, it could be concluded that, for the laboratory tests data sets used in this study, the so called "constants" in Rittinger and Bond equations (Equations 1 and 2) are a function of grinding product size P80, see Equation 5.

$$B, R = f(P80) \tag{5}$$

Therefore, B and R are variable coefficients (rather than constants) and Rittinger (1) and Bond (2) equations could be modified accordingly to equations 6 and 7, respectively.

$$E_{1-2} = 10 * f_R(x_2)\left(\frac{1}{x_2} - \frac{1}{x_1}\right) \quad \text{modified Von Rittinger} \tag{6}$$

$$E_{1-2} = 10 * f_B(x_2)\left(\frac{1}{\sqrt{x_2}} - \frac{1}{\sqrt{x_1}}\right) \quad \text{modified Bond} \tag{7}$$

Where:

x_1, x_2 are the product and feed particle size respectively, usually known as F80 and P80, µm

$f_R(x_2)$ Rittinger model variable coefficient, function of product size x_2.

$f_B(x_2)$ Bond model variable coefficient, function of product size x_2.

Applying the modified Bond and Rittinger equations improves the predictions significantly, as shown in Table 2. The results using a linear trend for the variable coefficients are shown in the third and fourth columns and with Polynomial/Power trends in the last two columns.

It can be observed that the total average model errors and standard deviations more than halved for both Bond and Rittinger models using linear variable coefficient compared to the models with fixed value constant. When the "best fit" variable coefficient trends (Polynomial/Power) were used, the errors were further reduced to below 5% in most cases (the average error was a bit higher for the Batch Ball mill test). Models are usually considered good if the errors are expected to be below 5%.

It is not possible to determine from this analysis which of the two models (modified Bond or modified Rittinger) may be better to use for fine grinding. Further analysis of the individual tests would be required to verify this. The results are expected to be published in follow up papers.

The experimental and Bond model predicted specific energy consumptions (kWh/t) for the SMD data set with the standard and modified models are compared in Figure 4. The error reduction can be clearly observed. Similar comparison was obtained for the other laboratory tests for both Bond and Rittinger models. The small errors confirm that the modified models could be used to describe the laboratory test results discussed in this work.

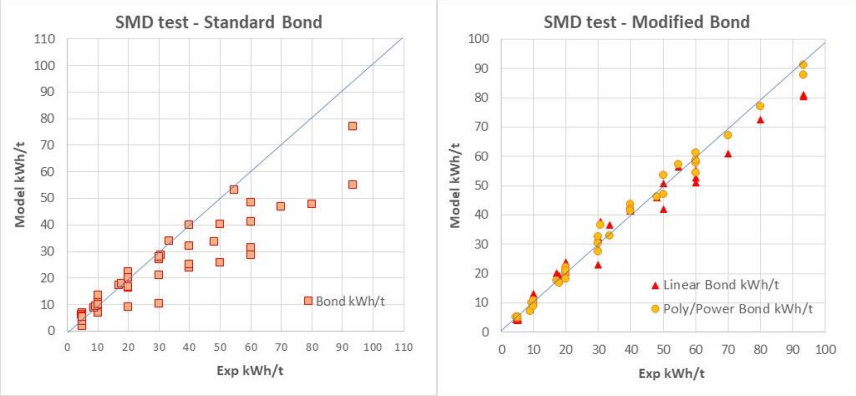

Figure 4 Standard and Modified Bond model predictions for SMD tests

CONCLUSION

Fine grinding consumes greater energy and often uses different technology (with different dominant breakage mechanisms) to coarser grinding applications. Bond and Rittinger size-energy relationships are commonly used for conventional coarser grinding applications, but when applied to data sets from fine grinding laboratory tests including Isamill, SMD, Levin, Tower mill and batch ball mill tests, the errors were high. The average model standard errors and standard deviations for each set of test data were in the range of 15 - 20%, and as such these models would not be usable.

It was found that the constants in the Bond and Rittinger models are strongly related to product size in most of the fine grinding cases investigated, and this was the major reason for poor model performance. Replacing the model constants with variable coefficients which are a function of product size dramatically improved the accuracy of the models, with errors reduced to mostly below 5% for both models. These small errors confirm that the modified Bond and Rittinger models with variable coefficient could be used to describe the fine grinding laboratory test results discussed in this work. Further analysis of the individual tests would be required to determine if either of the two models (modified Bond or modified Rittinger) is more suitable for modelling of fine grinding. The results of this analysis will be published in subsequent papers.

ACKNOWLEDGEMENT

The authors would like to thank Hatch for granting permission to publish this work.

REFERENCES

1. Gupta, A., Yan, D.S. (2016) Stirred mills – ultrafine grinding. In: A. Gupta, D.S. Yan (Eds.), Mineral Processing Design and Operations: An Introduction (Second Edition), Elsevier, ISBN: 9780444635921.
2. de Bakker, H. (2014) Energy use of fine grinding in mineral processing. Metall. Mater. Trans. E 1E, 8–19, https://doi.org/10.1007/s40553-013-0001-6.

3. Hukki, R.T. (1961) “Proposal for a Solomonic Settlement between the Theories of von Rittinger, Kick and Bond,” Transactions on AIME, Vol. 220, pp. 403-408.
4. Jankovic, A. (2003) Variables affecting the fine grinding of minerals using stirred mills, Miner. Eng. 16, 337–345, https://doi.org/10.1016/S0892-6875(03)00007-4.
5. Wills, B.A., Finch, J.A. (2016) Chapter 7 – Grinding mills. In: B.A. Wills, J.A. Finch (Eds.), Wills’ Mineral Processing Technology (Eighth Edition) - An Introduction to the Practical Aspects of Ore Treatment and Mineral Recovery, Butterworth-Heinemann, ISBN 9780080970530.
6. Lynch, A.J., Rowland, C.A. (2005) The History of Grinding, Society for Mining, Metallurgy and Exploration, ISBN: 9780873352383.
7. Mazzinghy, D.B., Alves, V.K., Schneider, L.C., Galery, R., Faria, P.M.C., Alvarenga, T. (2012) Predicting the size distribution in the product and the power requirements of a pilot scale Vertimill. In Proceedings of Procemin 2012 Conference. Santiago, Chile.
8. Glencore Technology, IsaMill™: Breaking the Boundaries [brochure], Available on line at: http://www.isamill.com/EN/Downloads/Brochures/IsaMillBrochure.pdf 2015.
9. Jankovic, A. (1999) Mathematical modelling of stirred mills, Ph.D. Thesis –University of Queensland, JKMRC, Brisbane, Australia.
10. Levin, J. (1989) Observations on the Bond standard grindability test, and a proposal for the standard grindability test for fine materials, J. South. Afr. Inst. Min. Metall. 89 (1), 13–21. ISSN: 0038/223X/3.00.

XV International Mineral Processing and Recycling Conference
17-19 May 2023, Belgrade, Serbia

OPTIMIZATION OF MICRONIZING ZEOLITE GRINDING USING ARTIFICIAL NEURAL NETWORKS

V. Nikolić#, M. Trumić, D. Tanikić
University of Belgrade, Technical Faculty in Bor, Bor, 19210, Serbia

ABSTRACT – The aim of the experiment was to determine the optimal grinding conditions for obtaining a powder with appropriate physico-chemical and microstructural characteristics that would find its potential application as a binder and ion exchanger in structural composites. The analysis of certain classes of zeolite size after micronization was performed through grinding kinetics. An artificial neural network was developed based on the obtained results, and then compared with the obtained experimental results.

Keywords: Zeolite, Micronizing Grinding, Specific Surface, Artificial Neural Networks.

INTRODUCTION

The process of micronizing grinding is intended to grind the mineral raw material to particles of micron size and thus prepare it for direct application or for further technological processing. The application of a prolonged micronization procedure in a certain time interval under certain conditions increases the specific surface area of the treated powder, improves the reactivity and pozzolanic activity of the zeolite material, increases the cation exchange capacity and agglomerates the samples. [1, 2]. The main problem related to mirconizing grinding at the industrial level is in the sustainability of this procedure in economic terms, so an ideal balance must be found between the achieved properties of the treated material on the one hand and the time and energy consumption for the process on the other.

Recently, artificial neural networks are increasingly used in modeling and optimizing the grinding process. Flament et al. (1993) [3, 4] in their paper considered the identification of the dynamics and reverse dynamics of a simulated grinding cycle, using neural networks. Ma et al. (2009) [5] developed a series of artificial neural networks (ANN) for the analysis and prediction of correlations between process parameters and morphological characteristics of nanocomposite WC-18 % MgO powders using the backward error propagation algorithm (BP). Ahmadzadeh and Lundberg (2013) [6] in their work tested different methods of predicting the wear of the lining from the mill, in the context of the remaining height and the remaining service life of the lining. In their second work, Ahmadzadeh and Lundberg (2013) [7] attempted to develop a method that predicts the remaining service life of a coating, without the need to stop the mill. Singh et al. (2013) [8] developed a wrestling neural network model to predict the distribution of the granulometric composition of grinding products using available grinding data for different chromite ore grindability. Terzić et al. (2017) [9] examined the mechano-

corresponding author: vnikolic@tfbor.bg.ac.rs

chemical activation of bentonite clay in an ultra-centrifugal mill, to obtain a material that is used as a binder and sorbent in building composites due to its physical-mechanical and microstructural characteristics. Terzić et al. (2017) [10] in their second work examined the mechano-chemical activation of natural clinoptilolite-type zeolite from seven deposits in an ultra-centrifugal mill, for the production of powder with appropriate physicochemical and microstructural characteristics that can be used as a binder and ion exchanger in structural composites. Farizhandi et al. (2020) [11] used a planetary mill to develop a rapid assessment procedure to identify the characteristics of powders and granular materials. The modeling of an artificial neural network in this paper aims to optimize the process of micronizing grinding (in order to obtain the shortest time of micronizing grinding, the lowest energy consumption), to obtain materials with the best properties.

EXPERIMENTAL

Materials

The paper plans to examine the dry micronization of zeolite, using modern methods for determining the physicochemical and mineralogical characteristics of micronized zeolite products, and changes in parameters that determine the operation of the vibrating mill with rings, as well as quality analysis of micronizing powder. Based on the obtained results of micronizing grinding, the results will be predicted using artificial neural networks, in order to determine the best grinding conditions and the optimal product.

The zeolite sample is gray, while the crystals are lithocrystalloclastic to crystalloclastic. It contains about 90 % zeolite, in a smaller amount quartz, feldspar, mica and calcite and traces of ilite. The zeolite sample was crushed in a laboratory jaw crusher to an upper limit size of 3.35 mm. For further research, four classes of size (-3.35+0; -3.35+2.36; -2.36+1.18; -1.18+0) mm and different starting masses (50 g, 100 g, 200 g) which were subjected to micronizing grinding.

Micronizing grinding

Micronizing grinding of zeolite was performed in a laboratory vibrating mill with rings of the type "SIEBTECHNIK TS-250", at a speed of 1000 rpm in a time interval of 20s, 45s, 75s, 120s, 300s, 900 seconds. The content of the size class (-5+0) μm and the specific surface area were monitored on each grinding product.

Modeling of artificial neural networks

In this research, models based on the Multi-Layer Perceptron were used, which in principle consist of three layers (input layer, hidden layer and output layer). The input values of this model were: size class, grinding time and initial mass of the sample, while the output values were: the content of the size class (-5+0) μm and the specific area.

RESULTS AND DISCUSSION

The increase in the time of micronizing grinding led to a change in the characteristics

of zeolite and the manifestation of differences between unground and ground zeolite. The results of micronizing grinding are shown in Tables 1-4.

Table 1 Content of the size class (-5+0) μm of the sample (-3.35+0) mm, after micronizing grinding, starting masses (50, 100 and 200) g

50 g						
Time	**20 s**	**45 s**	**75 s**	**120 s**	**300 s**	**900 s**
Size class (μm)	- 5 + 0	- 5 + 0	- 5 + 0	- 5 + 0	- 5 + 0	- 5 + 0
W (%)	95.90	97.40	95.86	94.08	81.04	80.18
Spec. surface area (m^2/kg)	1056.02	1070.77	1056.65	1036.41	895.96	888.22
100 g						
Time	**20 s**	**45 s**	**75 s**	**120 s**	**300 s**	**900 s**
Size class (μm)	- 5 + 0	- 5 + 0	- 5 + 0	- 5 + 0	- 5 + 0	- 5 + 0
W (%)	90.98	94.15	95.83	94.31	82.11	64.99
Spec. surface area (m^2/kg)	1006.26	1039.44	1055.46	1038.20	908.23	723.16
200 g						
Time	**20 s**	**45 s**	**75 s**	**120 s**	**300 s**	**900 s**
Size class (μm)	- 5 + 0	- 5 + 0	- 5 + 0	- 5 + 0	- 5 + 0	- 5 + 0
W (%)	83.22	92.49	93.48	93.39	90.76	71.49
Spec. surface area (m^2/kg)	922.29	1020.16	1031.95	1031.64	1001.81	797.52

Table 2 Content of size class (-5+0) μm of sample (-3.35+2.36) mm, after micronizing grinding, starting masses (50, 100 and 200) g

50 g						
Time	**20 s**	**45 s**	**75 s**	**120 s**	**300 s**	**900 s**
Size class (μm)	- 5 + 0	- 5 + 0	- 5 + 0	- 5 + 0	- 5 + 0	- 5 + 0
W (%)	93.03	95.71	94.63	91.64	81.03	76.78
Spec. surface area (m^2/kg)	1027.67	1053.86	1042.69	1012.06	897.11	852.43
100 g						
Time	**20 s**	**45 s**	**75 s**	**120 s**	**300 s**	**900 s**
Size class (μm)	- 5 + 0	- 5 + 0	- 5 + 0	- 5 + 0	- 5 + 0	- 5 + 0
W (%)	89.92	94.83	95.34	94.78	86.63	74.49
Spec. surface area (m^2/kg)	996.46	1046.60	1050.40	1045.26	957.48	826.11
200 g						
Time	**20 s**	**45 s**	**75 s**	**120 s**	**300 s**	**900 s**
Size class (μm)	- 5 + 0	- 5 + 0	- 5 + 0	- 5 + 0	- 5 + 0	- 5 + 0
W (%)	77.75	90.72	93.01	95.33	92.97	76.82
Spec. surface area (m^2/kg)	864.01	1002.84	1027.77	1050.04	1024.66	849.60

Table 3 Content of size class (-5+0) μm of sample (-2.36+1.18) mm, after micronizing grinding, initial masses (50, 100 and 200) g

50 g						
Time	**20 s**	**45 s**	**75 s**	**120 s**	**300 s**	**900 s**
Size class (μm)	- 5 + 0	- 5 + 0	- 5 + 0	- 5 + 0	- 5 + 0	- 5 + 0
W (%)	94.12	96.53	96.37	93.04	85.80	79.29
Spec. surface area (m^2/kg)	1039.29	1062.18	1060.31	1026.50	946.92	878.86
100 g						
Time	**20 s**	**45 s**	**75 s**	**120 s**	**300 s**	**900 s**

Table 3 continued Content of size class (-5+0) μm of sample (-2.36+1.18) mm, after micronizing grinding, initial masses (50, 100 and 200) g

Size class (μm)	- 5 + 0	- 5 + 0	- 5 + 0	- 5 + 0	- 5 + 0	- 5 + 0
W (%)	93.44	93.62	93.94	93.83	84.54	70.48
Spec. surface area (m^2/kg)	1029.96	1035.05	1037.55	1036.92	935.84	784.92
200 g						
Time	**20 s**	**45 s**	**75 s**	**120 s**	**300 s**	**900 s**
Size class (μm)	- 5 + 0	- 5 + 0	- 5 + 0	- 5 + 0	- 5 + 0	- 5 + 0
W (%)	81.80	92.42	95.61	95.69	93.65	75.18
Spec. surface area (m^2/kg)	906.09	1019.29	1054.08	1054.56	1032.70	833.96

Table 4 Content of size class (-5+0) μm of sample (-1.18+0) mm, after micronizing grinding, starting masses (50, 100 and 200) g

50 g						
Time	**20 s**	**45 s**	**75 s**	**120 s**	**300 s**	**900 s**
Size class (μm)	- 5 + 0	- 5 + 0	- 5 + 0	- 5 + 0	- 5 + 0	- 5 + 0
W (%)	96.28	96.15	92.75	91.72	86.98	82.84
Spec. surface area (m^2/kg)	1059.86	1058.75	1026.59	1015.20	961.18	919.22
100 g						
Time	**20 s**	**45 s**	**75 s**	**120 s**	**300 s**	**900 s**
Size class (μm)	- 5 + 0	- 5 + 0	- 5 + 0	- 5 + 0	- 5 + 0	- 5 + 0
W (%)	92.87	94.50	95.20	94.16	88.86	66.78
Spec. surface area (m^2/kg)	1025.54	1042.88	1049.27	1038.06	980.73	745.39
200 g						
Time	**20 s**	**45 s**	**75 s**	**120 s**	**300 s**	**900 s**
Size class (μm)	- 5 + 0	- 5 + 0	- 5 + 0	- 5 + 0	- 5 + 0	- 5 + 0
W (%)	82.41	92.72	94.37	93.87	90.60	76.17
Spec. surface area (m^2/kg)	912.77	1023.59	1040.74	1036.79	1001.55	844.26

As the time of micronized grinding increases, the content of the class (-5+0) μm and the specific surface area [7] increase until a certain grinding time, and after that it is assumed that agglomeration of samples occurs. For all samples, the optimal grinding time is between (45 and 75) seconds, during which time the sample is crushed and the specific surface area is increased, while after that time the specific surface area is reduced and the agglomeration is assumed.

Modeling of micronizing zeolite grinding

The input sizes of the models were: size classes (-3.35+0 mm; -3.35+2.36 mm; -2.36+1.18 mm; -1.18+0 mm), grinding time (20 s, 45 s, 75 s, 120 s, 300 s, 900 s) and the initial mass of the sample (50 g, 100 g, 200 g), while the output values were: content of the size class (- 5 + 0) μm and specific area. The database used for modeling artificial neural networks in Matlab was divided into three sets: a network training set (70 %), a validation set (15 %) and a testing set (15 %). Testing of the model showed that the network achieves good results, which is shown in Figure 1, having in mind a small set of input-output data. The accuracy of the results is confirmed by a very large coefficient R that ranges (0.989 - 0.997), which gives a satisfactory prediction accuracy.

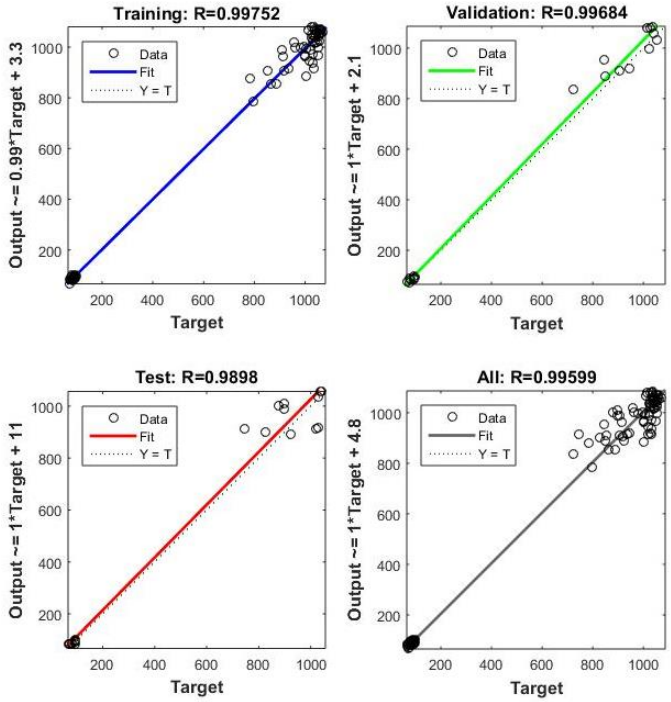

Figure 1 Experimentally obtained values of parameters i values obtained using the ANN model

Figures 2 and 3 show a comparison of the calculated values compared with the experimental data for the optimal artificial neural network.

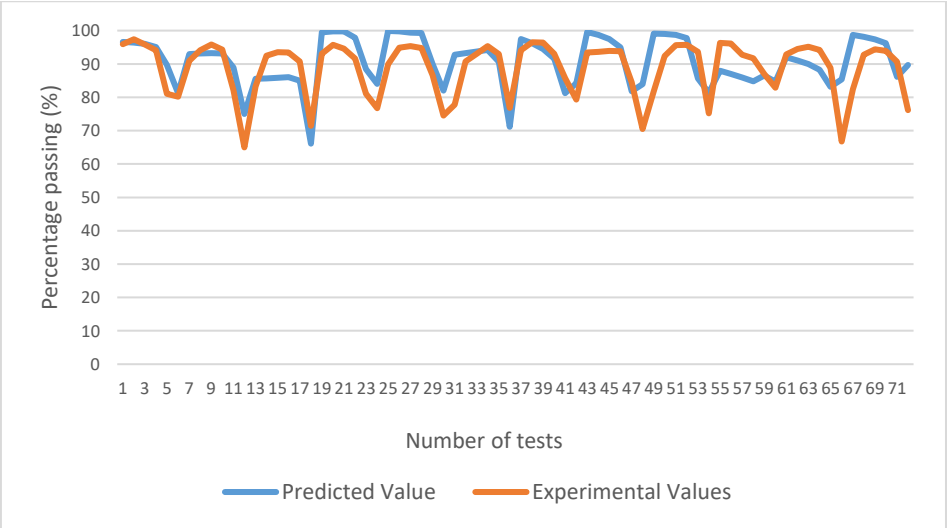

Figure 2 Comparative values of the content of the class (-5+0) μm obtained experimentally andusing the ANN model

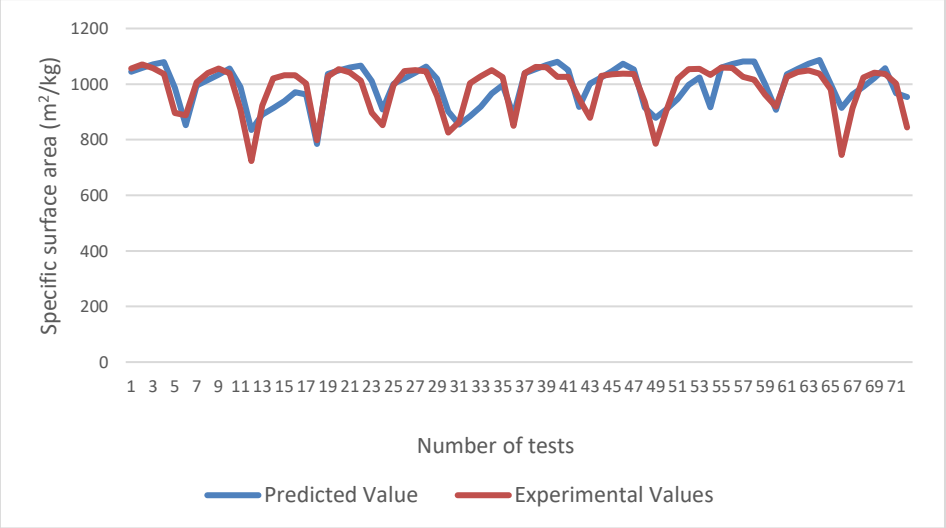

Figure 3 Comparative values of specific surface obtained experimentally and using the ANN model

From diagrams 2 and 3 it can be seen that the modeling of the network is well done, the neural network has well captured the trend of change of curves obtained on the basis of experimental results. It was calculated that the mean error of the obtained model for the content of the size class (-5+0) µm is about 6 %, and for a specific area about 4.5 %, which is considered a very good prediction.

CONCLUSION

The study presents a comprehensive approach of artificial neural networks that can predict the content of the size class (-5+0) µm and the specific surface with great certainty. Neural networks are applied to this grinding process because neural networks rely less on an accurate physical model. Neural networks can be ideal for modeling this complex grinding process, which is the correlation coefficient and confirmed by its predictive accuracy that ranges (0.989 - 0.997).

ACKNOWLEDGEMENT

"The research presented in this paper was done with the financial support of the Ministry of Education, Science and Technological Development of the Republic of Serbia, within the funding of the scientific research work at the University of Belgrade, Technical Faculty in Bor, according to the contract with registration number 451-03-47/2023-01/200131".

REFERENCES

1. Kang, S.J., Egashira, K. (1997) Modification of different grades of Korean natural zeolites for increasing cation exchange capacity. Applied Clay Science, 1-2, 131-144.
2. Villa, C., Pecina, E.T., Torres, R., Gómez, L. (2010) Geopolymer synthesis using alkaline activation of natural zeolite. Construction and Building Materials, 24 (11), 2084-2090.

3. Flament, F., Thibault, J., Hodouin, D. (1993) Neural network based control of mineral grinding plants. Minerals Engineering, 6 (3), 235-249.
4. Thibault, J., Flament, F., Hodouin, D. (1992) Modelling and Control of Mineral Processing Plants Using Neural Networks. IFAC Proceedings Volumes, 25 (17), 25-30.
5. Ma, J., Zhu, S.G., Wu, C.X., Zhang, M.L. (2009) Application of back-propagation neural network technique to high-energy planetary ball milling process for synthesizing nanocomposite WC-MgO powders. Materials and Design, 30, 2867-2874.
6. Ahmadzadeh, F., Lundberg, J. (2013) Application of multi regressive linear model and neural network for wear prediction of grinding mill liners. International Journal of Advanced Computer Science and Applications, 4 (5), 53-58.
7. Ahmadzadeh, F., Lundberg, J. (2013) Remaining useful life prediction of grinding mill liners using an artificial neural network. Minerals Engineering, 53, 1-8.
8. Singh, V., Banerjee, P.K., Tripathy, S.K., Saxena, V.K., Venugopal, R. (2013) Artificial Neural Network Modeling of Ball Mill Grinding Process. Journal of Powder Metallurgy & Mining, 2 (2):1-4.
9. Terzić, A., Pezo, L., Andrić, Lj., Pavlović, V.B., Mitić, V.V. (2017) Optimization of bentonite clay mechano-chemical activation using artificial neural network modeling. Ceramics International, 43, 2549-2562.
10. Terzić, A., Pezo, L., Andrić, Lj. (2017) Chemometric assessment of mechano-chemically activated zeolites for application in the construction composites. Composites Part B, 109, 30-44.
11. Farizhandi, A.A.K., Zhao, H., Chen, T., Lau, R. (2020) Evaluation of material properties using planetary ball milling for modeling the change of particle size distribution in a gas-solid fluidized bed using a hybrid artificial neural network-genetic algorithm approach. Chemical Engineering Science, 215, 1-10.

XV International Mineral Processing and Recycling Conference
17-19 May 2023, Belgrade, Serbia

THE EFFECT OF MICROWAVE RADIATION ON DRY GRINDING KINETICS OF BAUXITE ORE

E. Petrakis[#], K. Komnitsas
Technical University of Crete, School of Mineral Resources Engineering, Chania, Greece

ABSTRACT – The aim of this study is to evaluate the effect of microwave radiation on the grinding kinetics of Greek bauxite ores. In this respect, three mono-sized fractions, namely -3.35+1.70 mm, -0.850+0.425 mm and -0.212+0.106 mm, were prepared and ground individually in a laboratory-scale ball mill at different grinding periods. With the use of kinetic modeling, the breakage rate and breakage function parameters of the untreated and microwave-treated prior to grinding fractions were determined. The results showed that for a given grinding time the grindability of the products, as indicated by the characteristic particle size d_{80}, is improved with increasing power level from 0 to 800 Watt. Also, after microwave radiation about 10-13% increase in breakage rate was achieved. Breakage function parameters showed that more efficient breakage action is achieved when power of 800 Watt is applied to fractions prior to grinding.

Keywords: Grinding, Microwave Radiation, Breakage Rate, Breakage Function.

INTRODUCTION

In the mineral processing plants, the primary goal is to produce a desired product size and liberate the mineral(s) of interest from associated gangue minerals [1]. Comminution, also known as size reduction, which includes the two-unit operations of crushing and grinding, is necessary to obtain the desired product size distribution. Grinding consumes more energy than crushing when comparing the two operations and accounts for more than 50% of the total energy consumption in the mining industry.

With the aim of reducing energy consumption, a number of studies have focused on the optimization of operating parameters, e.g. ball size/shape [2-4], mill speed [5,6] and powder loading [7]. Besides, over the past decades, a growing interest has arisen in the ore pretreatment methods prior to comminution. The main objective of pretreating is to improve the grindability of the ore by creating intergranular cracks, which can reduce the energy required for grinding. Some of these pretreatment methods include thermal via furnace, microwave radiation, chemical additives, electric, magnetic, ultrasonic, as well as bio-milling [8]. Microwave treatment has been highlighted among them as a method for decreasing the costs associated with size reduction compared to conventional heating [9,10].

Microwaves are a form of electromagnetic energy with frequencies in the range of 300 MHz to 300 GHz. Microwave heating takes advantage of the ability of some materials to absorb electromagnetic energy in the microwave spectral range and transform it into

[#] corresponding author: evpetrakis@tuc.gr

heat. Due to the different thermal properties of the minerals present, these ores experience varying degrees of thermal expansion as a result of the differential thermal stresses produced within the lattice. Consequently, when an ore is exposed to microwave radiation prior to the comminution stage, fractures produced at the grain boundaries of two or more minerals expand at different rates and the breakage energy consumption is reduced [11,12].

In order to improve process efficiency, kinetic models based on population balance considerations have been widely applied to ball milling. Population balance modeling (PBM) is based on first-order kinetics and uses two functions, namely the breakage rate (or selection function) and the breakage function, according to Equations (1) and (2) [13].

$$\frac{dR_i(t)}{dt} = -S_i R_i(t) \tag{1}$$

$$B_{i,j} = \frac{log\,[(1-P_i(0)/(1-P_i(t))]}{log\,[(1-P_{j+1}(0))/(1-P_{j+1}(t))]} \tag{2}$$

where, R_i(t) is the mass fraction for size class *i* at grinding time *t*, S_i is the breakage rate of size class *i*, $B_{i,j}$ is the breakage function and represents the mass fraction less than the upper size of size class *i* resulting from primary breakage of size class *j,* and P_i(t) is the mass fraction less than size x_i at time *t*.

The breakage rate can be described by a power function of particle size, as shown in Equation (3),

$$S_i = a_T \cdot x_i^a \cdot q_i \tag{3}$$

where, a_T and *a* are parameters depending respectively on milling conditions and material type, while q_i is a correction factor; q_i is equal to 1 for small particles (normal breakage) and lower than 1 (abnormal breakage) for large particles.

The breakage function $B_{i,j}$ can also be represented by the following empirical Equation (4) [14],

$$B_{i,j} = \Phi_j \cdot \left(\frac{x_{i-1}}{x_j}\right)^{\gamma} + (1-\Phi_j) \cdot \left(\frac{x_{i-1}}{x_j}\right)^{\beta} \tag{4}$$

Φ_j, γ, and β are model parameters. Specifically, γ characterizes the relative mass of fines produced after breakage; lower values of γ imply more effective breakage action with high production of fines. In addition, higher values of Φ_j and β indicate that fractions close to feeding size are ground faster into undersize.

The objective of the present paper is to investigate the effect of microwave radiation on dry grinding kinetics of bauxite ores.

EXPERIMENTAL

Greek bauxite ore from the mining company Delphi-Distomon S.A. was the material used in the present study. The ore is a typical red-brown (Fe-rich) bauxite consisting of aluminum-bearing minerals. Chemical analysis through X-ray fluorescence (XRF)

spectroscopy showed that the main oxides present are Al_2O_3 and Fe_2O_3 assaying 56.85 and 22.97 wt%, respectively. The mineralogical analysis revealed that the main aluminum containing phases present in the ore are diaspore [α-AlO(OH)] and boehmite [γ-AlO(OH)], while the gangue minerals include hematite [Fe_2O_3], anatase [TiO_2] and kaolinite [$Al_2Si_2O_5(OH)_4$].

The received sample was initially crushed to -3.35 mm using a jaw crusher and the product obtained was sieved using a series of sieves to prepare three mono-sized fractions, namely -3.35+1.70 mm, -0.850+0.425 mm and -0.212+0.106 mm. Each fraction was used as feed to the mill. The grinding tests were carried out using a laboratory-scale ball mill operated at a constant speed of 66 rpm corresponding to 70% of its critical speed. Different grinding times, namely 0.5, 2, and 4 min were considered, while the mill charge was made up of stainless steel balls of three different sizes, i.e. 25.4, 12.7 and 6.5 mm. The ball and material filling volume was kept constant at 20% and 4%, respectively.

Microwave radiation was applied to the prepared material fractions using a kitchen-type oven of variable power (0-800 W) and a frequency of 2.45 GHz. Samples were placed in the oven in a microwave-transparent Pyrex glass beaker and exposed to microwave radiation for a short period of 3 min.

RESULTS AND DISCUSSION

Particle size distribution

The grinding tests conducted using mono-size fractions showed that the particle size distribution curves of the products vary depending on the microwave power level. In this regard, Figures 1a-c present the product particle size d_{80} as a function of grinding time for three feed fractions when different microwave power levels were applied prior to grinding. The results show that for a given grinding time the grindability of the products, as indicated by the characteristic particle size d_{80}, is improved with increasing power level from 0 to 800 Watt. The improvement is more pronounced for the products obtained after 4 min of grinding. Specifically, particle size d_{80} decreased by 1.4, 4.1 and 4.2% at grinding time 4 min for the -3.35+1.70 mm, -0.850+0.425 mm and -0.212+0.106 mm feed fractions when the power increased from 0 to 800 Watt.

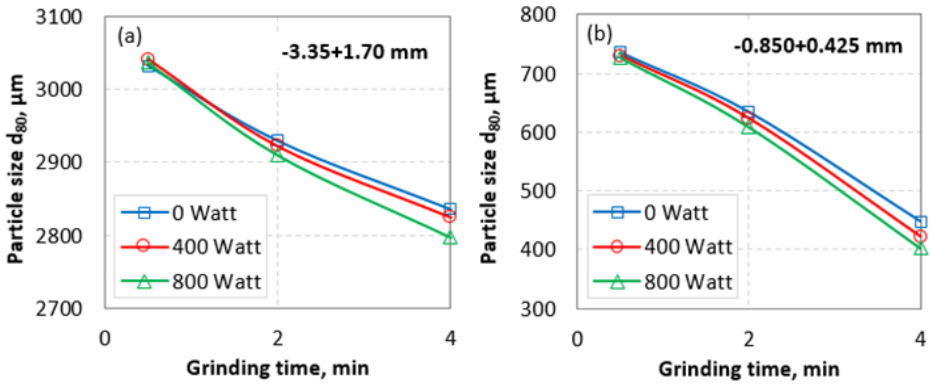

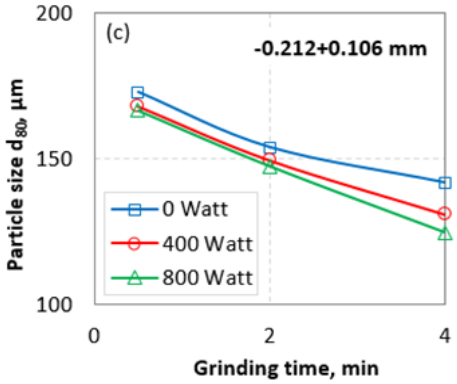

Figure 1 Product particle size d_{80} versus grinding time for three size fractions when different power levels were applied to feed fractions prior to grinding

Determination of the breakage rate and breakage function parameters

Figures 2a-c show in normal-log plots the remaining mass percentage for each feed fraction as a function of grinding time under the assumption that grinding exhibits first-order behavior.

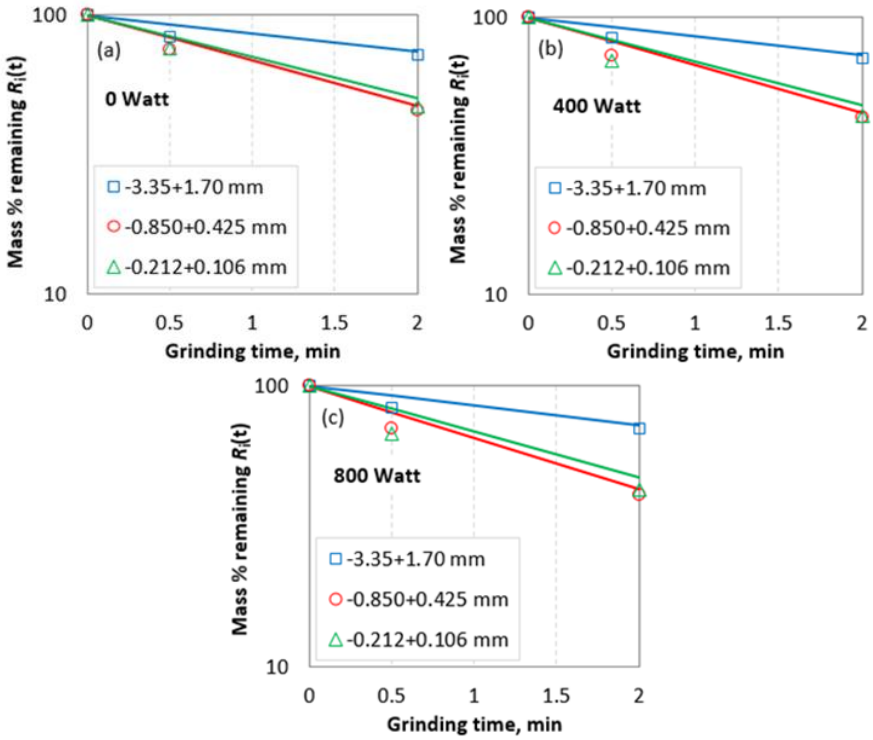

Figure 2 First-order plots of the mass (%) remaining vs. grinding time for three feed fractions when different power levels were applied to feed fractions prior to grinding

The results indicate that for a given power level, the breakage rate S_i determined from the slope of the straight lines increases with increasing feed fraction and then drops as the size becomes coarser. This implies that there is an optimum feed size (ranging from 0.66 to 0.70 mm) for which the breakage rate obtains its maximum value, but above this size coarse particles cannot be effectively ground by the grinding media. The maximum breakage rate determined was 0.38, 0.40 and 0.43 min^{-1} when respectively 0, 400 or 800 Watt was applied to feed fractions prior to grinding. The variation of breakage rate S_i with the upper feed size for different power levels is shown in Figure 3. It is apparent that the increase of S_i is linear up to the optimum size and the slope of this linear part for the different power levels remains almost constant. The beneficial effect of microwave radiation on the grindability of the three feed fractions is also shown in Table 1, which presents the S_i values along with the breakage rate parameters. More specifically, 10.1, 12.8 and 10.6% increase in the breakage rate was achieved respectively for the feed fractions -3.35+1.70 mm, -0.850+0.425 mm, -0.212+0.106 mm when power of 800 Watt was applied prior to grinding. The α_T parameter which indicates the breakage rate at size x_i=1 mm also increases with increasing power level from 0 to 800 Watt.

The BII method presented in Equation (2) was used to determine the values of breakage function $B_{i,j}$ from the size distribution obtained after short periods of grinding. Afterwards, the $B_{i,j}$ values were fitted into the empirical model presented in Equation (4) and the breakage function parameters Φ_j, γ and β were determined. As a rule of thumb, the number of parameters should be reduced for an optimal fitting, thus β parameter was kept constant and only two parameters, namely Φ_j and γ were adjusted to better fit the data.

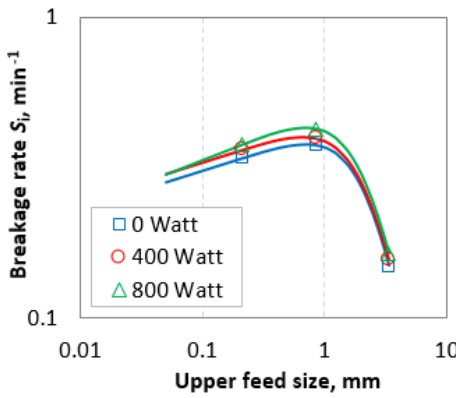

Figure 3 Variation of breakage rate S_i with feed size when different power levels were applied to feed fractions prior to grinding

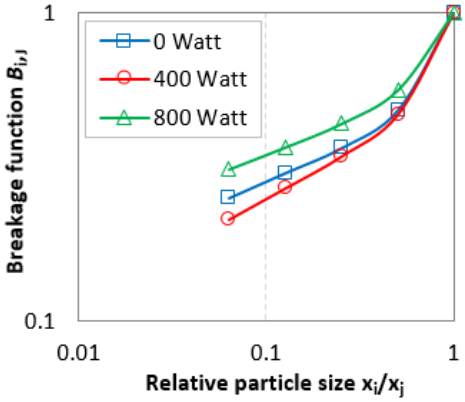

Figure 4 Breakage function $B_{i,j}$ versus relative particle size when different power levels were applied to feed fractions prior to grinding

Figure 4 presents, as an example, the breakage distribution plots of the -3.35+1.70 mm fraction when different power levels were applied prior to grinding. The model parameters shown in Table 1 reveal that γ is lower (0.26) when power of 800 Watt was applied to this fraction prior to grinding indicating more efficient breakage action with

high proportion of fines, e.g. the mass of the -106 μm fraction increased by about 1.5%. In addition, the higher value of Φ_j (0.63) implies that fractions close to feeding size are ground faster into undersize.

Table 1 Breakage rate and breakage function parameters

Power (W)	$S_{i/3.35}$ min^{-1}	$S_{i/0.850}$ min^{-1}	$S_{i/0.212}$ min^{-1}	a_T min^{-1}	a	$\Phi_{j/3.35}$	$\gamma_{/3.35}$	$\beta_{/3.35}$
0	0.149	0.376	0.341	0.420	0.133	0.53	0.28	3.50
400	0.156	0.396	0.364	0.450	0.133	0.54	0.33	3.50
800	0.164	0.424	0.377	0.490	0.165	0.63	0.26	3.50

CONCLUSION

The application of microwave radiation to bauxite ore fractions prior to grinding has a beneficial effect on their grindability. As indicated by the characteristic particle size d_{80} of the grinding products, finer particle size distribution is achieved when the power level increases from 0 to 800 Watt. Grinding kinetic modeling revealed that microwave radiation increases the breakage rate by 10-13 %. Breakage function parameters showed that more efficient breakage action with high proportion of fines is achieved when power of 800 Watt is applied to fractions prior to grinding.

REFERENCES

1. Petrakis, E., Komnitsas, K. (2021) Development of a Non-linear Framework for the Prediction of the Particle Size Distribution of the Grinding Products. Mining Metall. Explor., 38, 1253-1266.
2. Katubilwa, M.F., Moys, H.M. (2009) Effect of ball size distribution on milling rate. Miner. Eng., 22, 15.
3. Kolev, N., Bodurov, P., Genchev, V., Simpson, B., Melero, M.G., Menéndez-Aguado, J.M. (2021) A Comparative Study of Energy Efficiency in Tumbling Mills with the Use of Relo Grinding Media. Metals, 11, 735.
4. Liao, N., Wu, C., Li, J., Fang, X., Li, Y., Zhang, Z., Yin, W. (2022) A Comparison of the Fine-Grinding Performance between Cylpebs and Ceramic Balls in the Wet Tumbling. Mill. Minerals, 12, 1007.
5. Mulenga, F.K., Moys, M.H. (2014) Effects of slurry filling and mill speed on the net power draw of a tumbling ball mill. Miner. Eng., 56, 45-56.
6. Bian, X., Wang, G., Wang, H., Wang, S., Lv, W. (2017) Effect of lifters and mill speed on particle behaviour, torque, and power consumption of a tumbling ball mill: Experimental study and DEM simulation. Miner. Eng., 105, 22-35.
7. Shin, H., Lee, S., Jung, H.S., Kim, J-B. (2013) Effect of ball size and powder loading on the milling efficiency of a laboratory-scale wet ball mill. Ceram. Int., 39, 8963-8968.
8. Adewuyi, S.O., Ahmed, H.A.M., Ahmed, H.M.A. (2020) Methods of Ore Pretreatment for Comminution Energy Reduction. Minerals, 10, 423.
9. Fitzgibbon, K.E., Veasey, T.J. (1980) Thermally assisted liberation—a review, Miner. Eng., 3 (1/2), 181-185.

10. Omran, M., Fabritius, T., Mattila, R. (2015) Thermally assisted liberation of high phosphorus oolitic iron ore: A comparison between microwave and conventional furnaces. Powder Technol., 269, 7-14.
11. Sahyoun, C., Kingman, S.W., Rowson, N.A. (2004) High powered microwave treatment of carbonate copper ore. EJMP & EP, 4 (3), 175-182.
12. Somani, A., Nandi, T.K., Pal, S.K., Majumder, A.K. (2017) Pre-treatment of rocks prior to comminution – A critical review of present practices. Int. J. Min. Sci. Technol., 27, 339-348.
13. Austin, L.G., Klimpel, R.R., Luckie, P.T. (1984) Process Engineering of Size Reduction: Ball Milling. SME–AIME, New York.
14. Austin, L.G., Luckie, P.T. (1972) Methods for determination of breakage distribution parameters. Powder Technol., 5, 215–222.

XV International Mineral Processing and Recycling Conference
17-19 May 2023, Belgrade, Serbia

LSTM AND CNN COMBINATION BASED MODELLING APPROACH FOR PARTITION CURVE PREDICTION IN HYDROCYCLONES

M. H. Tyeb, S. Mishra, A. K. Majumder[#]
Indian Institute of Technology Kharagpur, Kharagpur, W.B., India

ABSTRACT – An attempt has been in this study to develop a novel artificial neural network (ANN) modelling approach for prediction of the complete partition curves at varying hydrocyclone design and operating conditions. Experimental data generated on a 50.8 mm diameter hydrocyclone test rig considering four primary process variables, was used for model development. The developed multi-output regression ANN model employed Long Short-Term memory (LSTM) and convolutional neural network (CNN) layers to process the sequential size distribution data. The model adequately predicted sets of partition coefficients based on the model inputs consisting of size distribution and process variable information.

Keywords: Hydrocyclone, LSTM, CNN, ANN, Partition Curve.

INTRODUCTION

The separation performance of hydrocyclones is typically assessed through a partition curve which is a graphical plot between particle sizes and their respective recoveries to the oversize product (partition coefficients). Characteristic parameters derived from the partition curves like the separation cut size (d_{50}) and the Ep value are used to quantitatively represent the particle separation behavior. Empirical models have been extensively developed by various researchers for the prediction of hydrocyclone process and performance parameters [1-3].

CFD and numerical modelling approaches have also been attempted by several researchers towards delivering phenomenological process models for hydrocyclones [4-6]. Some researchers have also adopted the artificial neural network (ANN) pathways to develop predictive models for hydrocyclone process and performance [7,8]. However, the CFD models inherently feature high computational complexity, especially when dealing with the hydrodynamic complexity of the multiphase bidirectional vortical flow prevailing inside hydrocyclones. Whereas other models aim to predict the separation performance only in simple parametric forms such as prediction of d_{50} and Ep values. Despite being characteristic parameters, d_{50} and Ep values fail to represent some common features of the partition curve like the bypass, fish hook, and overflow short circuiting, leading to loss of potentially crucial process information [9]. Thus, modelling of the complete partition curves across the full particle size spectrum is crucial for hydrocyclone process monitoring and optimization. The prediction of complete partition curves essentially warrants the prediction of discrete partition coefficients corresponding to different particle sizes for specific process conditions. This constitutes

[#] corresponding author: akm@mining.iitkgp.ac.in

a multi-output regression problem made complex by the plethora of impactful process variables. Artificial Neural Networks have the requisite versatility to handle such modelling challenges.

This study had the objective to develop a neural network modelling approach for the prediction of the entire partition curves, potentially allowing for enhanced process monitoring and optimization capability. The developed multi-output regression model which gave the partition coefficient values as its output, was trained and tested on the experimental data generated on a laboratory hydrocyclone test rig for this study.

MATERIAL AND METHODS

Experimental details

A detailed experimental study was carried out to generate relevant experimental data for different hydrocyclone operating conditions with pure silica sand slurry as the feed. A closed circuit hydrocyclone test rig consisting of a positive displacement pump and sump assembly with a hydrocyclone diameter of 50.8 mm was used for generating the requisite experimental data. The geometrical features of the hydrocyclone used for the experimentation along with the dimensional details are shown in figure 1(a). An illustrative sketch of the experimental test rig used is shown in figure 1(b).

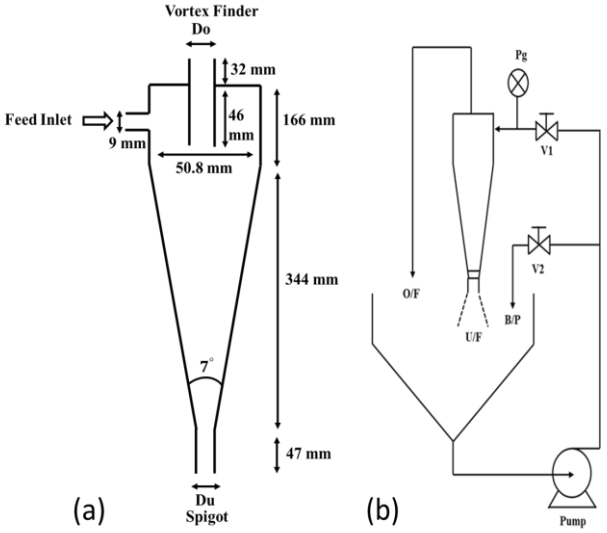

Figure 1 (a) Geometrical features of hydrocyclone used for experimentation (b) An illustrative sketch of the hydrocyclone test rig

For a given combination of spigot and vortex finder diameter, feed was tangentially introduced into the hydrocyclone system through the feed inlet at different levels of feed inlet pressures and feed solid concentrations. The feed solid characteristics remained consistent throughout the experimental runs. The details and the levels of the 4 primary design and operating variables considered for this study are provided in table 1.

Table 1 Details of the design and process variables in the experimental work

Experimental variables	Level values
Vortex Finder Diameter **(V)** (mm)	8, 11, 14
Spigot Diameter **(S)** (mm)	4.5, 6.4
Feed Solid Concentration **(C)** (wt.%)	1, 3, 5, 7, 10, 12.5
Feed inlet pressure **(P)** (N/m^2 $x10^4$)	6.9, 13.8, 20.7, 27.6, 34.5

For carrying out the experimental runs, 6 unique combinations of available vortex finder and spigot diameter were used. For every combination of vortex finder and spigot diameter, experiments were conducted for all five inlet pressure levels at different feed solid concentration levels. In each case of the outlet combinations, the feed solid concentration levels were increased and considered only up to the point of appearance of the roping phenomenon, so that all the experimental data considered for the modelling exercise corresponds to the spray discharge regime of the hydrocyclone. A total of 106 experimental data sets were generated on the hydrocyclone test rig and have been utilized for the modelling purposes. The samples collected from the experiments were analysed using a laser diffraction size analyser (Anton Paar 1099).

Neural Network Modelling

Before commencing with the modelling, the data sets of 15 random experimental conditions out of the 106 datasets generated, were isolated for testing purposes. The primary goal was to develop a model which can take the 4 primary design and operating variables along with the feed size distribution data as inputs, and then produce an output with the values of the partition coefficients corresponding to the size classes present in the input size distribution data. Thus, the input strategy of the model involved setting up two different parallel input layers for feeding the size distribution data and the 4 primary variables separately. The experimental results furnished a partition curve composed of 30 distinct points of particle size vs. partition values for each experimental run. For the sake of augmenting the volume of training data, 30 sets of randomly sampled 15 pairs of size and cumulative passing values, were generated and ascendingly sorted from each of the 91 experimental datasets considered for training. In this way, for each unique set of 4 primary variables, there now existed 30 different sets of 15 points essentially representing the same feed size distribution and partition curve, but with distinct set of points. This random sampling was believed to benefit the model training process as the model will get to learn the fact that for the same design and operating conditions, the partition curves may be plotted with different set of points but the overall relationship between size and partition values should remain the same. Feed size distribution data taken in the form of size (μm) vs. cumulative passing values was sequential in nature, and Long Short-Term Memory (LSTM] networks have been shown to be appropriate for sequence modelling and resolving the gradient scaling issues associated with recurrent neural network architectures [10]. Therefore, the feed size distribution was processed using an LSTM layer and a 1D CNN layer in series. The developed multi-output regression

model structure with details of data flow and the type and shape of different layers involved are shown in figure 2. Adaptive moment estimation (ADAM) algorithm was used with a dynamic learning rate for model optimization.

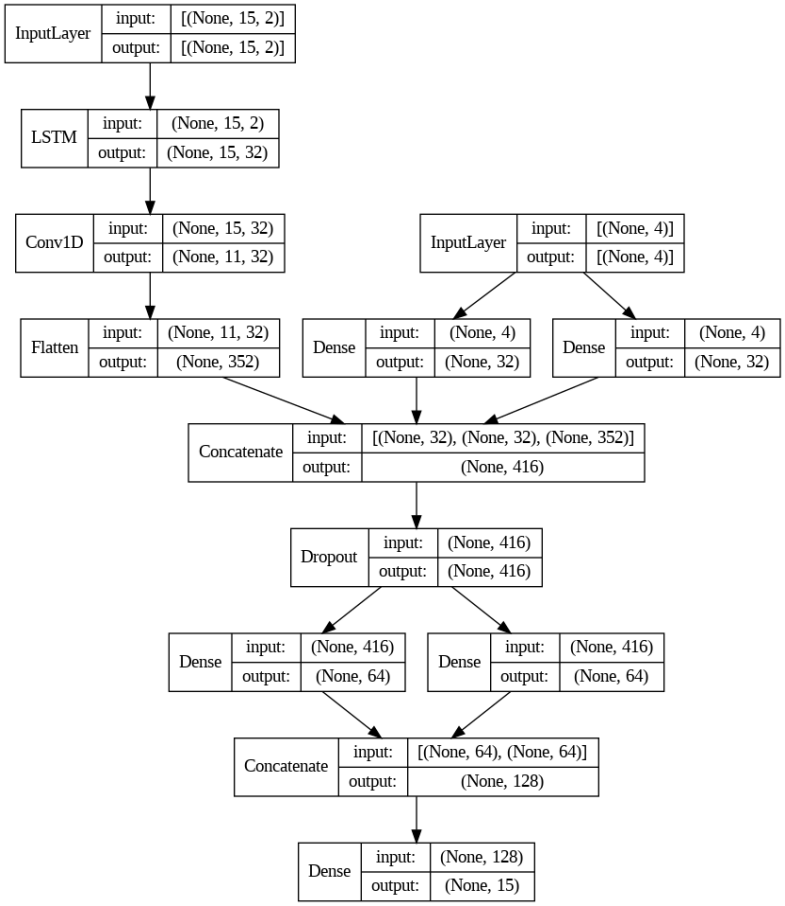

Figure 2 Developed neural network model structure with details of data flow and layer types and shapes

RESULTS AND DISCUSSION

The model was trained for 1500 epochs. The modelling dataset (excluding the test dataset isolated previously) was split into training and validation data set in a ratio of 80:20. The loss metric utilized was Mean square error (MSE) values. Dropout regularization was employed after the merger of the two parallel input layers. The evolution of training and validation loss with proceeding training epochs is shown in figure 3. It can be seen that no signs of overfitting are evident from figure 3 and that model training has proceeded smoothly and adequately. It can be observed from figure 3 that the validation loss was consistently smaller than the training loss throughout the training process. This may be due to the application of regularization techniques like

dropout which only affects the training process and not the validation process and thus, sometimes lead to higher training loss than validation loss [11].

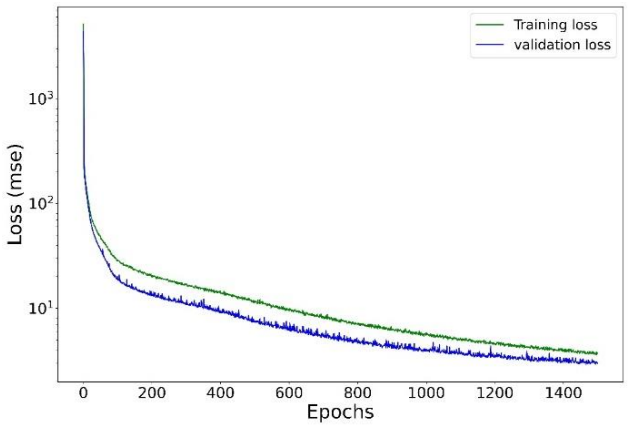

Figure 3 Training loss and validation loss evolution with the training epochs

Once successful model training was completed, the model was then used to predict the set of partition coefficient values for the test data which was not utilized for training and validation purposes. For the prediction of the complete partition curves with 30 data points, the trained model was utilized twice for each experimental data set by splitting each experimental dataset into random sets of 15 data points each, which were then fed to the model separately and the results were then combined for a full plot of the partition curves. The experimental vs. predicted partition coefficients for 2 of the 15 testing datasets have been shown in figure 4. The notations for the 4 primary variables depicted in the legend of figure 4 can be referred from table 1.

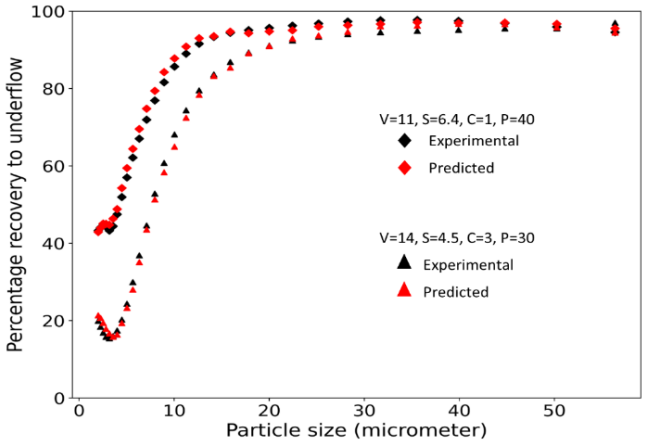

Figure 4 Experimental vs. predicted partition coefficients

It can be seen that the model successfully predicted even the features like bypass and the fish hook of the partition curves, providing a comprehensive prediction for the

particle partitioning behaviour across the size spectrum. The overall MSE in the predictions for the training and validation dataset combined was 2.73, while the overall MSE in the predictions for the test dataset was 10.78. As the predicted points were percentage values, the model's performance on unseen test data was found to be adequate.

CONCLUSIONS

The developed neural network modelling approach in this study has been demonstrated to be successful in predicting the partition coefficients corresponding to a discrete range of particle sizes, thereby allowing for the prediction of the complete partition curves. The model structure and the associated data input and processing strategies employed in this study may be extrapolated to include additional design and operating variables as model inputs for getting partition curve predictions for varying design and operating conditions for hydrocyclones.

REFERENCES

1. Lynch, A.J., Rao, T. (1975) Modelling and Scale Up of Hydrocyclone Classifiers, Proc.1 11th Int. Min.Proc.Cong., Cagliari.
2. Plitt, L.R, (1976) A Mathematical Model of the Hydrocyclone Classifier. *elM Bull.,* 69, 114-123.
3. Nageswararao, K, (1995) Technical Note - A Generalised Model for Hydrocyclone Classifiers. *AuslMM Proceedings,* No.2, 21.
4. Cullivan, J.C., Williams, R., Cross, R. (2003) Understanding the Hydrocyclone Separator Through Computational Fluid Dynamics. Chemical Engineering Research and Design, Vol. 81, 455-466. 10.1205/026387603765173718.
5. Hsieh, K.T., Rajamani, R.K. (1991) Mathematical model of the hydrocyclone based on physics of fluid flow. AIChE Journal, 37, 735-746.
6. Delgadillo, J., Rajamani, R. (2005) A Comparative Study of Three Turbulence-Closure Models for the Hydrocyclone Problem. International Journal of Mineral Processing, 77, 217-230. 10.1016/j.minpro.2005.06.007.
7. Fung, C., Wong, K., Eren, H. (1998) Developing a generalised neural-fuzzy hydrocyclone model for particle separation. 1, 334-337. 10.1109/IMTC.1998.679798.
8. Loggenberg, S., Schoor, G., Uren, K., van der Merwe, A. (2016) Hydrocyclone cut-size estimation using artificial neural networks. IFAC-PapersOnLine, 49, 996-1001. doi:10.1016/j.ifacol.2016.07.332.
9. Dueck, J., et al. (2013) The theoretical partition curve of the hydrocyclone. Miner. Eng., http://dx.doi.org/10.1016/ j.mineng.2013.10.004.
10. Hochreiter, S., Schmidhuber, J., (1997) Long Short-Term Memory, Neural Computation 9 (8), 1735–1780.
11. Chi, J., Liu, Y., Wang, V., Yan, J. (2022) Performance Analysis of Three kinds of Neural Networks in the Classification of Mask Images. Journal of Physics: Conference Series 2181, 012032. doi:10.1088/1742-6596/2181/1/012032.

XV International Mineral Processing and Recycling Conference
17-19 May 2023, Belgrade, Serbia

DETERMINATION OF LIMITING SETTLING VELOCITY IN THE SLURY PIPELINE FROM GRINDING PLANT, USING DIFFERENT APPROACHES – A CASE STUDY

I. Jovanović[1#], M. Ž. Trumić[2], J. Sokolović[2], M. S. Trumić[2], J. Nešković[3]
[1] Mining and Metallurgy Institute Bor, Bor, Serbia
[2] University of Belgrade, Technical Faculty in Bor, Bor, Serbia
[3] Mining institute, Zemun, Serbia

ABSTRACT – This paper examines three different approaches of determining limiting settling velocity of the particles in the specific case. The research was carried out for the hydraulic transport of the collective ground product from the semi-autogenous mill and the ball mill to the hydrocyclone battery, where pipeline diameter value is adopted form the plant. It was shown that in this case a satisfactory result is obtained by applying only one of the calculation methodologies, while the other two methodologies gave limiting settling velocities that are higher than the actual one.

Keywords: Slurry, Pipeline Diameter, Limiting Settling Velocity.

INTRODUCTION

One of the very frequently used methods of transport in the mining industry is the hydraulic transport of slurry. Slurry consists of a solid and a liquid phase (predominantly water). Homogeneous (non-settling) slurry (Fig. 1a) is mixture of solids and liquid in which the solids are uniformly distributed. A settling slurry can be defined as a pseudo-homogeneous or heterogeneous mixture. In pseudo-homogeneous mixture (Fig. 1b) all the particles are in suspension but concentration is greater towards the bottom. In heterogeneous mixture solids are not uniformly distributed and tend to be more concentrated in the bottom of the pipe. Heterogenous mixtures can be partly stratified (Fig. 1c) or completely stratified (Fig. 1d) [1].

Slurries containing essentially fine particles (predominantly less than 50 µm (0.05 mm) are generally considered non-settling and can normally be assessed without consideration for settling. (However, it must be noted that in high concentrations these slurries often exhibit non-Newtonian flow properties (or rheology) and require special consideration in determining suitable pump and system parameters.).

Slurries containing particles predominantly greater than 50 µm are generally considered settling (heterogeneous), which is the case in the majority of slurry pumping applications. Slurries containing solid particles essentially coarser than 50 µm are transported in suspension by a liquid in a pipe, providing the average velocity (v) that must be no less than the limiting settling velocity (v_L). [2].

corresponding author: ivana.jovanovic@irmbor.co.rs

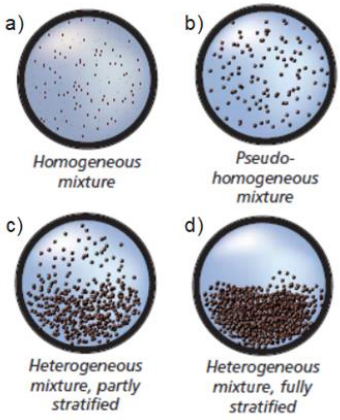

Figure 1 Types of hydraulic mixtures [1]

Limiting settling velocity is particularly important when calculating the diameter of the pipeline. At any velocity below v_L, solids are deposited in the pipeline. This may result in increased pipeline friction head loss, with reducing flow rate and may lead to a blockage of the pipeline [2, 3].

There is no explicit, mathematically derived form for determining the limiting settling velocity, but all forms are empirical or semi-empirical. They are the result of experimental research by different authors, who simulated different transport conditions, changing some of parameters. These parameters affect limiting settling velocity which can be determined by analytical methods [3]. Therefore, this research was carried out to examine how different the v_L values obtained by applying such empirical methodologies are in the specific case.

EXPERIMENTAL

For the purposes of the research, the grinding and classification plant in the Čukaru Peki Mine was selected and, within the plant, the centrifugal slurry pump that transports the collective ground product from the semi-autogenous mill and the ball mill to the hydrocyclone battery. For this purpose, the company Zijin installed a pump 350 MCR M120, manufactured by Weir Minerals, which general appearance is shown in Fig. 2.

Figure 2 MCR type pump Weir Minerals

Limiting settling velocity is calculated for the pipeline of the selected pump 350 MCR M120, which diameter was 500 mm. Calculation is performed using three different methodologies: (1) Durand-Condolios, (2) Evdokimov and (3) Cave. Formulas are given bellow [3, 4]:

(1) Durand-Condolios:

$$v_L = F_L\sqrt{2gD\,\frac{\rho_S-\rho_{LQ}}{\rho_{LQ}}} \tag{1}$$

(2) Evdokimov (for mean particle diameter $0.07 < d_{50} \leq 0.15$ mm):

$$v_L = \frac{\rho_S-\rho_{LQ}}{1700}\cdot\frac{4}{\pi}\cdot 0{,}2\cdot\left(1+2{,}48\cdot\sqrt[3]{p}\cdot\sqrt[4]{D}\right) \tag{2}$$

(3) Cave (valid if the pipeline diameter is greater than 200 mm):

$$v_L = 1{,}04\cdot D^{0{,}3}\cdot\left(\frac{\rho_S}{\rho_{LQ}}-1\right)^{0{,}75}\cdot ln\left(\frac{d_{50}}{16}\right)\cdot\left(ln\left(\frac{60}{C_v}\right)\right)^{0{,}13} \tag{3}$$

In the mentioned formulas (1) – (3), parameters have the following meaning and values for specified case:

v_L – limiting settling velocity, m/s
F_L – modified Froude number, read from a diagram in the literature [3, 4]; F_L = 1.04
g – acceleration of the Earth's gravity, m/s^2; g = 9.81 m/s^2
D – pipeline diameter, m; D = 0.5 m
ρ_S – solids density, kg/m^3; ρ_S = 3060 kg/m^3
ρ_{LQ} – liquid density, kg/m^3; ρ_{LQ} = 1000 kg/m^3
d_{50} – average particle size of solids, mm d_{50} = 0.15 mm
C_v – volume content of the solid phase, %; C_v = 29.37%
p – coefficient representing the mass ratio of solid and liquid phase (%), and is calculated according to the formula (4):

$$p = \frac{C_m}{(100-C_m)}\cdot 100\% \tag{4}$$

where C_m is mass content of the solid phase, C_m = 56.00%, and $p = \frac{56}{(100-56)}\cdot 100\% = 127.3\%$

In order to verify the diameter of the selected pipeline, it is necessary to determine the real slurry velocity of the hydraulic mixture through the pipeline. The real slurry velocity through the 500 mm diameter pipeline is calculated according to the formula (5):

$$v_R = \frac{V_S\cdot 4}{D^2\cdot\pi\cdot 3600} \tag{5}$$

Where:
v_R – real velocity, m/s
V_s – volumetric slurry flowrate, m^3/h; V_s = 2224.40 m^3/h

RESULTS AND DISCUSSION

The results of the calculation of the limiting settling velocity using different methodologies are given in the following text. According to Durand-Condolios approach, limiting settling velocity is: $v_L = 1.04 \cdot \sqrt{2 \cdot 9.81 \cdot 0.5 \cdot \frac{3060-1000}{1000}} = 4.675\ m/s$; Evdokimov formula gives: $v_L = \frac{3060-1000}{1700} \cdot \frac{4}{\pi} \cdot 0{,}2 \cdot \left(1 + 2{,}48 \cdot \sqrt[3]{127.3} \cdot \sqrt[4]{0.5}\right) = 3.546\ m/s$; and finaly, Cave's methodology provides $v_L = 1.04 \cdot 0.5^{0,3} \cdot \left(\frac{3060}{1000} - 1\right)^{0,75} \cdot ln\left(\frac{150}{16}\right) \cdot \left(ln\left(\frac{60}{29.37}\right)\right)^{0,13} = 3{,}112\ m/s$. Value of real slurry velocity is $v_R = \frac{2224{,}40 \cdot 4}{0{,}5^2 \cdot \pi \cdot 3600} = 3{,}147\ m/s$. Figure 3 presents the values of limiting settling velocities obtained through all three approaches in relation to the real velocity of the hydraulic mixture in the pipeline.

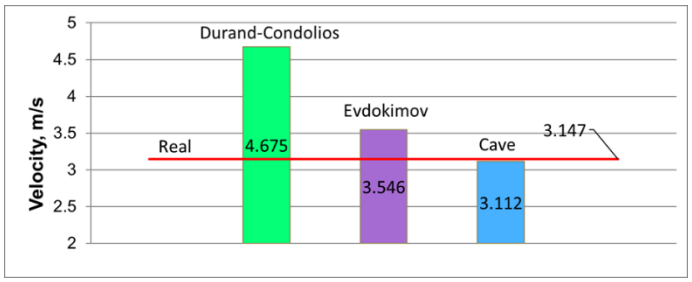

Figure 3 Limiting settling velocities vs. real velocity

As it can be seen from Fig. 3, the methodologies according to Durand-Condolios and Evdokimov give limiting settling velocities that are higher than the real one. Only Cave's methodology gives limiting settling velocity lesser than the real one, which satisfies the conditions for selecting the diameter of the pipeline. This issue can be expressed during the design of mineral processing plants, that is, during the design of devices for hydraulic transport, and can indicate the importance of choosing the calculation methodology of limiting settling velocity. However, as all the formulas are empirical, it cannot be stated with certainty whether the selected pipeline corresponds to the pulp transport conditions in the plant or not. Especially because it is a borderline case when it comes to the value of the pipeline diameter. More specific data can be obtained through laboratory research or by monitoring the operation of the plant in real conditions.

CONCLUSION

The research included determination of the particle limiting settling velocity in the pipeline, using three methodologies – by Durand-Condolios, Evdokimov and Cave in real conditions.

It was found that the first two approaches give the limiting settling velocity higher than the real, while the Cave procedure gave the value lesser than the real one. Since when selecting the diameter of the pipeline, it is necessary that the real velocity be higher than the limited settling, only in the third case is this condition fulfilled. However, it does not necessarily mean that the selected diameter of the pipeline does not correspond to the actual conditions of exploitation, because the formulas are empirical and the most adequate data can be obtained through laboratory tests or monitoring of plant operation.

ACKNOWLEDGEMENT

This work was financially supported by the Ministry of Education, Science and Technological Development of the Republic of Serbia, Grant No. 451-03-47/2023-01/200052.

REFERENCES

1. KETO Green Paper: Slurry Pumping 101 (2017) 23 pages; https://www.ketopumps.com/media/1365/keto-green-paper-slurry-101.pdf.
2. Warman Slurry Pumping Handbook (2000) Warman International LTD, 82 pages; https://www.pumpfundamentals.com/slurry/Warman_slurry_pumping.pdf.
3. Kolonja, B., Knežević, D. (2000) Transport u pripremi mineralnih sirovina, RGF Beograd, 363 pages (In Serbian).
4. Knežević, D., Kolonja, B., Stanković, R. (1996) Hidraulički transport mineralnih sirovina, RGF Beograd, 147 pages (In Serbian).

XV International Mineral Processing and Recycling Conference
17-19 May 2023, Belgrade, Serbia

FLOTATION OF POLYMETALLIC LEAD-ZINC ORES OF THE BAKALSKOYE DEPOSIT

N. Omarova#, R. Sherembayeva, A. Amirkhan, Zh. Ibraybekov, A. Nesipbay
NAO "Karaganda Technical University named after Abylkas Saginov",
Karaganda, Kazakhstan

ABSTRACT – Studies have been conducted to reduce the zinc content in lead concentrate during selective flotation of sulfide lead-zinc ores. It follows from the grinding kinetics that the optimal grinding tone is the mass fraction of the class -0.074 mm 62%. The possibility of flotation using a mixture of zinc sulfate and sodium thiosulfate as a depressor reagent of zinc minerals during flotation of lead-zinc ore in a closed cycle has been studied. With a ratio of their costs of 5:1, the mass fraction of lead in lead concentrate is 69.23%, zinc - 8.52% (versus 10.10% in the factory reagent mode).

Keywords: Flotation, Concentrate, Tailings, Extraction, Quality.

INTRODUCTION

Currently, about 50 metals are extracted from ores. Among 3,000 natural minerals, only 200-250 are of industrial importance. Deposits of lead-zinc ores are dispersed in the territories of many countries. According to the USGS, zinc reserves on Earth amount to about 200 million tons, while the largest, in which 16.5% of its world resources are concentrated, are located in China. Australia has quite noticeable shares - 10.5%, Peru - 9.5%, the USA - 7%, Mexico - 7% and Canada - 4%. Forecasted zinc reserves in Russia account for about 3.2% of the world (at least 63.2 million tons) [1-4]. The object of these studies are lead-zinc ores of the Akzhal deposit (Kazakhstan). The material composition of ore for the Akzhal processing plant has been studied. Technological tests were carried out by flotation methods of enrichment.

The mineralogy of the ore of the Akzhal deposit is simple. Its main ore minerals are represented by sphalerite, galena and pyrite. The host medium for the galena-pyrite-sphalerite association is mainly quartz-encrusted siderite and quartz-carbonate rocks. The ore sample of the section of the underground mine of the Akzhal deposit was studied, in particular, the mine ore of the Tsentralny section. The mass fraction of pyrite in the sample is about 1%. It forms in the non–metallic mass an interspersed texture of euhedral and subhedral very thin (0.001- 0.01 mm) and thin (up to 0.055 mm) crystals. Rare accretions of pyrite with sphalerite in the form of mutual boundary structures were noted. The mass fraction of sphalerite is approximately < 3%. It forms an interspersed texture of anhedral secretions ranging in size from the first microns to 0.2 mm in a non-metallic array, sometimes in fusion with galena or pyrite. The mass fraction of galena is about 1.5%. The mineral is observed in the form of small clusters of irregularly shaped

corresponding author: nazim48@mail.ru

secretions ranging in size from 0.001 to 0.25 mm, confined to the main rock-forming mass and developing in places along non-metallic veins. It occurs in fusion with sphalerite in the form of structures of mutual boundaries.

The aim of the research is to reduce the zinc content in lead concentrate during selective flotation of sulfide lead-zinc ores to improve the quality and extraction of lead concentrate, as well as to improve the quality and extraction of zinc concentrate in the zinc cycle.

THE EXPERIMENTAL PART. RESEARCH METHODS

The studies were carried out on mechanical flotation machines, the grinding tonin of the -0.074 mm class was 62-69%, the reagents used were of the HC brand.

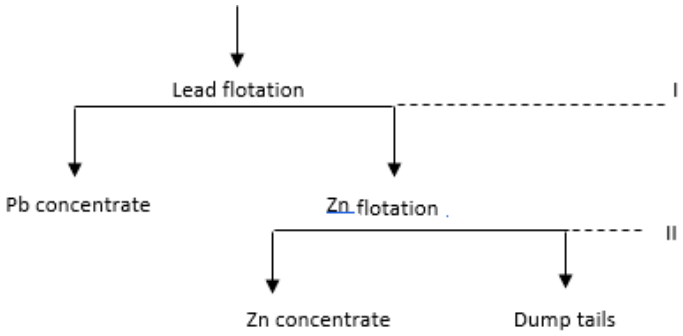

Figure 1 Scheme of flotation of sulfide lead-zinc ore in an open cycle

To study the flotation properties of ore, a scheme of an operating concentrating plant was implemented (Fig. 1). Studies were carried out to adjust the reagent regime using a mixture of zinc sulfate and sodium thiosulfate to depress sphalerite during flotation in the lead cycle [5-9]. The effect of grinding tonin on the quality of lead concentrate has been studied in advance, the results are presented in Table 1 [10]. Flotation was carried out in an open cycle (Fig. 1). The ratio of W:T was 3:1; reagent consumption, g/t: medium regulator – 30, zinc vitriol – 300, danaflot TM 067 – 30, T-92 – 25. From the results of the experiments (Table 1) it follows that with a grinding tone of -0.074 mm 62.00, 64.80 and 69.77% the separation efficiency of lead and zinc (lead concentrate) it was 57.1, 56.82 and 62.92%, respectively. Thus, the most optimal is the grinding tonin of 69.77%. The results of studies of the effect of the consumption of the suppressor reagent on the quality and extraction of lead concentrate are presented in Table 2.

The proposed reagent regime for selective flotation of lead-zinc ore in an open cycle (lead flotation): soda consumption as a reagent-regulator of the medium – 30 g/t, pH – 8.0, the ratio of zinc sulfate and sodium thiosulfate consumption 1:1, 2:1, 5:1, consumption of danaflot and foaming agent – at 25 g/t.

Thus, with an optimal grinding fineness of 69.77% of the -0.074 mm class and a 5:1 ratio of zinc sulfate and sodium thiosulfate consumption, a high separation efficiency of 79.07% is ensured. Studies in a closed cycle were carried out on a sample of lead-zinc ore of the Central section (Fig. 2-3).

Table 1 The results of experiments on the study of the effect of grinding tonina on technological indicators on the example of the ore of the Central site (factory mode)

Product	Yield, γ, %	Pb		Zn	
		β, %	ε, %	β, %	ε, %
Mass fraction of the class –0,074 mm 62.00%					
Pb concentrate	15.18	11.10	94.13	7.26	37.03
Zn concentrate	9.13	0.69	3.47	19.59	44.38
Tails	75.69	0.057	2.40	0.99	18.59
Ore	100.00	1.79	100.00	4.03	100.00
Mass fraction of the class –0,074 mm 64.80%					
Pb concentrate	16.79	9.07	92.29	3.72	35.47
Zn concentrate	15.73	0.23	2.19	16.02	54.54
Tails	67.48	0.13	5.52	0.68	9.99
Ore	100.00	1.65	100.00	4.62	100.00
Mass fraction of the class –0,074 mm 69.77%					
Pb concentrate	15.33	10.35	90.15	3.72	35.47
Zn concentrate	8.74	0.57	2.83	16.02	54.54
Tails	75.93	0.16	7.02	0.68	9.99
Ore	100.00	1.76	100.00	4.62	100.00

The mass fraction of lead in the ore is 1.72%, the grinding tonin is 69.77% of the class – 0.074 mm, the duration of the main flotation is 10 min, I re-cleaning – 5 min, II re-cleaning – 5 min, III re-cleaning – 3 min.

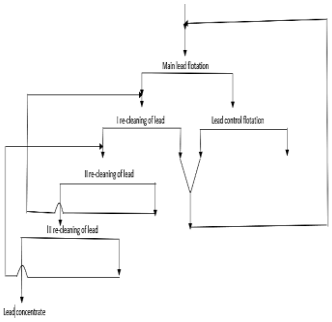

Figure 2 Lead flotation scheme

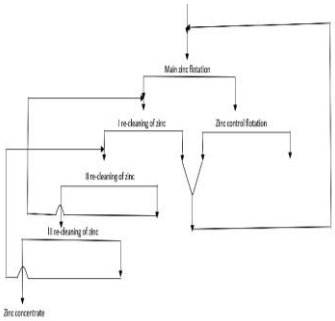

Figure 3 Zinc cycle flotation scheme

Experiments on flotation in a closed cycle were carried out under the following reagent regimes: — lead flotation: pH 8.0 at a flow rate of soda medium regulator 30 g/t; consumption, g/t: zinc sulfate – 300, danaflot – 12, frother – 25; — zinc flotation: pH 11.55 (lime to depress pyrite); consumption, g/t: copper sulphate – 240, danaflot – 45, frother – 45. The results of flotation of lead-zinc ore of the Central section are presented in Table 3 and 4. From the results obtained, it can be seen that with a ratio of zinc sulfate and sodium thiosulfate of 5:1, the mass fraction of lead in lead concentrate

is 67.95%, zinc - 8.86% (against 9.45% according to the factory reagent regime). The quality of the zinc concentrate is 56.24% by weight Zn (against 47.52% according to the factory reagent regime) with a mass fraction of lead in it of 1.64% (against 1.91% according to the factory regime).

Table 2 Results of experiments to study the effect of the consumption of the depressor reagent on the quality and extraction of lead concentrate (proposed mode)

Product	Yield, γ, %	Pb		Zn	
		β, %	ε, %	β, %	ε, %
The ratio of the costs of zinc sulfate (depressor) and sodium thiosulfate 1:1					
Pb concentrate	11.87	13.19	94.89	5.36	26.65
Zn concentrate	8.20	0.48	2.39	26.54	54.41
Tails	78.93	0.06	2.72	0.96	18.94
Ore	100.00	1.65	100.00	4.00	100.00
The ratio of the costs of zinc sulfate (depressor) and sodium thiosulfate 2:1					
Pb concentrate	10.54	14.99	94.04	3.88	15.12
Zn concentrate	6.54	0.55	2.14	27.33	46.70
Tails	82.92	0.08	3.82	1.75	38.09
Ore	100.00	1.68	100.00	3.82	100.00
The ratio of the costs of zinc sulfate (depressor) and sodium thiosulfate 5:1					
Pb concentrate	10.12	15.95	93.85	3.52	14.78
Zn concentrate	7.23	0.50	2.12	24.24	45.64
Tails	82.65	0.08	4.03	1.84	39.58
Ore	100.00	1.72	100.00	3.84	100.00

Table 3 Results of ore flotation of the Central section in a closed cycle (factory mode)

Product	Yield, γ, %	Pb		Zn	
		β, %	ε, %	β, %	ε, %
Pb concentrate	2.01	65.85	76.54	9.45	4.71
Zn concentrate	4.44	1.91	2.10	47.52	52.35
Tails	93.55	0.39	21.36	1.85	42.94
Ore	100.00	1.72	100.00	4.03	100.00

Table 4 Results of ore flotation of the Central section in a closed cycle (proposed mode) with a ratio of zinc sulfate and sodium thiosulfate 5:1

Product	Yield, γ, %	Pb		Zn	
		β, %	ε, %	β, %	ε, %
Pb concentrate	2.12	67.95	82.32	8.86	4.69
Zn concentrate	4.32	1.64	2.23	56.24	60.74
Tails	93.56	0.29	15.45	1.48	34.57
Ore	100.00	1.75	100.00	4.00	100.00

RESULTS AND DISCUSSION

Experiments on flotation in a closed cycle were carried out according to the scheme operating at the Akzhal processing plant (Fig. 2-3). The production of lead and zinc concentrates was carried out according to a selective flotation scheme. From the Table 1 it can be seen that with a grinding tone of -0.074 mm 62.00, 64.80 and 69.77%, the separation efficiency of lead and zinc in lead concentrate was 57.1, 56.82 and 62.92%, respectively.

The maximum separation efficiency is ensured by using the ratio of zinc sulfate (suppressor reagent) and sodium thiosulfate 5:1. At optimal grinding fineness 69.77% by weight class -0.074 mm and the ratio of consumption of zinc sulfate and sodium thiosulfate 5:1 separation efficiency was 79.07%. It was found that with an optimal ratio of zinc sulfate and sodium thiosulfate consumption of 5:1, the mass fractions of lead and zinc in lead concentrate are 67.95 and 8.86% with the extraction of 83.32 and 4.69%, respectively. The quality of zinc concentrate is 56.24% by weight. Zn with a mass fraction of lead in it of 1.64%, zinc extraction is 60.74%.

CONCLUSION

When conducting studies in a closed cycle to determine the consumption ratio of a mixture of reagents – depressors to improve the quality of lead concentrate, the optimal consumption ratio of zinc sulfate and sodium thiosulfate 5 was established :1. At the same time, the quality of lead concentrate is 67.95%, with 83.32% extraction.

REFERENCES

1. Abramov, A.A. (2005) Technology of processing and beneficiation of non-ferrous metals ores. Vol. 3, Bk. 1. Moscow: MGGU, 575 p.
2. Algebraistova, N.K., Prokopiev, I.V., Markova, A.S., Kolotushkin, D.M. (2017) Flow sheet and reactant treatment for lead-zinc ore bulk flotation. Gornyi Zhurnal. No. 1. 50–54. DOI: 10.17580/gzh/2017.01.10.
3. Telkov, S.A., Motovilov, I.Yu., Barmenshinova, M.B., Medyanik, N.L., Daruesh, G.S. (2019) Substantiation of gravity concentration to the Shalkiya deposit lead zinc ore. Fizikotekhnicheskie Problemy Razrabotki Poleznykh Iskopayemykh. No. 3. 99–105.
4. Gavrilova, T.G., Kondrat'ev, S.A. (2020) Effect of physisorption of collector on activation of flotation of sphalerite. Fizikotekhnicheskie Problemy Razrabotki Poleznykh Iskopayemykh. No. 3. 131–143.
5. Cveticanin, L., Lazic, P., Vucinic, D. (2018) Influence of galena grain size and collector concentration on recovery and flotation rate. Fiziko-tekhnicheskie Problemy Razrabotki Poleznykh Iskopayemykh. No. 3. 143–149.
6. Mütevellioğlu, N.A., Yekeler, M. (2019) Beneficiation of oxidized lead-zinc ores by flotation using different chemicals and test conditions. Fiziko-tekhnicheskie Problemy Razrabotki Poleznykh Iskopayemykh. No. 2. 162–168.
7. Troshkina, I.D., Zakharyan, S.W., Yun, A.B., Gedgagov, E.I. (2018) The recovery of rare metals from a sulphuric acid scrub solutions generated during the complex processing

of copper sulphide ore. Advances in chemistry research. Ed. J. C. Taylor. New York: Nova Science Publishers Inc., Vol. 45. 43–76.
8. Chanturiya, V., Kondratiev, S. (2019) Contemporary understanding and developments in the flotation theory of nonferrous ores. Mineral Processing and Extractive Metallurgy Review. Vol. 40, Iss. 6. 390–401.
9. Cvetićanin, L. (2017) Uticaj krupnoće galenita na kinetiku flotiranja: Doktorska disertacija. Univerzitet u Beogradu, Rudarsko-geološki fakultet, 215 p.
10. Omarova, N.K., Naguman, P.N., Sherembaeva, R.T. (2020) A flotation study for oxidized copper products in electrochemical sulfidation. Obogashchenie Rud. No. 1. 32–35. DOI: 10.17580/or.2020.01.06.

XV International Mineral Processing and Recycling Conference
17-19 May 2023, Belgrade, Serbia

THE APPLICATION OF THE DIELECTRIC BARRIER DISCHARGE (DBD) FOR THE IMPROVEMENT OF THE SEPARATION OF PYRITE AND ARSENOPYRITE

V. A. Chanturiya, I. Zh. Bunin, M. V. Ryazantseva[#]
Melnikov' Institute of Comprehensive Exploitation of Mineral Resources of RAS (IPKON), Russia

ABSTRACT – The mechanism for modifying the structural and chemical state of pyrite and arsenopyrite surfaces in the process of interaction with nonequilibrium plasma of dielectric barrier discharge (DBD) were defined. It consists in strengthening the acceptor and weakening the electron - donor properties of the pyrite surface and reducing the acceptor ability of arsenopyrite, which caused an increase in the sorption and flotation activity of pyrite and a decrease in that of arsenopyrite. In a monomineral flotation experiments, the increase in the recovery of pyrite was 27%, while the decrease in the yield of arsenopyrite was 10-12%. DBD pretreatment of the flotation concentrate samples from the gold concentrator ZIF 2 (Olimpiada ore field) reduced the recovery of arsenic to the concentrate by 10-11%, while the arsenic content of the concentrate decreased by 0.71-0.78%.

Keywords: Flotation, Pyrite, Arsenopyrite.

INTRODUCTION

This paper reports the results of our study of the relationship between the plasma treatment parameters implemented under exposure to dielectric barrier discharge (DBD) on the structural and chemical state of the surface, physicochemical (sorption capacity), and process properties (flotation activity) of pyrite and arsenopyrite. The study was carried out on monomineral (98-99%) fractions of pyrite and arsenopyrite (from Darasun, Krasnoyarsk Territory), as well as pyrite contained in the arsenopyrite concentrate of the Olimpiada deposit.

DBD treatment parameters were as follows: electrode voltage in the DBD generator cell - 20 kV, pulse duration - 8 μs, leading edge duration ~300 ns, pulse repetition rate - 16 kHz, interelectrode gap ~5 mm. When exposed to DBD low-temperature non-equilibrium plasma (LTP) in air, the gas temperature in the active zone of the discharge cell did not exceed the temperature of the dielectric barrier and stayed at room temperature for t_{treat} = 10 - 120 s.

When identifying the main patterns of changes in the structural and chemical properties of the pyrite and arsenopyrite surfaces under exposure to DBD, such methods as IR and XPS spectroscopy [1-4], as well as adsorption of acid-base indicators [5-7] were used. The sorption activity of minerals with respect to potassium butyl xanthate was studied using IR spectroscopy; in addition, flotation experiments were carried out [1-4].

[#] corresponding author: ryzanceva@mail.ru

EXPERIMENTAL

The use of spectroscopic methods traditionally used in research (IR and XPS spectroscopy) in order to describe the structural and chemical state of sulfide surfaces did not allow in this case to identify the features describing the state and patterns of changes in the phase composition of the surface with varying DBD parameters (treatment time). In this regard, to identify those, adsorption of acid-base indicators was used with different acidity values (pKa), selectively adsorbed on surface functional groups with corresponding pKa values [8-10] (Fig. 1). In accordance with [8], indicators with the lowest (usually negative) pKa values are selectively adsorbed on Lewis basic active centers (containing an unshared pair of electrons and capable of dissociative adsorption of water molecules with proton elimination).

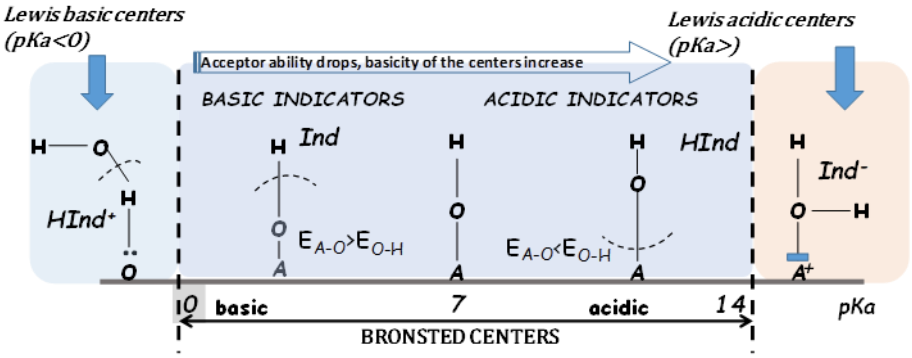

Figure 1 The scheme of the basic and acidic centers of the solid

With an increase in pKa values of the indicators, their selective adsorption occurs at Bronsted acidic centers (pKa = 0-7, surface OH groups with a tendency to proton cleavage), Bronsted basic (pKa = 7-14, surface OH groups with a tendency to cleavage of hydroxyl ion), and Lewis acidic centers (pKa > 14, atoms with a free orbital, capable of dissociative adsorption of water and hydroxyl capture).

RESULTS AND DISCUSSION

The content of the corresponding adsorption centers was determined from the change in the optical density of indicator solutions at wavelengths corresponding to the absorption maximum using a Shimadzu UV-1700 spectrophotometer. The experimental results are presented in Figure 2.

Our analysis of the obtained results made it possible to establish the following changes in the functional state of the mineral surface in the process of interaction with the DBD plasma of: in pyrite, the number of active centers with pKa = 12.8 and 8.8 increased by a factor of 1.5 and 1.5-1.8, respectively (from 8.7 to 12.7 µmol/g and from 21.3 to 39.3 µmol/g). At the same time, the pKa value of -0.29 and -4.4 decreased by a factor of 1.3 (from 41.5 to 32.3 µmol/g) and 1.4 times (from 36.9 to 29.2 µmol/g). In arsenopyrite, there was a decrease in the number of active centers with pKa = 12.8 and 8.8 by a factor of 1.9-3.0 (from 12.2 to 6.2 µmol/g) and 1.4-1.6 (23.8 to 15.9 µmol/g).

Based on the interpretation of the surface of a solid as a combination of acidic and basic centers of the Bronsted and Lewis types, and taking into account the results observed, it can be assumed that the DBD treatment of pyrite enhances the acceptor properties (this fact is indicated by the increase in the number of centers with pKa = 12.8 and 8.8, and in addition, weakens the electron-donating properties of the mineral surface (decrease in the number of centers with pKa = -0.29 and -4.4). At the same time, the acceptor properties of arsenopyrite weaken, as the number of centers with pKa = 12.8 and 8.8 decreases.

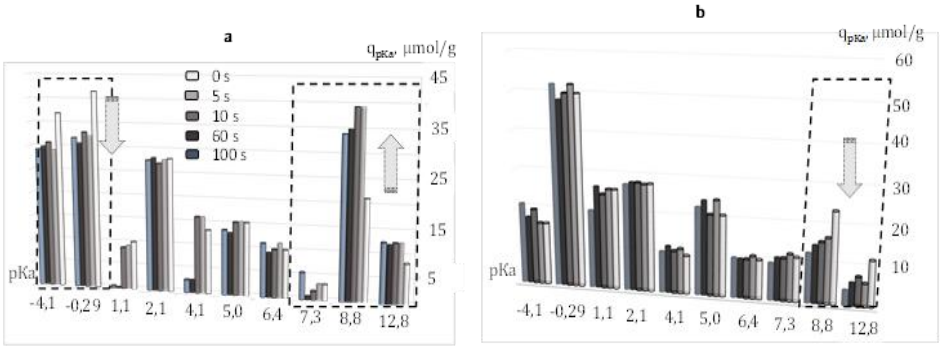

Figure 2 The distribution of the active centers at the pyrite (a) and arsenopyrite (b) surface after the DBD treatment

Thus, the obtained results indicate that DBD pretreatment of minerals is likely to promote an increase in the sorption activity of pyrite with respect to electron-donor collectors, for example, xanthate, and a decrease in BX adsorption on arsenopyrite surfaces. The conducted sorption experiments supported this hypothesis; the data obtained during the adsorption of acid-base indicators and the results of the sorption experiments are presented in Figure 3.

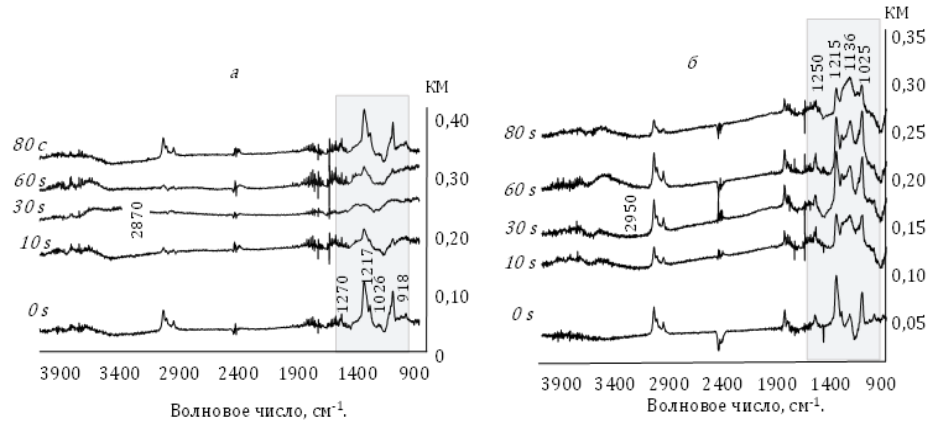

Figure 3 IR spectra of the arsenopyrite (a) and pyrite (b) before (0 s) and ater the DBD treatment

The figure demonstrates that DBD treatment of pyrite samples at t_{treat}= 10 - 60 s promotes an increase in BX adsorption on the mineral surface, which follows from an increase by a factor of 1.2-1.3 of the integral intensities of the absorption bands, which describe the stretching vibrations of both the C–H bond (2950 cm^{-1}) of the collector hydrocarbon skeleton and the 1025 cm^{-1}, 1136 cm^{-1}, 1215 cm^{-1}, and 1250 cm^{-1} bands relating to the vibrations of the bonds of the functional group of the reagent. A further increase in DBD treatment time (80-120 s) caused a decrease in the sorption activity of the mineral. The opposite trend describes changes in the sorption activity of arsenopyrite: the area under the spectral curve in the intervals corresponding to the absorption of the reagent adsorbed by the mineral surface decreases by a factor of 1.1-1.2.

Evidence on the effect of DBD on BX sorption on mineral surfaces is supported by the results of flotation experiments (Figure 4), which showed that under monomineral flotation, the increase in pyrite recovery is up to 27%, and the decrease in arsenopyrite recovery is 10-12%.

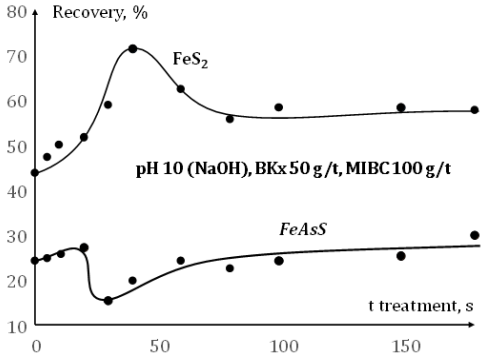

Figure 4 The floatability of the pyrite and arsenopyrite depending on the treatment duration (s)

Table 1 Results of flotation experiments

		g.	γ, %	β, %		
0	Conc.	27.57	55.17	4.62	50.70	
	Tails	22.40	44.83	5.33		49.30
	Σ	**49.97**	**100**	**4.72**		100
40 s	Conc.	22.65	46.60	3.86	39.94	
	Tails	25.95	53.39	5.07		60.05
	Σ	**48.60**	**100**	**4.51**		100
40 s	Conc.	22.78	48.05	3.91	39.41	
	Tails	27.22	51.95	5.61		60.58
	Σ	**48.29**	**100**	**4.78**		100

DBD treatment of the flotation concentrate samples from the gold concentrator ZIF 2, processing the Olimpiada ore, reduces (Table 1) the yield of arsenic to the flotation froth by 10-11%, while the arsenic grade of the concentrate decreases by 0.71-0.78%.

CONCLUSION

Thus, our study revealed a mechanism for modifying the structural and chemical state of pyrite and arsenopyrite surfaces in the process of interaction with nonequilibrium plasma of dielectric barrier discharge, which consists in strengthening the acceptor and weakening the electron-donor properties of the pyrite surface and reducing the acceptor ability of arsenopyrite, which caused an increase in the sorption and flotation activity of pyrite and a decrease in that of arsenopyrite. In a monomineral flotation circuit, the increase in the recovery of pyrite was 27%, while the decrease in the yield of arsenopyrite was 10-12%. DBD pretreatment of the flotation concentrate samples from the gold concentrator ZIF 2 (Olimpiada ore) reduced the yield of arsenic to the flotation froth by 10-11%, while the arsenic grade of the concentrate decreased by 0.71-0.78%.

REFERENCES

1. Chanturia, V.A., Bunin, I.Z., Ryazantseva, M.V., Khabarova, I.A. (2012) Influence of nanosecond electromagnetic pulses on phase surface composition, electrochemical, sorption and flotation properties of chalcopyrite and sphalerite. Journal of Mining Science, 48 (4), 732-740.
2. Chanturia, V.A., Bunin, I.Z., Ryazantseva, M.V., Khabarova, I.A. (2013) X-ray photoelectron spectroscopy-based analysis of change in the composition and chemical state of atoms on chalcopyrite and sphalerite surface before and after the nanosecond electromagnetic pulse treatment. Journal of Mining Science, 49 (3), 489-498.
3. Chanturia, V.A., Bunin, I.Z., Ryazantseva, M.V., Khabarova, I.A., Koporulina, E.V., Anashkina, N.E. (2014) Surface activation and induced change of physicochemical and process properties of galena by nanosecond electromagnetic pulses. Journal of Mining Science, 50, 573-586.
4. Chanturiya, V.A., Bunin, I.Z., Ryazantseva, M.V., Khabarova, I.A. (2013) Structural and phase transformations of sulfide mineral surfaces irradiated by nanosecond electromagnetic pulses. Bulletin of the Russian Academy of Sciences: Physics, 77 (9), 1096-1100.
5. Nechiporenko, A.P. et. all. (1985) Indicative method of the solid surface acidity investigation. Russian journal of general chemistry, 9, 1907-1912.
6. Nechiporenko, A.P. (1995) Donor–acceptor properties of the solid oxides and chalcogenides: Ph.D Thesis, St. Peterburg.
7. Ryazantseva, M.V., Bunin, I.Z. (2015) Modifying acid–base surface properties of calcite, fluorite and scheelite under electromagnetic pulse treatment. Journal of Mining Science, 51 (5), 1016-1020.
8. Tanabe, K. (1973) Solid acids and basic. Moscow: MIR.
9. Sychov, M.M., Nakanishi, Y., Mjakin, S.V. (2003) Surface properties of ZnS and AC powder electroluminescent phosphors, J. SID., 11 (1), 33-38.
10. Sychov, M.M., Mjakin, S.V., Nakanishi, Y., Korsakov, V.G., Vasiljeva, I.V., Bakhmetjev, V.V., Solovjeva, O.V., Komarov, E.V. (2005) Study of active surface centers in electroluminescent ZnS: Cu, Cl phosphors. Applied Surface Science, 244, 461-464.

XV International Mineral Processing and Recycling Conference
17-19 May 2023, Belgrade, Serbia

BASIC SELECTIVE REAGENT REGIMES FOR COMPLEX SULFIDE ORE FLOTATION

V. Ignatkina[#], A. Kayumov, N. Yergesheva, P. Chernova
National University of Science and Technology «MISiS», Moscow, Russia
NUST "MISiS"

ABSTRACT – Flotation is the main method of mineral processing of fine disseminated ores. Butyl xanthogenate is universal collector, but it has low selectivity of its action against iron sulfides. Chalcopyrite, molybdenum, gold, pyrite, arsenopyrite have been studied. Research methods were flotation, adsorption, potentiometric measurements, surface compounds by the IR ATR and TEM. The effect of the combination of short chain thionocarbamates and diisobutyl dithiophosphate is dependent on the ratio. It may reduce or increase the floatability of pyrite and arsenopyrite. The effect of the collectors depends on the redox conditions and ionic molecular composition. Hydrogen peroxide was used as oxidant and thiosulfate as reducing agent.

Keywords: Flotation, Selection, Collector, Redox Conditions.

INTRODUCTION

Flotation is the main method of mineral processing of fine-disseminated ores. Copper, molybdenum and gold are strategic metals in Russia. Copper, molybdenum, iron sulfides, as well as gold are present in various industrial types of ores such as porphyry copper, pyrite copper, gold sulfide.

The market value of pyrite and arsenopyrite depends on their gold content. The main reason of its refractoriness is due to the close interpenetration of minerals of fine disseminated ores.

The necessary difference between the flotation properties of non-ferrous and noble metal sulfides and ferrous sulfides requires a forced change in their technological properties to obtain high-quality monometallic concentrates for recovery from fine-disseminated ores [1,2].

The success of selective separation depends on the reagent regime in which the collector plays a critical role. The use of a combination of weak and strong collectors increases the contrast of technological properties. The effectiveness of the combination of collector composition depends not only on the qualitative and quantitative composition, but also on the composition of the liquid phase of the pulp, redox conditions [3-9].

The purpose of the report is to present the results of the study of the influence of the qualitative and quantitative composition of the sulfhydryl collector on the results of the floatability of sulfides from the environment.

[#] corresponding author: woda@mail.ru

MATERIALS AND METHODS

Materials

Table 1 provides information on the minerals used. Elemental composition was determined by XRD (EAGLE III, AMETEK, USA).

Table 1 The chemical composition of minerals, %.

Mineral	Cu	Fe	As	Mo	S	Au	Other	Total
Gold						90.0	10.0	100.0
Molybdenum		0.6		57.8	38.6		3.0	100.0
Chalcopyrite	32.9	30.9			35.6		0.6	100.0
Pyrite	0.2	45.9			53.8		0.1	100.0
Arsenopyrite	0.2	32.5	43.2		19.5		4.6	100.0

The specific surface area of the -44 +10 µm fraction was measured by low temperature nitrogen adsorption (Nova, Quantachrome Instruments, USA) and is, m^2/g: 1.982 molybdenum, 0.845 chalcopyrite, 0.440 pyrite, 0.555 arsenopyrite. Table 2 contains list of reagents.

Table 2 Reagents

Reagent	Technological purpose	Chemical formula	Characteristic
butyl xanthogenate – ButX	collector	$C_4H_9OCS_2K$	92 % activity
diisobutyl dithiophosphate – DTP	collector	$i(C_4H_9)_2O_2P_2Na$	56% activity
O-isopropyl N- methyl-thionocarbamate – ITC	collector	$iC_3H_7OCSNHCH_3$	98% activity non-ionic reagent
alkaline and acid	regulator pH	NaOH, $Ca(OH)_2$, H_2SO_4	chemical pure
sodium thiosulfate	modifier, reductant	$Na_2S_2O_3 \cdot 5H_2O$	chemical pure
hydrogen peroxide	modifier, oxidizer	H_2O_2	50% activity

Collector solution concentration was prepared based on pH water. All reagents were prepared at 100% activity.

Methods

Flotation was carried out in a Hallimond tube with a capacity of 50 ml, in which a system of glass capillaries allows to obtain individual air bubbles with a diameter of 1-2 mm. The duration of flotation was determined by the constant volume of displaced air. The duration of mixing with a modifier was 5 min, with a collector for MoS2 and Au was during 15 min, and other minerals were 3 min [2].

Potentiometric control was performed using an I-160MI ion meter to measure the pH of the medium and an I-160M to measure the redox potential (Eh). The pH measurements were performed with an ES-10603 electrode and an ESR-10103 reference electrode. An EPV-1 platinum electrode and an ESR-10103 (Ag/AgCl) reference electrode were used to measure Eh. The absolute adsorption of the collector was checked by measuring the initial and final concentration of a liquid phase during flotation through the Hallimond tube. Standard samples were prepared and a calibration curve was constructed using the built-in "Cary WinUV Software" (Cary 6000i).

Surface compounds on a flotation concentrate were studied by IR ATR with KRS 55° (Specord M80, Carl Zeiss-Jena, Germany, Soft Spectra).

Reagent film on the surface of a concentrate was studied by transmission electron microscopy (TEM) (JEM-2100, JEOL INCAx-sight Energy "OXFORD instruments", Japan).

RESULTS AND DISCUSSION

Butyl xanthogenate is most commonly used for a reagent regime of sulfide ores in flotation processing plants. In the reagent regime lime is an environmental regulator and iron sulfide flotation suppressant. It is believed that difficult to oxidize sulfides are not floated by ionogenic sulfhydryl collectors [1,6]. Figure 1 shows the floatability of gold, molybdenum, chalcopyrite, pyrite and arsenopyrite by ButX in different acid-base pH environments.

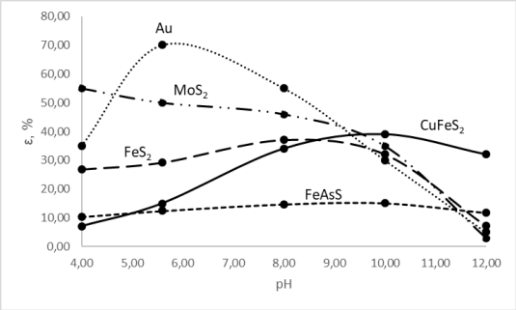

Figure 1 Effect of pH on recovery by ButX (10^{-4} M, Hallimond tube)

Figure 1 shows that gold and sulfides are well floated at pH 5-8 and chalcopyrite is better recovered at pH 9.5-10. It is well known that the floatability of chalcopyrite increases in an alkaline environment [1]. Natural gold is well floated by ButX in a neutral environment. Naturally oxidized molybdenum can be floated by ButX and not only by an apolar collector. Separately, pyrite has a greater flotation activity than chalcopyrite. This fact is in agreement with other researchers [5-9].

Figure 2 shows the highest pyrite floatability by ButX in neutral and slightly alkaline environments. Arsenopyrite floats more actively by DTP than ButX over the entire pH range.

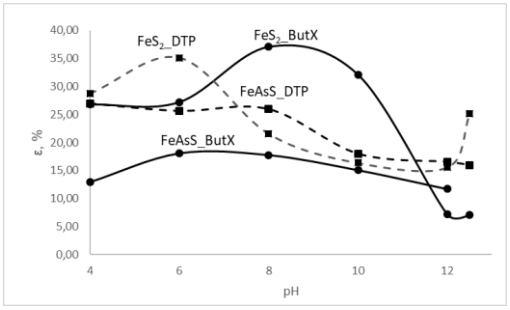

Figure 2 Effect of pH on FeS_2 and FeAsS recovery by collectors (ButX or DTP, 10^{-4} M)

In figure 2, it can be seen iron sulfides float better on DTP in an acidic environment. Arsenopyrite floats more actively on DTP than ButX over the entire pH range.

Figure 3 shows the results of pH and Eh control under flotation conditions in the Hallimond tube.

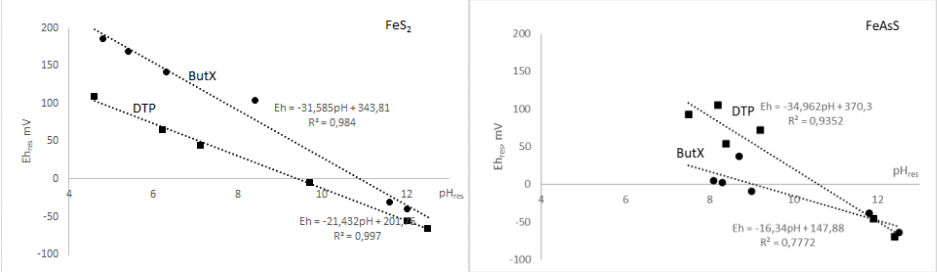

Figure 3 The relationship of Eh and pH

The analysis of pH and Eh allowed us to determine that the slope coefficient of the straight line is higher "ButX-FeS_2" (a = -31.585) than "DTP-FeS_2" (a = -21.432). Arsenopyrite has the inverse dependence of "DPT-FeAsS" (a = -34.962) is higher than with "ButX-FeAsS" (a = -16.34) flotation.

The effect of the collectors depends on the redox conditions and the ionic-molecular composition. Hydrogen peroxide was used as oxidant and thiosulfate as reducing agent (Figure 4). Figure 4 shows the influence of the concentration of the modifiers H_2O_2 and $Na_2S_2O_3$ on the recovery of MoS_2 by ButX.

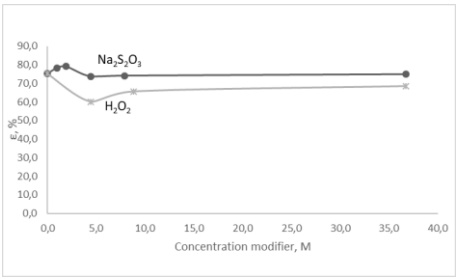

Figure 4 Effect of H_2O_2 and $Na_2S_2O_3$ concentration on MoS_2 recovery by ButX

There is a critical concentration ($4.4\text{-}10^{-3}$ M) of the modifier that corresponds to the minimum flotation activity. This concentration corresponds to the volume concentration of H_2O_2 (150 mg/l) and $Na_2S_2O_3$ (700 mg/l). In addition, as the modifier concentration increases, the recovery increases slightly, but less than with a collector.

IR-ATR spectra are shown in Figure 5. In the IR reflection spectrum of molybdenum, shifts of the characteristic bands of O-C-S bonds of ButX (1142, 1075, 1003 cm^{-1}) to the long wavelength region are identified: the band 1142 cm-1 is shifted to 1185 cm^{-1} (at 41 cm^{-1}) and from 1003 to 1025 cm^{-1} (at 22 cm^{-1}); there is a band at 1079 cm^{-1}. It indicates the coordination through sulfur of the solidophilic group of ButX, confirming the possibility of chemisorption of ButX on active centers of molybdenum with natural surface oxidation.

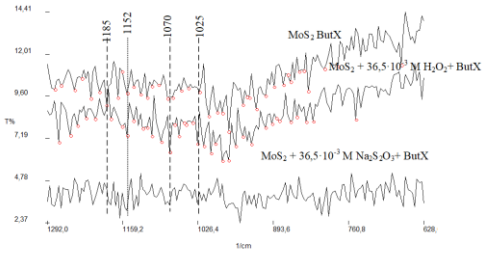

Figure 5 IR-ATR of molybdenum flotation concentrates under different reagent regimes

It is shown that preconditioning with hydrogen peroxide reduces the shift of the characteristic bands to the long wavelength region from 1185 to 1152 cm^{-1} (ButX 1142 cm^{-1}) and there are no bands at 1070 and 1025 cm^{-1}. However, there are no bands in the 1190-1150 cm^{-1} region, when the sample is preconditioned with thiosulfate, but there are bands at 1070 and 1025 cm^{-1}. Such a change in the wave numbers of the characteristic bands indicates a change in the type of coordination of the xanthate group with the molybdenum surface.

Figure 6 shows diagram of the effect of the part of ITC in combination DTP and pH on the recovery FeS_2, FeAsS. It shows that the effect of the combination of short-chain thionocarbamates and diisobutyl dithiophosphate is dependent on the ratio. It can decrease or increase the floatability of pyrite and arsenopyrite.

It was found that, on the one hand, 75% ITC in combination with DTP increases the recovery of pyrite and arsenopyrite (significantly) over a wide pH range. On the other hand, 70-60% ITC in combination with DTP reduces the extraction of pyrite and arsenopyrite.

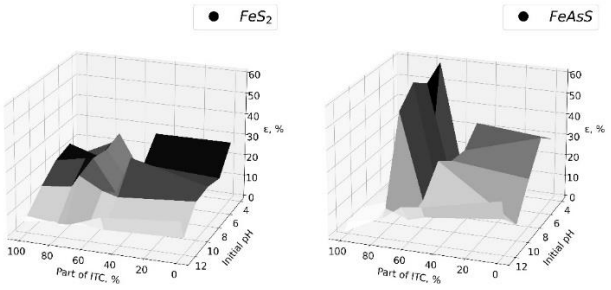

Figure 6 Diagram of the effect of the part of ITC in combination ButX or DTP and pH on the recovery of FeS_2, FeAsS

Control of adsorption by residual concentration showed that with increasing alkalinity, the individual adsorption of DTP on pyrite decreases by 2 orders of magnitude from $1.42\text{-}10^{-5}$ (pH=4) to $3.41\text{-}10^{-7}$ (pH=12) mol/m^2, the adsorption of ITC on pyrite does not change practically $1.56\text{-}10^{-4}$ mol/m^2. With increasing alkalinity, the adsorption of ButX on pyrite slightly decreases from $3.2\text{-}10^{-5}$ (pH=4) to $2.37\text{-}10^{-5}$ mol/m^2 (pH=10), in a highly alkaline medium, the residual concentration of ButX practically does not change. The residual concentration of ITC didn't change over the whole pH range.

The individual adsorption of booths is less than $9.0\text{-}10^{-7}$ mol/m^2 (pH=4) for arsenopyrite and increases slightly with increasing alkalinity, to $2.7\text{-}10^{-6}$ mol/m^2 (pH=12). The adsorption of DTP is higher for arsenopyrite $2.2\text{-}10^{-4}$ mol/m^2 (pH=4), with the increase of alkalinity, the adsorption of DTP decreases. The value of adsorption of ITC for arsenopyrite is slightly lower than on pyrite $1.2\text{-}10^{-4}$ mol/m^2 (pH=4), with increasing alkalinity, individual adsorption of ITC significantly decreases $8.1\text{-}10^{-6}$ mol/m^2 (pH 12). In general, the contribution of DTP is decisive for arsenopyrite. In the isomolar series, a pattern was confirmed that greater recovery corresponds to greater adsorption of components in the pH range 4-10; the maximum adsorption and recovery rates correspond to the proportion of 75% ITC for both combinations. It was found that PAX adsorbed on arsenopyrite was generally lower than on pyrite, but after the longest aeration and pH 7-8, pyrite recovery decreased. There are controversial results concerning adsorption of DTP on pyrite and arsenopyrite [5,7-9].

Figure 7 shows an image of chalcopyrite concentrate grains with surface films. The visualization shows that the part of ITC in the composition with ButX also has different surface films. This is consistent with the recovery results. It is an uniform thin film on the surface of the sulfide grains (chalcopyrite in the example) coincides with the highest floatability. The probability of an elementary act of flotation increases.

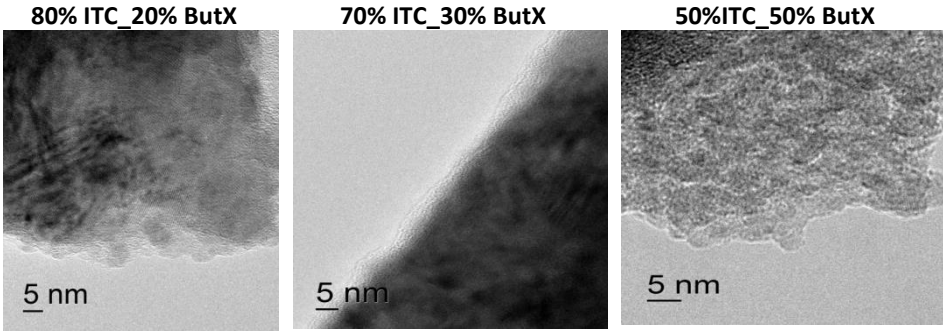

Figure 7 TEM. Surface films of collectors on flotation concentration of chalcopyrite at the Hallimond tube

CONCLUSION

It is shown that the qualitative-quantitative ratio in the composition is important with the redox conditions to maintain the contrast of flotation properties. The combination of ITC and DTP has certain requirements in use to ensure the flotation activity of either non-ferrous metal sulfides or iron sulfides. The proportion of ITC 75% corresponds to the maximum recovery of pyrite and arsenopyrite. However, there is a ratio of ionic sulfhydryl component to ITC at which the flotation activity of both iron sulfides is low, while the recovery of copper sulfides is high.

ACKNOWLEDGEMENT

The study was supported by the grant № 22-27-00102 from the Russian Science Foundation, https://rscf.ru/project/22-27-00102/.

REFERENCES

1. Klassen, V.I., Mokrousov, V.A. (1959) An Introduction to the Theory of Flotation. Gosgortehizdat, Moscow.
2. Ignatkina, V.A., Kayumov, A.A., Yergesheva, N.D. (2022) Floatability and Calculated Reactivity of Gold and Sulfide Minerals. Russian Journal of Non-Ferrous Metals, 63, 5, 473–481. https://doi.org/10.3103/S1067821222050054.
3. Castro, S., Lopez-Valdivieso, A., Laskowski J.S. (2016) Review of the flotation of molybdenite. Part I: Surface properties and floatability. International Journal of Mineral Processing, 148, 48-58. http://dx.doi.org/10.1016/j.minpro.2016.01.003.
4. Ignatkina, V.A., Bocharov, V.A., Puntsukova, B.T., Alekseychuk, D.A. (2010) Analysis of selectivity of thionocarbamate combinations with butyl xanthate and dithiophosphate. Journal of Mining Science, 46 (3), 324-332.
5. Forson, Ph., Skinner, W., Asamoah, R. (2021) Decoupling pyrite and arsenopyrite in flotation using thionocarbamate collector. Powder Technology, 385, 12–20. https://doi.org/10.1016/j.powtec.2021.02.057.
6. Mermillod-Blondin, R., Kongolo, M., de Donato, P., Benzaazoua, M., Barrès, O., Bussière, B. and Aubertin, M. (2005) Pyrite flotation with xanthate under alkaline conditions — Application to environmental desulfurization. Centenary of Flotation Symposium, Brisbane, QLD, 6 - 9 June 2005, 683-692.
7. Tapley, B., Yan, D. (2003) The selective flotation of arsenopyrite from pyrite. Minerals Engineering, 16, 1217–1220. https://doi.org/10.1016/j.mineng.2003.07.017.
8. Forson, P., Zanin, M., Skinner, W., Asamoah, R. (2022) Effect of pulp aeration and the critical importance of collector concentration Minerals Engineering 178, 107421 https://doi.org/10.1016/j.mineng.2022.107421.
9. Jiang, K., Liu, J., Wang Y., Zhang, D., Han, Yu. (2023) Surface properties and flotation inhibition mechanism of air oxidation on pyrite and arsenopyrite. Applied Surface Science, 610, 155476. https://doi.org/10.1016/j.apsusc.2022.155476.

XV International Mineral Processing and Recycling Conference
17-19 May 2023, Belgrade, Serbia

STUDIES ON THE FLOATABILITY CHARACTERISTICS OF LOW VOLATILE COKING COAL FINES USING X-RAY DIFFRACTION (XRD) ANALYSIS AS A DIAGNOSTIC TOOL

S. Chaudhuri[#], S. Maity, S. C. Maji, D. Roy, U. S. Chattopadhyay
Central Institute of Mining and Fuel Research (CSIR), Digwadih Campus, Dhanbad, India

ABSTRACT – The coking coal washeries in India are facing challenges to beneficiate the high ash coals of the lower seams due to the fact that the minerals are finely disseminated with the coal macerals and crushing to lower sizes is inevitable for its liberation. Once the coal is crushed to finer size, there is marked increase in the quantum of coal fines and to beneficiate these coal fines flotation is usually practiced globally. In the case of Indian coking coal fines, the floatability characteristics play a very important role and in the present investigation, attempts have been made to beneficiate the coal fines of a low volatile coking by froth flotation in laboratory scale. X-ray Diffraction (XRD) analysis was performed using an automated high-resolution multipurpose X-ray diffractometer with expert system Guidance software (Model: SmartLab X-ray Diffractometer; Make:Rigaku, Japan). The flotation tests are carried out and to understand the role of various minerals and its effect on flotation. XRD was used as a diagnostic tool.
It is found that the ash% of the 0.5mm raw coal fraction for the top size crushing 50mm to 0.5mm crushing are increased from 25.9% to 39.1% whereas the ash% of the Flotation cleans of these coal fines are increased from 16.9% to 29.6% at same reagent dosages. By XRD analysis it is observed that the non-crytalline part decreases from 80.2% to 68.1% whereas the percentage of quartz increases from 12.6% to 16.8% for the 0.5mm raw coal fraction for the top size crushing 50mm to 0.5mm fraction. The investigations have revealed that flotation characteristics are being deteriorated due to crushing of coal from coarser top size to finer top size and using XRD as a diagnostic tool it is possible to understand the role of minerals in flotation efficiency.

Keywords: Indian Low Volatile Coking Coal Fines, Froth Flotation, X-Ray Diffraction (XRD) Analysis.

INTRODUCTION

The National Steel Policy, 2017 has envisaged crude steel production around 300 million tonnes (Mt) by the year 2030-31 and forecasts coking coal demand of 161 Mtpa (million tonnes per annum) [6]. For the present and even in the foreseeable future conventional blast furnace technology will be the main route for iron and steel making and so will be importance of coking coal as an important raw material. Coking coal is used to produce coke which is used primarily as energy source and a reductant in blast furnace for the production of steel. The availability of indigenous good coking coal has almost become stagnant. At present about 85% of the current requirement of coking coal is met through imports. Relying on this trend, 35% of the demand during year 2030-31, i.e. 56.35 Mtpa of coal has to be made available from indigenous sources.

As the reserve of good quality coking coal of upper seams are almost depleted there

[#] corresponding author: sanjaycfri@yahoo.co.in

is need to enhance utilization of available resources of inferior indigenous coals as alternate choice. LVMC coal (low volatile medium coking or low volatile high rank coal) and low rank high volatile coals are new sources that can be used in coke-making as blends through processes of suitable beneficiation.

LVMC coals falls into the category of medium coking coal which are also known as non-linked washery coal (NLW) due to ash content greater than 35%. These coals belong to lower seams are more likely to be more mature (Rr >1.20%) and low volatile matter content (18-22%), low reactive content (30-45%), high inertinite content, having lower coking propensities with difficult cleaning characteristics. At present, these coals are being used in power sector. These coals generally occur in the lower seams of Jharia coalfield (combined seam V/VI/VII/VIII and even seam IV, III and II) and Karo group of seams (seam VI-XI) in the eastern part of East Bokaro coalfield.

The coking coal washeries generates huge quantity of coal fines in the form of slurry at the rate of 15-20% and these slurries are not processed further in most of the washeries because of so many reasons. One of the reasons is that most of the washeries originally designed to treat easy to wash upper seam coking coals did not initially include flotation circuit as the quality of fines produced were enriched in requisite macerals necessary for metallurgical coke. The raw coal fines were simply blended with the washed coarser coals to give steel plant cleans. With fast depletion of the good quality coals and deterioration in the quality of coal mined, the existing washeries suffer from severe technical constraints in terms of throughput and discharge capacities of individual washing units while treating the fines of 'difficult to wash' lower seam coals. As a result, a huge quantity of unwashed slurry having ash content between 30-40% is left as such and discharged as tailings to nearby ponds or lagoons, thereby polluting the surroundings. The estimated quantity may increase to as high as 4.75 Mt per annum, if the washeries operate with full designed capacity. The coal fines (below 0.5mm) having better coking propensity is a valuable prerequisite in preparing cleans for metallurgical coke. Though enriched in vitrinite content, the fines cannot be mixed directly with clean coal due to their high ash content (more than 25%) and of high percentage of silica content. [1]The slurry needs to be washed for enrichment of coking propensity and for utilization of total cleans as high valued component for metallurgical purposes [1].

Most of these vitrinite-rich fines could not be beneficiated properly due to varied reasons and are being used irrationally or remained dumped. Generation of fines is increasing by leaps and bounds which may increase to 25% to 30% in future due to adoption of size reduction and multistage washing. Obviously incorporation of flotation circuits with proper care & design is a necessity of the forthcoming washeries for the beneficiation of these inferior grade coal otherwise these vitrinite enriched coal fines will be misused or wasted as it is noticed in the most of the coking coal washeries presently.

In this context Froth Flotation a sensitive and economically viable process to tackle these coal fines of very difficult cleaning character. Flotation is a complex process that takes place in a turbulent three phase system and influenced by many chemical and hydrodynamic factors [2]. The manner in which these factors influence each other is not completely understood [3]. However, surface characteristics play the most important role since they form the basis on which separation is accomplished [4]. In the case of coal fines, the situation is aggravated by the highly heterogeneous nature of coal's surface

and the lack of widely accepted techniques for characterizing the surface properties of fine particles [5].

It is found that the quality and the flotability characteristics of coal fines have detoriarated due to crushing the coal from coarser top size to finer top size. An attempt has been made to understand the cause of detoriaration by XRD analysis of raw coal fines, clean coal fines and tailings fines of each fine coal is generated due to crushing the coal from coarser top size to finer top size.

The existing BCCL coking coal washeries such as DugdaII, Patherdih, Bhojudih, Sudamdih, Borora, Madhuband, Mahuda have already possessed fine coal beneficiation circuit as Flotation. In the scenario of private sector the Coking coal washeries belonged under Tata such as West BokaroII, West BokaroIII, Bhelatand and Jamadoba already have the fine coal beneficiation circuit as Froth Flotation and all the coal preparation plants have already adopted small size crushing of coal which generates the fine coal at the tune of 15-20%.

The Froth Flotation circuits are also being adopted for the new washeries of BCCL such as Madhuband (5.0Mtpa), PatherdihI (5.0 Mtpa), PatherdihII (2.5Mtpa), Bhojudih (2.0 Mtpa). The finer coal crushing is being adopted for all the new washeries of BCCL hence the generation of fines (below 0.5mm fractions) are being increased which is going to be a big challenge to beneficiate to a desired quality. The feed coal will be the LVCC/NLW coal with very difficult cleaning characteristics hence the coal fines so generated may be more difficult characteristics due to finer top size crushing which are going to be a big challenge to beneficiate for desired quality and quantity.

Coking coal is an essential input for production of iron and steel through blast furnace (BF) route. The cost of blast furnace (BF) coke accounts for more than 50% in production in hot metal through BF route. The reserves of coking coal in India is meager and good quality coals of upper seams are fast depleting leaving behind the inferior quality lower seam coal. Low volatile coking coal (LVCC), though the inferior in qualities but abundantly available in eastern part of the country may be an immediate choice. The LVCC(NLW) constitutes about 50% of the total coking coal reserves in India.

To meet the increased demand of coking coal concerted efforts have to be made to correct the imbalance between need and availability by increasing the production of coal of desired quality through better management of available resources of inferior grade low volatile coking coal (LVCC).

In the present investigation the coals collected from CIMFR pilot plant has been crushed at different top sizes from 50mm,25mm,13mm,6mm,3mm and 0.5mm and coal fines so generated from each top size crushing are collected. Attempts have been made to beneficiate these coal fines coal by froth flotation in laboratory scale. The tests are carried out by varying the process parameters. It is found that the quality and the flotability characteristics of coal fines have detoriarated due to crushing the coal from coarser top size to finer top size. An attempt has also been made to understand the cause of detoriaration by XRD analysis of raw coal fines, clean coal fines and tailings fines of each fine coal is generated due to crushing the coal from coarser top size to finer top size.

EXPERIMENTAL

Sample Source

Central Institute of Mining and Fuel Research, Digwadih Campus, Dhanbad has a 40 tph coal washing pilot plant having all sorts washing circuits and crushing systems. A lot of samples are used to come for testing purposes. Out of which one ROM coal of LVCC variety was collected.

Experimental Procedure

After proper mixing and followed by standard procedure of coning and quartering the representative parts were collected. Accordingly, six representative parts were taken and crushed at different top sizes such as 50mm, 25mm,13mm, 6mm, 3mm and 0.5mm. The coal size fractions below 0.5mm of each top size crushing are taken for the present investigation.

The sample was characterized with respect to proximate analysis and the results are given in Table 1. The Froth Flotation experiments were done as per standard procedure. Details experimental procedures are given below.

Table 1 Proximate analysis

	-0.5mm (X50 mm)	-0.5mm (X25mm)	-0.5mm (X13mm)	-0.5mm (X6mm)	-0.5mm (X3mm)	-0.5mm (X0.5mm)
Ash %	25.9	27.0	27.2	31.0	35.6	39.1
Moisture %	1.6	1.5	1.3	1.3	1.1	1.0
VM %	16.2	16.1	16.0	15.7	15.6	15.5
FC %	56.3	55.4	55.5	52.0	47.7	44.4
Total	100	100	100	100	100	100

Laboratory Flotation Studies

The laboratory flotation studies were carried out on the coal fines (- 0.5mm). Laboratory batch flotation studies were carried out in Denver D12 sub aeration flotation machine, with a cell capacity of 2.5 L. The studies were carried out keeping the RPM constant at 1500 and varying the collector and frother dosage as per requirement. About 250 gms of sample was taken and conditioned with required amount of collector at 40% solids concentration for 2 minutes. Then the slurry was adjusted to 10% solids concentration by adding fresh water and then frother was added and further conditioned for one more minute. The aeration was started by opening the air valve and the froth floated as concentrate was collected, dewatered, dried and weighed. The air dried concentrate/clean were sub sampled and ash content of each sample was determined. Flotation experiment results were showed in Table 2.

XRD analysis

X-ray Diffraction (XRD) analysis was performed using an automated high-resolution θ-θ multipurpose X-ray diffractometer (XRD) with expert system Guidance software

(Model: SmartLab X-ray Diffractometer; Make: Rigaku, Japan). The X-ray intensities of the samples are collected in the 2θ range of 10 – 80° with 3 kW sealed X-ray tube, CBO optics, D/teX Ultra 250 silicon strip detector. An X-ray amorphous sample holder is used for sample loading and the scan is made in continuous mode having scan speed of 10.40182o/min and step size of 0.01o. Analysis is done using PDXL2 software and ICDD data bank for mineral identification. XRD analysis results were enlisted in Table 3.

Table 2 Flotation results of coal fines generated at different top size crushing

Same dosages for all the six Flotation experiments	Below 0.5mm fraction (different top size crushing)	Clean Wt %	Clean ash %	Tail Wt %	Tail Ash %
Collector: - 1.25kg/t Frother :- 0.42 kg/t	-0.5mm (X50mm)	69.6	16.9	30.4	48.5
	-0.5mm (X25mm)	70.0	18.1	30	49.3
	-0.5mm (X13mm)	66.4	17.8	33.6	52.6
	-0.5mm (X6mm)	74.4	23.4	25.6	57.9
	-0.5mm (X3mm)	78.4	28.3	21.6	63.0
	-0.5mm (X0.5mm)	72	29.6	28	61.5

Table 3 XRD results of coal fines

Sample	Ash %	Non-Crys	Quartz	Kaolinite
X50mm Raw 0.5mm	25.9	71.5	12.6	13.5
X50mm Flotation. Cleans	17	80.2	7.5	10.1
X25mm Raw 0.5mm	27	70.3	12.6	15.2
X25mm Flotation. Cleans	15.1	79.4	8.7	10.3
X13mm Raw 0.5mm	27.2	70.1	13	15.2
X13mm Flotation. Cleans	18.7	77.2	8.9	10.9
X6mm Raw 0.5mm	31	65.9	14.6	17
X6mm Flotation. Cleans	21.8	75	9.0	12.6
X3mm Raw 0.5mm	35.6	60.8	16.2	20.1
X3mm Flotation. Cleans	21.4	75.3	10.7	14
X0.5mm Raw 0.5mm	39.1	57	16.8	23.6
X0.5mm Flotation. Cleans	28.5	68.1	12.8	16.3

RESULTS AND DISCUSSION

It is observed from the Table 1 that the ash contents of the -0.5mm fraction for the top size crushing 50mm, 25mm, 13mm are 25.9%, 27.0%, 27.2% respectively whereas the ash contents for the -0.5mm fraction for the top size crushing 6mm, 3mm ,0.5mm are 31.0%, 35,6%, 39.1% respectively. Hence it may be concluded from the proximate analysis that the quality of coal fines are deteriorated due to finer Top size crushing i.e. from x6mm and below.

The Flotation experiments (Table 2) are carried out for the coal fines which are generated from different top size crushing. It is observed that Flotation clean coal ash% has increased a lot from 16.9% (x50 mm), 18.1% (x25 mm), 17.8% (x13 mm) to 23.4%(x6 mm), 28.3% (x3 mm), 29.6%(x0.5 mm).

It may be concluded that due to finer top size crushing (x6mm and below) the quality of the coal fines has been deteriorated which is reflected during beneficiation process by Froth Flotation study.

Distribution of Non crystalline in coal fines by crushing the raw coal at coarser top size to finer top size

It is found that by crushing the raw coal coarser top size (50mm) to finer top size (0.5mm) the non-crystalline portion has decreased from 70.1 to 57 which indicated the proportion of pure coaly matters are being decreased whereas the proportion of mineral matters have been increased by crushing the coal to finer size due to its liberation from coal matrix.

During the beneficiation study of below 0.5mm fraction by Froth Flotation the contribution of non-crystalline in clean coal has also been decreased from 80.2 to 68.1 which reflects the deterioration of coal fines quality by crushing the coal coarser to finer.

Distribution of Quartz in coal fines by crushing the raw coal at coarser top size to finer top size

It is found that by crushing the raw coal coarser top size (50mm) to finer top size (0.5mm) the Quartz portion has increased from 12.6 to 16.8 which indicated that the proportion of mineral matters as quartz have been increased by crushing the coal to finer size due to its liberation from coal matrix.

During the beneficiation study of below 0.5mm fraction by Froth Flotation the contribution of quartz in clean coal has also been increased from 7.5 to 12.8 which reflects the deterioration of coal fines quality by crushing the coal coarser to finer.

Distribution of Kaolinite in coal fines by crushing the raw coal at coarser top size to finer top size

It is found that by crushing the raw coal coarser top size (50mm) to finer top size (0.5mm) the Kaolinite portion has increased from 13.5 to 23.6 which indicated that the proportion of Kaolinite has been increased by crushing the coal to finer size due to its liberation from coal matrix.

During the beneficiation study of below 0.5mm fraction by Froth Flotation the contribution of quartz in clean coal has also been increased from 10.1 to 16.3 which reflects the deterioration of coal fines quality by crushing the coal coarser to finer.

CONCLUSION

It is found that the ash% of the 0.5mm raw coal fraction for the top size crushing 50mm to 0.5mm crushing are increased from 25.9% to 39.1% whereas the ash% of the Flotation cleans of these coal fines increased from 16.9% to 29.6% at same reagent dosages. By XRD analysis it is observed that the non-crytalline decreases from 80.2% to 68.1% and the percentage of quartz increases from 12.6% to 16.8% whereas the percentage of kaolinite increases from 13.5% to 23.6% for the 0.5mm raw coal fraction for the top size crushing 50mm to 0.5mm fraction. The investigations revealed that

flotation characteristics are being deteriorated due to crushing of coal from coarser top size to finer top size and using XRD as a diagnostic tool it is possible to understand the role of minerals in increasing or decreasing the flotation efficiency.

ACKNOWLEDGEMENT

We are very much thankful to Director, CSIR-CIMFR for his kind permission to submit the paper to IMPRC-2023.

REFERENCES

1. Sinha, K.M.K., Chattopadhay, U.S., Sen K. (2000) Recycling and Treatment of Settling Pond Fines - A challenge to Industry and Environment. International Symposium on Processing of fines, (2), National Metallurgical Institute, Jamshedpur, India, 416-422.
2. Arnold, B.J., Aplan, F.F. (1986) The effect of clay slimes on coal flotation, part I: The nature of the clay. International Journal of Mineral Processing, 17 (3-4), 225-242.
3. Sagar, C.K., Mishra, P.K., Baranwal, P.K. (2003) Coal preparation - an overview. Journal of Mines, Metals and Fuels, 51 (1/2), 98-100.
4. Bonner, C.M., Aplan, F.F. (1993) The influence of reagent dosage on the floatability of pyrite during coal flotation. Separation Science and Technology, 28 (1-3), 747-764.
5. Taweel, A.M.A., Delory, B., Wozniczek, J., Stefanski, M., Andersen, N., Hamza, H.A. (1986) Influence of the surface characteristics of coal on its floatability. Colloids and Surfaces, 18 (1), 9-18.
6. Imam, Z., Saran, S., Mishra H.K. ICPC 2019, Paper 14.

XV International Mineral Processing and Recycling Conference
17-19 May 2023, Belgrade, Serbia

APPLICATION OF COLLECTOR BTF-15221 IN FLOTATION OF COPPER- AND GOLD - CONTAINING ORES

V. I. Ryaboi[1], V. P. Kretov[2#], E. D. Schepeta[3], I. V. Ryaboi[1], S. E. Levkovets[2]
[1] Mekhanobr-OR, Saint-Petersburg, Russia
[2] Kvadrat Plus, Togliatty, Russia
[3] Primorsky GOK, Vostok, Primorsky region, Russia

ABSTRACT – A new collector for flotation of sulfide ores BTF-15221 has been developed. The results of using BTF-15221 collector alone and in combination with potassium butyl xanthate (PBX) in the flotation of copper, copper-zinc, skarn scheelite-sulfide ore and two auriferous types of pyrite-arsenopyrite ores are as follows.

The use of BTF-15221 alone as a collector in the flotation of skarn scheelite-sulfide ore made it possible to increase recovery of copper by 1.21-3.0 gold - 3.55-17.41%, silver - 2.44-5.27, depending on the consumption of the collector (data from industrial tests). The use of BTF-15221 and PBX composition in the flotation of copper ores increases recovery of copper and gold by 3.7% and 6.15%, in the flotation of copper-zinc ores - the recovery of copper and zinc by 1.35% and 6.82%, and in the flotation of two types of pyrite- arsenopyrite ores - gold by 2.57% and 3.67% respectively.

The flotation performance when using BTF-15221 and PBX composition significantly depends on the ratio of collectors: the recovery of metals decreases with the increase of consumption of BTF-15221.

At the end of 2022, a commercial batch of the reagent in volume of 50 tons was produced, its introduction is planned at one of the enterprises of Russian Federation and its field trials at a factory in Kazakhstan.

Keywords: Flotation, Copper Ore, Copper And Zinc Ore, Gold Containing Ore, Pyrite, Arsenopyrite, Xanthate, Dithiophosphate Composition.

INTRODUCTION

A new collector for sulfide ores flotation was developed and named BTF-15221. The reagent is a composition of known collectors. The creation of the reagent was based on both the features of its components [1-5], and information on the collectors' compositions use [6-11].

One of the collector components is a dialkyldithiophosphate compound, which provides the reagent with some specific properties.

The reagent is readily soluble in water; its aqueous solutions can be stored for a long time without decomposition.

In the Russian Federation, the task of creating a collector capable of successful gold-containing pyrite-arsenopyrite ores flotation is currently urgent, therefore this reagent has been tested in flotation of similar ores from a number of mine fields in Russia and Kazakhstan.

corresponding author: vkretov@kvadratplus.ru

EXPERIMENTAL PART

Conducting flotation experiments in the flotation of sulfide ores is characterized by the following conditions.

Flotation of copper ores. The scheme included carrying out the roughing flotation during 10 min., the content of - 0.074 mm class is 72%. Reagents consumption in the regular experiment: Na2S 18 g/t; PBX 57 g/t (100%); T-92 frother 57 g/t; pH 7.85.

Reagents consumption using BTF-15221: BTF-15221 11.4 g/t (20%, hereinafter % of xanthate consumption), consumption of other reagents and conditions are similar to the regular experiment.

Flotation of copper-zinc ores. The flotation scheme included obtaining a copper head and conducting a collective copper-zinc flotation, the content of -0.074 mm class is 90%. Consumption of reagents in the collective cycle: PBX 45 g/t (100%), CaO 5 kg/t, Na2S 75 g/t, T-92 10 g/t.

Reagent consumption using BTF-15221: BTF-15221 9 g/t (20%) and 18 g/t (40%). Consumption of other reagents and conditions are similar to the regular experiment.

Flotation of skarn scheelite-sulfide ores. (Field tests stage). The processing scheme included the main cycle (roughing and scavenger flotation, separate recleaning of the main and control concentrates) and the selection cycle (the roughing and two scavenger flotations, two concentrate recleanings).

The ore was crushed to a fineness of 65-68% -0.074 mm class, conditioned with liquid glass in the amount 120 g/t, treated with 40 g/t of IMA-I413p a collector and 3 g/t of pine oil frother during 10 minutes. Then the roughing collective sulfide flotation was carried out during 10 minutes and the scavenger flotation for 10 minutes with the superinduction of a collector of 10 g/t, then the resulting concentrate was subjected to two recleanings.

During selection cycle, the bulk concentrate was treated in a conditioning tank with 5 g/t of activated carbon at normal temperature, then the roughing (10 min.), scavenger (10 min.) copper flotations and two recleanings (10 min. each) were carried out. In the roughing flotation 56-59 g/t of trisodium phosphate was added and 200 and 100 g/t of ferrous sulfate, pulp pH 7.4-7.9, were added in the 1st and 2nd recleaning, respectively.

The froth product of the second recleaning is a standard copper concentrate, the copper flotation tailings were sent to scheelite flotation.

Consumption of reagents using BTF-15221: at consumption of BTF-15221 50 g/t, consumption of activated carbon was 10 g/t, and at a consumption of BTF 75 g/t, consumption of activated carbon was 25 g/t. Consumption of other reagents remained similar to the default mode.

Flotation of auriferous arsenopyrite ore (I). The scheme included intermediate, roughing and scavenger flotation. Reagent consumption for the mentioned cycles, respectively: Potassium amyl xanthate (PAX) by Senmin 72.8 g/t, 20.8 g/t, 10.4 g/t; BTF-163 18.2 g/t, 5.2 g/t.2.6 g/t; Senfroth 1 g/t, 15 g/t, 15 g/t; C-7 12 g/t; soda in grinding 1400 g/t. Flotation time according to these cycles: 6 mins, 8 mins, 10 mins. Grinding size class 0.074 mm is up to 88%.

Reagents consumption using BTF-15221: BTF-15221 26 g/t by cycles is proportional to the consumption of PAX in the amount of 20% out of consumption of PAX, amyl xanthate in the amount of 130 g/t by cycles is proportional to the consumption of the

sum of PAX + BTF-163.

Flotation of auriferous and carbon-bearing pyrite-arsenopyrite ore (II). The flotation scheme included carbon flotation, which was carried out during 10 min at a flow rate of OPF-597 frother 80 g/t, the first stirring with reagents, intermediate flotation (3 min), concentrate regrinding, the second stirring with reagents, roughing flotation (7 min), scavenger flotation (14 min), primary cleaning (16 min) and secondary cleaning (14 min). During the first and second stirring consumption of reagents was as follows: soda 900 g/t and 400 g/t, liquid glass 50 g/t and 50 g/t, copper sulfate 160 g/t and 40 g/t, depressing agent A636 80 g/t and 80 g/t, PBX 100 g/t and 70 g/t, Aero-8045 20 g/t and 10 g/t, OPF-597 7 g/t and 7 g/t. In addition, 60 g of BPC and 8 g of Aero-8045 were sent to the scavenger flotation, and 80 g of A636 were sent to the primary cleaning.

Consumption of reagents using BTF-15221: the total consumption of BTF-15221 and PBX is given in Table. 5. BTF consumption on operations is proportional to the PBX consumption. Consumption of other reagents is similar to the default mode.

RESULTS AND DISCUSSIONS

The purpose of this study was to evaluate the flotation activity of the collector BTF-15221 and to establish the optimal conditions for its flotation effect.

When testing BTF-15221 collector, it was found that the flotation performance of its use is most often achieved when it is applied in composition with other collectors. In our researches the composition of this collector with PBX and PAX was used. Moreover, optimum results are only received at a certain ratio of xanthates and BTF-15221, with a narrow variation range of reagent concentrations in composition. The compositions of these reagents are characterized by both a decrease in the consumption of the initial xanthate and the preservation of its initial consumption. In order to assess the effect that the composition formulation has on flotation performance more clearly, in the tables with the test results of PBX and BTF-15221 compositions their consumption is presented as % from the initial xanthate consumption that is 100%. The actual consumption of reagents in g/t is given in description of the experimental part.

Table 1 shows the results of copper ore flotation with several compositions of BTF-15221 and PBX with different formulation.

The ore contained about 0.97% of copper and 0.27 g/t of gold. From the standpoint of economy in the composition, in addition to the flotation performance increase, it is necessary to minimize the consumption of xanthate and add more expensive additional collector BTF-15221 minimally in this case. With the decrease in xanthate consumption to 80% and its compensation by an equivalent consumption of BTF-15221, the use of composition made it possible to obtain a higher extraction of copper and especially gold (experiment 2). Increasing the xanthate consumption to 85% while maintaining the same consumption of BTF-15221 did not affect the flotation performance (experiment 3), while increasing the xanthate consumption to 90% made it possible to obtain an even higher copper recovery (experiment 4). A further increase in the consumption of xanthate to 100% at the taken consumption of BTF-15221 and an increase in the consumption of BTF-15221 to 30 g/t at a consumption of xanthate of 90 g/t did not affect the recovery of copper and gold, but somewhat reduced the content of copper and gold in the rough concentrate by means of output increase count. It is notable that the

recovery of gold in experiments 2-4 is disproportionately higher compared to the recovery of copper, which indicates the ability of BTF-15221 not only to increase recovery of gold associated with copper mineral, but also other auriferous forms (native, oxidized, sulfide, etc.). The noted feature determined the prospects for testing this reagent during the flotation of auriferous ores.

Table 2 shows the results of copper-zinc ore flotation.

Table 1 Flotation of copper ores results

№	Product name	Output, %	Content		Recovery, %		Collector consumption, %
			Cu, %	Au, г/т	Cu	Au	
1	Rough flotation concentrate	9.23	9.73	2.4	89.11	70.94	PBX 100%
2	Rough flotation concentrate	8.33	10.20	2.6	91.69	79.40	PBX-80% BTF- 20%
3	Rough flotation concentrate	10.50	8.17	2.0	91.77	77.28	PBX 85% BTF-15221 20%
4	Rough flotation concentrate	9.43	9.52	2.1	92.79	77.09	PBX 90% BTF-15221 20%

Table 2 Copper-zinc ore flotation results

№	Product name	Output, %	Content, %		Recovery, %		Collector consumption, %
			Cu	Zn	Cu	Zn	
1	Collective concentrate Cu-Zn	22.52	4.60	12.88	83.82	81.08	PBX 100%
2	Collective concentrate Cu-Zn	15.52	6.75	19.58	85.17	87.90	PBX 80% BTF-15221 20%
3	Collective concentrate Cu-Zn	14.89	6.88	20.42	83.58	86.28	PBX 60% BTF-15221 40%

The presented results indicate that the replacement of 20% xanthate consumption by an equal consumption of BTF-15221 allows to increase the recovery of both copper and zinc (experiment 2). At the same time, reducing the consumption of xanthate in the composition of less than 80% in experiment 3 significantly worsens the copper recovery. The results of this experiment allow us to conclude that BTF-15221 is a weaker collector compared to xanthate in the composition, when the proportion of BTF-15221 increased markedly, but is case the question arises: why does the extraction of metals increase in experiment 2, which will be discussed below.

Under laboratory conditions, the mode of application of BTF-15221 was worked out

in the flotation of skarn scheelite-sulfide ore, both as an independent collector and in combination with PBX.

After obtaining positive laboratory results in the flotation of skarn scheelite-sulfide ore, field tests were carried out on the use of BTF-15221 mainly as an independent collector and in a small volume in combination with xanthate.

Copper in the ores of the mine field is represented by chalcopyrite, sulfur by the main sulfide mineral pyrrhotine, arsenic by arsenopyrite. Gold is in a finely dispersed native state (basic size is 5-75 microns), in the form of thin adhesions on a quartz surface, the bulk of the metal is inside quartz particles, size 0.01-0.2 (0.3) mm and isomorphically replaces Fe, Cu, As in sulfides. Silver occurs in free form, in association with sulfides, in heavy metal carbonates, in quartz, and silicates. The mass fraction of copper in the head feed is 0.11-0.3%, the range of fluctuations for gold is 0.3-0.8 g/t, silver 1.7-8.5 g/t, sulfur 2.0-5.0 %, arsenic 0.04-0.17%.

The tests were carried out during 17 shifts, 1380 kg of the reagent were used for the tests. The test results are presented in table 3.

Table 3 Results of field testing of skarn scheelite-sulfide ore

№	Product name	Content				Recovery, %		
		Cu	As	Au	Ag	Cu	Au	Ag
Default mode								
1	Copper concentrate	16.81	1.33	15.08	384.5	74.29	33.03	61.13
Using reagent BTF-15221 consumption 50 g/t								
2	Copper concentrate	17.55	1.05	15.30	418.7	75.75	36.58	63.57
Using reagent BTF-15221 consumption 75 g/t								
3	Copper concentrate	17.08	0.29	24.70	372.2	77.34	50.44	66.40
Using reagent BTF-15221 consumption 59 g/t, PBX consumption 16 g/t								
4	Copper concentrate	17.99	1.08	25.50	429.2	78.44	47.41	67.87

Three modes were tested: at consumption of BTF-15221 in the amount of 50 g/t, equal to the regular consumption of IMA-I413P, at consumption of BTF-15221 in the amount of 75 g/t and at consumption of BTF-15221 in the amount of 58 g/t and PBX - 17 g/t (total 75 g/t).

With consumption of BTF-15221 in the amount 50 g/t, the increase in the recovery of metals into copper concentrate was: copper 1.46%, gold 3.55% and silver 2.44%. At the same time, the content of arsenic, which is limited, in the collected copper concentrate was lower than in the default mode.

With increase in consumption of BTF-15221 to 75 g/t, recovery of copper and precious metals increased markedly, and the content of arsenic in the concentrate, on the contrary, decreased by 3.6 times than with the consumption of BTF-15221 in the amount of 50 g/t.

When using the BTF-15221 and PBX composition, when the PBX content was about

27% of the BTF-15221 consumption, recovery of copper and silver increased slightly, but the arsenic content in the concentrate increased significantly, which noticeably reduces the cost of this concentrate.

The results of using the composition IMA-I413p and BTF-15221 and xanthate obtained in this study require some explanation. First of all, they indicate the absence of synergism in the action of these reagents composition. Given the synergy of action that might be expected with the introduction of small amounts of xanthate, the increase in the recovery of valuable metals should not have been accompanied by an equally high extraction of arsenopyrite [9,10].

Consequently, the obtained industrial results on the use of BTF-15221 indicate not only that it contributes to an increase in the recovery of copper and precious metals, but can be effectively used at certain consumptions in cases where it is necessary to reduce the arsenic content in concentrates.

In the above test results of BTF-15221 in the flotation of copper-bearing ores, when gold is present, it is shown that in compositions and separately it is a rather strong gold collector. In this regard, experiments on the use of the composition of xanthate and BTF-15221 in the flotation of two types of gold-containing arsenopyrite-pyrite ores were carried out.

The mineralogical composition of the tested arsenopyrite ore, containing about 3% of arsenopyrite as the main sulfide mineral, is represented 80% or more by quartz and silica-containing minerals (microcline and oligoclase), approximately 10% by silicates of mica group (biotite) and hydromicas. Pyrite and chalcopyrite in the form of isolated grains are present in small amounts.

Gold in the amount of 1.9-3.0 g/t is found in the ore in the form of simple gold arsenopyrite aggregates in quartz, or in the form of core or sieve clots in arsenopyrite.

When enriching this ore under industrial conditions, a combination of potassium amyl xanthate (PAX) in the amount of 104 g/t and BTF-163 collector of the dialkyldithiophosphate type in the amount of 26 g/t is used.

The results of arsenopyrite ore flotation using the xanthate and BTF-15221 composition are shown in Table 4.

As follows from the data in the table, an increase in the consumption of amyl xanthate in the composition from 104 g/t to 130 g/t and the replacement of BTF-163 collector with an equivalent amount of BTF-15221 makes it possible to increase the gold recovery by 2.57% at a higher degree of gold concentration.

Table 4 Flotation of auriferous arsenopyrite ore results

№	Product name	Output, %	Content of Au, g/t	Recovery of Au, %	Efficiency %	Concentration ratio
Default						
1	Total concentrate	15.25	10.73	84.29	70.41	5.53
PBX consumption – 130 g/t, BTF-15221 – 26 g/t						
2	Total concentrate	15.29	11.36	86.86	73.04	5.68

Similar results in gold recovery were also obtained by reducing the consumption of amyl xanthate to 110 g/t and increasing the consumption of BTF-15221 to 39 g/t.

Field tests using the composition of amyl xanthate and BTF-15221 are scheduled to be conducted on the enterprise processing this ore in 2023.

At present, gold- and carbon-bearing pyrite-arsenopyrite ores are a difficult object of enrichment in Russian Federation and Kazakhstan due to the difficulty of separating carbon components. In this regard, it seemed interesting to test the composition of xanthate and BTF-15221 during flotation of this type of ores. The following ore was used for the experiments: gold content 3.3 g/t, total sulfur 1.53%, sulfide sulfur 1.367%, total carbon 3.563%, organic carbon 2.626%, SiO2 content 67.99%, Al2O3 14.34%.

Table 5 Flotation of gold- and carbon-containing pyrite-arsenopyrite ore results

№	Product name	Output, %	Content			Recovery, %			Efficiency, %	Throughout recovery, %
			Au, g/t	C, %	C_{org}%	Au	C	C_{org}		
Default consumption: PBX – 230 g/t; A 8045 – 38 g/t.										
1	Total concentrate	5.69	86.97	5.74	5.25	90.82	8.20	9.97	90.03	95.63
Using A 8045. Consumption PBX 260 g/t, A 8045 30 g/t										
2	Total concentrate	5.98	83.00	7.47	7.27	89.85	11.94	15.64	88.77	94.74
Using BTF-15221. Consumption: PBX – 230 g/t; BTF-15221 – 46 g/t										
3	Total concentrate	5.24	99.0	4.11	3.61	94.49	5.38	6.11	94.44	98.36
Using BTF-15221. Consumption: PBX – 260 g/t; BTF-15221 – 30 g/t										
4	Total concentrate	5.41	97.91	3.28	3.16	91.59	4.68	5.79	91.47	96.80

Experiments with the composition of BTF-15221 and xanthate were carried out on this ore sample with a change in the consumption of both BTF-15221 and xanthate. The results of flotation tests are shown in Table 5. As follows from the data in the table, the highest technological results were obtained in experiment 3, when the standard consumption of xanthate was maintained and the consumption of BTF-15221 was increased by 20% compared to the consumption of the standard additional reagent A-8045. The recovery of gold both in the total concentrate of 94.49% and throughout recovery (total recovery of all products of the experiment without extraction into tailings) of 98.36% is noticeably higher than in the standard experiment: 90.82% and 95.63%, respectively. The selectivity of gold recovery in this experiment, estimated according to the carbon content in the concentrate, is noticeably higher than in the standard experiment.

Sufficiently high rates of gold recovery and selectivity were achieved in experiment 4 with the increased consumption of xanthate. The increase in gold recovery compared to the standard experiment was 0.77% and 1.74% compared to experiment 2, when the consumptions of the collectors are equal.

A number of features of BTF-15221 reagent effect can be explained by the presence

of a dialkyldithiophosphate compound in its composition. When BTF-15221 is used as a collector, the replacement of a part of the xanthate on the mineral surface with dialkyldithiophosphate present in BTF-15221 leads to a decrease in the mineral hydrophobicity, and as a consequence, to a deterioration in floatability, due to the fact that dialkyldithiophosphates are weaker collectors compared to xanthates. This disadvantage is compensated by an increase in xanthate consumption. It is known that dialkyldithiophosphates have surface activity not only at the liquid-gas interface, but also at the solid-gas interface. A noticeable increase in the concentration of dialkyldithiophosphate in the aqueous phase can also cause a decrease in the extraction of the mineral, since it is known that the decrease in the free energy of the mineral particle-air bubble system is the smaller, the lower the σl-g (surface tension) of the aqueous solution.

At the same time, it has been shown that the movement of dialkyldithiophosphate from the liquid-solid interface to the solid-gas interface, both on the contact perimeter and over the entire bubble area, leads to strengthening of the bubble-particle contact. This strengthening is due to an increase in the rate of thinning of the water film between the air bubble and the mineral particle [6].

Therefore, during flotation, the consumption of dialkyldithiophosphates and reagents containing dialkyldithiophosphates must be experimentally selected so that their positive effect at the solid-gas interface exceeds the possible negative effect at the liquid-gas interface, as well as their weaker hydrophobic effect on the mineral surface. compared to xanthates. The use of dialkyldithiophosphates in combination with strong collectors reduces their negative effect at the liquid-gas interface by reducing the consumption and explains how a positive effect with their low consumption can be achieved.

CONCLUSION

The presented experiment results on the use of BTF-15221 as a collector allow us to suggest that it can be successfully used in the flotation of various types of sulfide ores containing copper and precious metals.

A commercial batch of this reagent was made in the amount of 50 tons for its introduction at one of the factories in Russia, where they enrich auriferous arsenopyrite ores. It is also planned to conduct field tests of the reagent at one of the factories in Kazakhstan.

REFERENCES

1. Lewis A., (2018) Tectlote - novel chemistry for new sulfide collectors. A selective collector at natural pH for pyrite rich ores and ores containing sulfides, gold, silver and platinum group elements. XXIX IMPRC, Moscow, Paper 244.
2. Miki H., Hirajima T., Muta Y., Suyantara G.P.W., Sasaki K. (2018) Investigation of reagents for selective flotation on chalcopyrite and molybdenite. XXIX IMPRC, Moscow, Paper 663.
3. G. Lui, J. Xiao, X. Yang and H. Zhong. (2016) A review of flotation collectors: fundamentals to practice. XXVIII IMPRC, Canada Quebec, P ID 206.

4. Hreniuc P.N, Pasca I, Stevan O., Badescu G. (2013) New technologies to recover gold and silver from ores and concentrates incell-type column XV Balkan Processing Congress, Bulgaria, v.1, 466-475.
5. Lei Pan, Rol-Hoan Yoon. (2014) Direct measurement of hydrodynamic and surface forces in bubble particle. XXVII IMPRC, Santiago, Chile, V.1, P. 88.
6. Kondratyev S.A., Ryaboy V.I. (2016) Influence of desorbed species of xanthates and dialkyldithiophosphates on their collecting ability. XXVIII IMPRC, Canada Quebec, Paper 133.
7. Ryaboy V.I et al. Eurasian patent No 031517 The composition of the collecting reagents for the flotation of sulfide ores. Announced 12.08.2017, published 31.01.2019.
8. Roberts D. et al. USA patent No 5232581. Recovery of platinum group metals and gold by synergetic reaction between allylalkyl thionocarbamates and dithiophosphates. Announced 04.05.1992, published 03.08.1993.
9. Karimain A, Rezaei B., Masoumi A. (2013) The effect mixed collectors in the rougher flotation of sungun copper Life Science Journal, 10 (6s), 268-272.
10. Bradshow D.J, Harris P.J, O'Connor C.T. (1998) Synergetic interactions between reagents in sulfide flotation. J. of the South African Institute of Mining and Metallurgy, 189-194.
11. Kondratyev S.A. (2010) Assessment of the activity of collecting reagents during flotation, Obogashenie rud, No 4, 24-30.

XV International Mineral Processing and Recycling Conference
17-19 May 2023, Belgrade, Serbia

COMPARATIVE ANALYSIS OF REAGENTS FOR GOLD EXTRACTION FROM FLOTATION TAILS

I. Dervišević[1#], A. Dervišević[2], M. Tomović[1], J. Galjak[1]
[1] University of Pristina with temporary headquarters in K. Mitrovica, Faculty of Technical Sciences Kosovska Mitrovica, Serbia
[2] University of Novi Sad, Faculty of Technology, Novi Sad, Serbia

ABSTRACT – The importance of obtaining gold from low-quality ores and flotation tailings is continuously growing, not only due to the increase in demand for gold and high gold prices, but also due to raising social awareness of the importance of the circular economy, sustainable development and greening of the gold extraction process. The goal of this work is the development and implementation of alternative, environmentally less dangerous and harmful processes for the extraction of gold and other valuable metals, the reduction and efficient, economically justifiable and environmentally acceptable use of the generated amounts of waste as one of the key goals of the future development of society. The paper provides a comparative analysis of appropriate reagents for the extraction of gold and associated metals, with a focus on less harmful processes. The following methods were used for the characterization and analysis of the examined samples: Inductively Coupled Plasma with Optical Emission Spectroscopy (ICP-OES), X-ray diffraction (XRD) and X ray fluorescence spectroscopy (XRF) methods. As a result of this comparison, thiourea stands out as the most promising alternative reagent for the extraction of gold from the tested samples.

Keywords: Flotation Tailings, Gold Extraction, More Ecological Reagents.

INTRODUCTION

In the earth's crust, gold is present in a concentration of only 0.005 ppm. This low concentration is a major challenge for gold processing due to the need to upgrade by a factor of 3000 to 4000 to obtain commercial concentrations. And if it can be found in elemental form in some parts of the world, gold is often associated with silver, copper and other metals, it also occurs in sulphide ores such as pyrite, tetrahedrite, chalcopyrite and arsenopyrite [1]. Gold has excellent chemical resistance and electrical conductivity. These properties of gold make it a useful material for the electronics industry, where it is used as a coating for electrical contacts. The demand for this precious metal is constantly growing. In the last four decades, gold production in the world has doubled and new hydrometallurgical processes have been developed for its extraction. Strategic principles of future development, based on circular economy, sustainable development, cleaner technologies, more efficient, economical and ecological processes. The constant increase in demand for gold and price jumps on the economic market indicate that the recovery of gold from secondary raw materials is gaining more and more importance. The exceptional chemical resistance of gold becomes a disadvantage in

corresponding author: irma.dervisevic@pr.ac.rs

hydrometallurgical processes, and it is not easy to find reagents that can easily dissolve gold. Reagents that can dissolve gold, such as cyanide, chloride or sulfur complexes, are generally extremely aggressive and highly toxic to the environment [2,3]. In order to overcome environmental problems, new reagents for gold extraction, less toxic and new washing techniques, which are more suitable for further research in laboratory conditions, were tested [1,4]. All gold ore treatment processes, from concentration to gold refining process, create residues with residual gold content (tailings and waste sludge from various extraction processes, flotation, leaching processes, cyanidation, amalgamation, electrolysis, etc.). It is precisely the low content of gold in the ore that contributes to the generation of huge amounts of tailings and waste sludge, which not only reduce the efficiency of extraction, but also contribute to large economic losses and environmental problems [1].

This paper aims to present the procedure of efficient extraction of gold by more environmentally friendly hydrometallurgical procedures. The paper will present the results of gold extraction from the flotation tailings of the Lece mine, using different reagents, in order to point out their advantages and disadvantages in terms of extraction efficiency and impact on the environment and pollution.

GENERAL CHARACTERISTICS OF THE FLOTATION TAILINGS OF THE LECE MINE

The Lece mine is located in the territory of the municipality of Medveđa, in the immediate vicinity of the Lece village of the same name, at the foot of the Radan mountain. The Lece mine is located at an altitude of 525 m. It is a rugged landscape, which is part of the Lec volcanic complex with jewelry stone deposits that belong to the group of hydrothermal deposits and mineral resources. The geological structure of this ore area consists of rocks of the andesite complex of Tertiary age, formed during the Upper Oligocene and Miocene by the deposition of powerful andesite flows and deposits of their pyroclastites. The creation of deposits and ore occurrences of lead, zinc, gold and silver in the Lece region is genetically linked to the tectonic-magmatic processes of the Tertiary metallogenic epoch. Traces of old mining activities were found on the mountains of Radan and Majdan, which surround the settlement of Lece [5].

EXPERIMENTAL

Materials and Methods

The tested material consists of samples of "old" flotation tailings from the Lece mine, treated in laboratory conditions. The material was first treated by the method of gravity concentration (rotating cone) and magnetic separation, optionally: shredding, grinding and gravity concentration and magnetic separation.

X-ray fluorescence spectroscopy (XRF) was used to determine the chemical composition of the flotation tailings, and X-ray diffraction analysis (XRD) was used to determine the crystallographic structure of a material. To determine the content of the constituents of the solution and sediment, after treating the flotation tailings with different reagents, the methods Atomic Absorption Spectrophotometry (AAS) and Induced Coupled Plasma with Optical Electron Spectrometry (ICP-OES) were used.

RESULTS AND DISCUSSION

The process of gravity concentration involves the separation of tailings containing gold, which has a higher specific gravity, from the rest of the accompanying material. The efficiency of gravity concentration stems from the large difference in specific density between gold (19.3 g/cm^3) and other impurities with an average density of about 2.6 g/cm^3. The process of pre-concentration of gold is very important and should enable effective and economical further processing of gold, i.e. effective washing, precipitation and purification of gold by chemical methods [6]. The device for gravity concentration is created so that the movement of crushed ore material with gold particles is aimed at settling in the bottom of the device, unlike other ore material, which as a specifically lighter fraction, reaches the surface of the device.

The quality of the ore exploited in the Lece mine has changed over time. In period 1931-1941. quality of exploited ore: Pb 3.6%, Zn 6.5%, Au 4.7-9.4(g/t), while the 1953-1990. Pb 1.55%, Zn 3.43%, Au 3.78(g/t) and Ag 16.16(g/t) [7]. The chemical composition of the flotation tailings analyzed by the XRF method is shown in Table 1. The proportion of Au and Ag in the flotation tailings was determined by the ICP-OES method and is shown in the same Table 1.

Table 1 Chemical composition of the flotation tailings analyzed by the XRF and ICP-OES method

Elem.	SiO_2	Fe_2O_3	SO_3	Al_2O_3	K_2O	ZnO	CaO
Wt %	34.69	43.26	15.09	2.77	1.27	1.39	0.34
Elem.	P_2O_5	CuO	PbO	TiO_2	Cr_2O_3	Au ppm	Ag ppm
Wt %	0.18	0.47	0.31	0.15	0.09	1.12	5.46

Figure 1. shows the diagram of the XRD analysis of the flotation tailings sample, which shows the highest presence of quartz, as a tailings residue, which initiates mandatory gravity concentration pretreatment, followed by the presence of 3-amino-1,2,4-triazole, i.e. organic substances and fluorides used in the process of multi-stage ore flotation, in order to achieve selective separation in the pretreatment of gold extraction.

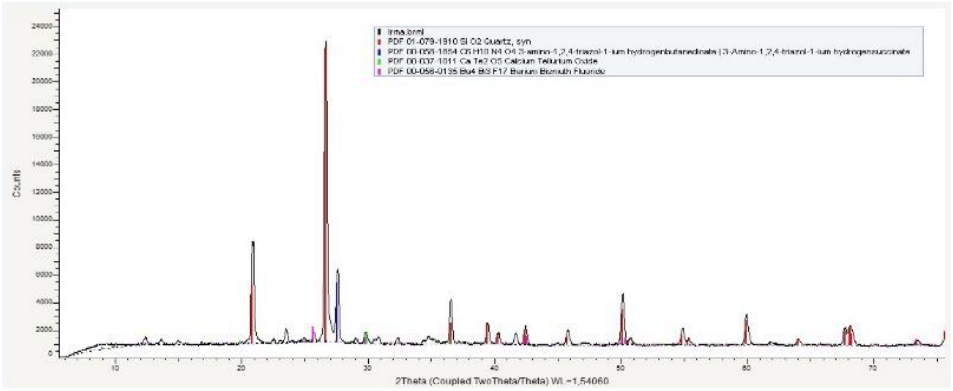

Figure 1 XRD analyzes of the flotation tailings sample

In the treatment of flotation tailings samples for gold extraction in laboratory conditions, conventional reagents were used, which are otherwise very aggressive, corrosive and harmful to the environment and human health, as well as less harmful and more suitable for the environment, so that a comparative test could be carried out analysis of their efficiency. Table 2 shows the characteristics of the reagents used.

Table 2 Characteristics of the reagents used for extraction gold

Reagents	Oxidants	Agents	Advantages	Disadvantages
Aqua Regia	O_2 Fe^{3+} Mg^{2+}	Cl^- NO_3^-	Acts as a strong oxidizing solvent for gold and other precious metals (Pt, Pd) remar-kable economic benefit.	Extremely toxic, harmful to environment and human health.
Cyanides	O_2	CN^-	Simple process, high yield, remarkable economic benefit, Industrial used.	No antiinterfere-nce, extremely toxic, harmful to environment and human health.
Thioslfate	O_2 $Cu(NH_3)_4^{2+}$	$S_2O_3^{2-}$	Rapid, high yield, strong antiinterference, slight equipment corrosion.	Large reagents consumption, complex gold recovery process.
Thiourea	Fe^{3+}, H_2O_2	$SC(NH_2)_2$	Rapid, high yield, strong antiinterference, preliminary industrialization.	Poor stability, large consumpti-on, strong corro-siveness, high cost.
Iodine–iodide	I_3^-	I^-	Non-toxic, rapid, high yield, ecofriendly.	High cost, poor industrial application, harsh conditions.

Pretreatment and leaching conditions are very important and affect the efficiency of gold extraction. Parameters such as reagent concentration, pH value, process temperature, aeration and mixing were monitored in all leaching trials. The optimal conditions and achieved level of leaching efficiency, in laboratory conditions, are shown in Table 3.

During the test, on average, in the first 1 - 2 hours, about 60% of the gold was leached, and in 12 hours, approximately 70%. The results of leaching achieved in 24h are shown in Table 3. Longer leaching time, after 24h, resulted in negligible gold leaching.

The experimental investigates were performed under conditions with variable pH values in a wide range and mostly at room temperature, except in the case when aqua

regia was used as a reagent. For leaching efficiency, a higher liquid-to-solid ratio increases the rate and quality of gold recovery.

Table 3 The optimal conditions and achieved level of leaching efficiency

Characteristics of reagents	pH	Leaching conditions	Leaching yield
Aqua regia concen. (HNO_3: HCl =1:3)	1.2	70 °C, 24h, 300 r/min, O_2	62.32%
NaCN (5.5-6.5kg/t)	11	25 °C, 24h, 400 r/min, O_2	61.08%
0.5 M Thioslfate, 0.2 M CuSO4, 1 M HN_3	9.5	25 °C, 24h, 400 r/min, O_2	68.87%
0.1 M Thiourea, 0.09 M $Fe_2(SO_4)_3$	1.25	25 °C, 24h, 400 r/min, O_2	66.43%
20 g/L KI, 4 g/L I_2	8.5	25 °C, 24h, 300 r/min, O_2	73.95%

The highest leaching efficiency was achieved using KI/I of 73.95% at pH 8.5, which is nontoxic and ecofriendly, but the price of this reagent is high. In contrast, the classical methods: cyanidation and the method with aqua regia, which are extremely aggressive and corrosive reagents, with a negative impact on the environment and human health, showed the maximum yield of leaching, respectively: 61.08% at a high pH value of 11, and 62.32% at an extremely low pH of 1.2. A leaching yield of 66.43% for thiourea required a pH of 1.25, and for thiosulfate, a yield of 68.87%, pH 9.5. Both processes are environmentally friendly, but require a large amount of reagents and the selectivity of gold leaching. Effective leaching of gold with thiosulfate requires a more complex process.

CONCLUSION

The paper examined the efficiency of gold extraction from the flotation tailings of the Lece mine with different reagents in order to determine the optimal leaching conditions and to see the basic advantages and disadvantages of each reagent in relation to the efficiency, economy and environmentalization of the process. The high selectivity of Au leaching with respect to other coexisting metals is a key advantage, but further research is needed to reduce the consumption of appropriate reagents.

ACKNOWLEDGEMENT

This research is supported by the Ministry of Education, Science and Technological development of the R. Serbia and s conducted as a part of project no. III 43007 and no. 37016.

REFERENCES

1. Marsden, J., House, I. (2006) The Chemistry of Gold Extraction: SME.
2. Mineral Commodity Summaries, “Gold Production in World” 2012_George_US Geological Survey.

3. US Department of Health and Human Services, "Toxicological Profile for Cyanide," 2006.
4. Syed, S. (2012) Recovery of Gold from Secondary Sources—A Review. Hydrometallurgy, 115, 30-51. http://dx.doi.org/10.1016/j.hydromet.2011.12.012.
5. Miladinović, Z.Ž. (2012) Mineragenetske karakteristike i potencijalnost juvelirskih mineralnih resursa Leckog vulkanskog kompleksa, Disretacija, RGF, Univerzitet u Beogradu.
6. Gül, A., Kangal, O., Sirkeci, A.A., Önal, G. (2012) Beneficiation of the Gold Bearing Ore by Gravity and Flotation. Int. J. Minerals, Metallurgy, and Materials, 19, 106-110. http://dx.doi.org/10.1007/s12613-012-0523-4.
7. https://web.archive.org/companies/lece/sr/2023/03/20.

XV International Mineral Processing and Recycling Conference
May 17-19, 2023, Belgrade, Serbia

TESTS WITH DIFFERENT FLOCCULANTS FOR CHROMIUM ORE TAILINGS

E. M. S. Silva[1#], A. C. Silva[1], J. M. B. S. Cabral[1], P. S. Oliveira[2], A. F. Nascimento[2], A. P. Vieira Filho[2], S. A. Santos[2]

[1] Modelling and Mineral Processing Research Lab, Federal University of Catalão, Catalão, Brazil

[2] Companhia de Ferro Ligas da Bahia (FERBASA), Andorinha, Brazil

ABSTRACT – Aqueous routes are of paramount importance in mineral processing. To adjust the solid contents, both concentrates and tailings, must be dewatered. A widely adopted method is the thickening, promoting the free settling of the mineral particles aided by coagulants or flocculants. This study analyzed the performance of different polyacrylamides as flocculants in the sedimentation of chromite tailings. Tests were carried out in graduated cylinders of 2.0 L for different types and dosages of flocculants and pHs. It was possible to make the settling more efficient with the addition of 30 g/t of BASF's Magnafloc 338 at pH 8.5, decreasing the average pulp turbidity from 740.33 NTU to 31.74 ± 1.16 NTU after a few minutes.

Keywords: Dewatering, Tailings, Chromite, Flocculation, FERBASA.

INTRODUCTION

Brazil is the 11th larger chromium producer, with Companhia de Ferro Ligas da Bahia (FERBASA) being the largest producer. The company operates two chromite mines, located in the Center-North region of the state of Bahia, Brazil, ninety miles away from each other: Ipueira mine in the Chromite District of Vale do Jacurici and the Coitezeiro mine in the Chromite District of Campo Formoso. The Figure 1 shows the FERBASA simplified flowsheet for the chromite sand production. The run of mine (ROM) ore is feed in a series of crushers (primary and secondary crushing in universal jaw crushers). The secondary crusher operates in a closed circuit with a double deck vibratory screen. The fine fraction (-10 mm) and the products referred as disseminated ore feeds a gravimetric plant, where it will be grinded (two stage grinding, with ball mills) and concentrated using spirals and magnetic separators to produce chromite sand, used as steel casting. This is a wet circuit; therefore, the chromite sand (concentrate) needs to be dried in ovens before expedition. The plant produces two different tailings: a coarse and a fine tailing, which also need solid-liquid separation (aka dewatering). The coarse tailing is composed by cyclones underflow, and the fine tailings are fed to conventional thickeners (see Figure 2). The solids percentage feed in the thickener is normally below 2%. According to Dahlstrom and Fitch [1], dewatering is common in mineral processes plants, mainly because water as the main medium for processing and transport ores. The thickener overflow is sent to ponds for free settling, indicating that the thickener operation is not

[#] corresponding author: eschons@ufcat.edu.br

optimized. According to Bolto and Gregory [2], after the flocculant is added to a colloidal suspension the particles need to be mixed with the reagent. Then the adsorption of the reagent on the particles surface occurs, followed by rearrangement of the adsorbed chains and, finally, the flocculation takes place by bridging flocculation. This process increases the settling speed of the solid particles. Nowadays an anionic high molecular weight polyacrylamide (PAM) is used as flocculant (10 g/t Flonex 910 SH manufactured by SNF Floerger diluted to 0.15%). This work aimed in reduce the solids in the thickener overflow by changing the PAM, flocculant dosage, and pulp pH.

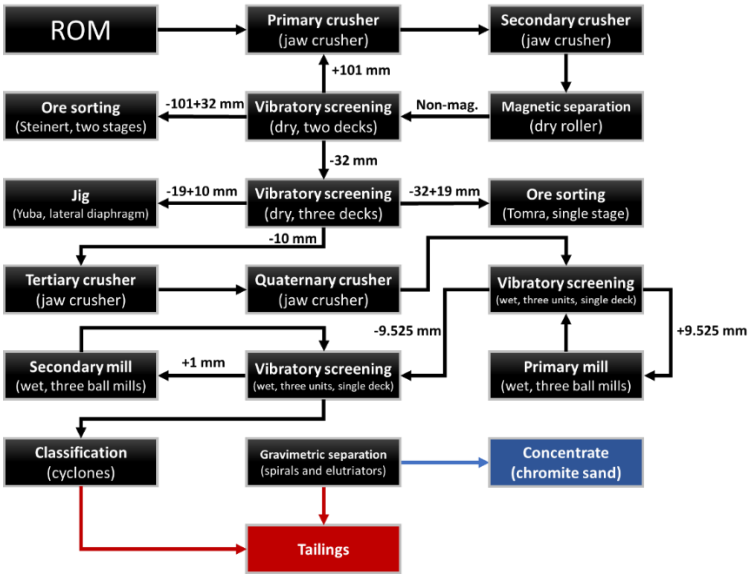

Figure 1 FERBASA simplified mineral processing flowsheet for the chromite sand production

Figure 2 View of one of the chromite tailings thickeners operating at Ipueira/FERBASA.

EXPERIMENTAL

Samples from the tailing thickener feed were collected oven dried and sent to wet screening particle size distribution determination. For that eight screens were used according to a Tyler series. The screening duration was 15 minutes, and 20 L of water were used. Sodium metasilicate (1% v./v.) was used as dispersant (6 mL). The fractions produced after the wet screening were sent to optical microscopy using a Bresser Biolux NV - Technic Professional Microscope. A head sample and two samples from the wet screening (+400# and -400#) were chemically analyzed in a Rigaku ZSX Primus IV x-ray fluorescence spectrometer at CRTI/UFG.

A flocculant screening was carried out with eleven different PAM (see Table 1) through sedimentation tests in graduated cylinders (2.0L of internal volume). The objective of this stage was to choose one PAM to be further assessed (optimization stage). According to Bolto and Gregory [2], flocculants are broadly characterized by their ionic nature: cationic, anionic, and non-ionic. Since the use of cationic polymers are not usually for mineral particles, only anionic (with different charge densities) and non-ionic flocculants were tested in this work. The flocculant dosage was fixed at 22.5 g/t for all flocculants and the solid percentage of 1.0% (w./v.). The pulp pH was not controlled, only measured, with average value of 8.5. The pulp turbidity was measured at seven different times (from 0 to 30 minutes every 5 minutes after initial agitation) using a Hanna portable turbidimeter model HI-93703 (0 to 1,000 NTU). Turbidity indicates the degree of attenuation that a beam of light undergoes when passing through water. This attenuation occurs by the absorption and scattering of light caused by suspended solid particles. This parameter was adopted since Brazilian regulations stablish that industrial water must be returning to environment with turbidity below 5 NTU [4].

Table 1 PAM used in the experimental test work.

Flocculant	Molecular weight	Charge	Manufacturer	Recommended dosage (g/t)
Magnafloc 10	Very high	Slightly anionic	BASF	2 – 200
Magnafloc 155	High	Anionic	BASF	2 – 500
Magnafloc 336	High	Anionic	BASF	50 – 200
Magnafloc 338	Moderated	Anionic	BASF	2 – 200
Magnafloc 351	High	Non-ionic	BASF	2 – 100
Magnafloc 919	Ultra-high	Anionic	BASF	2 – 200
Magnafloc 1011	Very high	Anionic	BASF	2 – 200
Magnafloc 3230	-	Low anionic activity	BASF	-
Rheomax DR 1050	-	Anionic	BASF	2 – 200
MKFLOC ASV 3060	High	Anionic	MK	-
FLONEX 910 SH	High	Anionic	SNF Floerger	10 – 15

Additional tests (optimization stage) were carried out in three different pHs (7.5, 8.5, and 9.5) and three dosages (15, 22.5, and 30 g/t) with the best flocculant selected after the screening. According to Nozaic et al. [3], there is a greater sensitivity to incorrect dosage of flocculants with turbidity, which motivated the dosage investigation. The two flocculants available at FERBASA (Flonex 910 SH and MKFLOC ASV 3060 manufactured by MK) were used as benchmark in all tests. The pulp turbidity was measured at three different times (0, 5, and 10 minutes) Sodium hydroxide and sulfuric acid (both 10%)

were used as pH regulators. Tap water were used throughout the experiments. All tests were carried out in triplicate. In total, thirty-three tests were carried out in the screening stage and eighty-one in the optimization stage.

RESULTS AND DISCUSSION

Figure 3 shows the tailings samples characterization. It is possible to notice that the tailings were very fine, with average of 96% of the mass below 400# (-38 µm). Regarding the chemical composition the tailings is composed by SiO_2 (35.66%), MgO (28.00%), Fe_2O_3 (8.18%), Cr_2O_3 (6.86%), Al_2O_3 (6.33%), and CaO (3.40%). The low chromium oxide content and the fine granulometry makes impossible to gravimetric recover the remaining chromium particles in the tailings. Figures 3c to 3f presents same optical microscopy images. It was possible to notice the presence of micas (vermiculite and/or muscovite).

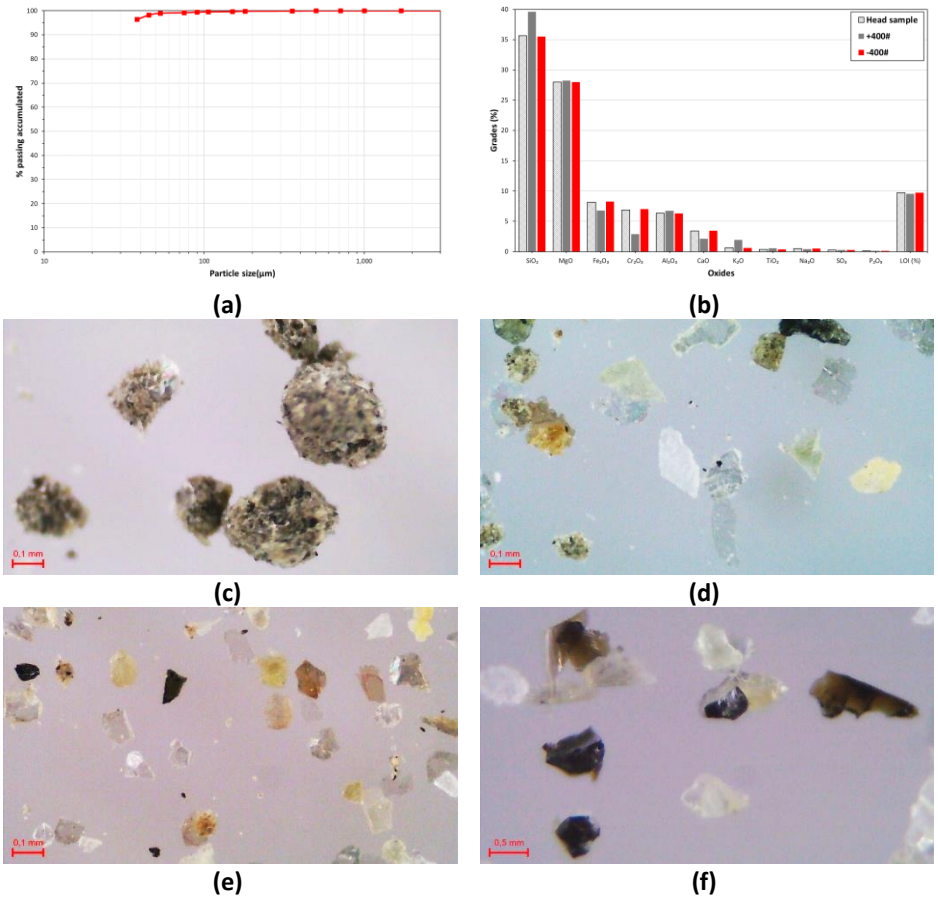

Figure 3 Tailings characterization: (a) particle size distribution, (b) XRF, and optical microscopy -45+80# (c), -140+170# (d), -200+270#, and -325+400# (f).

Figure 4 presents the flocculant screening results. It is possible to notice that the solid percentage of 1.0% (w./v.) produced pulps with initial turbidity in the reading range of the turbidimeter (< 1,000 NTU). The sedimentation tests results can be seen in Figures 4c and 4d. Since the initial turbidity its more than ten times the final turbidity, the figures were plotted with (4c) and without (4d) this point. The Magnafloc 388 was produced the best results in this stage, with final turbidity of 13.75 ± 2.87 NTU. The PAM used in Ipuera/FERBASA produced a residual water with turbidity almost three times higher (40.71 ± 5.76 NTU for Flonex 910 SH and 36.84 ± 0.77 NTU for MK Floc ASV 3060).

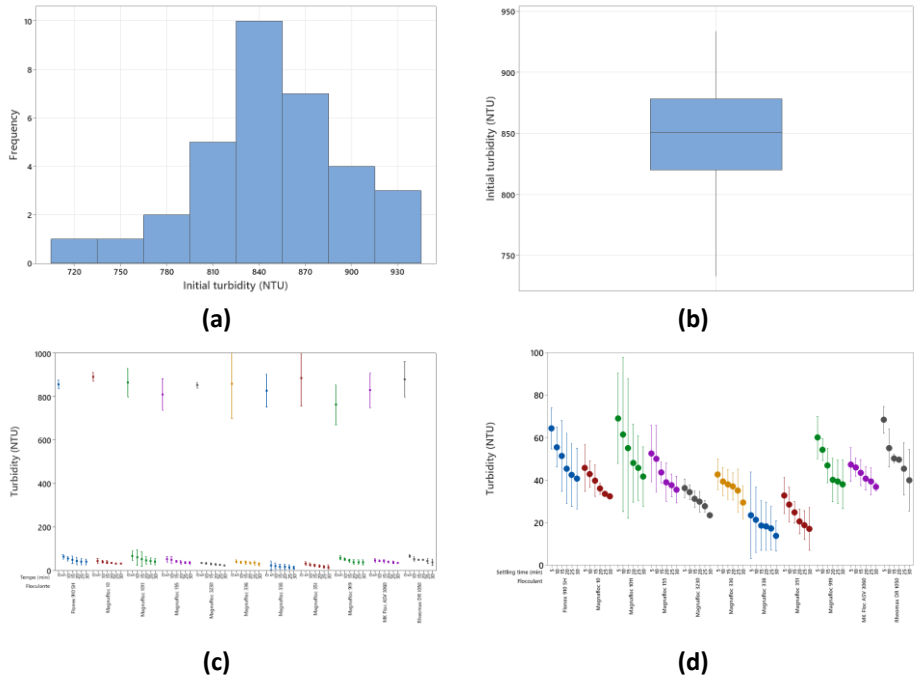

Figure 4 Results of the flocculant screening: initial turbidity histogram (a) and boxplot (b), and interval plot of turbidity with (c) and without (d) the initial turbidity.

Figure 5 present the results for the two flocculants used in Ipuera/FERBASA (Flonex 910 SH and MK Floc ASV 3060) versus the Magnafloc 338, manufactured by BASF. In general, the increase in the pH increased the final turbidity (after 10 minutes of settling) when using Flonex 910 SH, for all tested pH. Similar behavior was only seen with 30 g/t of MK Floc ASV 3060. Magnafloc 338, on the other hand, showed a decrease in the turbidity with the increase of the pH. The increase in the flocculant dosage produced small to no changes in the final turbidity for Magnafloc 338 and MK Floc ASV 3060. The lower final turbidity found for the Flonex 910 SH was 43.12 ± 0.38 NTU at pH 7.5 and 22.5 g/t. For the MK Floc ASV 3060 the best result found was 45.33 ± 0.58 NTU at pH 8.5 and 15 g/t. Magnafloc 338 lower final turbidity was 31.74 ± 1.16 NTU at pH 8.5 and 30 g/t. This result is 35.84% and 42.81% lower than the best results found for Flonex 910 SH and MK Floc ASV 3060, respectively.

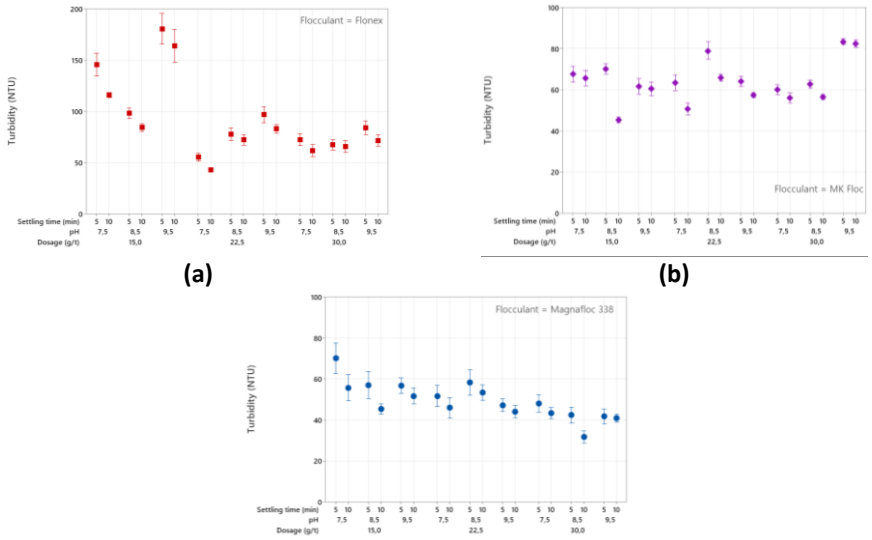

Figure 5 Results for the three tested flocculants: (a) Flonex 910 SH, (b) MK Floc ASV 3060, and (c) Magnafloc 338 for different dosages and pHs

CONCLUSION

The found results indicated that the change from high molecular weight anionic PAM such as to a Flonex 910 SH and MK Floc ASV 3060 to a moderated molecular weight anionic PAM (Magnafloc 338) can decrease the turbidity of the clarified effluent produced. Although no test could reduce the pulp turbidity below 30 NTU, the authors believe that an increase in the Magnafloc 338 dosage could produce even better results.

ACKNOWLEDGEMENT

The author would like to acknowledge FERBASA for the permission to carry out this work ant to allow the data publication. We also thank the CRTI/UFG, Federal University of Catalão and Modelling and Mineral Processing Research Lab (LaMPPMin).

REFERENCES

1. Dahlstrom, D.A., Fitch, B. (1985) Thickening. In: Weiss, N.L. SME Mineral Processing Handbook. SME Editor, New York.
2. Bolto, B., Gregory, J. (2007) Organic polyelectrolytes in water treatment. Water Research, 41 (11), 2301-2324.
3. Nozaic, D.J., Freese, S.D., Thompson, P. (2001) Long term experience in the use of polymeric coagulants at Umgeni Water. Water Supply, 1 (1), 43-50.
4. Viana, D.B., Daniel, M.H.B., Magalhães, T.B. (Org.) (2016) Diretriz Nacional do Plano de Amostragem da Vigilância da Qualidade da Água para Consumo Humano. Brasília: Ministério da Saúde, p. 53.

XV International Mineral Processing and Recycling Conference
17-19 May 2023, Belgrade, Serbia

STUDY ON THE APPLICATION OF HIGH-EFFICIENCY AND ENVIRONMENT-FRIENDLY COPPER COLLECTOR TO ASSOCIATED COPPER IN AN IRON ORE

C. Ouyang[#], B. Lv, K. Jia, Y. Yang
Serbia Zijin Mining, Bor, Serbia

ABSTRACT – The associated copper of a large iron ore mainly exists in the form of natural copper. The processing plant has used xanthate as the copper flotation collector for many years. However, due to the excessive xanthogenate ion in the tailings monitoring well, the copper flotation operation was stopped; this study. In view of the nature and characteristics of natural copper, the high-efficiency and environmentally friendly copper collector CYC-20 is used for process research. The laboratory closed-circuit test results show that the use of CYC-20 instead of the butyl xanthate process can obtain copper grades through one rough, two fine and one sweep. The copper concentrate with 17.20% and a recovery rate of 74.48%. Industrial test results show that using CYC-20 as copper collection, the copper concentrate grade has been increased from 13.57% to 17.04%, and the recovery rate of copper metal has been increased 7.68%, and the effect of improving technical indicators is significant.

Keywords: Environmental Protection, Associated Natural Copper, Collector.

INTRODUCTION

In recent years, with the increasing emphasis on ecological economy, the requirements for clean production of mineral processing are increasing. In order to reduce the impact of flotation reagents on the surrounding water quality, the replacement of traditional reagents such as xanthate with new reagents that are clean, environmentally friendly and free of water pollution has received increasing attention. In the early mine construction, the anti-seepage treatment measures for the tailings pond were not perfect. The use of xanthate as a collector for copper flotation would cause some xanthate ions to diffuse to the surrounding groundwater with the tailings pond water, causing water pollution. As a result, the production cannot run smoothly.

In this study, a detailed copper flotation collector test was carried out according to the properties of the associated copper ore in an iron ore. The purpose is to obtain copper flotation collectors with less using dosage, poor water solubility, less residues of chemicals in tailings water, and good collection performance which can replace the widely used xanthate and reduce the risk of environmental pollution. And carry out industrial tests at the production site according to the research results [1-5].

MATERIALS AND METHODS

The ore used in this research was taken form Shandong province of China. The iron

[#] corresponding author: Chongzhong Ouyang:542198726@qq.com

grade is 30.77%, and the Cu grade is 0.098%. The main gangue components are SiO_2, followed by Al_2O_3, CaO and MgO (Table1).

Table 1 The chemical analysis results [%]

element	TFe	FeO	Fe_2O_3	Cu	Co	TiO_2
content	30.77	2.70	40.99	0.098	0.021	0.38
element	CaO	MgO	MnO	Na_2O	K_2O	S
content	7.96	6.87	0.24	0.52	0.63	0.19
element	SiO_2	Al_2O_3	P	LOI		
content	20.16	7.44	0.043	8.29		

*LOI - loss on ignition

The chemical reagents used in this research are all industrial products.

Optical microscope analysis

The sample was boiled, roughly ground, finely ground, and polished to obtain a qualified light sheet, and then the microstructure of the sample was analyzed using the German Leica DMI 5000M.

Chemical phase analysis

Chemical phase analysis is mainly based on the different solubility or dissolution speed of various compounds in the solvent, through the method of selective dissolution, the content of a certain element in the sample in the presence of various compounds is respectively determined, so as to obtain the content of the compound in the sample.

Flotation test

The flotation test samples were taken directly form the production site, and the flotation test was carried out using XFD (Fig. 1) series laboratory hanging-trough flotation machines.

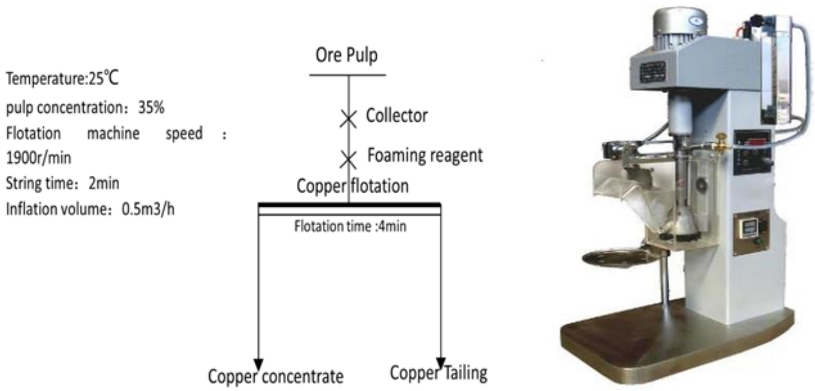

Figure 1 The flotation test flow chart and XFD flotation machine

In this paper, the collector type test and condition test of flotation reagents are evaluated by one roughing selection. The flotation temperature was 25 °C, the pulp concentration was 35%, the flotation machine speed was 1900 r/min, each addition of chemicals was stirred for 2 min, and the flotation aeration volume was 0.5 m3. The test flow chart is shown in Figure 1.

RESULTS AND DISCUSSION

Microscopy and dissociation results

Microscopy analysis results

The copper minerals in the ore are mainly natural copper, and there are also a small amount of copper blue and bornite.

The natural copper content is relatively high. The natural copper mineral in the ore sample is copper red, rose red, Irregular granular or agglomerate, the crystal size is generally 0.01 ~ 0.04 mm, the small one can be less than 0.005 mm, and the thick one can reach 0.15 mm (Fig. 2-a~b). In addition to single particles, some are closely inlaid with hematite, limonite or gangue to form conjoined bodies of different proportions (Fig. 2-c~d).

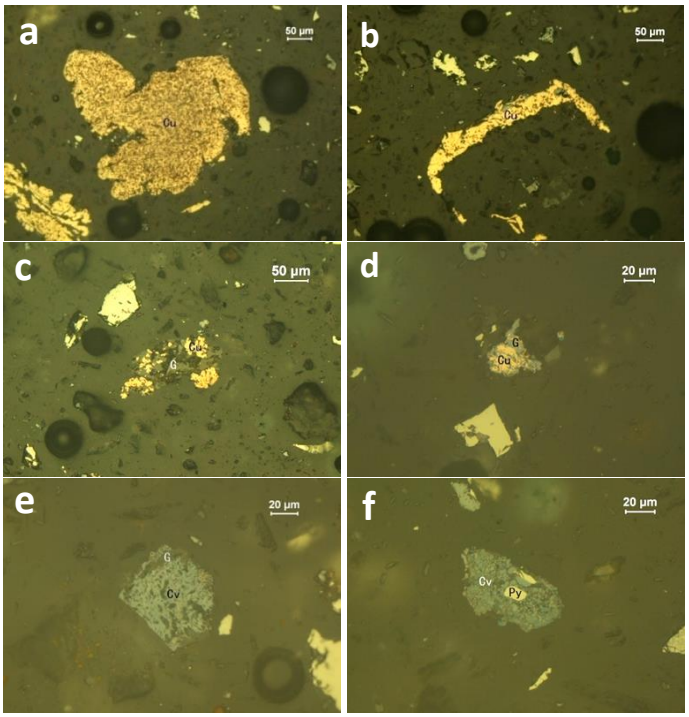

Figure 2 (a~b) Irregular mass of natural copper (Cu) and short-veined natural copper (Cu) wrapped in fine-grained gangue ;**(c~d)** Fine-grained natural copper (Cu) and gangue (G) mixed inlaid Fine-grained natural copper (Cu) and gangue (G) closely inlaid; **(e~f)** Fine-grained gangue wrapped in agglomerated copper blue (Cv), pale rose-bornite

Granular pyrite (Py) encapsulated in irregular agglomerated copper blue (Cv).

Copper blue is the most important secondary copper sulfide mineral in the sample, which is light blue, amorphous and granular, and some of the particles are wrapped with bornite remnants to form composite copper minerals. The inside of the aggregate is often wrapped with fine-grained gangue or pyrite, and some hematite fillings can be seen along the edges, between grains or fissures (Fig. 2-e~f), and the particle size is generally 0.01 to 0.04 mm.

Bornite is one of the secondary copper sulfide minerals in the sample. The content is not high, irregular granular, light rose color, often closely inlaid with chalcopyrite to form composite copper minerals, mainly chalcopyrite to replace residual The form is wrapped in bornite.

Copper mineral dissociation analysis results

The determination results show that the degree of dissociation of copper minerals (including natural copper, bornite, cerulis, etc.) in the sample is poor, and only 72.7% of them are monomer producers (Table 2).

Table 2 The dissociation of copper mineral

monomer	conjoined body			
	>3/4	3/4~1/2	1/2~1/4	<1/4
72.7	15.0	2.2	6.6	3.6

Flotation testing results

The effect of different collector reagents

In this research, commonly used copper flotation collectors such as Butyl xanthate (BX), Ammonium dibutyl dithiophosphate (ADD), O-isopropyl ethylthiocarbamate (Z200), Sodium diethyldithiocarbamate (SN-9) were used to compared with Dodecanethiol (DOD). the dosage of collector is 100 g/t, 2# oil is used as the foaming agent, and the dosage is 20 g/t; The test process is shown in Figure 1, the test results are shown in Figure 3.

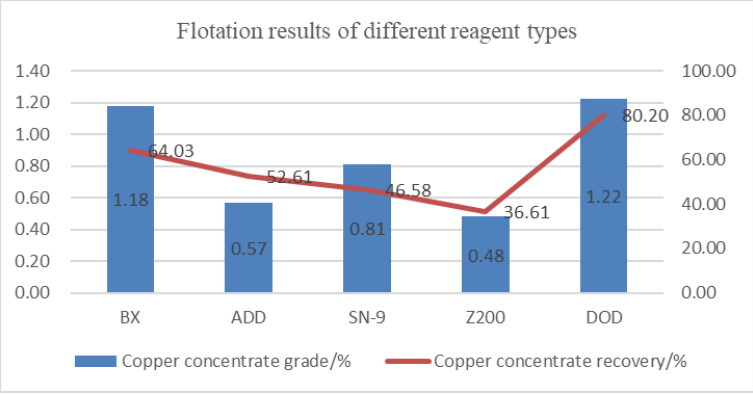

Figure 3 The flotation results of different reagents

The above results show that BX can obtain rough concentrates with a copper grade of 1.18% and a recovery rate of 64.03%; The concentrate grade and recovery rate of ADD, SN-9, Z200 are generally low, indicating that the separation effect of this type of copper minerals is poor; The copper crude concentrate with a grade of 1.22% and a copper recovery rate of 80.20% by DOD is higher than the flotation index of BX.

As shown in Figure 4, through electron microscope scanning analysis of the tailings flotated by xanthate, it is found that some natural copper particles with a particle diameter of up to 200um are found in the flotation tailings. This part of the particles is due to the good extension of natural copper. In the grinding process, it is easy to produce large particle flakes, and the collecting ability of collectors such as xanthate is insufficient, and these large particles cannot be effectively floated.

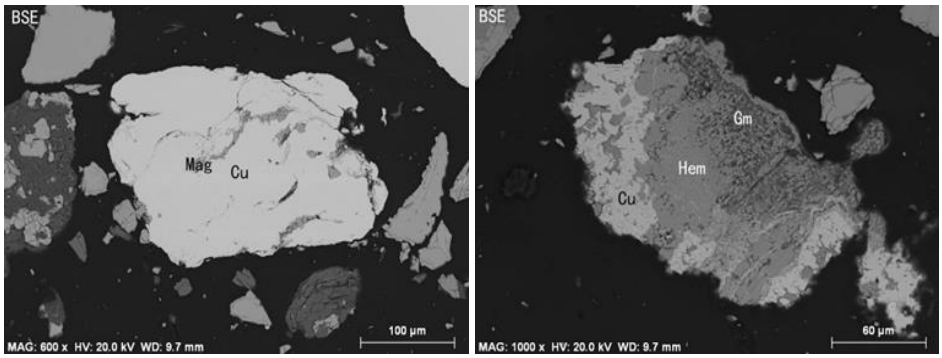

Figure 4 Electron microscope scanning analysis of the tailings flotated by xanthate

The effect of the CYC-20 dosage

CYC-20 was used to replace butyl xanthate as collector for copper flotation of the ore, and the flotation conditions were further optimized. First, the CYC-20 dosage test was carried out under the condition that the 2# oil consumption remained unchanged at 30 g/t, and the results were shown in Fig. 5.

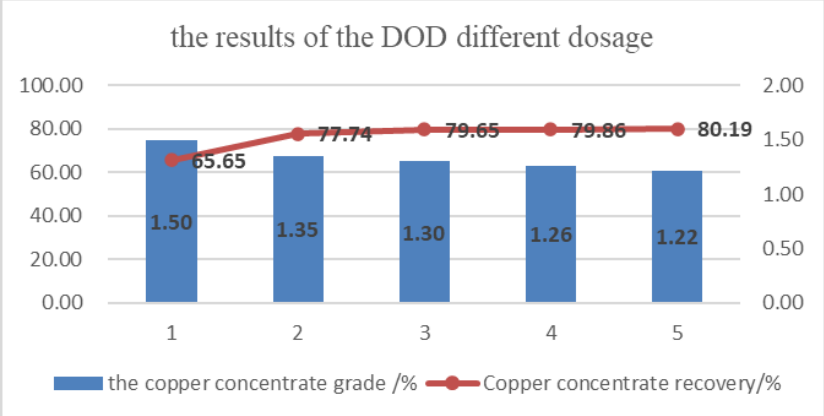

Figure 5 the results of the DOD different dosage

The above results show that: When DOD dosage gradually increased from 60 g/t to 100 g/t, the yield of coarse concentrate increased from 5.99% to 7.50%, the copper grade decreased from 1.500% to 1.22%, but the copper recovery increased from 65.65% to 80.19%, and the concentrate grade gradually decreased as the amount of collector CYC-20 continued to increase. However, the recovery rate of copper is basically unchanged, so it is more appropriate to choose 100 g/t CYC-20.

Closed-circuit test of copper flotation collector CYC-20

Under the condition that the amount of CYC-20 is 100 g/t and the amount of foaming agent 2# oil is 20 g/t, the closed-circuit test of copper flotation is carried out by using the closed-circuit process of one roughing, two cleaning and one sweeping, and the middling ore is returned successively. The test process is shown in Figure 3.1-1, and the test results are shown in Table 3.

Table 3 The results of closed-circuit test [%]

reagents/ $g \cdot t^{-1}$	Product name	Yield	Copper grade	Copper recovery
CYC-20 100 $2^{\#}$ oil 20	Concentrate	0.54	17.20	74.48
	Tailing	99.46	0.03	25.52
	Feed	100.00	0.12	100.00

The closed-circuit test results showed that copper concentrate with copper grade of 17.20% and working recovery of 74.48% could be obtained by using CYC-20 as copper collector instead of butyl xanthate, through one roughing, two refining and one sweeping process in sequence.

CYC-20 industrial application test

The comparison results of preliminary laboratory tests and field verification tests show that the use of CYC-20 as collector for copper flotation not only effectively improves the separation index of copper flotation, but also does not pollute the water quality due to its characteristics of insolubility in water, low density, close binding with solid, etc. Therefore, after further communication with the concentrator and environmental protection department. It was decided to use copper flotation collector CYC-20 to replace xanthate for industrial implementation in order to solve the problem of excessive xanthan ions from the source.

Comparison of indicators during Industrial commissioning

The copper flotation production indicators during the whole commissioning period and the same period in 2019 are statistically compared, and the results are shown in Table 4. Copper flotation separation index during industrial commissioning and in the same period of 2019. The above results show that: Compared with the same period in 2019, the grade of copper concentrate increased from 13.57% to 17.04%, and the recovery of copper metal increased from 65.88% to 73.56%. The technical index improved significantly.

Table 4 Copper flotation separation index during industrial commissioning and at the same time in 2019 [%]

Processing	Copper grade of concentrate	Copper recovery of concentrate
Xanthate Flotation	13.59	73.56
CYC-20 flotation 2020.05~2020.06	17.04	65.88

CONCLUSION

1. The process of replacing butyl xanthate with CYC-20 is adopted. Under the condition that the dosage of CYC-20 is 100 g/t and the dosage of 2# oil is 30 g/t, copper concentrate with copper grade of 17.20% and recovery of 74.48% can be obtained through one roughing, two refining and one sweeping.

2. Copper flotation separation index during industrial commissioning and in the same period of 2019. The above results show that: Compared with the same period in 2019, the grade of copper concentrate increased from 13.57% to 17.04%, and the recovery of copper metal increased from 65.88% to 73.56%. The technical index improved significantly.

REFERENCES

1. Bruckard, W.J., Sparrow, G.J., Woodcock, J.T. (2011) A review of the effects of the grinding environment on the flotation of copper sulphides [J]. International Journal of Mineral Processing, 100 (1-2), 1-13.
2. Lee, K., Archibald, D., McLean, J., et al. (2009) Flotation of mixed copper oxide and sulphide minerals with xanthate and hydroxamate collectors [J]. Minerals engineering, 22 (4), 395-401.
3. Vazifeh, Y., Jorjani, E., Bagherian, A. (2010) Optimization of reagent dosages for copper flotation using statistical technique [J]. Transactions of Nonferrous Metals Society of China, 20 (12), 2371-2378.
4. Guang-Yi, L., Hong, Z., Liu-Yin, X., et al. (2011) Improving copper flotation recovery from a refractory copper porphyry ore by using ethoxycarbonyl thiourea as a collector [J]. Minerals Engineering, 24 (8),817-824.
5. Hassanzadeh, A., Karakaş, F. (2017) Recovery improvement of coarse particles by stage addition of reagents in industrial copper flotation circuit [J]. Journal of Dispersion Science and Technology, 38 (2), 309-316.

XV International Mineral Processing and Recycling Conference
17-19 May 2023, Belgrade, Serbia

KINETIC STUDIES OF THE ADSORPTION POLYACRILAMIDE-BASED FLOCCULANTS ON NATURAL GOETHITE, QUARTZ AND CLAY MINERALS

S. Sredić, Lj. Tankosić[#]
University of Banja Luka, Faculty of Mining, Prijedor, Bosnia and Herzegovina

ABSTRACT – Studying the adsorption kinetics of flocculants on natural minerals in real systems can provide useful information to explain the mechanisms. The aim of this study was to improve knowledge about the mechanism of flocculent binding to the surface of different real minerals, which is important in the mineral processing processes of iron ores. A commercial anionic flocculent was used for the settling of fine particles of natural samples of goethite, quartz and clay minerals in this study. The pseudo-first order, pseudo-second order and intraparticle diffusion models were used to analyze experimental results in kinetic studies. In all 3 systems, the highest correlation coefficients were obtained for the pseudo-second order kinetic model. Also, the equilibrium adsorption capacity obtained theoretically from the kinetic model of the pseudo-second order is much closer to the experimentally obtained equilibrium capacity in all three cases.

Keywords: Goethite, Quartz, Clays, Flocculants, Polyacrylamide, Kinetics.

INTRODUCTION

Selective flocculation is promising process used to beneficiate valuable minerals for fine and ultrafine particles, but also in the process of purification of waste water and drinking water [1-4]. The process of flocculation usually consists of several steps (preparation materials and conditions for flocculation, flocs forming and separation of flocs from not flocculated material). The biggest problem is choosing the flocculant to achieve the highest selectivity. This is especially pronounced in heterogeneous systems such as sludges in mineral processing. Sludge produced by processing of iron ore often still contains a relatively high concentration of iron minerals, as well as quartz and clay minerals, as tailings. It is difficult to achieve selectivity in such heterogeneous systems unless the individual components are first examined. The mechanism of action of flocculants in complex heterogeneous systems is relatively unknown and mostly based on assumptions. Polyacrylamides are classified into three types, nonionic, anionic, and cationic, with respect to their charges induced by the different functional groups along their chains. The utilization of polyacrylamides-based flocculants in a mineral processing is widely mentioned in literature [5-7]. Polyacrylamides are known to be effective flocculants against iron mineral particles. Adsorption of PAM on mineral particles has a partially electrostatic character, and partially another type of bonding, probably hydrogen bonding between the polymer molecules and the hydroxyl groups on the surface of minerals [8-10]. However, they do not show good selectivity in many natural systems. Studying the adsorption kinetics of flocculants on natural minerals in real

[#] corresponding author: ljiljana.tankosic@rf.unibl.org

systems can provide useful information in order to better understand the factors that influence the velocity of the adsorption process. In the process of selective flocculation, study of adsorption can provide useful information about the mechanism of action on individual minerals and thus help in choosing the conditions under which satisfactory selectivity can be expected. The presented work includes the study of the adsorption of an anionic polymer, polyacrylamide, on a series of well-characterized natural minerals to determine the similarities and differences between them in relation to interactions with the flocculant.

Several mathematical models have been introduced to describe the optimized fitting of adsorption kinetics. In general, these mathematical models can be divided into two groups: (a) kinetic models which describes the interactions between the adsorbate molecules and active sites on the adsorbent surface and (b) diffusion models which assumes that diffusion steps control the overall rate because the interaction between the adsorbate and the active sites is instantaneous in relation to diffusion [11-13].

MATERIALS AND METHODS

Materials

The natural raw material samples used in this study was taken from Omarska mine (Republic of Srpska, Bosnia and Herzegovina) and labeled as “goethite”, “quartz” and “clay”. The samples were hand-picked and carefully selected for further analysis. The mineralogical and chemical analyses were recently performed for obtaining more precise mineral determination [14], and major mineralogical compositions are given in table 1.

Table 1 Major mineral compositions of the natural samples labeled as “goethite”, “quartz” and “clay”

Sample	Major mineral composition
“Goethite”	Goethite (~86%) which dominate over hematite (~10%) and with minor contents of quartz (~4%).
“Quartz”	Quartz (~93%) which dominates over illite-sericite (~6%) and with minor contents of hematite (~1%).
“Clay”	Quartz (~50%) and clay minerals (~44%) which dominates over minor goethite (~4%), chloritoid (~2%) and hematite.

As flocculant, anionic polyacrylamide type SUPERFLOC A100, manufactured by Kemira, was used. Flocculant was prepared as 0.1% solutions in distilled water. Preparation of flocculant for all experiments was carried out in the same way according to the instructions provided by the manufacturer of reagents [15].

Batch Adsorption Tests

Adsorption capacity tests were carried out in a batch process by varying the dosage of polymer with a constant amount of adsorbents, 10 g/dm^3. The initial concentration of the flocculant in the solutions examined during the adsorption and kinetic studies were always identical, used the prepared stock solution (~20 mg/dm^3), whose

concentration was constantly verified with analytical precision at the beginning of every experiments. Three solutions were performed by adding the flocculant in the amount corresponding to the dosage of: 50 mg/kg, 100 mg/kg and 250 mg/kg. The test procedure was as follows: in 100 cm^3 of distilled water, 1 g of the prepared sample (natural samples of "goethite", "quartz" and "clay") and the appropriate amount of flocculant were added. Each suspension was mixed for 1h at a room temperature (25 ± 1 °C) and pH≈7, the samples were filtered and determined equilibrium concentrations of flocculant. Preliminary sedimentation experiments have shown that flocculation occurs rapidly (within 1 minute), and that 60 minutes is sufficient to achieve thermodynamic equilibrium of the system. Since the determination of equilibrium adsorption capacity can be a problem in practice, for safety reasons, equilibrium concentrations were measured after 24 hours. After this time, suspensions were filtered and solutions were analyzed to determine PAM concentrations. The amount of adsorbed flocculant was calculated according to equation: $q_{eq} = (C_0-C_t)$ V/m, where q_{eq} represented the adsorption capacity of PAM A100 on certain mineral (mg/g), C_0 initial content of PAM A100 (mg/dm^3), C_t final mass concentration (after adsorption) of PAM A100 (mg/dm^3), V-volume of solution (dm^3) and m- mass of the adsorbent (g). Kinetic studies were carried out at same condition with a dosage of 100 mg/kg of flocculant. Each suspension was mixed for 1h at a room temperature. 10 ml of the supernatant (which was filtered through a 0.45 µm pore diameter cellulose nitrate filter) was collected at various time intervals from 0 to 60 minutes and analyzed for the determination of PAM.

Mathematical models

There are a large number of mathematical models for describing the kinetics of the adsorption process [16-17]. A pseudo-first-order model, a pseudo-second-order model, and a Weber-Morris diffusion model (the most commonly used reaction kinetic and diffusion models) were used in this study.

Pseudo-first order kinetics model

The linear form of the equation describing the pseudo-first order kinetics model (known as the Lagergren equation) is as follows:

$$ln(q_{eq} - q_t) = lnq_{eq} - k_1 t \quad (1)$$

where are: q_{eq} - equilibrium adsorption capacity (mg/g), q_t - adsorption capacity at time t (mg/g), k_1 - first order reaction rate constant (min^{-1}) and t - time (min).

Pseudo-second order kinetics model

The pseudo-second order kinetics model is most often represented by the following linear form:

$$t/q_t = 1/k_2 q_{eq}^2 + 1/q_{eq} t \quad (2)$$

where are: q_{eq} - equilibrium adsorption capacity (mg/g), q_t - adsorption capacity at time t (mg/g), k_2 - second order reaction rate constant (g/mg min) and t - time (min).

Weber-Morris diffusion model

The Weber-Morris diffusion model is commonly used for porous adsorbents to describe intraparticle diffusion and has the following form:

$$q_t = k_{id} t^{0.5} + C \quad (3)$$

where: q_t - adsorption capacity at time t (mg/g), k_{id} - intraparticle diffusion rate constant ($mgg^{-1}min^{-0.5}$) and C -segment indicating the thickness of the boundary layer (mgg^{-1}).

Analytical method

Determination of polyacrylamide A100 level was made by using an UV VIS 1800 Shimadzu spectrophotometer, measured at 190 nm [18], with a 1 cm quartz glass cell. Distilled water was used as a "blank" during calibration. All results represent the mean values of the three measurements.

RESULTS AND DISCUSSION

Adsorption capacity

The use of chemical reagents in mineral processing is often necessary, but carries certain environmental risks. Therefore, the first task is to determine the smallest effective amount of reagent, in this case flocculant based on anionic polyacrylamides. Three dosages of PAM A 100 (50 mg/kg, 100 mg/kg and 250 mg/kg) were selected for testing the effect of the amount of reagent on the adsorption capacity, based on preliminary settling experiments. Dosages of less than 50 mg/kg have been shown to cause weaker flocculation effects, and dosages of more than 250 mg/kg are not acceptable for ecological reasons. The dependences of the amount of adsorbed flocculant A100 on samples of “goethite”, “quartz” and “clay” for different dosage of flocculant are shown in Figure 1.

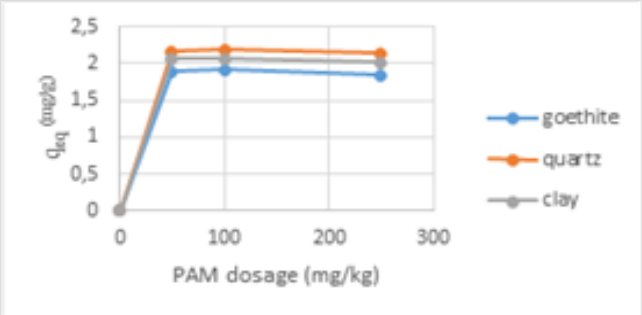

Figure1 Amount of PAM A100 adsorbed onto natural goethite, quartz and clay against of polymer dosage (pH ≈ 7; t ≈ 25 °C)

It can be seen that the concentration does not significantly affect the amount of adsorbed flocculant per unit mass of the adsorbent in all three cases and further experiments were performed with a dosage of 100 mg/kg. This suggests that the adsorption rate is not only influenced by the adsorbate concentration but also by the adsorption mechanism. The adsorption capacity of the tested samples was 1.92 mg/g for "goethite", 2.06 mg/g for "clay" and 2.19 mg/g for "quartz".

Kinetic studies

Adsorption kinetics models provide important information about adsorption mechanisms. Kinetics actually studies the decrease in adsorbate concentration (for example, in this case flocculant PAM A100) over time. Since this process takes place in several phases and surface and intraparticle diffusion control the adsorption kinetics, using mathematical models, useful data on the adsorption of polyacrylamide on "goethite" can be given. To address the adsorption in real system, three sets of kinetic adsorption experiments were performed with all mine sludge components labeld as "goethite", "quartz" and "clay" under the same experimental conditions. The adsorption kinetic models are used to analyze experimental results in order to determine the mechanism of adsorption and the step that determines the speed of the process. This step can be the chemical reaction itself, diffusion or mass transfer across the phase boundary.

The dependence of adsorption capacities of three natural minerals on time is shown in Figure 2.

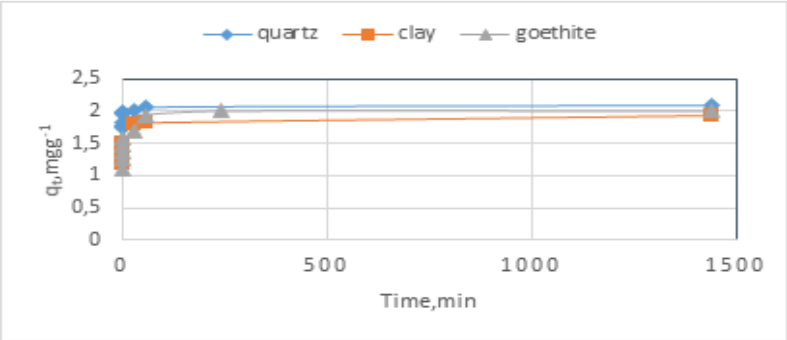

Figure 2 Adsorption kinetics for PAM onto different adsorbents ("goethite", "quartz" and "clay") at ambient temperature and pH ≈ 7

As we can see, the adsorption takes place in two steps. The adsorption initially proceeds very rapidly and occurs more slowely afterwards. The first step can be explained by the rapid adsorption on the external surface. At the beginning, high number of free adsorption sites, such as positive metal ions, negative oxygen ions and OH groups, are available. The equilibrium is established already after 30 minutes and after that the increase in adsorption is almost negligible. Hence, adsorption of anionic polymers on the surface of mineral particles can be explained by a combination of electrostatic bonding between the functional group of the polymer and oppositely charged sites on

the particle surface and hydrogen bonding between functional groups such as -NH_2 and -OH groups.

This has been confirmed by settling experiments, where flocculation becomes visible in the first minute. The reason for that is most likely the steric effect. Large molecules of polyacrylamide very quickly approach, occupy or block places on mineral surfaces that are free for adsorption, which significantly slows down further adsorption. For the selection of the best adsorption kinetic model, the data obtained experimentally within 60 minutes were taken. The data were processed by the linear regression method and shown in Figures 3-5. The characteristic parameters of the adsorption kinetics for all three examined models, as well as the correlation coefficients (R^2), obtained from the linearized equations of these isotherms in the Microsoft Excel program, are given in Table 2.

From the values of the correlation coefficients, which are indicators of the applicability of an individual model (as close as possible to 1), it can be seen that a very high degree of correlation is obtained for the pseudo-second order model. Also, the equilibrium adsorption capacites obtained theoretically from the kinetic model of the pseudo-second order are much closer to the experimentally obtained equilibrium capacities. The adsorption of flocculant A100 onto three different minerals most likely takes place according to the pseudo-second order model. This is, in a way, expected, given that it is a heterogeneous surface, and most of the tested reactions on heterogeneous surfaces occur precisely according to this kinetic model. The lowest degree of correlation is obtained when the intraparticle diffusion model is applied. From Fig. 5 we can see nonzero intercepts, indicating that the rate-limiting step not involves intraparticle diffusion. In this case it is obvious that intraparticle diffusion does not determine the adsorption rate most likely due to the size of flocculant molecules, which prevents macro-, meso- and microporous diffusion. So, it is possible to talk only about surface adsorption. In order to compare the behavior of all sludge components, in the same way and under the same conditions, the adsorption kinetics of polyacrylamide onto natural samples of goethite, quartz and clay were examined. From the values of the correlation and agreement coefficients of theoretically and experimentally obtained equilibrium adsorption capacities, it can be seen that a very high degree of correlation is obtained for the pseudo-second order model in all three cases. A slightly better agreement with intraparticle diffusion model in the case of the clay sample could be attributed to the layered structure of the illitic type of clay.

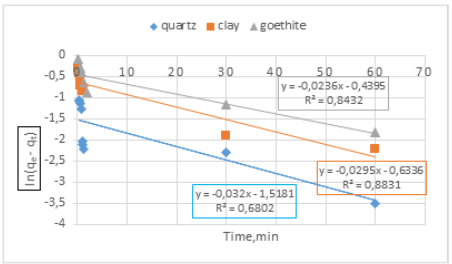

Figure 3 Pseudo-first order model

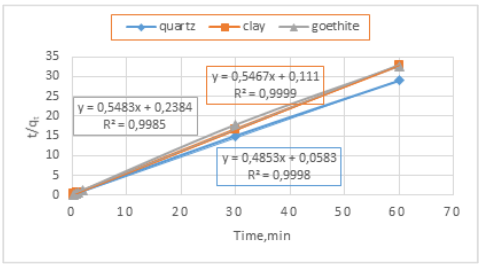

Figure 4 Pseudo-second order model

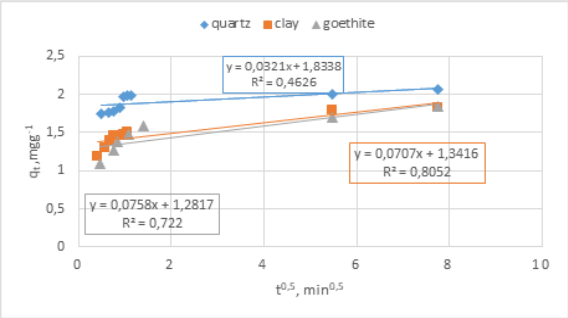

Figure 5 Weber-Morris diffusion model

In general, it can be said that the study of adsorption kinetics of A100 flocculant onto natural samples of goethite, quartz and clay showed that in all three cases these systems behaved very similarly. Adsorption of anionic PAM on mineral particles has a partially electrostatic character, and partially another type of bonding, probably hydrogen bonding between the polymer molecules and the hydroxylic groups on the surface of minerals.

Table 2 Kinetic parameters for adsorption of anionic PAM on natural quartz and clay

Kinetic models	Kinetic parameters		
Pseudo-first order	k_1 (min^{-1})	q_{max} (mgg^{-1})	R^2
Goethite	0.0236	0.6444	0.8432
Quartz	0.0320	0.2191	0.6802
Clay	0.0295	0.5307	0.8831
Pseudo-second order	k_2 ($gmg^{-1}min^{-1}$)	q_{max} (mgg^{-1})	R^2
Goethite	1.2600	1.8238	0.9985
Quartz	4.0397	2.0606	0.9998
Clay	2.6901	1.8292	0.9999
Weber-Morris Intraparticle diffusion	k_{id} ($mg\ g^{-1}min^{-0.5}$)	C (mgg^{-1})	R^2
Goethite	0.0758	1.2817	0.722
Quartz	0.0321	1.8338	0.4626
Clay	0.0707	1.3416	0.8052

CONCLUSION

The kinetic of the adsorption polyacrylamide-based flocculant on natural minerals (goethite, quartz and clay) has been investigated at same condition of pH, temperature, adsorbent amount and adsorbate dosage. The adsorption performs very quickly in all three cases with the establishment of equilibrium after 60 minutes. The equilibrium adsorption of anionic PAM from solution onto the surface of natural goethite, clay and quartz in real conditions was 1.92, 2.06 and 2.19 mg/g, respectively.

It was shown that the adsorption data with the pseudo-second-order model fit best in all three cases. The equilibrium adsorption capacity obtained theoretically from the

kinetic model of the pseudo-second order for natural goethite, clay and quartz is much closer to the experimentally obtained equilibrium capacity than that obtained from the other models. In general, it can be said that the study of adsorption kinetics of anionic flocculant PAM on natural samples of goethite, quartz and clay showed that in all three cases these systems behaved very similarly. The flocculation of fine particles of goethite, quartz and clay occurs rapidly at low concentrations of anionic polyacrylamide caused by electrostatic forces, hydrogen bonds and the formation of bridges between polymer molecules. Consequently, the anionic polyacrylamide used in small amounts can be effective at pH ≈ 7 to accelerate the settling of industrial sludge containing fine particles of goethite, quartz and clay, but selectivity cannot be expected under these conditions.

REFERENCES

1. Sarma, J., Rajkhowa, S., Mahiuddin, S. (2022) Upgradation of Iron Ore Fines and Slime by Selective Flocculation Using Surface-Active Agents, Settling Study, and Characterization of the Beneficiation Waste for Value Addition. Journal of Chemistry, Article ID 6451187, 13 p, https://doi.org/10.1155/2022/6451187.
2. Yu, Y., Zhao, C., Liu, X., Sui, M., Meng, Y. (2017) Selective flocculation of pollutants in wastewater using pH responsive HM-alginate/chitosan complexes. Journal of environmental chemical engineering, 5(6), 5406-5410, doi.org/10.1016/j.jece.2017.10.025.
3. Kumar, R., Mandre, N.R. (2017) Recovery of iron from iron ore slimes by selective flocculation. Journal of the Southern African Institute of Mining and Metallurgy, 117(4), 397-400, doi.org/10.17159/2411-9717/2017/v117n4a12.
4. Su, T., Chen, T., Zhang, Y., Hu, P. (2016) Selective Flocculation Enhanced Magnetic Separation of Ultrafine Disseminated Magnetite Ores, Minerals, 86(6), 1-12, doi:10.3390/min6030086.
5. Szewczuk-Karpisz, K., Krasucka, P., Boguta, P., Skic, K., Sokołowska, Z., Fijałkowska, G., Wiśniewska, M. (2019) Anionic polyacrylamide efficiency in goethite removal from aqueous solutions: goethite suspension destabilization by PAM, International Journal of Environmental Science and Technology 16, 3145-3154, doi.org/10.1007/sl 3762-018-2064-5.
6. Sadangi, J.K., Sahoo, A.K., Sushobhan, B.R. et al. (2020) Effect of anionic flocculant on settling rate of iron ore ultra-fines, Materials Today: Proceedings, 30(2), 316-321, doi.org/10.1016/j.matpr.2020.01.594.
7. Lew, J.H., Matar, O.K., Müller, E.A., Maung, M.T.M., Luckham, P.F. (2022) Adsorption of Hydrolysed Polyacrylamide onto Calcium Carbonate, Polymers, 14, 405. doi.org/10.3390/polym14030405.
8. Drzymala, J. (2007) Mineral processing, Foundations of theory and practice of minerallurgy, Wroclaw University of Technology, 449-462.
9. Moody, G. (1992) The use of polyacrylamides in mineral processing, Minerals Engineering, 5(3-5), 479-492, https://doi.org/10.1016/0892-6875(92)90227-Z.
10. Peng, Y., Jin, D., Li, J., Wang, C. (2020) Flocculation of mineral processing wastewater with Polyacrylamide, 6th International Conference on Energy Science and Chemical Engineering IOP Conf. Series: Earth and Environmental Science 565, 012101, doi:10.1088/1755-1315/565/1/012101.

11. Liang, G., Nguyen, A.V., Chen, W., Nguyen, T.A.H., Biggs, S. (2017) Interaction Forces between Goethite and Polymeric Flocculants and their Effect on the Flocculation of Fine Goethite Particles, Chemical Engineering Journal, doi.org/10.1016/j.cej.2017.10.107.
12. Pholosi, A., Naidoo, E.B., Ofomaja, A.E. (2020) Intraparticle di_usion of Cr(VI) through biomass and magnetite coated biomass: A comparative kinetic and diffusion study. S. Afr. J. Chem. Eng. 32, 39–55.
13. Zhu, S., Ye, Z., Liu, Z., Chen, Z., Li, J., Xiang, Z. (2021) Adsorption Characteristics of Polymer Solutions on Media Surfaces and Their Main Influencing Factors. Polymers, 13, 1774. doi.org/10.3390/polym13111774.
14. Tankosić, Lj., Tančić, P., Sredić, S., Nedić, Z., Malbašić, V. (2017) Characterization of natural raw materials in the processing of iron ore from Omarska mine. Proceedings of International Symposium "Mining and Geology Today", Belgrade, Serbia, 316-330.
15. Cytec Industries Inc, Cytec Mining Chemicals Handbook, 1976, 1989, 2002, pp. 187-202, https://www.911metallurgist.com/wp-content/uploads/2017/03/2002-cytec-mining handbook 924751.pdf.
16. Worch, E. (2012) Adsorption technology in water treatment–fundamentals, processes and modeling, Walter de Gruyter GmbH & Co. KG, Berlin/Boston.
17. An, B. (2020) Cu(II) and As(V) Adsorption Kinetic Characteristic of the Multifunctional Amino Groups in Chitosan, Minerals, 8, 1194, doi:10.3390/pr8091194.
18. Gibbons, M.K., Örmeci, B. (2013) Quantification of polymer concentration in water using UV-VIS spectroscopy. Journal of Water Supply: Research and Technology – AQUA, 62(4), pp. 205-213.

XV International Mineral Processing and Recycling Conference
17-19 May 2023, Belgrade, Serbia

COLUMN LEACHING OF LOW-GRADE COPPER SULFIDE ORE WITH SULFURIC ACID

G. D. Bogdanović[1#], D. Marilović[1], B. Nikolić[2], S. J. Petrović[3]
[1] University in Belgrade, Technical faculty in Bor, Bor, Serbia
[2] Jiuzhou International Construction doo Bor, Bor, Serbia
[3] Mining and Metallurgy Institute Bor, Bor, Serbia

ABSTRACT – The paper presents the results of leaching of low-grade copper sulfide ore with average Cu content of 0.33% and an oxide content of about 7%. The experiments were carried out in sulfuric acid solution and with the addition of Fe(III) ions that had the role of oxidant. During the leaching period of 23 days, with sulfuric acid, the concentration of copper in the solution ranged from 0.05 to 0.230 g/dm^3, and iron from 0.125 to 0.350 g/dm^3. With the addition of Fe(III) ions to the process, the concentration of copper in the solution moved in the same range. These results show that a longer period is needed for the oxidation and dissolution of this raw material.

Keywords: Leaching, Copper, Sulfuric Acid, Fe(III) ions.

INTRODUCTION

Due to the low content of copper in natural deposits, today more attention is paid to the possibility of treating low-grade raw materials. Extraction of copper from such raw materials is in most cases achieved by the leaching process [1]. Percolation leaching is used for heap leaching, leaching of dump, or "in situ" leaching, i. e. it is used for leaching of raw materials that contain a low content of useful components [1,2]. For the leaching process, it is necessary to determine the chemical and mineralogical composition of the raw material.

Sulfuric acid is most often used as an agent for the leaching of copper minerals [3], and Fe(III) ions as an oxidant [4]. Copper sulfide minerals in an acidic medium is based on the following stoichiometric reactions:

Covellite:

$$CuS + Fe_2(SO_4)_3 = CuSO_4 + 2FeSO_4 + S^0 \quad (1)$$

Chalcocite:

$$Cu_2S + 2Fe_2(SO_4)_3 = 2CuSO_4 + 4FeSO_4 + S^0 \quad (2)$$

Chalcopyrite:

$$CuFeS_2 + 2Fe_2(SO_4)_3 = CuSO_4 + 5FeSO_4 + 2S^0 \quad (3)$$

$$CuFeS_2 + 2Fe_2(SO_4)_3 + 2H_2O + 3O_2 = CuSO_4 + 5FeSO_4 + 2H_2SO_4 \quad (4)$$

corresponding author: gbogdanovic@tfbor.bg.ac.rs

The dissolution of copper oxide minerals in acidic solutions is carried out mainly without the presence of oxidants, and can be represented by the following stoichiometric reactions:

Cuprite:

$$Cu_2O + H_2SO_4 \rightarrow CuSO_4 + Cu + 2H_2O \quad (5)$$

$$Cu_2O + \frac{1}{2}O_2 + 2H_2SO_4 \rightarrow 2CuSO_4 + 2H_2O \quad (6)$$

Tenorite:

$$CuO + H_2SO_4 = CuSO_4 + H_2O \quad (7)$$

Azurite and Malachite:

$$Cu_3(OH)_2(CO_3)_2 + 3H_2SO_4 = 3CuSO_4 + 2CO_2 + 4H_2O \quad (8)$$

$$Cu_2(OH)_2CO_3 + 2H_2SO_4 = 2CuSO_4 + CO_2 + 3H_2O \quad (9)$$

The paper presents the influence of sulfuric acid and iron (III) ions as oxidant on the leaching of low-grade copper ore.

EXPERIMENTAL

Characterization of the sample

The ore sample was dried at room temperature and crushed. Particle size distribution was determined by the sieve analysis on the standard Retsch sieve series. The granulometric composition of the sample is shown in Figure 1.

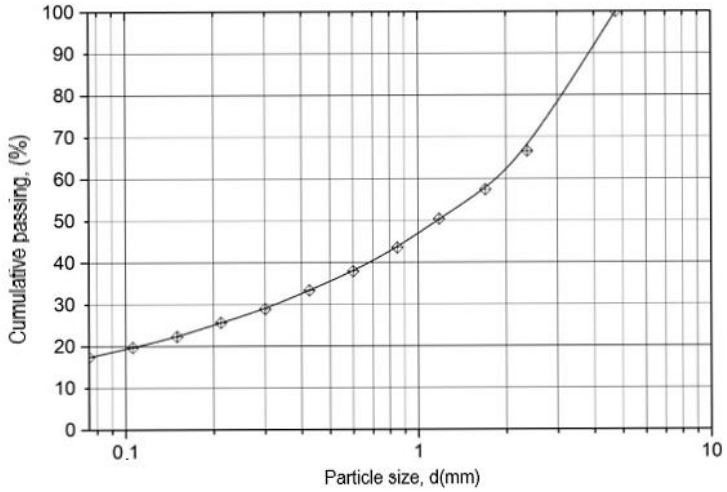

Figure 1 Particle size distribution of ore

Chemical composition of the initial sample (class -4.75 +0.00 mm) is presented in Table 1.

Table 1 Chemical composition of ore

El.	Cu_{tot}	Cu_s	S	Fe	Fe_2O_3	Al_2O_3	CaO	MgO	Na_2O	K_2O	SiO_2	Zn	Ni	Mn
%	0.33	0.306	1.24	4.21	6.02	18.58	0.76	2.28	1.18	3.16	59.78	0.011	<0.007	0.052

Based on the obtained qualitative mineralogical analysis, the following mineral composition was determined: pyrite, chalcopyrite, covellite, cuprite, chalcocite, magnetite, rutile, goethite, galena, sphalerite and gangue minerals. The most present minerals were pyrite and chalcopyrite.

Column leaching

The leaching experiments were carried out in PVC columns, 110 mm in diameter and 1000 mm in height. In each column was added 7 kg of ore. At the top of the ore layer a layer of silica was placed for the uniform distribution of the acid solution. The leaching agent used in the experiment was 0.03 mol/dm^3 sulfuric acid solution. When the influence of oxidants was tested, the experiments were performed with the addition of 3 g/dm^3 Fe(III) ions, at a solid:liquid ratio of 1:1. The flow rate of the solution through the column during the experiment was from 8 to 10 ml/min. The ore leaching in the columns was done for 23 days. After 10 days of leaching, the flow of the leaching solution was stopped and the ore was exposed to an oxidation cycle for a period of 7 days. After the oxidation period, the sulfuric acid solution was again passed through the raw material layer in the column until the end of the leaching period.

Figure 2 Apparatus for percolation leaching

At certain time intervals, 20 cm^3 of the leaching solution was sampled. Copper and iron concentrations in the solution were analyzed by Hanna HI 83200 Atomic Adsorption Spectrophotometer and Inductively Coupled Plasma Optical Emission Spectrometer (ICP-OES, Perkin Elmer Optima 8300).

RESULTS AND DISCUSSION

The results in Figure 3 show that after the initial period, which corresponds to the leaching of copper oxide, the leaching rate decreases. For the sample treated only with sulfuric acid (Fig. 3a), the concentrations of Cu and Fe in the solution increased with time in the first 11 days, and the concentration of copper was 0.158 g/dm^3, and the concentration of iron was 3.037 g/dm^3. The next 7 days were followed by an oxidation period. After this period, the raw material layer in the column was re-washed with a leaching solution. The concentration of Cu in the solution after the period of oxidation slight increase and reached the value of 0.182 g/dm^3 and the concentration of iron in the solution remained the same (Fig. 3 a).

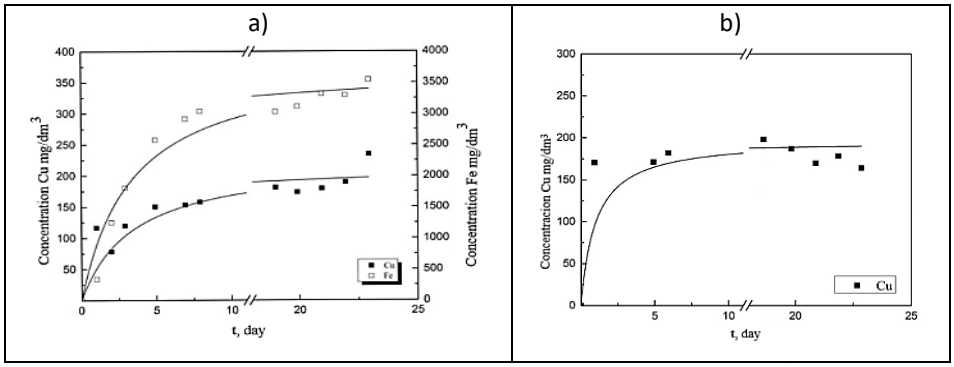

Figure 3 Concentration of Cu and Fe vs. time leaching with 0.03 mol/dm^3 H_2SO_4 solution (a) and concentration of Cu vs. time leaching with 0.03 mol/dm^3 H_2SO_4 and 3 g/dm^3 Fe(III) ions (b)

Simultaneously with the leaching of copper oxide minerals, the process of oxidation of copper sulfide minerals takes place. Since leaching is a slow process, dissolved oxygen in the leaching solution and Fe^{3+} ions, formed by leaching of iron oxide compounds and pyrite oxidation, can also act as oxidants for copper sulfides. Under real conditions, microorganisms present in the ore can oxidize Fe^{2+} to Fe^{3+} ions, which can affect the leaching rate of copper sulfide minerals. Therefore, percolation leaching of copper on a heap or on a dump can last for years, depending on the size of the heap, i.e. the dump, the copper content in it and the used copper mineral leaching agent. Oxidation of chalcopyrite (reactions 3 and 4) leads to the formation of elemental sulfur and sulfate as the final product. Elemental sulfur formed can act as a passivating layer on the surface of a mineral that leads to slow down the dissolution rate [5-9].

During the leaching of ore in the solution of 0.03 mol/dm^3 H_2SO_4 and 3 g/dm^3 Fe (III) ions, the concentration of copper in solution after 11 days was 0.187 g/dm^3 and after the oxidation period there was a small change in the concentration of copper in the solution (Fig. 3b).

Final copper extraction after 23 days in the sulfuric acid solution was 7.11%, and the extraction of oxide Cu was 97.87%. Under the tested conditions, the iron extraction value was 7.88%. Since during the column leaching a low extraction of total copper was obtained, and copper oxide minerals were not completely leached, it can be assumed

that there was a higher consumption of acid due to the occurrence of other reactions with carbonate minerals or iron minerals. As a result of these reactions, the formation of reaction products can prevent contact of the solution with the copper minerals [10,11].

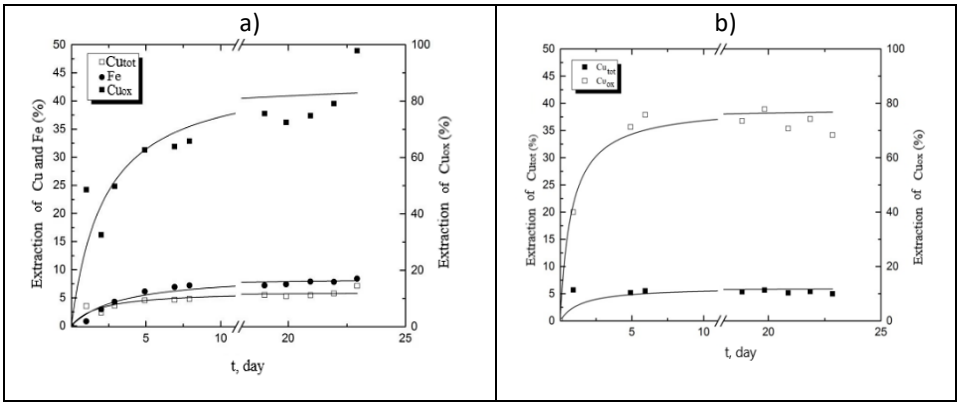

Figure 4 Extraction of Cu and Fe vs. time leaching with 0.03 mol/dm^3 H_2SO_4 solution (a) and Extraction of Cu vs. time leaching in 0.03 mol/dm^3 H_2SO_4 and 3 g/dm^3 Fe(III) ions

The final copper extraction with the addition of Fe(III) ions was about 5.6%, while the extraction of oxide copper was about 69%. It can be seen that the addition of Fe(III) ions slightly affects the leaching of copper. Considering that copper in the sample is mostly in the form of chalcopyrite, the degree of oxidation and leaching of this raw material was very low. It can be assumed that another type of processing should be used to treat such raw material.

CONCLUSION

Percolation leaching of low-grade sulfide ore in columns performed with sulfuric acid with and without oxidants, with a period of oxidation of the sample in the columns, did not give satisfactory results. The best result was obtained by leaching with 0.03 mol/dm^3 H_2SO_4 without the addition of oxidants. After 23 days of leaching in the column, the concentration of copper in the solution was 0.235 g/dm^3 and the extraction of total copper was 7.11%. Considering the content of oxide minerals in the examined raw material was 7.27%, it can be concluded that the oxidation of sulfide minerals did not succeed, even part of the oxide copper remained unleached. Analyzing the obtained results, it can be concluded that another type of processing should be used for this kind of raw material.

Acknowledgment

The research presented in this paper was done with the financial support of the Ministry of Science, Technological Development and Innovation of the Republic of Serbia, within the funding of the scientific research work at the University of Belgrade, Technical Faculty in Bor, Grant No. 451-03-47/2023-01/200131 and Mining and Metallurgy Institute Bor, Grant No. 451-03-47/2023-01/200052.

REFERENCES

1. Ilankoon I.M.S.K., Tang Y., Ghorbani Y., Northey, S., Yellishetty, M., Deng, X., McBride, D. (2018) The current state and future directions of percolation leaching in the Chinese mining industry: Challenges and opportunities. Minerals Engineering, 125, 206-222.
2. Bogdanović, G.B., Stanković, V.D., Trumić, M.S., Antić, D.V., Trumić, M.Ž. (2016) Leaching of Low-Grade Copper Ores: A Case Study For „Kraku Bugaresku Cementacija" Deposits (Eastern Serbia). Journal of Miningand Metallurgy, 52 A (1) 45-56.
3. Sun, X-L., Cen, B-Z., Yang, X-Y., Liu, Y-Y. (2009) Technological conditions and kinetics of leaching copper from complex copper oxide ore. Journal of Central South University of Technology, 16, 936−941.
4. Li, Y., Kawashima, N., Li, J., Chandra, A.P., Gerson, A.R. (2013) A review of the structure, and fundamental mechanisms and kinetics of the leaching of chalcopyrite. Advances in Colloid and Interface Science, 197-198, 1-32.
5. Munoz. P.B., Miller. J. D., Wadsworth, M.E. (1979) Reaction mechanism for the acid ferric leaching of chalcopyrite. Metallurgical Transactions B10, 149-158.
6. Dutrizac, J.E. (1981) The dissolution of chalcopyrite in ferric sulfate and ferric chloride media. Metallurgical Transactions, 12B, 371-378.
7. Mateos, F. B., Perez, I. P., Mora, F. C. (1987) The passivation of chalcopyrite subjected to ferric sulfate leaching and its reactivation with metal sulfides. Hydrometallurgy, 19, 159-167.
8. Hackl, R.P., Dreisinger, D. B., Peters, E., King, J. A. (1995) Passivation of chalcopyrite during oxidative leaching in sulphate media. Hydrometallurgy 39, 25-48.
9. Bogdanović, G. D., Antonijević, M. M., Šerbula, S. M., Milić, S. M., (2007) Elektrohemijsko ponašanje halkopirita u rastvorima sumporne kiseline, Zaštita materijala 48 (3), 39-48.
10. de Oliveira, C.; de Lima, G.F.; de Abreu, H.A. Duarte, H.A. (2012) Reconstruction of the Chalcopyrite Surfaces: A DFT Study. The Journal of Physical Chemistry C, 116, 6357–6366.
11. O'Connor, G.M., Eksteen, J.J. (2020) A critical review of the passivation and semiconductor mechanisms of chalcopyrite leaching. Miner. Eng., 154, 106401.

XV International Mineral Processing and Recycling Conference
17-19 May 2023, Belgrade, Serbia

AN INFLUENCE OF MECHANICAL ACTIVATION ON THE COPPER LEACHING KINETICS OF BERZELIANITE

K. Gáborová[1,2], M. Achimovičová[1#], M. Hegedüs[3], O. Šestinová[1]
[1] Institute of Geotechnics, Slovak Academy of Sciences, Košice, Slovakia
[2] Technical University, Faculty of Materials, Metallurgy and Recycling, Institute of Metallurgy, Košice, Slovakia
[3] Synthon, Ltd., Blansko, Czech Republic

ABSTRACT – In this paper, the structure, phase composition, chemical composition and leaching of berzelianite (Cu_2Se) were studied. Mechanical activation of Cu_2Se in a planetary ball mill resulted in increasing its specific surface area. The influence of milling time on the particle size distribution and the size of the specific surface was studied by particle size distribution analysis and specific surface area measurements. The leaching kinetics of non-activated and mechanically activated samples in 20-40% HNO_3 solutions were examined. The maximum yield of copper almost 80% was achieved after 120 min of leaching in 40% HNO_3 at 25 °C for the sample mechanically activated for 30 min.

Keywords: Berzelianite, Mechanical Activation, Acid Leaching, Copper.

INTRODUCTION

Copper is one of the oldest and most widely used metals in the world. Industrial use of copper due to its excellent properties of corrosion resistance, conductivity, and malleability. Nowadays, copper and its alloys are used in various fields such as building construction, electrical, and electronic devices [1].

As a traditional type of extractive metallurgy process for copper production, pyrometallurgical processes have been used to process sulphide minerals with a high grade of copper. However, increasingly strict regulations for environmental protection require the development of more selective and efficient hydrometallurgical processes for the extraction of copper from mineral ores [2]. All this leads to increased interest in the extraction of copper from low-grade sulphides in aqueous solutions. Moreover, there has been a growing interest in secondary copper sulphides as the dominant mineral source of copper [3].

The effect of mechanical activation on the reactivity of MeS has been studied for many years. Milling caused an increase in the specific surface area of the studied sulphide minerals and their crystal structure become disordered. The surface layers were significantly heterogeneous from a morphological and energetic point of view. This was because of broken chemical bonds, which subsequently affected the reactivity of sulphides in the acid-leaching process [4].

corresponding author: achimovic@saske.sk

This study aimed to investigate the effect of mechanical activation on the leachability of copper from berzelianite (Cu_2Se) – a natural Cu-bearing selenide mineral using diluted nitric acid (HNO_3) as a leaching agent.

EXPERIMENTAL

Material

Mineral berzelianite, Cu_2Se, from Chelopech, Bulgaria was used as an input material. Mechanical activation was conducted in the laboratory planetary ball mill Pulverisette 6 (Fritsch, Germany) under the following conditions: 5 g of sample was added to a tungsten carbide milling chamber (inner volume: 250 ml) with 50 tungsten carbide balls of 10 mm in diameter. The mechanical activation was carried out for 5, 15, and 30 min with a rotation speed of 400 rpm under the Ar-atmosphere.

The quantitative determination of major and minor elements in the input material was realized using SPECTRO XEPOS (Spectro, Germany). The chemical composition of the input material is given in Table 1.

Table 1 XRF analysis of mineral Cu_2Se

Element/Oxide	*Content, %*	*Element/Oxide*	*Content, %*
Cu	44.12	Na	1.39
Se	27.08	Ta	0.71
Ca	6.03	Fe	0.17
Al	4.23	Si	0.15
Mg	1.17	Σ	104

The samples were characterized by X-ray (XRD) diffraction analysis (D8 Advance diffractometer Bruker, Germany) using Cu-Kα radiation to identify the phase composition during mechanical activation and the Diffracplus Eva tool ICDD-PDF 2 database has been utilized.

The specific surface area (S_A) measurements were determined by the low-temperature nitrogen adsorption method in a Gemini 2360 sorption apparatus (Micromeritics, USA) and particle size distribution analysis (PSD) was performed by a laser diffraction system using Mastersizer 2000E particle size analyzer (Malvern Pananalytical, UK).

Leaching

The batch leaching was carried out in a 500 ml three-necked glass reactor into which 200 ml of leaching solution and 2 g of sample were added. As the leaching solutions, 20, 30, and 40% HNO_3 were used. The leaching was performed at an ambient temperature 25 °C. The stirring speed was set to 180 rpm. Aliquots (2 ml) of the solution were withdrawn at an appropriate time interval (5-120 min) for the determination of the content of dissolved copper by the atomic absorption spectrometry method using a spectrometer 240 FS/240 Z (Varian, Australia).

RESULTS AND DISCUSSION

In Figure 1**,** the XRD patterns of unmilled and milled samples for various milling times, t_M are shown. The pattern of the unmilled sample (t_M=0 min) represented the input Cu_2Se, dominated by Cu-bearing phases, cubic berzelianite, $Cu_{2-x}Se$ (6-0680) and tetragonal umangite, Cu_3Se_2 (01-071-0045) and contained also a considerable amount of trigonal calcite phase, $CaCO_3$ (01-071-3699). The other three patterns demonstrated mechanically activated berzelianite for 5, 15, and 30 min, respectively.

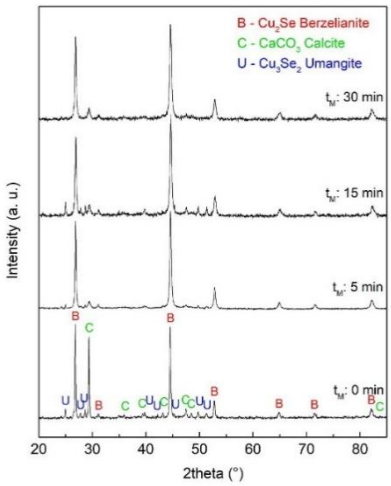

Figure 1 XRD patterns of unmilled and milled Cu_2Se for various milling times, t_M

The quantitative analysis of the non-activated sample pointed to the presence of approximately 35 wt.% of the $CaCO_3$ phase. The analyses of the mechanically activated samples were complicated due to the lower crystallinity and possibly also by the presence of an amorphous phase. On average, the Cu and Se content was slightly higher than the measured one by XRF analysis. This may be due to the impossibility of assigning all diffraction peaks in the patterns or by the presence of amorphous $CaCO_3$ created by milling. The latter was also manifested as a significant drop in the intensity of the $CaCO_3$ phase even after 5 min of milling. Consequently, a notable difference between the elemental composition (as determined from XRD) was calculated for unmilled and milled material samples (Table 2). The amorphization effect during mechanical activation is further supported by a reduction in intensities of the peaks belonging to the berzelianite and their broadening after 30 min of mechanical activation. The average values of the elemental composition for all analysed samples (Cu - 46.6%, Se - 34.2%, Ca - 9.0%) are relatively close to the determined from XRF analysis. Amorphization of the material is therefore believed as the main reason for the observed differences.

Table 3 illustrates the parameters of PSD analysis of non-activated and mechanically activated berzelianite with various milling times. Upon mechanical activation d_{10}, d_{50}, and d_{90} values decreased significantly, and the S_A values increased from 0.12 to 1.66 $m^2 \cdot g^{-1}$ for 5 min activated sample, which is more than a 10-fold increase of the reaction surface. After prolonged milling, the slight decrease in the S_A after 30 min of milling might be

assigned to a common agglomeration phenomenon. The value of the median particle size distribution, d_{50} finally dropped to approximately 16 μm. There were no significant changes between the 15 and 30 min activated sample, so the mechanical activation process was no longer prolonged. A fast decrease in particle size distribution might well correspond to the presence of a brittle calcite phase, which is easily crushed into smaller particles [5].

Table 2 The average mass of the most abundant elements in the studied unmilled and milled samples of berzelianite determined from XRD Rietveld analysis; t_M-milling time

Average mass of the element (wt.%)	t_M***=0 min***	t_M***=5 min***	t_M***=15 min***	t_M***=30 min***
Cu	39.1	50.7	48.3	49.0
Se	29.0	37.0	35.8	35.4
Ca	13.5	6.6	7.8	7.7
R_{wp} factor %*	6.99	6.11	7.11	7.21

*the final R_{wp} factor as calculated from HighScore Plus software.

Table 3 Representative particle sizes distribution and specific surface area (S_A) values of non-activated and mechanically activated berzelianite; t_M-milling time

Berzelianite/ t_M ***(min)***	d_{10} **(μm)**	d_{50} **(μm)**	d_{90} **(μm)**	S_A **m²/g**
Cu_2Se/0	31.88	227.10	508.64	0.12
Cu_2Se/5	3.06	19.57	78.91	1.66
Cu_2Se/15	2.98	14.50	74.28	1.43
Cu_2Se/30	3.42	16.38	69.72	1.43

Non-activated berzelianite was subjected to the leaching in diluted HNO_3 with various concentrations at a temperature of 25 °C. As shown in Figure 2, the recovery of copper, ε_{Cu} in 30% and 40% HNO_3 reached a maximum of only 28-30.5% after 120 min of leaching. At this point, the reaction seems to be almost stopped. In the 20% HNO_3 leaching agent, the leaching process was too slow and the leaching dependence appeared to have a sigmoidal character. The recovery of copper in 30% and 40% HNO_3 increased almost twice compared to the leaching in 20% HNO_3. To obtain higher recovery with the non-activated sample, the leaching time would have to be increased by order an of hours.

As it is obvious from Figure 3, the recovery of copper increased considerably for the mechanically activated berzelianite samples even at ambient temperature. The highest copper extraction was accomplished with a mechanically activated sample for 30 min, yielding 76.7%. Hence, the recovery of copper significantly improved compared to the unmilled berzelianite. In general, the reaction kinetics appeared to be extremely fast in the first 10-20 min before they slowed down. These results imply that the copper recovery from berzelianite was positively affected by mechanical activation. The result follows the already demonstrated effect of ball milling on the activation of minerals for extractive hydrometallurgy. Several papers focused especially on metal-bearing sulphides have been published in the past [6,7]. Although the high yields were obtained with the mechanically activated sample, at some point, the reaction appeared to stop

eventually and does not proceed to completion. This phenomenon can be explained in two ways:

1. The reaction system contains two completely different fractions of particles, out of which, one is readily dissolved in the leaching medium. Once the small particles are dissolved, the fraction of bigger particles follows slower kinetics,
2. Upon ball-milling, only the surface of the material is activated. Once the surface of the disordered structure is leached out, the non-activated core of the particle remains intact in the leaching medium or dissolves at a considerably slower rate.

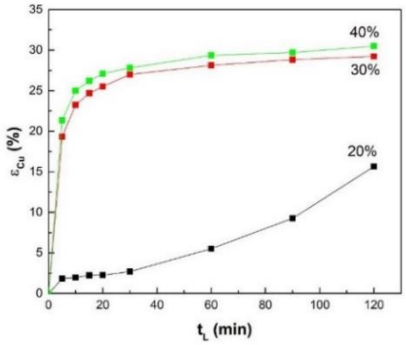

Figure 2 Copper recovery, $\varepsilon_{Cu,}$ into leachate vs. leaching time, t_L for non-activated berzelianite. Milling time - 0 min, leaching temperature – 25 °C, HNO_3 concentrations are given next to the leaching curves

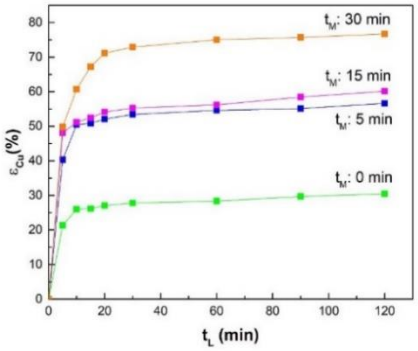

Figure 3 Copper recovery, ε_{Cu} into leachate vs. leaching time, t_L for non-activated and mechanically activated berzelianite with various milling time, t_M; leaching temperature-25 °C, leaching agent-40% HNO_3

Before, it was shown by [8] that for metal sulphides, the reaction kinetics and mechanism of activation depend strongly on material properties, inner crystal structure, and the cleavage of the minerals. This will most probably apply in the same way to selenides. The exact mechanism or the cause for the apparent slow-down of the leaching might not be deductible from the measured data. Since the curves of mechanically activated samples (5 and 30 min) have not contained the bimodal distribution, the first explanation is not much probable. Considering the increase in reaction kinetics and total yields, activation of the surface is more reasonable. In the end, the following kinetics can also be a combination of these two factors.

CONCLUSION

In this work, the influence of mechanical activation by milling on the kinetics of copper leaching from berzelianite, Cu_2Se was studied. XRD analysis of mechanically activated Cu_2Se confirmed that due to mechanical activation, amorphization of mineral phases of berzelianite occurred. With the time of mechanical activation, the specific surface area of the Cu_2Se sample milled for 30 min increased significantly compared to the non-activated sample, more than 10 times. Its mean particle size distribution, d_{50} also decreased almost more than 14 times. By leaching the non-activated sample in 40% HNO_3 at ambient temperature, a maximum copper recovery of 30% was achieved after 120 min of leaching. Using a mechanically activated sample for 30 min, the copper recovery increased to almost 80% under the same leaching conditions. Leaching kinetics is influenced by increasing the reaction-specific surfaces of mechanically activated samples.

ACKNOWLEDGEMENT

This work was realized within the frame of the Slovak Research and Development Agency under contract No. APVV-18-0357, and by the Slovak Grant Agency VEGA (projects 02/0036/23, 02/0136/23).

REFERENCES

1. Davenport, W.G., King, M., Schlesinger, M.E., Biswas, A.K. (2002) Extractive metallurgy of copper. 5th. Edition, Elsevier, Great Britain.
2. Havlík, T. (2014) Hydrometallurgy: Principles and applications. Elsevier.
3. Xing, W.D., Lee, M.S. (2017) Leaching of gold and silver from anode slime with a mixt. of hydrochloric acid and oxidizing agents. Geosystem Engineering, 20(4), 216-223.
4. Baláž, P. (2003) Mechanical activation in hydrometallurgy. International journal of mineral processing, 72(1-4), 341-354.
5. Sulimai, N.H., Rani, R.A., Khusaimi, Z., Abdullah, S., Salifairus, M.J., Alrokayan, S., Rusop, M. (2018) Effect of ball-milling to the surface morphology of $CaCO_3$. AIP Conference Proceedings, 1963(1), 020057.
6. Godočíková, E., Baláž, P., Boldižárová, E. (2002) Structural and temperature sensitivity of the chloride leaching of copper, lead and zinc from a mechanically activated complex sulphide. Hydrometallurgy, 65(1), 83-93.
7. Achimovičová, M., Baláž, P., Briančin, J. (2006) The influence of mechanical activation of chalcopyrite on the selective leaching of copper by sulphuric acid. Metalurgija, 45(1), 9-12.
8. Hu, H.P., Chen, Q.Y., Yin, Z.L., He, Y.H., Huang, B.Y. (2007) Mechanism of mechanical activation for sulfide ores. Transactions of Nonferrous Metals Society of China, 17(1), 205-213.

XV International Mineral Processing and Recycling Conference
17-19 May 2023, Belgrade, Serbia

USE OF COPPER POWDER AS A REDUCING AGENT IN THE LEACHING PROCESS OF $LiCoO_2$

D. Medić[1#], I. Đorđević[2], M. Nujkić[1], A. Papludis[1], V. Nedelkovski[1], S. Alagić[1], S. Milić[1]

[1] University of Belgrade, Technical Faculty in Bor, Bor, Serbia
[2] Elixir Prahovo Ltd, Prahovo, Serbia

ABSTRACT – In this study, the possibility of using copper powder as a reducing agent in the process of cathode material leaching from spent lithium-ion batteries (LIBs) was examined. The copper powder was obtained by grinding copper foil, which is used in LIBs as a current collector. Optimal leaching efficiency of 99.84% for lithium and 99.99% for cobalt was achieved by using 0.4 mol/L phosphoric acid with 0.2 g of copper powder, during the leaching time of 30 min, and at 80°C. Leaching results indicated that copper powder could be used as an effective reducing agent to recover lithium and cobalt.

Keywords: LIBs, Current Collector, Phosphoric Acid, Cobalt, Lithium.

INTRODUCTION

Due to the existing energy crisis and increasing environmental pollution, developing clean and sustainable energy is the biggest challenge today. Lithium-ion batteries (LIBs) have found application in many branches of industry as "green technology" [1]. However, with the popularization and development of electric cars and portable electronic devices, the amount of spent LIBs is rapidly increasing. In addition to the fact that spent LIBs represent a significant secondary source of many valuable metals, their improper disposal can seriously worsen the quality of the environment [2].

Lithium cobalt oxide ($LiCoO_2$) was the first commercialized cathode material, but it still represents the basis for the development of LIBs. For high efficiency of LIBs recycling, complete dissolution of the cathode material is necessary. In the leaching studies published so far, sulfuric acid with hydrogen peroxide as a reducing agent was most often used to dissolve the cathode material [3-5]. The advantage of using hydrogen peroxide in the reductive leaching process is that only oxygen and water are obtained by its decomposition, and thus no additional impurities are introduced into the leaching system. However, hydrogen peroxide decomposes at high temperatures in the presence of sulfuric acid, which reduces the efficiency of cathode material leaching. Considering that the standard electrode potential of $LiCoO_2$ reduction is 2.13 V, it can be concluded that iron, copper, and aluminum, which are integral parts of LIBs, can be used as reducing agents in the leaching process [6]. Ghassa *et al.* [7] investigated the possibility of using iron scrap, obtained from the metal casing of LIBs, in the leaching process of

corresponding author: dmedic@tfbor.bg.ac.rs

$LiCo_{1/3}Ni_{1/3}Mn_{1/3}O_2$ in sulfuric acid. The results of their study indicated that the extraction rate of cobalt increased significantly by adding 6 g/L of iron scrap to the leaching system. Also, it was noted that the presence of iron scrap has no significant effect on the degree of lithium extraction, which is explained by the fact that the lithium extraction process does not require a reducing atmosphere. Porvali *et al.* [8] investigated the combined effect of Fe^{2+} ions and copper scrap on the kinetics of $LiCoO_2$ leaching in sulfuric acid and came to the conclusion that Fe^{2+} ions act as a reducing agent, whereby Fe^{3+} ions are formed, which are converted back to Fe^{2+} ions by oxidation of copper to Cu^{2+}.

In the aforementioned studies, the reduction properties of copper and iron were examined in the process of dissolving the cathode material in a sulfate medium. The aim of this work is to examine the possibility of using copper powder as a reducing agent during the leaching of $LiCoO_2$ in phosphoric acid.

EXPERIMENTAL

Preparation of cathode material and copper powder

To test the possibility of using copper powder as a reducing agent, 17 spent LIBs were collected. The spent LIBs were first disassembled into individual LIBs cells and then discharged using a 5.5 Ω resistance wire. The cathode material was obtained by separating $LiCoO_2$ from aluminum foil in a two-stage thermal treatment at 580°C and 630°C. In order to obtain the copper powder, the anode material was mechanically removed from the copper foil. The obtained copper foil was crushed in a laboratory mill.

Leaching tests

Cathode material leaching experiments were performed in a 600 ml glass laboratory beaker with a double bottom. The leaching apparatus was equipped with a condenser to prevent evaporation of the leach solution and a thermometer to control the temperature. 200 ml of leaching solution of a certain concentration is first thermostated to the desired temperature.

When the desired temperature was reached, 2.0 g of cathode material (with and without the addition of 0.2 g of copper powder) was added to the reactor and the mixer was turned on with a controlled number of revolutions. Leach solutions (1.0 ml of solution) were sampled at precisely determined time intervals (5, 15, 30, 45, and 60 min), filtered, and diluted to 50 ml in volumetric flasks.

An optical emission spectrometer with inductively coupled plasma (ICP-OES) Optima 8300, Perkin Elmer, USA was used to determine the content of Li and Co in the initial cathode material, as well as to monitor the content of the mentioned metals in leach solutions.

RESULTS AND DISCUSSION

The contents of cobalt and lithium in the initial cathode material determined by ICP-OES were 47.91% and 6.97%, respectively.

Leaching of the cathode material in H_3PO_4

The influence of copper powder on the degree of extraction of Co and Li

In order to examine the influence of copper powder on the degree of extraction of Li and Co, leaching experiments were performed in a solution of 0.4 mol/dm^3 H_3PO_4 with and without the addition of 0.2 g of copper powder, at a temperature of 80°C, at a stirring speed of 600 rpm and process duration of 30 min. The obtained results are shown in Figures 1a and 1b.

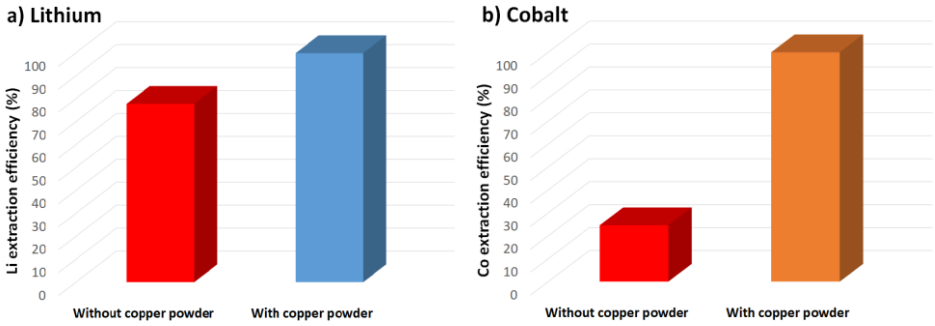

Figure 1 Effect of copper powder on Li and Co extraction

From Figures 1a and 1b, it can be seen that in the absence of copper powder, the degrees of Li and Co leaching were 77.73% and 24.58%, respectively. However, when the copper powder was added to H_3PO_4, the degree of Li leaching increased from 77.73% to 99.84%, while the degree of Co leaching increased from 24.58% to 99.99%. In this study, H_3PO_4 probably acted as a chelating agent, whereby Li and Co were extracted from the cathode material through a complexation process. The low level of Co extraction in the absence of copper powder is probably due to the fact that Co in $LiCoO_2$ is in the form of Co^{3+}, which is poorly soluble in an acidic medium, and for its dissolution, the presence of a reducing agent [9], i.e. copper powder, is necessary. Namely, in an acidic environment, Cu can be oxidized with oxygen from the air according to the following reaction [8]:

$$2\mathrm{Cu} + 4H^+ + O_2 \rightarrow 2\mathrm{Cu}^{2+} + 2H_2O \quad (1)$$

Taking into account the values for the electrode potentials of Cu of 0.34 V and $LiCoO_2$ of 2.13 V, it can be assumed that the dissolution of Cu in an acidic environment can also be a result of galvanic corrosion, where electrical contact between Cu and $LiCoO_2$ is necessary [6,8]. Since it is a complex system, for a more detailed analysis of the role of Cu powder in the process of extracting Li and Co from the cathode material, it is necessary to conduct additional experiments, which will be the subject of research in our next paper.

The influence of temperature on the degree of extraction of Li and Co

The influence of temperature on the degree of extraction of Li and Co was investigated in the range from 35°C to 80°C in a solution of 0.4 mol/dm^3 H_3PO_4 with the

addition of 0.2 g of copper powder, at a mixing speed of 600 rpm and duration of the process of 30 min. The test results are shown in Figure 2.

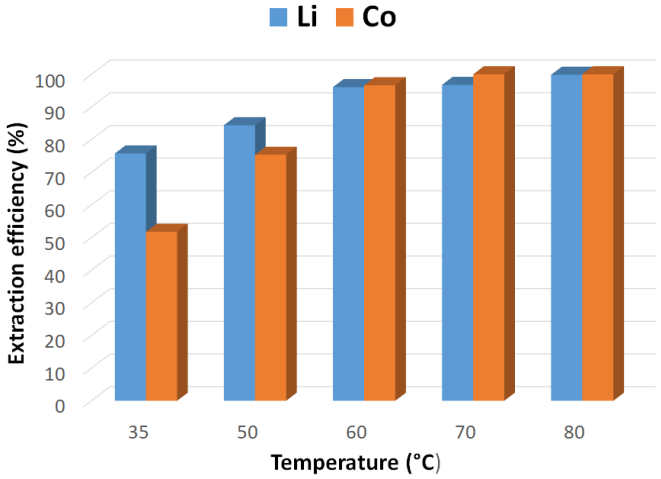

Figure 2 Effect of temperature on Li and Co extraction

From Figure 2 it can be seen that an increase in temperature leads to an increase in the degree of extraction of both tested metals. The maximum extraction values of Li and Co of 99.84% and 99.99%, respectively were achieved at a temperature of 80 °C. Similar results were obtained by Pinna *et al.* [10] when examining the effect of temperature on the degree of dissolution of $LiCoO_2$ in H_3PO_4 in the presence of H_2O_2 as a reducing agent.

The influence of time on the degree of extraction of Li and Co

The influence of time on the degree of extraction of Li and Co was investigated at a temperature of 80°C in a solution of 0.4 mol/dm^3 H_3PO_4 with the addition of 0.2 g of copper powder, at a mixing speed of 600 rpm (Figure 3).

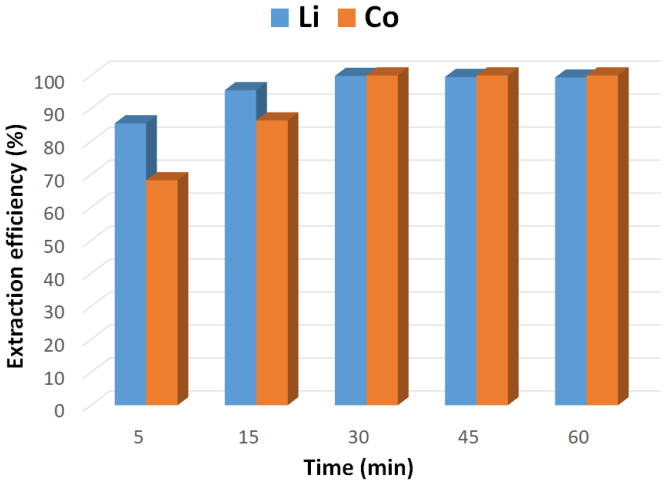

Figure 3 Effect of time on Li and Co extraction

The obtained results indicated that the degree of extraction of Li and Co increased with the increase in the duration of the leaching process, especially in the first 30 min. After 30 min, the degree of extraction of Li and Co reached a value of about 100%. For this reason, a time of 30 min can be considered the optimal time for the leaching process of the cathode material. The increase in the degree of metal extraction with an increase in the duration of the process can be related to the well-known fact that increasing the contact time between the solid and liquid phases increases the degree of dissolution of the solid phase [10].

CONCLUSION

Based on the conducted experiments, it can be concluded that copper powder is an effective reducing agent in the process of cathode material leaching in phosphoric acid. In the presence of copper powder, the degree of Li extraction increased from 77.73% to 99.84%, while the degree of Co extraction increased from 24.58% to 99.99%. The greater influence of copper powder on the Co extraction process was probably due to the fact that the Li extraction process does not require a reducing atmosphere. The obtained results were achieved at an optimal temperature of 80°C and a duration of the process of 30 min.

ACKNOWLEDGEMENT

The research presented in this paper was done with the financial support of the Ministry of Science, Technological Development and Innovation of the Republic of Serbia, within the funding of the scientific research work at the University of Belgrade, Technical Faculty in Bor, according to the contract number 451-03-47/2023-01/ 200131.

REFERENCES

1. Zhang, B., Xu, Y., Makuza, B., Zhu, F., Wang, H., Hong, N., Long, Z., Deng, W., Zou, G., Hou, H., Ji, X. (2023) Selective lithium extraction and regeneration of $LiCoO_2$ cathode materials from the spent lithium-ion battery. Chemical Engineering Journal, 452, 139258.
2. Wang, J., Liang , Z., Zhao, Y., Sheng, J., Ma, J., Jia, K., Li, B., Zhou, G., Cheng, H.M. (2022) Direct conversion of degraded $LiCoO_2$ cathode materials into high-performance $LiCoO_2$: A closed-loop green recycling strategy for spent lithium-ion batteries. Energy Storage Materials, 45, 768-776.
3. Zhu, S., He, W., Li, G., Zhou, X., Zhang, X., Huang, J. (2012) Recovery of Co and Li from spent lithium-ion batteries by combination method of acid leaching and chemical precipitation. Transactions of Nonferrous Metals Society of China, 22, 2274-2281.
4. Sun, L., Qiu, K. (2011) Vacuum pyrolysis and hydrometallurgical process for the recovery of valuable metals from spent lithium-ion batteries. Journal of Hazardous Materials, 194, 378-384.
5. Nayl, A.A., Elkhashab, R.A., Sayed, M.B., El-Khateeb, M.A. (2014) Acid leaching of mixed spent Li-ion batteries. Arabian Journal of Chemistry, 10, S3632-S3639.

6. Chernyaev, A., Partinen, J., Klemettinen, L., Wilson, B.P., Jokilaakso, A., Lundström, M. (2021) The efficiency of scrap Cu and Al current collector materials as reductants in LIB waste leaching. Hydrometallurgy, 203, 105608.
7. Ghassa, S., Farzanegan, A., Gharabaghi, M., Abdollahi, H. (2020) The reductive leaching of waste lithium ion batteries in presence of iron ions: Process optimization and kinetics modelling. Journal of Cleaner Production, 262, 121312.
8. Porvali, A., Chernyaev, A., Shukla, S., Lundström, M. (2020) Lithium ion battery active material dissolution kinetics in Fe(II)/Fe(III) catalyzed Cu-H_2SO4 leaching system. Separation and Purification Technology, 236, 116305.
9. Meng, Q., Zhang, Y., Dong, P. (2017) Use of glucose as reductant to recover Co from spent lithium ions batteries. Waste Management, 64, 214-218.
10. Pinna, E.G., Ruiz, M.C., Ojeda, M.W., Rodriguez, M.H. (2017) Cathodes of spent Li-ion batteries: Dissolution with phosphoric acid and recovery of lithium and cobalt from leach liquors. Hydrometallurgy, 167, 66-71.

XV International Mineral Processing and Recycling Conference
17-19 May 2023, Belgrade, Serbia

REMOVAL OF HEAVY METAL IONS FROM MULTIMETALLIC SOLUTION BY MODIFIED OAT STRAW

J. Dimitrijević[1#], S. Jevtić[2], A. Marinković[2], M. Simić[1], M. Koprivica[1], J. Petrović[1]
[1] Institute for Technology of Nuclear and Other Mineral Raw Materials, Belgrade, Serbia
[2] Faculty of Technology and Metallurgy, University of Belgrade, Belgrade, Serbia

ABSTRACT – In this paper, the ability of waste biomass as an adsorbent was investigated. Oat straw was chosen as the starting raw material. In order to improve the adsorption capacity this material was modified with selected deep eutectic solvent (DES). Changes in the structure of the native and modified samples were examined using the SEM analysis. The efficiency of the adsorption of heavy metal ions from a multimetal solution was tested on the modified oat straw. The maximum obtained capacities of lead, copper and zinc ions were 77mg/g, 29.5mg/g and 44.1mg/g, respectively. The obtained results showed that adsorption follows pseudo-second-order kinetics model that imply chemisorption as a rate controlling step.

Keywords: Adsorption, Oat Straw, DES Solution, Biomass Modification.

INTRODUCTION

The rapid technical and technological development in recent years has led to greater use of natural waters and their contamination. Various branches of industry such as pharmaceuticals, mining, mineral processing, production of artificial fertilizers and construction materials, oil refining and ferrous metallurgy are among the main polluters of the environment [1]. On that occasion, heavy metals, organic components, dyes, pesticides, drugs, which have a harmful effect on the environment, enter the waterways. Due to their toxicological and chemical properties, heavy metals represent a major problem for the preservation of the environment. They are toxic, non-degradable in water and soil, subject to bioaccumulation, which leads to reaching the food chain. Heavy metals in smaller quantities are necessary for the normal functioning of the organism, while to a greater extent they cause serious damage or can have a lethal effect. Accordingly, more and more attention is being directed to research related to the preservation of the environment in order to reduce or completely prevent the pollution by heavy metals [1-3].

Different traditional methods such as: sedimentation, oxidation-reduction, ion exchange, coagulation and flotation, membrane filtration and others have been greatly used for the removal of pollutants from waste water [3,4]. Traditional technologies also have disadvantages such as economic profitability due to high operating costs, insufficient selectivity, producing large amount of waste sludge, the increasing

corresponding author: j.dimitrijevic@itnms.ac.rs

attention of the scientific public is focused–in finding more adequate and accessible solutions [4,5].

An increasing number of researches are directed towards the development of alternative remedies for the removal of semi-titanium from water. One of the increasingly applicable alternative methods is biosorption. Biosorption is a technique characterized by high efficiency, accessibility, economic profitability, selectivity and ecological acceptability for the removal of heavy metals from wastewater [1,4,5]. Easily available, cheap, waste natural materials are used, due to their physical and chemical characteristics; they bind pollutants to the surface. In order to increase the additional adsorptive properties, different methods of biomass modification are used to increase the binding surface and the number of active binding sites. Various alkaline and acid modifications are widely used. Recently, there has been an increasing use of environmentally acceptable deep eutectic solvents (DES) as innovative green liquid for the treatment of lignocellulosic biomass, in order to obtain the desired characteristics for potential further application [6,7]. DES solvents consist of hydrogen bond donors and acceptors, which affect biomass degradation, that is, partial or complete degradation of lignin from biomass. The biomass after the interaction with the DES gives a more porous structure in comparison with the native sample [8].

Oat straw is a readily available, inexpensive bio-waste generated after harvesting of oats. Due to the large production of straw after the harvest, are more and more attention is being directed to its further application. Precisely for this reason, in this paper, the modification of oat straw with DES solvent as an adsorbent for liquid metals from water resources was examined. In order to examine the influence of the modification on the sorbent SEM analysis was performed. The paper presents the results obtained after the application of modified oat straw for the removal of lead, copper and zinc from a multi-metallic solution.

EXPERIMENTAL

The oat straw used in this research was obtained after the oat harvest in Banat (a region in Serbia). The straw was collected directly from the field, washed a couple of times to avoid impurities and dried at room temperature. The dried oat straw was ground, sieved and dried to a constant mass at 105°C.

In order to degrade lignocellulose in oat straw, DES solvent was used. The DES solvent is prepared by mixing the ionic liquid choline arginate (IL) and a sufficient amount of urea. The reaction was carried out in a reflux condenser with constant stirring at 40°C [9]. Obtained modified oat straw was dried in a dryer to constant mass and used for further adsorption experiments.

The $Pb(NO_3)_2x6H_2O$, $Cu(NO_3)_2x3H_2O$ and $ZnSO_4x7H_2O$ were used for the preparation of the working solution. All used chemicals were of analytical grade.

Morphological characteristics of the sample before and after modification were investigated by scanning electron microscopy (SEM) using Jeol JSM-6610LV, at 20 keV. Before recording, the samples were dried at 105°C, impregnated with gold and placed on a carbon.

Adsorption experiments were performed in a batch system. The experiment was carried out at room temperature and pH value 5. The influence of contact time was

tested in different time intervals from 15 to 1440 min. About 0.04 g of modified oat straw and 40 ml of multi-metal solution were added to 100 ml Erlenmeyer flasks. The initial concentrations of lead, zinc and copper were 1mM, 1,5mM and 1.5 mM, respectively. The suspensions were stir on an orbital shaker mixed at room temperature at 250 rpm and filtered. At the end of the adsorption experiment, the metal concentration in the filtrates was measured by the ASS method on a Perkin Elmer 900T.

RESULTS AND DISCUSSION

The morphological characteristics of the material before and after modification were examined with a scanning electron microscope (SEM). Figure 1 shows the results of the analysis. According to the SEM micrograph, it was observed that there was a change in the appearance of the surface of the modified sample. Changes on the surface are caused by degradation of lignocellulose after modification with DES. An increase in the number of channels, voids and pores is observed compared to the relatively smoother appearance of native oat straw. In oat straw, a smaller number of cavities and channels are observed [1,10,11]. Figure 1b, which represents the modified sample, shows numerous cavity channels and a more heterogeneous structure compared to the native sample. The results obtained in this way support the fact that the use of degradability of DES leads to the degradation of lignocellulose. [10] A surface with more pores and channels is more suitable for adsorption due to the easier possibility of ion diffusion, as well as more sites for metal binding.

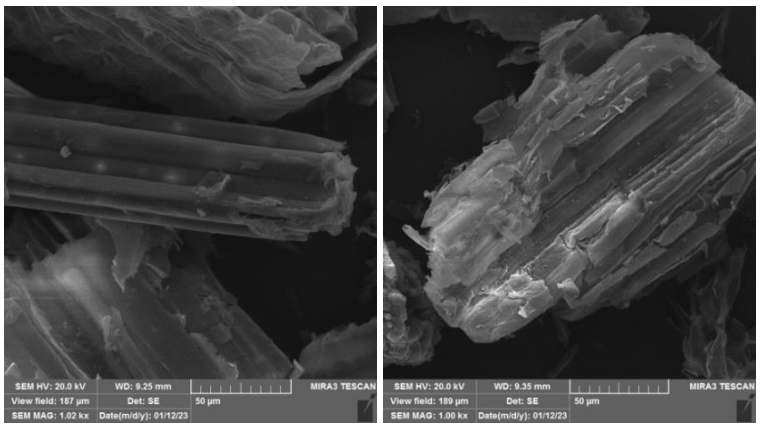

Figure 1 SEM images of oat straw before and after modification with DES

Preliminary adsorption tests revealed that the modified oat straw has a higher affinity for metal ion binding than the native one. Accordingly, the influence of time was examined only on the modified material. The influence of contact time on the adsorption of each metal is shown separately in the Figure 2. The results indicate that with increasing time, the efficiency of removing metal ions from the aqueous solution also increases. After 4 hours, there were no significant changes in the capacity. The maximum capacities for lead, zinc and copper are 77mg/g, 29.5mg/g and 44.1mg/g

respectively. The obtained results indicate that the binding sites on the surface of the adsorbent are filled due to high competition between the site ions in the solution [12]. Similar results were obtained by Cherono et al. [13], which also has a slight trend of decreasing capacity for certain metals after 24 h, which is noticeable here for zinc. The multiple efficiency of metal ion removal was faster on the beginning, which is attributed to the larger number of active sites that become filled over time. Adsorption efficiency is highest for lead ions.

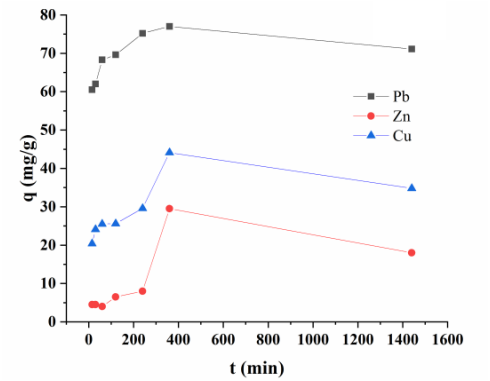

Figure 2 The effect of time during the adsorption of lead, copper and zinc ions using modified oat straw

Figure 3 shows graphs representing the pseudo first and pseudo second kinetic models for the adsorption of lead, copper and zinc metals from a multimetal solution after adsorption of modified oat straw. Based on the obtained results, it can be concluded that the adsorption kinetic for all metals follows pseudo second-order kinetic model. This is supported by the data presented in Table 1. Obtained values (Table 1) suggesting that chemisorption was an important mechanism responsible for the binding of investigated metal ions to the modified oat straw surface [14]. The results obtained during this study support the fact that the modification process with DES was successful.

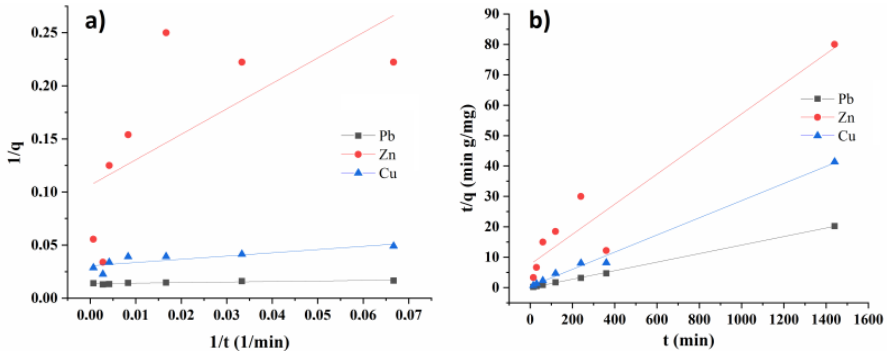

Figure 3 Curves of kinetic adsorption of metals on modified oat straw a) pseudo first models b) pseudo second models

Table 1 Kinetic parameters

Modified oat straw	Pb	Zn	Cu
$q_{eq,\ exp}$ [mg/g]	77.00	29.5	44.1
Pseudo-First-Order Model			
$q_{eq,cal}$ [mg/g]	73.42	9.40	32.77
k_1 [1/min]	3.69	22.53	9.99
R^2	0.8055	0.4517	0.6992
Pseudo-Second-Order Model			
$q_{eq,cal}$ [mg/g]	71.38	20.21	35.43
κ_2 [g/mg min^{-1}]	0.2914	0.0065	0.0007
R^2	0.9994	0.9129	0.9939

CONCLUSION

In this work, the possibility of using modified oat straw as a biosorbent for the removal of heavy metals from waste water was investigated. In order to improve the adsorption capacity of oat straw, it was modified with DES solvent. In order to compare the structural characteristics of the material before and after modification, characterization was performed using SEM analysis. Based on the obtained results, it was observed that there are changes in the structure, i.e. degradation of lignocellulose. Adsorption experiments performed on modified oat straw showed that adsorption follows pseudo-second-order kinetics and approaches chemisorption as binding mechanism. Results from this study indicate that competition between ions from multimetal solution for binding sites on adsorbent surface occurs. Besides, under these conditions, the best ability of lead removal was achieved.

ACKNOWLEDGEMENT

The authors are grateful to the Ministry of Science, Technological Development and Innovation of the Republic of Serbia for the financial support (contract no. 451-03-47/2023-01/200023).

REFERENCES

1. Simić, M., Petrović, J., Šoštarić, T., Ercegović, M., Milojković, J., Lopičić, Z., Kojić, M., (2022) A Mechanism Assessment and Differences of Cadmium Adsorption on Raw and Alkali-Modified Agricultural Waste. Processes, 10 (10), 1957.
2. Yao Z.Y., Qi J.H.,Wang L.H. (2010) Equilibrium, kinetic and termodynamic studies on the biosorption of Cu(II) onto chestnut shell. Journal of Hazardous Materijals, 137-143.
3. Solisio C., Al Arni S., Converti A. (2019) Adsorption of inorganic mercury from aqueous solution onto dry biomass of Chlorella vulgaris: kinetic and isotherm study, Environ Technol, 40, 664-672.
4. Fan, L., Miao, J., Yang, J., Zhao, X., Shi, W., Xie, M., Wang, X., Chen, W., An,X., Luo, H., Ma, D., Cheng, L. (2022) Invasive plant-crofton weed as adsorbent for effective removal of copper from aqueous solution. Environmental technology & innovation,

26, 102280.
5. Petrović, J., Stojanović, M., Milojković, J., Petrović, M., Šoštarić, T., Laušević, M., Mihajlović, L.M. (2016) Alkali modified hydrochar of grape pomace as a perspective adsorbent of Pb^{2+} from aqueous solution. Journal of Environmental Management, 182, 292-300.
6. Zhang, Y., Meng, Y., Ma, L., Ji, H., Lu, X., Pang, Z., Dong, C., (2021) Production of biochar from lignocellulosic biomass with acidic deep eutectic solvent and its application as efficient adsorbent for Cr (VI). Journal of Cleaner Production, 324, 129270.
7. Xu, H., Dong, C., Wang, W., Liu, Y., Li B., Liu, F. (2023) Machine learning prediction of deep eutectic solvents pretreatment of lignocellulosic biomass. Industrial Crops and Products, 196, 116431.
8. Jose, D., Tawai, A., Divakaran, D., Bhattacharyya, D., Venkatachalam, P., Tantayotai, P., Sriariyanun, M. (2023) Integration of deep eutectic solvent in biorefining process of lignocellulosic biomass valorization. Bioresource Technology Reports, 21, 101365.
9. Wang, Y., Zhang, J.W., Yang, J.Y., Li, M.L., Peng, F., Bian, J. (2022) Efficient fractionation of woody biomass hemicelluloses using cholinium amino acids-based deep eutectic solvents and their aqueous mixtures. Bioresource Technology, 354, 127139.
10. Lai, P., Zhou, H., Niu, Z., Li, L., Zhu, W., Dai, L. (2023) Deep eutectic solvent-mediated preparation of solvothermal carbon with rich carboxyl and phenol groups from crop straw for high-efficient uranium adsorption. Chemical Engineering Journal, 457, 141255.
11. Gollakota, R.K.A., Munagapati, S.V., Shu C.M., Wen, J.C. (2022) Adsorption of Cr (VI), and Pb (II) from aqueous solution by 1-Butyl-3-methylimidazolium bis(trifluoromethylsulfonyl)imide functionalized biomass Hazel Sterculia (Sterculia Foetida L.). Journal of Molecular Liquids, 350,118534.
12. Gupta V., Nayak A., Agarwal S., Tyagi I. (2014) Potential of activated carbon from Waste Rubber Tire for the adsorption of phenolics: effect of pre-treatment conditions. Journal of Colloid and Interface Science, 417, 420-430.
13. Cherono F., Mburu Nj., Kakoi B. (2021) Adsorption of lead, copper and zinc in a multi-metal aqueous solution by waste rubber tires for the design of single batch adsorber. Heliyon, 7 (11), e08254.
14. Kakoi B., Kaluli J.W., Ndiba P., Thiong G., (2016) Removal of lead (II) from aqueous solution using natural materials: a kinetic and equilibrium study. J. Sustain. Res. Eng., 3 (3), 53-62.

XV International Mineral Processing and Recycling Conference
17-19 May 2023, Belgrade, Serbia

A PROCESS TO DECREASE THE CLAY COATING OF IRON ORE LUMPS AND FINES BY THE APPLICATION OF DISPERSANTS

M. R. Rath, A. S. Patra[#], S. K. Kumar, M. Mukherjee, A. Chatterjee, A. Ranjan, A. K. Bhatnagar, A. K. Mukherjee
Tata Steel Ltd., Jamshedpur, Jharkhand, India

ABSTRACT – Modern day mining practices generate a large quantity of fines along with the intended lumps. Fine particles are generated during comminution and transportation process too. These fine particles tend to stick together and with coarser particles due to their high surface energy (high surface area). Hence mere washing does not remove all clay coatings effectively. The present work relates to the application of organic dispersants to enhance the effectiveness of water in the scrubbing action to wash the clay coatings more effectively. It was observed that alumina and silica could be reduced by 0.2-0.3% in addition to that by washing with water alone.

Keywords: Alumina Reduction, Dispersant, Beneficiation.

INTRODUCTION

There is a requirement of about 1.5 tonnes of iron ore for every ton of hot metal produced by the blast furnace route. This iron ore is provided in the form of lumps, pellets, and sinter. Pellets and sinters are produced from fines. Pellets are generally produced from the dry fines whereas sinters are produced from the wet fines less than 10 mm. The preferred alumina for the feed to blast furnace is less than 2.5%. Hence, the mined ore needs to be beneficiated to produce the required sizes and specifications so as to meet the blast furnace requirements. The run of mine ore is thus crushed, screened to get the required size fractions, and washed and classified by drum scrubbers and screw classifiers to reduce the alumina content as per blast furnace norms. In the washing process in the cylindrical drum scrubbers water is generally used in the ration of 1:1 with the ore with variations of around 10-15%. The simplified flowsheet has been shown in Figure 1 below depicting the drum scrubbers and screw classifiers. Other beneficiation techniques are deployed for low grade ore like jigging, dense media separation, magnetic separation, froth flotation etc and all these are well known beneficiation techniques. The choice of the beneficiation treatment depends on the nature of the gangue present and its association with the ore structure. Most of these are usually deployed for fine particle beneficiation where they separate Iron ore from alumina/silica. But none of these processes can reduce surface coatings from the ore better than the scrubbers and that too across all size ranges. However, the ultrafine clay particles containing alumina and silica adhere to each other and to relatively coarser particles with great strength due to their high surface energy (high surface are due to extremely fine and ultrafine size).

[#] corresponding author: abhay.shankar@tatasteel.com

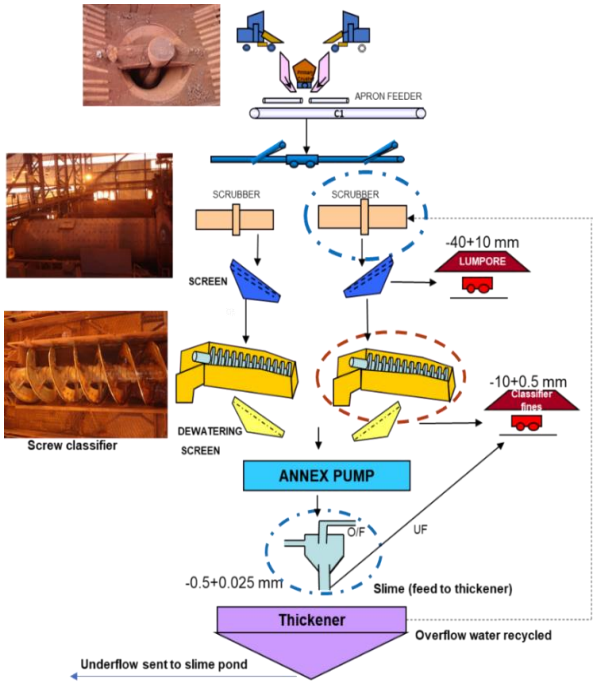

Figure 1 Simplified flowsheet of iron ore beneficiation wet plant

Moreover, the removed ultrafine particles may re-adhere to the other particles as stated before in the subsequent stages of washing process. Hence, to make the scrubbing or washing action more effective, so that the surface clay coatings are removed more efficiently and effectively, a process needs to be developed. There are different works on beneficiation of iron ore by different methods. For e.g., U.S. No. 4,410,431 claims a method of dewatering a wet, particulate mineral mass which comprises treatment of the wet mineral with a composition comprised of a surfactant having a hydrophile-lipophile balance number of from about 6.0 to 12.0, and a quantity ("surfactant absorption inhibitory amount") of a fatty acid substance such as tall oil fatty acid. Preferred surfactants are composed of the reaction product of one mole of primary aliphatic alcohol containing from 6 to 13 carbon atoms with two to seven moles of ethylene oxide. Tridecyl alcohol is specifically mentioned as a useful alcohol for ethoxylation. However, this work does not discuss dewatering.

- The objective is to develop a process for alumina reduction in iron ore lumps and fines irrespective of their size.
- The objective is to enhance the washing efficiency of water to remove clay coatings more effectively.
- The objective is to propose suitable organic reagents which will improve the washing efficiency of water in the scrubbing process.
- The objective is to suggest appropriate dosage, addition points of the reagent to maximise alumina reduction and minimise downstream issues.

EXPERIMENTAL

Figure 1 describes the simplified flow sheet of the plant. Iron ore is mined from its resources (ROM) and fed to the primary crusher for first step size reduction as is depicted in figure 1. The crushed ore is stacked as primary surge pile from where it is screened into +40mm and -40mm size fractions. The oversize that is +40mm fraction goes to the secondary crusher. The -40mm product goes to the drum scrubber for washing. Washing of iron ore is practised to clean the clay coatings and the associated liberated gangue minerals. To remove the clay coatings, effective scrubbing action is necessary which is provided in the drum scrubber. Also, the fine clay minerals sticking to the iron ore lumps adsorb much moisture. The scrubbing action in the drum scrubber is therefore essential to remove the clay coatings as far as possible. After this the lumps are screened, the fines (less than 10mm) go to the screw classifier where again the ultra-fines are separated from the fines ore. The cut off size in the classifier is 0.5 mm as depicted in Figure 1. The better the separation better is the fines product with respect to gangue (Alumina, silica) and moisture content. The ultra-fines tend to stick to the fines and can adsorb good amount of water owing to their large surface area and high hydration energy. This separation or classification step is mandatory in the dewatering process. Finally, the ore fines are passed through a vibrating dewatering screen to shed away as much water as possible.

The new process invention incorporates the dosing of organic surfactant to improve the alumina reduction as well as dewatering efficiency of the plant circuit. It reduces the overall alumina and moisture in the lumps and fines ore [1-3].

Probable mechanism of action

Iron ore is washed to remove the clay coatings as far as possible. Drum scrubbers and screw classifiers are normally used for scrubbing and washing of ores to reducing the clay content or coating (alumina and silica are the major gangue in the clay) on the surface of iron ore (both lumps and fines). However, the fine particles or coatings are difficult to remove by mere washing with water. These fine particles tend to stick together and with coarser particles due to their high surface energy (high surface area). Hence mere washing does not remove all clay coatings effectively. Addition of surface-active reagents help to increase the washing efficiency of iron ore fines. Some examples of surfactants are given below in Figure 2. One important point however is that all organic surfactants may not be dispersants. Only those reagents that are able to adsorb on the mineral surfaces and impart charge so that the surfaces now repel each other may act as effective dispersants. The surfactant adsorbs on the mineral surface via its charged hydrophilic functional groups. The adsorption process renders the mineral the same charge as that of the reagent. When all the surfaces become charged, they repel each another and tries to move away from one another and are effectively washed by water. The probable mechanism has been present in figure 3. However, the dispersants are effective for ultrafine particles which are less than 50 microns. If bigger size particles contain alumina/silica they cannot be removed by dispersants. These are useful to remove surface coatings which are basically extremely fine sized particles and liberated ultrafine particles [4-6].

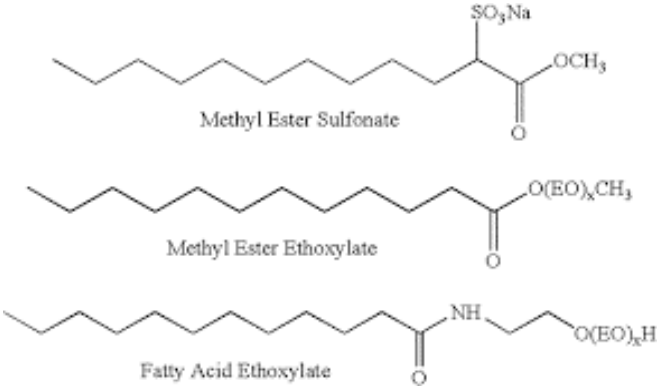

Figure 2 examples of surfactants and their structure

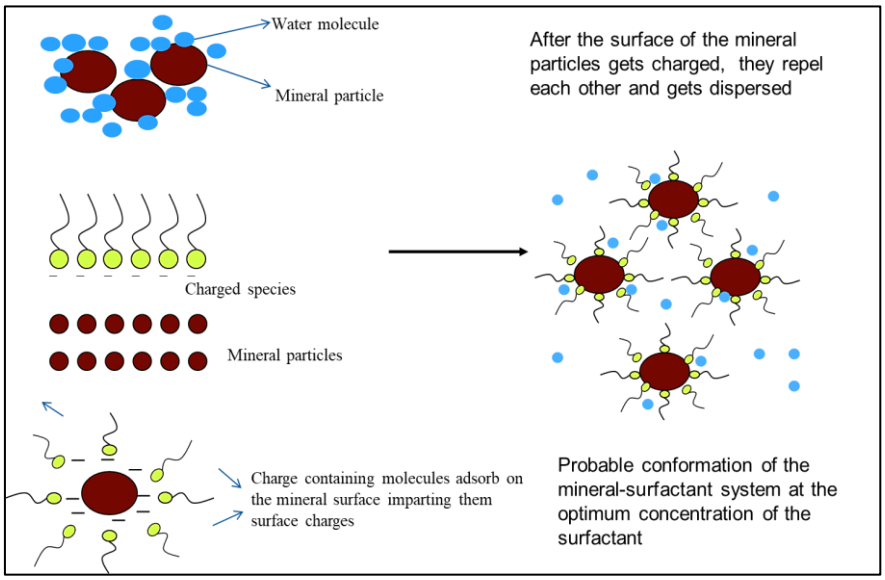

Figure 3 Probable phenomena occurring at the Mineral - water interface

The run of mine iron ore is crushed to -40 mm size using primary and secondary crusher. Thereafter, iron ore less than 40 mm size is mixed with surfactant solution in the drum scrubber. The surfactant dosed can vary from 0.25-1% concentration. The ore is treated with water and surfactant solution in the drum scrubber. Similar dosing is also provided in the screw classifier which allows us the freedom to use the reagent as per our requirements. If the feed ore is of good quality, the lumps generated are already of good quality. Hence, dispersant may not be required for the lumps. In this scenario, the dispersant is used in the screw classifier which enables further alumina reduction in fines ore. However, the alumina reduction is always better when the dispersant or surfactant is used in the drum scrubber. Surfactant solution can be mixed directly with iron ore in screw classifier, or the surfactant solution and iron ore can be mixed simultaneously both in scrubber and in the classifier [7-10].

Lab test with the selected dispersant

The process was tested and evaluated with organic dispersants or surfactants such as alcohol ethoxylates, Di(2-Ethylhexyl) Sodium Sulfosuccinate and Polyethylene glycol 4000(PEG). All of these surfactants when used as per the current process gave positive results as depicted in table 1. The lab tests were performed by simulating the whole process followed in the plant that is scrubbing, separation and screening. The same process was carried out with scrubbing by different surfactant solutions. Then the effectiveness of the different processes was evaluated. Out of the given surfactants, Di(2-Ethylhexyl) Sodium Sulfosuccinate gave best results with respect to alumina reduction. Further, concentration of the surfactant solution played an important role in the process. Surfactant solution with a concentration in the range of 10-20 ppm (w.r.t. dry solids) showed good results as depicted in the Table 1. with respect to alumina and silica reduction. We had taken different feed samples with varying alumina and silica range to study the effect of Di(2-Ethylhexyl) Sodium Sulfosuccinate on alumina and silica reduction. Table 1 shows that there is further reduction in alumina and silica in all the cases when dispersant as used than when washed with water alone. The difference in reduction is represented as delta reduction.

Table 1 Table depicting the analysis of ore when washed with water and washed with dispersant

Feed			Normal water washed		Difference (Normal water wash-ROM)		Washed with dispersant		Difference (Chemically wash-ROM)		Delta Alumina	Delta Silica
Fe %	SiO_2 %	Al_2O_3 %	SiO_2 %	Al_2O_3 %	SiO_2 %	Al_2O_3 %	SiO_2 %	Al_2O_3 %	SiO_2 %	Al_2O_3 %		
55.49	5.77	7.15	5.67	6.95	0.1	0.2	5.49	6.45	0.28	0.7	0.5	0.18
47.52	9.09	10.95	8.81	9.52	0.28	1.43	7.16	9.14	1.93	1.81	0.38	1.65
63.05	1.55	3.61	1.42	3.39	0.13	0.22	1.37	3.22	0.18	0.39	0.17	0.05
55.15	3.7	7.84	2.81	7.03	0.89	0.81	2.67	6.61	1.03	1.23	0.42	0.14
62.2	2.35	4.26	1.89	3.98	0.46	0.28	1.83	3.85	0.52	0.41	0.13	0.06
57.31	3.54	6.27	3.11	5.72	0.43	0.55	3.01	5.24	0.53	1.03	0.48	0.1

Plant Trials with selected dispersant

Based on the lab data plant trials were taken for more than 3 months in different phases and varying different parameters like dosing positions, reagent dosages at Noamundi wet processing plant. The dosing points at drum scrubber have been shown below in figure 4 and dosing point at classifier at figure 5.

Figure 4 Dosing Point and Dosing System at Scrubber

Figure 5 Dosing Point and Dosing System at Classifier

RESULTS AND DISCUSSION

- The analysis of 15 days trial has been presented in tables below. As per Wet ROM Alumina, total number of data has been classified into three different bands i.e., <3.5% Alumina, 3.5-5.0% Alumina, and > 5.0% Alumina.
- The Alumina % in Classifier Fines, Lumps and corresponding delta Alumina reduction in Classifier Fines and Lumps are given below in Table 2, 3 and 4.
- In order to understand the efficacy of dispersant in Alumina reduction, the trial period data has been compared with past data (period: 21 days pre-trial and post-trial data) having similar level of Wet ROM Alumina in three different Alumina bands. Ref. Table 2,3 and4 below.

Table 2 Comparison of alumina reduction in alumina band less than 3.5%

Parameters	Alumina Class	Data Count (Shift-wise)	Avg. Wet ROM Alumina % (Calculated)	Classifier Fines Alumina % (Avg.)	Delta Classifier Fines Alumina	Lumps Alumina% (Avg.)	Delta Lumps Alumina%
Baseline Data	<3.5	11	3.24	3.03	0.21	2.58	0.66
Plant Trials (15 days)		11	3.17	2.82	0.35	2.03	1.14
Delta Reduction					0.14	0.55	0.48

Table 3 Comparison of alumina reduction in alumina band of 3.5-5%

Parameters	Alumina Class	Data Count (Shift-wise)	Avg. Wet ROM Alumina % (Calculated)	Classifier Fines Alumina % (Avg.)	Delta Classifier Fines Alumina	Lumps Alumina% (Avg.)	Delta Lumps Alumina%
Baseline Data	3.5-5	28	4.33	4.02	0.21	3.17	1.16
Plant Trials (15 days)		23	4.24	3.64	0.60	2.93	1.31
Delta Reduction					0.39	0.24	0.15

From the tables 2, 3 and 4, we can clearly see that there is an additional alumina reduction in the fines and lumps across all alumina feed ranges than when washed with water alone. Hence, the laboratory data was vetted in actual plant conditions.

Table 4 Comparison of alumina reduction in alumina band of >5%

Parameters	Alumina Class	Data Count (Shift-wise)	Avg. Wet ROM Alumina % (Calculated)	Classifier Fines Alumina % (Avg.)	Delta Classifier Fines Alumina	Lumps Alumina% (Avg.)	Delta Lumps Alumina%
Baseline Data	>5	8	5.29	4.52	0.21	3.72	1.57
Plant Trials 15 days)		12	5.62	4.87	0.75	3.81	1.81
Delta Reduction					0.54	-0.09	0.24

In the figure 6 and 7 we can see a visible difference in the texture and colour of the fine and lumps when washed with water and water and dispersant together.

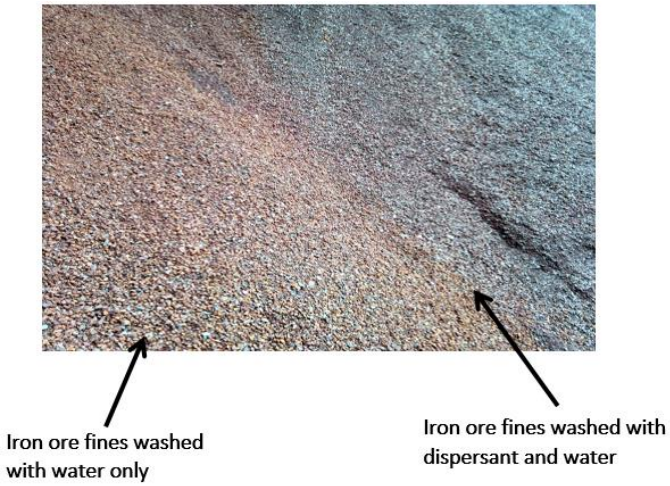

Figure 6 Image of iron ore fines washed with only water and water and dispersant together

Figure 7 Image of iron ore lumps washed with only water and water and dispersant together

CONCLUSION

In the sized ore and classifier fines, alumina has decreased considerably in majority of the cases by the application of dispersant. Dispersant application is an effective solution for the reduction of alumina in iron ore fines. This requires minimum open and can be deployed parallelly across units once the effectiveness of the dispersant is established.

ACKNOWLEDGEMENT

Authors thankfully acknowledge the financial support from Tata Steel Ltd., Jamshedpur to carry out the lab work as well as plant trials. We acknowledge the support of persons involved in the plant trials and analysis. We also sincerely acknowledge the support of chemical labs of Tata Steel for their support.

REFERENCES

1. Somasundaran, P., Kunjappu, J.T. (1989) In-situ investigation of adsorbed surfactants and polymers on solids in solution. Colloids and Surfaces, 37, 245-268.
2. Dibrov, I.A., Voronin, N.N., Klemyatov, A.A. (1998) Froth flotation extraction, a new method of metal separation from aqueous solutions. International Journal of Mineral Processing, 54 (1), 45-58.
3. Ma, M. (2012) Froth flotation of iron ores. International Journal of Mining Engineering and Mineral Processing, 1 (2), 56-61.
4. de Andrade Lima, L.R.P., Bernardez, L.A., Barbosa, L.A.D. (2007) Characterization and treatment of artisanal gold mine tailings. Journal of Hazardous Materials, 150 (3), 747-753.
5. Johnson, S.L., Wright, A.H. (2003) Mine void water resource issues in Western Australia: Western Australia, Water and Rivers Commission. Hydrogeological Record Series, Report HG 9, 1-93.
6. Lottermoser, B. (2007) Mine wastes: characterization, treatment and environmental impacts. Springer, 304.
7. Puttock, S.J., Fuile, A.J., Fell, C.J.D., Robins, R.G., Wainv, M.S. (1985) Role of surface effects in the dewatering of alumina trihydrate. American Institute of Chemical Engineers Journal, 31 (7), 1213-1216.
8. Pradip, P. (2006) Processing of alumina rich Indian iron ore slimes. International Journal of Minerals, Metals and Materials Engineering, 59 (5), 551-568.
9. Somasundaran, P., Krishnakumar, S. (1997) Adsorption of surfactants and polymers at the solid liquid interface. Colloids and Surfaces A: Physicochemical and Engineering Aspects, 123-124, 491-513.
10. Stroh, G., Stahl, W. (1990) Effect of surfactants on the filtration properties of fine particles, Filtration & Separation, 27 (3), 197-199.

XV International Mineral Processing and Recycling Conference
17-19 May 2023, Belgrade, Serbia

SURFACTANTS AND THEIR FUNCTIONS ON NANO- POWDER SYNTHESIS

H. Kurama[1], S. Kurama[2#]
[1] Eskisehir Osmangazi University, Mining Engineering Department, Eskisehir, Turkey
[2] Eskisehir Technical University, Materials Science Engineering Department, Eskisehir, Turkey

ABSTRACT – Nanoparticles have been drawn attention more than 20 years and this interest looks like to continue in near future. One of the challenging tasks to manage the production of nanomaterials/powders with controlled structure is the stabilization of particles and disturbing them in homogenously, which has played important roles in the advancement of targeted product, used in wide variety of industrial applications.
In this paper, the fundamental concept of colloidal stability and the role of surfactants in powder processes are briefly presented. A special attention has given to investigation of grinding aid on the magnetic properties of MgB_2 synthesized by high-energy ball mill.

Keywords: Colloidal Stability, Grinding Aids, High-energy Ball Mill, MgB_2.

INTRODUCTION

In recent years, the interest to production of nanostructured materials has gained worldwide prominence due to their existing and/or potential applications in a wide variety of technological areas such as electronics, catalysis, ceramics, magnetic data storage, structural components etc. The main reason of this can be attributed to their unusual properties based on the high concentration of atoms in interfacial structures and the relatively simple ways of their preparation [1-3]. Nanocrystalline materials are generally characterized by a large volume fraction of grain boundaries. Because of the extremely small size of the grains and increased fraction of the atoms located in the grain boundaries, allow significant improvement of the mechanical, chemical and physical properties of the powder and thus the material exhibits enhanced combinations of physical, mechanical, and magnetic properties compared to conventional coarse-grained counterparts. Synthesis of nanoparticle is complex processes. There are three main categories of nanoparticle synthesis and these are vapor phase, solution precipitation and solid-state processes. Although, all three processes are widely used in practice, the more common and oldest one is solid state. In this process, nanoparticles generally subjected to heat treatment followed by milling which carried out to get an average particle size of 100 nm or less.

The usage of mechanical energy dates backed to early ages of humanity, it was used crush bones, grains, shells and to produce food, pigments and weapons. However, with

Corresponding author: skurama@eskisehir.edu.tr

the beginning of nineties, the discovery of new class of solids based on crystallites with an average size in the nanometer range and very active surface of them has been lead to re-gaining of it for material synthesis [4]. Within the grinding processes, the mechanical milling or alloying is one of the most preferred and earliest techniques to produce nano-sized powders. However, the stabilization of particles and disturbing them in homogenous arrangement is the common challenge to increase the efficiency of milling to obtain required grain size, homogeneous size distribution and milling yield [5,6]. Most of the synthesis routs, these are act as important factor to develop the product with desirable properties. As indicated above, although, decreased grain size provoke the tailoring of particles with a different surface structures, in the nanometer size range, the particles have a strong tendency to agglomerate owing to their relatively large specific surface area, which cause enhancement of their van der Waals interactions. Therefore, in the last years, a broad range of techniques in chemistry and physical chemistry has been offered to stabilize inorganic nanoparticles or to self-assemble them in a controlled manner. The use of surfactants and /or grinding aids as the stabilizing agents in the preparation of nano powders has been recognized as an effective way for the synthesis of various nanomaterials, inter-metallic compounds and ceramic nanocomposites from solid state.

Colloidal stability

The term colloidal stability can simply be defined as the ability of dispersion to resist coagulation. This issue has been traditionally the primary focus of colloidal science at least dating back to the ancient Egyptians [7]. It is well known that if the particles are small enough, the van der Walls force between particles in a dispersion is usually attractive due to the Brownian motion, hence it is expected that these particles will be continually colliding with one another and they will remain as individual particles only if those collisions do not result in permanent association. Therefore, if there are no repulsive interactions between particles, especially at short interparticle separation, the dispersion will be unstable [8,9]. One of the concerned ways to ensure the required stability is known an electrostatic stability. The stability in this case will be depending on the nature of electrostatic force that results when the electrical double layers of two particles overlap, if it is repulsive, serves to counteract the attraction. The stability of the system based on the total potential energy of interaction between particle surfaces (VT) was previously well modeled by DLVO theory given in Eq. (1):

$$VT = VA + VR + VS \tag{1}$$

Where, VA is representing the sum of these van der Waals attractive and VR is electrical double layer repulsive forces that exist between particles. The combination of these two functions is the fundamentals of the DLVO theory. However, the potential energy occurred by the solvent, VS, is also makes a marginal contribution to the total potential energy over the last few nanometers of separation. The theory proposes that an energy barrier resulting from the repulsive force prevents the approaching of two particles one another and adhering them together. Therefore, if the particles have a sufficiently high repulsion, the dispersion will resist flocculation and the colloidal system

will be stable. The interaction energy curves of the type shown in Fig. 1, are useful construct for developing quantitative measures of kinetic stability. The van der Waals forces dominates at both large and small separation, however, in former case its value may be too small to be significance. At small VR must approach a finite magnitude, whereas the absolute value of the VA increases very markedly and hence is expected to pull the surface into a deep attractive well, which called the primary minimum. On the other hand, the secondary minimum is only occurred at larger distance where a much weaker and potentially reversible adhesion between particles exists [8].

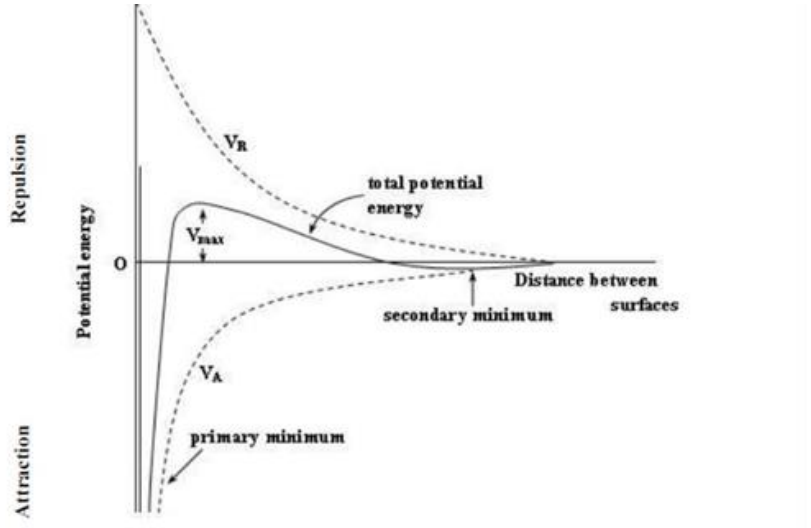

Figure 1 A variation of free energy diagram with particle separation according to DLVO theory [8]

Although, it is relatively easy to control the dispersion stability of sub-micron particles with the electrical double layer, which can be tuned by the surface potential of particles and the counter ion concentration. As recently reported by Kamiya et al. [7] for the nanoparticles, it is became difficult to improve their dispersion stability using only the DLVO interactions due to the existing relatively small potential barrier between them. Furthermore, the concentration of the particles should also have to take into account. When the concentration of particles is high and their separation is smaller than this distance, the particles will be trapped by the van der Waals force and form aggregates. In order the overcome these problems, surface modification of nanoparticles with polymeric surfactants or other agents is also one of the most preferred methods both in research studies and industry to improve the dispersion stability (steric stabilization). In this case, the stability is imparted by adsorption or attachment of polymer molecules onto the surface of colloidal particles. Steric stabilization is widely exploited industry because offers several distinct advantages over electrostatic stabilization. Compared to electrostatic stabilization, polymeric stabilization offers additional advantages in the synthesis of nano powders particularly when the narrow size distribution is required. Polymer layer adsorbed on the surface of particles serves as diffusion barrier to growth

of nuclei and the diffusion limit growth would reduce the size distribution of system. The comparison of these two options is given in Table 1.

Table 1 Electrostatic and steric stabilization comparison [9]

Electrostatic stabilization	Steric stabilization
Addition of electrolytes causes coagulation	Insensitive to electrolytes in case of non-ionic polymers
Usually effective in aqueous system	Equally effective for both aqueous and non-aqueous dispersion
More effective at low concentration of the dispersion	Effective at both low and high concentrations
Coagulation is not always possible	Reversible coagulation is more common
Freezing of dispersion induces reversible coagulation	Good freeze-thaw stability

A common explanation mechanism for the steric stabilization is entropic stabilization theory in which, it is assumed that a second surface approaching the adsorbed layer is impenetrable. Thus, the adsorbed layer is compressed and the polymer segments present in the interaction region lose configurationally entropy. That is, the polymer segments occupy fewer possible configurations in the compressed state than in the uncompressed state. This reduction in entropy increases Gibbs free energy change (ΔG), producing the net effect of repulsion between the particles and thus allow the particles stable.

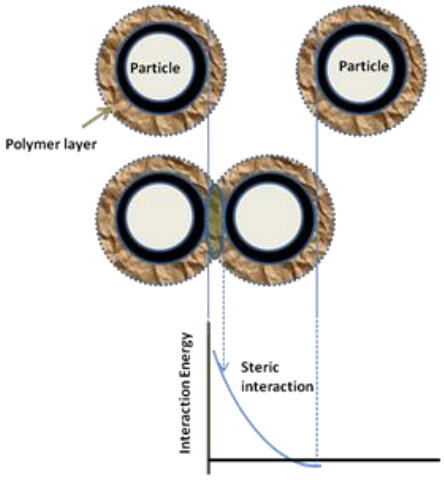

Figure 2 Schematic representation of polymer layer overlap

The application of steric stabilization in dispersing ceramic particles in non-aqueous media and the basic concepts has recently been reviewed by Shi [10]. According the concerned stabilization works on ceramic powders such as Al_2O_3 and Fe_2O_3 in xylene or Fish oil, $BaTiO_3$ in an ethanolmethyl ethyl ketone solution, polyamides on dispersing TiO_2

and Fe_2O_3, it was stated that functional groups, such as carboxyl, hydroxyl, amine, and ester groups in the molecular polymer structure generally play an important role in steric stabilization. Polymers containing carboxyl groups turn out to be the most effective steric stabilizers because carboxyl groups are supposed to interact strongly with basic sites, often present on the particle surface. On the other hand, the long chain hydrocarbons in the molecular structures extend from the surface into nonaqueous solvent act as good moieties in nonaqueous media.

The experiments conducted on the steric stabilization shown that the best steric stabilizers are amphipathic block or graft copolymers [11]. Block copolymers are a specific class of copolymers, in which the chemically distinct monomer units are grouped in discrete blocks along the polymer chain (Fig. 3). The result is that different homopolymers chains are joined in a head-to-tail configuration. Therefore, a block polymer is a linear arrangement of blocks of different monomer composition.

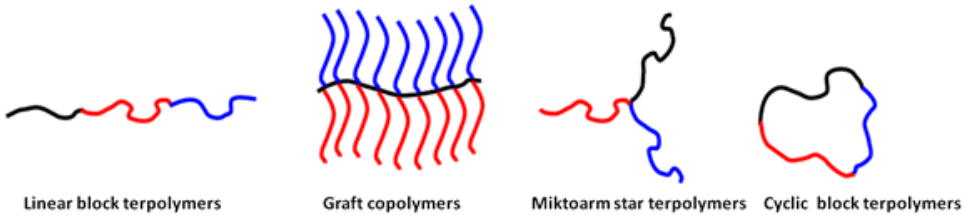

Figure 3 Representative architectures of linear block terpolymers, “comb” graft polymers, miktoarm star terpolymers, and cyclic block terpolymers

At least two chemically bounded homopolymer components, one of which soluble in the dispersion medium, while the others are nominally insoluble. The anchor polymer, serves to attach to soluble species to the colloidal particles. The soluble chains, which project away from the particle surface into the dispersion medium, are responsible for the observed colloidal stability (Fig. 4).

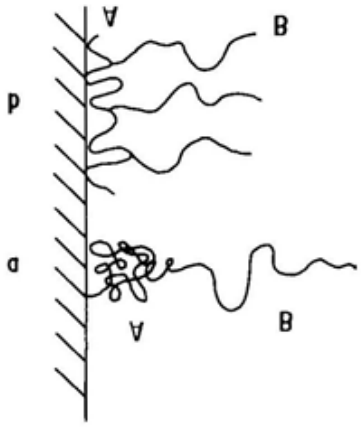

Figure 4 Examples of (a) block copolymers and (b) graft copolymers used as stabilizers; A is the anchor group, and B is the soluble group providing the steric barrier

However, it should be taking into consideration that, the anchoring must be adequate, the surface coverage must be complete and the thickness of the steric layers must be sufficiently large. The quality of solvent (i.e., solvent-polymer interaction) can also clearly affect the interaction force. In a good solvent, polymer segments favor contacts with the solvents. The self-assembly of amphiphilic block copolymers has been a popular topic in fields such as thermoplastic elastomers, nano-cargo drug delivery, lithography, biomedical/pharmaceutics, mesaporous materials. Although the self-assembly of amphiphilicis is more complicated than block copolymers self-assembly in bulk. The application detail of these polymers can be found in review [11]. Especially for ordered mesoporous materials, the research interest was started with the successful synthesis of porous silicates in the 1990s. Nowadays, with the help of several attempts, it has spread to a variety of framework compositions including metal oxides, non-oxide inorganic, and carbon. This group of materials exhibits periodically aligned structures and uniform cavities with sizes ranging from micro- (<2 nm), to meso- (2–50 nm), to macro-pores (>50 nm) which lead to very high surface areas (up to 1500 m^2/g). With these unique features, porous materials present great value for applications in energy conversion and storage, catalysis, drug delivery, gas capture, and water purification. Steric stabilization of colloidal particles is achieved by attaching (grafting or chemisorptions) macromolecules to the surfaces of the particles.

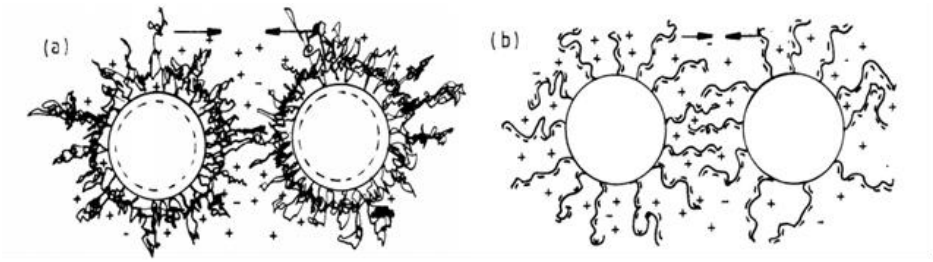

Figure 5 Schematic illustration of electrostatic stabilization, charged particles with non-ionic polymers (a); polyelectrolytes attached to uncharged particles (b)

Steric stabilization for powder stabilization can also applied as combined with electrostatic stabilization (Fig. 5). In which, polymers are attached to a charged particle surface; a polymer layer would form as discussed above. In addition, an electrical potential adjacent to the solute surface would retain. When two particles approach each other both electrostatic repulsion and steric repulsion would prevent agglomeration**.**

Grinding aids

Different from the course grinding, as the grinding proceeds into an ultrafine region, it becomes more and more difficult to obtain further reduction in size because a grind limit is approached. A practical grind limit exists for most systems is mainly depending on the tendency of the product particles to re-aggregate and established physical equilibrium between aggregation and fragmentation [12]. Especially in dry grinding, particle-particle interactions rise with increasing product fineness hence reduce the product throughput, increase the specific power consumption, make difficult to reach

certain product fineness and complicate the process control. Therefore, in many industrial dry fine-grinding processes, grinding aids are added into the process to handle these problems [4,12-14]. In this context, inorganic salts with multivalent ions or complex anions may be concerning as grinding aids. Adsorption of multivalent ions on the particles to increase the electrical repulsion between them is possibly the major reason for their influence. However, some of these reagents are reported to act only preventing ball coating but not aggregation of particles. Instead of inorganic salt usage, surfactants have been widely reported as effective grinding aids. Historically, for cement industry, where the huge amounts of cement clinker are dry ground in ball mills, therefore, considerably more efforts have been performed in to developing of suitable grinding aids and still these are continuing to find reagents that are more suitable both inorganic salt and surface active agents [15]. The first commercial use of grinding aids in the cement industry came about 50 year's ego. Since then several examples of grinding aids used in cement industry were reported in literature such as amines, organosilicones, organic acetates, propylene glycol, calcium sulfate, urea, carbon blacks, and wool grease. Katsioti et al [16], released a study on the various cement grinding aids and their impact on grindability and cement performance. The evaluation tests using with commercial grinding additives, triethanolamine hydrochloride, triethanolamine, propanol, benzene, benzenamine, acetamide, indicated that in all cases the addition of grinding aids resulted in improvement of the specific surface and grindability index. It was also proposed that additives have ability not only to reduce resistance to comminuting, but also an ability to prevent agglomeration, powder coatings of ball, and mill. Recently, in the study performed by Toprak et al [17], three grinding aids and three mixed products (grinding aid-strength enhancer) were tested around a cement grinding circuit at the same cement type (CEM II A-M (LW) 42.5 R) to select the most appropriate option. It was reported that the production rate of the circuit and the 28-day strength of the cement could be increased by 24% and 3.5% respectively with the selection of an appropriate chemical. In addition, the studies concluded that triethanolamine-based chemical had better performance parameters than the other types.

Other than these, some examples; polysiloxane in the grinding of ultra-porcelain and talc, silicones in the bail milling of quartz and limestone, acetones in nitromethane benzene, carbon tetrachloride and hexane in vibratory milling of ground glass, marble and quartz, and wool grease in the milling of gypsum, limestone, and quartz cloud also be given attractive applications. Grinding aids especially in dry micro-fine grinding processes remarkably increase the grinding energy efficiency, bring down the limit of grinding, prevent the agglomeration of ground particles, avoid grinding media coating and improve material transport [18,19]. Recently, Gokcen at al. [20] investigated the amine based various grinding aids (BMA 1923, BMA 1517, KATPLAST 54 and GRACE XS 304) effects on the fine grinding of sodium feldspar (albite) in stirred mill. The authors reported that all grinding aids were determined to be effective for micro-fine grinding of albite at some extent. The decreased energy conception was explained by amine chemistry. It tends to adsorb on the solid surface by their polar functional group, thus decreasing the surface energy, or to coat the external surfaces of the fine dispersed particles, thereby preventing their agglomeration, or to act as a lubricant on the shell of the mill and media to prevent powder coating thus influencing their flowability.

As a conclusion, according to several reports in literature, an effective way of the improving grinding efficiency is the use of special chemicals as grinding aids. This effect was mainly attributed the previous mechanisms proposed by Rehbinder and Westwood [21,22]. Rehbinder's mechanism based on adsorption-induced surface energy changes and Westwood's mechanisms based on adsorption induced mobility of near-surface dislocations. Addition of chemical agents to reduce the effective surface energy of the solid particles should, based on the above concept, enhance the grinding process, According to Westwood, the Rehbinder effect is more likely due to changes in the electronic states near the surface and point and line defects caused by the adsorption of the additives on the solid. Such changes are known to influence the specific interactions between dislocations and point defects that control the dislocation mobility and hence the hardness. A more recent study conducted by Prziwara et al [14], several grinding aids on dry fine grinding of limestone in a laboratory vibration mill were investigated. It was reported that all of the investigated grinding aids influence the grinding efficiency. However, the formation of agglomerates is not necessarily linked to the product fineness. Furthermore, a strong impact of certain grinding aids on the flowability of the product powder was determined. Moreover, a direct relation between surface energy and powder flowability as well as agglomeration behavior is supported the above mechanisms. Then summarized that such a behavior could be possible only when plastic deformation is dominant in fracture thus cannot be used in explaining the interactions in tumbling mills where the impact fracture prevails.

Mechanical alloying and MgB_2 synthesis

Mechanical Alloying (MA) is described as a high energy milling process, in which the powder particles are subjected to repeated cold welding, fracturing, and re-welding. Due to ability of the providing of creating pressure to enhancement of the thermodynamic and kinetic reactions between solid particles, in recent years, it has gaining as a most preferred solid-state method for powder preparation. In comparison with wet processes, MA approach has a great deal of well-known inherent advantages because of its being both economical and technically simple to perform mass productivity and its tremendous flexibility to generate nanocrystalline powders [23,24]. The usage of MA for the synthesis of nanomaterials dates back to the preparation of oxide dispersion strengthened solids (ODS). Although, the milling process was called as “mechanical alloying”, it was not widely accepted at that time that this milling process was a true alloying process. Later Koch et al. [25] published a landmark paper, demonstrated that mechanical milling could facilitate true alloying, and the outcome of the alloying can be a metastable material. This was the milestone of the widening of MA for the preparation of the amorphous alloys, superconducting materials, rare permanent magnets, superplastic alloys and intermetallic compounds. Within these practiced efforts, the production of MgB_2 can be given as example of attractive usage of MA. The discovery of the superconductivity of MgB_2 with a critical temperature of 39 K in 2001, has offered the promise of important large-scale applications at around 20 K [26]. Specifically, lack of weak-links at the grain boundaries, relatively high-critical temperature (*Tc*) of 39 K, improved critical current density (*Jc*) and the low cost of the starting materials make MgB_2 a promising candidate super conductor for wide range of practical applications. Nevertheless, observed rapid

drops of *Jc* at increased magnetic field has been limited the wide usage of the pristine MgB_2. The lack of sufficient defects at flux-pinning centers was suggested as main reason of this rapid decline [27-30]. Apart from the several attempts that perform to overcome this limitation, usage of MA has received more interest as an economical and effective method. During MA, heavy deformation is introduced into the particles. This is manifested by the presence of a variety of crystal defects such as dislocations, vacancies, stacking faults and increased number of grain boundaries hence leads to improving of the critical currents and magnetic flux pinning ability of the product. The presence of this defect structure also helps to enhancement of the diffusivity of solute. However, as indicated above parts, true alloying among powder particles can occur only when a balance is maintained between cold welding and fracturing of particles [23]. Therefore, preventing of the agglomeration of the powders especially at the initial stage of milling is plays an important role to obtain nano sized alloyed powder with homogeneous particle size dispersion. Zu et al. [31] reported that the microstructure and the *Jc* values of the MgB_2 samples affected from the ball milling media. In this report, different media, such as acetone, ethanol, and toluene has been used in milling stage. It was suggested that ball milling of B with toluene was a highly effective method to enhance the *Jc* performance of MgB_2 under high field. This affect was attributed to prevention of the oxidation of B powder during milling, and the small grain size was effective for enhancing flux pinning at the grain boundaries. The recent report released by Wu et al. [32], with using the SPEX mill also showed that a bulk form of MgB_2 with improved magnetization properties could be synthesized in a relatively short time and lower sintering temperature. It was reported that the highest Jc, approximately $2.3 \cdot 105$ A/cm^2 (-258.15 °C =15 K, 3 T) could be obtained for the samples milled for 5 hrs. and sintered at 750 °C for 1 hr.

In our previous paper [33], the effects of the process control agent (toluene) usage at relatively lower milling time (2 hrs.) and sintering Temperature (630 ^oC) on the product size, morphology and conversion level of precursor powders to MgB_2 was investigated. The MgB_2 samples used in this study were pre-alloyed by mechanical milling of magnesium (99.8 wt% purity) and amorphous boron (95 wt% purity) powders in a SPEX 8000D mills. The mixture powder were subsequently cold pressed. The powder was then sintered in a tube furnace under Ar-atmosphere. The experimental results showed that usage of toluene during milling step resultant with the decreasing of mean particle size of the powder mixture. Compared to other variables such as increase on the ball to powder ratio and milling time, ball diameter this affect was found to be more dominant. As can be seen in Fig. 6 the usage of toluene leads to relatively different grain. morphology of the sintered products. The observed more spherical and coarser particles for the sample which ball /powder ratio of 3, and sintered at 2 hrs. (Fig. 7-a) could be attributed to reflection of the agglomerated particles at previous dry milling. On the other hand, for the sample milled with toluene (Fig. 7-b) the relatively finer particle size of the milled could visible. This effect became more dominant for the sample milled with lover size of balls. This result was attributed to prevention of the surface coating and the agglomeration of particles in each run. Details on the sample preparation and the effect of sintering parameters on bulks samples can be found in elsewhere.

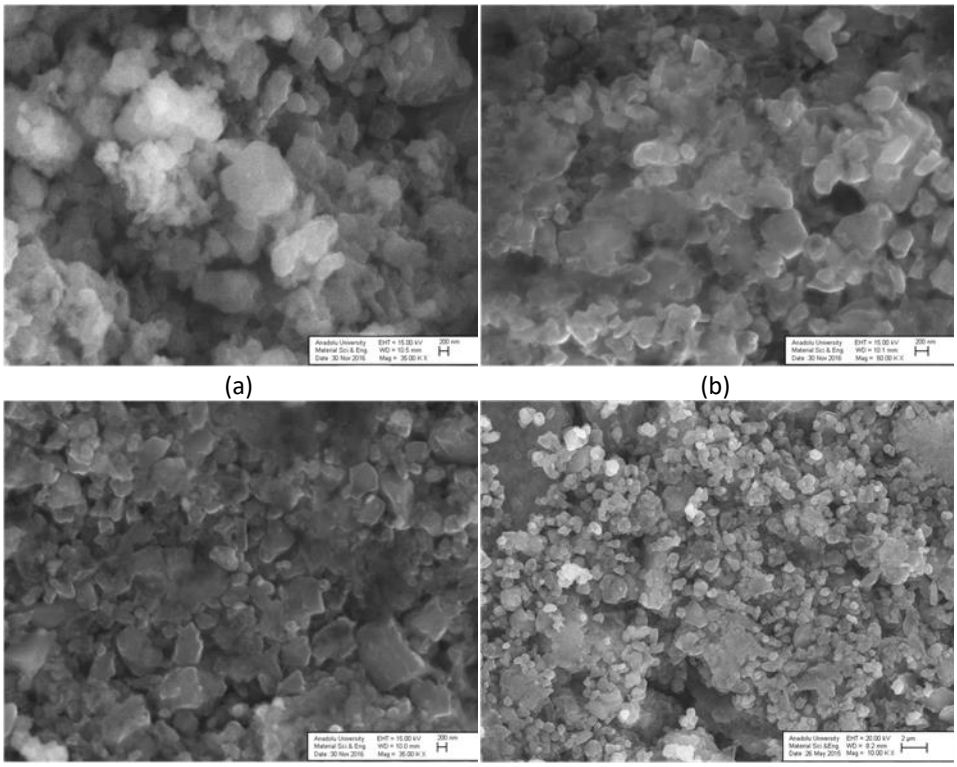

(a) (b)

(c) (d)

Figure 6 SEM images of samples ball /powder ratio of 3, and sintered at 2 hrs with standard ball without toluene (a), with toluene (b), ball /powder ratio of 3, and sintered at 2 hrs with fine ball (5 mm) without toluene (c), with toluene (d)

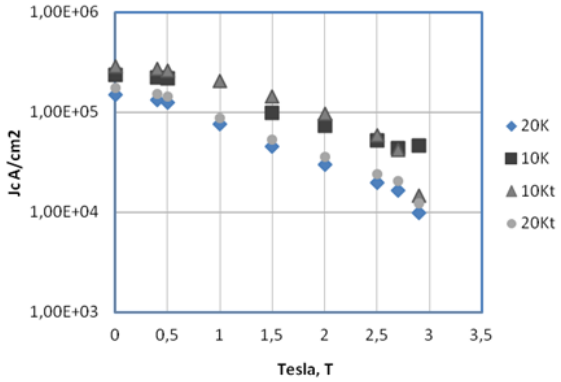

Figure 7 The variation of the calculated Jc values according the applied magnetic fields

Although, previous results clearly revealed the benefit of toluene usage in milling stage, these results should be supported with magnetization measurements. Therefore, in the following part, superconducting characterization of the toluene assisted (T- A) and

dry milled samples were presented to discuss how the grinding aid usage affects the final properties of product. The superconducting characterization of the samples was performed using a Quantum Design Physical Properties Measurement System (PPMS having Vibrating Sample Magnetometer (VSM) attachment. The *Jc* values of samples were calculated by extended Bean's critical state model [34] given below;

$$Jc = 20\Delta M \,/\, L_1(1 - L_1/3L_2) L_1 < L_2 \quad (2)$$

Where, ΔM is the width of the magnetic hysteresis loop and L, 1 and 2 are the thickness and width of the sample, respectively.

CONCLUSION

In the recent years, the demand for ultrafine particles as raw materials particularly in chemical, cement, ceramic, paint, and pharmaceutical industries and or demand for nano powders as precursor for composite material synthesis have increased a lot due to the specific properties of nanoparticles, where products with high homogeneity or solubility are often required. Among product properties, particle fineness, expressed by the median size or the width of the particle size distribution is prime importance. In these attempts, although, decreased grain size provoke the tailoring of particles with a different surface structures, the particles in this size range have a strong tendency to agglomerate owing to their relatively large specific surface area. Therefore, in this study, the fundamental concept of colloidal stability and the role of surfactants in powder processes mainly mechanical milling or alloying are briefly presented. The review was supported with selected applications to guide the researchers. A special attention has given to investigation of grinding aid on the magnetic properties of MgB_2 synthesized by high-energy ball mill.

The use of special chemicals to provide particle stability promises to be a broadly applicable method.

REFERENCES

1. Gleiter, H. (2000) Nanostructured materials, Basic concept and microstructure. Acta Mater., 48.
2. Murty, B.S., Ranganathan, S. (1998) Novel materials synthesis by mechanical alloying/milling. Int. Mater. Rev., 43: 101.
3. Balaz, P., Godocikova, E., Krilova, L., Lobotk, P., Gock, E. (2004) Preparation of nanocrystalline materials by high-energy milling. Mater. Sci. & Eng. A, 386: 442.
4. Fuerstaneu, D.W. (1995) Grinding aids, Kona, 13.
5. Suryanarayana C. (2001): Mechanical alloying and milling. Prog. Mater. Sci., 2001, 46:1.
6. Meyers, M.A., Mishra, A., Benson, D.J. (2006) Mechanical properties of nanocrystalline materials. Prog. Mater. Sci., 51: 427.
7. Kamiya, H., Iijima, M. (2010): Surface modification and characterization for dispersion stability of inorganic nanometer-scaled particles in liquid media, Sci. Technol. Adv. Mater. 11: 044304, 7.
8. Hunter, R.J. (1986) Foundation of Colloidal Science, 1 Oxford: Clarendon.

9. Himenez, P.C., Rajagopalan R. (1997) Principle of Colloidal Surface Chemistry. New York: Marcel Dekker Inc.
10. She, J. (2002): Steric Stabilization, http://muri.lci.kent.edu/References/NIM_Papers/stabilization_of_NP_suspensions/2002_Shi_steric_stabilization.pdf (22.03.2023).
11. Feng, H., Lu, X., Wang, W., Kang, N-G., Mays, J.W. (2017) Block copolymers: Synthesis, self-assembly, and applications, Polymers, 9, 494; doi:10.3390/polym9100494.
12. Somasundaran, P. (1978) Theories of Grinding, Ceramic Processing Before Firing, Edited by George Onoda, Jr. and Larry Hench Copyright 1978, by John Wiley & Sens. Jnt.
13. Schubert H. (1998) Effects of fluid and additives on grinding processes, Aufbereitungstechnik 8: 115–120.
14. Prziwara, P., Breitung-Faes S., Kwade A. (2018) Impact of grinding aids on dry grinding performance, bulk properties and surface energy, Advanced Powder Technology 29 416–425.
15. Guo, Yan-mei, Sun Shao-fei, (2017) The effect on the performance of cement grinding aid components, Journal of Materials, Processing and Design, 1: (1).
16. Katsioti, M., Tsakiridis, P.E., Giannatos, P., Tsibouki, Z. Marinos, J. (2009) Characterization of various cement grinding aids and their impact on grindability and cement performance, Construction and Building Materials, 23: 1954–1959.
17. Toprak, A. N., Altun, O., Aydogan, N., Benzer, H. (2014) The influences and selection of grinding chemicals in cement grinding circuits, Construction and Building Materials 68: 199–205.
18. Paramasivam R., Vedaraman R. (1992) Effect of physical properties of liquid aids on dry grinding. Powder Technol. 70: 43–50.
19. Hasegawa, M., Kimata, M., Shimane, M., Shoji, T., Tsuruta, M. (2001) The effect of liquid additives on dry ultrafine grinding of quartz. Powder Technol. 114: 145–151.
20. Gokcen H.S., Cayirll S. Ucbas Y., Kayaci K. (2015): The effect of grinding aids on dry micro fine grinding of feldspar, International Journal of Mineral Processing 136:42-44
21. Rehbinder, P.A. (1931) Verminderung der ritzhärte bei adsorption grenzflächenaktiver stoffe, Zeitschrift für Physik 72: 191–205
22. Macmillan, N.H., Westwood A.R.C. (1973): Surface charge-dependent mechanical behavior of non-metals, Office of Naval Research Project NR-O32-524, RIAS, Martin Marietta Corp., Baltimore, September 1973
23. Suryanarayana, C. (2008) Recent developments in mechanical alloying, Reviews 18, I3, 203-21
24. Zahrani, E.M., Fath, M.H. (2009) The effect of high-energy ball milling parameters on the preparation and characterization of fluorapatite nanocrystalline powder, Ceramics International 35 2311–2323
25. Koch, C.C., Cavin, O.B., Mckamey C.G., Scarbrough J.O. (1983) Preparation of amorphous Ni60Nb40 by mechanical alloying. Appl. Phys. Lett., 43, 1017
26. Nagamatsu, J., Nakagawa, N., Muranaka, T., Zenitani, Y., Akimitsu, J. (2001) Superconductivity at 39 K in magnesium diboride. Nature, 410, 63
27. Prinkhna, T.A. (2009) Properties of MgB_2 bulk, ⟨https://arxiv.org/ftp/arxiv/papers/0912/0912.4906.pdf (22.03.2023)

28. Rogado, N., Hayward, M. A., Regan, K. A., Wang, Y., Ong, N.P., Zandbergen, H.W., Rowell, J.M., Cava, R. J. (2002) Low temperature synthesis of MgB_2, J. Appl. Phys. 91, 274-277
29. Whaßler, C.R., Birajdar, B., Gruner, W., Herrmann, M., Perner, O., Rodig, C., Schubert, M., Holzapfel, B., Eibl, O., Schultz, L. (2006) MgB_2 bulk and tapes prepared by mechanical alloying: influence of the boron precursor powder, Supercond. Sci. Technol. 19, 512–520
30. Ma, Z., LİU, Y. (2011) The varied kinetics mechanisms in the synthesis of MgB_2 from elemental powders by low-temperature sintering, Materials Chemistry and Physics 126 114–117)
31. Xu, X., Kim, J.H., Yeoh, W.K., Zhang, Y., Dou, S.X. (2006) Improved Jc of MgB_2 superconductor by ball milling using different media, Supercond. Sci.Technol.19 L47–L50
32. Wu, Y.F., Lu, Y.F, Li, J.S., Chen, S.K., Yan, G., Pu, M.H, Li, C.S., Zhang, P.X. (2007) The microstructures and superconducting properties of MgB_2 bulks prepared by a high-energy milling method, Physica C 467 38-42
33. Kurama, H., Erkus, S., Gasan, H. (2017) The effect of process control agent usage on the structural properties of MgB_2 synthesized by high energy ball mill, Ceramics International 43: S391–396
34. Bean, C. P. (1962) Magnetization of Hard Superconductors, Physical Review Letters 8 250-253. http://dx.doi.org/10.1103/PhysRevLett.8.250 (22.03.2023)

XV International Mineral Processing and Recycling Conference
May 17-19, 2023, Belgrade, Serbia

METHODS FOR PROCESSING NATURAL AND ANTHROPOGENIC COPPER-NICKEL RAW MATERIALS IN THE ARCTIC

A. Goryachev[#], D. Makarov
Institute of North Industrial Ecology Problems – Separate subdivision of the Federal State Budgetary Institution of Science of the Federal Research Center «Kola Science Center», Apatity, Russian Federation

ABSTRACT – The research has been carried out on the enrichment of Murmansk region copper-nickel raw materials, that have been processed by heap leaching and low-temperature roasting, followed by water leaching. A high recovery of nickel and copper into solution has been achieved. The prospects of using these methods in the Arctic conditions have been shown.

Keywords: Low-temperature Roasting, Heap Leaching, Sulfuric Acid Granulation, Copper, Nickel.

INTRODUCTION

The economy of the Murmansk region (North-Western part of the Russian Federation) is dominated by mining industry, and the copper-nickel industry plays a significant role in the economic development of the region. Most of sulfide copper-nickel ores deposits and occurrences is located in the western part of the region, a smaller part – in the central part, and in the eastern part only occurrences of poor copper-nickel mineralization are known [1]. A number of deposits considered as promising for processing by alternative enrichment methods are associated with the ore-magmatic systems of Monchegorsk pluton. Monchegorsk pluton consists of two branches. One branch is represented by the Nittis-Kumuzhya-Travyanaya massifs, the other – by the Sopcha and Nud-Poaz massifs. At the Nud II and Nud Terrasa deposits, a nested disseminated type of mineralization is developed, the sulfide matrix of the ore is formed by pyrrhotite, that contains ingrowths of pentlandite [2]. From a technological point of view, the Allarechensk technogenic deposit, located in the Pechenga region, also attracts attention. This object is a rock dump formed as a result of the primary Allarechensk deposit development. During the development of a primary deposit, overburden and host rocks were dumped into a dump, the volume of rocks in the dump reached 6,700 thousand m^3. The main ore-forming minerals are: pyrrhotite, pentlandite, chalcopyrite and magnetite.

In addition to a significant number of deposits in the region, large stocks of copper-nickel enrichment waste have been accumulated. For example, JSC «Kola GMK» currently operates one tailing dump at the enrichment plant in the city of Zapolyarny. The tailing dump covers an area of approximately 1,033 hectares and receives about 7 million tons

[#] corresponding author: a.goryachev@ksc.ru

of tailings per year. During its operation, it has accumulated about 330 million tons (or 226 million m^3) of tailings. The tails are characterized by the predominance of the -0.1 mm fraction, a significant proportion is the -0.044 mm fraction [3]. The mineral composition of the tailings is dominated by serpentines (60%), and there are also pyroxenes, amphiboles, talc, chlorite, quartz, and feldspars. The main ore minerals are magnetite, pyrrhotite, pentlandite, chalcopyrite. When processing copper-nickel ores, the loss of nickel with tailings is about 25% of the initial content in the ore [4]. Thus, the processing of finely dispersed tailings is of particular practical interest. Interest in sulfide-containing enrichment wastes is also due to the need to reduce environmental impact, in particular – water bodies pollution with metal ions. Non-ferrous metal and iron sulfides are oxidized during waste storage to form sulfuric acid, while heavy metals are converted into water-soluble salts.

For efficient processing of the above-mentioned copper-nickel raw materials, the development of alternative enrichment methods is required, since physical enrichment methods – flotation, gravity and magnetic separation are ineffective for processing such raw materials. It has been established that implementation of an enrichment technology is determined by the characteristics of the copper-nickel raw materials – the mineralogical composition and the initial content of the valuable component. For the processing of substandard raw materials, in particular, industrial waste, the content of non-ferrous metals in which does not exceed 1%, the heap leaching method seems promising [5]. Successful industrial trials for metals recovery from copper-nickel ores by heap leaching were carried out by Talvivaara Mining Company plc, Finland. This method has been used to recover nickel, cobalt, zinc, copper, manganese and uranium, providing experience with heap leaching in severe climate conditions. As studies show, it is advisable to grind the ore before heap leaching to a particle size of <8 mm [6, 7]. In the case of enrichment tailings, on the contrary, the accumulated experience justifies the need to enlarge the material in order to increase the pile filtration properties [8]. The difficult climatic conditions of both the Murmansk region and the entire territory of the Russian Arctic make it difficult to operate the heap all year round. It is advisable to carry out preliminary preparation of raw materials (granulation) before a long period of below-zero temperatures, storage of the granules during winter time and subsequent leaching in the warm season [9, 10].

In the case of copper-nickel ores with a content of non-ferrous metals >1%, as well as rough concentrates, the method of low-temperature roasting of ore with ammonium sulfate seems promising. Conducted studies on the roasting of copper-nickel raw materials with ammonium sulfate $(NH_4)_2SO_4$ made it possible to establish that metal sulfides and oxides are able to react with the formation of water-soluble sulfates. Previously, this compound has been used to recover manganese from low-grade carbonate manganese ore, to process spent lithium-ion batteries, and to process converter slag to recover nickel, cobalt, and copper. Processing of substandard and low-grade sulfide and mixed ores by low-temperature roasting followed by water leaching can be considered as promising and environmentally friendly process. This process is characterized by a high degree of metals recovery, the selectivity of the reactions occurring during the roasting process, energy efficiency and low cost [11, 12].

EXPERIMENTAL

In the course of the study, methods for processing the following raw materials were considered: a) copper-nickel ores enrichment tailings of the Kola GMK JSC, b) ores of the Nud Terrasa and Nud II deposits, c) ores of the Allarechensk technogenic deposit (hereinafter referred to as TD).

To carry out experiments on the processing of copper-nickel tailings, sulfuric acid granulation of tailings was carried out, followed by leaching according to the following scheme: grinding of raw materials → granulation of raw materials using sulfuric acid → irrigation of the obtained granules with an oxidizer → storage of granules for six months → heap leaching of granules. Content of metals in tailings, %: Ni – 0.20, Cu – 0.07, Fe – 14.1. During the experiment, the tailings were granulated using an experimental granulator FL015-1K-02 («Dzerzhinsktechnomash» LLC, Dzerzhinsk, Russia). A 30% sulfuric acid solution was chosen as a binder, the S:L ratio varied from 4:1 to 9:1. The resulting granules were 3-4 mm in diameter and 1-1.5 mm thick. The granules were irrigated with a 0.5% sulfuric acid solution containing the Fe^{3+} oxidizer in an amount of 2 g/L, the ratio of granules and oxidizer = 5:1. After applying the oxidant, a storage step followed, when excess moisture was removed and the granules gained strength. The goal set in the work implies the development of an approach to tailings processing adapted to the climatic conditions of the Far North.

For this reason, an assessment was made of the effect of negative temperatures on the process of storing granules with subsequent leaching during the warm period. Samples were preliminarily stored for six months in a freezer at -15 °C. After long-term storage, the pellets were processed by heap leaching. To simulate the process of heap leaching, the granules were placed in glass percolators with a diameter of 45 mm. The load weight was 180 g, the height of the layer of granules was 110 mm. Distilled water with a volume of 50 ml was supplied to the layer of granules five times a week for 20 days. This was followed by the stage of sulfuric acid leaching, during which 50 ml of a 2% solution of sulfuric acid was applied to the surface of the heap with the same frequency. The ambient temperature during the leaching was approximately +19 °C. The duration of heap leaching was 40 days.

Ore from the Nud Terrasa and Allarechensk TD deposits with a non-ferrous metal content of <1% was processed using the heap sulfuric acid leaching method. For leaching tests, samples of Nud Terrasa ore with a Ni content of 0.42% and Cu 0.15% and Allarechensk TD ore with a Ni content of 0.52% and Cu 0.74% were used. The ore was crushed to a fraction of -3+1 mm and placed in glass percolators with a diameter of 27 mm. The weight of the ore loaded into the percolator was 220 g, 25 ml of a 2% sulfuric acid solution were fed into the columns with ore three times a week. The duration of the experiments was 80 days. Heap leaching modeling studies were carried out at an ambient temperature of approximately +19 °C.

In the course of experiments on low-temperature roasting, the copper-nickel ore was mixed with ammonium sulfate (chemically pure, GOST 3769-78) and ground the resulting mixture in a BMU-100 ball mill (HT Machinery Co., Ltd., Harbin, China). For the research, ore from two deposits was used – Nud II deposit ore with a content of Ni 0.45% and Cu 0.39% and the Allarechensk TD ore with a content of Ni 5.8% and Cu 2.9%. The mixture was fired for 240 minutes at various temperatures in a SNOL 3/11 muffle furnace («NPF

Thermiks» LLC, Moscow, Russia). The firing temperature was varied from 300 to 500°C in steps of 50°C. Heating to the desired temperature took 60 min. After roasting, the clinker was cooled in the open air for 60 min. Then the clinker was leached in distilled water heated to ≈ +80°C for 40 min with constant stirring at an intensity of 230 min^{-1} using an MV-6 overhead mixer («NV-LAB» Ltd., Moscow, Russia). In productive solutions, during the experiments, the concentrations of copper and nickel in solutions were measured according to the standard PND F 14.1:2:4.140-98 by atomic absorption spectrometry with electrothermal atomization. In experiments on heap leaching, the pH values of solutions were controlled using an I-160 MI ionometer («Izmeritelnaya Tekhnika» LLC, Moscow, Russia).

RESULTS AND DISCUSSION

During the copper-nickel tailings granulation, granules with a strength of >3.5 MPa were obtained. The most solid were the granules obtained at the ratio S:L = 4:1, the strength of these granules was 4.7 MPa. However, the granules prepared at this ratio were also characterized by high caking (48%), that is expressed in the formation of large shapeless agglomerates. According to the totality of physical characteristics, the ratio S:L = 6:1 was chosen as the optimal one for granulation.

To study the effect of the ratio of raw materials and binder in the granulation process on the subsequent recovery of metals into solution, three samples of granules were taken, prepared at a ratio of S:L = 4:1, 6:1, 9:1 and stored for six months at a temperature of -15 °C. In the course of aqueous leaching of granules prepared at a ratio of S:L = 4:1, the pH value of the pregnant solutions varied from 3.11 to 5.29, the average pH value of the solutions was 4.10. Low pH values of the pregnant solutions at an early stage of aqueous leaching indicate the formation of highly concentrated areas of granules saturation with sulfuric acid. The average concentration of metals in the productive solutions was 72.4 mg/L nickel and 6.5 mg/L copper.

In the course of the experiment with tailings granulated at a ratio of 4:1, 12.3% nickel and 3.3% copper were recovered into solution during aqueous leaching. During the sulfuric acid leaching of granules, the average pH value of the productive solutions was 1.80. The average nickel concentration in the solution was 107.8 mg/l, and that of copper was 19.6 mg/l. By the end of the experiment, 21.2% nickel and 10.2% copper were recovered. Thus, 33.6% nickel and 13.5% copper were recovered from tailings granulated at a ratio of S:L = 4:1 for 40 days of leaching, including water and sulfuric acid stages.

Reducing the binder consumption, the ratio S:L = 6:1 at the granulation stage made it possible to achieve the following results. The average pH value of pregnant solutions at the stage of aqueous leaching was 4.38, the values changed during the experiment in the range from 3.86 to 5.56. The average concentration of metals in the solution during the experiment was 129.5 mg/L for Ni and 6.8 mg/L for Cu. By the end of water leaching, 27.5% nickel and 3.4% copper recovered from the granules into solution, while a significant part of the granules retained its original shape. In the course of sulfuric acid leaching, the average pH value of pregnant solutions was 1.85. The average concentration of nickel in the solution over 20 days of leaching was 82.9 mg, copper – 10.7 mg/L. Leaching with a solution of sulfuric acid yielded 16.9% nickel and 5.5% copper by the end of the experiment. Thus, for 40 days of leaching, the total recovery was: 44.4%

nickel and 8.9% copper.

The granules obtained at the ratio S:L = 9:1 were characterized by relatively low strength. During the water leaching of the granules, the pregnant solutions pH value varied from 3.90 to 6.41, the average value was 4.64, that is higher compared to the solutions obtained after leaching of the granules prepared at S:L = 4:1 and 6:1. The average concentration of nickel in solution was 89.1 mg/L, copper – 5.5 mg/L. As a result of water leaching of the granules, 18.3% nickel and 0.1% copper were recovered. When leaching with a sulfuric acid solution, the pregnant solutions average pH was 1.87. The average concentration of nickel in the solution was 77.2 mg/L, copper – 8.6 mg/L. During sulfuric acid leaching, 15.8% nickel and 4.4% copper were recovered from the granules. Thus, 34.1% nickel and 4.5% copper were recovered from the tailings granulated at the ratio S:L=9:1 during 40 days of the experiment.

Comparison of the results of granulation at different ratios of S:L made it possible to establish that the granules obtained at a ratio of S:L = 4:1 are characterized by high caking, that does not provide proper contact with the leaching agent. A low solution filtration rate was noted during aqueous leaching of granules. When using the ratio S:L = 9:1, softening of the granules occurs, leading to the effect of clogging and, as a result, to a deterioration in the filtration of the solution. Thus, the considered variants of the S:L ratios (4:1 and 9:1) are not optimal due to the low quality of the obtained material and the relatively low level of metals recovery into solution during subsequent heap leaching. When using the ratio S:L=6:1, it was possible to obtain granules with better physical characteristics. In addition, from granules prepared at this ratio, the nickel recovery was maximum. Research on the processing of tailings by granulation followed by leaching is ongoing.

Processing of the ore of the Allarechensk TD and the Nud Terrasa deposit by the method of sulfuric acid heap leaching made it possible to achieve the following results. The concentration of metals in the pregnant solutions during the processing of Allarechensk TD ore averaged 114.6 and 70.7 mg/L for nickel and copper, respectively. The concentration of metals in the productive solutions naturally decreased as the experiment duration increased and by the end of the experiment did not exceed 50 mg/l. For 100 days of leaching, 10.22% nickel and 4.44% copper were recovered from the ore.

During processing the Nud Terrasa deposit ore, the average nickel concentration in solutions was 114.2 mg/l, copper – 32.7 mg/l. By the end of the experiment, 12.80% nickel and 10.20% copper were recovered from the Nud Terrasa deposit ore. Thus, over the same period of heap leaching, the recovery of copper from the Nud Terrasa deposit ore was significantly higher. This indicates the need for additional activation of the grains surface of sulfide minerals of the Allarechensk TD ore, in particular, chalcopyrite, which is the main concentrator of copper.

The processing of ore with a higher initial content of non-ferrous metals was carried out using ammonium sulfate. It is known that the process of thermal decomposition of ammonium sulfate occurs in the temperature range of 155-450 °C, so this compound can contribute to the intensive conversion of non-ferrous metal sulfides into the sulfate form during low-temperature roasting of the mixture. At atmospheric pressure, ammonium sulfate decomposes to form a melt based on NH_4HSO_4 hydrosulfate and an ammonia-

enriched gas phase. It can be argued that in the process of low-temperature roasting at temperatures of 300-500 °C for four hours, several ammonium compounds that make up the melt come into contact with ore particles. This condition is met only with the access of atmospheric oxygen. Experiments carried out in an autoclave without constant air access showed that during low-temperature firing for four hours, no melt formation occurs [13].

During the roasting of a mixture of Nud II deposit ore with a particle size of <100 μm and ammonium sulfate at a ratio of 1:2, it was found that with an increase in the roasting temperature, the recovery of metals during subsequent aqueous leaching increases. The smallest recovery of metals was noted at a roasting temperature of 300 °C, 12.5% of nickel was recovered, and less than 13.5% of copper. A significant increase in the recovery of metals was noted at a temperature of 400 °C, 33.6% nickel and 34.6% copper were recovered into solution during leaching. A further increase in the roasting temperature did not lead to a significant increase in the recovery of metals. Taking into account the sharp increase in recovery after roasting the mixture at 400 °C, it was reasonable to consider ways to intensify the transition of metals into a water-soluble form at a given temperature. An increase in the consumption of ammonium sulfate led to a more intensive metals recovery into solution. At a ratio of 1:7, by the end of the experiment, 56.7% nickel and 52.1% copper were recovered. To further increase the metals recovery, the mixture was grinded to finer fractions before roasting. The recovery of metals increased as the particle size of the mixture decreased. From the <40 μm fraction, 73.5% nickel and 72.1% copper were recovered.

According to the results of experiments with the Allarechensk TD ore, with varying roasting temperature, it was found that at a temperature of 300 °C, the minimum recovery of metals occurs in the studied roasting temperature range, 17.0% nickel and 18.9% copper are recovered during water leaching. As in the case of Nud II ore, an increase in the roasting temperature led to an increase in the recovery of metals. The highest recovery of nickel was achieved at a roasting temperature of 450 °C, with almost 44% going into solution. The reasons for a not so significant increase in metals recovery, especially nickel, with an increase in temperature above 450 °C can be explained by a decrease in the amount of the reagent involved in the reaction due to the decomposition of ammonium sulfate and ammonium hydrosulfate with the formation of SO_2 and NH_3. The effect of the concentrate:ammonium sulfate ratio on the recovery of metals into solution was studied at a temperature of 400 °C. An analysis of metal recovery using different ratios of concentrate and ammonium sulfate showed that the highest recovery of nickel was achieved at a ratio of 1:7, 79% recovered into solution. The recovery of copper also tended to increase with an increase in the proportion of ammonium sulfate in the roasted mixture. At a ratio of 1:2, 36% of copper was recovered, while at a ratio of 1:9 – 79%. In order to increase the recovery of non-ferrous metals into solution, the influence of the particle size was analyzed. The experiments were carried out at an optimum temperature of 400 °C and a concentrate:ammonium sulfate ratio of 1:7. When the mixture was ground to a particle size of <50 μm, 87.1% nickel and 81.4% copper were recovered. Finer grinding made it possible to increase the recovery of non-ferrous metals, 91.5% nickel and 94.8% copper were recovered into solution.

CONCLUSION

The conducted studies show the prospects of processing copper-nickel raw materials of the Murmansk region by alternative methods of enrichment. Severe climatic conditions are not a barrier to the use of the proposed enrichment processes.

Copper-nickel tailings can be processed by heap leaching. The principal possibility of using sulfuric acid granulation as a method of preliminary preparation of raw materials before subsequent leaching is shown. The storage conditions of ore material in the winter period with the conversion of non-ferrous metals into a soluble form and subsequent leaching in the summer period are simulated. Using this approach will significantly reduce capital and operating costs and make the processing of substandard raw materials profitable.

Laboratory tests of heap sulfuric acid leaching showed the effectiveness of the method for processing copper-nickel ores with substandard content of non-ferrous metals. The leaching of non-ferrous metals from the ore of the Nud II deposit was especially intensive. This is probably due to the structural features of the ore of this deposit. When the ore was crushed, the sulfide grains opened up better and became available for leaching. The application of the method will make it possible to involve in the processing of currently unclaimed raw materials, allowing to obtain additional economic benefits and minimizing the negative impact on the environment.

Empirically, the prospects for processing the ore of the dump of the Allarechensk deposit by roasting with ammonium sulfate have been shown. Sintering at 400 °C at a ratio of ore and ammonium sulfate = 1:7 makes it possible to recover more than 80% of the target metals into solution. It must be taken into account that the temperature of 400 °C is lower than the temperature of traditional pyrometallurgical processes. In addition, there is the possibility of regenerating the reagent by capturing the off-gases - SO_2 and NH_3. Low-temperature roasting of sulfide raw materials with ammonium sulfate, provided that the process is optimized, can also be considered promising for the processing of low-grade ores due to high selectivity, relatively low energy consumption, and low cost.

ACKNOWLEDGEMENT

The authors are grateful to L. P. Kudryavtseva and I. R. Elizarova for the chemical analysis of the solutions. The work was carried out within the framework of research topics Nos. 122022400093-9 and 1021051803680-5.

REFERENCES

1. Yakovlev, Yu., Yakovleva, A., Neradovskiy, Yu., Osokin, A., Balabonin, N., Dokuchaeva, V., Orsoev, D., Distler, V. (1981) Mineralogy of copper-nickel deposits of the Kola Peninsula (Gorbunov G. I.), L.: Nauka, Leningrad, 352.
2. Pripachkin, P., Neradovskiy, Yu., Fedotov, Zh., Nerovich, L. (2013) Cu-Ni-PGE and Cr deposits of the Monchegorsk region, Kola Peninsula, Russia. In: Geological tour guide (Voytekhovskiy Yu. L.) GI KSC RAS, Apatity, 44.

3. Makarov, D., Makarov, V., Vasil`eva, T., Farvazova, E. (2004) Changes in the content of Ni, Cu, Fe, Mg in the copper-nickel ores enrichment tailings during its storage. Engineering ecology, 1, 18-28.
4. Chernousenko, E., Neradovskiy, Yu., Kameneva, Yu., Vishnyakova, I., Mitrofanova, G. (2018) Improving the efficiency of flotation enrichment of refractory sulfide copper-nickel ores of the Pechenga ore field. Journal of Mining Science, 6, 173-179.
5. Khalezov, B. (2013) Heap leaching of copper and copper-zinc ores (domestic experience): monograph. RiO UrB RAS, Ekaterinburg, 346.
6. Svetlov, A., Makarov, D., Pripachkin, P., Usov, A., Potokin, A., Goryachev, A. (2018) Methods of increasing the recovery of non-Ferrous metals from the low-grade copper-nickel ores for heap leaching. Inzynieria Mineralna, 19, 173-177.
7. Yanishevskya, E., Fokina, N., Goryachev, A., Krasavtseva, E. (2020) Biohydrometallurgical processing methods for low-grade sulfide ores in the Arctic. Inzynieria Mineralna, 2 (1), 221-224.
8. Khabirov, Ye., Shadrunova, I., Garkavi, M. (2007) Formation of granules from sulfide tailings for heap leaching. Mining informational and analytical bulletin journal (scientific and technical journal), 309-314.
9. Goryachev, A., Makarov, D., Svetlov, A. (2021) Sulfuric acid granulation of copper-nickel tailings in the climatic conditions of the Murmansk region. Mineralogy of technogenesis – 2021, 22, 116-125.
10. Markovich, T., Razvorotneva, L. (2011) Oxidative leaching of sulfide Udokan ore with the participation of oxygen compounds of nitrogen under cryogenic condition. Vestnik ONZ RAS,3, NZ6071.
11. Goryachev, A., Chernousenko, E., Potapov, S., Tsvetov, N., Makarov, D. (2021) A Study of the feasibility of using ammonium sulfate in copper–nickel ore processing. Metals, 11 (422), 1-11.
12. Liu, X.W., Feng, Y.L., Li, H.R., Yang, Z.C., Cai, Z.L. (2012) Recovery of valuable metals from a low-grade nickel ore using an ammonium sulfate roasting-leaching process. International Journal of Minerals, Metallurgy, and Materials, 19 (5), 377-383.
13. Goryachev, A., Makarov, D., Belyaevskiy, A. (2020) Low-temperature roasting of copper-nickel ores with ammonium sulphate as a perspective method for processing such raw materials. Mineralogy of technogenesis – 2020, 21, 144-151.

XV International Mineral Processing and Recycling Conference
17-19 May 2023, Belgrade, Serbia

DAM BREACH ANALYSIS USING HEC-RAS: A CASE STUDY OF COPPER AND GOLD "ČUKARU PEKI" MINE DAMS

Y. Yuankun, D. Mirović#
Serbia Zijin Mining d.o.o., Bor, Serbia

ABSTRACT – In order to predict the maximum discharge of the rupture (RMD), it is very important to evaluate the statistical data of the influence of the configuration of the dam breach on the most relevant parameters which are needed to be representative enough to get the conclusions. This study summarizes the main points in already finished project that carry out dam breach analysis for the pyrite depostits pond, flotation tailings pond and the accumulation for the collection of leachate, on a Čukaru Peki dams using a one-dimensional hydraulic model called Hydraulic Engineering Center's River Analysis System (HEC-RAS). This study should also serve to extricate the main factors for future conversion of variables in order for better prediction of the dam failures.

Keywords: Dams, Hydraulic, Rupture, Statistics, Flotation.

INTRODUCTION

Without the exiting of the dams constructions, it wouldn't have existed the way of safeguarding water supply, where the water demands since the oldest times are continuously increasing. Structure of the dams has been made to serve also for water supply, irrigation, agriculture, industry, power generation and the most important and purposeful, the flood control. Also the dam constructions have the opposite side, where it can harm the environment or violate human safety. "A dam failure is defined by ICOLD (International Commission for High Dams) 2015 as „Collapse or movement of part of a dam or its foundation, so that the dam can't retain water" [1].

The main purpose of the present study is to provide an example of one so far succesful framework of the the final probabilistic dam breach model which will be generated into Analysis System for serving in further data. The mainly considered informations are the dam's height, age and a reason of the failure. The enhanced reliability of predicted breach hydrographs is of major importance regarding the quality of risk quantification induced by dam failures [2].

EXPERIMENTAL

Documentation: ˝The Mining and Processing of the Upper Zone, Timok Cu-Au Project˝, ˝Feasibility Study˝, ˝Rakita Exploration d.o.o.˝, 2019. [3], is the basis of the ˝Čukaru Peki˝ copper and gold deposit dam breach project, in which the stability of the system of three dams, located in a row and practically on the upper part of the Grčava river, is examined. The most downstream dam is located about 1 km (as seen in the

corresponding author: dusica.mirovic@zijinmining.rs

airline) from the confluence of the Grčava river into the Bor river. The investigation of the stability of the system of three dams was also the basis of this study. Due to the high resistance to flow and the geometry itself, the Rgot gorge has a very significant effect on the spread of the flood wave caused by the collapse of dam 3 (the one that was formed from the collecting of leachate reservoir).

When calculating the hydraulic consequences of dam collapse, mathematical models of hydrodynamic calculations are used in the world, which are based on solving the complete or extended 1-D Barré de Saint-Venant (1871) equations that describe the unsteady flow of water in open streams. Hydrodynamic mathematical models that use the complete Saint-Venant equations differ in that they use implicit or explicit numerical schemes of finite increments (differences) when linearizing the equations. Also, hydrodynamic calculation models can differ according to the entered boundary and contour conditions in the model, the degree of preprocessing and postprocessing of the calculation results, and the degree of quick visualization of the obtained results.

The use of the HEC-RAS hydraulic calculation model in the present study is complemented by the use of a GIS application due to the great possibilities during preprocessing with the DEM (Digital Elevation Model) terrain model and displaying geospatial information, where is the ability to create various types of maps and visualize calculations is excellence. Therefore, the input data, when making hydrodynamic calculations of the best situation on the ground, would imply the possession of topographic maps and/or ortho-photo and satellite images of the terrain.

If one of the hydraulic models isn't able to process GIS data formats, there are special external modules for integration into the GIS environment. One of the additions to the HEC-RAS module that was used for the subject study was HEC - GeoRAS, for pre-processing and post-processing of input data.

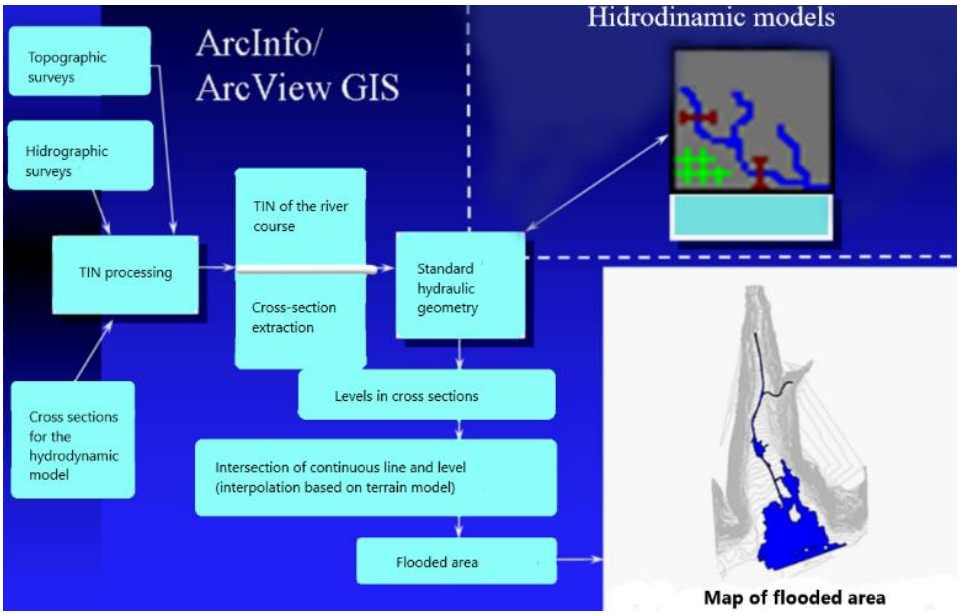

Figure 1 Methodology (Illustration of the workflow adopted in this paper) [4]

The methodology of applying the mentioned hydrodynamic mathematical models for performing the dam break analysis is shown in Fig. 1. Furthermore, the methodology presented above and displayed by the steps, was adopted as an optimal combination of hydraulic modeling, model simulation, and floodplain mapping, which were carried out for the purposes of the subject study.

Model HEC-RAS is globally applied throughout the world.

RESULTS AND DISCUSSION

The study reports the scenario due to the piping and overtopping failure modes, downstream from the most upstream dam to ensure accumulation for pyrite concentrate, which is more than 22 km, to the profile in the settlement of Vržogrnac, directly upstream from the confluence of the Bela Reka and Timok.

When the calculations begin, that is, when the demolition of the most upstream dam begins, the water level in the most downstream reservoir is 236.0 mnm. The water level in this reservoir for collecting leachate increases due to the activation of the safety spillway on the upstream dam of the flotation tailings pond, that is, due to the demolition of the most upstream dam, and then the demolition of the dam of the flotation tailings pond. When the level in the reservoir for collecting seepage water reaches the level of the crown of the dam of 238.0 mnm, the water overflows and the development of the breccia in the body of this dam begins.

The third variant of the calculation generates the most catastrophic consequences on the downstream river section, considering that it describes a situation in which the sequential collapse of three dams occurs, where the collapse of the most upstream dam initiates the collapse of the remaining two dams, so the whole phenomenon can be visualized as a domino effect.

Table 1 provides an overview of selected characteristic cross-sections in which the details of the calculations for Variants 3 will be presented, as well as in some segments Variants 2, in order to describe the wave characteristics for these two variants in more detail.

Table 1 The characteristic cross sections of the Variant 2. and Variant 3.

No	No of cross section	Name of cross section	Stationary [km]
1	77.6	Dam 1-pyrite concentrate deposit	0+000
2	67.5	Dam 2-flotation wasteland	1+213
3	58.5	Dam 3- reservoir for the collection of leachate	1+670
4	52	Before confluence in Bor river	2+554

According to the analysis of the numerical model calculation results, from the aspect of hydraulic consequences, when it comes to the area threatened by the demolition of the dams on the Grčava river, from the most upstream dam, along the entire Grčava river, to the mouth of the Borska river and along the Borska river, to the junction of the

Borska and Kriveljska rivers (up to cross-section 39.6), the system for informing and alerting the population relies on the relevance of the results of Variant 3 [5]. These results are authoritative for determining the maximum flow, the time of the appearance of the wave front and, consequently, the speed of the wave front, but also the time of the appearance of maximum levels and maximum flows along the downstream river section.

The results of this variant, which considers the movement of the mixture wave, created by the collapse of all three dams, are authoritative for the maximum levels that have appeared. For easier identification, the dams are numbered from 1 to 3, viewed in the downstream direction.

On the downstream river section, 2 more cross-sections were selected in the event of the demolition of 3 dams in a row, as provided for in Variant 3 of the calculation.

The first downstream cross-section is located before the confluence of the Grčava River with the Borska River and it is profile 52, which is located at station 2+554 km, viewed from the pyrite concentrate accumulation dam, for which station 0+000 km was adopted. The second downstream cross-section is located before the confluence of the Borska river and the Kriveljska river, and it is profile 39.6., which is located at the station 4+902 km, seen from the dam for accumulating pyrite concentrate, for which the station 0+000 km was adopted.

The time of the appearance of the wave front, the time of the appearance of the maximum level and the time of appearance of the maximum flow in the section downstream of the most downstream dam for accumulating leachate (Dam 3), from the moment of the demolition of the most downstream of the 3 dams on Grčava, for Variant 3, is shown in Figure 2.

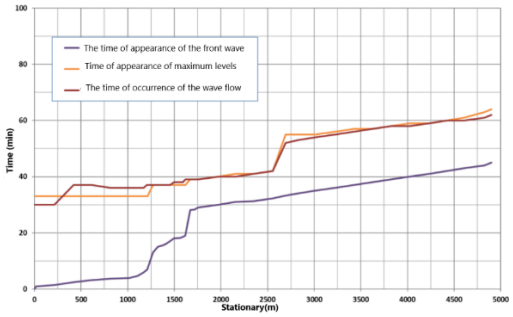

Figure 2 The time of appearance of the front wave, maximum levels and flow of waves – Variant 3

Dam 2 begins to collapse 26 minutes after the collapse of the most upstream dam 1, and dam 3 begins to collapse 28 minutes after the collapse of the most upstream dam 1, that is, from the beginning of the calculation.

The cumulative mean velocity of wave front propagation in the section downstream from the most downstream dam for accumulating leachate (Dam 3), from the moment of the collapse of the most downstream of the 3 dams on Grčava, for Variant 3 and Variant 2, is constant until Dam 2 begins to collapse 26 minutes, and Dam 3, 28 minutes after the demolition of the most upstream Dam 1, i.e. from the beginning of the calculation.

The maximum flow that occurs in the section of Dam 1 is 1395 m^3/s, in the section of Dam 2 it is 1768 m^3/s, as well as in the section of Dam 3 it is 1789 m^3/s, which means that the maximum flows are realized at the moment of completion of the development of the breccia in the body dam.

The section downstream from the junction of the Borska and Kriveljska rivers was treated as more critical from the point of view of possible hydraulic consequences in the previously prepared documentation [5], and up to this junction, viewed upstream along the Borska and Grčava rivers, the authoritative results presented in the subject documentation. The cumulative velocity of the wave front has a constant decreasing trend in the downstream direction. Thus, from the cross section immediately downstream of Dam 3, where the velocity exceeds 100 m/s, at the most downstream section, at a distance slightly greater than 1250 m, this velocity drops to about 4 m/s. The cumulative speed of the wave front for Variant 3 and Variant 2 of the calculation has relatively similar values, except in the cross-sections immediately downstream of Dam 3.

The maximum mean wave speed in cross-sections downstream of Dam 3 has a general trend of decreasing in the downstream direction, so that from 6 m/s, it in the downstream section amounts to slightly over 2 m/s, in the Variant 3 calculation. The maximum mean wave speed in the cross-sections for the Variant 3 calculation is about 4 m/s higher, than it is the case with the Variant 2 calculation, and the amplitude of the differences ranges from 0.7 m/s to only 0.02 m/s.

Table 2 shows the most important calculation results in the selected characteristic sections, which illustrate the characteristics of the wave created by the collapse of the dams for Variant 3 of the calculation.

Table 2 Calculation results in selected characteristic cross-sections

No	No of cross section	Cross section name	Stationary [km]	Max level (up/down) [mnm]	Time of occurrence of front wave [sec]	Time of occurrence of max level [sec]	Time of occurrence of max flow [sec]
1	77.6	Dam 1	0+000	19.00/291.21	0	0	1800
2	67.5	Dam 2	1+213	291.21/246.73	432	1980	2220
3	58.5	Dam 3	1+670	244.65/235.74	1680	2340	2340
4	52	Before confluence in Bor river	2+554	216.05	1938	2520	2520
5	39.6	Before joint with Krivelj river	4+902	196.26	2700	3840	3720

CONCLUSION

Regulation and flood control maintained with the constructions of the dams, are usually constructed in the river or stream basins to derive, retain or store the water runoff. Also, another type of dams are constructed in aim to retend the large amounts of different types of tailings. In case if this type of materials runs out, the inundated area and the maximum depth are very high in the overtopping failure scenario and pose a greater threat to the downstream region.

Real dam break risk analysis requires for reliable breach models capable to predict possible breach outflow hydrographs. The challenge to predict a worst case scenario, which still is regarded as a physically feasible event, is of particular interest for engineering applications. By contrast, seeking for more accurate breach models often loses sight of reliably predicting less probable events [6].

By reusing the same data from the previous project, the focus is on the proposed framework itself and adding the new one for the three dams in a row, there has been generated the next conclusions:

The worst case scenario will be if all three dams together were demolished on the Grčava River, as described in the analyzes for Variant 3 of the calculation;

The results for variant 3 of the calculation are authoritative for marking the flood area and creating a population information system in the section along the most upstream dam (dam 1), further to the confluence of the Grčava river with the Borska river and at the end, along the Bor river, to the junction with the Krivelj river. Although based on the results for variant 3, in the case of the demolition of all three dams in a row, which is described as the variant with the greatest consequences, only individual buildings and part of the Bor-Zaječar road, i.e. the section of the Slatina-Rgotina road, on the section from the Grčava confluence to the Bor river, will be found in the flooding zone to the junction of the Bor river with the Krivel river, which will undergo significant damage.

REFERENCES

1. ICOLD (1995-2001) Tailing dams and Waste lagoons – Committee, Bulletin 121.
2. Rico, M., Benito, G., Salgueiro, A.R., Diez-Herrero, Pereira, H.G. (2007) Reported tailing dam failures-A review of the European incidents in the worlwide context.
3. Rakita Exploration d.o.o. (2019) The Mining and Processing of the Upper Zone, Timok Cu-Au Project˝, ˝Feasibility Study˝.
4. US Army Corps of Engineers (2014) Using HEC-RAS for Dam-Break Studies.
5. Institut za rudarstvo i metalurgiju Bor (2017) Dopunski rudarski projekat, Proširenje flotacijskog jalovišta Veliki Krivelj na Nulto polje, Projekat proboja brana i poplavnog talasa, Elaborat o prolomu brana flotacijskog jalovišta "Veliki Krivelj" po proširenju jalovišta na ¨NULTO˝ polje, Knjiga I: Opšti deo sa hidrauličkim proračunima.
6. Peter, S.J., Siviglia, A., Nagel, J., Marelli, S., Boes, R.M., Vetsch, D., Sudret, B. (2018) Development of probabilistic dam breach model using Bayesian inference. Water Resources Research, 54 (7), 4376-4400.

XV International Mineral Processing and Recycling Conference
17-19 May 2023, Belgrade, Serbia

MANAGEMENT OF FLOTATION TAILINGS AS MINING WASTE ON THE COPPER AND GOLD MINE "CUKARU PEKI"

A. Milovanović Brkić#, Y. Yuankun, N. Buđelan
Serbia Zijin Mining DOO, Bor, Serbia

ABSTRACT – This paper presents the characterization of flotation tailings, the process of formation of flotation tailings in the process of preparing mineral raw materials. This paper also shows two methods according to waste management steps that are applicable for the management of flotation tailings on safe and effective way in the "Čukaru Peki" copper and gold mine.

Keywords: Flotation Tailings, Disposing, Characterization, Reuse.

INTRODUCTION

Mining activities produce larger quantities of waste and have more adverse environmental impacts than waste from any other human activity [1].

Mining wastes are defined herein as solid, liquid or gaseous by-products of mining, mineral processing, and metallurgical extraction. They are unwanted, have no current economic value and accumulate at mine sites. Mine wastes are commonly classified according to their physical and chemical properties and according to their source as solid mining, processing and metallurgical wastes and mine waters [2].

Mining wastes have been accumulating for thousands of years, and their rate of production has accelerated in step with increases of the human population to an estimated worldwide production rate of 350×10^9 t year^{-1} [3].

Mining waste is one of the largest waste streams in the EU. It can contain large quantities of dangerous substances. Mining and processing of copper ores cause degradation and pollution of land due to deposition of large mining wastes (overburden and flotation tailings) as well as Acid Mine Drainage (AMD) formation.

Mining waste management in the European Union is regulated with "Directive 2006/21/EC of the European Parliament and of the Council of 15 March 2006 on the management of waste from extractive industries and amending Directive 2004/35/EC" and its accompanying documents [5].

Directive 2006/21/EC on the management of waste from extractive industries aims to prevent or reduce as far as possible any adverse effects on the environment, in particular on water, air, soil, fauna and flora and the landscape, and any resultant risks to human health, brought about as a result of the management of waste from the extractive industries. The Directive covers the management of waste resulting directly from prospecting, extraction, treatment and storage of mineral resources and from quarrying.

corresponding author: ana.brkicmilovanovic@zijinmining.rs

Serbia is a country with a rich tradition in every area, including mining. Centuries of mining in our country have generated waste which we define as mining waste and which has mostly been disposed at ore mining locations. The management of mining waste in the Republic of Serbia is related to the "Law on Mining and Geological Exploration" ("Official Gazette of the RS", No. 101 of December 8, 2015, 95 of December 8, 2018 - other laws and 40/2021).

The "Law on Mining and Geological Explorations" in the section "Management of mining waste" defines what is not mining waste (Article 145).

The development of the mining waste management plan is related to the "Decree on the conditions and procedure for issuing a permit for waste management, as well as criteria, characterization, classification and reporting on mining waste". The Regulation was published in the Official Gazette of the RS No. 53/2017, and entered into force on January 1, 2020, and its adoption is related to Article 144, paragraph 2, of the aforementioned Law.

The aforementioned Regulation is harmonized with the European "Directive 2006/21/EC of the European Parliament and of the Council of 15 March 2006 on the management of waste from extractive industries and amending Directive 2004/35/EC" and its accompanying documents.

This paper focuses on the management of the solid waste produced at modern "Čukaru Peki" mine in Serbia.

STUDY SITE

The Bor mining area is one of the important copper-producing areas in Serbia. Copper mines are mostly responsible for mining waste forming. The Čukaru Peki" copper mine, as the part of the Zijin Mining Group, is located in Eastern Serbia, near city of Bor.

During the technological process of ore mining and flotation concentration of useful minerals at the "Čukaru Peki" mine, several types of mining waste are generated that differ in their physical, chemical, mineralogical and toxicological characteristics.

In the process of preparing mineral raw materials in the "Čukaru Peki" mine, during the ore flotation process, after extracting useful minerals, flotation tailings are formed.

This waste is generated as barrens with a low, residual, concentration of useful minerals. It is extracted in the form of pulp with a low concentration. This mining waste has two ways of disposal, namely transport to a tailings dump, or use for backfills.

ORIGIN AND CHARACTERISTICS OF FLOTATION TAILINGS AS MINING WASTE:

The process of formation of flotation tailings

Flotation tailings represent waste that is created in the process of flotation concentration of useful copper sulphide minerals and accompanying useful products such as pyrite, gold and silver. Flotation is preceded by a comminution process (crushing and grinding) in order to free useful minerals from their natural connection with useless ones.

The flotation process at the "Čukaru Peki" mine takes place in two stages. Start with "fast" flotation. Fast flotation of copper minerals produces copper concentrate 1. The

tailing of fast copper flotation goes to rough copper mineral flotation in two stages and scawenger flotation in two stages. The rough concentrate go to copper cleaners and give us copper concentrate 2. The flotation process continues by flotation of pyrite from the tailings from the copper flotation cycle. The rough pyrite concentrate is send to cleaning process, and the tailings of the basic concentrate goes to pyrite scawenger flotation, at the end of which we get the final tailings. With this process, in addition to copper concentrate, depyritized (desulfurized) tailings with favorable characteristics are also obtained.

Tailings preparation after flotation continues with flocculation and thickening in a radial thickener. Two products are obtained here: relatively clear water is obtained as an overflow, which is returned to the process, and as sand, a thickened tailings that is transported.

Characteristics of flotation tailings

Physical and mechanical characteristics

From the results of the granulometric composition, determined by laser in the laboratory grain size is:

90% below 224.357 μm

50% below 40.436 μm

10% below 5.790 μm. [6]

For copper mines, this is a very fine opening, which indicates that it is not realistic to expect that a size class suitable for the construction of peripheral dykes can be extracted from this material. At the same time, this size justifies the Investor's decision to thicken this tailings in a radial thickener using flocculants before depositing.

Chemical and mineralogical composition of flotation tailings

According to its chemical and mineralogical composition, the tailings represent a typical silicate tailings with the predominant participation of silicon and significant participation of aluminum and iron. Quartz like silicon carrier is a very stable and desirable element in flotation tailings, while aluminum is mostly bound to clay minerals (kaolinite, alunite), and iron is preferentially bound for residual pyrite. [7]

Involvement of hazardous components

Table 1 shows the share of hazardous components in flotation tailings. The obtained results show that the participation of highly toxic, toxic and dangerous elements is far below the limit values, and according to the content of dangerous components, flotation tailings are characterized as non-hazardous mining waste.

Table 1 Hazardous components in flotation tailings [6]

Element	The content in total	The limit values
Hg, Total very toxic	<0.00001	1%
As,Ni,Cd,Total toxic	0.00677	3%
Cu,V,Mo,Pb,Cr,Yn,Co,Hazardous	0.14211	25%

Leaching tests

The leaching tests of flotation tailings were done in two ways. The first results were obtained by tests in accordance with the Serbian standard SRPS.EN 12457-2:2008, which was developed on the basis of European standards, and the second on the basis of the TCLP procedure of the American agency EPA.

Table 2 Results of leaching test of flotation tailings [6]

	Unit of measure	Test results	Value for non-hazardous waste
El. conductivity	µS/cm	975	
pH		9.02	6-13
Sb	mg/kg dm	0.12	0.7
As	mg/kg dm	<0.20	2
Ba	mg/kg dm	0.59	100
Cu	mg/kg dm	0.19	50
Cd	mg/kg dm	<0.04	1
Mo	mg/kg dm	0.17	10
Ni	mg/kg dm	<0.07	10
Pb	mg/kg dm	<0.20	10
Se	mg/kg dm	<0.04	0.5
Cr	mg/kg dm	<0.05	10
Zn	mg/kg dm	<0.04	50
Hg	mg/kg dm	<0.005	0.2
Cl^-	mg/kg dm	1207.7	15,000
F^-	mg/kg dm	1.0	150
SO_4^{2-}	mg/kg dm	4,750.0	20,000

Table 3 Results of leaching test of flotation tailings and cement mix [8]

	Unit of measure	Test results (64 days of the test)	Value for non-hazardous waste
El. conductivity	µS/cm	78-320	
pH(25C)		7.94-11.42	<6
Sb	mg/kg dm	<0.3	0.3
As	mg/kg dm	0.72	1.3
Ba	mg/kg dm	3.36	45
Cu	mg/kg dm	0.27	45
Cd	mg/kg dm	<0.2	0.2
Mo	mg/kg dm	0.27	7
Ni	mg/kg dm	0.25	6
Pb	mg/kg dm	0.72	6
Se	mg/kg dm	<0.4	0.4
Cr	mg/kg dm	0.18	5
Zn	mg/kg dm	0.18	30
Hg	mg/kg dm	0.02	0.1
Cl^-	mg/kg dm	255.68	10,000
F^-	mg/kg dm	6.73	60
SO_4^{2-}	mg/kg dm	241.94	10,000

It can be stated that all the tests performed show that the level of leaching from the flotation tailings is below the reference values of the standards according to which the tests were performed. All this indicates that tailings can be classified as non-hazardous waste. Table 2 shows the results of leaching tests according to the standard SRPS.EN 12457-2:2008.

Leaching tests of the mixture of flotation tailings and cement in the ratios 6:1, 10:1 and 25:1 were performed in accordance with the NEN 7345 standard for monolithic waste. Table 3 shows the results of a 10:1 mix as an example.

Neutralization and acid potential of flotation tailings

The results of determining the acid and neutralization potential of the flotation tailings of the "Čukaru Peki" mine, using the static test EN 15875, which is adjusted for sulfides, are shown in Table 4.

The results of testing the acid and neutralization potential of flotation tailings show that there are natural conditions for the formation of acidic drainage water (ARD), which can be seen from the ratio of neutralization and acid potential (acidic is three times higher), but this should be additionally monitored and investigated because it is neutralization potential close to zero, which indicates that there are theoretical conditions for the formation of acidic drainage waters, but that this is not certain given the different rate of dissolution of the accompanying rocks and the possibility of practical action to prevent acidification.

Table 4 Results of determining the acid and neutralization potential [6]

Parameter	Unit	Test results	The limit values
Acid potential (AP)	H^+ mol/kg	8.33	
Neutralization Potential (NP)	H^+ mol/kg	0.16	
Ratio (coefficient) of neutralization potential (NPR)	H^+ mol/kg	0.02	<1, there are conditions for ARD
Net Neutralization Potential (NNP)	H^+ mol/kg	-8.17	
Acid potential (AP)	($CaCO_3$) kg/t	416.25	
Neutralization Potential (NP)	($CaCO_3$) kg/t	1.67	
Net Neutralization Potential (NNP)	($CaCO_3$) kg/t	7.75	-20-+20, should be further examined

*Note: ARD – acid rock drainage.

Waste classification and index number

Index number of flotation tailings according to the Waste Catalog 01 04 99: 01 – Mining, 04 - Waste from physical and chemical processing of minerals for the non-ferrous industry, 99 - Waste not otherwise specified.

According to all its characteristics, flotation tailings can be classified as non-hazardous mining waste, except for its neutralizing acid potential, according to this characteristic, there are theoretical conditions for the formation of acidic drainage waters, which should be further investigated.

Based on the examination of monolithic waste from mix of flotation tailings and

cement, all three ratios showed that the character of the waste is non-hazardous. The index number of the waste according to the catalog is 19 03 07- solidified waste. As such, this waste can be used as a construction material in the environment.

MANAGEMENT OF FLOTATION TAILINGS AS MINING WASTE

Based on the steps in the waste management hierarchy at the "Čukaru Peki" mine, we have two management methods for flotation tailing that are applicable for this type of waste.One is reuse of flotation tailing,and other is material disposal.

Reuse of flotation tailing

The flotation tailings are reused as a component in the pit backfill. It is planned to use about 63% of the generated tailings, and the annual amounts change depending on the capacity of the Mine.

The backfill used to fill the excavation spaces in the pit is formed by mixing flotation tailings and Portland cement. The consistency of the mixture should ensure the pumpability of the mixture to the filling site and rapid solidification. The expected concentration of the solid phase at the exit from the radial thickener is 55%, and at the exit from deep cone 72% by mass. In order to speed up this process, a flocculant is added to the paste thickener. The tailings that we separate after the flotation cycle are first thickened in the radial thickener, and then transported by pumps to the deep cone thickener. The thickened product from the thickener pastes can be transported by pipelines by gravity directly into the receiving silos in front of the paste mixer, and there is also the possibility of transport to the tailings silo. Transport of the thickened tailings to the silo is carried out by centrifugal sludge pumps, and the overflow of the thickeners goes by gravity to the return water basin.

From the silos for tailings, the material is transported by gravity into the receiving troughs, in which water is added to regulate the solid phase. From the receiving troughs, the material goes to the mixers by gravity. Portland cement is transported to cement silos by trucks. Each of the cement silos is equipped with a hydraulic silo under which a feeder with rotating rollers and a scale is located. Beneath the scales are spiral feeders with which the cement is dosed into the mixer.

The mixing system consists of two horizontal mixers, one with paddles and the other with a spiral, for better mixing and a more homogeneous texture. After the preparation of the paste, the backfill is transported by gravity into the receiving slopes of the wells, from where it is further transported through the well pipelines to the pit rooms [7].

Depositing tailings at the flotation tailings dump

When the needs of pit fillings are met, the remaining part of the tailings is sent to the tailings dump. The location of the tailings is located in the Bor river basin, where the flow and quality of the water have been greatly affected by the surrounding historical mining activities. The chosen location of tailings enables the concentration of pollution sources, which facilitates management with a minimal negative impact on the environment.

The flotation tailings has a two-layer geosynthetic barrier in order to protect the soil

and groundwater. The waterproof barrier also has the role of protecting the slopes on which the tailings rely from the aspect of stability because it protects them from the influence of leachate and prevents erosion and instability.

The flotation tailings dam is natural and has a stepped shape. It can meet tailings storage requirements for the 13-year life of the flotation plant. The total height of the dam is 59 m, the total volume of tailings is 9,672x106 m^3. On the downstream slope of the dam, there is an embankment made of rolled stone whose width in the crown is 4m. On the upstream slope of the stone embankment, a geotextile of 400 g/m^2 and a filter layer of sand and gravel is placed.

The upstream side of the dam is lined with a layer of clay 0.3 m thick, a non-woven geotextile 400 g/m^2 is placed on the clay, and a textured HDPE geomembrane 2 mm thick goes over the geotextile. As already mentioned, the results of the acid and neutralization potential of the flotation tailings show that there are natural conditions for the formation of acidic drainage water ARD, this coating prevents pollution by acidic drainage waters, because in case of leakage from the tailings, they are collected in the reservoir for the collection of leachate located downstream from flotation tailings. The bottom of the tailings pit is on level ground, which is also protected by a geotechnical layer and an HDPE geomembrane. The drainage system is located at the bottom of the flotation tailings and consists of HDPE drainage pipes DN200 mm, DN300 mm, DN400 mm. They are placed in the filter layer and wrapped with geotextile. After passing through the dam, the DN400 mm drainage pipe flows into a concrete channel with a trapezoidal cross-section, which conducts the water to the drainage water reservoir [7].

CONCLUSION

The generation of flotation tailings cannot be avoided because the share of the useful component is very subordinate in relation to the total ore.

About 63% of the flotation tailings are planned for pit filling, and the remaining 37% are sent to the tailings. It is very important to note the characteristic of the flotation tailings through the examination of the acidic potential, according to which it is a dangerous waste. The design of the flotation tailings completely eliminated the possibility of acidic drainage water entering the environment.

REFERENCES

1. Blight, G. (2011) Mine waste: A brief overview of origins, quantities, and methods of storage. In: Waste, Academic Press, 77-88.
2. Lottermoser, B.G., (2010) Mine Wastes - Characterization, Treatment and Environmental Impacts, Third Edition, Springer Heidelberg Dordrecht London New York.
3. Vallero, D.A., Blight, G. (2019) Mine Waste: A brief overview of origins, quantities, and methods of storage. In: Waste, Academic Press, 129-151.
4. https://environment.ec.europa.eu/topics/waste-and-recycling/mining-waste_en.
5. EC Directive, (2006) Directive 2006/21/EC of the European Parliament and of the Council on the management of waste from the extractive industries, European

Commission Environment (ECE). Official Journal of the European Communities, L 102/15, 11.4.2006, Brussels.
6. Institute of Mining and Metallurgy Bor (2022) No.3222/22, Report on examination of flotation tailings.
7. Serbia Zijin Mining DOO Bor (2022) Updated mining waste management plan.
8. Institute of Mining and Metallurgy Bor (2019) No.32296/19, Test reports of monolithic waste from flotation tailings and cement.

XV International Mineral Processing and Recycling Conference
17-19 May 2023, Belgrade, Serbia

GEO-STABLE DISPOSAL OF COAL COMBUSTION BYPRODUCTS

N. Pavlovic[#], F. Palkovits, A. Hall
Responsible Mining Solution, Suite 460-688 W. Hastings Street, Vancouver, BC V6B 1P1, Canada

ABSTRACT – Coal combustion produces two byproducts known as fly ash and bottom ash. Both products are deposited in tailings storage facilities (TSF) in dry and wet forms (slurry consistency). The fly ash at slurry consistency is usually mixed with bentonite to minimize the water seepage to the TSF foundations. Dewatering and geotechnical tests were carried out to find the suitable dewatering process and to identify geotechnical parameters for fly ash disposal on the TSF. Dewatering the fly ash to a paste consistency ($C_w \approx 68\%$) reduces the water seepage and the TSF footprint area and improves both TSF stability and water management.

Keywords: Paste, Dewatering, Fly Ash, Bottom Ash.

INTRODUCTION

Coal Combustion Byproducts (CCBs) are commonly known as fly ash (FA) and bottom ash (BA) and are produced by utility boilers as coarse and fine granulated unburned residues [2]. These products might or might not have pozzolanic properties depending on the properties of the coal. Due to their properties and process management, CCBs have been drawn public and regulatory concerns [1]. Also, tailings storage facility (TSF) permitting can be very costly and was identified as an additional concern due to the boundaries that are often in close proximity to local utilities and agricultural fields. Additional matters raised by authorities are radioactivity, detrimental chemical elements (mercury), long-term legal liabilities due to potential dam failures, water demand, ground and underground water impact, etc. [2].

CCBs are usually managed in dry or wet form. The dry form relies on haul trucks for transportation from the coal plants to the TSF. This approach causes dust issues, which requires additional suppression systems. Likewise, the wet form utilizes hydro transport of diluted slurry and discharge on the TSF where the particles settle to various degrees. The wet form demands water, which could be an issue especially in arid parts of the world [2].

Paste technologies were identified as a potential solution where CCBs could be converted into the paste range for disposal. The paste consistency at low (250 mm/10" slump) and high density (175 mm/7" slump) is the typical range for non-segregating and slumpable material that contains a small (interstitial) water quantity, which does not bleed upon disposal. Slump is normally measured using an ASTM 30.5 cm (12 inch) slump cone, a standard tool used in the concrete industry [2]. From the particle size distribution

[#] corresponding author: npavlovic@rmscorp.ca

(PSD) perspective, materials that can produce paste typically have a minimum of 15% passing the 20 µm threshold [2]. The fines fraction in soil mechanics is defined as the portion of the soil passing 74 µm. As such, paste requires to be pumped by positive displacement piston pumps for the paste to be conveyed in the plug flow regime with the interstitial water and the 20 µm fines acting as the major lubricant. The paste consistency with the water sensitivity test and typical pipe discharge are presented in Figure 1 and 2, respectively.

Figure 1 High (175mm/7") and Low (250mm/10") Density Paste Consistency

Figure 2 Typical Pipe Discharge of The Paste Tailings

Conventional FA slurry disposal relies on bentonite addition to minimize the water infiltration or seepage to the TSF foundation. This paper outlines an alternative solution for FA disposal avoiding bentonite addition, reducing the size of the TSF footprint area and improving TSF stability.

EXPERIMENTAL

In the industry, fly ash is typically neutralized by adding lime to remove SO_2, which produces neutralized FA (NFA) dominated by gypsum ($Ca_3OH_{4.5}H_20$) with a minor calcium hydrate component ($Ca_2OH_3.H_2O$). The final ash stream with lime produces diluted NFA slurry at a concentration by weight (C_w) of about 10%. The diluted NFA stream as such is transported by pipeline to the TSF [2]. The laboratory testing and investigation of the NFA sample included PSD, mineralogical and chemical composition, rheological characterization including water sensitivity test (slump vs. C_w) and water retention

(bleed) test. PSD and mineralogy of the material drive the materials ability to exhibit paste transport characteristics. Dewatering (solid-liquid separation) testing included: thickening (flocculant type and dosage, feed density dynamic test) and centrifuge. These tests aimed at identifying the preferred densification process for the NFA slurry. Static and dynamic thickening testing configurations are presented in Figure 3.

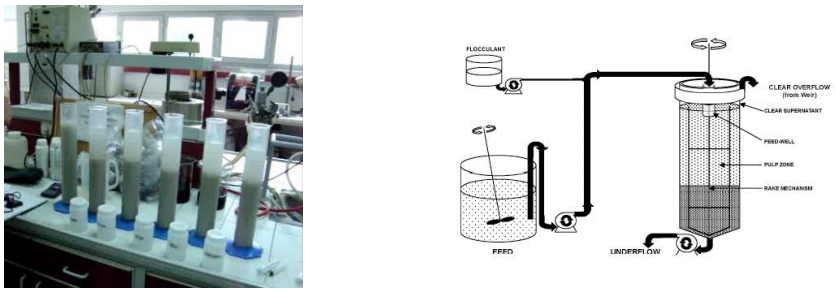

Figure 3 Static and Dynamic Thickening Test

Beyond dewatering testing, a geotechnical testing campaign was also executed on both the NFA and BA samples. Geotechnical testing for BA included classification testing (PSD and specific gravity), permeability, compaction, and triaxial compression testing. The testing program for NFA included classification testing (PSD, Atterberg limits and specific gravity), column settling (drained and undrained), slurry consolidation permeability testing, and triaxial compression testing. Rheological testing was not executed on BA samples.

RESULTS AND DISCUSSION

The PSD graph is displayed in Figure 4. Specific gravities (SG) of 2.58 and 2.62 were determined for BA sample and NFA samples, respectively. The BA sample appears to be coarser than NFA due to the process conditions. Pozzolanic properties were not observed in either sample.

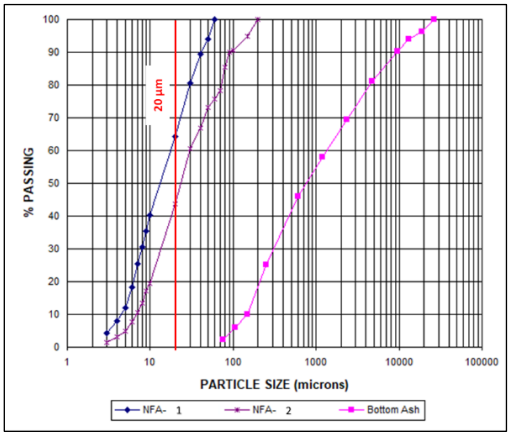

Figure 4 PSDs

The water sensitivity and water retention (bleed) tests are illustrated in Figure 5 and 6, respectively.

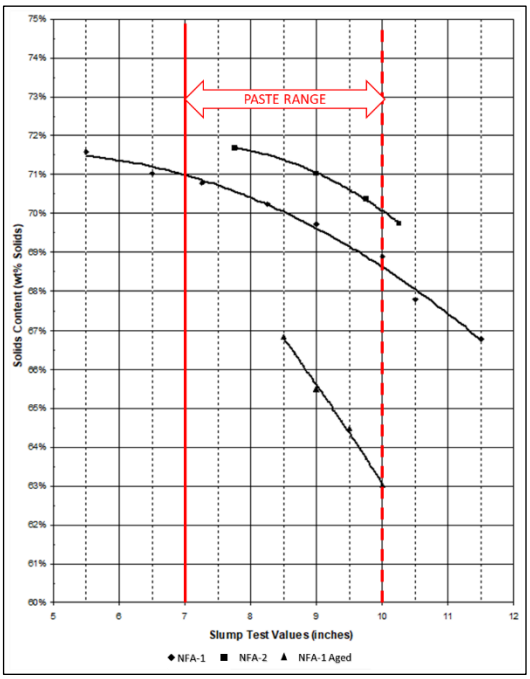

Figure 5 Water Sensitivity / Slump Test

The high and low paste densities report to C_w of 71% (72% upper limit) and C_w of 69% (67% lower limit), respectively. The NFA samples showed good paste qualities due to high content of sub 20 µm particles, which makes it very transportable through the pipeline. It was observed that the FA sample at slurry consistency agglomerated, showing lumping after an aging process of several months. The NFA slurry and paste samples are presented in Figure 7.

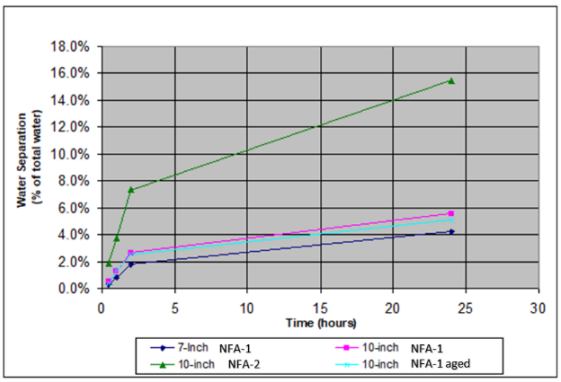

Figure 6 Water Retention (Bleed) Test

NFA Slurry at C_w = 9% NFA Paste at C_w = 68%

Figure 7 FA - Low Density Paste (10”/250mm slump)

The NFA paste sample showed strong water retention, which indicates non-segregating properties. This means NFA paste can be left to idle in the pipeline for several hours. Thickening testing results are tabulated in Table 1. Available thickener types are illustrated in Figure 8.

Table 1 Dewatering Testing Results and Estimates

Description	Density – C_w (%)	Source
Slurry (Unthickened)	10%	Plant discharge
*HRT	50% - 55%	Testing
*HCT	-	Not Considered
*PT	62% - 65%	Testing / Estimate
*PPSM	67% - 69%	Testing
Centrifuge	70%	Testing
Vacuum Filtration	73% - 74%	Estimate

*HRT – High Rate Thickener, *PT – Paste Thickener, HCT – High Compression Thickener
*PPSM – Paste Production Storage Mechanism (thickener).

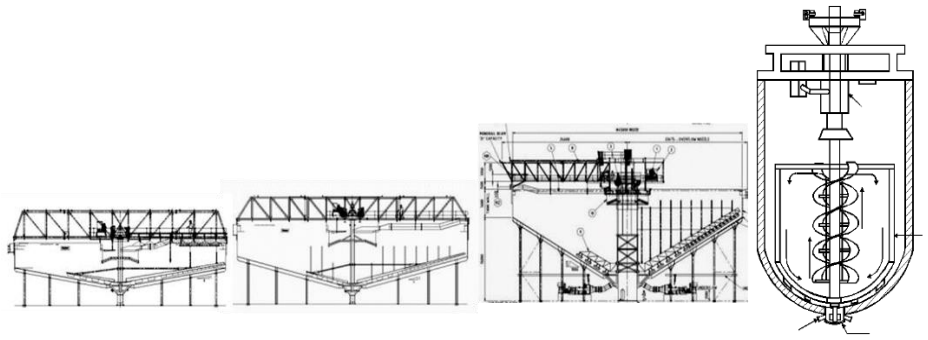

HRT HCT PT PPSM

Figure 8 Thickener Types

The thickening test showed that the NFA sample can be efficiently thickened by PPSM which outperformed the other thickeners. Due to its geometry and rake (spiral) mechanism, the PPSM would be able to densify the NFA up to low density (10”/250mm

slump) paste that would be transported by piston pumps. It appears that the NFA paste would be prepared without filters and mixer application.

Geotechnical testing results indicated that unamended NFA sample behaves as non-plastic silt with trace of fine to medium sand size. The results of the column settling tests indicate that the unamended NFA settles relatively quickly and achieves settled dry densities up to 1.12 t/m^3. The initial test simulated deposition as paste with slightly lower density than the paste plant design target at C_w of 68% for a 10" (250 mm) slump.

The initial dry density target was 1.11 t/m^3 representing a material deposited at C_w of 66%. The test results show rapid compression under increasing loading, approaching a relatively constant ultimate dry density of 1.3 t/m^3.

CONCLUSION

The PSD and rheological testing showed that paste can be produced quickly from the NFA slurry. The NFA is non-plastic silt that is able to settle and consolidate quickly after deposition. In the paste form the NFA would compress very quickly in response to loading from deposition at a dry density of 1.12 t/m^3 (C_w of 68% solids) up to final dry density of 1.3 t/m^3. Bentonite addition, in the powder form, to the NFA sample was initially considered to reduce the permeability and seepage of the NFA. However, bentonite modifies NFA from non-plastic to high plastic silt or high plastic clay. To maintain the transport of bentonite modified NFA, the water should be added which, in turn, reduces the C_w of 68% to 53% and lower, dictated by the pumping distances.

The application of dewatering by PPSM eliminates bentonite modified NFA and allows unamended NFA to be deposited on the TSF with significant water savings. The unamended NFA paste aims to reduce the entrained water, increase ash storage density, simplify operations, and improve economics. The substantial reductions in seepage water losses can be accomplished by converting dilute slurry to paste deposition. This approach reduces water inflows to the TSF and removes the need to manage large quantities of free water. Also, it reduces the risk for water losses to the TSF foundation.

TSF dam raises and increasing TSF footprint were identified as a main drawback for bentonite modified NFA option. Likewise, the paste NFA with PPSM application reduces the dam raises and the overall TSF footprint, which were identified as great benefits.

REFERENCES

1. Palkovits, F. (2007) Paste Technology Offers Coal Combustion Byproducts Solutions. World Coal. Pittsburgh, USA, Proceedings, 21-25.
2. Palkovits, F., Criswell, G., Johnson, J. (2004) Paste Fly Ash Management to Reduce Impoundment Seepage and Improve Storage Efficiency. Denver, USA, SME Annual Meeting, 04-103.

XV International Mineral Processing and Recycling Conference
17-19 May 2023, Belgrade, Serbia

TAIL WAGGING THE DOG-WHY INTEGRATED SOLUTIONS ARE BETTER-TAILINGS AND BACKFILL DISPOSAL

N. Pavlovic[#], F. Palkovits, A. Hall
Responsible Mining Solution, Suite 460-688 W. Hastings Street, Vancouver, BC V6B 1P1, Canada

ABSTRACT – Historically, conventional tailings management had not considered integrating management approaches. There has been a significant number of tailings dams failures over the past two decades. Also, mining companies developed their own strategies to mitigate environmental and social issues. The proper selection procedure of dewatering technology, TSF design, tailings transport and mine backfill type should be established at the project onset. The procedure as such provides a good foundation for feasibility design and concurrently mitigates social and environmental impacts and improves company's reputations.

Keywords: Tailings, Integration, Management, Backfill, Paste.

INTRODUCTION

World demand for metals has been increasing over the past two decades. Likewise, development of mineral properties has never been more difficult. Resistance to resource development occurs within communities globally based on environmental, social and cultural aspects in additional to project specific legacy issues [1].

There have been over 60 incidents related to the failures of the tailings storage facility (TSF) dams. The number of incidents increases to over 70 when including heap leaching, pipeline leaks and ruptures and environmental containment breaches. The most significant failures such as Mount Polly (2014, Canada), Samarco (2015, Brazil), Brumadinho (2020, Brazil) and Baia Mare (1999, Romania) received global coverage. These global incidents attracted non-government organizations, government regulatory bodies etc. [3]

Due to catastrophic events and the environmental consequences, in some countries, the permitting process became very critical. Concurrently, for mining companies, the permitting process became as important as the technical and economical aspects. To avoid catastrophic incidents, the permitting process includes the best available technologies (BAT) and best available practices (BAP), process design and testing programs that support process design and overall concept.

Large multi-national mining companies, such as Vale, Barrick, Rio Tinto, Newmont and BHP are very sensitive to reputational risk and are seeking ways to implement integrated waste management strategies. Many of these companies have internally developed global environmental and social standards and they are actively developing new technologies to reduce environmental and social impacts [1].

[#] corresponding author: npavlovic@rmscorp.ca

The main objectives of integrated waste management strategies are to:

- Minimize and consolidate the surface footprint of the tailings storage facility (TSF);
- Reduce acid rock drainage and metals leaching (ARD/ML) impact;
- Improve long term stability of the TSF and dams;
- Minimize impact on ground and underground water;
- Minimize operating cost (OPEX) that can be more important than capital cost (CAPEX);
- Improve mine productivity with quality engineered backfill; and
- Providing long term economic and amenity benefit to local communities;

The following aspects characterize the Base Case (conventional tailings disposal):

- The TSF increases in height with conventional slurry disposal;
- Mine rock handling remains as today where some is deposited into exhausted Pits; trucked to surface; or placed underground; and
- The mine backfill consists of hydraulic fill (CHF) with some waste rock.

This study outlines an integrated tailings management strategy that utilizes a common dewatering process for surface disposal and underground backfill. An integrated system will be compared with the Base Case that is a conventional tailings management practice.

EXPERIMENTAL

In order to support the process design i.e., process flow diagrams (PFDs), technical solutions, concepts etc., a proper material testing campaign should be executed at the onset of the project. It should be noted that the concept designs and PFDs are the core of the engineering process; however, the material testing campaign is a convincing approach for supporting the overall project concept. It should be noted that the process design is tailored to concurrently meet the surface disposal criteria and backfill strength requirements. In accordance with the integrated tailings management approach, the testing campaign for the process, surface disposal (geotechnical) and backfill strength should be carried out in parallel.

A typical testing campaign that is required for process design includes material characterization, rheology (water sensitivity, static and dynamic viscosity), thickening (flocculant type and dosage, feed density, static and dynamic tests), vacuum filtration (disc and belt) and pressure filtration. Also, for long distance transport and underground distribution system design, flow loop testing can be conducted to determine friction losses and flow resistance. Concurrently, the results are used for equipment sizing and for creating operating envelops enabling the equipment to meet the process upset conditions. Some testing apparatus are presented in Figure 1.

Surface disposal testing is determined based on the nature of the material and consists of Atterberg tests, Proctor tests, hazard tests, acid base accounting etc. These tests aim to establish the plastic limits of the material, ultimate dry density for the given TSF volume, acid rock drainage and metal leaching (if material contains high sulphide i.e., pyrite, pyrrhotite etc.). These tests aim to establish the TSF design

parameters for the certain terrain topography, social and environmental conditions etc. There are several types of underground backfill: crushed rock fill (CRF); hydraulic backfill (HF) and paste fill (PF). Also, the co-disposal of waste rock and paste fill is another one type of backfill.

(1) (2) (3) (4)

Figure 1 12" (300mm) ASTM Cone (1), Brookfield Device (2); Thickening Test (3) and Backfill Strength Testing Machine Apparatus

Testing for backfill strength, also known as unconfined strength (UCS) is determined by breaking cylinders with a frame press as presented in Figure 1 (4). Prior to that, the cylinders are prepared with high density paste (175 mm slump) and low density paste (250 mm slump) that are mixed with a certain binder content and left to reside in the curing chamber that simulates underground conditions.

Prior to cylinder preparation with paste backfill, the underground backfill strength requirement is determined by rock mechanics engineering based on the underground and rock conditions, stope sizes, mining methods etc. Regarding the backfill strength, the curing days (cylinders breaking period) are determined to meet underground mining plan. Also, different binder types and mixtures i.e., cement, ground granulated blast furnace slag (GGBFS), fly ash etc. are tested to determine the best binder from environmental and economic perspectives.

RESULTS AND DISCUSSION

The process testing results gained through the process testing campaign are used for sizing the equipment and tailoring the PFD to meet both surface disposal and mine backfill requirements. There are different parameters that are considered such as: life of mine (LOM) plan, geology, hydrology, terrain topography, TSF configuration, underground mine design, mining methods etc. The dewatering plant or paste plant location is primarily selected to satisfy the paste backfill to underground stopes with minimum energy where gravity delivery is preferred; however, paste pumps can be utilized when required. Depending on the TSF location the common dewatering plant location for surface disposal and mine backfill affect the tailings transport which is dictated by the preferred disposal method i.e., thickened tailings, paste, filter cake etc. An example of an integrated tailings management PFD is displayed in Figure 2.

Usually, the paste backfill plant with an integrated tailings management system operates on an "either/or" scenario. When backfill is required (line 1) the paste plant would produce cemented paste backfill. The paste would be produced by mixing the filter cake, thickened tailings and binder and delivered underground either by gravity or via

paste pumps. When paste backfill is not required, the same plant could be used for producing filter cake (line 2) that is transported to the TSF followed by dozing and compacting (dry stacking). Filter cake conveying by grasshopper arrangement (Figure 3) is also possible and is dictated by the terrain topography, paste plant location etc.

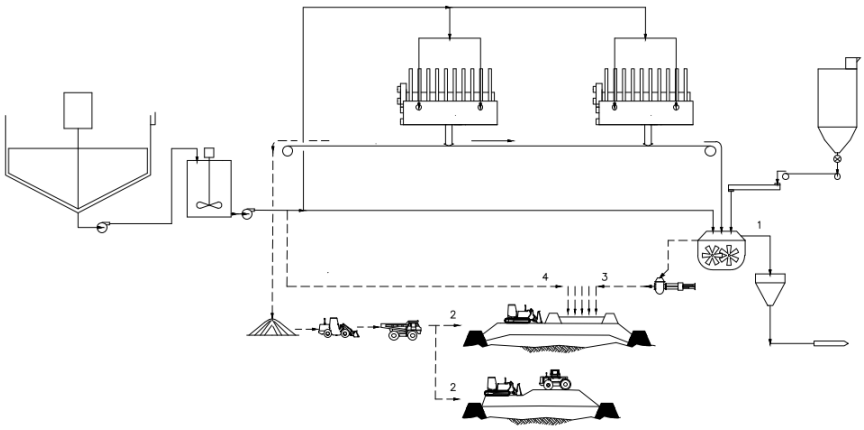

Figure 2 Simplified Integrated Tailings Management Process Flow Diagram

Figure 3 Grasshopper Conveyors Arrangement

Surface paste disposal (line 3) alone is also possible without binder addition where the paste pumps are used for paste delivery to the TSF. The paste deposition is performed in thin layers to concurrently allow dissipation of the flow and quick tailings desiccation. This method allows the paste layer to dry and gain strength. One successful example of this approach is MATSA mine in Southern Spain (Figure 4) [2]. This method reduces oxygen ingress to the tailings which mitigates ARD/ML.

Figure 4 Subaerial Paste Deposition for High Sulphide Tailings

A co-disposal of the filter cake and paste (lines 2 and 3) though a paddock system can be accomplished by filter cake deposition to create cell embankments allowing the paste to be deposited within the cell perimeter. Additionally, co-disposal of the filter cake and thickened tailings (lines 2 and 4) is also possible. In this case the thickened tailings would be deposited within the cell perimeter. In both co-disposal cases, any water or run-off would drain through the embankments enabling the paste or thickened tailings to dry and gain the strength. Thin layer disposal of paste is illustrated in Figure 5.

Lastly, thickened tailings disposal alone (line 4) without a paddock arrangement is another possible solution for an integrated tailings management system, when underground backfill is not required. The thickened tailings could also be deposited in thin layers allowing dissociation and drying. It should be noted that the "either/or" scenario is valid only when the full tailings capacity discharged from the concentrator is used to meet underground backfill throughput. Beyond the paste densities and underground requirements, one of the drivers could be hydraulic transport of the paste backfill which is driven by the underground distribution (piping) system (UDS). The UDS is sized to accommodate and convey the paste backfill at a nominal velocity range from 1 m/s to 1.5 m/s. Mine requirements, paste densities and size of the UDS drive "either/or" operating scenario for the common dewatering plant serving both surface disposal and mine backfill.

Figure 5 Paste Deposition in Thin Layers for High Sulphide Tailings (MATSA mine)

Likewise, there are the mining operations that operate with higher ore throughputs and produce greater amounts of tailings, for instance with both open pit and underground mines feed a single mill. In this case, the tailings synergies are determined to primarily meet underground backfill requirements allowing the rest of the tailings to report to the TSF, including while backfilling. In this case, the paste or dewatering plant would not operate under "either/or" scenario; however, the paste plant would operate when backfill is required, otherwise the overall dewatering plant would be utilized for the surface production.

Concurrently, the waste rock generated through the mining operations could be used for underground backfill purposes in co-disposal with low density paste and co-disposed on the surface either with low density paste or thickened tailings. Beyond the tailings process technology selection, the TSF type selection should be performed in parallel with each technology (thickened tailings, paste, filter cake or co-disposal). Both components (dewatering technology and TSF type) aim to suite the tailings characteristics, terrain topography and satisfy the LoM requirements.

From an economical perspective, CAPEX, OPEX and net present cost (NPC) are determined for the Base Case and each alternative. Compared to the Base Case, thickened tailings, paste, and filter cake disposal reduce the TSF footprint, lower TSF dam requirements and increase water recovery. Moreover, the tailings synergy between surface disposal and underground backfill allows about 50% of tailings generated over the LoM to be stored underground, which affects the TSF size and overall cost. An additional assessment of the Base Case and integrated tailings management alternatives should be carried out through a strength, weaknesses, opportunities and threats (SWOT) analysis. The SWOT analysis includes technical, environmental, social, and economical criteria.

CONCLUSION

Historically, tailings management systems were considered separately without any integration with underground mining design. However, this paper argues for an approach that evaluates sustainable integrated tailings management systems versus conventional tailings disposal (the Base Case).

Does it make sense for each mine to change their tailings management operating philosophy? The answer is “yes”. However, to stay on the right path, there is a procedure to be followed and satisfied at the project onset. This procedure encompasses a parallel assessment of dewatering technologies and TSF type that suit each considered technology as well as backfill type and selection for underground mines. This screening procedure includes economic evaluation, risk assessment and overall SWOT analysis. Process dewatering technology and transportation/distribution systems for each considered technology should be investigated together in order to properly arrive at an optimized and integrated design that achieves all of the objectives at minimal cost.

Lastly, the final integrated tailings management system should encompass a properly selected dewatering technology, tailings or waste transportation system (hydraulic, conveying etc.), tailings storage facility design and backfill type.

REFERENCES

1. Palkovits, F. (2007) Integrated Waste Management Strategy. In: Paste Conference.
2. del Pozo, G., Fimbres, F., Wilson, S., Gutierez del Olmo, A., Darby, A. (2007) Integration of Paste Management within a Mining Project to Respond to Operational and Permitting Needs - The Aguas Teñidas Mine in Southern Spain. In: Australian Centre for Geomechanics.
3. Dieh, P. (2022) List of tailings dam and mine waste failures - https://www.wise-uranium.org/mdaf.html.

XV International Mineral Processing and Recycling Conference
17-19 May 2023, Belgrade, Serbia

POSITION OF COPPER WITHIN URBAN MINING - RECOVERING POTENTIAL FROM MINE TAILINGS

V. Alivojvodic[1#], N. Petrovnijevic[2]
[1] The Academy of Applied Technical Studies Belgrade, Serbia
[2] Institute for Technology of Nuclear and Other Mineral Raw Materials (ITNMS), Belgrade, Serbia

ABSTRACT – Due to population growth and urbanization, accompanied by rapid technological development, the need for more material resources has multiplied. Demand for specific materials is growing particularly fast. One of these minerals is copper. Besides its quality for conducting electricity, this metal is crucial to a greener world. It founds application in managing electric vehicles, smart grids, and renewable energy systems. A wide span of its utilization requires an adequate and continuous supply of copper. A key solution for this lies in urban mining, which implies reusing and recovering raw materials from waste materials in the technosphere. One type of free voluminous waste that is difficult to dispose of safely is tailing ponds, an additional reason for recycling. Recycling copper from tailing ponds is an economically and environmentally acceptable form of waste reuse based on the principles of the circular economy by using already disposed waste, reducing current and future pollution, reducing remediation costs, and converting toxic waste into a free resource.

Keywords: Copper, Urban Mining, Circular Economy, Integral Treatment.

INTRODUCTION

Due to population growth and urbanization, accompanied by rapid technological development, the need for more material resources has multiplied. Almost all the contemporary technologies prioritized in today's accompanying industry production trends (wind turbines, solar PV systems, batteries, grid technologies, hydrogen electrolyzes) require an increased supply of metals and minerals. To meet growing demand, the European Commission has proposed an ambitious set of measures for materials considered 'critical' or 'strategic'. Copper has become part of both categories, according to the last Commission report from 2023 [1,2].

Why is copper so important? Unlike most other materials, copper can be perpetually recycled without losing performance or quality. It is identical to mined copper (with its infinite life cycle, it is a truly circular material) [3]. Copper is evolved as one of the essential metals in contemporary life and is the benchmark for conducting electricity. This metal has become a greener world key element [4]. Most copper (70 percent) is used worldwide for electrical/conductivity applications and communications.[5] Electric vehicles (EVs) use up to four times than gasoline vehicles [6]. As electric cars become more mainstream, enormous amounts of copper will be needed [7].

S&P Global points out that more copper is used in the energy transition will also open

corresponding author: valivojvodic@atssb.edu.rs

more "opportunities for recycling", such as when EVs are scrapped. Recycled production will come to represent about 22% of the total refined copper market by 2035, up from about 16% in 2021, while at the same time mature mines, the quality of ore is deteriorating, meaning output either slips or more rock has to be processed to produce the same amount. Meanwhile, new deposits are getting trickier and pricier to find and/or develop [8], as stated in Bloomberg reported sources [4].

Based on the global copper stocks and flows model, developed by the Fraunhofer Institute, it is estimated that two-thirds out of the 550 million tones of copper produced since 1900 are still in productive use, with approximately about 100 million tones estimated to remain in tailings ponds [5,9].

MATERIALS AND METHODS

There are enormous amounts of material in the anthropo-sphere. The potential of the anthropogenic stock (urban mine) can be defined as the sum of all used or stored materials contained in products by society over a comparatively long time (among many others, this includes buildings, electronic goods, waste, and mine tailings) [10]. While all material extracted from geological deposits enters the urban mine, urban mining cannot increase the number and amount of materials within the anthropogenic stock. Only the outflow products and material recovered from landfills and tailings ponds can be used to obtain new goods [10]. From the quantitative point of view, urban mining is currently equivalent to the recycling of end-of-life products. In contrast, material recovery from landfills and tailings ponds is negligible (the reprocessing mine tailings is a topic of increasing importance but remains a niche) [3,11]. A significant part of it never leaves mining deposition sites, so the large engineered dams and dyke facilities called tailings ponds contain this residual material stored for decades [10].

RESULTS AND DISCUSSION

The current potential for raw material production from the urban mine depends on the outflow of buildings, infrastructures, and products from service into waste management and recycling, together with the recovery from tailings ponds and landfills [12].

Urban stocks the stocks of urban copper resources that exist in long-lived uses like building wiring and batteries, according to authors of *Industrial ecology and sustainable engineering*, can be identified with good information on inputs and outputs in order to take the difference to compute stocks over time. The standing stock (the difference) can be calculated when input/output information for an extended period is assembled.

Information about the amounts is essential, but the material locations within the city can also be of practical usage (more accessible collection and reuse of the material). It could help anticipate environmental problems of dissipated material for environmentally toxic materials [12]. To plan wisely further recovery potential of urban copper resources, the information on its generation, locations, discarded periods, and expected availability is of great importance.

There is a gap between the raw material production potential given by *the urban mine* and the amounts of raw materials effectively recovered [10]. This follows from the

challenges – from organizational to technological to economic – facing the recovery of raw materials from a highly diverse and highly complex resource base distributed worldwide [10].

Potentials hidden in mininig tailings Copper production begins with the extraction of copper-bearing ores in mining or recycling of scrap metal. The ores are processed into copper concentrate, which can be further treated onsite or sold to a smelter [5].

During 2018, the global demand for copper was $23.6x10^6$ t. By the end of 2027, the market is estimated to grow to $29.8x10^6$ t, with an annual increase of 2.6%. World copper reserves are estimated at 5.6 billion tons. The largest estimated reserves are in Chile, which in 2018 was also the largest producer of copper with $5.8x10^6$ t [13].

Production of one ton of copper, for example, generates about 110 tons of tailings and roughly 200 tons of overburden [14]. Human civilization pays dearly for the need for metals [15]. The huge amounts of mining waste that are generated represent a great danger to the environment [16]. The disposal of mining waste destroys arable land and, forested areas, surface and underground water courses [17]. Scattered small particles from mining dumps, carried by the wind, fall on crops or households, so the negative effects of mining are reflected on all living resources: soil, water, air, as well as food production through the accumulation of toxic substances. In addition to the surface, toxic elements are also dispersed in-depth and thus disrupt ecosystems in a wider area but also disrupt plant and animal communities and their habitats [18].

Mining waste also represents a potential resource of valuable metals which, if unused or improperly deposited, is one of the primary environmental pollutants. Ore, with a lower percentage of copper, also has a larger share of the waste fraction. With the opening of new mines, additional quantities of tailings will inevitably be formed. It is necessary to emphasize that due to the higher percentage of the waste fraction, the required area for its disposal will grow faster than in the earlier period when the ore was richer (Table 1).

Table 1 Ore Grades Slump (globaly) [4]

Year	Copper grade
1900	2.0 %
2000	1.0 %
2020	0.7 %
2030	0.5 %

*Table shows concentration of copper in ore

The fact is that scientific and technological development has enabled the valorization of valuable components from raw materials in which the copper content is around 0.2-0.3%, which was not economically profitable in the past, so it can be expected that secondary sources of copper such as flotation tailings will represent an essential source of raw materials for copper production [19]. In addition, it is undoubtedly important to consider the energy savings related to the copper ore processing process itself (Figure 1).

The revaluation of metals from low-quality ore or tailings is justified because it is more economically and environmentally acceptable to use existing stocks than to start a new mine and production. In this way, resources are saved for future generations. By treating already disposed amounts of waste, environmental contamination, the emission of toxic metals, and the formation of acidic mine waters are reduced [20].

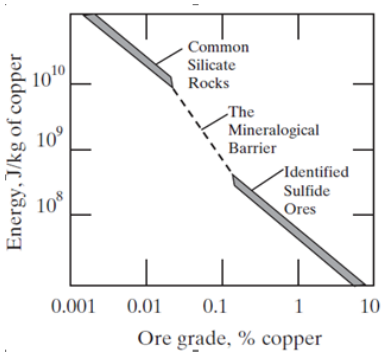

Figure 1 The energy necessary to recover copper from its ores and by atomic substitution from common silicate minerals [12]

Apart from Cu, the concentration of other valuable elements, such as Zn, Ag, and Au, is deficient, but the total amount in the disposed of tailings is significant. That was the reason for severe analysis and finding the possibility of their valorization.

Although until now, direct exploitation from flotation tailings was not economically justified. Applying appropriate integral treatment with acidic mine water from such as Lake Robule, formed near Bor (Serbia), would become ecologically justified and recommended which was the subject of previous investigations [21, 22].

Table 2 Tailing pond – Characteristics of input raw material [22]

Consequences of waste disposal	**Benefits of integral treatment**
- *a source of fine dust which can contain harmful chemical elements* - *healthy risks* - *constant danger of possible breakage or overflow of dams and leakage of flotation pits* - *source of acid mine water*	- *metal revalorization* - *economically viable* - *there is no formation of new acidic mine water* - *reduced pollution and* - *reduces costs for remediation*

In this way, the consumption and utilization of raw waste materials would increase.

Concern for the sustainable development of mining is justified, and it is necessary to consider the balance of social, economic, and environmental risks [23]. Bearing in mind all the negative consequences that can be caused by large amounts of permanently deposited flotation tailings, the conclusion is that this problem could be solved by adequate additional treatment of the tailings to reduce the concentration of residual heavy metals as potential polluting elements, with lowering of tailings deposited at the site [24].

CONCLUSION

Copper supplies decreasing daily, and opening of new mining sites is not neither favorable nor feasible in all circumstances. Opening of new mining sites means transport and installation of new equipment and mechanization, possible tectonically moves, destruction of landscape, higher carbon emission etc. All of these raising costs and vulnerability of environment. Urban mining is recognized as main mechanism for

valorization of already disposed waste streams ant it implies valorization of dispose waste and recycling of copper from it. Tailing ponds as secondary materials contain a large percentage of metals, and for this reason great attention is paid to the development of technologies for their processing in order to obtain metals of high purity. It is necessary to emphasize that previous extracted ore, primary ore, had higher copper content and less percentage of waste fraction, which is not situation nowadays. Previously deposited tailings, as secondary raw material, have similar percentage of copper as nowadays ore. This indicates that modernization of extraction technology should be implemented in treatment of already deposited flotation tailing waste not for new mining sites. By applying modern technologies, it is possible to significantly reduce the amount of these already disposed waste materials and reduce costs of treatment and reduce energy consumption. Processing of secondary raw materials compared to the production of metals from primary raw materials has several advantages: much smaller investments compared to the processing of primary raw materials, production of high-purity metals with a high level of utilization, lower energy consumption, preservation of natural resources, and lower costs of wastewater and gas treatment. Urban mining represents ecological and economic progress in implementing the principles of Circular economy, by which it is achieved: rational use of waste raw materials, reduction of the amount of waste materials and the emission of pollutants as well as the costs of disposal and storage space, formation of new by-products and possible to receive compensation from their sale, but also to replace expensive products with by-products.

REFERENCES

1. The European Commission (2023) Proposal for a regulation of the European Parliament and of the Council establishing a framework for ensuring a secure and sustainable supply of critical raw materials, COM(2023)160.
2. European Commission (2023) Study on the Critical Raw Materials for the EU, Final Report.
3. Tercero Espinoza, L., Rostek, L., Loibl, A., Stijepic, D. (2020) The promise and limits of Urban Mining. Fraunhofer ISI, Karlsruhe.
4. James Attwood (2022) A Great Copper Squeeze Is Coming for the Global Economy, September, BNN Bloomberg (https://www.bnnbloomberg.ca/a-great-copper-squeeze-is-coming-for-the-global-economy-1.1821990).
5. Copper Alliance (2023) Copper Life Cycle https://copperalliance.org/sustainable-copper/about-copper/copper-life-cycle/(accessed March 2023).
6. Majuba Hill Copper (2023) Copper In Electric Vehicles, article, https://www.majubahillcopper.com/copper-in-electric-vehicles/.
7. LePan, N. (2018) How Much Copper is in an Electric Vehicle? Visual Capitalist, https://www.visualcapitalist.com/how-much-copper-is-in-an-electric-vehicle/.
8. Bloomberg (2022) Why investors are selling copper and how a looming shortage will affect the economy, article, www.thenationalnews.com/business/2022/09/24/why-investors-are-selling-copper-and-how-a-looming-shortage-will-affect-the-economy/.
9. Glöser, S., Soulier, M., Tercero Espinoza, L.A. (2013) Dynamic analysis of global copper flows. Global stocks, postconsumer material flows, recycling indicators & uncertainty evaluation. Environmental Science & Technology, 47, 6564–6572.

10. The International Copper Association, ICA (2020) Urban Mining: The next frontier in the circular economy? https://www.euractiv.com/section/energy-environment/opinion/urban-mining-the-next-frontier-in-the-circular-economy/.
11. Winterstetter, A., Wille, E, Nagels, P., Fellner, J. (2018) Decision making guidelines for mining historic landfill sites in Flanders. Waste Management.
12. Graedel, T.E., Allenby, B.R. (2010) Industrial ecology and sustainable engineering, Prentice Hall, ISBN-13: 978-0-13-600806-4.
13. International Copper Study Group (2019) www.icsg.org, (accessed March 2023).
14. Das, R., Choudhury, I. (2013) Waste Management in Mining Industry. Indian Journal of Scientific Research, 4 (2), 139-142.
15. Stanković, S. (2016) Mikrobiološki diverzitet kiselog jezera Robule i uticaj jezerske vode na oksidaciju sulfidnih mineral. Doktorska disertacija, Rudarsko-geološki fakultet, Beograd.
16. Sheoran, A.S., Sheoran, V. (2006) Heavy metal removal mechanism of acid mine drainage in wetlands: A critical review. Minerals Engineering, 19 (2), 105–116.
17. Mudd, G.M., Patterson, J. (2010) Continuing pollution from the Rum Jungle U-Cu project: A critical evaluation of environmental monitoring and rehabilitation. Environmental Pollution, 158 (5), 1252–1260.
18. Spasić, N., Stojanović, B., Nikolić, M. (2012) Uticaj rudarstva na okruženje i revitalizacija degradiranog prostora. Arhitektura i urbanizam, 75-85.
19. Onuaguluchi, O., Eren, O. (2012) Recycling of copper tailings as an additive in cement mortars. Construction and Building Materials, 37, 723-727.
20. Antonijević, M.M., Dimitrijević, M.D., Stevanović, Z.O., Šerbula, S.M., Bogdanović, G.D. (2008) Investigation of the possibility of copper recovery from the flotation tailings by acid leaching. Journal Hazardous Materials, 158 (1), 23–34. DOI: 10.1016/j.jhazmat.2008.01.063.
21. Petronijevic, N. (2023) Ispitivanje mehanizma neutralizacije kiselih rudničkih voda korišćenjem flotacijske jalovine i letećeg pepela. Doktorska disertacija, Univerzitet u Beogradu, Tehnološko-metalurški fakultet, Beograd.
22. Petronijevic, N., Alivojvodić, V., Sokić, M., Marković, B., Stanković, S., Radovanović, D. (2020) Sustainable mining towards accomplishing circular economy principles. Journal of Applied Engineering Science, 18 (4), 493-499. doi: 10.5937/jaes0-27460.
23. Mudd, G.M. (2007) Global trends in gold mining: Towards quantifying environmental and resource sustainability. Resources Policy, 32 (1-2), 42-56.
24. Stanković, V., Milošević, V., Milićević, D., Gorgievski, M., Bogdanović, G. (2018) Reprocessing of the olf flotation tailings deposited on the Bor tailings pond- a case study. Chemical Industry and Chemical Engineering Quarterly, 24 (4), 334-344. DOI: 10.2298/CICEQ170817005S.

XV International Mineral Processing and Recycling Conference
17-19 May 2023, Belgrade, Serbia

BACTERIOSTATIC ACTIVITY OF GEORGIAN HEULANDITE ENRICHED WITH BIOLOGICALLY ACTIVE METALS

V. Tsitsishvili[1], N. Dolaberidze[2], N. Mirdzveli[2#], M. Nijaradze[2], Z. Amiridze[2], B. Khutsishvili[2]

[1] Georgian National Academy of Sciences, Tbilisi, Georgia (Saqartvelo)
[2] Petre Melikishvili Institute of Physical & Organic Chemistry at Ivane Javakhishvili Tbilisi State University, Tbilisi, Georgia

ABSTRACT – Heulandite-containing tuff from the Rkoni plot of the Tedzami-Dzegvi deposit, Eastern Georgia, characterized by a Si/Al ratio of 3.6 was enriched with silver (130 mg/g), copper (63-72 mg/g) and zinc (30-58 mg/g) as a result of ion exchange reactions. Bacteriostatic activity of obtained samples against *Escherichia coli*, *Staphylococcus aureus*, hay bacteria *Bacillus subtilis*, pathogenic fungal yeast *Candida albicans* and fungus *Aspergillus niger* was studied by the disk-diffusion method, and it is shown that mixtures of silver, copper and zinc forms in a molar ratio 1:1 exhibit the greatest activity against staphylococcus, and mixture of copper and zinc forms – against other studied microorganisms.

Keywords: Heulandite, Silver, Copper, Zinc, Bacteriostatic.

INTRODUCTION

Among the materials advanced for the creation of new bactericidal substances, zeolites $M_x[Al_xSi_yO_{2(x+y)}]\cdot mH_2O$, in which alkali or alkaline-earth metal ions M are partially replaced by bioactive metal ions (Ag^+, Cu^{2+}, Zn^{2+}, etc.), are recognized as promising [1,2]. Biocidal formulations containing zeolites do not cause allergic reactions in humans; they are nontoxic, odorless, and considered to be safe for the environment [3].

The intensity of research on metal-containing zeolites (MZs) increased at the beginning of the 21st century, they continue to this day and are reflected in numerous publications; it has been shown that synthetic and natural zeolites enriched with bioactive metals exhibit antimicrobial activity against a wide range of microorganisms. As a result of studies of silver-, copper- and zinc-containing zeolites, it was found that the silver-containing zeolites are the most active. However, the disadvantages of the use of silver ions have been noted – silver is an expensive metal, and Ag^+ is not stable in aqueous solutions, tends to be reduced to Ag^0 and reacts with sulfate and other anions forming insoluble salts [4], so in some cases the benefits of silver ions are not so obvious. Thus, Zn^{2+} and Cu^{2+} loaded samples of synthetic zeolite X showed excellent antimicrobial activities against three bacteria – gram-negative *E. coli* and *Pseudomonas aeruginosa*, gram-positive *S. aureus*, a yeast *C. albicans* and a fungus *Aspergillus niger* [5]; according to the recent results [6], Cu-X is more active against *S. aureus*, Zn-X – against *E. coli*, although the zinc form of synthetic zeolite A is inactive [7].

corresponding author: nato.mirdzveli@gmail.com

In most studies applying natural zeolites for preparation of bactericidal materials, heulandite-clinoptilolite of various origins was used, and results for bioactive metal-enriched clinoptilolites are also inconsistent. On the one hand, it was found that the diameters of the zones of inhibition of the growth of *E. coli* by the Ag-, Cu-, and Zn-forms of clinoptilolite from Gördez, Turkey, at an exchange level of ~0.2 are approximately the same and amount to 12 mm, the maximum zone of inhibition by Ag^+ ions is 14 mm, and by Cu^{2+} ions – 13 mm [8]. On the other hand, natural clinoptilolite from Mare Baia, Romania (CLI, [9]) was "activated" by Cu^{2+} and Zn^{2+} ions and tested on antimicrobial activity against *E. coli*, *S. aureus* and *C. albicans*, but only Cu-CLI and only against *E. coli* appeared to be active [10].

The purpose of the study was to obtain bactericidal materials using Georgian natural heulandite-clinoptilolite, to study their properties and use them as a filler for the production of bactericidal paper.

MATERIALS AND METHODS

Heulandite-clinoptilolite-containing rock from the Rkoni plot of Tedzami deposit (Eastern Georgia) was 1) grinded using a planetary mill (Pulverisette 7, Fritsch Laboratory Instruments, Germany), 2) fractionated to a size less than 0.044 mm (325 US mesh) using a set of sieves, 3) washed with diluted HCl solution (0.025 N) to remove clay impurities and improve ion-exchange properties, and 4) dried under static conditions, in air and/or in a thermostat at a temperature of 95-100 °C; prepared sample was named as HCR.

Ion exchange reactions were carried out as follows: powder of HCR and analytical grade silver (I) nitrate $AgNO_3$, copper (II) chloride dihydrate $CuCl_2{\cdot}2H_2O$, and zinc (II) chloride $ZnCl_2$ purchased from Merck KGaA, Darmstadt, Germany) were mixed in different weight ratios (1:1.5 for silver, 1:1.5 and 1:2.55 for copper, 1:1.2 and 1:2 for zinc) and thoroughly grinded in an agate mortar for 10 minutes for $AgNO_3$-containing mixture, and for 15 minutes for $CuCl_2$ or $ZnCl_2$-containing mixtures. The solid mixture was then transferred to a filter and washed with distilled water until the complete disappearance of nitrate or chlorine anions, after which the modified samples were first dried in air and then in a thermostat; samples are labeled as AgHCR, CuHCR, and ZnHCR (silver-, copper-, and zinc-containing heulandite-clinoptilolite, respectively).

Chemical composition of studied zeolites was calculated from the X-ray energy dispersive (XRED) spectra obtained from scanning electron microscope JSM6510LV (Jeol, Japan) equipped with X-Max 20 analyzer (Oxford Instruments, UK). The crystalline phase was identified by powder X-ray diffraction (XRD) patterns obtained from a modernized Dron-4 X-ray diffractometer (USSR) employing the Cu-K_α line (λ = 0.154056 nm). The samples were scanned in the 2Θ range of 5° to 50° with a 0.02° step at a scanning speed of 1°/min. Fourier transform infrared spectra were collected by a 10.4.2 FTIR spectrometer (Perkin-Elmer, UK) over the range of 400–4000 cm^{-1} with a resolution of 2 cm^{-1} using the KBr pellet technique for sample preparation.

Bacteriostatic properties of zeolite samples were determined by the disk diffusion (Kirby-Bauer) method in standard conditions using the cultures of Gram negative bacterium *Escherichia coli* (strain ATTC 8739), Gram-positive bacteria *Staphylococcus aureus* (ATTC 6538) and *Bacillus subtilis* (ATTC 6633), fungal pathogenic yeast *Candida albicans* (ATTC 10231) and a fungus *Aspergilus niger* (ATTC 16404 – *A. brasiliensis*).

RESULTS AND DISCUSSION

Chemical composition of obtained samples is given in Table 1; the achieved content of bioactive metals is close to the maximum values calculated from the ion exchange isotherms obtained on Turkish clinoptilolite [8]. The hydrated ions of copper and zinc in solution are known to have the same regular configuration $M(H_2O)_6^{2+}$, size and diffusion coefficients [39], but under "solid" ion exchange conditions, the incorporation of zinc ions into the structure of clinoptilolite is difficult.

Table 1 Chemical composition of original (HCR) and modified zeolite samples

Sample	Averaged empirical formula of dehydrated zeolite	Bioactive metal content	
		mg/g	mmol/g
HCR	$(Na_{0.25}K_{0.06}Ca_{0.19}Mg_{0.15})[AlSi_{3.6}O_{9.2}]$	-	-
AgHCR	$(Na_{0.11}K_{0.06}Ca_{0.10}Mg_{0.09})[AlSi_{3.6}O_{9.2}]$	130	1.2
$CuHCR_1$	$(Na_{0.08}K_{0.06}Ca_{0.03}Mg_{0.04})[AlSi_{3.9}O_{9.8}]$	63	1.0
$CuHCR_2$	$(Na_{0.03}K_{0.05}Ca_{0.02}Mg_{0.02})[AlSi_{4.1}O_{10.2}]$	72	1.14
$ZnHCR_1$	$(Na_{0.10}K_{0.06}Ca_{0.13}Mg_{0.13})[AlSi_{3.65}O_{9.3}]$	30	58
$ZnHCR_2$	$(Na_{0.07}K_{0.05}Ca_{0.05}Mg_{0.07})[AlSi_{3.8}O_{9.6}]$	0.46	0.89

The greatest change in the silicate modulus Si/Al and leaching of aluminum atoms (up to 10%) occurs when copper Cu^{2+} ions are introduced into the zeolite structure; when silver Ag^{+} ions are introduced, the modulus does not change. Ion exchange takes place with the participation of magnesium Mg^{2+} and sodium Na^{+} ions, calcium Ca^{2+} ions are also involved in the process, but relatively heavy and large potassium ions do not participate in ion exchange reactions.

Comparison of the powder XRD patterns of the initial and modified samples (Figure 1) confirms the retention of the crystal structure of the heulandite-clinoptilolite during ion-exchange reactions; no changes in the pore system and specific surface area were fixed.

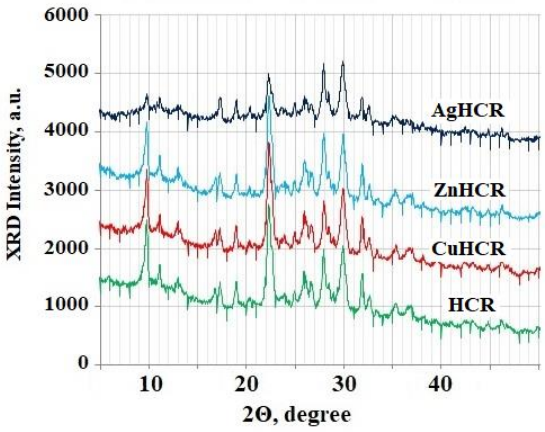

Figure 1 Powder X-ray diffraction patterns of the HCR and its modified forms enriched with silver (AgHCR), copper (CuHCR) and zinc (ZnHCR)

Results of the disk-diffusion test are given in the Table 2: silver-containing heulandite-clinoptilolite shows bacteriostatic activity against all microorganisms used; sample $CuHCR_1$ with a relatively low copper content is inferior to it in activity, and sample $CuHCR_2$ with an increased copper content shows significantly higher activity, especially against staphylococcus and fungi. The zinc-containing form $ZnHCR_1$ is inactive against *E. coli* and staphylococcus, but has weak bacteriostatic activity against other microorganisms, an increase in the amount of bioactive metal makes sample $ZnHCR_2$ the most active against all applied microorganisms.

Table 2 Diameter (mm) of zones of inhibition of the growth of microorganisms by metal-containing zeolites

Microorganism	Sample				
	AgHCR	$CuHCR_1$	$CuHCR_2$	$ZnHCR_1$	$ZnHCR_2$
Escherichia coli	21	15	36	0	35
Staphylococcus aureus	19	19	53	0	52
Bacillus subtilis	30	21 – 36*	41	19	42
Candida albicans	20.5	15	54	15*	61
Aspergillus niger	25	14*	65	17	69

*Secondary grouth.

However, the picture of bacteriostatic activity, especially with the participation of the zinc-containing form, changes dramatically in the case of using mechanical mixtures of metal-containing heulandites, and this is shown in Figures 2-4.

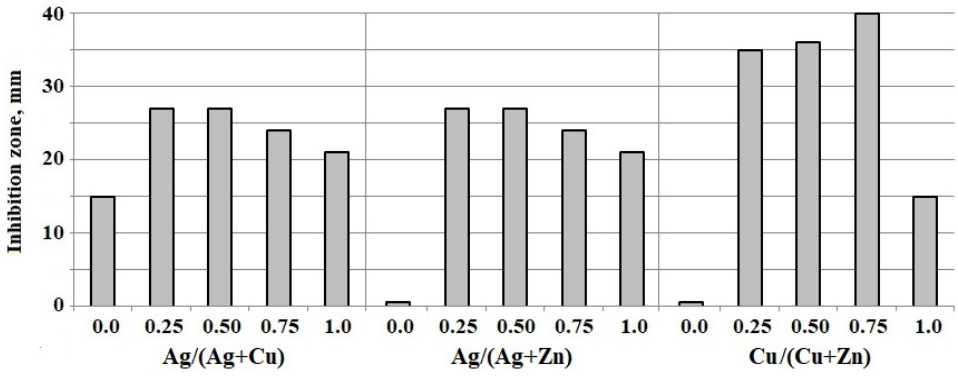

Figure 2 Inhibition zones of *E. coli* growth by AgHCR, $CuHCR_1$, $ZnHCR_1$ and their mixtures in different molar ratios

Despite the fact that the low-zinc form $ZnHCR_1$ is inactive to *E. coli*, even a small addition of the silver AgHCR or copper $CuHCR_1$ form dramatically increases the activity; the highest bacteriostatic activity is observed for the ¼ZnHCR + ¾CuHCR mixture (Figure 2). The synergistic effect is also manifested in relation to the both gram positive bacteria (Figure 3), the mixtures ¼AgHCR+¾CuHCR, ½AgHCR+½ZnHCR and ¼CuHCR+¾ZnHCR have the greatest activity against staphylococcus, and mixtures of copper and zinc forms are moslt effective against hay bacillus *B. subtilis*.

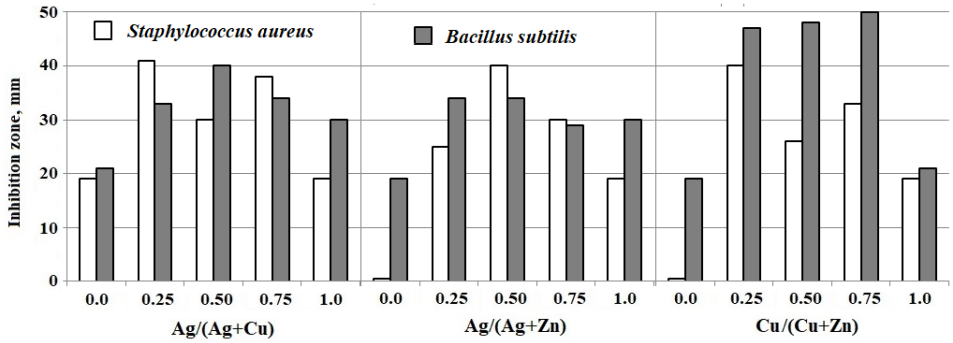

Figure 3 Inhibition of Gram positive bacteria growth by AgHCR, $CuHCR_1$, $ZnHCR_1$ and their mixtures in different molar ratios

In inhibiting the growth of fungi (Figure 4), mixtures with the AgHCR show low activity, the most effective are mixtures of CuHCR and ZnHCR, which is very important from a practical point of view, to replace expensive silver (approx. 770 $/kg, December 2022) with cheaper copper (10 $/kg) and zinc (3 $/kg).

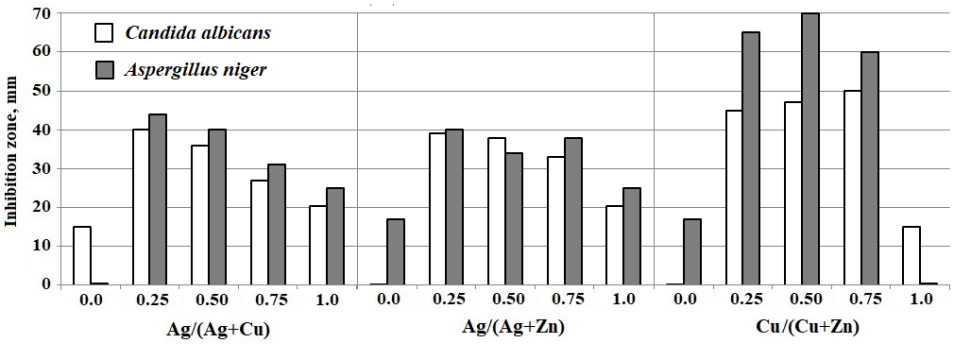

Figure 4 Inhibition of fungi growth by AgHCR, $CuHCR_1$, $ZnHCR_1$ and their mixtures in different molar ratios

As follows from the data obtained, a mixture with a high copper content, Cu/Zn = 3, is the most effective against *E. coli* and hay bacillus, while the zone of inhibition is two times higher than that of the silver-containing form. On the contrary, against staphylococcus and *C. albicans*, the most effective is a mixture with a high zinc content, Zn/Cu = 3, and the maximum inhibition of the growth of *A. niger* is caused by a mixture with equal amounts of copper and zinc.

CONCLUSION

As a result of the conducted research, it was established that solid-state ion-exchange reactions between Georgian natural heulandite-clinoptilolite and salt of corresponding transition metal followed by washing results in zeolite materials with a fairly high content of bioactive metals (silver up to 130, copper 72, and zinc 58 mg/g) and exhibiting bacteriostatic activity against *Escherichia coli*, *Staphylococcus aureus*, hay bacteria

Bacillus subtilis, pathogenic fungal yeast *Candida albicans* and fungus *Aspergillus niger*. It is shown that mixtures of silver, copper and zinc forms in a molar ratio 1:1 have the greatest activity against staphylococcus, and mixture of copper and zinc forms – against other studied microorganisms. According to these results and taking into account that copper and zinc ions are more stable than silver ions, it is very promising to use copper- and zinc-enriched forms of heulandite as fillers for the production of bactericidal paper and for other purposes.

ACKNOWLEDGEMENT

This work was supported by Shota Rustaveli National Science Foundation of Georgia (SRNSFG) [grant number AR-22-610 "Production of paper with bactericidal and improved surface properties"].

REFERENCES

1. Díez-Pascual, A.M. (2018) Antibacterial activity of nanomaterials. Nanomaterials*,* 8*,* 359-365.
2. Azizi-Lalabadi, M., Alizadeh-Sani, M., Khezerlou, A., Mirzanajafi-Zanjani, M., Zolfaghari, H., Bagheri, V., Divband, B., Ehsani. A. (2019) Nanoparticles and zeolites: Antibacterial effects and their mechanism against pathogens. Curr. Pharm. Biotechnol., 20(13), 1074-1086.
3. Król, M., Syguła-Cholewińska, J., Sawoszczuk, T. (2022) Zeolite-supported aggregate as potential antimicrobial agents in gypsum composites. Materials, 15, 3305, 1-11.
4. Vergara-Figueroa, J., Alejandro-Martín, S., Pesenti, H., Cerda, F., Fernández-Pérez, A., Gacitúa, W. (2019) Obtaining nanoparticles of Chilean natural zeolite and its ion exchange with copper salt (Cu^{2+}) for antibacterial applications. Materials, 12(13), 2202-2220.
5. Tekin, R., Bac, N. (2016) Antimicrobial behavior of ion-exchanged zeolite X containing fragrance. Micropor. Mesopor. Mat., 234, 55–60.
6. Yao, G., Lei, J., Zhang, W., Yu, C., Sun, Z., Zheng, S., Komarneni, S. (2019) Antimicrobial activity of X zeolite exchanged with Cu^{2+} and Zn^{2+} on Escherichia coli and Staphylococcus aureus. Environ. Sci. Pollut. Res. Int., 26(3), 2782-2793.
7. Milenkovic, J., Hrenovic, J., Matijasevic, D., Niksic, D., Rajic, N. (2017) Bactericidal activity of Cu-, Zn-, and Ag-containing zeolites toward *Escherichia coli* isolates. Environ. Sci. Pollut. Res., 24(6), 20273-20281.
8. Top, A., Ülkü, S. (2004) Silver, zinc, and copper exchange in Na-clinoptilolite and resulting effect on antibacterial activity. App. Clay Sci., 27(1-2), 13-19.
9. Đolić, M.B., Rajaković-Ognjanović, V.N., Štrbac, S.B., Rakočević, Z.Lj., Veljović, Đ.N., Dimitrijević, S.I., Rajaković, L.V. (2015) The antimicrobial efficiency of silver activated sorbents. Applied Surface Science, 357A, 819-831.
10. Dolic, M.B., Rajakovic-Ognjanovic, V.N., Strbac, S.B., Dimitrijevic, S.I., Mitric, M.N., Onjia, A.E., Rajakovic, L.V. (2017) Natural sorbents modified by divalent Cu^{2+}- and Zn^{2+}-ions and their corresponding antimicrobial activity. *New Biotechnology*, 39, 150-159.

XV International Mineral Processing and Recycling Conference
17-19 May 2023, Belgrade, Serbia

THERMAL STABILITY OF NATURAL HEULANDITE-CHABAZITE MIXTURES

V. Tsitsishvili[1#], M. Panayotova[2], N. Dolaberidze[3], N. Mirdzveli[3], M. Nijaradze[3], Z. Amiridze[3], B. Khutsishvili[3], N. Dzhakipbekova[4], S. Sakibayeva[4]

[1] Georgian National Academy of Sciences, Tbilisi, Georgia (Saqartvelo)

[2] Department of Chemistry, University of Mining & Geology "St. Ivan Rilski", Sofia, Bulgaria

[3] Petre Melikishvili Institute of Physical & Organic Chemistry at Ivane Javakhishvili Tbilisi State University, Tbilisi, Georgia

[4] M. Auezov South Kazakhstan University, Shymkent, Kazakhstan

ABSTRACT – The study of thermal stability of tuffs from the Rkoni plot of the Tedzami-Dzegvi deposit (Eastern Georgia) and the Chankanay deposit (Almaty region, Kazakhstan), containing heulandite and chabazite, showed that partial amorphization of the heulandite phase begins at ≈300°C, transition to the heulandite B was not observed, but formation of the 9.GB.05 group minerals was confirmed, the complete collapse occurs at ≈700°C; the chabazite is stable up to ≈900°C; the volume of micropores in the Rkoni sample (Si/Al=3.6, HEU/CHA≈8) decreases monotonically with an increase in the calcination temperature, in the Chankanay sample (Si/Al=2.9, HEU/CHA≈1) it reaches a maximum after calcination at 800°C.

Keywords: Heulandite, Chabazite, Tedzami-Dzegvi, Chankanay.

INTRODUCTION

Thermal stability is an important characteristic of zeolites, aluminosilicates of the general formula $M_x[Al_xSi_yO_{2(x+y)}]\cdot mH_2O$ ($M^+ = Na^+, K^+, \ldots ½Ca^{2+}, ½Mg^{2+}, \ldots$), which have a unique set of molecular-sieve, sorption, ion exchange and catalytic properties.

Thermal stability is often a critical factor in the catalytic applications of zeolites [1], and this problem from 1960-ies is usually solved by the use of ultra-stable high-silica (Si/Al>>1) zeolites [2]. The cationic content also affects the thermal properties of zeolites and It is known that K^+ may thermodynamically stabilize a certain zeolitic frameworks, and this is used in the cement industry [3]. To improve the properties of natural zeolites, preliminary heat treatment is used [4], and the stability of the zeolite framework also plays an important role. On the other hand, acid treatment is also used to modify zeolites, and pre-heat treatment may affect the acid resistance of the sample.

The purpose of this work was to consider the thermal stability and accompanying processes in zeolites from the deposits of Georgia and Kazakhstan, selected for thermal and acid-base modification to create new bactericidal zeolite filter materials for purification and disinfection of water from various sources. Recently, Georgian zeolite has been used for the production of bactericidal adsorbents [5], while Kazakhstani zeolite has been successfully used in fish-breeding [6].

corresponding author: nato.mirdzveli@gmail.com

EXPERIMENTAL

Heulandite-clinoptilolite-containing rock from the Rkoni plot of Tedzami-Dzegvi deposit (Eastern Georgia) and the zeolitic tuff of Chankanay deposit (Kazakhstan, Almaty region) were grinded using a standard crusher, fractionated to the particle size 1-1.4 mm or 14-16 mesh, washed with distilled water or dilute HCl solution (0.025 N) to remove clay impurities, and dried up at a temperature of 95-100°C. The main characteristics of rocks according to the results of their study [7] are given in Table 1.

Table 1 Characteristics of the studied zeolite-containing rocks

Characteristic	Sample from	
	Rkoni	Chankanay
Zeolite phase content (%)	90	70
Empirical chemical formula	$Na_{0.25}K_{0.06}Ca_{0.19}Mg_{0.15})[AlSi_{3.6}O_{9.2}]\cdot 3H_2O$	$Na_{0.115}K_{0.079}Ca_{0.228}Mg_{0.175})[AlSi_{2.96}O_{7.92}]\cdot 3H_2O$
HEU/CHA*	8	1
Impurities per Al atom	$Fe_{0.2}$, $Ca_{0.14}$	$(SiO_2)_{\approx 1}$, $Fe_{0.33}$, $Ca_{0.17}$

*HEU – content of heulandite ($M_8(H_2O)_{24}[Al_8Si_{28}O_{72}]$), CHA – content of chabazite ($M_{12}(H_2O)_{40}[Al_{12}Si_{24}O_{72}]$).

Heat treatment of the prepared zeolites was carried out in a muffle furnace B400/410 (Naberthem, Carl Stuart's group) in the temperature range of 200 – 800°C for 1 hour, after which the samples were placed in desiccators with $CaCl_2$ until complete cooling.

Chemical composition of samples was calculated from the X-ray energy dispersive (XRED) spectra obtained from scanning electron microscope JSM-6490LV (Jeol, Japan) equipped with INCA Energy 350 XRED analyzer. Powder X-ray diffraction (XRD) patterns were obtained from D8 Endeavor diffractometer (Bruker, Germany).

RESULTS AND DISCUSSION

According to the XRED spectra, chemical composition of the surface of the calcined samples undergoes slight changes, which are most reflected in the Si/Al molar ratio (see Figure 1) – in the temperature range of 400-500°C, dealumination is observed; at higher temperatures, the modulus Si/Al returns to its previous values.

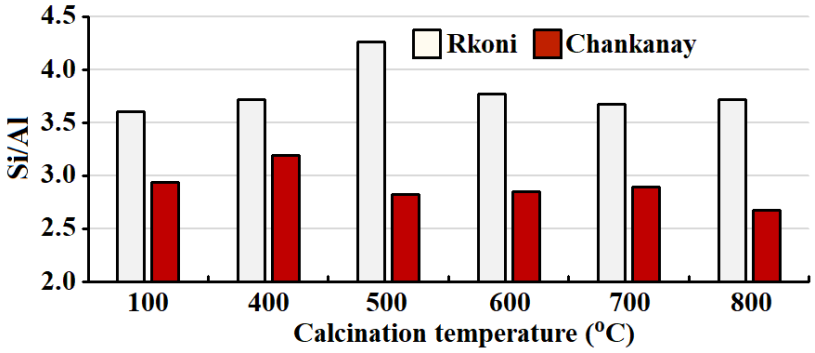

Figure 1 The Si/Al molar ratio in calcinated samples

At room temperature under conditions of normal humidity, the framework, cations and water molecules of zeolite are in equilibrium, on heating water is released from the structure and such dehydration is accompanied with other processes (phase transitions, etc.) which establish equilibrium under the new conditions. Generally, dehydrated zeolites are metastable, and the temperature of thermal decomposition depends upon the duration and rate of heating, presence of traces of water, etc. [8, p. 25-25].

According to the data of thermal analysis [9], the measured total weight loss (15.09%) in Georgian sample, a high-silica heulandite (Si/Al=3.6) containing relatively high content of sodium exchangeable ions, is in good agreement with the calculated (15.5%) based on the empirical chemical formula (see Table 1) and crystal chemical data of heulandite **|**$Ca_4(H_2O)_{24}$**| [**$Al_8Si_{28}O_{72}$**]-HEU** [10, pp. 156-157]. Most of the water (≈60% of the total water content) is continuously lost at temperatures below ≈250 °C, and then part of the remainder (≈24%) is slowly dehydrated up to 650 °C; the DTA and DTG curves show slow endothermic changes between room temperature and 250 °C, but do not have a sharp endothermic peak at ≈340 °C, which is considered a hallmark of heulandite [8, pp. 26, 47-48, Fig. 1.14]. Apparently, in the heulandite sample from Rkoni plot, there is no transition to the "sluggish" heulandite B first described by Koizumi [11].

In a more detailed study by Pechar and Rykl [12], it was shown that the heulandite structure is stable up to 280°C, at higher temperature the transformation into the modification of heulandite B occurs, from the temperature of 470 °C upwards the amorphous phase begins to be formed, from which at the temperature exceeding 500°C a mixture of quartz and minerals of the 9.GB.05 group wairakite ($Ca[Al_2Si_4O_{12}]\cdot 2H_2O$) and/or anorthite ($Ca[Al_2Si_2O_8]$) starts to appear.

Powder X-ray diffraction patterns of Georgian heulandite calcined at different temperatures (Figure 2) show following: in the temperature range up to 200°C, the patterns do not change, at higher temperatures the peaks begin to broaden, than the intensity of the heulandite peaks decreases, a broad band and a sharp peak of quartz (2Θ = 26.6°) appear (Figure 2b), which confirms the formation of an amorphous phase and the minerals indicated in [12]; at temperatures above 750°C, heulandite peaks collapse into a broad band, overlapping the sharp peaks of chabazite and quartz (Figure 2c).

Thus, the decomposition of the main zeolite phase of the sample (HEU) starts at approximately 300°C, as for high-silica heulandites [1, p. 49], while the impurity phase (CHA) is stable at temperatures above 800°C.

The presence of a large amount of impurities (quartz, oxides of iron and calcium) leads to a rather low value of the total weight loss (≈6%) in the Kazakhstan zeolite, while the dehydration process occurs in a very wide temperature range: the third part of the water molecules leaves the framework up to a temperature of 200°C, about half of the water molecules are lost up to 660°C, the remaining small part is lost at higher temperature up to 1000°C in two stages.

Powder XRD patterns of calcined Kazakhstani zeolite (Figure 3), which contains much more chabazite and additionally quartz, did not provide such a detailed picture as for Georgian heulandite: broadening of the peaks and a change in their intensity is observed only at temperatures above 400°C, a broad band appears at temperatures above 500°C and reaches its maximum intensity after calcination at 800°C, overlapping the sharp peaks of chabazite and quartz (Figure 3b).

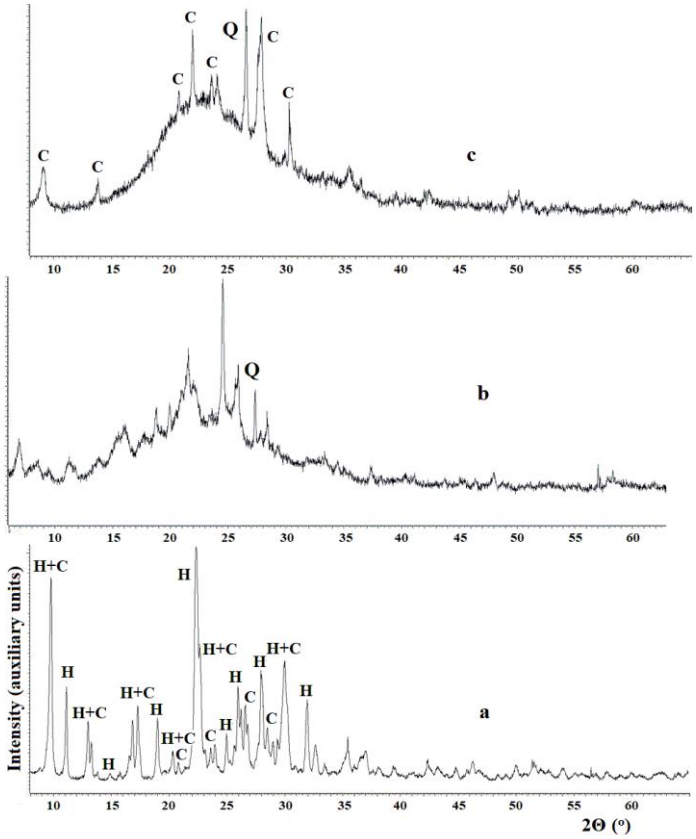

Figure 2 XRD patterns of Georgian heulandite calcined at 100 (a), 500 (b) and 800 (c)°C

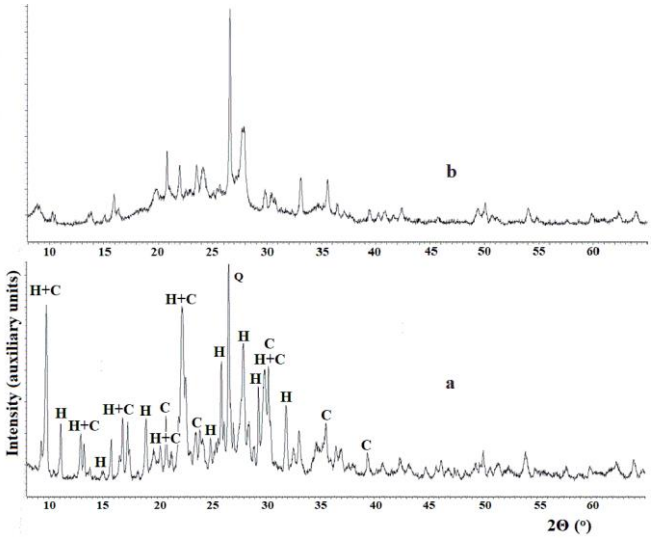

Figure 3 XRD patterns of Kazakhstani zeolite calcined at 100 (a) and 800 (c)°C

The DTA curve show low-temperature (103°C) and high-temperature (629, 701 and 835°C) associated with dehydration, but did not show a weak exo effect at 960°C, which is characteristic of chabazite [8, Fig. 1.14]. At this temperature, the material no longer contains framework water and is partially amorphized, formation of leucite $(K,Na)AlSi_2O_6$ occurs at temperatures above 1100°C as described in [13].

The difference between heat-treated Georgian and Kazakhstani zeolites is most pronounced in their sorption capacity for water vapor (Figure 4).

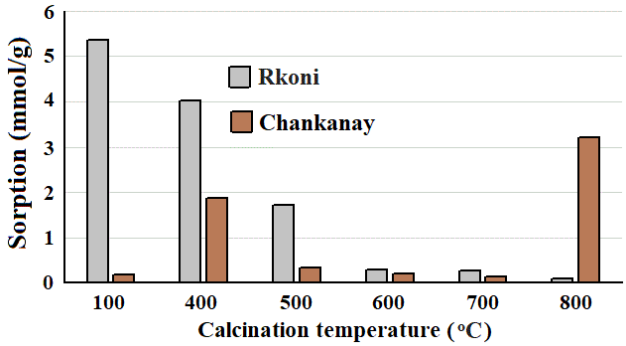

Figure 4 Water sorption (p/p_0=0.4, 20°C) of Georgian (Rkoni) and Kazakhstani (Chankanay) zeolites calcined at different temperatures

Value of water sorption at relative pressure p/p_0=0.4 represents sorption capacity in micropores, and this indicator for the Georgian zeolite decreases monotonically with an increase in the calcination temperature; for the Kazakhstani sample it significantly increases after calcination at 400°C, then decreases, but reaches a maximum after calcination at 800°C. However, although changes in the pore systems of the studied zeolites are directly related to their thermal stability, the study of the state of pores as a result of heat treatment is a separate topic.

CONCLUSION

It is found that partial amorphization of the heulandite phase in the Rkoni sample begins at ≈300°C, transition to the metastable heulandite B is not observed, but formation of the 9.GB.05 group minerals and quartz is confirmed, the complete collapse of the HEU crystal structure occurs at ≈700°C. The chabazite phase in both samples is stable up to ≈900°C. The volume of micropores available for water molecules in the Rkoni sample (HEU/CHA≈8) decreases monotonically with an increase in the calcination temperature, thereby demonstrating a gradual destruction of the adsorbent structure; in the Chankanay sample (HEU/CHA≈1) this volume reaches two maxima (after calcination at 400 and 800°C) due to structural changes.

ACKNOWLEDGEMENT

This work was supported by the International Science and Technology Center (ISTC) under the project GE-2506 "Scientific substantiation of the possibility of creating new bactericidal zeolite filter materials for purification-decontamination of water from various sources".

REFERENCES

1. Hardi G.W., Maras M.A.J., Riva Y.R.R., Rahman S.F. (2020) A review of natural zeolites and their applications: Environmental and industrial perspectives. International Journal of Applied Engineering Research, 15(7), 730-734.
2. Li, Y., Yu, J. (2021) Emerging applications of zeolites in catalysis, separation and host–guest assembly. Nature Reviews Materials, 6, 1156–1174.
3. Ma, B., Lothenbach, B. (2021) Synthesis, characterization, and thermodynamic study of selected K-based zeolites. Cement and Concrete Research, 148, 106537.
4. Grela, A., Kuc, J., Bajda, T. (2021) A review of the application of zeolites and mesoporous silica materials in the removal of non-steroidal anti-flammatory drugs and antibiotics from water. Materials, 14(17), 4994, 1-24.
5. Tsitsishvili V., Dolaberidze N., Nijaradze M., Mirdzveli N., Amiridze Z., Khutsishvili B., Virsaladze K., Kapanadze T. (2021) Properties of Georgian heulandite-clinoptilolite and its application for production of bactericidal adsorbents. Scientific collection “InterConf”, 59, 633-642.
6. Paritova A.E., Sarsembayeva N.B., Buralhiev B., Slyamova A.E. (2013) An experimental study of the effect of natural zeolite of Chankanay deposits on fish-breeding and biological and hematological parameters of the body of fish. Global Veterinaria, 11(3), 348-351.
7. Tsitsishvili, V., Panayotova, M., Miyamoto, M., Dolaberidze, N., Mirdzveli, N., Nijaradze, M., Amiridze, Z., Klarjeishvili, N., Khutsishvili, B., Dzhakipbekova, N., Harutyunyan, L. (2022) Characterization of Georgian, Kazakh and Armenian natural heulandite-clinoptilolites. Bull. Georg. Natl Acad. Sci., 16(4), 115–122.
8. Tsitsishvili G.V., Andronikashvili T.G., Kirov G.N., Filizova L.D. (1991) Natural zeolites. Ellis Horwood, Chichester (UK).
9. Tsitsishvili V., Machaladze T., Dolaberidze N., Nijaradze M., Mirdzveli N., Djakipbekova N., Harutyunyan L. (2022) Dehydration and structural transformations during thermal treatment of Georgian, Kazakhstani and Armenian natural heulandite-clinoptilolites. Scientific collection “InterConf”, 136, 356-364.
10. Baerlocher Ch., McCusker L.B., Olson D.H. (2007) Atlas of zeolite framework types. 6th revised edition, Elsevier, Amsterdam.
11. Koizumi, M. (1953) The differential thermal analysis curves and the dehydration curves of zeolites. Mineralogical Journal, 1(1), 36-47.
12. Pechar, F., Rykl, D. (1985) Study of the thermal stability of the natural zeolite heulandite. Chemical Papers, 39(3), 369-377.
13. Lee, E.-H., Kim, J.-M., Oh, M.-K., Kim, M.-J., Lee, K.-Y., Kim, K.-W., Kim, H.-J., Kim, I.-S., Chung, D.-Y., Moon, J.-K., Choi, J.-W. (2017) Thermal decomposition of chabazite-Cs and chabazite-PCFC-Cs zeolite. Proceedings of the Korean Radioactive Waste Society Conference, 311-312.

XV International Mineral Processing and Recycling Conference
17-19 May 2023, Belgrade, Serbia

COMPOSITION OF GEORGIAN AND KAZAKHSTANI NATURAL HEULANDITES

V. Tsitsishvili[1], M. Panayotova[2], N. Dolaberidze[3], N. Mirdzveli[3#], M. Nijaradze[3], Z. Amiridze[3], N. Klarjeishvili[3], N. Dzhakipbekova[4]

[1] Georgian National Academy of Sciences, Tbilisi, Georgia (Saqartvelo)
[2] Department of Chemistry, University of Mining & Geology "St. Ivan Rilski", Sofia, Bulgaria
[3] Petre Melikishvili Institute of Physical & Organic Chemistry at Ivane Javakhishvili Tbilisi State University, Tbilisi, Georgia
[4] Mukhtar Auezov South Kazakhstan State University, Shymkent, Kazakhstan

ABSTRACT – To create bactericidal zeolite filter materials for water purification and disinfection, heulandite-containing tuffs from the Rkoni plot of the Tedzami-Dzegvi deposit (Eastern Georgia) and the Chankanay deposit (Almaty region of Kazakhstan) were selected. According to the results of quantitative determination of zeolite content by thermochemical method, in Georgian tuff (Si/Al=3.6) it reaches 90%, in Kazakhstani tuff (Si/Al=2.9) it is up to 70%. Powder X-ray diffraction patterns show that the zeolite phase consists of two types: HEU as the main and CHA as a minor in the Rkoni sample, while the Chankanay sample contains heulandite and chabazite in comparable amounts, quartz and iron oxides as impurities.

Keywords: Heulandite, Chabazite, Tedzami-Dzegvi, Chankanay.

INTRODUCTION

The purpose of drinking water and waste water treatment is to remove of dissolved and suspended pollutants, and technically this is carried out, as a rule, by adsorption of these substances on activated carbon, clay minerals, biopolymers, and zeolites [1-3]. Zeolites are aluminosilicates of general formula $M_x[Al_xSi_yO_{2(x+y)}]\cdot mH_2O$ ($M^+ = Na^+, K^+, \ldots$ $½Ca^{2+}, ½Mg^{2+}, \ldots$) and have open, "framework" structure with cages and channels that determine molecular-sieve, sorption and other properties; zeolites adsorb a variety of heavy metals and ammonia, and remove a wide range of pollutants. Natural zeolites are usually characterized by a developed system of meso- and macropores in which large organic molecules, supramolecular aggregations, and even microorganisms can be adsorbed or immobilized. Natural zeolites outperform conventional granular materials in water purification, they are cost-effective, abrasion resistant, non-toxic and environmentally friendly, especially in the treatment of acid mine drainage, landfill leachate, nuclear fallout, urban runoff and other special wastewater streams [1]. Heulandite-clinoptilolite is one of the most widespread natural zeolites, it is well studied and widely used as an adsorbent, ion exchanger and catalyst in industry,

corresponding author: nato.mirdzveli@gmail.com

construction, medicine, agriculture and environment protection [3-5]. Among natural zeolites, heulandite-clinoptilolites are the most widespread, studied and widely used in many countries of the world. Heulandite-clinoptilolites belong to the HEU group of zeolites (crystal chemical data $|Ca_4(H_2O)_{24}|$ $[Al_8Si_{28}O_{72}]$-**HEU** [6]), but the chemical composition of their varieties is characterized by remarkable changes in the Si/Al ratio (from 2.7 to 5.5) as well as in the content of exchangeable cations [7].

The aim of this study was to characterize heulandites of Georgian and Kazakhstani origin selected for implementation of the project "Scientific substantiation of the possibility of creating new bactericidal zeolite filter materials for purification-+decontamination of water from various sources" granted by the International Science and Technology Center.

EXPERIMENTAL

Heulandite-clinoptilolite-containing rock from the Rkoni plot of Tedzami-Dzegvi deposit (Eastern Georgia), used for production of bactericidal adsorbents [8], and the zeolitic tuff of Chankanay deposit (Kazakhstan, Almaty region), successfully used in fish-breeding [9], were studied. Quantitative determination of zeolite content in rocks was carried out by Belitski's thermochemical method [10].

Preparation of zeolite samples included 1) grinding of rock using a standard crusher, 2) fractionation of obtained material using a set of sieves according to the standard requirements for filtering material for water purification (the particle size 1-1.4 mm or 14-16 mesh), 3) washing with distilled water or dilute HCl solution (0.025 N) to remove clay impurities, and 4) drying of the prepared samples under static conditions, first in air and then in a thermostat at a temperature of 95-100 °C.

Chemical composition of zeolites was calculated from the X-ray energy dispersive (XRED) spectra obtained from scanning electron microscope JSM-6490LV equipped with INCA Energy 350 XRED analyzer (see Figure 1),

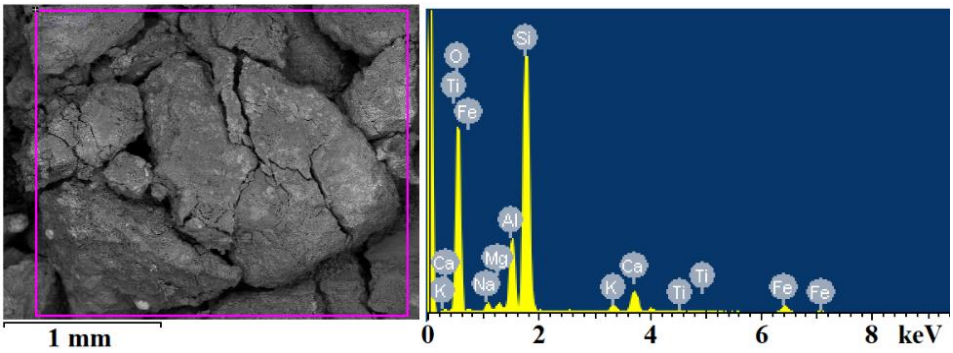

Figure 1 SEM image and typical XRED spectrum of raw heulandite

Powder X-ray diffraction patterns were obtained from modernized diffractometer Dron-4 (USSR) and X-ray diffractometer D8 Endeavor (Bruker, Germany) both employing the Cu-K_α line (λ = 0.154056 nm); the samples were scanned in the 2Θ range of 5° to 80° with a 0.02° step at a scanning speed of 1°/min.

RESULTS AND DISCUSSION

According to the results of quantitative determination of zeolite content by thermochemical method, in Georgian rock it reaches 90%, in Kazakhstani tuff it is up to 70%. Chemical composition described by averaged empirical formulas and scientific weight ion exchange capacity (SWIEC) of the studied samples are given in Table 1.

Table 1 Chemical composition and scientific weight capacity of the studied samples

Characteristic	Sample from	
	Rkoni	Chankanay
Empirical formula*	$Na_{0.25}K_{0.06}Ca_{0.19}Mg_{0.15})$ $[AlSi_{3.6}O_{9.2}]\cdot 3H_2O$	$Na_{0.115}K_{0.079}Ca_{0.228}Mg_{0.175})$ $[AlSi_{2.96}O_{7.92}]\cdot 3H_2O$
SWIEC (meqv/g)	3.03	3.43

*When processing the XRED data, the number of oxygen atoms in the zeolite lattice was taken based on the total number of Si and Al atoms as $AlSi_xO_{2(1+x)}$, and the number of oxygen atoms in water molecules was rounded to the nearest integer as $Al(H_2O)_n$.

According to the EDS data, the sample from the Rkoni plot is a high-silica heulandite (Si/Al=3.6) containing relatively high content of sodium exchangeable ions, while the sample from the Chankanay deposit is calcium heulandite (Si/Al≈3). In addition, XRED spectra (Figure 1) show the presence of titanium and iron atoms. The titanium content in Georgian heulandite is one atom per 240±20 aluminum and silicon atoms, Kazakhstani zeolite contains approx. two times less titanium, and since this value remains unchanged for ion-exchanged Georgian samples [8], there is reason to believe that titanium atoms are part of the zeolite crystal lattice. On the contrary, iron atoms (0.2 and 0.33 per Al atom in samples from Rkoni and Chankanay, respectively) and a part of the calcium atoms compose micrometric amorphous or crystalline impurity inclusions visible in the layered XRED images (Figure 2).

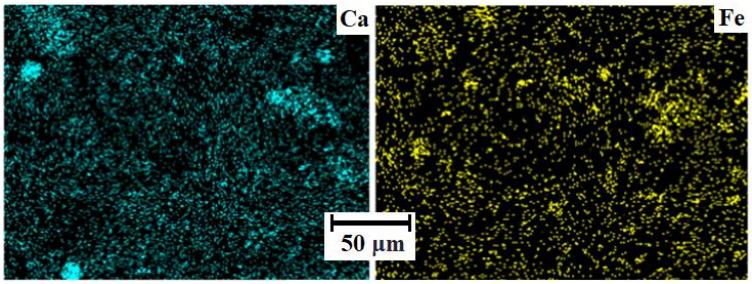

Figure 2 Layered XRED images of calcium (left) and iron (right) distribution

The scientific weight ion exchange capacity of the zeolite from Rkoni is close to the calculated one for the structure of heulandite HEU (3.08 meqv/g), the capacity of the zeolite of the Chankanay deposit is higher due to the higher aluminum content

Powder X-ray diffraction patterns of these tuffs show that the zeolite phase consists of two types of zeolites: HEU as the main and CHA (crystal chemical data $|Ca_6(H_2O)_{40}|[Al_{12}Si_{24}O_{72}]$-**CHA** [6]) as a minor in the Rkoni sample, while the Chankanay sample contains both HEU and CHA in comparable amounts.

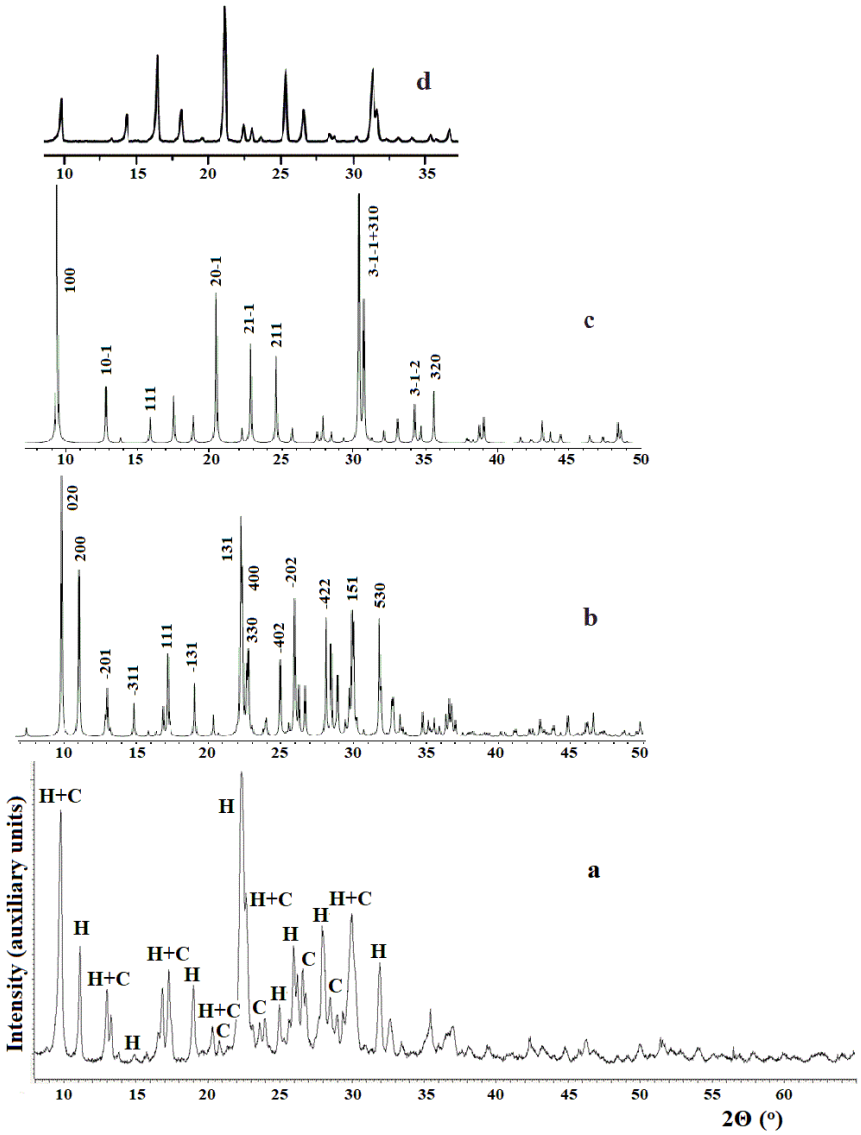

Figure 3 Powder XRD pattern of the Rkoni zeolite (**a**), simulated patterns of heulandite (**b**) and chabazite (**c**) from [11], experimental pattern of chabazite (**d**) from [13]

The assignment of peaks to HEU (H) and CHA (C) types in the powder X-ray diffraction pattern of the Rkoni sample is shown in Figure 3; simulated XRD patterns of heulandite (Figure 3b) and chabazite (Figure 3c) with respective Miller hkl indices are taken from a collection of simulated XRD powder patterns [11]. The simulated pattern of chabazite is based on the data for the potassium form of chabazite with a molar ratio of Si/Al=2.44 [12], but current studies in the field of chabazite synthesis [13] show that the position and intensity of the peaks on XRD patterns strongly depend on the nature

and amount of compensating ions; therefore, the experimental pattern of high-silica chabazite (Figure 3d) is also taken into account.

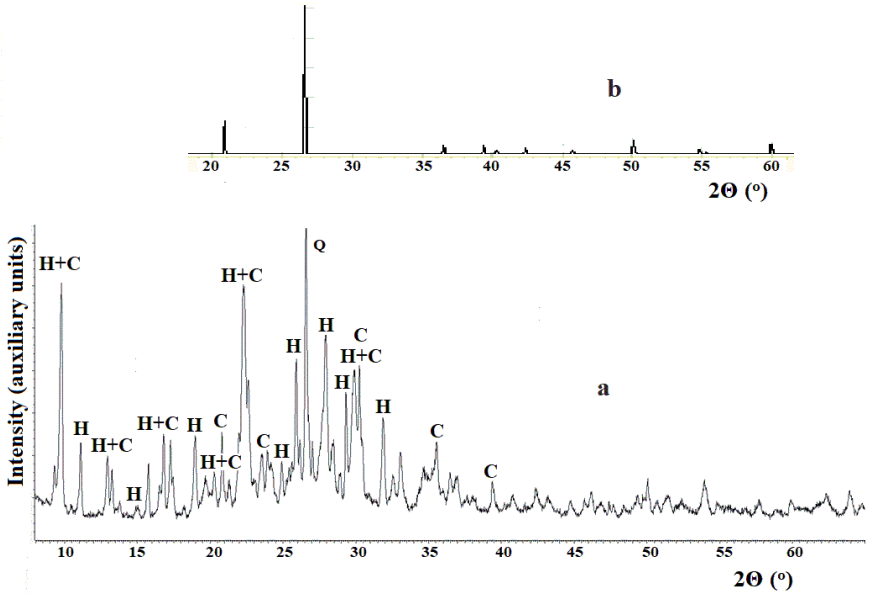

Figure 4 Powder XRD pattern of the Chankanay zeolite (**a**) and pattern of quartz (**b**)

The same simulated and experimental patterns were used for the assignment of peaks in the powder XRD pattern of the Chankanay sample shown in Figure 4; peaks of chabazite (C) have higher intensity comparable to the peaks of heulandite (H). A strong peak at 2Θ ≈ 26.7°, which persists even after calcination of the sample at 800 °C, is attributed to the (011) reflection of quartz (Q); XRD pattern (Figure 4b) is taken from the RRUFF database (https://rruff.info/quartz/R100134).

CONCLUSION

Zeolite phase content in Georgian tuff from the Rkoni plot of the Tedzami-Dzegvi deposit reaches 90%, consists of two types: HEU as the main and CHA as a minor, its chemical composition is described by empirical formula $Na_{0.25}K_{0.06}Ca_{0.19}Mg_{0.15})[AlSi_{3.6}O_{9.2}]\cdot 3H_2O$, main impurities are iron and calcium oxides, 0.2 and 0.14 per Al atom, respectively; zeolite phase content of Kazakhstani tuff from the Chankanay deposit is up to 70% with chemical composition $(Na_{0.115}K_{0.079}Ca_{0.228}Mg_{0.175})[AlSi_{2.96}O_{7.92}]\cdot 3H_2O$, in which HEU, CHA and the major impurity of quartz are in comparable amounts, ≈35%, ≈35%, and ≈30%, respectively, minor impurities are $Fe_{0.33}$ and $Ca_{0.167}$ per Al atom.

ACKNOWLEDGEMENT

This work was supported by the International Science and Technology Center (ISTC) under the project GE-2506 "Scientific substantiation of the possibility of creating new bactericidal zeolite filter materials for purification-decontamination of water from various sources".

REFERENCES

1. Delkash M., Bakhshayesh B.E., Kazemian H. (2015) Using zeolitic adsorbents to cleanup special wastewater streams: A review. Micropor. Mesopor. Mat., 214, 224-241
2. Anjum, M., Miandad R., Waqas, M., Gehany, F., Barakat, M.A. (2016) Remediation of wastewater using various nanomaterials. Review. Arabian Journal of Chemistry, 12(8), 4897-4919.
3. Hardi G.W., Maras M.A.J., Riva Y.R.R., Rahman S.F. (2020) A review of natural zeolites and their applications: Environmental and industrial perspectives. International Journal of Applied Engineering Research, 15(7), 730-734.
4. Kraljević Pavelić S., Simović Medica J., Gumbarević D., Filošević A., Pržulj N., Pavelić K. (2018) Critical review on zeolite clinoptilolite safety and medical applications in vivo., Frontiers in Pharmacology, 9, 1350.
5. Cataldo E., Salvi L., Paoli F., Fucile M., Masciandaro G., Manzi D., Masini C.M., Mattii G.B. (2021) Application of zeolites in agriculture and other potential uses: a review. Agronomy, 11, 1547-1561.
6. Baerlocher Ch., McCusker L.B., Olson D.H. (2007) Atlas of zeolite framework types. 6th revised edition, Elsevier, Amsterdam.
7. Tsitsishvili G.V., Andronikashvili T.G., Kirov G.N., Filizova L.D. (1991) Natural zeolites. Ellis Horwood, Chichester (UK).
8. Tsitsishvili V., Dolaberidze N., Nijaradze M., Mirdzveli N., Amiridze Z., Khutsishvili B., Virsaladze K., Kapanadze T. (2021) Properties of Georgian heulandite-clinoptilolite and its application for production of bactericidal adsorbents. Scientific collection “InterConf”, 59, 633-642.
9. Paritova A.E., Sarsembayeva N.B., Buralhiev B., Slyamova A.E. (2013) An experimental study of the effect of natural zeolite of Chankanay deposits on fish-breeding and biological and hematological parameters of the body of fish. Global Veterinaria, 11(3), 348-351.
10. Belitsky I.A., Berenstein B.G., Gorbunov A.V., Drebuschak V.A., Seretkina Yu.V., Chelishchev N.F. (1988) Quantitative determination of zeolite content in rocks. Thermochemical method. Institute of Geology and Geophysics, Siberian Branch of the USSR Academy of Sciences, Novosibirsk (in Russian).
11. Treacy M.M.J., Higgins J.B. (2001) Collection of simulated XRD powder patterns for zeolites. Elsevier, Amsterdam-London-New York-Oxford-Paris-Shannon-Tokyo.
12. Calligaris M., Nardin G., Randaccio L. (1983) Cation site location in hydrated chabazites. Crystal structure of potassium- and silver- exchanged chabazites. Zeolites, 3, 205-208.
13. Dang L., Le S., Lobo R., Pham T. (2020) Hydrothermal synthesis of alkali-free chabazite zeolites. Journal of Porous Materials, 27, 1481-1489.

XV International Mineral Processing and Recycling Conference
17-19 May 2023, Belgrade, Serbia

NANOCRYSTALLIZATION OF POTASSIUM NIOBIUM GERMANATE GLASSES

S. Matijašević[1#], S. Grujić[2], V. Topalović[1], J. Stojanović[1], J. Nikolić [1], V. Savić[1], S. Zildžović[1]

[1] Institute for Technology of Nuclear and other Mineral Raw Materials, 86 Franchet d' Esperey St, 11000 Belgrade, Serbia

[2] Faculty of Technology and Metallurgy, 4 Karnegijeva St.,11000 Belgrade, Serbia

ABSTRACT – This paper presents the effect of K_2O content on phase composition of the nanocrystallized niobium germanate glasses. It was shown that the exothermal peak temperature, T_p, shifted toward the higher temperatures with increasing content of K_2O. Such increase of K_2O content causes a decrease of GeO_2 content in the primary phases. The crystals below 100 nm were detected in the samples.

Keywords: Crystallization, Content of K_2O, Niobium Germanate Glasses.

INTRODUCTION

Transparent or slightly opalescent crystallizes glasses with second-order optical non-linearity are of great scientific and industrial interest [1-3]. Nanocrystallzation of glasses is an effective method for fabrication of such materials. Developing techniques for creating nanostructures is an area that requires substantial effort. In this study, the attention was focus on K_2O-Nb_2O_5-GeO_2 glasses, because various potassium germanate-based crystals show a second harmonic generation [4]. For this investigation the glass composition $18.86K_2O{\cdot}53.22Nb_2O_5{\cdot}27.92GeO_2$ (wt%) was selected. The influence of K_2O content on phase composition of the nanocrystallized glasses was studied.

EXPERIMENTAL

The starting materials used are reagent grade GeO_2, K_2CO_3, and Nb_2O_5. The appropriate batch compositions were melted in an electric furnace Carbolite BLF 17/3 at 1200°C for 1 h in a Pt crucible. The melts were cast on a steel plate and cooled in air. The chemical analysis was performed using spectrophotometer AAS PERKIN ELMER Analyst 703. The method of atomic absorption spectrophotometry (AAS) was used to determine the content of oxides in glass, after the destruction of the sample by NaOH, composition was determined by analyzing the content of their cations in solution. The measurement uncertainty is 0.86%.

The peak temperature of crystallization T_p was determined by DTA run of glass powder with Netzsch STA 409 EP instrument and Al_2O_3 powder as the reference

corresponding author: s.matijasevic@itnms.ac.rs

material in a static air atmosphere. In the experiments, a constant weight (100 mg) of the samples were heated at rate β = 10 °C/min. Powdered glass samples of particle sizes < 0.038 mm were used. Before the DTA experiment, the device was calibrated with quartz standard purity of 99.995% of known crystallization temperature.

The experiments with bulk glass samples were performed in a two-stage regime. The samples were heated at a heating rate β =10 °C/min up to the desired temperature at which they were maintained for different times in an electric furnace, Carbolite CWF 13/13, with automatic regulation and a temperature accuracy of $\pm$ 1°C. The heat treatment temperatures were in the range T_c = 600 – 800 °C. Finally, the samples were removed from the furnace and then crushed in an agate mortar. Powdered samples were used for X-ray analyses and fractures (fracture surfaces) of the crystallized samples were analyzed by Scanning electron microscope (SEM).

Identification of the phase crystallized was performed with the Powder X-ray diffraction (XRD) analysis.

The Philips PW-1710 automatic diffractometer with the following characteristics was used for measurement: - X-ray tube Cu LFF 40 kW; 32 mA; - graphite monochromator and proportional counter with xenon; - recording area (2θ) from 4 to 70° (scan time from 0 to 5 s). The intensities of diffracted CuKα1 X-rays (λ = 0.154060 nm) were measured at room temperature.

The Powder Cell Program was used for determination of primary phases and crystallite dimensions of all determined phases were calculated using MAUD software [5, 6]. A Jeol JSM 6460 microscope was used for the SEM investigations.

RESULTS AND DISCUSSION

The glass mixture for obtaining the selected glass composition was melted in an electric furnace. The resulting melts were poured on a steel plate and cooled in the air. During cooling, the melt solidified into a transparent, homogeneous, and colorless glass. XRD analysis confirmed the quenched melts to be vitreous (figure not shown). The results of the chemical analysis of the investigated glasses are listed in Table 1.

Table 1 Chemical composition of the glasses

Sample	Composition [wt%]			
	K_2O	Nb_2O_5	GeO_2	$\sum$
G-10	18.25	57.48	24.27	100
G-15	19.52	57.24	23.24	100
G-25	20.30	56.97	22.73	100
G-28	22.71	54.59	22.70	100

The results of the chemical analysis show that a glasses with the content of K_2O: 18.25 (G-10), 19.52 (G-15), 20.30 (G-25) and 22.71 (G-28) (%wt) were obtained by addition of 1, 2 and 4 wt% K_2O to glass G-10.

In Figure 1, the DTA curves of these samples recorded at heating rate β=10 °C/min in the temperature range of 400-800°C are shown. At these curves the exothermal temperature peaks which correspond to the crystallization of glass were registered.

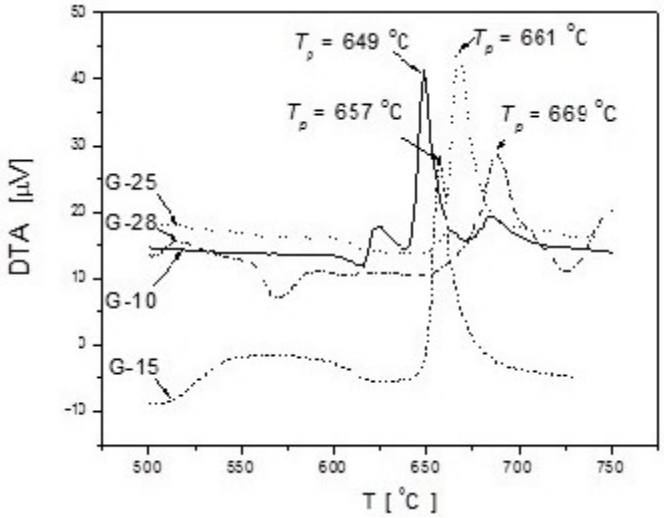

Figure 1 DTA curves recorded for the glasses G-10, G-15, G-25 and G-28.

As can be seen in Figure 1, the exothermal peak temperature, T_p, shifted toward the higher temperatures with increasing content of K_2O. Such behaviour indicates the formation of different crystalline phases during crystallization of these glasses.

To determine the phases appeared the experiments under isothermal conditions were performed with bulk samples.

In two-stage regime the samples were first treated isothermally at the nucleation temperature between T = 600-630°C, for different times.

The crystallization temperatures were in the range T_c=650-800°C. The samples were kept at the crystallization temperatures for different times, in the range t_c=1-100 h. The XRD patterns of the crystallized glass samples G-10, G-15, G-25 and G-28 are shown in Figure 2.

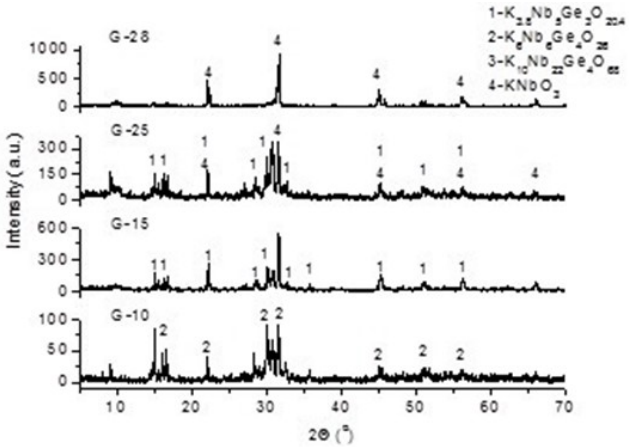

Figure 2 Powder XRD patterns for the crystallized samples of glasses G-10, G-15, G-25 and G-28. The numbers (1-4) designate the primary phases

It can be seen that several crystalline phases appeared in the samples which clearly demonstrated a primary crystallization of these glasses. The phase which is present in a largest amount crystallizes as primary one. Other phases appear as secondary ones. These results shows that the role of some phases changed with increasing K_2O content. In the sample with 18.23 wt% of K_2O, a primary $K_6Nb_6Ge_4O_{26}$ phase appeared. Otherwise, in the samples with 19.52 and 20.30 wt% of K_2O the primary phase is $K_{3.8}Nb_5Ge_3O_{20.4}$ while in the sample with highest K_2O content of 22.71 wt% only the $KNbO_3$ phase appeared.

The results show that such compositions of glasses are very sensitive on changes of K_2O content. By increasing of K_2O content as primary germanate phases with low contents of germanium oxide appeared, while in the glasses with K_2O content > 20 wt% the primary phase does not contain germanium oxide. Such behaviour confirms that an increase of K_2O content causes the change of kinetics and mechanism of the phases formation which indicates a very complex crystallization behaviour of these glasses. Figure 3, shows SEM micrograph of compact sample of G-10 glass composition processed at nucleation temperature during 24h.

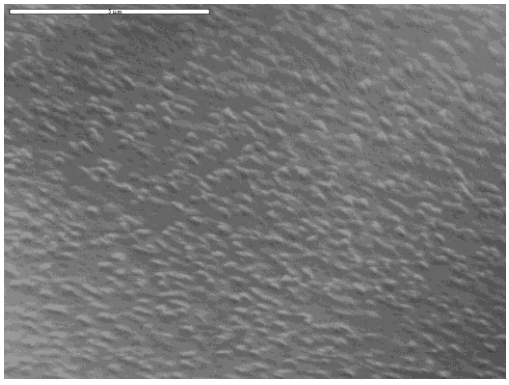

Figure 3 SEM micrography of glass treated at temperature T = 650 °C, t = 24 h, the length of the bar is given in the pictures (5 μm), fracture surfaces are captured

The samples crystallized are slightly opalescent and the dimensions of crystals were below 100 nm indicating a glass nanocrystallization (SEM micrographs).

CONCLUSION

The results presented in the study showed that these glasses crystallized with primary crystallization. By increasing K_2O content the germanate phases with low content of germanium oxide were appeared as primary ones. The nanocrystallization of these glasses was registered and crystals dimensions below 100 nm were observed.

ACKNOWLEDGEMENT

The authors are grateful to the Ministry of Science, Technological Development and Innovation of Serbia for financial support (grant contract No.: 451-03-47/2023-01/200023 and 451-03-47/2023-01/200135).

REFERENCES

1. Matijašević, S.D., Tošić, M.B., Grujić, S.R., Stojanović, J.N., Živanović, V.D., Nikolić, J.D. (2011) The effect of K2O on the Crystallization of Niobium Germanate glasses. Sci. Sinter, 43 (1), 47-53.
2. Guedes, L.F.N., Marcondes, L.M., Evangelista, R.O., Batista, G., Mendoza, V.G., Cassanjes, F.C., Poirier, G.Y. (2020) Effect of alkaline modifiers on the structural, optical and crystallization properties of niobium germanate glasses and glass-ceramics. Opt. Mater., 105, 109866.
3. Matijašević, S., Savić, V., Topalović, V., Stojanović, J., Nikolić, J., Zildžović, S., Grujić, S. (2022) The complex crystallization of potassium-niobium-germanate system. In 53th International October Conference on Mining and Metallurgy-IOCMM 2022. Bor, Sebia, Proceedings, 97-100.
4. Narita, K., Takahashi, Y., Benino, Y., Fujiwara, T., Komatsu, T. (2004) Prominent Nanocrystallization of $25K_2O{\cdot}25Nb_2O_5{\cdot}50GeO_2$ Glass. J.Am.Ceram.Soc., 87, 113-118.
5. Kraus, W., Nolze, G. (2000) Powder Cell for windows 2.4, www.CCP14.ac.uk.
6. Lutterotti, L. (2009), MAUD version 2.074, http://www.ing.unitn.it/~maud/.

XV International Mineral Processing and Recycling Conference
May 17-19, 2023, Belgrade, Serbia

ESTIMATING THE ACCURACY, PRECISION, AND RECALL OF THE HAND-SORTING OF A BRAZILIAN CHROMIUM ORE

A. C. Silva[1#], E. M. S. Silva[1], P. S. Oliveira[2], A. F. Nascimento[2], A. P. Vieira Filho[2], D. B. Carvalho Neto[2]

[1] Federal University of Catalão, Modelling and Mineral Processing Research Lab, Catalão, Brazil

[2] Companhia de Ferro Ligas da Bahia (FERBASA), Senhor do Bonfim, Brazil

ABSTRACT – For many decades FERBASA, the Brazilian major producer of chromium ore and its alloys, relayed on hand-sorting, not only for chromite concentration, but also to estimate the ROM grade. In this work an experiment was carried out to evaluate the accuracy, precision and recall of this methodology. To do so, thirty-two rock samples were collected and submitted to hand-sorting. The found results indicated that the accuracy was 27.45%, the precision 27.22%, and the recall 26.76%, too low to the considered as a valid methodology.

Keywords: Hand-sorting, Error Estimation, Chromite, Brazilian Ore, FERBASA.

INTRODUCTION

Brazil is the 11th larger chromium producer, with Companhia de Ferro Ligas da Bahia (FERBASA) being the largest producer. The company operates two chromite mines, located in the Center-North region of the state of Bahia, Brazil, 90 miles away from each other: Ipueira mine in the Chromite District of Vale do Jacurici and the Coitezeiro mine in the Chromite District of Campo Formoso. Operations in Coitezeiro began in 1961, using the open pit mining method, which is still being used. Ipueira mine operations began in 1973, initially as an open pit mining, and later, through underground methods. Most of the ore production is consumed internally at the Pojuca metallurgical plant, to produce ferrochrome and ferrosilicon chrome alloys. The Figure 1 shows the FERBASA simplified flowsheet. The run of mine (ROM) ore is feed in a primary and secondary crushers (both universal jaw crushers). The secondary crusher operates in a closed circuit with a double deck vibratory screen. The oversize (+101 mm) returns to the secondary crusher, the midsize material (-101+32 mm) feeds the Steinert ore sorter circuit, composed by two ore sorters operating in series and in closed circuit, models XSS 200 430 V12U and KSS 200 520 MS XT. The -32 mm fraction (undersize) feeds a triple deck vibratory screen. The first deck oversize (-32+19 mm) feeds a TOMRA Sorting Solutions ore sorter, model COM TERTIARY XRT 1200/B. All ore sorters operate with 160 keV, 160 kV and 0,5 mA (Steinert) and 10 mA (Tomra). The -19+10 mm feeds two Yuba jigs (lateral diaphragm) operating in parallel. Finally, the undersize fraction (-10 mm) and the products referred as

corresponding author: ancarsil@ufcat.edu.br

disseminated ore feeds a gravimetric plant, where it will be grinded (two stage grinding, with ball mills) and concentrated using spirals and magnetic separators to produce chromite sand, mainly used as steel casting.

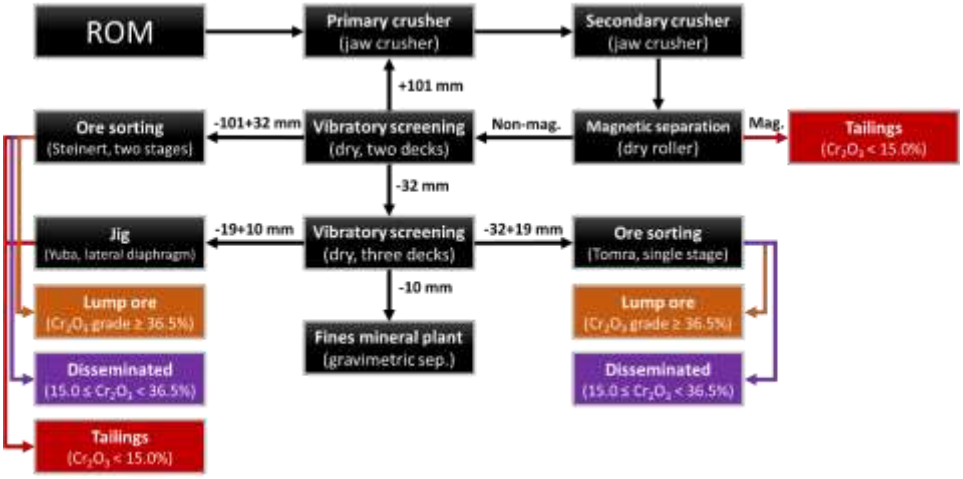

Figure 1 FERBASA simplified mineral processing flowsheet

Hand-sorting is the oldest ore separation process used by mankind. The sorting of ores is a universal practice, with color being the main separation criterion used to obtain concentrates. The list of ores that were, or are still manually separated, is extensive, including asbestos, barite, magnesite, diamond and semi-precious stones, mica, limestone, etc. [1].

According to Salter and Wyatt [2], hand-sorting of rocks and mineral products has been conducted since ancient times and numerous mining historians have described the practice in detail. The author pointed out that the romantic imagery (but real misery) of the work belied what became a very efficient concentration method. Even complex high-grade ores have been concentrated. The Cornish tin/sulfide ores were sorted into six fractions based on their mineralogy, whilst at Clausthal in Germany during the late nineteenth century up to 16 classes of products were hand-sorted [3].

Taggart [3] described many hand-sorting operations of the early twentieth century but as ore grades and liberation sizes decreased, the scale and economics of processing operations changed, and new technology was introduced, hand-sorting became impractical, impossible, or too expensive.

According to Salter and Wyatt [2], by the late 1960s and early 1970s hand-sorting was largely abandoned [4, 5] and it is now accepted that complex and low-grade ore characteristics, together with free market economics, preclude the application of hand-sorting except in rare circumstances.

Cutmore and Eberhardt [6] apud Varela et al. [1] conducted a literature review from 1960-2000 and found more than 1,300 papers describing various aspects of the hand-sorting of ores.

Hand-sorting has been part of FERBASA's operations since the beginning. Initially, all chromite ore was hand-sorted, an operation that demanded many collaborators working

simultaneously. Since November 2013, the introduction of the ore sorters and the mineral processing plant changed entirely this operation. However, they kept hand-sorting samples in order to estimate the grade of the ore. In this methodology, rock samples are separated by size and labeled as lump ore (Cr_2O_3 grade ≥ 36.5%), disseminated (36.5% > Cr_2O_3 grade ≥ 15.0%) and tailings (Cr_2O_3 grade < 15.0%), as seen in Figure 2. In this work the hand-sorting methodology was investigated, in order to evaluate its error.

Figure 2 Hand-sorting in FERBASA. Rocks are manually classified according to their lithology and size

EXPERIMENTAL

Rocks from two different sources (ROM and a tailing stockpile) were sampled (approximately 100 kg of each source) and sent to the ore sorters circuit. The products were then resampled resulting in thirty-two rock samples, which were photographed, weighted, and randomly aligned on top of a table. FERBASA works were them asked to move the samples to the correct line, labeling them as lump ore (green line on the table), disseminated (orange) or tailing (red), as seen in Figure 3.

The works could interact with only one rock at the time. The experiment ended after all samples were sorted. The time need to perform the hand-sorting were also measured. In total 46 workers were submitted to the text, with different academic backgrounds and from areas in the company, such as geology (two workers), engineering (two workers) and hand-sorting area.

After the experiment the samples were crushed in a jaw crusher, grinded in a puck mill (also known as a rig mill or shatterbox) and chemically analyzed in a Rigaku ZSX Primus III+ dispersive x-ray fluorescence spectrometer. Therefore, the samples were labeled as lump ore, disseminated and tailings according to the Cr_2O_3 grade (chemically labeling) and according to the workers.

RESULTS AND DISCUSSION

Figure 4 shows the samples characterization. It is possible to notice that the samples masses were distributed according to the Cr_2O_3 grade, not showing any bias. The Cr_2O_3 grade, however, presented a trimodal distribution, with a positive asymmetry (or skew) for the low grades (tailings), negative asymmetry for the high grades (or lump ore) and normal distribution for the middle grade ore (disseminated).

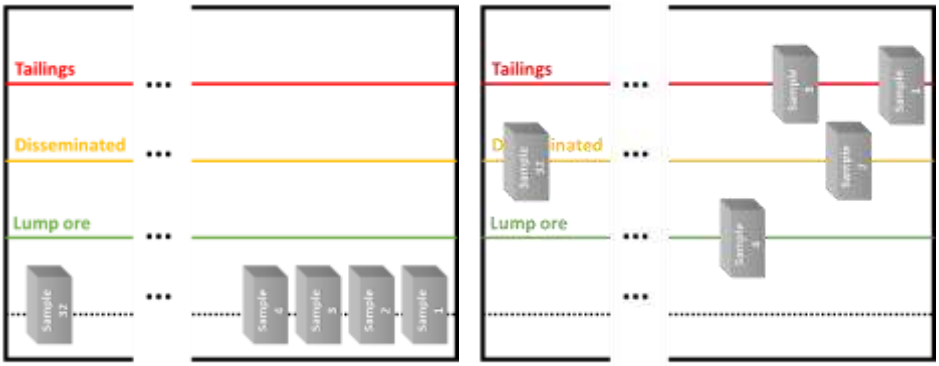

(a) (b)

Figure 3 Hand-sorting experiment: (a) initial setup and (b) end of the experiment, after all thirty-two samples were sorted

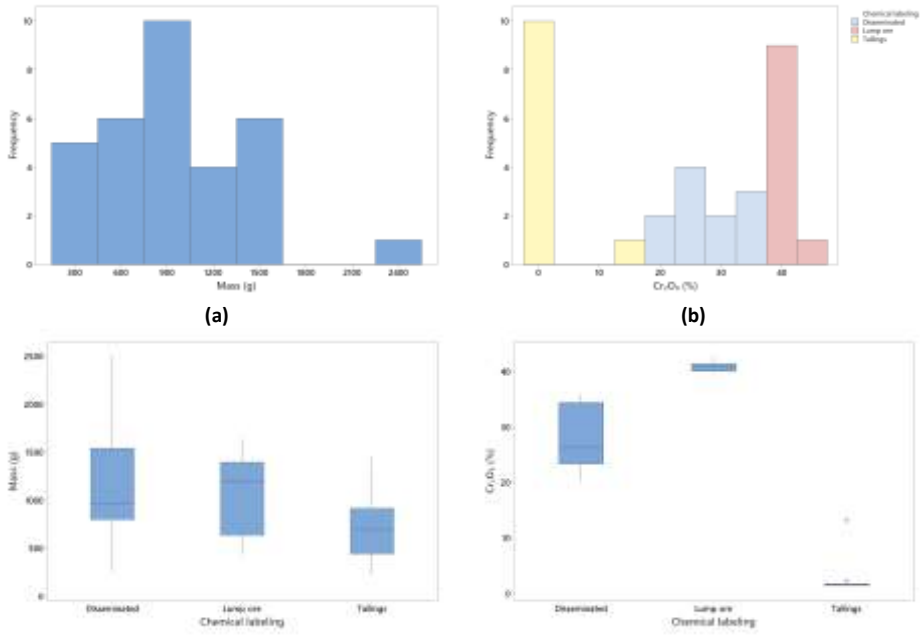

(a) (b)

(c) (d)

Figure 4 Samples characterization: histograms of mass (a) and Cr_2O_3 grade (b) and boxplots of mass (c) and Cr_2O_3 grade (d) according to the chemical labeling

Figure 5 presents Six samples used in the tests: two tailings (Cr_2O_3 = 1.6% 5a and 1.5% 5b), disseminated (34.3% 5c and 13.1% 5d), and lump ore (42.2% 5e and 41% 5f).

Figure 5 Six samples used in the tests: tailings (a and b), disseminated (c and d), and lump ore (e and f)

Figure 6 presents the experiment results as a confusion matrix. The numbers indicate the percentage of the samples that were labeled chemically and by hand-sorting. The best result was obtained for the disseminated ore, with 40.12% of the samples corrected sorted by the workers. However, for the lump ore the result was only 20% and for the tailings 21.54%. The found accuracy was 27.45%, the precision (ratio between the true positives and the sum of true positives and false positives) was 27.22%, and the recall (defined as the ratio between the true positives and the sum of true positives and false negatives was 26.76%.

Since the samples were collected as products of the ore sorters, an indirect result of this work was the evaluation of the machines performance. Figure 5 presents a confusion matrix between the chemical labeling of the samples and the origin of them, as ore sorter products. The found accuracy was 92.10% (an increase of 335.52% when compared to the hand-sorting), the precision was 92.31% (339.13% higher), and the recall was 92.46% (345.52% higher).

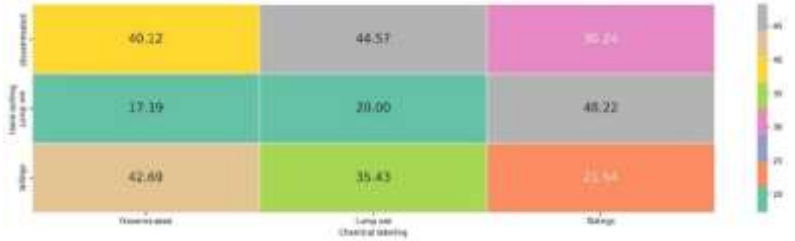

Figure 6 Confusion matrix: chemical labeling versus hand-sorting

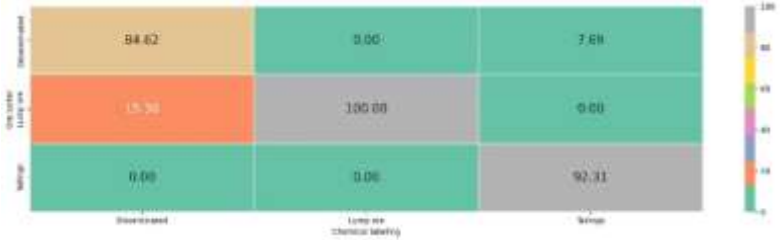

Figure 7 Confusion matrix: chemical labeling versus ore sorter products

CONCLUSION

The found results indicated that the hand-sorting may have served its purpose in the past. However, nowadays the low accuracy and precision does not allow its you anymore, specially to provide data that lead to any kind of decision making. Therefore, it is strongly recommended that FERBASA use chemical assays to measure chromium content in the ore and products.

ACKNOWLEDGEMENT

The author would like to acknowledge FERBASA for the permission to carry out this work ant to allow the data publication. We also thank the Federal University of Catalão and Modelling and Mineral Processing Research Lab (LaMPPMin).

REFERENCES

1. Varela, J.J., Riedel, F., Wotruba, H., Petter, C.O. (2005) Estado da arte da triagem ótica no processamento mineral. In: XXI ENTMME. Natal, Brazil, Proceedings, 577-584.
2. Salter, J.D., Wyatt, N.P.G. (1991) Sorting in the minerals industry: past, present and future. Minerals Engineering, 4(7-11), 779-796.
3. Taggart, A.F. (1945) Handbook of mineral dressing. New York, John Wiley.
4. Carson, D.L., Moir A.T. (1961) The separation of waste rock. In: VII Comm. Mitt. Metall. Inst. Congr. Johannesburg, South Africa, Proceedings.
5. Freer, J.S., Bohme, R.C. (1984) The role of waste sorting in the South African gold mining industry. In: Intern. Conf. Recent Advances in Miner. Sci. Technol. Johannesburg, South Africa, Proceedings.
6. Cutmore, N.G., Eberhardt, J.E. (2002) The Future of Ore Sorting in Sustainable Processing. ln: Green Processing Conference. Cairns, Australia, Proceedings, 287-289.

XV International Mineral Processing and Recycling Conference
17-19 May 2023, Belgrade, Serbia

SCANNING FLATBED OPTICAL ORE QUALITY ANALYZER

V. V. Morozov[1#], Y. P. Morozov[2], G. Zorigt[3], D. Lodoy[3], E. Jargalsaikhan[4], I. V. Pestriak[1]

[1] National University of Science and Technology "MISiS", Moscow, Russian Federation

[2] Urals State University of Mining, Ekaterinburg, Russian Federation

[3] Erdenet Mining Corporation SOE, Erdenet city, Orkhon province, Mongolia

[4] Erdenet Institute of Technology, Erdenet city, Mongolia

ABSTRACT – The modern systems for the optical analysis of or provide a basis for effective optimization of ore processing, based on the principle of advanced measurement and control. To improve accuracy of ore mineralogical composition determination, the new optical techniques and facilities have been developed. Such systems provide highly accurate measurements of ore composition. The original flatbed facility for visual analysis of fine-crushed ore has been developed, being incorporated in the existing system of ore sampling and analysis. Application of the flatbed facility renders possible high accuracy of ore mineralogical composition determination and technological regime of flotation process.

Keywords: Ore Processing, Mineral Composition, Ore Grade Estimation, Optical Analyser.

INTRODUCTION

In-stream analysis of ore grade can be implemented on the basis of continuous measurement of the mineral composition directly in-stream, i. e. at a conveyor, or using "sample-now-analyse-later" system (in-stream sampling with the following analysis). In-stream analysis of incoming ore grade is the new trend in effective control of ore benefication processes [1,2]. This is realized based on radiometric measurements in X-ray and visible spectrum regions, in which mineral components of the initial ore become apparent. An important advantage of such methods is in-stream measuring ore parameters, including mass fractions of individual minerals.

The implemented researches proved feasibility of the processed ore grade evaluation based on the results of determination (measurements) of the material composition of the initial ore and products of its flotation, using X-ray fluorescence analyzers [3,4]. Adequate evaluation of the ore grade is only possible with in-stream measuring the mineralogical composition parameters, such as degree of ore oxidation and the ratio of the major mineral phases. Analysis of ore grade can be implemented on the basis of continuous measurement of the mineral composition [5].

EXPERIMENTAL. TECHNIQUE OF OPTICAL-BASED ESTIMATION OF ORE GRADES

At the Erdenet processing plant, the new method for the ore diagnostics, based on

corresponding author: dchmggu@mail.ru

the mineralogical composition analysis was tested. High precision of the optical spectrum-based estimation is achieved using special devices, installed in the sampling and the sample analysis flow sheet.

For this, the special flatbed facility was developed. The facility includes a table for placing the sample, made of transparent glass, light flux source, optical system and optical converter (Fig. 1).

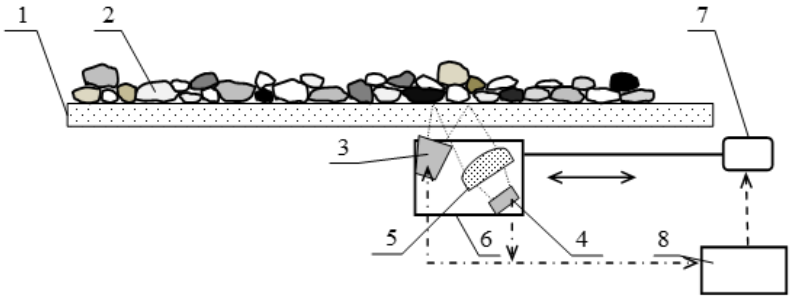

Figure 1 Flatbed facility for optical spectrum-based estimation of mineral composition of ore : 1 - table for placing of the ore sample; 2 - ore sample; 3 - light flux source; 4 - optical converter; 5 - optical system; 6 - carriage; 7 - drive; 8 - processor

The measurement technique involves preparing the ore sample, forming the measurement area in the form of a flat portion of the sample, illumination of sample and capture of the images of the formed flat portion of the sample in the visible spectrum range. The sample illumination and image capturing is carried out bottom-upwards in the two-dimensional scanning mode. Due to the sample "flattening", the sample roughness is considerably decreased. As a result, an almost planar parallel surface with uniform illumination without shaded areas is formed. This provides the high definition of the images with subsequent high accuracy of the mineral.

The most important spectral characteristics, hue and saturation (HSV), are determined on the basis of basic parameters. Via image software processing, computer databases of individual minerals were created. The spectral characteristics of minerals in visible light are the source of information for estimation of ore mineralogical composition (Fig. 2).

Figure 2 Image of Copper-Molybdenum Ore and the Recognition Results.
1 - chalcopyrite; 2 - bornite; 3 – bornite, 4 - chalcocite

RESULTS AND DISCUSSION

As can be seen from Fig. 3, the spectral characteristics of minerals become more resolvable when using the two-parameter recognition system "color - saturation" in HSV format. Full-scale application of the HSV format capabilities considerably increases the feasibility of determining the minerals, which reaches 0.95, even for complex systems such as chalcopyrite - pyrite or chalcocite - covellite, bornite.

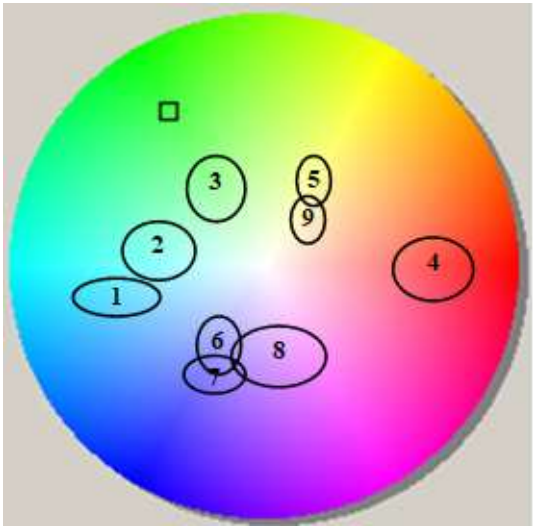

Figure 3 Color characteristics of minerals in HSV format (hue - saturation): 1 - azurite; 2 - turquoise, 3 - malachite; 4 - cuprite; 5 - chalcopyrite; 6 - chalcocite; 7 - bornite; 8 - covellite; 9 - pyrite

The effectiveness of recognition is great, even for spectrally similar minerals such as covellite and bornite. The intergrowth size in the image is 1 mm.

Based on the spectrum-based mineralogical estimation, mass fractions of oxidized copper and ferrum minerals, primary and secondary copper sulphide, pyrite, quartz, sericite, and other minerals, the presence and ratio of which characterizes ore grade, are determined.

The optical spectrum-based estimation technique is very advantageous when assessing the ore oxidation level. In the optical spectrum-based estimation method, the ore oxidation level is calculated as the ratio of total intensity of the reflected light from the oxidized copper minerals to the intensity of the reflected light from all the sulphide copper minerals.

The calculation of ore grade was carried out using a multi-criteria method calculations [6]. Ore is presented as a mixture of the five types and the contribution of each ore type to the summary ore should be determined. The mathematical model provides for calculation of the incoming ore affiliation by six (or more) significant parameters (for instance, copper, molybdenum and iron contents in the ore, the proportions of oxidized copper minerals, secondary sulphide copper minerals, primary copper minerals in the ore.

The essence of calculation of the shares of ore affiliation to a certain type(s) consists of the fact that, for the incoming ore, the degree of "similarity" to each of the five known ore types can be determined, and, proportionally to this degree (affiliation), fractions of each of these five types in the incoming ore can also be determined. For this purpose, distances between the point, the coordinates of which describe the incoming ore parameters, and points, the coordinates of which describe the ore types, identified as basic by technologists, are initially determined (Fig. 4).

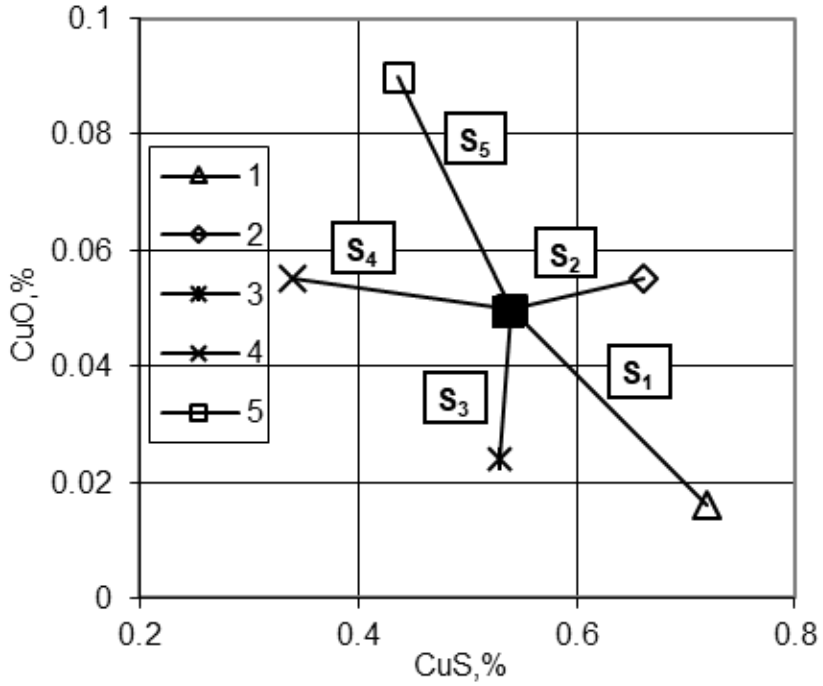

Figure 4 An example of ore composition assessment in two-dimensional space: 1, 2, 3, 4, 5 – the ore types; 6 (■) - currently produced ore; S_1, S_2, S_3, S_4, S_5 - differences between the parameters of the currently produced ore and the parameters of the ore types 1, 2, 3, 4, 5. CuO - oxidised copper minerals; CuS - sulphide copper minerals

The factors of significance of the specific measured ore parameters are adaptively adjustable parameters. The starting base for their adjustment is the checking information on the actual ore grade, obtained from the analysis of samples taken and analysed using classical techniques [6].

To calculate the required parameters of grinding and flotation, special studies were carried out on the most pronounced samples of the typical ores, and the process parameters for their grinding and flotation were developed. The simulation results made it possible to select the following ore types: - Massive Primary Ore (MPO); - Mixed Secondary Sulphidised Ore (MSSO); - Lean Pyritised Ore (LPO); - Mixed Seriticitised Ore (MSO) and Mixed Oxidised Ore (MOO). When determining the grade of ore, the parameters of typical ores presented in Table 1 are used.

Table 1 Parameters of typical ores used in determining the grade of the current ore

Параметры	Types of ore				
	MPO	MSSO	LPO	MSO	MOO
The ratio of the mass fractions of primary and secondary copper sulfides	2.1	0.50	0.45	0.75	0.57
The ratio of the mass fractions of primary and oxidized copper minerals	18.5	15.4	21.4	10.4	17.6
The ratio of the mass fractions of chalcopyrite and pyrite	0.77	1.5	0.45	0.86	0.67
Mass fraction of copper in ore, %	0.53	0.57	0.39	0.55	0.52
Mass fraction of molybdenum in ore, %	0.015	0.028	0.013	0.02	0.025
Mass fraction of iron in ore, %	1.50	1.09	1.15	1.22	1.30
Mass fraction of sericite in ore	0.12	0.15	0.1	0.17	0.34
Mass fraction of porphyry minerals,%	0.45	0.40	0.48	0.39	0.22
Absorption capacity to collector, %	66.7	76.9	63.5	80.1	84.1

At the same time, the simulation results enabled calculation of the optimum parameters of the process mode for each ore grade (Table 2).

Table 2 Preset functions in the grinding and flotation processes control systems

Process variable – set of control functions	MPO	MSSO	LPO	MSO	MOO
Grinding size, % of –74 μm grain size	67.5	64.5	67.0	66.0	66.0
Water supply to the mill, t/m^3h	1.65	1.74	1.71	1.75	1.75
Pulp density %	43.5	41.0	41.5	40.0	40.0
Collector consumption	10.0	12.0	13.0	17.5	10.0
Frother consumption	13.0	16.0	16.0	19.0	13.0
Lime consumption	1100	1300	1300	1300	1100

The value of the parameters SF for each parameter of the process was calculated as a weighted average of the parameters values for each “typical” ore type (SF_i) taking into account the weight contribution of the given technological type in the ores mixture using Equation (1):

$$SF = \Sigma\gamma i SFi \quad (1)$$

where γ_i - relative weight fraction of an ore of tecnological type i in the summary ore mixture incoming to processing.

The calculated preset functions were used as baseline in the systems of automatic control of grinding and flotation processes at the Erdenet processing plant. Using the ore grade determination increased effectivity of the automatic control, as it allowed a fast response to changes in the incoming ore grade. Applying the ore grade estimation algorithm enabled an increase of the control stability. Maintaining the optimum degree of ore grinding and optimization reagent regime of the flotation process provides

increasing recovery of copper and molybdenum into concentrates by 0.3% and 1.1%, respectively, as well as decreasing the consumption of reagents by 2–3%.

CONCLUSIONS

At the Erdenet processing plant (Mongolia), systems and algorithms of flotation process control, based on an advanced system of estimating the processed ore grade, have seen further progress. The scanning flatbed optical quality analyzer for automatic measurement of the ore mineralogical composition by in-stream sampling with later analysis were tested. The control algorithm uses data of ore grade and the accumulated information about the optimal process parameters for flotation. The introduction of this system reduces losses of valuable components and reagent consumption.

REFERENCES

1. Patel, A.K., Chatterjee, S., Gorai, A.K. (2017) Development of machine vision-based ore classification model using support vector machine (SVM) algorithm. Arab J Geosci. 10, 107-113.
2. Horrocks, T., Wedge, D. Holden, E.J. et al. (2015) Classification of gold-bearing particles using visual cues and cost-sensitive machine learning. Math Geosci. 47, 521–545.
3. Ganbaatar, Z., Morozov, V.V., Delgerbat, L., Duda, A.M. (2017) Management of copper-molybdenum ore enrichment processes using advanced quality control. Mining Sciences and technologies, 1, 40-48.
4. Chatterjee, S. (2013) Vision-based rock-type classification of limestone using multi-class support vector machine. Appl Intell 39, 14–27.
5. Morozov, V., Morozov, Y., Ganbaatar, Z., Delgerbat, L. (2019) Optimization of the Optical Methods of Ore Grade Analysis at Mineral Processing. Insights Min Sci technol. 1 (2), 555-560.
6. Morozov, V., Ganbaatar, Z., Delgerbat, L., Morozov, Y. (2018) Modern method and systems of optical ore grade analysis by processing of copper-molybdenum ores. In: Proceedings of 29th international mineral processing congress, IMPC 2018. Moscow, Russia. Proceedings, 52-60.

XV International Mineral Processing and Recycling Conference
17-19 May 2023, Belgrade, Serbia

CHARACTERIZATION, ENRICHMENT TEST AND VALORIZATION OF IRON ORE FROM NABEBA (NORTH – CONGO)

B. B. Tchouffa[1#], N. J. Ndemou[2], M. G. F. Ntsama[3]
[1] University of Douala, Douala, Cameroon
[2] Xplortec SA, Yaounde, Cameroon
[3] Aureus Mining Cameroon, Yaounde, Cameroon

ABSTRACT – The objective of this paper is to investigate the potential for beneficiation of the Nabeba iron ore located in northern Congo. Samples were taken from the three major deposits on this permit and sent to the laboratory for particle size, chemical and mineralogical analyses before undergoing treatment by magnetic separation. These analyses reveal the presence of Hematite, Magnetite, Sinerite, Bimessite, Fluorapatite, Garronite, Goethite, Greenalite and Eucryptite in the Nabeba iron ore, with average Fe_2O_3 contents of around 65.05%. The iron content recovered after magnetic separation in the crude iron ore samples ranges from 79.5 to 91.8% wt.

Keywords: Nabeba, Iron Ore, Characterisation, Magnetic Separation, Enrichment.

INTRODUCTION

The Mbalam-Nabéba iron ore deposit is located between the Republic of Cameroon (Mbalam) and the Republic of Congo (Nabéba). It is one of the structuring projects contributing to the overall objective of the emergence of Cameroon and Congo. According to a study carried out by Sundance Resources, the characteristics of the Mbalam-Nabéba iron ore make it a product of superior quality to the world reference in the field. The mining industry is an activity that involves the extraction and processing of various minerals that represent an industrial and economic pole, and plays an important role in the global economy [1]. It is a unique industry because of the complex impact it can have on local economic development, on the environment, and on the socio-cultural profiles that are often typical of the vast mining areas of a particular country or region [2]. Some minerals such as silica (Mbalam iron ore), alumina (Nabeba iron ore), phosphorus, Sulphur or carbon which are frequently found as a constituent of iron ore, are extremely harmful elements in ferrous metallurgy as they increase the brittleness and decrease the ductility of iron and steel products, and as the price of iron ore increases, it is necessary to dephosphorise iron ore to a level that meets international standards [3]. The main aim of this work is to determine the factors and methodology for the enrichment of the iron ore deposit (Mbalam-Nabeba) which embodies two neighbouring countries, Cameroon and Republic of Congo named as Mbalam iron ore project.

corresponding author: tchouffab@yahoo.com

EXPERIMENTAL

The sampling campaign was carried out at the level of the main deposits using the trench method. The sampling took place at different points corresponding to the different zones and layers of the deposit. The sampling points are shown in Figure 1 below:

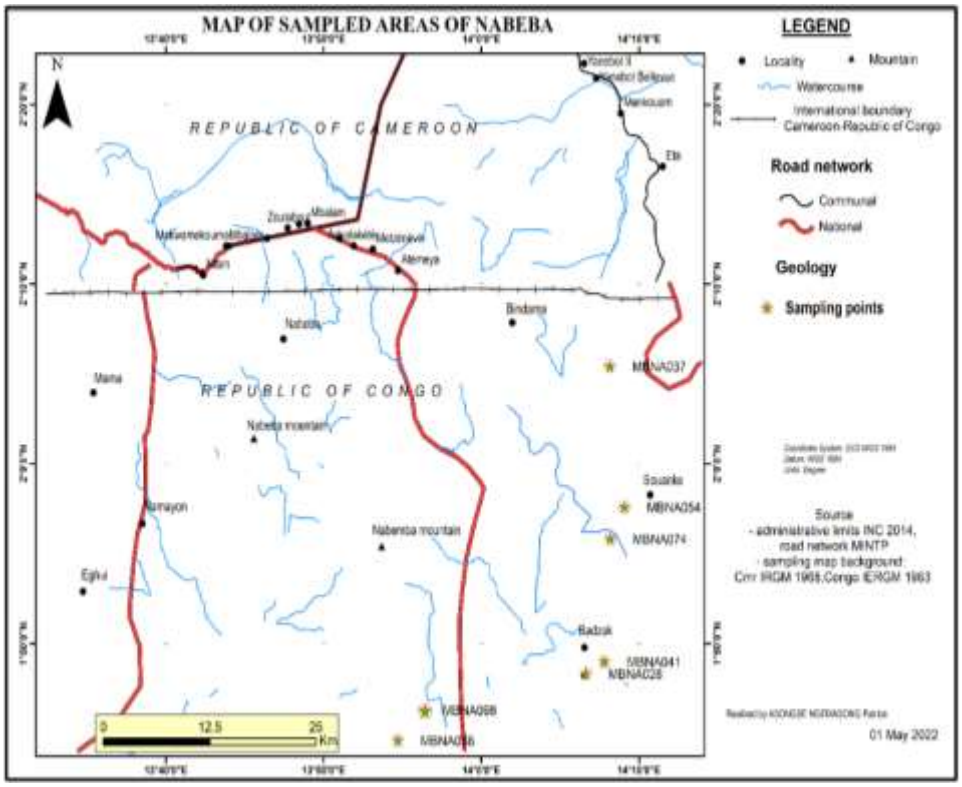

Figure 1 Sampling map of the studied area

It is a mechanical treatment that serves to reduce the dimensions of the raw material to a granularity of the order of a few millimeters. A FRITSCH type jaw crusher was used, which is available at the Nkolbisson Minerals Processing Laboratory. Crushing does not reduce the diameters of the grains of different samples to a diameter of less than 1mm. Generally, fragmentation by crushing is followed by a drying and grinding operation to prepare the samples for the various subsequent analyses such as particle size analysis. The purpose of drying is either to eliminate or to reduce the humidity of the samples by evaporation, and to facilitate the grinding operation and the other mechanical preparation steps of the Nabeba iron ore samples in the dry state. The oven used is brand and it is used for drying crushed samples at 1050°C ±5 for 24 hours.

Characterization consists of determining the oxide and element composition of the iron ore. To achieve this objective, a series of characterization methods are carried out such as: XRD, XRF, ATD/ATG, from this stage we can consider a valuation method. The

laboratory used has two powder diffractometers, brand Bruker, one operating with a copper tube (λ=1.54Å) and the other with a cobalt tube (λ=1.79Å). Various accessories are available, making it possible to vary the sample environments (stage for the analysis of samples in capillary, chamber allowing the control of the temperature and the relative humidity, accessory of "micro-diffraction", sample holders for samples sensitive to the atmosphere…). X-ray fluorescence (XRF) is an analytical technique that can be used to determine the chemical composition of a wide variety of sample types, including solids, liquids, slurries, and loose powders. X-ray fluorescence is also used to determine the thickness and composition of layers and coatings. It can analyze elements ranging from beryllium (Be) to uranium (U) in concentration. Our samples intended for chemical analyzes were prepared at the Mineral Processing Laboratory in Nkolbisson (Yaoundé, Cameroon). For each sample, 100 g are taken for quartering. Then 10 g are taken to make pellets for the actual analysis. The major elements were analyzed by X-ray fluorescence (XRF), by the Phillips PW 1840 brand device and the trace elements by mass spectrometry coupled to the induction plasma (ICP-MS) on a mass spectrometer VG- Plasma Quad STE ICP at the OMAC laboratory in Ireland of the ALS Geochemistry group.

The separation test envisaged for Nabeba iron ore is magnetic separation and magnetizing roasting, used in order to obtain a concentrate rich in hematite or magnetite and the reduction of the contents of certain harmful elements such as phosphorus (P), and this before and after heat treatment by magnetizing roasting. The quantity required for magnetic separation tests and magnetizing roasting is 0.5 Kg per sample. Each sample is divided into 05 sub-samples by mass, corresponding to each roasting temperature, therefore 20 sub-samples in total. A quantity of 500 g of natural coal (coke) to be used as fuel is crushed using a laboratory crusher to less than 1 mm, and ground manually using a mortar to a size < 0.71 mm. The coal prepared (coke) and mixed with the iron ore sub-samples in a proportion of 5% by mass of each ore sub-sample is mixed with natural coal (coke). For each sample, the mixture is placed in five stainless crucibles covered with stainless steel lids to protect the sample from re-oxidation and heated to 500°C, 600°C, 700°C, 800°C and 900° respectively. Covered for 30 minutes. This manipulation applies to the 20 sub-samples. After the roasting time has elapsed, the crucibles are cooled to room temperature.

RESULTS AND DISCUSSION

Mineralogical and chemical characterization

The results of X-ray diffraction on the concentrate of the four granulometric classes resulting from the laboratory operations consist mainly of magnetite (Fe_3O_4) and hematite (Fe_2O_3). However, some traces (weak inclusions) of Sinnerite, Bimessite, Fluorapatite, Garronite, goethite, Greenalite and Eucryptite are observed. The analysis of this sample shows the greater proportion of Magnetite at the highest intensity making it known that, the sample was principally of magnetite. It contained some minor traces (weak inclusions) of minerals like Hematite, Fluorapatite and Bimessite.

XRF produces an assay by giving information on the chemical composition of given sample(s) without indicating what phases they are present in the given sample(s)

rather, the rates are presented in percentages as seen on the table 1 below. This table shows the proportion of Fe between 40.44 – 51.65%; Fe_2O_3 between 57.82 – 73.85% and low fraction of P and S.

Table 1 Chemical Analyses of samples of Nabeba iron ore deposit

Sample	Al_2O_3	Fe	Fe_2O_3	K_2O	MgO	MnO	Na_2O	P	S	SiO_2
MBNA028	8.54	40.44	57.82	0.078	0.24	0.05	0.027	0.076	0.037	25.8
MBNA037	8.77	42.85	61.26	0.044	0.1	0.051	0.018	0.083	0.043	22.1
MBNA041	8.61	44.99	64.32	0.055	0.09	0.051	0.043	0.035	0.046	19.75
MBNA054	7.47	47.95	68.55	0.042	0.09	0.055	0.052	0.079	0.044	18.95
MBNA074	6.58	46.88	67.03	0.031	0.08	0.058	0.024	0.030	0.032	20.5
MBNA088	6.08	43.71	62.5	0.029	0.16	0.073	0.028	0.063	0.027	25
MBNA098	5.26	51.65	73.85	0.031	0.07	0.053	0.035	0.087	0.027	15.6

Magnetic separation

The results of the magnetic separation after grilling of crude samples enumerated below (**table 2**). This table illustrates the levels of magnetic fractions, non-magnetic fraction, mass yield to concentrate, mass yield of the non-magnetic fraction and variation of temperature. At a higher temperature of 900˚C for the majority of samples, we experienced high magnetic fraction with mass yield to concentrate columns and vice versa for non-magnetic fraction and mass yield of the non-magnetic fraction columns. In some cases, we had the highest magnetic fraction at 900˚C example MBNA28.

Table 2 Results of magnetic separation after magnetizing grilling for crude sample

Sample	Grilling temperature (°C)	Mass (gram)			Mass yield (%)	
		Feed	**MF**	**NMF**	**yc**	**Гr**
MBNA28	500	120	108	12	**90**	**10**
MBNA28	600	120	109.2	10.8	**91**	**9**
MBNA28	700	120	114	6	**95**	**5**
MBNA28	800	120	116.4	3.6	**97**	**3**
MBNA28	900	120	117.6	2.4	**98**	**2**

*MF: Magnetic Fraction; NMF: No Magnetic Fraction; yc: Mass yield for magnetic fraction; Гr: Mass yield for no magnetic fraction.

CONCLUSION

The application of low-intensity magnetic separation is effective for the recovery of the ferriferous fraction of the Nabeba ore but the quality of the concentrates is insufficient as long as the phosphorus is not eliminated. The magnetizing roasting operation allowed samples rich in hematite to be reduced to magnetite, which facilitates its extraction by magnetic separation.

The quality of the roasting and magnetic separation products must be determined to evaluate the performance of the magnetic separation process. Several samples were prepared for different characterization analyzes and of separation, but they are not all used, for lack of the means of analysis and the characterization.

ACKNOWLEDGEMENT

The authors of this manuscript would like to express their gratitude to the LIEC for the quality of the analyses produced.

REFERENCES

1. Nouioua, D., Merbai, H., Malek, N. (2016) Influence du broyage sur les caractéristiques chimiques et minéralogiques du minerai de phosphate de Kef Essennoun. Mémoire de Master, UAMB, 76p.
2. Belkacemi, A., Kacel, M., AYADI, B. (2014) Caractérisation et élaboration d'un schéma de traitement de tuf de remila (Bejaia). Mémoire de Master, UAMB, 67p.
3. Bersi, M., Saibi, H., Chabou, M.C. (2016) Aerogravity and remote sensing observations of an iron deposit in Gara Djebilet, southwestern Algeria. Journal of African Earth Sciences, 116, 134-150.

XV International Mineral Processing and Recycling Conference
17-19 May 2023, Belgrade, Serbia

LABORATORY BENEFICIATION TECHNOLOGY AND DEVELOPMENT RESEARCH ON TITANIUM MAGNETITE ORE

A. K. Jia, B. S. Đorđević[#], C. C. Ouyang, D. B. Lv
Serbia Zijin Mining Doo Bor, Bor, Serbia

ABSTRACT – The iron ore it was investigate very often, mostly about his valorization from the crude ore. On representative test sample, conducted process mineralogy study and laboratory beneficiation test study. The iron in titanium magnetite form accounts for 52.39%. Crude ore was processed by coarse dry pre-separation stage grinding - stage magnetic separation process and coarse dry pre-separation stage grinding-elutriation process. The pre-separation stage grinding-stage magnetic separation process was conducted on crude ore at -12 mm and -20 mm sizes, iron concentrate with TFe grade above 65% and recovery rate TFe above 53%, with the elutriation process magnetic separation concentrate can be increased TFe grade to above 66% for final grinding fineness of -0.074 mm 75%.

Keywords: Titanium Magnetite Ore, Magnetic Separation, Elutriation, Dry pre-separation.

INTRODUCTION

Titanomagnetite ores are currently one of the leading industrial types of iron ore deposits and the main type of mineral raw material for obtaining vanadium ilmenite-titanomagnetite type of these ores is an important source of titanium production. They traditionally belong to the late magmatic class of magmatic deposits, spatially and genetically associated with ultrabasite-basite complexes. Titanomagnetite deposits are explored in many countries around the world: South Africa, Canada, Norway, China, Ukraine. In Russia, they are known in Karelia, the Kola Peninsula and the Urals, in Western and Eastern Siberia. In the structure of titanium and vanadium reserves, titanomagnetite ores have a considerable share: abroad 6.5% of the confirmed reserves of iron ores, about 60% of TiO_2 and over 90% of V_2O_5 reserves are associated with this industrial type, in Russia these figures are respectively 13.48 and 92% [1,2]. As iron mineral products have expanded their use, so has the need to investigate the best valorization techniques. The most widely used titanium product is titanium dioxide (TiO_2), being used as pigment, as filler in paper, plastics and rubber industries, and as flux in glass manufacture. [3] The main titanium containing minerals are ilmenite, rutile, and leucoxene. Ilmenite supplies about 91% of the world's demand for titanium minerals. Most of the magnetite is produced as a by-product of iron ore processing. Low grade titanium dioxide contains a lot of unwanted materials. Beneficiation is the process of removing unwanted laterites materials in an ore (referred to as gangue) to increase its economic value. For the enrichment of iron minerals, the gangues components need to be eliminated through beneficiation are mainly SiO_2, CaO

[#] corresponding author: sanjajb8@gmail.com

and MgO, secondarily Al_2O_3. The content of deleterious impurities is relatively low such as phosphorus and sulfur, which have a minimum effect on the quality of iron concentrate.

MATERIALS AND METHODS

Material

The ore samples belongs to low-phosphorus, low-sulfur, low-grade original vanadium titanium magnetite. All the samples are blended (loop heap method for 6 times), quartered and divided into process mineralogy research sample, pre-separation discarding sample and preparation sample; different sizes of ore samples are produced with different crushers and different aperture screens: Φ250×400mm jaw crusher-screen analysis is used for (-70+0) mm and (-55+0) mm ore samples, Φ125×250mm jaw crusher-screen analysis is used for (-35+0) mm, (-20+0) mm and (-12+0) mm ore samples, all the samples are quartered again with Φ200×240mm roller crusher and crushed into -3 mm, followed by 3 times of coning and one quartering, the final test samples are collected for spectrum semi-quantitative analysis, multi-element analysis, iron phase analysis. The main element available to be recovered from the ore is iron with grade of 16.34%; the content of TiO_2 and V_2O_5 is 1.17% and 0.16%, which can be used for comprehensive utilization. The ratio of Ore TFe/FeO is 1.60. It is ascertained through microscopic identification, X-ray diffraction analysis and scanning electron microscopy analysis that the mainly iron mineral in the ore is titanium magnetite, occasionally existed in martite and limonite. The content of titanium minerals is relatively low in the majority of ilmenite, followed by sphene, metal sulfide occasionally existed including pyrite, chalcopyrite and pyrhotite. Gangue minerals are mainly in pyroxenite and amphiboles, followed by plagioclase and chlorite, and other trace minerals such as apatite, zircon and sericite, etc.

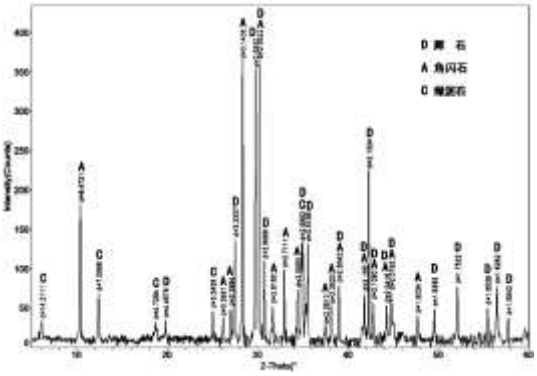

Figure 1 X-ray Diffraction Analysis (XRD) Atlas of LIMS Tailing

Method

Mainly conduct test research on single full magnetic process and combined process of magnetic-gravity separation is shown in Fig. 2. Both of the two processes have their

own characteristics. Single full magnetic separation process is simple and easy to operate with high automation level. Magnetic-gravity combined process with the same grade of concentrate can properly increase the final grinding fineness with the help of elutriation magnetic separation combined process, which is beneficial to decrease concentrate mixture and widely applied in industry. For research is used equipment for grinding tests Φ200mm×240mm Rod Mill and Φ200mm×240mm Ball Mill. For full magnetic process and combined process of magnetic-gravity separation is used Low-intensity Magnetic Roller Separator Φ600mm×450mm, shell surface field intensity 0.15T, Φ400mm×300mm Drum Type Wet Magnetic separator, shell surface field intensity ≤0.2T and Φ100mm elutriation magnetic separator.

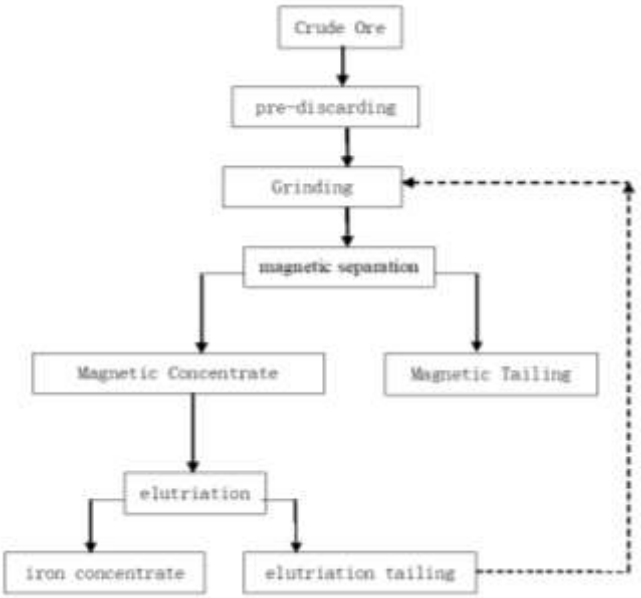

Figure 2 Pre-separation- stage grinding-magnetic separation-elutriation principle process

RESULTS AND DISCUSSION

Primary Magnetic Field Intensity Test

The grinding fineness increased from -0.074 mm 20.5% with the increase of magnetic field intensity, the tailing with yield of 76.38%÷61.26% can be discarded, thus it is proper to select rougher magnetic field intensity of 0.2T combined with industrial production reality.

Magnetic separation concentrate grade generally decreased with the increase of magnetic field intensity at secondary grinding fineness of -0.074 mm 75.00% while the concentrate yield varied a little. Thus, it is proper to select 0.12T÷0.15T as magnetic field intensity after synthetically considering concentrate grade and recovery.

Table 1 Different magnetic separation tests are conducted at grinding fineness of -0.074 mm of 20.5%

Magnetic Field Intensity/T	Product Name	Yield	TFe Grade	TFe Recovery
0.10	Magnetic Concentrate	23.62	55.19	67.92
	Magnetic Tailing	76.38	8.06	32.08
	Feed	100.00	19.19	100.00
0.15	Magnetic Concentrate	25.25	54.05	70.12
	Magnetic Tailing	74.75	7.78	29.88
	Feed	100.00	19.46	100.00
0.20	Magnetic Concentrate	29.08	46.87	71.34
	Magnetic Tailing	70.92	7.72	28.66
	Feed	100.00	19.10	100.00
0.30	Magnetic Concentrate	38.74	38.28	76.06
	Magnetic Tailing	61.26	7.62	23.94
	Feed	100.00	19.50	100.00

Table 2 Different magnetic field intensity tests are conducted at grinding fineness of -0.074 mm 75%

Magnetic Field Intensity/T	Product Name	Yield	TFe Grade	TFe Recovery
0.12	Concentrate	66.01	65.63	92.38
	Tailing	33.99	10.52	7.62
	Feed	100.00	46.90	100.00
0.15	Concentrate	66.10	65.21	92.47
	Tailing	33.90	10.35	7.53
	Feed	100.00	46.62	100.00
0.18	Concentrate	66.92	64.98	92.99
	Tailing	33.08	9.91	7.01
	Feed	100.00	46.77	100.00
0.20	Concentrate	67.21	64.72	93.10
	Tailing	32.79	9.83	6.90
	Feed	100.00	46.72	100.00

Elutriation test

Elutriation tests are conducted on magnetic separation concentrate at different grinding fineness's to probe the possibilities of obtaining qualified concentrate and decrease grinding energy consumption at coarse grinding fineness. The concentrate grade is further increased, elutriation field intensity appearing value is 10500, ascending water speed is 4.6 cm/s. Elutriation can increase concentrate grade to some extent, and iron concentrate with TFe grade of 66.01% can be obtained through elutriation at secondary grinding fineness of -0.074 mm 75%.

Table 3 Elutriation Test Results on Magnetic Separation Concentrate with Different Fineness %

Grinding Fineness/ -0.074 mm	Product Name	Yield	TFe Grade	TFe Recovery
45.00	elutriation concentrate	90.75	63.67	93.31
	elutriation tailing	9.25	44.82	6.69
	Feed	100.00	61.92	100.00
55.00	elutriation concentrate	90.50	64.75	93.54
	elutriation tailing	9.50	42.61	6.46
	Feed	100.00	62.64	100.00
61.25	elutriation concentrate	91.46	65.16	94.50
	elutriation tailing	8.54	40.63	5.50
	Feed	100.00	63.06	100.00
75.00	elutriation concentrate	84.50	66.01	85.84
	elutriation tailing	15.50	59.41	14.16
	Feed	100.00	64.98	100.00

BENEFICIATION PROCESS TEST

Dry Pre-separation-stage grinding- stage magnetic separation

Dry pre-separation-stage grinding-stage grinding magnetic separation (full magnetic) can be conducted on crude ore with (-12+0) mm, (-20+0) mm. Iron concentrate with yield of 13.95%, TFe grade of 65.03%, TFe recovery of 53.74%, mFe recovery of 98.30% can be obtained through dry pre-separation-stage grinding-stage magnetic separation on (-12+0) mm crude ore at secondary grinding fineness of -0.074 mm 75%. Iron concentrate with yield of 13.91%, TFe grade of 65.03%, TFe recovery of 54.31%, mFe recovery of 98.08% can be obtained through dry pre-separation-stage grinding-stage magnetic separation on (-20+0) mm crude ore. Thus, the obtained iron concentrate grade are generally the same after the dry pre-separation-stage grinding-stage magnetic separation process on (-12+0) mm and (-20+0) mm at the same final grinding fineness of -0.074 mm 75%. The dry pre-separation-stage grinding-stage magnetic separation process test is conducted on crude ore (-12+0 mm) at final grinding fineness of -0.074 mm 85% to satisfy contract and design requirement. In other study is reported that the yield of the magnetic concentrate increases with the increase in magnetic intensity but simultaneously the grade of the concentrate decreases. Though the percentage recovery of Fe is increased but the grade of the concentrate is not appreciable. In this study on the raw ore at 4900 gauss magnetic intensity, a concentrate of 49.67% yield with 55.48% Fe recovery is produced with a grade of only 59.92% Fe. [4]

Dry Pre-separation-stage grinding- stage magnetic separation-elutriation process

Dry pre-separation-stage grinding-stage magnetic separation-elutriation concentrate recovery-elutriation tailing regrinding and re-separation (magnetic separation and gravity separation) process test is conducted on crude ore (-12+0) mm, results are shown in Table 4. Iron concentrate with yield of 13.92%, TFe grade of 64.97%, TFe recovery of

53.58%, mFe recovery of 98.18% can be obtained through dry pre-separation-stage grinding-magnetic separation-elutriation on -12+0 mm crude ore at secondary grinding fineness of -0.074 mm 61%. The dry pre-separation-stage grinding-magnetic separation-elutriation process test is conducted on crude ore (-12+0) mm at secondary grinding fineness of -0.074 mm 85% and elutriation tailing regrinding fineness of -0.074 mm 95% combined with the requirement for iron concentrate sizes showed in table 5.

Table 4 Dry Pre-separation-stage grinding-magnetic separation process on (-12+0) mm crude ore

Product name	Yield	Grade		Recovery		Yield	Grade		Recovery	
		TFe	mFe	TFe	mFe		TFe	mFe	TFe	mFe
Concentrate	13.92	64.97	61.36	53.58	98.18	**13.91**	65.05	61.56	54.31	98.08
Tailing	86.08	9.10	0.18	46.42	1.82	86.09	8.84	0.19	45.69	1.92
Crude Ore	100.00	16.88	8.70	100.00	100.00	100.00	16.66	8.73	100.00	100.00

Table 5 Dry Pre-separation-stage grinding-magnetic separation process test results on (-12+0) mm crude ore %

Product name	Yield	Grade		Recovery		Yield	Grade		Recovery	
		TFe	mFe	TFe	mFe		TFe	mFe	TFe	mFe
Concentrate	13.92	64.97	61.36	53.58	98.18	13.47	66.34	63.15	52.94	97.77
Tailing	86.08	9.10	0.18	46.42	1.82	86.53	9.18	0.22	47.06	2.23
Crude Ore	100.00	16.88	8.70	100.00	100.00	100.00	16.88	8.70	100.00	100.00

CONCLUSION

Ores in these areas belong to original low-phosphorus low sulfur lean vanadium-titanium magnetite, the iron in titanium magnetite form accounts for 52.39%. Iron minerals is mainly titanium magnetite, occasionally existed martite and limonite. Gangue minerals is mainly pyroxenite and amphiboles, followed by plagioclase and chlorite. The pre-separation-stage grinding-stage magnetic separation process was conducted on crude ore at -12 mm and -20 mm sizes, iron concentrate with TFe grade above 65% can be obtained at final grinding fineness of -0.074 mm 75%, which is increased to above 66% with the elutriation process on magnetic separation concentrate.

REFERENCES

1. Alikulov, Sh.Sh., Azimov, O.A., Toshnazarov, A.Kh. (2022) Development of Processing Technology for Titano-magnetite Ores of Tebinbulak Deposit. Journal of Pharmaceutical Negative Results, 13(8).
2. Kharlamov, V.S., Nikolaenko, V.P. (2005) Enrichment of ores of ferrous metals.
3. Bykhovskiy, L.Z., Tigunov, L.P., Pakhomov, F.P. (2009) Ilmenite and titano-magnetite deposits of Russia in connection with ultrabasic and mafic complexes. Proceedings of the III-international conference, Russia, Ural, pp. 93-96.
4. Jena, M.S., Tripathy, H.K., Mohanty, J.K., Mohanty, J.N., Das, S.K., Reddy, P.S.R. (2015) Roasting Followed by Magnetic Separation: A Process for Beneficiation of Titano-Magnetite Ore. Separation Science and Technology, 50: 1221–1229.

XV International Mineral Processing and Recycling Conference
17-19 May 2023, Belgrade, Serbia

INVESTIGATION OF THE POSSIBILITY OF VALORIZATION OF TWO BORATE SAMPLES FROM THE DEPOSIT "POBRĐE" – BALJEVAC

D. S. Radulović#, V. Jovanović, B. Ivošević, D. Todorović, S. Milićević, M. Marković
Institute for Technology of Nuclear and Other Mineral Raw Materials (ITNMS)
Belgrade, Serbia

ABSTRACT – Boron is a rare element from the group of non-metals and it occurs in nature in over 250 boron-bearing minerals-borates. Turkey has the largest borate reserves and is their largest producer. Serbia has significant borate resources, for now without exploitation and processing. This paper presents the results of investigating two borate samples from the deposit "Pobrđe. The following properties were determined on borate samples: free and hygroscopic moisture, granulometric composition, chemical composition, mineralogical analysis by size classes, and XRD analysis.

Keywords: "Pobrđe" Deposit, Boron Minerals, Properties.

INTRODUCTION

Boron is a rare element from the group of non-metals (concentration of 10 ppm in the upper continental crust) [1,2]. Boron occurs in nature in over 250 boron-bearing minerals-borates, which are defined as any compound containing boric oxide (B_2O_3). The most important boron minerals in commercial terms are: borax(tincal), kernite, ulexite, colemanite [3]. Approximately 75% of the world's boron reserves are located in Turkey, which is also the largest producer of borates (Table 1) [2].

Table 1 World reserves and production of borates [4,5]

Countries	**Total Reserve (Thousand ton B_2O_3)**	**Distribution (%)**	**Productions of borate concentrates, t (2019.)**
Turkey	948,712	73.4	4,000,000
Russia	100,000	7.7	80,000
USA	80,000	6.2	1,300,000
Peru	22,000	1.7	111,108
Argentina	9,000	0.7	80,000
China	36,000	2.8	250,000
Bolivia	19,000	1.5	214,500
Chile	41,000	3.2	352,225
Kazakhstan	15,000	1.2	500,000
Serbia	21,000	1.6	/
TOTAL	**1,291,712**	**100**	

corresponding author: d.radulovic@itnms.ac.rs

Starting in 2014, Boron was marked as "critical" in the European Commission's assessment study for the E.U. [6,7]. Four main sectors of boron mineral application represent 86% of its world annual consumption: 1. Glass sector -1.17 Mt B_20_3; 2. Ceramics sector -280,000 B_20_3 3. Agriculture sector 240,000 B_20_3 4. Detergents sector -45,000 B_20_3 [8,9]. There are several borate deposits in Serbia: Piskanja - 11.8 Mt [10], Pobrđe - about 150,000 t [11] and it is counted on the possible production of boron from the jadarite mineral [9].

Boron ore from the "Pobrđe" deposit was exploited by "Ibar Coal Mines". After mining, the borates ore was crushed and then sieved on a screen with an opening of 30 mm. Commercial borate concentrate was obtained from the size class +30 mm by hand picking. The size class -30+0.00 mm was discarded to the landfill as tailings. "Elixir group", the largest producer of mineral fertilizers in the Balkans, bought 7-8,000 tons of this raw material and transferred it to the "Elixir Zorka" factory in Šabac. Here, after grinding, this raw material is used as an additive for mineral fertilizer. The "Elixir group" wanted to examine the possibility of obtaining boron mineral concentrates both from run-of-mine ore and from the -30+0.00 mm class. The goal of these tests would be to obtain K/B_2O_3 with a B_2O_3 content of over 35% and a middling product that would have a B_2O_3 content of 7-10% for the fertilizer industry. In order to determine the possibility of conducting magnetic separation tests, detailed physical-chemical and mineralogical characterization was performed.

EXPERIMENTAL (MATERIALS AND METHODS)

Two representative borate samples were taken for these investigations. The run-of-mine borate ore sample had an upper size of limit -280+0.00 mm, mass m=130 kg, and the -30+0.00 mm class sample had a mass of m= 82 kg. On both samples, free moisture was determined. After that, both samples were crushed to a size of -10+0.00 mm, and physico-chemical and mineralogical properties of these samples were determined. The following were determined on the samples: hygroscopic moisture, granulometric composition, chemical composition, mineralogical analysis by size classes, and XRD analysis. Mineralogical analysis by size classes was performed on a polarizing microscope "JENAPOL-U", Carl Zeiss-Jena, with a measuring device. X-ray diffraction (XRD) analysis was performed on a "PHILIPS" X-ray diffractometer, model PW-1710.

Determination of moisture content and granulometric composition of borate ore samples

The content of free moisture in the run-of-mine sample was 2.39% and hygroscopic 0.21%; in the sample of the size class -30+0.00 mm the content of free moisture was 2.51% and the hygroscopic 0.22%.

The granulometric composition for both samples was determined by sieving on a Tyler series of sieves, with the last sieve having an aperture of 0.1 mm. All the weights of the sieves oversize together with the sieve undersize of the last sieve were measured. Granulometric analysis showed that: - for the run-of-mine sample of the borate ore, after three-stage comminution, the d_{95} is 6.895 mm, while the d_{50} is 2.323 mm; - for a borate

sample of the size class -30+0.00 mm, after comminution, d_{95} is 6.773 mm, while d_{50} is 2.193 mm.

Chemical analysis of the borate samples

The chemical composition of both borate samples was determined by chemical analysis. In both samples, the content of the B_2O_3, and secondary components was determined, before all Fe_2O_3. Loss of ignition at 800 °C is shown. The chemical compositions of borate samples are shown in Tables 3 and 4.

Table 2 Chemical composition of the run-of-mine borate ore

Comp.	B_2O_3	SiO_2	Al_2O_3	Fe_2O_3	CaO	MgO	Na_2O	K_2O	TiO_2	LOI at 800°C
Cont.,%	32.21	15.20	4.05	1.61	20.30	3.75	1.06	0.57	0.168	21.03

Table 3 Chemical composition of the borate, size class -30.0+0.00 mm

Comp.	B_2O_3	SiO_2	Al_2O_3	Fe_2O_3	CaO	MgO	Na_2O	K_2O	TiO_2	LOI at 800°C
Cont.,%	21.05	21.60	6.09	2.38	20.13	4.83	1.16	0.83	0.33	23.26

Chemical analysis showed that these two borate samples are significantly different from each other. Namely, the starting sample of the borate ore has a much higher boron content (B_2O_3 content 32.21%), compared to the -30+0.00 mm size class sample (B_2O_3 content 21.05%). The starting sample also has a lower content of Fe_2O_3 -1.6% and sample of the size class -30+0.00 mm, has content of Fe_2O_3 -2.38%.

Qualitative-quantitative mineralogical investigation of borate samples

Quantitative-qualitative mineralogical analysis was performed using an optical polarization microscope and X-ray diffraction analysis on several different samples of borate ore. Mineralogical analysis by size class was carried out on crushed borate samples with a size of -10 mm, in order to determine intergrowth and liberations of minerals in each class of the borate samples. These data made it possible to define the size of the class in which boron minerals can be separated from tailings minerals. X-ray diffraction (XRD) analysis was performed on both borate samples after micronization, on the basis of which the mineral composition of the samples was determined.

Mineralogical analysis by size classes of run-of-mine borate sample and borate sample size class -30+0.00 mm

Both borate samples were sieved into the following narrow size classes: -10.00+9.52 mm; -9.52 +7.93 mm; -7.93 + 6.35 mm; -6.35 + 5.00 mm; -5.00 + 4.00 mm; -4.00 + 3.36 mm; -3.36 + 2.83 mm; -2.83 + 2.38 mm; -2.38 +1.6 mm; -1.6 + 1.19 mm; -1.19+0.00 mm. Mineralogical analysis by size classes for both borate samples was performed by examination with an optical polarization microscope. This analysis, for both borate samples, determined that the liberations of boron minerals of over 80% are achieved in the size class -2.83+0.00 mm. Mineralogical analysis by size class of the borate sample of

class -30+0.00 mm showed that this sample has a very dirty surface. The dust stuck to its mineral surfaces, despite crushing and dry sieving.

Mineralogical analysis by X-ray diffraction method

Mineralogical, X-ray diffraction analysis was used to determine and monitor the phase composition of both borate samples. The samples were analyzed on a "PHILIPS" X-ray diffractometer, model PW-1710, with a curved graphite monochromator and a scintillation counter. The intensities of diffracted CuKα X-rays (λ=1.54178Å) were measured at room temperature in intervals of 0.02° 2θ and time of 1 s in the range from 4 to 65 °2θ. The X-ray tube was loaded with a voltage of 40 kV and a current of 30 mA, while the slits for directing the primary and diffracted beams were 1° and 0.1 mm. The following text shows the obtained results.

The run-of-mine borate sample - X-ray diffraction method

X-ray analysis determined the following mineral composition of the examined sample: colemanite, howlite, quartz, carbonate minerals (calcite, dolomite), clay minerals (smectite)/chlorites, analcime, jarandolite, and weddellite. The absolutely dominant mineral in the analyzed sample is colemanite. After colemanite, quartz is more significantly present, as well as carbonate minerals (dolomite is more dominant than calcite), clay minerals (smectite), analcime, howlite, and jarandolite are less abundant. The semiquantitative share of crystalline phases (minerals) is as follows: colemanite 55-57%, carbonates 18-20% (dolomite 15-17%, calcite ≤ 2-3%), smectites/chlorites ~ 10%, analcime 8-10%, quartz 1-2%, other boron minerals (howlite and jarandolite in total ~ 5%). Weddelite is present in the trace. The diffractogram of the tested sample is presented in Figure 1.

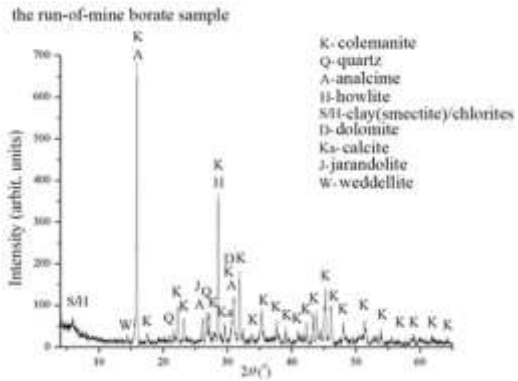

Figure 1 Powder diffractogram of the run-of-mine borate sample

Borate sample of size class -30+0.00 mm - X-ray diffraction method

X-ray analysis determined the following mineral composition of the examined sample: colemanite, howlite, quartz, carbonate minerals (calcite, dolomite), clay minerals (smectite)/chlorites, analcime, and jarandolite.

The absolutely dominant mineral in the analyzed sample is colemanite. After colemanite, quartz is more significantly present, as well as carbonate minerals (dolomite is more dominant than calcite), clay minerals (smectite), analcime, howlite, and jarandolite are less abundant. The semiquantitative share of crystalline phases (minerals) is as follows: colemanite 35-37%, carbonates 30-32 (dolomite 20-22, calcite ≤ 10%), smectites/chlorites 10-12%, analcime 8-10%, quartz ≤ 5%., other boron minerals (howlite and jarandolite in total ~ 5%). The diffractogram of the tested sample is presented in Figure 2.

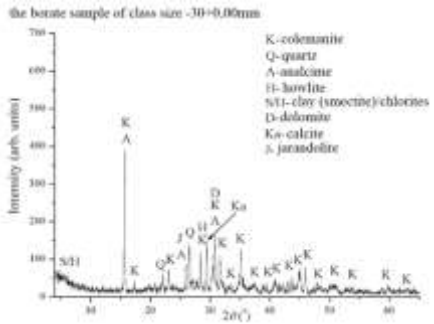

Figure 2 Diffractogram of the borate sample of size class -30+0.0 mm

RESULTS AND DISCUSSION

Physico-chemical and mineralogical investigations represent the basis for further technological tests that should define the processing procedure of both types of borates. These investigations showed that borates are very complex in terms of their mineral composition. Namely, in addition to boron minerals, they also consist of alumino-silicate tailings, oxide carbonate minerals, zeolite (of the analcime type), and organic matter. Based on the mineralogical analysis, the same minerals are present in both borate samples, Figure 1, Figure 2. According to the mineralogical analysis, the content of boron minerals is higher in the run-of-mine borate sample (B_2O_3-55-57%, Figure 1), than in the borate sample of the size class -30+0.00 mm (B_2O_3- 35-37%, Figure 2).In order to examine and determine the possibility of the separation of minerals one from another, it is necessary that the minerals have some different properties by which they can be separated from each other. Regarding their physical-mechanical properties, hardness by Mohs scale, specific mass, etc. the minerals present in the sample have similar properties. According to the specific mass (density), all these minerals have a specific mass of about 2.5 g/cm^3, except montmorillonite, whose specific mass ranges from 2-2.7 g/cm^3. Chamosite has a higher specific mass than the mentioned minerals with a specific mass of 3.2 g/cm^3. This fact tells us that it would be difficult to separate these minerals by gravity concentration because they are close in density (specific mass).

CONCLUSION

According to the chemical compositions of the minerals present in the borate samples, it can be stated that some of these minerals contain iron, especially smectites,

and chlorites. These minerals can be separated from boron minerals using high-intensity magnetic separation. In addition, montmorillonite itself does not contain iron, but in nature very often binds it to itself, either between lamellae, or by isomorphic replacement, or sometimes both ways. For this reason, montmorillonite very often belongs to the minerals that can be separated by magnetic separation from boron minerals. In any case, in accordance with the mineralogical tests by size classes, the mineral raw material for this purpose should be comminute to a size of -2.83 mm, when the boron mineral is free from accompanying minerals. And after this phase, it is necessary to sieve the raw material prepared in this way into the appropriate size classes that can be subjected to magnetic separation. Through tests, it is necessary to determine the most optimal induction of the magnetic field, during which the magnetic separation of boron and accompanying minerals by size classes is achieved. With these tests, it is necessary to determine the optimal size range of classes that can be subjected to magnetic separation, as well as the last class that cannot be subjected to dry magnetic separation due to its fineness.

ACKNOWLEDGEMENT

This paper is part of the research according to the research funding agreement financed by the Ministry of Education, Science and Technological Development of the Republic of Serbia in 2023 under the number 451-03-47/2023-01/200023.

REFERENCES

1. https://www.britannica.com/science/boron-chemical-element.
2. Helvacı, C.(2017) Borate deposits: An overview and future forecast with regard to mineral deposits. Boron 2 (2), 59 - 70.
3. Flores, H.R., Mattenella, L.E., Kwok, L.H. (2006) Slow release boron micronutrients from pelletized borates of the northwest of Argentina. Minerals Engineering, 19, 364–367.
4. http://www.etimine.com/boron-minerals/.
5. Indian Minerals Yearbook (2020) (Part- III: Mineral Reviews) 59th Edition, BORON MINERALS.
6. Roskill (2015) Information services boron: global industry markets and Outlook thirteenth edition. https://roskill.com/market-report/boron/ (accessed May 2019).
7. European Commission (2014) Report on Critical Raw Materials for the EU. Report of the Ad-Hoc Working Group on Defining Critical Raw Materials. EC, Brussels, Belgium, 41.
8. Mermer, C. (2020) Addressing potential resource scarcity for boron mineral: A system dynamics perspective. Journal of Cleaner Production, 270, 122192.
9. Rio Tinto plc 2019, 2018 annual report: London, United Kingdom, Rio Tinto plc, February 27, 300 p. (Accessed April 5, 2019, at http://www.riotinto.com/documents/RT_2018_Annual_report.pdf.).
10. Tim, D. (2018) Erin Ventures enters into strategic partnership to advance its boron project: Junior Mining Network, June 18. (Accessed May 10, 2019, at https://www.juniorminingnetwork.com/junior-miner-news/press-releases/1256-tsx-venture/ev/48398-erin-ventures-enters-strategic-partnership-to-advance-its-boron-project.html.)
11. Geological elaborate on boron mineral reserves in the "Pobrđski potok" deposit near Baljevac in Serbian (Geostim, Aničić Stojan, dipl.ing.geol., Beograd, 2008. god.).

XV International Mineral Processing and Recycling Conference
17-19 May 2023, Belgrade, Serbia

STUDY OF ORE SAMPLES FROM THE ZLATÉ HORY DEPOSIT (HRUBÝ JESENÍK Mts., SILESIA, CZECH REPUBLIC)

S. Hredzák[1#], M. Matik[1], O. Šestinová[1], A. Zubrik[1], D. Kupka[1], S. Dolinská[1], I. Znamenáčková[1], M. Sisol[2], M. Marcin[2], L. Pašek[3]

[1] Institute of Geotechnics of the Slovak Academy of Science, Košice, Slovakia
[2] Institute of Earth Resources, Faculty of Mining, Ecology, Process Control and Geotechnologies, Technical University of Košice, Košice, Slovakia
[3] DIAMO state enterprise, Directorate of state enterprise, Department of Mining, Czech Republic

ABSTRACT – The contribution deals with characterization of 4 samples from Zlaté Hory ore district. Regarding all samples sphalerite was found as the main valuable mineral. Even in sample 1 Zn content attains 18.34 %. Its surrounding is represented by quartz, muscovite, chlorite and plagioclase. The content of pyrite is also significant.

Keywords: Zlaté Hory, Ore characterization, Sphalerite.

INTRODUCTION

Current period is characteristic by high demand for minerals, especially for metals. This situation generates activities connected with reassessment of known up to now non-commercial deposits and also abandoned mining fields.

Zlaté Hory (transl.: Gold Mountains) belongs to old mining fields probably mined in the period BC. A florescence of gold mining started in the 16th century, and in the 20th century Cu-Pb-Zn(±Au, Ag) ores were intensively exploited [4-5].

Thus, with regard on given situation about mineral resources and within the frame of bilateral cooperation 4 samples of ore have been studied.

EXPERIMENTAL

The samples of ore were subjected to chemical analysis and XRD study. So as to chemical analyses, SiO_2 content was assayed gravimetrically (GA). Carbon and sulphur were determined using a CHNS Vario MACRO Cube analyzer (Elementar Analysensysteme GmbH, Hanau, Germany). The sulfanilamide (C = 41.81 %, N = 16.26 %, H = 4.65 %, S = 18.62 %) was used as the CHNS standard. Fe, Mn, Zn, Pb and Cu have been analyzed by AAS using the device VARIAN AA240FS (Australia). Other elements were assayed by XRF technique carried out by a table XRF spectrometer Spectro Xepos model XEPO3 (Spectro Analytical Instruments, GmbH, Germany) at the measuring range ^{11}Na–^{92}U.

corresponding author: hredzak@saske.sk

XRD study was performed using D8 Advance diffractometer (Bruker, Germany), working with Cu Kα radiation at voltage 40 kV and current 40 mA. The data were collected over the angular range 5°<2θ<80° with measuring steps 0.03° and a counting time 5s. Measured diffractograms were processed using programs Diffracplus Basic and Excel. The databases such as webmineral, handbookofmineralogy and the Arizona library were also used at mineral phases identification [1-2]. The abbreviations of minerals were applied after [8].

Optical observations were performed by monocular microscope LEVENHUK (magnification max. ca 30x).

RESULTS AND DISCUSSION

The results are introduced in Tables 1-3. XRD patterns of float and sink products are presented in Figs. 1-4. Similarly, the examples are documented in Fig. 5.

Table 1 Major rock elements

sample	SiO_2	Al_2O_3	CaO	MgO	TiO_2	K_2O	Na_2O
	GA	XRF	XRF	XRF	XRF	XRF	XRF
1	52.82	3.76	2.74	3.48	0.14	0.69	6.33
2	53.18	16.39	0.13	14.38	0.56	0.41	0.88
3	59.4	16.42	0.15	7.01	0.63	2.12	1.84
4	53.62	12.36	0.0014	2.43	0.38	3.12	2.16

Table 2 Target elements

sample	Fe	Mn	Zn	Pb	Cu	S	C
	AAS	AAS	AAS	AAS	AAS	CHNS	CHNS
1	3.19	0.22	18.34	0.75	0.024	12.02	0.935
2	8.68	0.21	2.61	0.05	0.061	3.68	0.215
3	5.48	0.11	2.71	0.13	0.110	4.52	0.195
4	12.85	0.02	4.70	0.42	0.290	15.70	0.215

Table 3 Selected trace elements in ppm

sample	Cd	Cr	V	Ni	As	Sb	Ba
	XRF	XRF	XRF	XRF	XRF	XRF	XRF
1	1150	214	67	305	trace	55	220
2	190	62	115	100	8	67	228
3	210	585	165	129	21	73	607
4	260	365	110	185	124	66	480

Sample 1: Quartz is dominant mineral accompanied by sphalerite. It is needed to mention after considering Zn content that sphalerite strongly prevails over pyrite, their peaks overlapping and it is often difficult to discriminate them only after diffractogram. The other significant minerals are plagioclase (albite), muscovite, chlorite (chamosite), dolomite, ankerite, and probably galena. Zn and Pb content attain 18.34 % and 0.75 %, respectively.

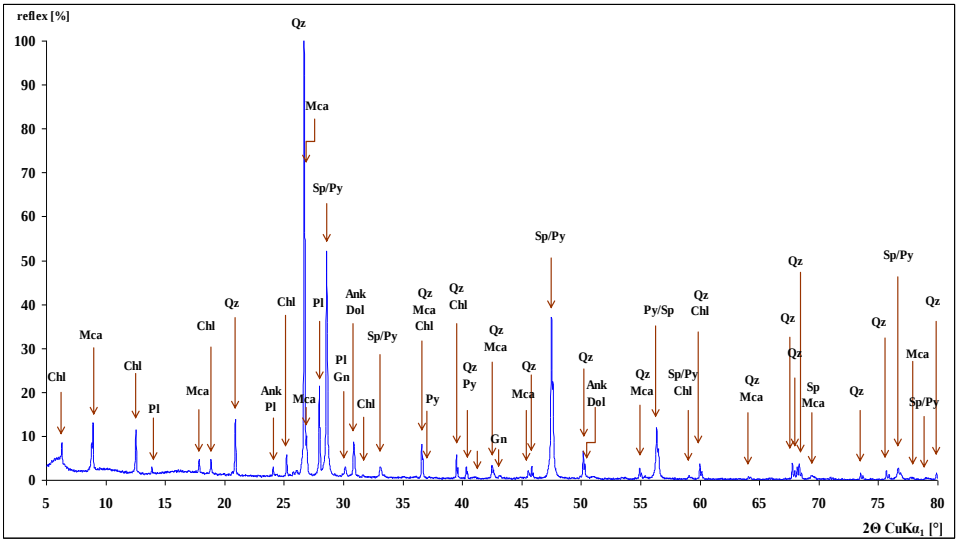

Figure 1 XRD pattern of sample 1

Qz – quartz, Chl – chlorite, Mca – muscovite, Pl – Plagioclase, Py – pyrite, Sp – sphalerite, Gn – galena, Ank – ankerite, Dol – dolomite

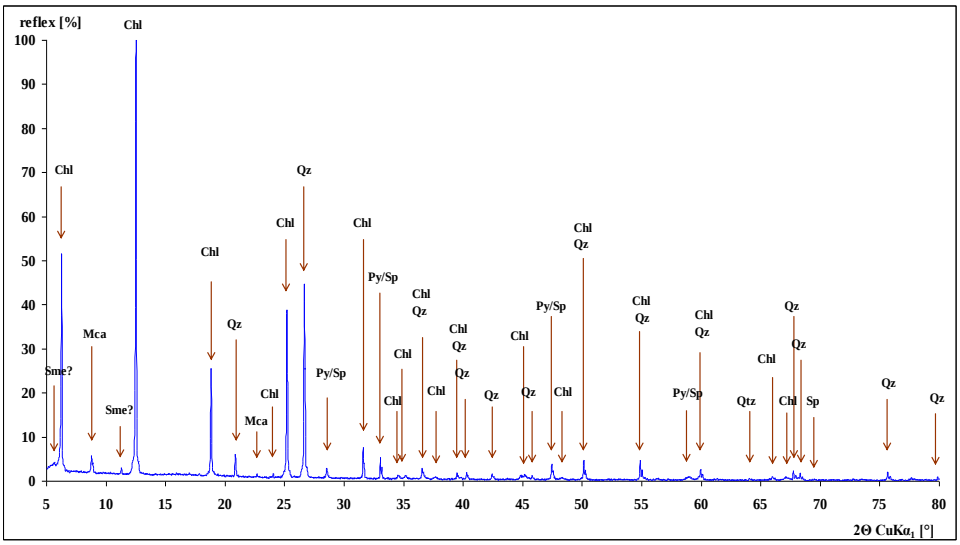

Figure 2 XRD pattern of sample 2

Qz – quartz, Chl – chlorite, Mca – muscovite, Py – pyrite, Sp – sphalerite, Sme - smectite

Sample 2: Chlorite is dominant mineral accompanied by quartz. Low peaks of muscovite, pyrite and sphalerite can be observed. Also some smectite (saponite and/or sauconite) occurs. The sample is without plagioclase. The content of MgO is far highest, namely 14.38 %, as to iron it runs 8.68 %, the both on the account of chlorite abundance in sample. Zn content is 2.61 %.

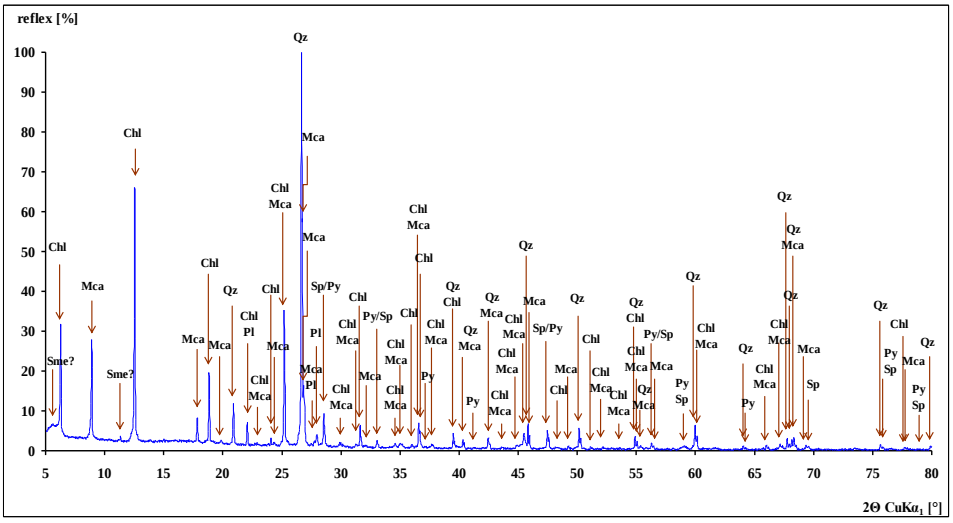

Figure 3 XRD pattern of sample 3

Qz – quartz, Chl – chlorite, Mca – muscovite, Pl – Plagioclase, Py – pyrite, Sp – sphalerite, Sme - smectite

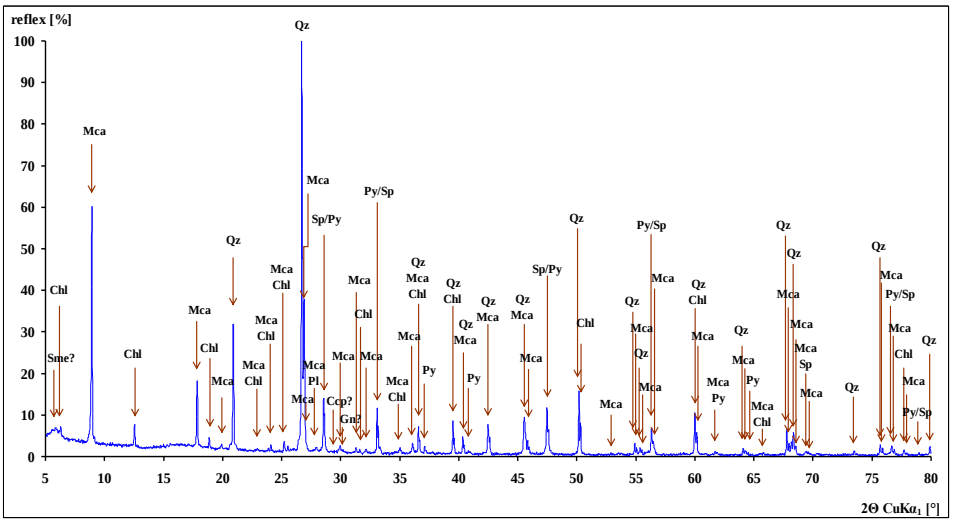

Figure 4 XRD pattern of sample 4

Qz – quartz, Chl – chlorite, Mca – muscovite, Pl – Plagioclase, Py – pyrite, Sp – sphalerite, Sme – smectite, Gn – galena, Ccp - chalcopyrite

Sample 3: Quartz is dominant mineral accompanied by chlorite. Muscovite is also significant. The other minerals are pyrite, sphalerite, plagioclase (albite), and smectite. Fe and Zn content is 5.48 % and 2.71 %, respectively.

Sample 4: Quartz is dominant mineral accompanied by muscovite. The other minerals are pyrite, sphalerite, chlorite. Peaks of plagioclase (albite), chalcopyrite and galena can be observed. The sample has the highest content of Fe, namely 12.85 %, furthermore contents of Zn, Pb and Cu are 4.7 %, 0.42 % and 0.29 %, respectively.

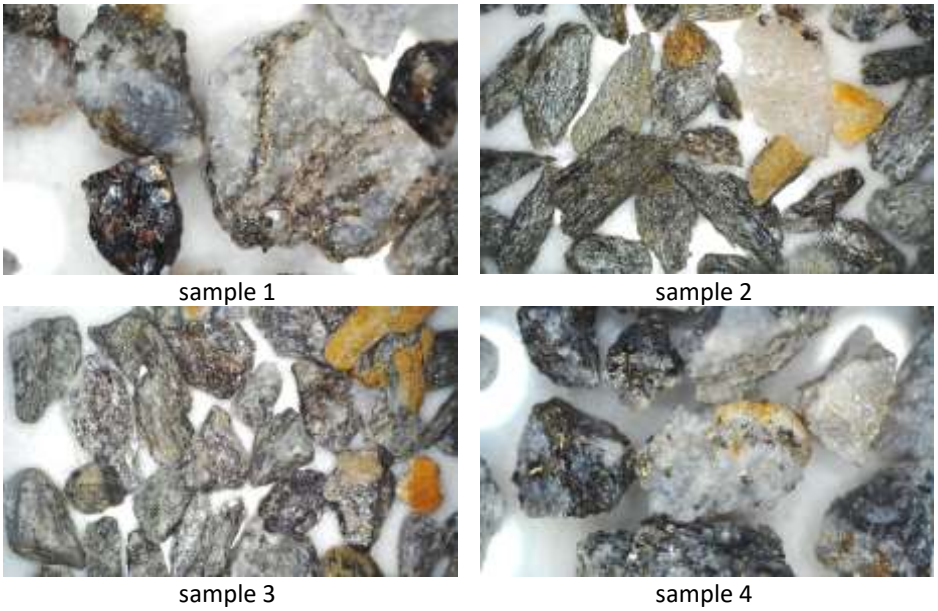

Figure 5 Samples of ore from Zlaté Hory (grain size of +2–5 mm)

As to mineral composition obtained results are in concordance with data after [3, 6-7]. Only sample 1 has extremely high content of zinc or more precisely sphalerite. Samples 2-3 with higher content of chlorite contain only small amount metalliferous or better said valuable minerals, i.e. pyrite and sphalerite. This pair is typical for all mining district. Moreover, comparing to [6] no barite was detected, but in sample 1 carbonates such as dolomite and ankerite were identified.

CONCLUSION

The study was performed with the aim to verify content of valuables in the ore from the Zlaté Hory deposit. As to metalliferous minerals pyrite and sphalerite were detected in all four samples. As to galena and chalcopyrite only small peaks were observed in diffractograms. Associated gangue minerals are represented mainly by quartz, chlorite (chamosite), muscovite, ± plagioclase, dolomite, ankerite and smectite. The samples 1 and 4, especially 1, the both ones can be considered as promising. Samples 2 and 3 contain high amount of chlorite. Finally, cleaner findings will be formulated after investigation of gravity concentrates.

ACKNOWLEDGEMENT

This work was supported by the Slovak Scientific Grant Agency for the projects VEGA VEGA2/0167/21 and 2/0116/23.

This study has received funding from the European Institute of Innovation and Technology (EIT), a body of the European Union, under the Horizon 2020, the EU Framework Programme for Research and Innovation (Project BioLeach: Innovative Bio-treatment of RM, grant number: 18259).

REFERENCES

1. Anthony, J.W., Bideaux, R.A., Bladh, K.W., Nichols, M.C. (eds.) (2004-2020) Handbook of Mineralogy, Mineralogical Society of America, Chantilly, VA 20151-1110, USA. http://www.handbookofmineralogy.org/. 2004-2020.
2. Barthelmy, D. (1997-2014). www.webmineral.com.
3. Fojt, B., Hladíková, J., Kalenda, F. (2001) Zlaté Hory in the Silesia - the largest ore district in the Jeseniky Mts., Czech Republic. Part 2: C. Geology D. Mineralogy E. Geochemistry of stable isotopes. Acta Mus. Moraviae, Sci. geol., 86, 3-58. (in Czech)
4. Fojt, B., Večeřa, J. (2000) Zlaté Hory in Silesia - the biggest are district in the Jeseniky Mts., Czech Republic. Part 1.: A. History of mining B. Review of published works. Acta Mus. Moraviae, Sci. geol., 85, 3-45. (in Czech)
5. Novák, J. (1988) Development of gold mining in the Zlaté Hory area. In: Proceedings of UNIGEO, government enterprise Ostrava, 34/1988, 89-106. (in Czech)
6. Vrlíková, V., Čablík, V., Janáková, I. (2019) Possibilities of Obtaining Metals from Polymetallic Ore from Zlate Hory. Inżynieria Mineralna - Journal of the Polish Mineral Engineering Society, July–December/2019, 33-37.
7. Vrlíková, V., Čablík, V., Hredzák, S., Matik, M., Briančin, J., Zubrik, A., Dolinská, S., Znamenáčková, I., Šestinová, O. (2019) The possibility of sulfide concentrate preparation from polymetallic ore. In: Situation in Ecologically Loaded Regions of Slovakia and Central Europe: The XXVIII-th Scientific Symposium with International Participation, Hrádok at Jelšava, Slovakia, October 24-25, 2019. Proceedings (ed. Hredzák, S.), Slovakian Mining Society, Košice 2019, 214-219.
8. Warr L.N. (2021) IMA–CNMNC approved mineral symbols. Mineralogical Magazine 85, 291–320. https://doi.org/10.1180/mgm.2021.43

XV International Mineral Processing and Recycling Conference
17-19 May 2023, Belgrade, Serbia

COMPARISON OF THE RESULTS OF SEPARATION OF DIFFERENT COALS IN THE ANTHRACITE MINE "VRSKA CUKA"

J. Sokolović[1], I. Ilić[1#], D. Krstić[2]
[1] University of Belgrade, Technical Faculty in Bor, Bor, Serbia
[2] Grammer System d.o.o., Aleksinac, Serbia

ABSTRACT – This paper presents the comparative results of the study of the efficiency of the separation of coal in the anthracite mine "Vrska Cuka". Industrial and laboratory tests of the possibility of gravity separation were carried out with the aim of verifying the sharpness of the separation in the process of coal separation, as well as assessing its impact on the technological indicators of the process. Parallel research was carried out on two different samples of raw coal: from the anthracite mine "Vrska Cuka" and the lignite mine "Lubnica". The Ecart probable values are Ep=97.5 kg/m^3 and 40 kg/m^3, respectively. Such results only confirm the fact that grain size affects the value of Ep, that is, that coarser-grained products are separated better, more efficiently than finer-grained products.

Keywords: Vrska Cuka, Lubnica, Gravity Separation, Coal.

INTRODUCTION

Anthracite mine "Vrska Cuka" Avramica is located about 10 km from Zajecar in eastern Serbia. The mine has a modern separation that was completed in 1994. The industrial plant comprises of a complex technological process for gravity and flotation concentration of raw coal. Size fractions over 0.5 mm are treated by dense-medium processes, whereas flotation has been proposed for sizes finer than 0.5 mm [1].

The gravitational concentration of coal is carried out in the two-part separator "BSRI - 1200" with a spiral and electromagnetic valve for separating the sink fraction. In this device for separation, two different size fractions of anthracite coal can be treated at the same time, namely: (- 30 + 5) and (- 5 + 0.5) mm [1,2]. In the separation plant, lignite with different characteristics from the Lubnica mine is washed, too. The aim of this study is to perform a comparative analysis of the results of separation of different coals. Research was carried out on two different samples of raw coal: from the anthracite mine "Vrska Cuka" and the lignite mine "Lubnica".

EXPERIMENTAL

The samples for experimental tests were collected from separation process in the anthracite mine "Vrska Cuka". As in the separation of the "Vrska Cuka" anthracite mine, different coal assortments from the "Lubnica" mine are washed, the samples from the "Lubnica" mine were collected in the same way and from the same sampling points from the coal separation plant [3].

corresponding author: iilic@tfbor.bg.ac.rs

The particle size analysis by size fractions and the float-sink analysis by density fractions were perfomed in order to characterize the raw coal. The laboratory float-sink analysis were performed on the raw coal and all products (float and sink prodcuts) of coal separation. The analysis was performed using an inorganic heavy liquid (solutions of $ZnCl_2$ of density ranging from from 1300 to 1850 kg/m^3). All obtained size fractions and density fractions were analyzed on the ash content.

RESULTS AND DISCUSSION

Particle size analysis

The particle size analysis and ash content in size fractions of raw coal from the "Vrska Cuka" and "Lubnica" are given in Table 1.

Table 1 Particle size distribution of raw coal [3]

Particle size d (mm)	Vrska Cuka		Lubnica	
	Mass %	Ash %	Mass %	Ash %
+30	0.00	0.00	1.63	67.24
-30+15	10.66	40.01	61.58	39.41
-15+10	29.09	41.71	28.80	32.75
-10+5	21.38	41.12	2.96	38.87
-5+0	38.87	33.49	5.03	52.42
∑	100.00		100.00	

The results of the analysis of the particle size distribution of the raw coal sample from the "Lubnica" mine show that this sample is significantly coarser-grained compared to the raw coal from the "Vrska Cuka" anthracite mine, and that in this sample there are dominant participation of coarse size classes, even particles with a size above 30 mm.

Float-Sink analyses

The results of float-sink analysis of a raw coal from anthracite mine "Vrska Cuka" as well as products of separation (separation coal as float fraction and tailing as sink fraction) are shown in Table 2 [3].

Table 2 Float-sink analysis of a raw coal and products of separation of coal from anthracite mine "Vrska Cuka"

Specific gravity kg/m^3	Raw coal (feed) (%)		Separated coal (float) (%)		Tailing (sink) (%)	
	Mass %	Ash %	Mass %	Ash %	Mass %	Ash %
-1300	6.19	6.79	4.78	3.38	0.38	3.82
-1400	27.37	9.83	40.50	3.77	11.37	4.48
-1500	8.57	18.20	17.63	13.00	4.31	14.64
-1600	7.64	34.00	9.58	24.16	3.40	25.47
-1700	8.85	40.29	5.07	29.13	3.81	32.15
-1850	10.86	53.64	2.95	41.32	3.77	40.62
+1850	30.51	68.82	19.49	80.07	72.96	80.91
∑	100.00		100.00		100.00	

By separation of raw anthracite coal, it can be noticed that depending on the quality, in the range of separation densities between 1400 and 1800 kg/m^3, the mass yield of the float coal is from 34% to 65%. For instance, the separation of raw coal on the density 1600 kg/m^3, it can be achieved mass yield of coal, Im = 49.78% with average ash content, p = 14.60%.

Based on the results, it can be seen that the fractions below 1500 kg/m^3 have a significant mass share of about 63% with an ash content of 8.68% in the separated coal product.

The fraction above 1850 kg/m^3, with the largest mass share in tailings (sinking product) which is 72.96% and with an ash content of 80.91%.The results of float-sink analysis of a raw coal from lignite mine "Lubnica" as well as products of separation by the density fractions are shown in Table 3 [3].

Table 3 Float-sink analysis of a raw coal and products of separation of coal from lignite mine "Lubnica"

Specific gravity kg/m^3	Raw coal (feed) (%)		Separated coal (float) (%)		Tailing (sink) (%)	
	Mass %	Ash %	Mass %	Ash %	Mass %	Ash %
-1300	23.95	10.75	51.66	8.78	0.77	13.23
-1400	11.90	20.01	32.25	19.40	2.73	23.27
-1500	29.96	40.76	11.78	41.01	4.72	41.39
-1600	11.48	54.83	3.41	55.59	20.96	57.40
-1700	4.25	57.87	0.82	56.54	23.52	64.05
-1850	12.20	63.43	0.08	52.74	30.93	73.99
+1850	6.26	73.51	0.00	0.00	16.37	82.02
∑	100.00		100.00		100.00	

The float-sink analysis of the raw lignite coal shows a low degree of separability for the tested raw material, the mass yield at a density of 1400 kg/m^3 is 35.80%. The ash content at this density is about 14%.

The results of float-sink analysis of the sample of separated coal show that the fraction -1300 kg/m^3, which amounts to 51.66%, is dominant in this product. The ash content in this fraction is about 9%.

Determination of separation efficiency

The partition or distribution curve is useful in assessing the efficiency or sharpness of the coal separation [5]. The partition curve or Tromp curve (introduced by Tromp in 1937) is obtained by plotting the partition coefficient against the mean of its density range [6].

The separation density or cut point (ρ_{50}) and the probable error of separation (E_P) can both be calculated from the partition curve [5].

The probable error of separation (E_P) is defined as half the difference between the S.G. where 75% is recovered in the sinks and the S.G. at which 25% is recovered in the sinks [5].

The mass yield was calculated using the Grumbrecht method. Figure 1 and Table 4 show the results.

Table 4 Calculation of mass yield of Grumbrecht methods – Vrska Cuka

Specific gravity	Feed raw coal (%)	Separation coal (float) (%)	Tailing (sink) (%)				
kg/m³	U	K	J	U - J	K - J	(U – J) (K – J)	(K – J)²
-1300	6.19	4.78	0.38	5.81	4.40	25.58	19.36
-1400	27.37	40.50	11.37	16.00	29.13	466.16	848.56
-1500	8.57	17.63	4.31	4.26	13.32	56.79	177.42
-1600	7.64	9.58	3.40	4.24	6.18	26.19	38.19
-1700	8.85	5.07	3.81	5.04	1.26	6.36	1.59
-1850	10.86	2.95	3.77	7.09	-0.82	-5.81	0.67
+1850	30.51	19.49	72.96	-42.45	-53.47	2269.85	2859.04
∑	100.00	100.00	100.00			2845.12	3925.47

$$Im = \frac{2845.12}{3925.47} \cdot 100 = 72.48\% \quad (1)$$

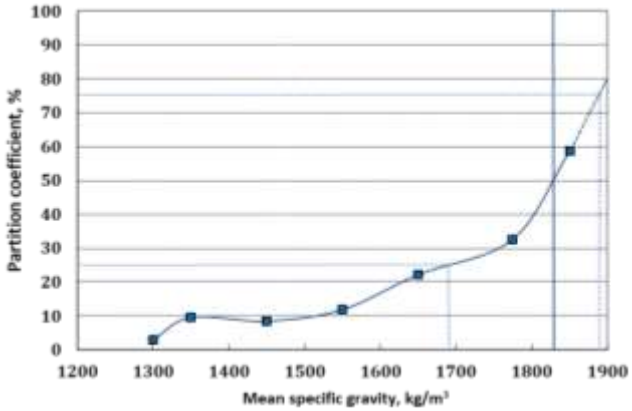

Figure 1 Partition curve for gravity separation of raw coal from the anthracite mine "Vrska Cuka" [3]

From the partition curve, the separation density or ρ_{50} is 1835 kg/m^3. The probable error of separation or the Ecart probable (Ep) is expressed as:

$$E_p = \frac{\rho_{75} - \rho_{25}}{2} = \frac{1890 - 1695}{2} = 97.5\ kg/m^3 \quad (2)$$

Table 5 compares theoretical and practical data for the gravity separation of raw coal from the "Vrska Cuka" anthracite mine.

Table 5 Compared theoretic and industrial values for gravity separation of raw coal

	Theoretic values	Industrial values
Mass yield (wt. %)	68.40	72.48
Average ash (%)	23.51	24.60
ρ_p (kg/m³)	1835	1835
E_p (kg/m³)	0	97.5

The results of the calculation of mass yield of Grumbrecht methods as well as partition curve for gravity separation of raw coal from the lignite mine "Lubnica" are shown in Table 6 and Figure 2.

Table 6 Calculation of mass yield of Grumbrecht methods – Lubnica

Specific gravity	Feed raw coal (%)	Separation coal (float) (%)	Tailing (sink) (%)				
kg/m³	U	K	J	U - J	K - J	(U – J) (K – J)	(K – J)²
-1300	23.95	51.66	0.77	23.18	50.89	1179.58	2589.79
-1400	11.90	32.25	2.73	9.17	29.52	270.71	871.43
-1500	29.96	11.78	4.72	25.24	7.06	178.23	49.84
-1600	11.48	3.41	20.96	-9.48	-17.55	166.40	308.00
-1700	4.25	0.82	23.52	-19.27	-22.70	437.45	515.29
-1850	12.20	0.08	30.93	-18.73	-30.85	577.94	951.72
+1850	6.26	0.00	16.37	-10.11	-16.37	165.46	267.98
∑	100.00	100.00	100.00			2975.76	5554.06

$$Im = \frac{2975.76}{5554.06} \cdot 100 = 53.58\% \quad (3)$$

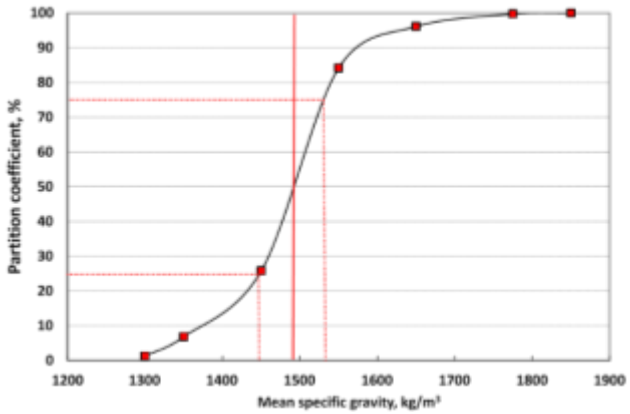

Figure 2 Partition curve for gravity separation of raw coal from the lignite mine "Lubnica" [3]

From the partition curve, the separation density or ρ_{50} is 1490 kg/m^3. The probable error of separation or the Ecart probable (Ep) is expressed as:

$$E_p = \frac{\rho_{75} - \rho_{25}}{2} = \frac{1530 - 1450}{2} = 40\ kg/m^3 \quad (4)$$

Table 7 compares theoretical and practical data for the gravity separation of raw coal from the "Lubnica" lignite mine.

Table 7 Compared theoretic and industrial values for gravity separation of raw coal

	Theoretic values	Industrial values
Mass yield (wt. %)	62.81	53.58
Average ash (%)	25.39	18.02
ρ_p (kg/m^3)	1490	1490
E_p (kg/m^3)	0	40

CONCLUSION

In this paper are shown results of the parallel research conducted on two different samples of raw coal: from the anthracite mine "Vrska Cuka" and the lignite mine "Lubnica". The achieved results in the process of separation of coal from the "Vrska Cuka" anthracite mine are as follows: mass yield is 72.48%, while the average ash content in the separated coal is 24.60%. It was determined that the separation density is ρ_p=1835 kg/m^3. The probable error of separation or the Ecart probable (Ep) value is Ep=97.5 kg/m^3, confirming that the technological process of coal separation works with a reduced sharpness of separation.

Based on the results obtained in the lignite coal separation process, it can be concluded that the separation efficiency was better. The Ecart probable (Ep) is 40 kg/m^3. At a density of 1490 kg/m^3, the mass yield is 53.58% with an ash content of 18.02% in the separated coal. Such results only confirm the fact that grain size affects the value of Ep, that is, that coarser-grained lignite coal are separated better, more efficiently and with significantly greater precision than finer-grained anthracite coal.

ACKNOWLEDGEMENT

"The research presented in this paper was done with the financial support of the Ministry of Education, Science and Technological Development of the Republic of Serbia, within the funding of the scientific research work at the University of Belgrade, Technical Faculty in Bor, according to the contract with registration number 451-03-47/2023-01/200131".

REFERENCES

1. Stanojlovic, R., Markovic, Z.S., Milanovic, D., Trumic, G. (1995) The technology for valorization of coal from old discard of antracite mine "Vrska Cuka". In: Proceedings of the 6th Balkan Conference on Mineral Processing. Ohrid, Macedonia, Proceedings, 418-421.
2. The Main Mining Project of separation for concentration of coal from the anthracite mines "Vrska Cuka" - Avramica, Book I, Technology and mechanical project, Institute for Copper, Bor. (In Serbian)
3. Krstic, D. (2019) Verifikacija i ispitivanje mogućnosti poboljšanja tehnološkog procesa separacije uglja u rudniku antracita "Vrška Čuka". Graduated thesis, University of Belgrade, Technical Faculty in Bor, Bor. (In Serbian)
4. Sokolović, J. (2020) Practicum in physical methods of concentration, Technical Faculty in Bor, Bor. (In Serbian)
5. Gupta, A., Denis Yan, D. (2016) Chapter 16 - Gravity Separation. In: Mineral Processing Design and Operations (Second Edition), Elsevier, 563-628.
6. Tromp, K.F. (1937) New methods of computing the washability of coals. Glückauf, 37, 125-131.

XV International Mineral Processing and Recycling Conference
17-19 May 2023, Belgrade, Serbia

A COMPUTATIONAL TOOL FOR PREDICTION OF JIG CONCENTRATOR OPERATING PARAMETER TO GET IMPROVED YIELD OF CONCENTRATE

R. R. Bandaru[1#], A. Kumar[2], J. M. Korath[2], M. R. Rath[1]
[1] P&L Noamundi, Tata Steel Limited, Noamundi
Tata Steel Limited, Jamshedpur, India
[2] Automation Division, Tata Steel Limited, Jamshedpur, India

ABSTRACT – Jig-concentrators are widely used in mineral processing for enhancing the grade value of ore through gravitational separation process. In-order to understand the effect of various operating parameters on performance of the jig concentrator, a first principles based mathematical model has been developed. The design parameters of an operating Jig along with typical feed characteristics and operating parameters were used for model development and testing. The governing equations for the momentum balance are solved numerically. The model predicts the spatial and velocity distribution of both iron bearing particles and gangue particles in the Jig chamber. Model is used to simulate Jig performance under varying conditions of input feed's physio-chemical properties and machine operating variables like pulse/suction pressures, stroke length/frequency, bed depth etc. Using this model, optimal operating set points are arrived at for a given feed characteristics and operating constraints of the plant. The testing and validation of the model has been done at Noamundi beneficiation plant of TATA Steel, wherein the set point for jig bed depth predicted by model provide 5% to 8% more yield as comparison to set points as per existing standard operating procedure.

Keywords: Jig Concentrators, Gravity Separation.

INTRODUCTION

Jig concentrators are commonly used in mineral processing as the said concentrator provide an efficient and effective method to separate heavy minerals from lighter ones by means of gravity separation. In the jigging process the Separation mechanism is based on enhanced gravity which takes advantage of particle size and density of feed material or ore. The phenomenon that assists in the operation of a jig concentrator is known as the "stratification process". The jig concentrator is a gravity separation device that uses the principle of settling velocity difference between the mineral particles to separate them based on their specific gravity. The stratification process occurs when the heavy mineral particles sink to the bottom of the jig bed due to their higher settling velocity, while the lighter particles are carried upwards by the pulsating water flow. As a result, the heavy minerals are concentrated in the lower layer of the jig bed, while the lighter minerals are concentrated in the upper layer. The pulsating water flow in the jig concentrator creates an upward and downward motion, which helps to separate the minerals [1]. This motion causes the particles to move through the jig bed and collide with each other, which further enhances the stratification process. Overall, the

corresponding author: bandaru.reddy@tatasteel.com

stratification process is a crucial phenomenon that assists in the operation of the jig concentrator, as it allows for the efficient separation of minerals based on their specific gravity and liberation percentage of ore mineral and gangue mineral at certain size distribution of minerals which are best suits for jigging operation. It is well known that quality or grade of ore decreases day by day during mining which deteriorate the liberation characteristic of jig feed ore and hence, the performance of jig in terms of separation efficiency is decreases. To overcome the decrease in separation efficiency of jig concentrators various mathematical model has been proposed which leads to optimise the operating parameters of jig concentrators. The proposed model by different researchers is focused mainly on the gravimetric concentration criteria process in Jigs which are either based on energy conservation method or discrete elemental method. The said models will try to execute the different operating variables which affect the trajectories of particles, and such variables are feed water rate, amplitude (stroke length), frequency (number of strokes per second) of oscillating flow, feed rate etc and provide the optimal set point for such variables for jigging process [2,3]. But such optimal set point is good for lab scale or pilot scale jigging process and might not give good separation efficiency at plant scale jigging process, this is happening because, the existing theories or models assumed that the flow pattern of stratified jig bed is uniform and consisting idealized behaviour of flow. The main disadvantage with such model of jigging process is that, when the constants of the model are calibrated for a specific operating condition, the same model cannot be used to predict condition far from the calibrated conditions, hence the expected output will far from the predicted output.

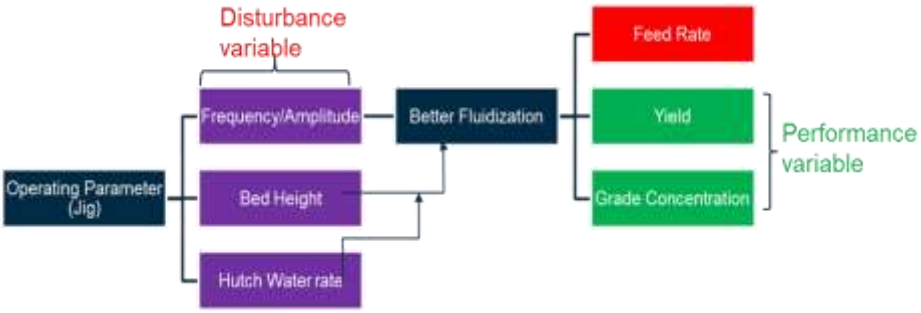

Figure 1 Generalized operating practices of Jig Concentrator

The fig. 1 represents the general operating practices of jig concentrator at plant scale wherein the disturbance variable is main pain area which determine the fluidization tendency for better performance of jig concentrators. During the actual plant operation due to variation suction pressure, pulsation pressure, frequency, and other operating parameters disturbance noises predominant and due to this uniform stratification of jig bed and ideal flow characteristic of motion of particle will never achieved. Hence, herein a hybrid model has been developed which consist of advanced machine learning technique as well as 1st principle mathematical modelling techniques and the model is successfully implemented at Noamundi Ore Processing Plant TATA Steel Ltd. Noamundi Ore Processing Plant is set a JIG plant with capacity 350 TPH for beneficiation of Iron ore wherein the iron ore consist of ore mineral as Hematite, Goethite, etc as heavy mineral

and Silica, Alumina, Kaolinite. etc are gangue mineral or light mineral. In this present model the machine learning techniques handled the non-linear disturbance function for various operating parameters and its out put will become input parameter for 1st principle mathematical modelling, thus the whole computational logic is run in series wherein the main output of this method is to provide optimal set point of bed depth at the gate valve of jig at real time of jigging operation. The set point provided by the model enhance the yield of jig process by 5-10%, recovery of jig process by 14-18% and separation efficiency by 7-12% for treatment of iron ore which particle size are -10+1 mm and mean sizes varies from 4.5 mm to 6 mm.

METHODS AND MATERIAL

Mathematical models are an important component of the final "complete model" of a system which is actually a collection of conceptual, physical, mathematical, visualization, and possibly statistical sub-models. The domain of validity is determined by the simplifying assumptions made during the modelling process and therefore is strongly and directly related with the goals of the modelling process. The methodology for modelling of jigging process is performed by tracking the fluid flow and particle motion having profile of sinusoidal wavefront while stratification of jig bed which are carried out by forming a set of ordinary/partial differential equations in time for each particle, consisting of equations for position, velocity, and masses of species.

The approaches used in formulation of 1st principle mathematical model are Particle transport modelling and design consideration of jig concentrator. Particle transport modelling is a type of multiphase model, where particulates are tracked through the flow in a Lagrangian way, rather than being modelled as an extra Eulerian phase. The full particulate phase is modelled by just a sample of individual particles by applying ordinary differential governing equation with a function of time. The equations generated are then integrated using a simple integration method to calculate the behaviour of the particles as they traverse the flow domain. The fluid and feed properties are taken from the start of the time step. For the particle momentum, would correspond to the particle velocity at the start of the time step which include pressure-velocity coupling method. In the calculation of all the forces, many fluid variables, such as density, viscosity, pressure and velocity are needed at each position vector of the particle trajectory. These variables are always obtained accurately by calculating the element in which the particle is traveling, calculating the computational position within the element, and using the underlying shape functions of the discretisation algorithm to interpolate from the vertices to the particle position.

The equation of motion for feed particles in a jigging process can be determined as follows governing equation:

$$\frac{\partial x_p}{\partial t} = v_p \tag{1}$$

$$m_p \frac{\partial v_p}{\partial t} = m_p \left(1 - \frac{\rho}{\rho_p}\right) g + F_p \tag{2}$$

Where x_p is the particle position tracing while sinusoidal motion up-to the jig length, m_p is the mass and ρ_p is the density of particle, v_p the instantaneous velocity of the particle. The term F_p represents the force caused by solid-liquid interaction. In the most general case, it could constitute of the following contributors modelled using governing equation formulas as follows:

$$F_p = F_1 + F_2 + F_3 + F_4 + F_5 + F_6 \tag{3}$$

The first term F_1 represent the drag force that was derived with assumption of uniform velocity and pressure field:

$$F_1 = 0.5\rho C_d \frac{\pi d^2}{4} |u - v_p|(u - v_p) \tag{4}$$

Similarly, F_2, F_3, F_4, F_5 and F_6 represents mechanical force Fby solid-liquid-solid interaction, viscous force, shear interaction force, lift force and force due to pressure gradient respectively and such forces are formulated accordingly after that, apply all the force value in the equation (2) of motion of particle:

$$\begin{aligned} m_p \frac{\partial v_p}{\partial t} = m_p \left(1 - \frac{\rho}{\rho_p}\right) g + 0.5\rho C_d \frac{\pi d^2}{4} |u - v_p|(u - v_p) + 0.5 \frac{m_p \rho}{\rho_p} \frac{d(u - v_p)}{dt} \\ + a1 * d^2 \sqrt{\pi \rho \mu} \int_{t_0}^{t} \frac{1}{\sqrt{t - \tau}} \frac{d(u - v_p)}{d\tau} \pm a2 * d^2 \sqrt{\mu \rho \gamma} (u - v_p) \\ - \frac{1 - \varepsilon}{\varepsilon} v_p \alpha \nabla p \end{aligned} \tag{5}$$

The above equation 5, is main governing equation for track the particle through out the jig bed has fixed design with length, width and depth, and such velocity of particle is measure as per design evaluation of said jig concentrator in 3- dimensional structure. The change in particle velocity is calculated by integrating Eq. (5) through fourth-order R-K method at each time instant updating the position of particles after the interaction with the water stream velocity i.e., u .

In this simulation, the water stream velocity is assumed to be a pulsating with harmonic wave and can be estimated by following governing equation:

$$Pi + 0.5\rho_l u_i^2 = P_u + 0.5\rho_p {v_0}^2 + (\rho_p - \rho) g sin\theta L + \vartheta \tag{6}$$

$$u = u_i \pm 2\pi f l \sin 2\pi f t \tag{7}$$

Where, Pi and P_u is pulse pressure and suction pressure respectively and 'ϑ' is termed as wall loss factor.

Herein, during actual operation of jig plant instantaneous fluctuation in suction pressure, pulse pressure and pulse frequency are observed which leads to disturb the sinusoidal movement of water stream and particle movement. Hence, before discretising

the Eq. (7) it is necessary to evaluate linear control limit for suction pressure, pulse pressure and frequency. Such linear correlation for said parameters is estimated by using advance machine learning techniques wherein MIMO methods is used on random forest optimization algorithm methods. The score value of such ML techniques optimization on MIMO is more than 96% in test data set, whereas the score value on unseen data set is around 95%.

The density distribution along the depth of a fluidized bed system for a solid-liquid interphase in Jig concentrator can be described using the Richardson-Zaki equation. This equation relates the pressure drop across the bed to the fluid velocity and the properties of the solid particles and liquid. The Richardson-Zaki equation is given by: ΔP/L = [α(1-ε)^2ρ_l u_m^2]/ε^3 + [150(1-ε)^2μ_l u_m]/(ε^3d_p)ρ_l where: ΔP/L is the pressure drop per unit bed length α is the Richardson-Zaki coefficient, which depends on the shape and size of the solid particles ε is the bed voidage ρ_l is the density of the liquid u_m is the fluid velocity through the bed μ_l is the viscosity of the liquid d_p is the diameter of the solid particles in the bed The density distribution can be obtained by integrating the Richardson-Zaki equation along the depth of the fluidized bed system for through out of jig length. The density of the bed at a particular depth can be calculated by dividing the mass of the solid particles and liquid in the bed by the volume of the bed at that depth. The mass of the solid particles and liquid can be calculated from the voidage, the density of the solid particles and liquid, and the volume of the bed. It should be noted that the density distribution in a fluidized bed system for a solid-liquid interphase can be affected by various factors, such as the solid particle size distribution, the liquid viscosity, and the properties of the solid particles and liquid. Therefore, the Richardson-Zaki equation may need to be modified or supplemented with other equations to account for these factors and accurately predict the density distribution in a specific fluidized bed system for a solid-liquid interphase.

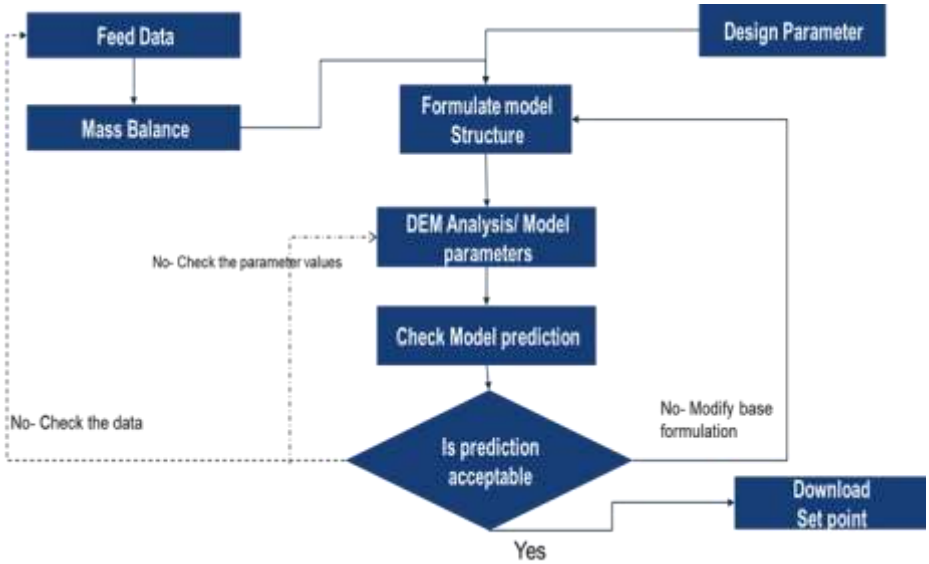

Figure 2 Process flow architecture for Hybrid -model of jig Simulator

Hence the distribution of density and particle velocity profile in Jig bed which evaluate by using Richardson-Zaki equation and Hybrid model respectively will determine the optimal set point for jig bed depth to gate valve from where the concentrate and reject separate out which triggered to high yield and high recovery of concentrate material. The hybrid modelling approach consist of three steps which are as follows:

a. Calculation of MIMO for operational parameters by using ML techniques
b. Calculation of 1st principle method for particle velocity
c. Calculation of density distribution throughout jig bed.

After considering all such steps, the architecture of jig simulator for processing of hybrid model is represented in Fig. 2. Here in Fig. 2 the checks box represents the term "Is prediction acceptable" considering two steps which are as follows:

a. Maximum score for optimization solution achieves or not through ML techniques.
b. Optimal density distribution is achieved or not w.r.t velocity distribution of particle.

RESULTS AND DISCUSSION

It is necessary to validate the model before its application for the numerical study at real time plant scale. The comparison between the plant and numerical results has also been made for the performance of jig concentrator, such as concentrate density, yield % and separation efficiency.

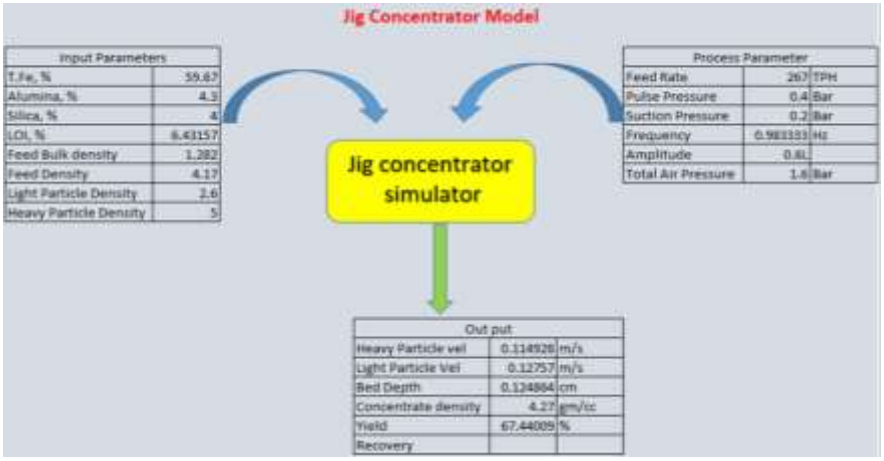

Figure 3 Overview of Jig Simulator Output

The Fig. 3, represents the schematic of jig simulator which provides an optimal set point of operating variable on Jig bed height at gate valve. This simulator gives optimum jig bed height based on feed characteristic and other variable like pulse rate, pressure, feed rate etc., so that at discharged end of jig, enriched and highly liberated material as concentrate can be achieved with better recovery. Wherein it is important to get proof of concept of said simulator at real time plant operation, hence shadow mode practice was opted to test the model at plant scale operation whose output is represented below.

Table 1 Testing of jig Model output at Noamundi Plant Tata steel

Yield Comparison for Jig (Model prediction vs Actual mode of operation - $ days trial at Noamudi-Tata Steel)							
Shift operation	**Test Condition**	**Feed Density**	**Conc Density**	**Bed Height (actual, mm)**	**Plant Yield Actual, %**	**Frequency (Hz)**	**Feed Rate (TPH)**
B1	Plant SOP	4.23	4.43	135	76.21	59	296
B2	Model	4.23	4.48	130	77.37	59	290
A1	Plant SOP	4.38	4.5	135	80.05	59	275
A2	Model	4.38	4.58	128	82.13	59	282
A1	Plant SOP	4.42	4.51	130	85	60	300
A2	Model	4.42	4.55	126	85.23	60	300
B1	Plant SOP	3.78	4.02	140	65	59	256
B2	Model	3.78	4.12	132	68	59	259

The above table 1 represents the establishment for proof of concept of the said jig model w.r.t standard operating practices of Jig plant. Herein, the set point for jig bed height at gate valve provided by model is showing better output in terms of concentrate density as well as yield and recovery %. In the furtherance, after implementing the web-based application of jig model at automation level 2 following output has been seen which are tabulated below:

Table 2 Results of Implemented Jig model Vs standard operating practices of Jig concentrator

Date: 27/06/22	**Jig Feed**				**Jig Concentrate**				**Mineralogical output**				
Set point (by)	**Wt. (T)**	**Fe, %**	**SiO_2, %**	**Al_2O_3, %**	**Wt. (T)**	**Fe, %**	**SiO_2, %**	**Al_2O_3, %**	**Yield, %**	**Fe, Recovery %**	**Alumina Red**	**Fe Improvement**	**Separation Efficiency**
Model	1039	59.62	3.49	5.27	809	60.4	3.39	4.4	77.86	78.88	0.87	0.78	9.64
Std. Practice (SOP)	762.00	59.71	3.27	4.97	566	61.41	3.02	4.45	74.28	76.39	0.52	1.70	9.06

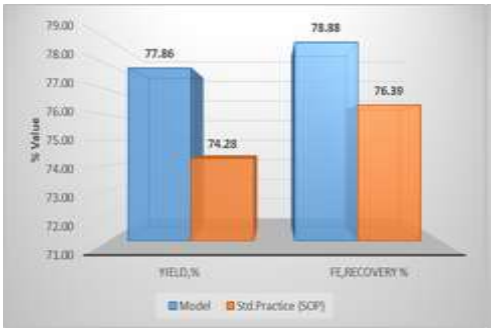

Figure 4 Yield and recovery Model Vs SOP of jig

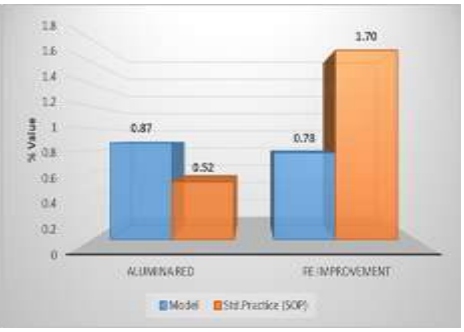

Figure 5 Mineralogical output Model vs SOP of Jig

The table 2 represents the output of online implemented jig model value at real time stamp and its comparison has also made with standard operating practices (SOP),

wherein the set point of bed depth at gate valve by jig model and Jig SOP is 133 and 137 respectively. The Fig. 4 & Fig. 5 represents characteristic output (Yield % and Fe-recovery %) and mineralogical output respectively in terms of Model based set point to jig bed depth as well as Jig SOP based jig bed depth. Herein, the improvement in yield and recovery is observed by 4 to 10% respectively when set point of jig bed is carried by jig model w.r.t Jig SOP, as well as reduction in gangue is also observed subsequently.

CONCLUSION

The hybrid model is well suited for get better optimization solution of any process equipment, herein also the hybrid model developed for jig simulator represents the better output.

The shadow mode testing as well as real time online implemented solution testing of Jig model provides optimal set point for jig bed depth to gate valve of jig concentrator, wherein improved yield as well as recovery are observed for the jig concentrate.

The Jig model will recommend the optimal jig bed height based on fluidization methodology. As per tests carried out based on the plant trial inferences that overall yield is of jig is improved by 4 to 6%, as well as Fe-recovery also increased by 4 to 8%.

The Alumina reduction (gangue reduction) while shadow mode testing and online testing is also observed in acceptable range when Jig plant is run at set point recommended by Jig Model.

ACKNOWLEDGEMENT

I would like to give my hearties thanks to Mr. Abhishek kumar Das (Senior CAM, Noamundi, Tata Steel Ltd) and Chandan kumar Lal Das (Senior Technologist, Automation Tata Steel Jamshedpur) for their immense support on online integration of jig model. I would like to grateful to Mr. Atul Bhatnagar (GM (OMQ), Noamundi, Tata Steel Ltd), Mr. Mithun Mukherjee (Senior Manager, Natural resource Department Noamundi, Tata Steel Ltd) and Ms. T Nandini (Senior manager Quality Noamundi, Tata Steel Ltd) for their valuable support and technical guidance on this novel approach.

REFERENCES

1. Viduka, S.M., et al. (2013) International Journal of Mineral Processing, 123, 108-119.
2. Mishra, B.K., Mehrotra, S.P. (1998) Miner. Eng., 11, 511–522.
3. Zhu, H.P., Zhou, Z.Y., Yang, R.Y., Yu, A.B. (2008). Chem. Eng. Sci., 63, 5728–5770.

XV International Mineral Processing and Recycling Conference
17-19 May 2023, Belgrade, Serbia

RELATIVE PREDICTION ERROR OF FLOTATION INDICES BY ANFIS MODELS

I. Jovanović[1#], V. Conić[1], D. Milanović[1], F. Nakhaei[2], S. Krstić[1]
[1] Mining and Metallurgy Institute Bor, Bor, Serbia
[2] North West University, School of Chemical and Minerals Engineering, Potchefstroom, South Africa

ABSTRACT – This paper describes performances of three different ANFIS models trough the important statistical parameters – relative prediction error, its standard deviation and its mean. Copper content in the ore feed, collector dosage and frother dosage were selected as input parameters to estimate the copper grade and recovery in the final concentrate, and the copper content in the final tailings of the flotation plant. For each output parameter one ANFIS model is developed. Evaluation of the proposed models were performed on the basis of real process data collected by the multiannual monitoring of industrial flotation plant operation in "Veliki Krivelj Mine". The results showed that the proposed ANFIS methodology is the most suitable for prediction of copper recovery in the final concentrate, given that the smallest relative prediction errors with their smallest standard deviation (SDE = 0.11) were obtained in this case.

Keywords: Flotation modeling, Relative prediction error, ANFIS.

INTRODUCTION

Adaptive Neuro-Fuzzy Inference System – ANFIS is an integration system in which neural networks are applied to optimize the fuzzy inference system. ANFIS constructs a series of fuzzy if–then rules with appropriate membership functions to produce the stipulated input–output pairs. The initial fuzzy rules and membership functions are first set by using human expertise about the outputs to be modeled. Then, ANFIS can modify these fuzzy if–then rules and membership functions to minimize the output error measure or explain the input–output relationship of a complex system. To describe the architecture of ANFIS, two fuzzy if–then rules are considered [1]:

Rule 1: If (x is A_1) and (y is B_1) then ($z_1 = p_1x + q_1y + r_1$),
Rule 2: If (x is A_2) and (y is B_2) then ($z_2 = p_2x + q_2y + r_2$),

where x and y are the inputs, A_i and B_i are the fuzzy sets, z_i (i = 1, 2) are the outputs within the fuzzy region specified by the fuzzy rules, and p_i, q_i, and r_i are the parameters determined during the training process. To implement these two rules, the architecture of ANFIS has five layers, as shown in Fig. 1.

It can be seen from the Figure 1 that the square stands for an adaptive node, and a circle indicates a fixed node. Nodes labeled with M are performed as multipliers, nodes

corresponding author: ivana.jovanovic@irmbor.co.rs

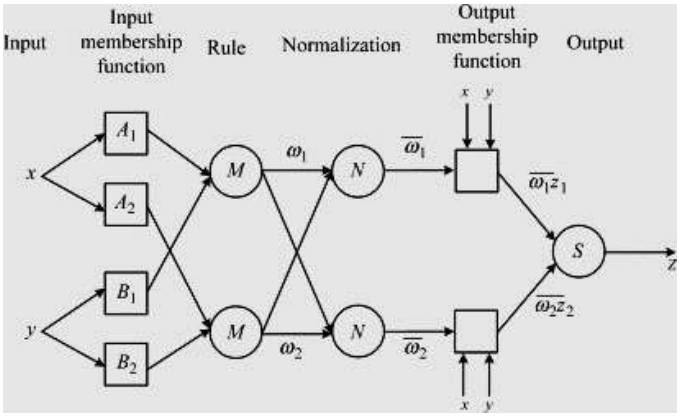

Figure 1 Architecture of the ANFIS [1].

labeled with N play a normalization role to the fuzzy strengths from the previous layer, where parameters ω_i represent fuzzy strengths. Single fixed node labeled with S represents output and performs the sum of the incoming signals [1].

EXPERIMENTAL

Experimental procedure was performed in virtual conditions, using the MATLAB programming language. A total of three models (which bear the labels ANF1, ANF2 and ANF3) have been developed using the ANFIS Editor Graphical User Interface. The independent variables in each model were: the copper content in the feed ore (FCU), collector dosage in the rough flotation stage (PXR) and dosage of frother (FRT). Other variables are considered constant due to different reasons (for more information see [2]) The dependent variables were: the final copper concentrate grade (CCU) in the ANF1 model; recovery of copper in the final concentrate (RCU) in the ANF2 model; and the final tailings grade (TCU) in the ANF3 model.

Model development and testing was based on the real process data, collected from the flotation plant "Veliki Krivelj" during the multi-annual monitoring. Performances of the proposed models were performed in Microsoft Excel through several statistical parameters that describe the validity of the model such as: correlation coefficient, determination coefficient, root mean square error, absolute error. Detailed description of the development of these models as well as a presentation of the mentioned statistical parameters is given in the literature [2, 3]. This paper deals with relative prediction error of these models, together with its standard deviation and its mean.

Relative prediction error (ε_r), serve as the criteria for evaluating the predictive properties of models, and is calculated according to the Formula (1):

$$\varepsilon_r = \frac{Y-X}{X} \quad (1)$$

Where *X* is the measured value, *Y* is the predicted value.

Standard deviation of relative error SDE shows how much, on average, the elements of the dataset deviate from the arithmetic mean of that dataset and is expressed by

Formula (2):

$$SDE=\sqrt{\frac{\sum_{i=1}^{n}(x-\mu)^2}{n}} \quad (2)$$

where *n* presents the number of elements in the dataset, μ is mean (average value) of the dataset and *x* is the i-th member of the dataset.

RESULTS AND DISCUSSION

Relative prediction error can provide a good insight into the effectiveness of the predictive model, because it is used as a basis for comparing parameters that are expressed in different measurement units and different value ranges. Figure 2 present the relative prediction errors of the ANFIS models. The red lines on the charts represents mean (μ), green lines value μ + 1 SDE and purple lines value μ − 1 SDE. Table 1 presents values of SDE and μ for each model.

Table 1 Relative prediction error parameters using ANF1 ANF2 and ANF3 models

Statistical Parameter	Technological Indices of the Flotation Process		
	CCU	RCU	TCU
Standard deviation of relative prediction error, SDE	0.1995	0.1103	2.4568
Mean of relative prediction error, μ	0.0086	0.0785	1.7066

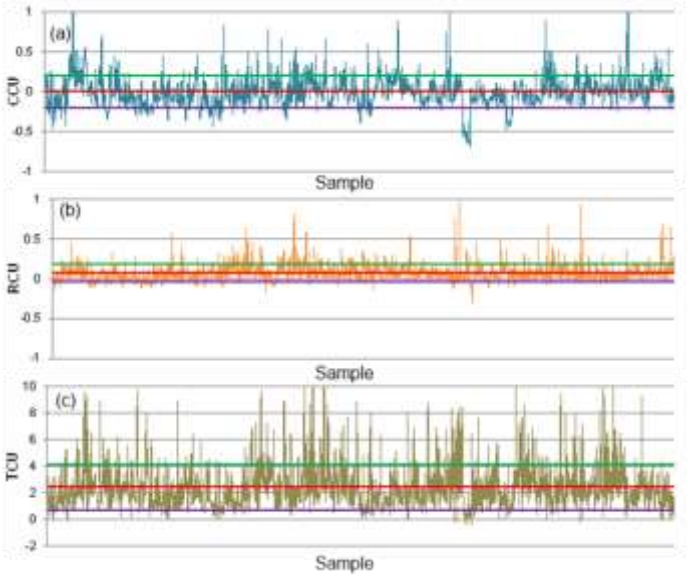

Figure 2 Relative prediction errors of flotation technological indices according to the (a) ANF1, (b) ANF2 and (c) ANF3 models

By visual analysis of the charts in Figure 2, it can be observed that the smallest relative prediction error is obtained when modeling RCU, and the highest when modeling TCU. The relative prediction error of ANF2 model has the smallest standard deviation (Table 1), and 79.3% of the results are in the range ± 1 SDE. When it comes to relative prediction errors of CCU and TCU, 75.6% and 78.2% of the results are within ± 1 SDE, respectively. A low standard deviation indicates that the values tend to be close to the mean (also called the expected value) of the set, while a high standard deviation indicates that the values are spread over a wider range. It should also be noted that the TCU relative prediction error is mostly positive, which means that the values predicted by the model are, as a rule, slightly higher than the real ones (offset error). This result indicates that the additional fine tuning of the model is needed. Mean of the ANF1 model is the smallest ($\mu = 0.0086$), but this can be attributed to approximately the same number of positive and negative values of relative prediction error, which can be observed from Figure 2(a).

CONCLUSION

Performances of three different ANFIS models that predict copper flotation process indices (concentrate grade, tailings grade and Cu recovery in concentrate) are evaluated trough their relative prediction error, its standard deviation and its mean. Evaluation of the proposed models were performed on the basis of real process data. The results showed that the smallest relative prediction error with the smallest standard deviation is obtained by applying the ANFIS predictive methodology to the Cu recovery variable. On the other hand, it turned out that this methodology is the least suitable for predicting of tailings grade.

ACKNOWLEDGEMENT

This work was financially supported by the Ministry of Education, Science and Technological Development of the Republic of Serbia, Grant No. 451-03-47/2023-01/200052..

REFERENCES

1. Lei, Y. (2017) Individual intelligent method-based fault diagnosis. Chapter 3 in Intelligent Fault Diagnosis and Remaining Useful Life Prediction of Rotating Machinery. Elsevier, pp. 67-174.
2. Jovanović, I. (2016) Model of an Intelligent System of Adaptive Control the Ore Processing System, PhD Dissertation, Faculty of Mining and Geology, Belgrade, p. 217 (in Serbian).
3. Jovanović, I., Nešković, J., Petrović, S., Milanović, D. (2018). A hybrid approach to modeling the flotation process from the “Veliki Krivelj” plant. Mining and Metallurgy Engineering Bor 1-2/2018, ISSN 2334-8836, pp. 1–10.

XV International Mineral Processing and Recycling Conference
17-19 May 2023, Belgrade, Serbia

APPLICATION OF VIKOR METHOD FOR SELECTION OF COLLECTOR IN PORPHYRY COPPER ORE FLOTATION

Z. Štirbanović[1#], R. Stanojlović[1], J. Sokolović[1], D. Stanujkić[1], N. Ćirić[2], I. Miljanović[3], G. Popović[4]

[1] University of Belgrade, Technical Faculty in Bor, Bor, Serbia
[2] Zijin Bor Copper d.o.o, Copper Mine Majdanpek, Majdanpek, Serbia
[3] University of Belgrade, Faculty of Mining and Geology, Belgrade, Serbia
[4] University Business Academy in Novi Sad, Faculty of Applied Management, Economics and Finance, Belgrade, Serbia

ABSTRACT – The selection of appropriate flotation collector is of the crucial importance especially for the complex ores like porphyry copper ores that are distinguished with lower copper grades and higher pyrite content. In this paper are presented the results of selection of flotation collector for porphyry copper ore from "Severni Revir" ore deposit in Copper Mine Majdanpek. The selection was performed between two collectors (Z11 and AP3404) with 3 different dosages (25; 35; 45 g/t) and their mixture with SKIK in different mass ratio. The VIKOR method was applied for the rating of 10 alternatives by 5 criteria: mass yield, copper grade in concentrate, sulfur grade in concentrate, copper recovery, and collector expenses (dosage and price). Based on the results of the analysis, alternative A8 which represents the mixture of three collectors Z11, AP3404, and SKIK with following dosage 20+8+8 g/t was selected as the best alternative.

Keywords: Porphyry Copper Ore, Flotation, Collector, Selection, VIKOR Method.

INTRODUCTION

The main characteristics of porphyry copper ore deposits are large quantities with lower copper grade, as well as high content of pyrite [1]. Pyrite as iron sulfide mineral is often associated with copper minerals and it is difficult to achieve their efficient separation especially if pyrite is activated with copper ions [2].

One of the ways to provide good selectivity of copper minerals from pyrite is to select appropriate flotation collector which will provide good floatability of copper minerals and efficient selectivity towards pyrite and other sulfide minerals.

Xanthates are mostly used collectors in copper flotation and they can be applied alone or in combination with other collectors, such as dithiophosphates or thionocarbamates, which are normally used for flotation of secondary copper minerals or in the case when flotation is performed at lower pH [3].

The selection of an appropriate collector is essential for the efficiency of the flotation process [4]. Certain minerals have similar properties in terms of floatability, so it is necessary to select a suitable collector that has a selective effect and that enables their efficient separation [5]. The selection of collectors in copper flotation is in close

corresponding author: zstirbanovic@tfbor.bg.ac.rs

correlation with the nature and appearance of copper minerals and other sulfides that are associated with them. Recovery of useful components as well as flotation time is also recognized as important parameters when choosing a collector [6-8]. Since the collectors are organic compounds, their impact on both human health and the environment can be very large [9-11], so it is necessary to take this aspect into account as well. The price and consumption of the collector always have an influence when choosing, because economic profitability is very important.

As can be seen, there are a large number of factors that have an impact and should be taken into account when choosing the optimal collector to be used in the flotation of a porphyry copper ores. Precisely for these reasons, it is necessary to apply some of the methods that will facilitate the process of selection the flotation collector, such as multi criteria decision making (MCDM) methods.

MCDM methods present very efficient tool which can simplify selection process when large number of criteria is involved, and for that reason are being used for selection in various areas of life, science and industry. Therefore, these methods have also found applications in mineral processing in recent years, starting from selection of equipment [12,13], technologies [14,15], reagents [16, 17], etc.

In this paper are presented the results of selection of flotation collector for porphyry copper ore from "Severni Revir" ore deposit in Copper Mine Majdanpek.

METHODOLOGY

Rougher flotation tests were carried out on of porphyry copper ore samples from "Severni Revir" ore deposit in Copper Mine Majdanpek and the influence of different collectors and their dosages on flotation indicators were investigated [18].

The data obtained in the study were used for the selection of the most appropriate collector for flotation of porphyry copper ore from this ore deposit. The selection was performed between two collectors (Z_{11} and AP3404) with 3 different dosages (25; 35; 45 g/t) and their mixture with SKIK in different mass ratio (Table 1).

Table 1 Alternatives for the selection of flotation collector

Alternative	Collector	Dosage
A_1	Z_{11}	25 g/t
A_2	Z_{11}	35 g/t
A_3	Z_{11}	45 g/t
A_4	AP3404	25 g/t
A_5	AP3404	35 g/t
A_6	AP3404	45 g/t
A_7	Z_{11}+AP3404	20+16 g/t
A_8	Z_{11}+AP3404+SKIK	20+8+8 g/t
A_9	Z_{11}+AP3404+SKIK	18+10+8 g/t
A_{10}	Z_{11}+AP3404+SKIK	18+12+6 g/t

Criteria that were used for selection and their weights are given in Table 2.

Table 2 The weights of selection criteria

Criteria	Weight
C_1 – Mass yield (%)	0.1
C_2 – Copper grade in concentrate (%)	0.2
C_3 – Sulfur grade in concentrate (%)	0.15
C_4 – Copper recovery (%)	0.35
C_5 – Collector expenses (dosage and price)	0.2

The ratings of alternatives in relation to the selected criteria are shown in Table 3.

Table 3 The ratings of alternatives in relation to the selected criteria

	C_1	C_2	C_3	C_4	C_5
	max	max	min	max	min
A_1	16.39	1.39	19.87	83.45	3
A_2	14.63	1.55	21.58	83.06	4
A_3	15.61	1.42	22.72	81.19	5
A_4	14.08	1.54	15.99	79.43	5
A_5	14.44	1.58	17.92	83.57	6
A_6	17.31	1.32	20.32	83.70	7
A_7	14.82	1.55	22.83	84.14	6
A_8	15.26	1.52	24.81	84.96	4
A_9	14.88	1.50	21.92	81.76	5
A_{10}	14.09	1.57	23.43	81.03	6

The selection was made by using VIKOR method.

VIKOR method

The VIKOR method was proposed by Opricovic and Tzeng in 2004 [19], and it can be also mentioned as a prominent and often used MCDM method. VIKOR means Multicriteria Optimization and Compromise Solution (VIsekriterijumska optimizacija i KOmpromisno Resenje, in Serbian).

The procedure of evaluating alternatives using the VIKOR method can be explained using the following steps:

Step 1. Determine the best x_j^* and worst x_j^- value for each criterion as follows:

$$x_j^* = \begin{cases} max_j x_{ij} & j \in \Omega_{max} \\ min_j x_{ij} & j \in \Omega_{min} \end{cases}, \text{ and} \quad (1)$$

$$x_j^- = \begin{cases} min_j x_{ij} & j \in \Omega_{max} \\ max_j x_{ij} & j \in \Omega_{min} \end{cases} \quad (2)$$

where x_{ij} denotes rating of alternative *i* in relation to criterion *j*, Ω_{max} and Ω_{min} denote set of maximization and minimization criteria, respectively.

Step 2. Determine average S_i and group R_i score for each alternative as follows:

$$S_i = \sum_{j=1}^{n} w_j \left(x_j^* - x_{ij}\right)/\left(x_j^* - x_j^-\right), \text{ and} \quad (3)$$

$$R_i = max_j\left[w_j \left(x_j^* - x_{ij}\right)/\left(x_j^* - x_j^-\right)\right], \quad (4)$$

where w_j denotes the weight of criterion *j*.

Step 3. Determine the overall ranking index Q_i as follows:

$$Q_i = \nu\frac{(S_i - S^*)}{(S^- - S^*)} + (1-\nu)\frac{(R_i - R^*)}{(R^- - R^*)}, \quad (5)$$

where: S_j and R_j denotes the average and the worst group score of alternative *i*, respectively, $S^* = min_i S_i$, $S^- = max_i S_i$, $R^* = min_i R_i$, $R^- = max_i R_i$, and ν is significance of the strategy, which value is usually set to be 0.5.

Step 4. Rank the alternatives, sorting by the value Q_i in decreasing order. The alternative with the minimum value of Q_i is the most appropriate alternative.

RESULTS AND DISCUSSION

In this numerical illustration two collectors with three different dosages and their mixtures, shown in Table 1, are evaluated. Ten alternatives, shown in Table 1, were evaluated based on the five criteria shown in Table 2. Table 2 also shows the weights of the criteria.

The ratings of the alternatives in relation to the criteria are shown in Table 3. The optimization directions of the criteria are also shown in Table 3.

The best and worst value for each criterion, determined using Eq. (1) and Eq. (2) are shown in Table 4.

Table 4 The best and worst value for each criterion

	C_1	**C_2**	**C_3**	**C_4**	**C_5**
	max	max	min	max	min
x_j^*	17.31	1.58	15.99	84.96	3
x_j^-	14.08	1.32	24.81	79.43	7

Based on the data from Table 3 and Table 4, the average S_i and group R_i score for each alternative were determined, using Eq. (3) and Eq. (4). The calculated values are shown in Table 5. Table 5 also shows the overall ranking index Q_i, calculated using Eq. (5) and ν = 0.5, as well as the ranks of each considered alternatives.

From Table 5, it can be seen that the alternative denoted as A_8 was selected as the most acceptable alternative. Alternative A_8 represents the mixture of three collectors Z_{11}, AP3404, and SKIK with following dosage 20+8+8 g/t. As it can be seen from Table 3, the copper recovery rate obtained with this mixture was the highest 84.96%. Mass yield and copper grade in concentrate were 15.26% and 1.52% respectively, which were not the

highest obtained values but also not the lowest. The sulfur content in the concentrate was the highest indicating lower selectivity but since the weight of this criterion was not very high it did not influence the overall ranking of alternative A_8. Considering all it can be concluded that the criterion C_4, i.e. copper recovery had the most influence during selection of flotation collector by application of VIKOR method which was expected since it was assigned the highest weight.

Table 5 The overall ranking index and rank of considered alternatives

	S_i	R_i	Q_i	Rank
A_1	0.336	0.146	0.097	3
A_2	0.371	0.120	0.096	2
A_3	0.629	0.239	0.752	8
A_4	0.581	0.350	0.920	10
A_5	0.360	0.150	0.142	4
A_6	0.553	0.200	0.551	7
A_7	0.418	0.150	0.233	5
A_8	0.310	0.150	0.065	1
A_9	0.540	0.203	0.536	6
A_{10}	0.633	0.249	0.780	9

CONCLUSION

Flotation collectors play very important role in flotation process of complex ores such as porphyry copper ores that are distinguished with lower copper grades and higher pyrite content, thus it is important to select collector which will provide good selectivity of copper minerals from pyrite. By selection of appropriate flotation collector, good floatability of copper minerals and efficient selectivity towards pyrite and other sulfide minerals can be achieved.

During the selection large number of criteria should be taken into consideration, making the selection process difficult. Therefore, the solution to the problem can be application of MCDM methods which can simplify selection process when large number of criteria is involved.

The selection of flotation collector for porphyry copper ore from “Severni Revir” ore deposit in Copper Mine Majdanpek was the aim of the study which results are presented in this paper. Two collectors (Z11 and AP3404) with 3 different dosages (25; 35; 45 g/t) and their mixture with SKIK in different mass ratio were applied for rough flotation tests and the results obtained were then used as the base for the selection. The VIKOR method was applied for the rating of 10 alternatives by 5 criteria: mass yield, copper grade in concentrate, sulfur grade in concentrate, copper recovery, and collector expenses (dosage and price). Based on the results of the analysis, alternative A_8 which represents the mixture of three collectors Z11, AP3404, and SKIK with following dosage 20+8+8 g/t was selected as the best alternative. The criterion C_4, i.e. copper recovery was recognized as the most influential during the selection of flotation collector by the VIKOR method which was not surprising since it was assigned the highest weight.

ACKNOWLEDGEMENT

The authors would like to acknowledge the Ministry of Science, Technological Development and Innovation of the Republic of Serbia for the financial support of scientific research at the University of Belgrade, Technical Faculty in Bor according to the contract with registration number 451-03-47/2023-01/ 200131.

REFERENCES

1. Wills, B., Finch, J. (2016) Wills' mineral processing technology: An introduction to the practical aspects of ore treatment and mineral recovery. 8th Ed., Elsevier Science: New York, USA.
2. Mu, Y., Peng, Y., Lauten, R.A. (2016) The depression of copper-activated pyrite in flotation by biopolymers with different compositions. Minerals Engineering, 113, 96-97.
3. Bulatovic, S.M. (2007) Handbook of Flotation Reagents: Chemistry, Theory and Practice. Volume 1: Flotation of Sulfide Ores, Elsevier.
4. Kawatra, S.K. Flotation Fundamentals, http://www.chem.mtu.edu/chem_eng/faculty/kawatra/Flotation_Fundamentals.pdf
5. Ignatkina, V.A. (2011) Selection of Selective Collectors for Flotation of Minerals with Similar Flotation Properties. Russian Journal of NonFerrous Metals, 52 (1), 1-7.
6. Ackerman, P.K., Harris, G.H., Klimpel, R.R., Aplan, F.F. (1987) Evaluation of Flotation Collectors for Copper Sulfides and Pyrite, I. Common Sulfhydryl Collectors. International Journal of Mineral Processing, 21, 105-127.
7. Ackerman, P.K., Harris, G.H., Klimpel, R.R., Aplan, F.F. (1987) Evaluation of Flotation Collectors for Copper Sulfides and Pyrite, II. Non-Sulfhydryl Collectors. International Journal of Mineral Processing, 21, 129-140.
8. Ackerman, P.K., Harris, G.H., Klimpel, R.R., Aplan, F.F. (1987) Evaluation of Flotation Collectors for Copper Sulfides and Pyrite, III. Effect of Xanthate Chain Length and Branching. International Journal of Mineral Processing, 21, 141-156.
9. Chen, S., Gong, W., Mei, G., Zhou, Q., Bai, C., Xu, N. (2011) Primary biodegradation of sulfide mineral flotation collectors. Minerals Engineering, 24, 953-955.
10. Chockalingam, E., Subramanian, S., Natarajan, K.A. (2003) Studies on biodegradation of organic flotation collectors using Bacillus polymyxa. Hydrometallurgy, 71,249-256.
11. Deo, N., Natarajan, K.A. (1998) Biological removal of some flotation collector reagents from aqueous solutions and mineral surfaces. Minerals Engineering, 11 (8), 717-738.
12. Štirbanović, Z., Stanujkić, D., Miljanović, I., Milanović, D. (2019) Application of MCDM methods for flotation machine selection. Minerals Engineering, 137, 140-146.
13. Sitorus, F., Brito-Parada, P.R. (2020) Equipment selection in mineral processing - A sensitivity analysis approach for a fuzzy multiple criteria decision making model. Minerals Engineering, 150, 106261.
14. Stanujkic, D., Kazimieras Zavadskas, E., Karabasevic, D., Milanovic, D., Maksimovic, M. (2019) An approach to solving complex decision-making problems based on IVIFNs: A case of comminution circuit design selection. Minerals Engineering, 138, 70-78.
15. Magdalinović, N., Štirbanović, Z., Stanujkić, D., Sokolović, J. (2021) Selection of copper-pyrite flotation circuit design by applying the Preference Selection Index

Method.In: Proceedings of XIV International Mineral Processing and Recycling Conference. Belgrade, Serbia, Proceedings, 136-141.
16. Kostović, M., Gligorić, Z. (2015) Multi-criteria decision making for collector selection in the flotation of lead–zinc sulfide ore. Minerals Engineering, 74, 142-149.
17. Kursunoglu, S., Kursunoglu, N., Hussaini, S., Kaya, M. (2021) Selection of an appropriate acid type for the recovery of zinc from a flotation tailing by the analytic hierarchy process. Journal of Cleaner Production, 283, 124659.
18. Sokolović, J., Stanojlović, R., Andrić, Lj., Štirbanović, Z., Ćirić, N. (2019) Flotation studies of copper ore Majdanpek to enhance copper recovery and concentrate grade with different collectors. Journal of Mining and Metallurgy, Section A: Mining, 55 (1), 53–65.
19. Opricovic, S., Tzeng, G.H. (2004) Compromise solution by MCDM methods: A comparative analysis of VIKOR and TOPSIS. European Journal of Operational Research, 156 (2), 445-455.

XV International Mineral Processing and Recycling Conference
17-19 May 2023, Belgrade, Serbia

RANKING OF FLOTATION TAILINGS POND IN EASTERN SERBIA USING THE AHP METHOD

S. Milutinović[#], Lj. Obradović, S. Petrović , S. Magdalinović, I. Svrkota
Mining and Metallurgy Institute Bor, Bor, Serbia

ABSTRACT – From the aspect of technology, the flotation tailings pond represents a necessary mining facility. From the point of view of the environment, a real danger to the ecological factors of the environment, whether they are in operation or the disposal process has been completed. In this paper, the AHP method was used to rank the tailings ponds in Bor and Majdanpek, so that a clear picture is obtained of which tailings pond should be paid the most attention in terms of taking all preventive measures to prevent accidents.

Keywords: Tailings, Tailings Pond, AHP, MCDM.

INTRODUCTION

Flotation tailings ponds are dynamic structures that continuously evolve during their time of exploitation, and for a good number of years after the end of exploitation [1]. They must be seen as living objects that reflect all-natural events in the environment and all events caused by human activities. Protection of general natural assets is one of man's biggest challenges every day. Exploitation and processing of natural resources such as mineral deposits contribute to the transformation of the natural environment. Several activities designed to maintain balance are undertaken by the concept of integrated order. One of them is the use of comprehensive tailings pond monitoring systems. Despite the monitoring, system crashes still happen.

In Europe, public concern about the risk and potential impacts of existing (operating, inactive, and abandoned) tailings ponds has been growing since recent incidents such as the large-scale tailings spill in Spain in 1998 [2], the Baia Borsa tailings (Romania)) contaminated with heavy minerals spilled in March 2000 [3], etc. These and other experiences show that the emphasis should be placed on prevention and not on responding after the incident. By predicting the potential risk, the environmental impact can be reduced and the actual costs optimized.

In the paper [4] a detailed review and re-evaluation of known historical cases of accidents at tailings ponds in Europe and the world was carried out. The main aim of the work was to improve the understanding of tailings pond incidents and to establish relationships and trends based on (known) historical tailings pond accidents in Europe as well as in the world.

In this paper, the AHP method was used to rank the tailings ponds in Bor and Majdanpek, so that a clear picture is obtained of which tailings pond should be paid the

[#] corresponding author: sandra.milutinovic@irmbor.co.rs

most attention in terms of taking all preventive measures to prevent accidents at these flotation tailings ponds. The decision that will be made will have a significant impact on the business in terms of achieving technical, environmental, and economic goals.

EXPERIMENTAL

The application of the AHP method is very broad, with the possibility of adaptation to specific circumstances.

In the paper [5] a detailed procedure and definition of the AHP method are given, so in this part of the paper, only the experimental part of the application of this method will be given.

The analyzed area of Eastern Serbia has six flotation tailings ponds, one of which is an accidental tailings pond. The comparison was made for six tailings ponds, namely the Veliki Krivelj tailings pond (Field 0, 1, 2), the RTH tailings pond, and two tailings ponds in Majdanpek (Valja Fundata and the Šaški Potok accidental tailings pond).

The Veliki Krivelj tailings dump is a valley-type tailings dump and occupies space in the former bed of the Kriveljska River. Downstream from the tailings pit is the village of Oštrelj, and upstream is a conveyor system for transporting tailings from the Krivelj mine to the old open pit in Bor and the Veliki Krivelj open pit. This tailing dump consists of three fields. Field 1 was created by closing the valley of the Kriveljska river with two barrier sand dams, upstream dam 1 and downstream dam 2. In 1990, the tailings pond was expanded downstream, occupying additional space in the bed of the Kriveljska river - a new tailings dump or Field 2. To contour the new tailings pond, it was enough to build only one dam - dam 3. To provide adequate space for the further disposal of tailings from the Veliki Krivelj flotation, at the beginning of 2015, the construction of the Zero Field upstream of field 1 was started.

The flotation tailing dump in the area of the old surface mine RTH (after the mine it is a tailings pit and got the name - ore body H) has been in operation since 1985. The tailings pit has the shape of an ellipse with the approximate direction of the central axis east-west.

Since the beginning of the operation of the copper mine in Majdanpek, flotation tailings have been deposited in two tailings ponds - Valja Fundata and Šaški Potok. The tailings pond "Valja Fundata" dates back to 1961 and is the main tailings pond, and it was named after the stream of the same name, Valja Fundata. This tailings pond was formed in the valley of the Valja Fundata stream, which starts immediately in front of the copper flotation in Majdanpek and extends in a southerly direction for about 1300 m, where two new branches flow into it. At a distance of about 1800 m, this valley changes its direction to the west, where it joins another larger branch. Then, at about 2400 m from the flotation, this valley widens considerably and enters a new branch, which eventually ends with a rocky limestone barrier. The original purpose of the "Šaški Potok" tailings pond was to deposit part of the tailings of the supplementary plant in the form of sand from secondary hydro cyclones. As such, this tailing pond has been in operation for several years and about 8.5 Mm^3 of flotation tailings were deposited in it, mostly in the central area of the tailings pond. Considering the various difficulties that arose during the operational work of this tailings pond, as well as different conceptions of its purpose and technical construction, after a comprehensive review of the entire situation related to

the disposal of tailings from RBM flotation, it was decided that this tailings pond will serve only for accidental discharges in the future in case of unforeseen downtimes and breakdowns.

The basic criteria for the selection of tailings for this work are:

- Area of the tailings pond (m^2) – A larger area of the tailings pond automatically means that the tailings pond is more dangerous.
- Volume of the tailings pond (m^3) - The larger the volume of the tailings pond, the less favorable the tailings pond.
- Proximity to surface waters (km) - If surface waters (rivers, streams, etc.) were observed near the tailings dump, their distance from the tailings dump was determined. The closer a river or stream is to a tailings pond, the less favorable the tailings pond is.
- Proximity to agricultural land (km) - If agricultural land was observed near the tailings dump, its distance from the tailings dump was determined. The closer an agricultural land is to a tailings pond, the less favorable the tailings pond is.
- Proximity of protected natural areas (km) - If a protected natural area (cave, etc.) was observed near the tailings dump, its distance from the tailings dump was determined. The closer an area is to a tailings pond, the less favorable the tailings pond is.
- Proximity to cities and settlements (km) - If a settlement was observed near the tailings dump, its distance from the tailings dump was determined. The closer a settlement is to a tailings pond, the less favorable the tailings pond is.

Other criteria, such as harmful and dangerous substances in tailings, stability of dams, environmental protection, economic aspect, etc. were not taken into account in this paper.

RESULTS AND DISCUSSION

The initial decision matrix is shown in Table 1.

Table 1 The initial decision matrix

	Name of tailings pond	Area of the tailings pond (m^2)	Volume of the tailings pond (m^3)	Proximity to surface waters (km)	Proximity to agricultural land (km)	Proximity of protected natural areas (km)	Proximity to cities and settlements (km)
Alternative/ criterion		K1	K2	K3	K4	K5	K6
A1	Veliki Krivelj-Field 0	424,193.00	15,200,000.00	2	1	27	3
A2	Veliki Krivelj-Field 1	2,321,823.00	135,300,000.00	2	1	27	1.5
A3	Veliki Krivelj-Field 2	1,347,567.00	87,500,000.00	2	1	27	1.5
A4	RTH	700,462.00	53,562,878.00	2	0.5	27	1.5
A5	Valja Fundata	4,726,514.00	364,950,000.00	0.5	2	14	1
A6	Šaški potok	365,606.00	21,250,000.00	3.5	2	14	3

The evaluation of six flotation tailings ponds A1, A2, A3, A4, A5, and A6 was carried out based on the six evaluation criteria K1, K2, K3, K4, K5 and K6 that were previously mentioned.

The first step is to define the weighting factors (preference factors) of the considered criteria using Saaty's scale [6], after which their mathematical calculation should be performed. After that, the consistency of the decision maker should be checked [7], which is shown in Table 2, as well as the value of the preference vector. Based on the results, we see that the random CR consistency index is <10%, which satisfies the conditions.

Table 2 Consistencies of the decision maker and the value of the preference vector

	K1	K2	K3	K4	K5	K6	Preference vector	Consistencies of the decision maker	
K1	1	0.33	0.14	0.14	0.14	0.11	0.023105	6.128457338	λmax
K2	3	1	0.14	0.14	0.14	0.11	0.034486	6	n
K3	7	7	1	1	1	0.33	0.178521	1.24	RI
K4	7	7	1	1	1	0.33	0.178521	0.025691468	CI
K5	7	7	1	1	1	0.33	0.178521	0.020718925	CR
K6	9	9	3	3	3	1	0.406846	2.071892544	%

The next step in the analysis is the evaluation of alternatives in relation to the defined criteria.

The first sub-criterion to be analyzed is the area of the tailings pond. All necessary input values, as well as preference values and consistency of the decision maker, for the calculation of alternatives according to the criterion of the tailings area are shown in Table 3.

Table 3 Values according to the criterion - tailings area

K1		A1	A2	A3	A4	A5	A6	Preference vector	Consistencies of the decision maker	
424,193.00	A1	1	0.14	0.2	0.33	0.11	1	0.023507614	6.597345816	λmax
2,321,823.00	A2	7	1	5	3	0.11	7	0.19744616	6	n
1,347,567.00	A3	5	0.2	1	3	0.11	5	0.091562837	1.24	RI
700,462.00	A4	3	0.33	0.33	1	0.11	3	0.051033157	0.119469163	CI
4,726,514.00	A5	9	9	9	9	1	9	0.612942617	0.096346099	CR
365,606.00	A6	1	0.14	0.2	0.33	0.11	1	0.023507614	9.634609942	%

Calculations are made in the same way for the other sub-criteria shown in Tables 4-8.

Table 4 Values according to the criterion - tailings volume

K2		A1	A2	A3	A4	A5	A6	Preference vector	Consistencies of the decision maker	
15,200,000.00	A1	1	0.14	0.2	0.33	0.11	1	0.023508	6.597346	λmax
135,300,000.00	A2	7	1	5	3	0.11	7	0.197446	6	n
87,500,000.00	A3	5	0.2	1	3	0.11	5	0.091563	1.24	RI
53,562,878.00	A4	3	0.33	0.33	1	0.11	3	0.051033	0.119469	CI
364,950,000.00	A5	9	9	9	9	1	9	0.612943	0.096346	CR
21,250,000.00	A6	1	0.14	0.2	0.33	0.11	1	0.023508	9.63461	%

Table 5 Values according to the criterion - Proximity to surface water

K3		A1	A2	A3	A4	A5	A6	Preference vector	Consistencies of the decision maker	
2	A1	1	1	1	1	3	0.14	0.094427	6.051013	λmax
2	A2	1	1	1	1	3	0.14	0.094427	6	n
2	A3	1	1	1	1	3	0.14	0.094427	1.24	RI
2	A4	1	1	1	1	3	0.14	0.094427	0.010203	CI
0.5	A5	0.33	0.33	0.33	0.33	1	0.14	0.038999	0.008228	CR
3.5	A6	7	7	7	7	7	1	0.583292	0.822788	%

Table 6 Values according to the criterion - Proximity to agricultural land

K4		A1	A2	A3	A4	A5	A6	Preference vector	Consistencies of the decision maker	
1	A1	1	1	1	3	0.11	0.11	0.052143	6.057498	λmax
1	A2	1	1	1	3	0.11	0.11	0.052143	6	n
1	A3	1	1	1	3	0.11	0.11	0.052143	1.24	RI
0.5	A4	0.33	0.33	0.33	1	0.11	0.11	0.025921	0.0115	CI
2	A5	9	9	9	9	1	1	0.408825	0.009274	CR
2	A6	9	9	9	9	1	1	0.408825	0.927384	%

Table 7 Values according to the criterion - Proximity to protected natural areas

K5		A1	A2	A3	A4	A5	A6	Preference vector	Consistencies of the decision maker	
27	A1	1	1	1	1	9	9	0.236925	5.986655	λmax
27	A2	1	1	1	1	9	9	0.236925	6	n
27	A3	1	1	1	1	9	9	0.236925	1.24	RI
27	A4	1	1	1	1	9	9	0.236925	0.002669	CI
14	A5	0.11	0.11	0.11	0.11	1	1	0.026149	0.002152	CR
14	A6	0.11	0.11	0.11	0.11	1	1	0.026149	0.215239	%

Table 8 Values according to criteria - Proximity to cities and settlements

K6		A1	A2	A3	A4	A5	A6	Preference vector	Consistencies of the decision maker	
3	A1	1	5	5	5	3	1	0.320217	6.177695	λmax
1.5	A2	0.2	1	1	1	3	0.14	0.072662	6	n
1.5	A3	0.2	1	1	1	3	0.14	0.072662	1.24	RI
1.5	A4	0.2	1	1	1	3	0.14	0.072662	0.035539	CI
1	A5	0.33	0.33	0.33	0.33	1	0.14	0.041028	0.028661	CR
3	A6	1	7	7	7	7	1	0.420768	2.866055	%

Table 9 Final report of parameters

Alternative/ criterion	K1	K2	K3	K4	K5	K6	RANK	RANK	Name of tailings pond
A1	0.023508	0.023508	0.094427	0.052143	0.236925	0.320217	6	1	Valja Fundata
A2	0.197446	0.197446	0.094427	0.052143	0.236925	0.072662	2	2	Veliki Krivelj-Field 1
A3	0.091563	0.091563	0.094427	0.052143	0.236925	0.072662	3	3	Veliki Krivelj-Field 2
A4	0.051033	0.051033	0.094427	0.025921	0.236925	0.072662	5	4	Šaški potok
A5	0.612943	0.612943	0.038999	0.408825	0.026149	0.041028	1	5	RTH
A6	0.023508	0.023508	0.583292	0.408825	0.026149	0.420768	4	6	Veliki Krivelj-Field 0
Ki	0.47134	0.32739	0.058321	0.058321	0.058321	0.026306			

Table 9 shows the last step in the application of the AHP method, which is the weighting of the calculated significance coefficients of the alternatives in the choice according to different criteria, and the significance coefficient (preference) of those criteria

CONCLUSION

During the construction of the flotation tailings pond, there are various changes related to the characteristics of the material to be deposited, the method and conditions of transport, deposition, environmental protection, water removal, changes in the groundwater level in the surrounding area, etc. Because of all this, it is impossible to predict all the influencing elements that occur at the beginning of the construction of the tailings pond, so auscultation or observation is necessary.

Based on the results obtained by the AHP analysis, it can be seen that the dangers to people and the environment in the vicinity of the tailings dump mainly depend on the size of the tailings dump, so the Valja Fundat tailings dump is in the first place in terms of risk to the environment. Then comes Veliki Krivelj tailings - Field 1 and Field 2. The other three places are occupied by accidental tailings Šaški Potok in Majdanpek and tailings RTH and Veliki Krivelj - Field 0 in Bor (Table 9.).

The selection of flotation tailings ponds can be based on other criteria, such as stability of dams on flotation tailings ponds, chemical hazard, presence of erosion, etc., and not only on those given in this paper, so different results can be obtained using the AHP method.

ACKNOWLEDGEMENT

This work was financially supported by the Ministry of Education, Science and Technological Development of the Republic of Serbia, contract no. 451-03-47/2023-01/ 200052.

REFERENCES

1. Milutinović, S., Svrkota, I., Obradović, Lj., Mikić, M. (2022) Oskultacija flotacijskih jalovišta. In: 13. Simpozijum sa međunarodnim učešćem “Rudarstvo 2022”, Privredna komora Srbije, 12–17.
2. Meharg, A.A., Osborn, D., Pain, D.J., Sánchez, A., Naveso, M.A. (1999) Contamination of Doñana food-chains after the Aznalcóllar mine disaster. Environmental Pollution, 105 (3), 387–390. https://doi.org/10.1016/S0269-7491(99)00033-0.
3. The Cyanide Spill at Baia Mare, Romania.
4. Rico, M., Benito, G., Salgueiro, A.R., Díez-Herrero, A., Pereira, H.G. (2008) Reported tailings dam failures: A review of the European incidents in the worldwide context. Journal of Hazardous Materials, 152 (2), 846–852.
5. Milutinović, S., Mikić, M., Stojanović, M. (2021.) The use of multicriteria decision-making methods in determining the optimal solution in the form of selection the priority in exploitation the ore deposit in Eastern Serbia. https://doi.org/10.5937/mmeb2101063M
6. Saaty, T.L. (1988) What is the Analytic Hierarchy Process? Mathematical Models for Decision Support, 109–121. https://doi.org/10.1007/978-3-642-83555-1_5.
7. Orašanin, G.S., Vučijak, B.S. Multi-criteria optimization in planning water supply. Tehnika, 68 (4), 768–774.

XV International Mineral Processing and Recycling Conference
17-19 May 2023, Belgrade, Serbia

SIMPLE FUZZY MODELS FOR PREDICTION OF FLOTATION INDICES

I. Jovanović[1#], V. Conić[1], J. Sokolović[2] D. Kržanović[1], D. Radulović[3]
[1] Mining and Metallurgy Institute Bor, Bor, Serbia
[2] University of Belgrade, Technical faculty in Bor, Bor, Serbia
[3] Institute for Technology of Nuclear and Other Mineral Raw Materials, Belgrade, Serbia

ABSTRACT – This paper presents the development and validation of two simple copper flotation models based on fuzzy logic (Mamdani and Takagi-Sugeno fuzzy inference system). Given that the Cu flotation process contains a large number of variables (especially inputs), models are called simple, because they contain only three input and three output variables. Input variables are feed grade, collector consumption in the roughing stage and overall frother consumption. Output variables are final concentrate grade and recovery as well as final tailings grade. The training and evaluation of the proposed models were accomplished on the basis of real process data from the industrial flotation plant of "Veliki Krivelj Mine". The results showed that the proposed fuzzy models well describe the behavior of the industrial flotation plant in a wide range of circumstances (correlation coefficient $R > 0.89$ in all cases). There is almost no difference between the results, whether Mamdani and Takagi Sugeno fuzzy inference system is applied.

Keywords: Fuzzy model, Flotation, Copper ore

INTRODUCTION

Many of the unit processes in mineral processing, (such as flotation) are multivariate systems and have nonlinear characteristics. Traditionally, they have been controlled using linear controllers such as proportional-integral-derivative (PID) controllers. These simple controllers are often acceptable if the process operation is restricted to a small region around the nominal operation point. Different control techniques should be used when high performance is required over a range of operation conditions. Fuzzy logic control is an alternative to realize nonlinear, multivariable control strategies [1].

For the purpose of the current research, the two most common FIS types were established: the Mamdani fuzzy inference system marked as EMM and the other based on the Takagi-Sugeno fuzzy inference system, marked as ESM. There are some differences between them.

The ESM model is made by the appropriate transformation of the EMM model. The output of the Takagi-Sugeno is linear or constant, but the output of Mamdani is the membership function. The final stage is the defuzzification in which the fuzzy results are translated to crispy form values [2].

corresponding author: ivana.jovanovic@irmbor.co.rs

EXPERIMENTAL

Simple (Elementary) Fuzzy Logic Model based on Mamdani Inference System (EMM)

This model was developed using the Fuzzy Logic Toolbox program module, which serves to generate fuzzy logic reasoning systems. The model is called simple or elementary, because it contains only three input variables and, as a result, a base with a relatively small number of fuzzy rules.

The basic methodological features of the EMM model are: (1) Mamdani inference system; (2) application of the AND (minimum) fuzzy operator in all rules; (3) implication method – minimum; (4) aggregation method – maximum; (5) defuzzification method – centroid; (6) number of rules – 63.

The input variables in the model are feed grade (FCU), collector consumption in the rough flotation stage (PXR) and frother (FRT). Output variables are concentrate grade (CCU), tailings grade (TCU), and concentrate recovery (RCU). Other parameters were considered constant due to different reasons. More details about this model development are given in literature [3]. Figure 1 presents some of the resulting surfaces provided by the model.

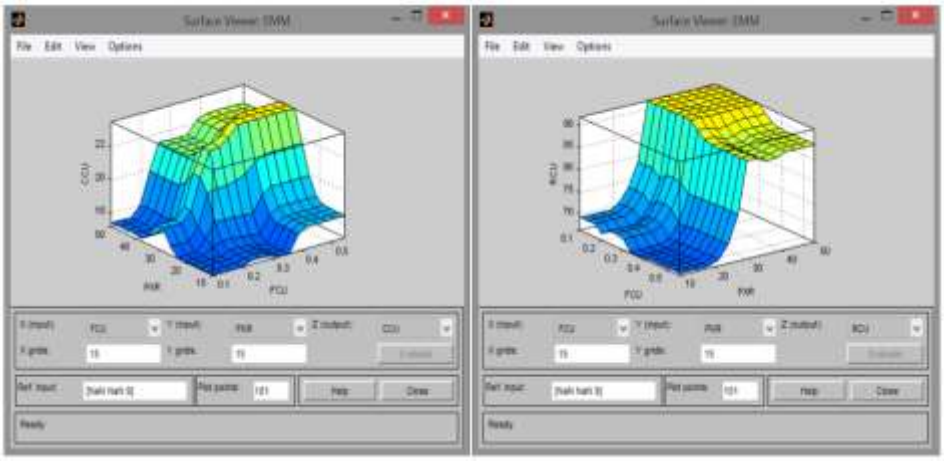

Figure 1 Resulting surfaces of the EMM model: left – dependence of the concentrate grade on the feed grade and collector consumption in roughing stage; right – dependence of copper recovery in the final concentrate on the feed grade and consumption in roughing stage

The resulting surfaces in Figure 1 show a logical sequence of cause-and-effect relationships between the considered variables. Namely, increasing the dose of the collector first leads to an increase, and then to a decrease in the grade of the concentrate, while the recovery of copper in the concentrate increases.

This shape of the resulting surfaces, indicates the adequacy of the fuzzy rules, given that the trends of the values of the dependent variables correspond to the real behavior of industrial flotation system.

Simple (Elementary) Fuzzy Logic Model based on Takagi-Sugeno Inference System (ESM)

The elementary Takagi-Sugeno model is formed by the appropriate transformation of the EMM model. Its main features are: (1) Takagi-Sugeno inference system; (2) application of the AND (minimum) fuzzy operator in all rules; (3) implication method – product; (4) aggregation method – sum; (5) defuzzification method – weighted average; (6) number of rules – 63. More details about this model development are given in literature [3]. Figure 2 shows resulting surfaces of the ESM model, respectively.

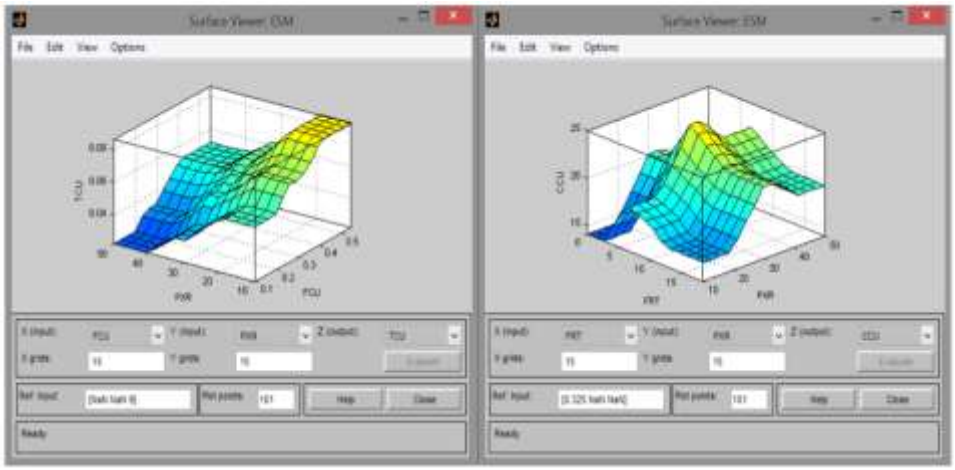

Figure 2 Resulting surfaces of the ESM model: left – dependence of tailings grade on copper content in the feed and collector consumption in roughing stage; right – dependence of the concentrate grade on the consumption of the collector in the roughing stage and the consumption of the frother

By observing the surfaces shown in Figure 2, it can be concluded that they represent the real process to a good extent. The copper content in the tailings increases with an increase of the copper content in the feed and decrease of the consumption of the collector, while a peak corresponding to the maximum grade of the concentrate can be observed on the surface on the right. This peak is coupled with the optimal consumptions of the collector and frother, which is also clearly visible in Figure 2.

RESULTS AND DISCUSSION

Evaluation of models was carried out in the MATLAB software package, by entering the real values of the input process variables from the industrial flotation plant "Veliki Krivelj" and generating the corresponding outputs predicted by the models. With the aim of determining the ability of each of the models to reliably predict the technological indicators of the flotation process based on the given input parameters, a regression analysis was performed in the Microsoft Excel program. As part of the regression analysis, the correlation between the real process values of recovery, concentrate grade and tailings grade with those obtained according to the models was considered.

Tables 1 and 2 show the results of the regression analysis for both models, while Figures 3 – 4 show their prediction errors of technological parameters. The prediction error (ε), which served as one of the criteria for evaluating the predictive properties of the model, was calculated according to the Formula (1):

$$\varepsilon = y_{pr} - y_{re} \quad (1)$$

Where:
y_{pr} – predicted value of flotation index
y_{re} – real value of flotation index

Table 1 Statistical analysis of actual and predicted values using the EMM model

Statistical parameters	Technological indices of the flotation process		
	Concentrate grade	Concentrate recovery	Tailings grade
Correlation coefficient R	0.98136	0.98943	0.89995
Determination coefficient R^2	0.96307	0.97896	0.80992
RMSE	3.87144	11.69683	0.03050

Table 2 Statistical analysis of actual and predicted values using the ESM model

Statistical parameters	Technological indices of the flotation process		
	Concentrate grade	Concentrate recovery	Tailings grade
Correlation coefficient R	0.98219	0.99537	0.90220
Determination coefficient R^2	0.96470	0.99077	0.81396
RMSE	3.98479	8.14911	0.02582

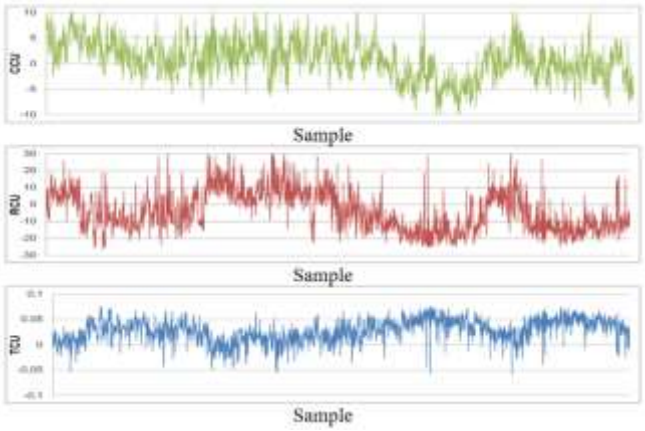

Figure 3 Prediction errors of technological indices according to the EMM model

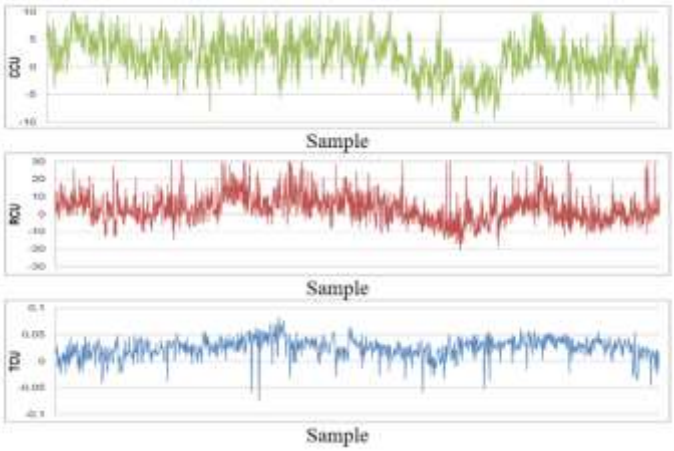

Figure 4 Prediction errors of technological indices according to the ESM model

By observing the trend of the prediction error of the concentrate grade, it can be concluded that the error mostly "oscillates" around the value of zero, which is expected. The only major deviation from this trend can be seen on the right half of the diagram, which, according to estimates, corresponds to the beginning of the last third of the observed time period of plant operation. In that period, prediction errors are mostly negative, which may indicate changes in the operating mode of the plant. These changes can be caused by various factors, which were not taken into account during modeling, such as, for example, changes in the fineness of grinding and/or regrinding due to the occurrence of softer or harder batches of ore, changes in the quality of the reagents themselves, etc. Furthermore, by looking at the trend of recovery error, it was observed that a positive recovery error (predicted values are higher than actual) is quite well followed by a negative tailings grade error. The reverse is also true – a negative recovery prediction error is followed by a positive tailings grade prediction error. Given that the recovery of copper in the concentrate and the content of copper in the tailings are in direct connection, this indicates a good general setting of the model, as well as the potential influence of process factors that were considered constant during the modeling. For the results obtained by the regression analysis of the ESM model, it can be stated that they are very similar to the results from the EMM model. Correlation coefficients are almost the same (about R = 0.98), as well as root mean square errors (RMSE is 3.87 and 3.98 for EMM and ESM, respectively). This points to the fact that in this case it does not make much difference whether the Mamdani or Takagi-Sugeno methodology was applied.

CONCLUSION

In this study, the metallurgical parameters of an industrial copper flotation plant were predicted by two fuzzy logic models (Mamdani and Takagi-Sugeno). The obtained correlation coefficients are very high, which generally indicates a good correlation between the actual and predicted values of the output variables. The significant deviations between actual and predicted values most likely occurred due to the

fluctuations in real process data that can be caused by various factors. By comparing the results of Mamdani and Takagi Sugeno fuzzy inference systems, it can be inferred that they demonstrate very similar predictive performance.

ACKNOWLEDGEMENT

This work was financially supported by the Ministry of Education, Science and Technological Development of the Republic of Serbia, Grant No. 451-03-47/2023-01/200052.

REFERENCES

1. Ding, L., Gustafsson, T., Su, F. (1999) Application of Fuzzy Control to a Flotation Process IFAC Proceedings Volumes, Volume 32, Issue 2, pp. 6998-7003
2. Jovanović, I., Nakhaei, F., Kržanović, D., Conić, V., Urošević, D. (2022) Comparison of fuzzy and neural network computing techniques for performance prediction of an industrial copper lotation circuit. Minerals, 12(12), 1493
3. Jovanović, I. (2016) Model of an Intelligent System of Adaptive Control the Ore Processing System, PhD Dissertation, Faculty of Mining and Geology, Belgrade, p. 217 (in Serbian).

XV International Mineral Processing and Recycling Conference
17-19 May 2023, Belgrade, Serbia

DEVELOPMENT OF A VIBRATION SENSOR-BASED ONLINE MONITORING SYSTEM FOR DETECTING ROPING IN HYDROCYCLONES

S. Mishra, M. H. Tyeb, A. K. Majumder#
Indian Institute of Technology Kharagpur, Kharagpur, W.B., India

ABSTRACT – In this study, we have attempted to develop a vibration sensor-based online monitoring system for detecting roping in hydrocyclones. A laboratory-scale hydrocyclone was operated at spray and rope discharge conditions, and simultaneously, vibration signals were captured using a commercially available accelerometer attached to the spigot region. Further, a novel methodology was adopted for differentiating the vibration characteristics acquired during the spray and rope discharge conditions. Based on this, it is proposed that a threshold limiting vibration value can be set for predicting the onset of roping and, thereby, incorporating remedial strategies to prevent any possible choking hazards in hydrocyclones.

Keywords: Hydrocyclone, Roping, Vibration Sensor, Online Monitoring, Condition Monitoring.

INTRODUCTION

In mineral processing industries, hydrocyclones are chiefly utilized for solid-liquid separation. Correspondingly, hydrocyclones are vulnerable to roping conditions; a condition where the underflow discharge profile attains the shape of a rope, owing to the small spigot sizes and less solid handling capacity [1,2]. In hydrocyclones, the phenomenon of roping has been attributed either to elevated levels of feed solid concentration or to relatively coarser size particles in the feed resulting in high underflow solid concentration [3-5]. Thus, the attainment of roping leads to significant product degradation due to an increase in the classification size [5]. Further, roping, if not prevented, may lead to spigot choking, which can cause the equipment to stop and sometimes the plant to shut down, resulting in heavy losses.

Due to the aforementioned problems, timely monitoring of the hydrocyclone underflow discharge profile is necessary for a continued operation. However, this is frequently made difficult by industrial site restrictions and is seldom possible by direct manual inspections. In addition, the challenge is multiplied by manifolds while monitoring the underflow discharge profiles of the hydrocyclones placed in series and/or clusters. This suggests that a near real-time and online hydrocyclone underflow discharge monitoring tool for the detection of roping is a sine qua non.

Several hydrocyclone underflow discharge monitoring techniques have been reported in the literature for detecting the onset of roping, which includes tomography [6,7], image processing [3,8,9], acoustics [10], and vibration-based techniques [3,10-12]. However, these have not yet found significant industrial applications due to their inherent limitations as reported by Mishra and Majumder [10]. They also reported that

corresponding author: akm@mining.iitkgp.ac.in

the vibration-based monitoring technique stands apart from other techniques due to the advantages of being non-intrusive, non-invasive, robust, less complex, and cost-effective, that are pre requisite for any industrial applications. In the past few years, some studies have been reported to diagnose the roping in hydrocyclones using vibration-based sensors [3,11-13]. However, despite these studies, to the best of the authors' knowledge, widespread industrial use of a vibration sensor-based online monitoring system for the detection of roping in hydrocyclones is still unknown. This is because the literature lacks a robust algorithm that can be applied for detecting roping in industrial hydrocyclones. Moreover, heavy financial aspects associated with sophisticated vibration-based sensors have also limited their industrial applicability. Recently, Mishra et al. [13] proposed an algorithm to diagnose the onset of roping in a laboratory-based small-diameter hydrocyclone using a commercially available vibration-based sensor. The present work was carried out on similar grounds to achieve the following objective.

- To develop a methodology for classifying the rope and spray discharge condition in the hydrocyclone by identifying differences in its vibration characteristics.

EXPERIMENTAL

To carry out the aforesaid objective, an experimental investigation was carried out in a closed-circuit test rig equipped with a 50.8 mm diameter hydrocyclone with vortex finder and spigot diameter 8 mm and 4.5 mm respectively. Table 1 enlists the operating conditions that were chosen for carrying out the experiments, which suggests that the hydrocyclone was operated with a gradual increase in the feed solid concentration until roping was established in the underflow. It was observed that the spray discharge condition prevailed till 11.2% feed solid concentration while roping was established at 12% and 12.5% feed solid concentration.

A commercially available and calibrated 3-axis digital MEMS accelerometer (ADXL-345) with a sensitivity of ±8g was attached to the outer wall of the spigot of the hydrocyclone and was used to record vibration data concurrently for each experimental run. Vibration data samples in acceleration (g) values were gathered for 30 seconds at a frequency of 1 kHz. Moreover, vibration data were collected twice for each level of feed solid concentration for experimental repeatability. Figure 1 shows the experimental hydrocyclone laboratory setup depicting the location of the accelerometer and the data acquisition system. It is to be noted that for the current study, the vertical axis was considered as the Y-axis and the X-Z plane as the horizontal plane as shown in the figure 1.

Consequently, the raw vibration signal was analyzed in the frequency domain through frequency spectrum and power spectral density (PSD) plots. For this, the time domain signal was considered as a sum of sinusoids of amplitude A_i, frequency f_i, time t and phase difference ϕ_i as shown in equation 1.

$$x(t) = \sum_{i=1}^{N} A_i \cos(2\pi f_i\, t + \emptyset_i) \quad (1)$$

The time domain vibration signal was then converted to the frequency domain using Discrete Time Fourier Transform (DTFT), as shown in equation 2.

$$X(f) = \sum_{n=0}^{N-1} x(n)\, e^{-\frac{j2\pi fn}{N}}, f = 0,1,2 \ldots \ldots (N-1) \quad (2)$$

where n is the number of samples, f the frequency, $X(f)$ is a complex vector of length N, which can be represented as $X(f) = X_a(f) + jX_b(f)$, where $X_a(f)$ is the real component and $X_b(f)$ is the imaginary part of the complex data in the frequency domain.

Table 1 Operating parameters for carrying out the experimental runs

Feed Solid Concentration (wt.%)	Feed Inlet Pressure (×10^4 N/m^2)	Feed Particle Size (d_{50}) (μm)	Feed Solid Density (g/cc)
6%, 8%, 8.8%, 9.6%, 10.4%, 11.2%, 12%, 12.5%	17	16	2.56

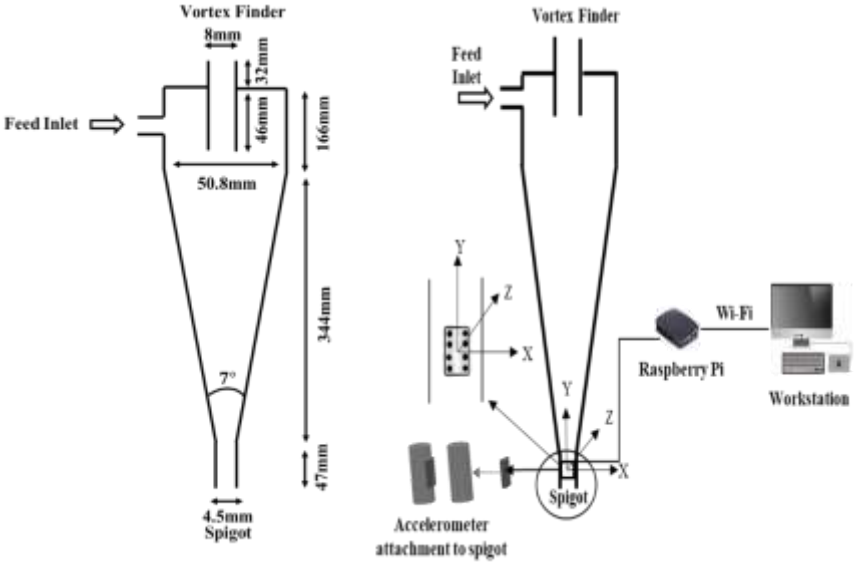

Figure 1 Hydrocyclone schematic and experimental setup

RESULTS AND DISCUSSION

To differentiate the hydrocyclone vibration characteristics at different feed solid concentration, the frequency spectrum and the subsequent power spectral density was computed following the methodology as discussed hereunder.

Roping detection by frequency spectrum

Figure 2 below shows the frequency spectrum obtained along the X-axis for different levels of feed solid concentration. It can be observed from Figures 2(a)-2(f) that no significant vibration peaks prevailed below 100 Hz frequency when the hydrocyclone was

operated with spray discharge condition in the underflow. However, once roping is established at 12% feed solid concentration, multiple peaks prevail below 100 Hz frequency. This observation suggests that, along the horizontal axis, the rope discharge condition is accompanied by high amplitude vibration in the low-frequency range. Neesse et al. [8] also reported a similar observation, who proposed rope and spray discharge conditions to be associated with low and high-frequency vibration, respectively. This observation is explained by the oscillating frequency of the air core during spray and rope discharge conditions, as reported by Banerjee et al. [14].

Roping detection by power spectral density (PSD)

Figure 3 below shows the PSD curves obtained along the X-axis for different levels of feed solid concentration. It can be observed from the figure that for the spray discharge condition, the intensity of vibration is lowered below the 100 Hz frequency range. In contrast, high-intensity vibration prevails for the rope discharge condition at this frequency range. Thus, it implies that the vibration energy along the horizontal axis is higher when the hydrocyclone is operated at rope discharge condition than the spray discharge. It is because once roping is attained, the oscillating behaviour of the air core is enhanced along the horizontal plane, as reported by Banerjee et al. [14].

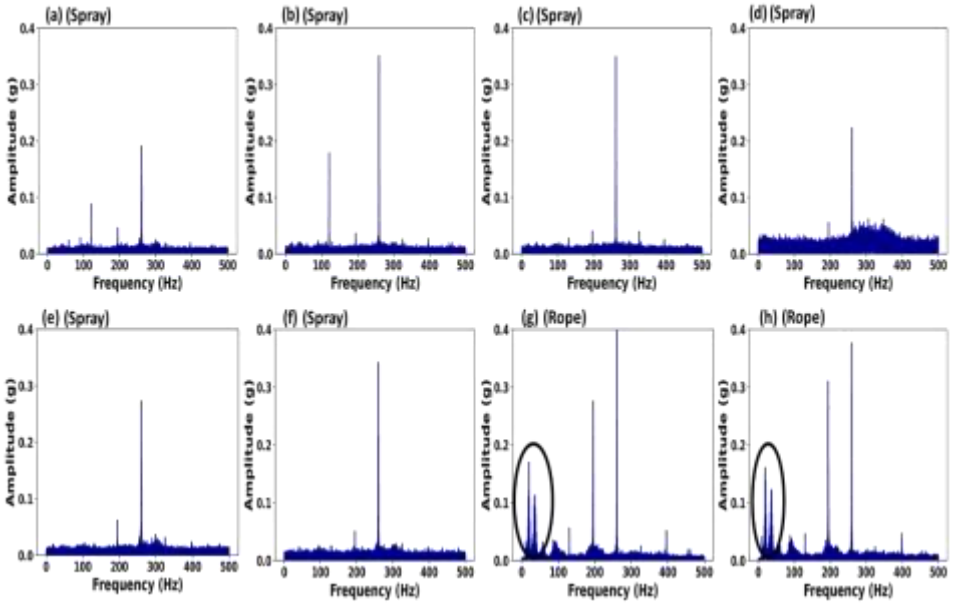

Figure 2 Frequency spectrum for (a) 6% (b) 8% (c) 8.8% (d) 9.6% (e) 10.4% (f) 11.2% (g) 12% (h) 12.5% feed solid concentration

It is inferred from the above understanding that low amplitude vibration prevails below the 100 Hz frequency range when the hydrocyclone is operated at spray discharge condition in the underflow. On the contrary, vibration is of high amplitude in this frequency range when the hydrocyclone is operated at rope discharge condition.

Similarly, vibration energy below the 100 Hz frequency range is increased for rope discharge conditions as compared to the spray discharge. These differences in the vibration characteristics of the spray and rope discharge condition can potentially be utilized for the online detection of roping in the hydrocyclone to prevent choking hazards. A threshold limiting vibration value can be set for predicting the onset of roping and, thereby, incorporating remedial strategies prior to rope discharge condition.

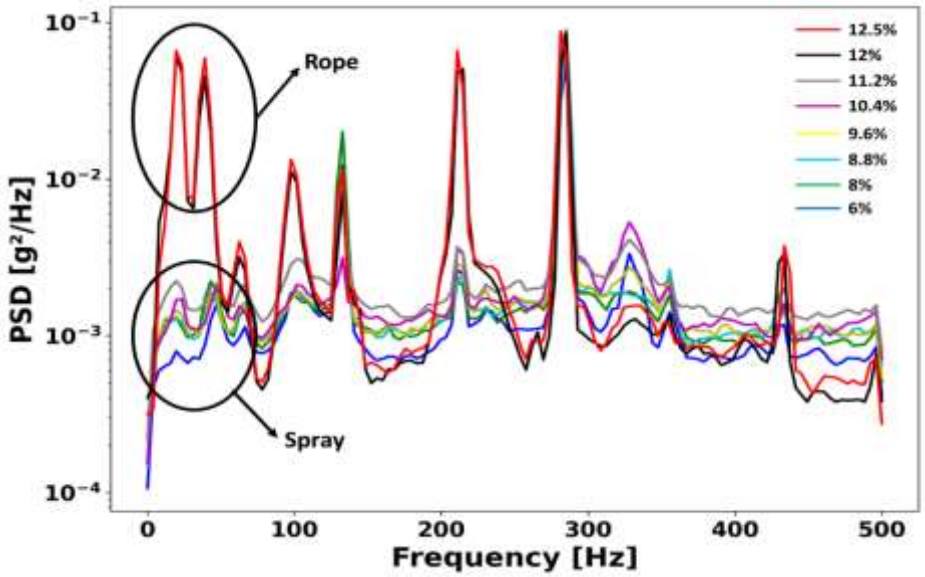

Figure 3 Power Spectral Density (PSD) plots with increase in the feed solid concentration (wt.%)

Contrary to these observations, Mishra et al. [13] reported that the vibration intensity along the spigot region increases for the spray discharge regime and is minimum when roping ensues. However, it is noteworthy that they analyzed the vibration characteristics along the vertical axis whereas in this work the differences in the vibration characteristics are shown along the horizontal axis. Thus, this work does not contradict the findings reported by Mishra et al. [13].

CONCLUSION

From the aforementioned results and discussions, the following conclusions are drawn.

i. The differences in the vibration characteristics acquired during the spray and rope discharge condition reveal that the methodology proposed in this work is suitable for diagnosing the onset of roping in the hydrocyclone.

ii. A threshold limiting vibration value can be set based on the developed methodology work for predicting the onset of roping in the hydrocyclones. It will help to incorporate remedial strategies to prevent any possible choking hazards in operating hydrocyclones.

REFERENCES

1. Mular, A.L., Jull, N.A. (1980) The selection of cyclone classifiers, pumps and pump boxes for grinding circuits. Mineral Processing Plant Design, AIME, New York, 376-91.
2. Plitt, L.R., Flintoff, B.C., Stuffco, T.J. (1987) Roping in hydrocyclones. In: P. Wood (Editor), Proceedings of the 3rd International Conference on Hydrocyclones, Oxford, BHRA. Elsevier, Amsterdam, Paper A-3, 21-34.
3. Dubey, R.K., Singh, G., Majumder, A.K. (2017) Roping: Is it an optimum dewatering performance condition in a hydrocyclone? Powder Technology, 321, 218-31.
4. Daza, J., Cornejo, P., Rodriguez, C., Betancourt, F., Concha, F. (2020) Influence of the feed particle size distribution on roping in hydrocyclones. Minerals Engineering, 157, 1-14.
5. Davailles, A., Climent, E., Bourgeois, F., Majumder, A.K. (2012) Analysis of swirling flow in hydrocyclones operating under dense regime. Minerals Engineering, 31, 32–41.
6. Williams, R.A., Jia, X., West, R.M., Wang, M., Cullivan, J.C., Bond, J., Faulks, I., Dyakowski, T., Wang, S.J., Climpson, N., Kostuch, J.A., Payton, D. (1999) Industrial monitoring of hydrocyclone operation using electrical resistance tomography. Minerals Engineering, 12 (10), 1245-1252.
7. Gutierrez, J.A., Dyakowski, T., Beck, M.S., Williams, R.A. (2000) Using electrical impedance tomography for controlling hydrocyclone underflow discharge. Powder Technology, 108, 180–84.
8. Neesse, T., Schneider, M., Golyk, V. Tiefel, H. (2004) Measuring the operating state of the hydrocyclone. Minerals Engineering, 17 (5), 697-703.
9. Van Vuuren, M.J., Aldrich, C., Auret, L. (2011) Detecting changes in the operational states of hydrocyclones. Minerals Engineering, 24 (14), 1532-44.
10. Mishra, S., Majumder, A.K. (2022) Online techniques for performance and condition monitoring of hydrocyclone: present status and the future. Mineral Processing and Extractive Metallurgy Review, doi.org 10.1080/08827508.2022.2047042.
11. Nayak, D.K., Das, D.P., Prasad, S., Behera, S.K., Sadangi, J.K. (2020) Prevention of Hydrocyclone Choking Through Detection of Sub-Hz Frequency Shift of Vibration Signal. Journal of Vibration Engineering & Technologies, 8, 517 – 28.
12. Wang, G., Liu, Q., Wang, C., Dong, L., Dai, D., Shen, L. (2020) Study of Blockage Diagnosis for Hydrocyclone Using Vibration-Based Technique Based on Wavelet Denoising and Discrete-Time Fourier Transform Method. Processes, 8 (4), 440-54.
13. Mishra, S., Tyeb, M.H., Majumder, A.K. (2022) Development of a vibration sensor-based tool for online detection of roping in small-diameter hydrocyclones. Mineral Processing and Extractive Metallurgy Review.
14. Banerjee, C., Chaudhury, K., Cid, E., Bourgeois, F., Chakraborty, S., Majumder, A., Climent, E. (2022) Oscillation dynamics of the air-core in a hydrocyclone. Physics of Fluids, 34 (09), 1-15.

XV International Mineral Processing and Recycling Conference
17-19 May 2023, Belgrade, Serbia

THE IMPROVEMENT OF MINERAL PROCESSING – CASE STUDY

B. Farkaš[1#], A. Hrastov[2], E. Orbanić[3]
[1] Faculty of Mining, Geology and Petroleum Engineering, Zagreb, Croatia
[2] RUDAR PROJEKT d.o.o, Zagreb, Croatia
[3] KAVA export-import d.o.o., Fažana, Croatia

ABSTRACT – The efficiency of the processing plant of a quarry can be improved by using modern analytical methods. For example, mineral processing in the "Tambura" quarry was analysed by comparing several models of mineral processing (existing condition, modified condition, new process model). Based on the cost and profit analysis, an optimal model for improving mineral processing was selected.

Keywords: Quarry Tambura, Mineral Processing, Production, Optimisation, Process Efficiency.

INTRODUCTION

The process of mineral processing requires maximum utilisation of the mining equipment and machinery used. By analysing the existing machinery and equipment used for mineral processing, their efficiency can be determined and ways to improve the analysed process can be identified. Various authors have explored the concepts of improvement and optimisation using different methods [1,2,3], and this paper focuses on the improvement of mineral processing. The effectiveness of the machinery and equipment used, the maximum production quantities, the costs, the required investments, and the profit were analysed. The optimisation process was carried out using the example of processing technical building stone in the "Tambura" quarry in Croatia. Based on the analysis, a way to improve mineral processing with minimum investment and maximum production was shown, also the loading and transport machinery were used in mineral processing [4].

EXPERIMENTAL (MATERIALS AND METHODS)

Site location

The quarry of technical building stone "Tambura" (Figure 1) is located in Istria, Republic of Croatia, northwest of the city of Pula and covers an area of 3.79 ha.

Basic assumptions for the mineral processing

The planned annual exploitation at the "Tambura" quarry amounts to 50,000 m^3 of mineral raw material, which has to be crushed and classified in the mineral processing.

corresponding author: branimir.farkas@rgn.hr

For models A and B, actual production data were used, while for model C an average value of 4,166.67 m^3 of the fractions to be processed in one month with the new method was used.

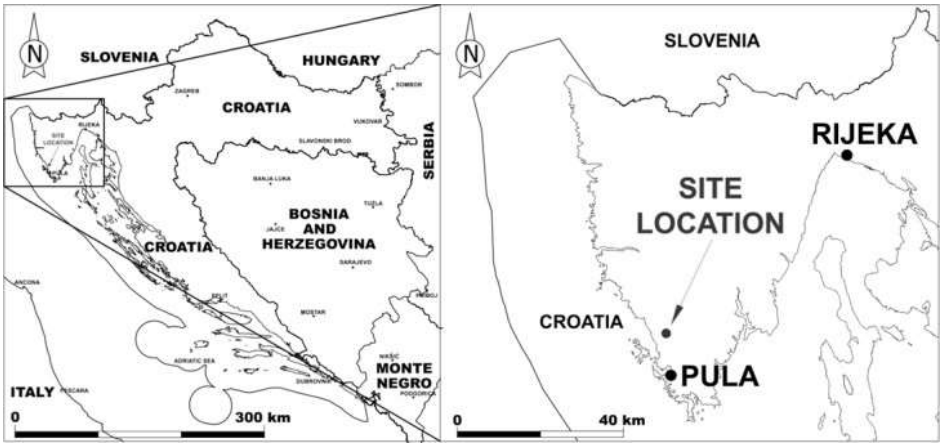

Figure 1 Quarry "Tambura" [5]

The mineral processing production process was analysed using three models [4]: Model A (existing production process), Model B (existing production process with 50% changes) and Model C (new production model).

The effective working hours were calculated to obtain the required working hours of the new machinery for Model C. The calculation for Model A and B was not done because real data was used. The calculation for Model C was based on the manufacturer's data (technical specifications) for each machine to determine the theoretical fuel consumption based on the total working time.

The working time in the quarry is 241 working days in 8-hour shifts, so the effective annual working time is 1,928 hours. The total annual working time (T) of each machine was calculated using equation (1) and the effective working time (T_{ef}) was calculated using equation (2). In equation (1), Q represents the annual amount of material to be exploited, and Q_p represents the capacity of a given machine. T_d in equation (2) stands for the number of working days per year in the "Tambura" quarry.

$$T = \frac{Q}{Q_p}, h \tag{1}$$

$$T_{ef} = \frac{T}{T_d}, h \tag{2}$$

Models of mineral processing

The processing plant for all three models consists of a number of machines: a rotary crusher, a mobile vibrating screen and a separation plant. The working hours were calculated for a number of machines, not for each machine individually.

Fuel consumption (N) was calculated for each model using equation (3), which

depends on the total amount of material produced (M_{uk}) and the total fuel consumption (G_{uk}).

$$N = \frac{G_{uk}}{M_{uk}}, \frac{l}{m^3} \tag{3}$$

For Model C, machinery with similar or improved characteristics compared to Models A and B and a different course of mineral processing were considered. (Figure 2c). The analysis was carried out on the basis of the defined maximum annual extraction quantity and the technical data of the new machinery. Only machines that consume fuel (excavator, loader and generator) were included in the analysis. For these machines, the hourly fuel consumption (g_h) was calculated, which depends on the engine power (P), the fuel consumption (s_g), and work inequality coefficient (k_g), according to equation (4).

$$g_h = P \cdot s_g \cdot k_g, \frac{l}{h} \tag{4}$$

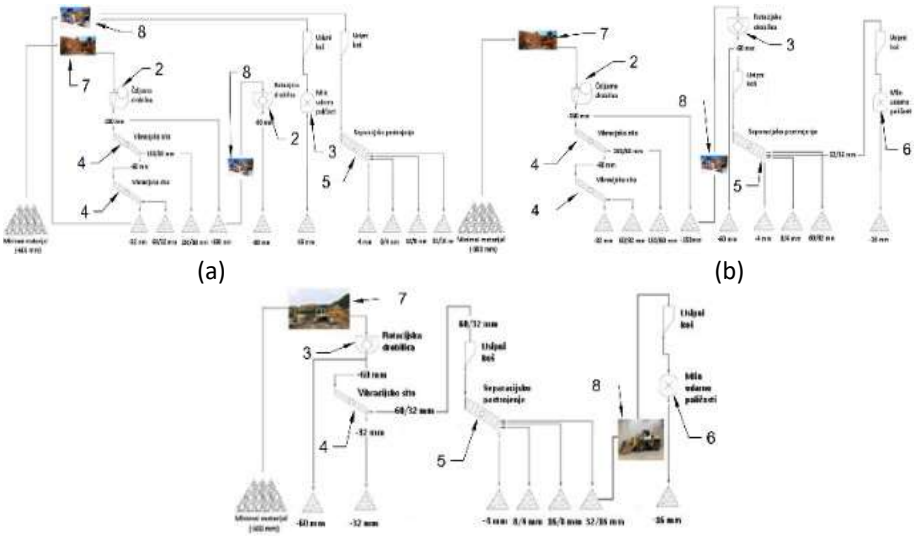

(a) (b)

(c)

Figure 2 The mineral processing: (a) Model A, (b) Model B, (c) Model C

The total annual fuel consumption (G_{uk}) for the generator, excavator and loader was calculated using equation (5) and the consumption rate (N) using equation (3).

$$G_{uk} = \frac{T}{g_h}, l \tag{5}$$

In order to improve mineral processing, the following parameters were taken into account: the amount of material produced, the fuel consumption for machinery operation, and the efficiency of the production process. The machines used in mineral processing at the "Tambura" quarry for each model are listed in Table 1.

Table 1 "Tambura" quarry machinery

Machinery		Models		
		Model A	Model B	Model C
1	Diesel generator	+	+	+
2	Crusher (jaw)	+	+	-
3	Crusher (rotary	+	+	+
4	Vibrational sieve	+	+	+
5	Separational facility	+	+	+
6	Beater mill	+	+	-
7	Excavator	+	+	+
8	Loader	+	+	+

Figure 2 shows schematically the production process of mineral processing for Models A, B and C. The machines used in each model are identified by numbers from 1 to 8, as in Table 1.

RESULTS AND DISCUSSION

Results

By using machinery for Model A (Table 1) in the production process of mineral processing (Figure 1a), a total of 5,200.08 m^3 of fractions were produced during October and November. The fuel consumption is real data from which the fuel rate consumption (N) was calculated according to the equation (3). Table 2 shows the total fuel consumption for each machine that uses fuel in the production process of Model A, with respect to the produced quantities of fractions.

Table 2 Fuel consumption in relation to quantity of material – Model A

Machinery	Fuel consumption (l)	Quantity of material (m^3)	Rate (l/m^3)
Loader	3 180.00	5 200.08	0.61
Excavator	5 200.00	5 200.08	1.00
Generator	7 050.00	5 200.08	1.36
TOTAL	15 430.00	5 200.08	2.97

The machinery in the mineral processing for Model B (Table 1 and Figure 2b) produced a total of 5,431.62 m^3 of fractions during October and November. Table 3 shows the total fuel consumption for Model B, and the consumption rate was calculated according to the equation (3).

Table 3 Fuel consumption in relation to quantity of material – Model B

Machinery	Fuel consumption (l)	Quantity of material (m^3)	Rate (l/m^3)
Loader	2 600.00	5 431.62	0.48
Excavator	5 250.00	5 431.62	0.97
Generator	6 850.00	5 431.62	1.26
TOTAL	14 700.00	5 431.62	2.71

The assumption for Model C is that machinery in the mineral processing (Table 1 and Figure 2c) produced 8,333.34 m^3 of fractions during October and November. The following hourly fuel consumption is assumed: 24.60 l/h for the loader, 28.80 l/h for the excavator, and 45.00 l/h for the generator [4]. Based on this, the fuel consumption was calculated with respect to the quantity of the material (Table 4).

Table 4 Fuel consumption in relation to quantity of material – Model C

Machinery	Fuel consumption (l)	Quantity of material (m^3)	Rate (l/m^3)
Loader	16 081.48	8 333.34	0.32
Excavator	21 705.13	8 333.34	0.43
Generator	53 035.71	8 333.34	1.06
TOTAL	90 822.33	8 333.34	1.82

Discussion

Based on the results for Models A, B, and C, the costs of equipment and the revenues that can be achieved depending on the quantity of produced finished fractions of technical building stone were analysed. The costs at the "Tambura" quarry consist of fuel costs (average price 1.5 €/L), equipment maintenance costs (3,700 €) [4], and necessary investments in the new equipment (for Model C), and their structure and percentage shares are shown in Table 5.

Table 5 Cost structure

Cost structure	Model A		Model B		Model C	
	EUR	%	EUR	%	EUR	%
Fuel	138 870.00	97.40	132 300.00	97.28	136 233.49	15.51
Equipment maintenance	3 700.00	2.60	3 700.00	2.72	3 700.00	0.42
New equipment	0.00	0.00	0.00	0.00	738 541.00	81.07

A comparative analysis of Models A, B and C is presented graphically (Figure 3) with the aim of improving the mineral processing. The total machinery costs (in red), the revenue from the sale of fractions (in green), which is based on the average selling price of 1 m^3 of mineral raw material of 4.65 €/m^3 [4], and the profit as the difference between revenue and costs (in yellow) are shown.

The costs (142,570.00 €) and profit (145,082.23 €) for Model A are almost equal, which means that this method of mineral processing is at the profitability threshold, and the profit is 2,512.23 €. In Model B, the restructuring of the mineral processing process results in higher production of fractions, resulting in sales revenue of 151,542.20 €, and reduced costs of 136,000.00 €, ensuring a higher company profit of 15,542.20 €. Model C, due to its significant investment in new equipment, generates a negative difference between profit (232,500.00 €) and costs (878,474.49 €), i.e. a financial loss of 645,974.49 €.

Figure 3 Mineral processing - model analysis

CONCLUSION

Using the "Tambura" quarry as an example, three different models for improving the mineral processing process were analysed. Model A represents the current state and organisation of the equipment used for mineral processing. Model B uses the same equipment but with a reorganised mineral processing approach, while Model C represents a completely new mechanisation.

In conclusion, the following points can be made:

- By reorganising existing processes, improvement opportunities can be identified that can increase production efficiency without requiring additional financial investment.
- Model B is the optimal model for improving mineral processing as it does not require financial investment but yields the highest profit.
- Before investing in new equipment and mechanisation, it is necessary to determine the financial feasibility of the new process by analysing the profit with the new projected investments.

REFERENCES

1. Trojanowska, J., Kolinski, A., Galusik, D., Varela, M.L.R., Machado, J. (2018) A Methodology of Improvement of Manufacturing Productivity Through Increasing Operational Efficiency of the Production Process. In: Hamrol, A., Ciszak, O., Legutko, S., Jurczyk, M. (eds) Advances in Manufacturing. Lecture Notes in Mechanical Engineering. Springer, Cham. 23-32.
2. Farkaš, B., Hrastov, A. (2021) Multi-criteria analysis for the selection of the optimal mining design solution - a case study on quarry “Tambura”. Energies, 14 (11), 3200.
3. Matiskova, D. (2013) Working Process Optimization and Minimization of Production Costs. Strojarstvo, 55 (3), 231-235.

4. Orbanić, M. (2021) Analiza procesa pridobivanja i oplemenjivanja mineralne sirovine na primjeru površinskog kopa "Tambura", Sveučilište u Zagrebu, (Diplomski rad) Rudarsko-geološko-naftni fakultet, Zagreb, 54.
5. Farkaš, B., Hrastov, A. (2022) Comparative analysis of the mining works performance on the quarry "Tambura" In: 8th Balkan mining congress. Belgrade, Serbia, Proceedings, 125-131.

XV International Mineral Processing and Recycling Conference
17-19 May 2023, Belgrade, Serbia

IMPROVED ON-LINE FAILURE PREDICTION METHOD OF COAL INJECTION SYSTEM USED IN A SPONGE IRON ROTARY KILN

T. Mohit[1], P. Patel[1], P. Kaushal[1], J. Sahoo[1], V. Arumuru[1], B. Deo[1#], M. Jain[2], R. Manchanda[2]

[1] Indian Institute of Technology, Bhubaneswar, Jatni, Odisha, India
[2] Tata Steel Long Products Limited, Joda, Odisha, India

ABSTRACT – Improvements have been carried out in the advanced prediction and warning of the failure in the injection system of a coal-fired rotary kiln by using both Fast Fourier Transform (FFT) and Wavelet transform. It better helps to decide on the timely replacement of lance, thereby avoiding product quality fluctuation. Rejections (due to the low quality of the sponge) can be lowered, and coal consumed per ton of ore can be reduced.

Keywords: Sponge Iron Rotary Kiln, Coal Injection System, Wavelet Transform, Fast Fourier Transform.

INTRODUCTION

The details of the sponge iron plant and coal injection system have been given in the previous work [1]. Internal wear of the coal injection pipe takes place because of friction due to the movement of coal inside the pipe. This wear is aggravated by high temperatures (1000-1400 K) prevailing inside the kiln. The portion of the stainless coal injection pipe protrudes inside the kiln up to +2 meters. After some use, when the pipe cracks or bends, it directly changes the 'coal throw' pressure and the also coal trajectory /profile inside the kiln. The trajectory of coal inside the kiln decides the amount of coal combusted in different regions along the length and hence also the corresponding temperatures. Therefore the failure of injection pipe due to wear and deformation is a cause of great concern for maintaining product quality and productivity.

There is no direct way to physically see the wear of the pipe and also the wear of the tip of the coal injection lance inside the furnace. In the previous work results of wavelet transform were presented [1]. In the present work data of a new campaign is analysed as a random check to confirm the applicability of an improved method developed which uses both wavelet transform and an in-depth analysis of Fast Fourier Transform. The procedure of knowing actual failure as well as advanced warning of impending failure, as developed in this work can be used in other similar applications like rockets/engines fired with propellants, supersonic nozzles in steelmaking etc.

EXPERIMENTAL METHODS: FAST FOURIER AND WAVELET TRANSFORMS

Fourier transform is used to compute the FFT amplitude of the data which provides

corresponding author: bdeo@iitbbs.ac.in

information about the irregularities in the system by raising the amplitude when it encounters an abnormality.

i) The data has been divided day-wise and also a sliding window analysis is performed for n+-m data points.
ii) The FFT of these divided data has been computed and plotted and the maximum amplitude for each day has been recorded.
iii) Comparing the record books of the plant to relate the failure of the lance with the computed FFT amplitude.

The wavelet analysis was explained in the previous work [1]. The procedure of signal analysis is as follows:

i) The input data is normalized to make the scalogram visualization easier.
ii) The scales are adjusted for the features to be visible clearly.
iii) Once the final scalogram is obtained we compare the record books of the plant to relate the failure of the lance with the computed maximum amplitude.
iv) The maximum amplitude (day-wise) is checked for patterns to understand how the system progresses to failure.
v) It is found that the failure is not abrupt but it approaches gradually with a visible increase in amplitude and is not abrupt.

RESULTS AND DISCUSSION

After performing the continuous wavelet transform (CWT) on the given data, the program outputs a scalogram. Scalogram is an effective tool to visualize failure. The horizontal axis of the scalogram is given by 'time and date' (referring to the particular day of plant operation) and the severity of failure is indicated by the change in color of the contour (blue being normal functioning to yellow/red being an indicator to approaching damage). We choose the absolute CWT axis to be in the range of 0.02 to 0.4 and not from 0-0.40 as it included a few bluish-white peaks which are caused due to cleaning as a part of the plant maintenance. In the scalogram (Figure 1), we observe major peaks on 29th June, 30th June, and 1st July. From the data archives of the DRI plant, we know that there has been an operational shutdown of about 87 minutes on 28th June 2021 and 29th June 2021 combined. From Figure 2 we can see that the highest amplitude of all days was observed on 30th June 2021 and thus RF1 must have failed on this day as it shows the maximum pressure deviation and this hasn't been associated with any kind of maintenance work. From the plots above we can infer that the system approaches failure over some time and is not abrupt. The lance RF1 under observation was changed on 7th July 2021 after making a visual observation which caused a pressure fluctuation resulting in a rise in amplitude on this day.

No high-intensity contours have been observed in the scalogram (Figure 3) and maximum amplitude plot (Figure 4). We checked the output of the scalogram with the record books of the plant and found that there were no abnormalities observed in the lance of RF2, as our model also predicted. Thus there is no failure in the case of RF2. This indicates that the system does not raise false alarms in the case of normal functioning.

The comparison plot (Figure 5) between the lance of RF1 and RF2 for the average FFT amplitude recorded each day shows that RF2 had some abrupt changes from 28th June 2021 to 2nd July 2021 but these changes haven't reached amplitudes as high as in case of

RF1 lance where there was recorded failure. RF2 hasn't failed when we match it with the logs of the plant's record books.

RF1 Pipe images

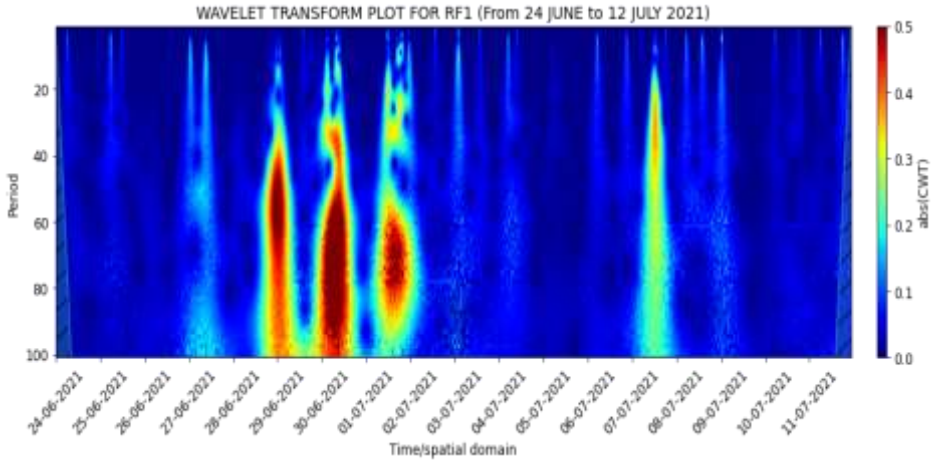

Figure 1 Continuous wavelet transformation of the pressure data for the period (24th June to 11th July 2021) shown in the graph for lance RF1

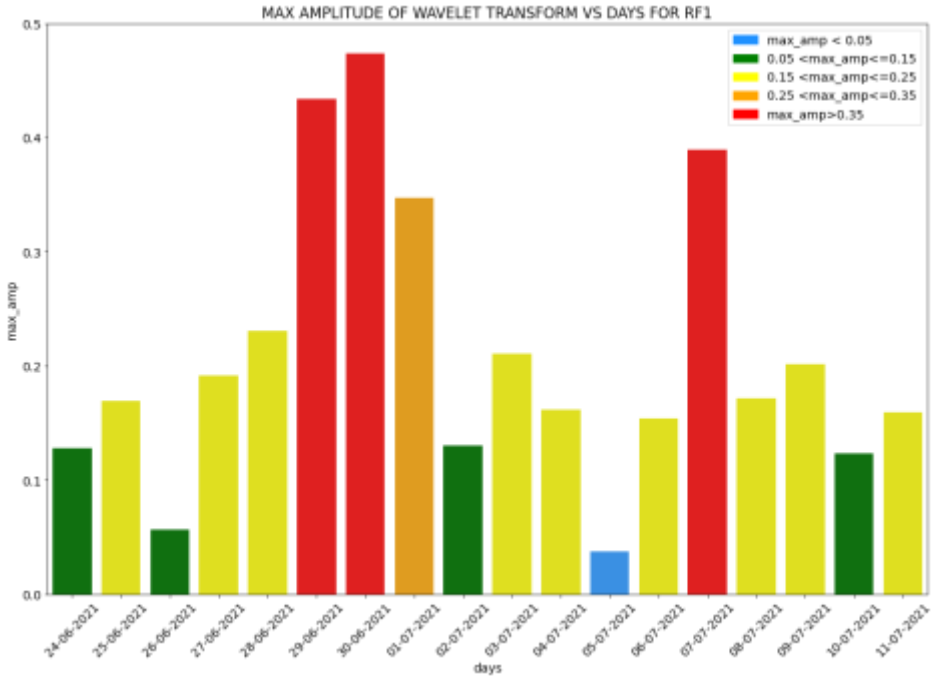

Figure 2 The above bar plot shows the maximum amplitude of wavelet transforms each day for the period (24th June to 11th July 2021) in lance RF1

RF2 Pipe images

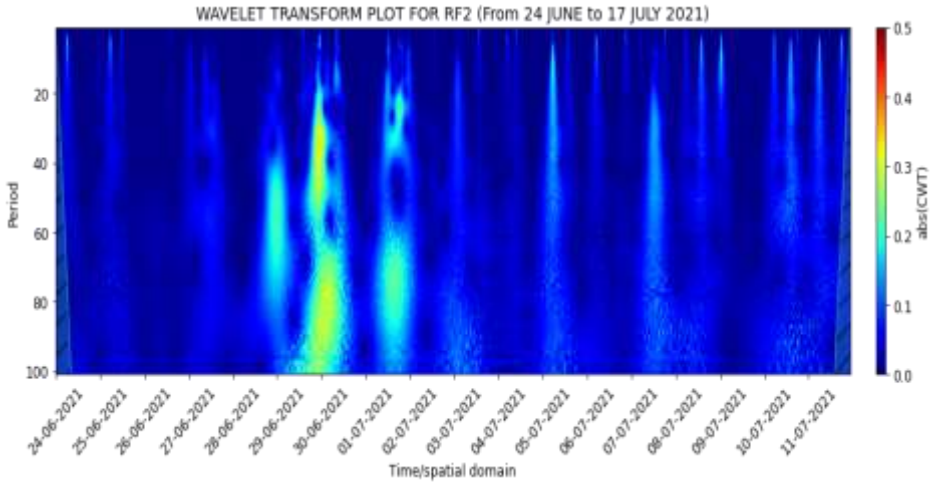

Figure 3 Continuous wavelet transformation of the pressure data for the period (24th June to 11th July 2021) shown in the graph in lance RF2: peaks having yellow/red color indicate lance failure

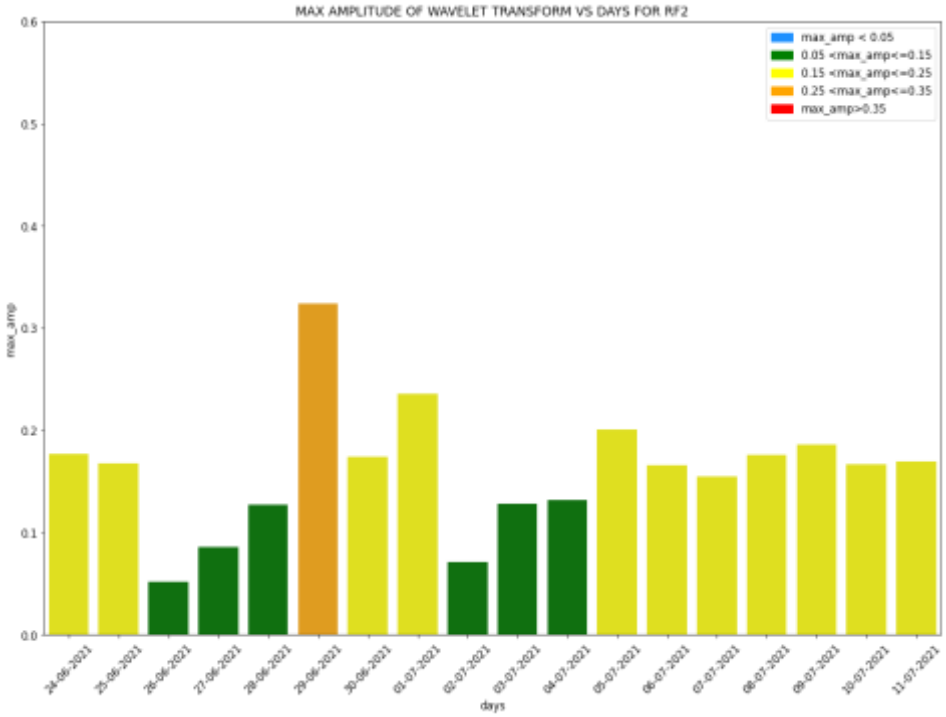

Figure 4 The bar plot shows the maximum amplitude of wavelet transforms each day for the period (24th June to 11th July 2021) in lance RF2

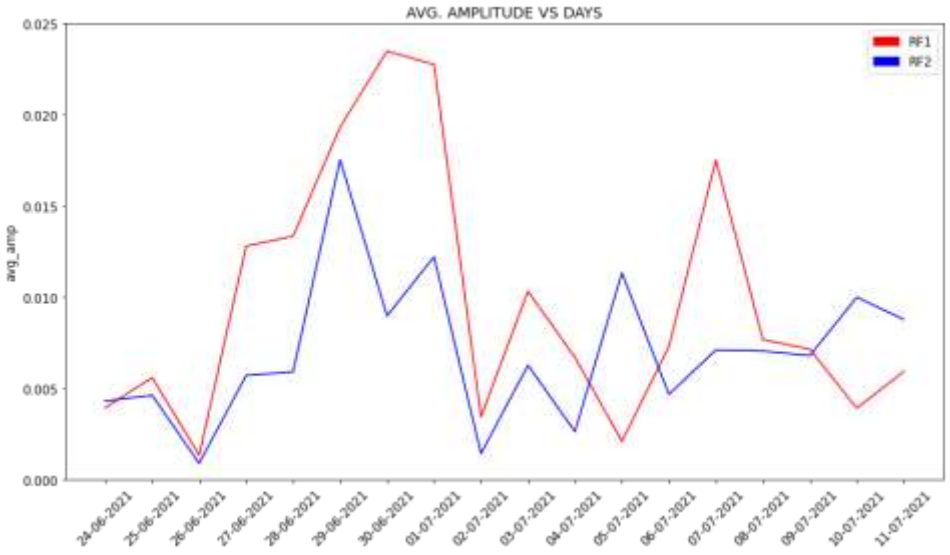

Figure 5 Average amplitude from FFT Vs Days graph for RF1 and RF2

CONCLUSION

The focus of the present work was on the dynamic analysis of online coal injection pressure in a sponge iron rotary kiln and relating them to the occurrence of lance failures. The results show that it is advantageous to use wavelet transform in combination with patterns developed in FFT. As an extension of this work, the effect of changes in moisture and mean particle size of coal can also be studied through the same procedure.

REFERENCES

1. Kaushal, P., Patel, P., Mohit, T., Deo, B., Jain, M., Manchanda, R.K., Naik, M. (2022) On-line Failure Detection during Coal Injection by Wavelet Analysis of Pressure Signal. In: International Conference on Advances in Materials and Manufacturing Technology. Chandigarh, India.
2. Shah, C., Choudhary, P., Deo, B., Malakar, P., Sahoo, S.K., Pothal, G., Chattopadhyay, P. (2018) Conventional and AI Models for Operational Guidance and Control of Sponge Iron Rotary Kilns at TATA Sponge. In: Soft Computing for Problem Solving. Springer, Singapore, Proceedings, 461-469.
3. Deo, B. (2018) Kinetics of dissolution of lime in steelmaking slags. In: The 3rd International Conference on Science and Technology of Iron and Steelmaking. Kanpur, India, Proceedings, 123-126.
4. Borah, S., Mondal, S., Choudhary, P., Deo, B., Sahoo, S.K., Malakar, P., Pothal, G., Chattopadhyay, P. (2019) Operation Of Coal Based Sponge Iron Rotary Kiln To Reduce Accretion Formation And Optimize Quality And Power Generation. In: AISTech. Cleveland, USA, Proceedings, 727-734.
5. Mondal, S., Borah, S., Choudhary, P., Deo, B., Sahoo, S.K., Malakar, P., Pothal, G., Chattopadhyay, P. (2019) Quality Prediction and Control in Coal-Fired Rotary Kilns at

TATA Sponge Iron Ltd. In: AISTech conference. Cleveland, USA, Proceedings, 719-726.
6. Khatri, P., Choudhary, P., Deo, B., Malakar, P., Bose, S.S., Pothal, G., Chattopadhyaya, P. (2019) Determination Of Surface Moisture And Particle Size Distribution Of Coal Using OnLine Image Processing. In: International Mineral Processing Conference. Belgrade, Serbia, Proceedings, 44-50.
7. Deo, B., Choudhary, P., Bose, S.S. (2021) Control of Post Combustion to Stabilize Power Generation in a Sponge Iron Plant. In: 7th Virtual International Conference on Science, Technology, and Management in Energy. Belgrade, Serbia, Proceedings, 213-218.
8. Burgess, J. (2018) Wavelets: Principles, Analysis, and Applications. Nova Science Publishers, Hauppauge, NY.

XV International Mineral Processing and Recycling Conference
17-19 May 2023, Belgrade, Serbia

IMPACT ON THE ENVIRONMENT AND RECULTIVATION OF THE OPEN MINE AND LANDFILLS IN SOUTH MINING DISTRICT – MAJDANPEK

M. Mikić#, R. Rajković, S. Trujić, D. Kržanović, M. Jovanović
Mining and metallurgy institute Bor, Bor, Serbia

ABSTRACT – During long period of copper exploatation in Majdanpek, Serbia, the impact of mining activities on the environment was multifaceted: degradation of the land - mostly forest, air pollution, water and soil. This paper presents mining impact analysis and measures to protect the environment from the impact of the open pit and landfills in South Mining District.

Keywords: mining, environmental protection, measures.

INTRODUCTION

The concept of pollution means the imission of pollutants (dust, gases) in the atmosphere of the open pits. The air pollutions, carried by wind streams from open pits, threaten the space in the direction even out of the open pits or the environment around them. Chemical pollutants that occur in the atmosphere of open pits are formed as the result of technological processes in order to obtain the ore and in case of mass blasting, loading, transport, crushing and at the effect of natural factors - winds [1]. The matters in the form of gases and dust get into the atmosphere of the environment from the open pits. The major air pollutants arising from the open cast mining operations include total suspended particulate (TSP) matter and particles with an equivalent aerodynamic diameter less than 10 microns (PM10) [2].

Air pollution in the area of open pit mines depends on the extent of annual production and intensity of pollutant emission, terrain configuration around the open pit mines and climatic parameters [3]. In this case, the entire area of open pit mine and landfills are source of environmental pollution. Outside the mining objects, the dust is spread by wind, usually in the direction of the dominant winds and the air pollution dispersion plume is formed [3]. The highest air pollution from the open pits is on their edge while moving away from the edge of pits in direction of winds blowing; the air pollution is reduced or diluted (dispersion) [1]. This rule is applied to dust because gases are mainly diffused. Imission of dust in the environment of the open pits and landfills depends on the size of dust particles that are dispersed from these objects by the wind currents. The largest particles (greater than 10 mm) begin to deposit near the edges of mining objects, while the finer particles smaller than 10 mm (PM10, PM2.5) are transported by the wind energy in the direction of its blowing and deposited away from the edge. The finest particles, dispersed by the wind currents from the open pits are not deposited, but remain flying in the air.

corresponding author: miomir.mikicrmbor.co.rs

The open pits are line source of dust for immediate surroundings. Removal of dust from the open pits depends on natural ventilation scheme that can be: flow, recirculation, convective and inverse. The TSP and PM10 levels in the open pit mining regions reduce the air quality and can cause silicosis, black lung (CWP), and increased mortality. They also reduce the visibility and affect surrounding flora and fauna [4]. Particles in the air are also known to play a critical role on climate [5], human health [6] and multi-phase atmospheric processes [8,9].

Due to the complexity of mining activities on the floors of the open pit South Mining District and large amounts of water on the bottom of the open pit and specificity of the flotation tailing dump facilities and unpredictability of the exact time and place of possible emergence of an accident and size of accidents, it is necessary to formulate the protection measures of working and living environment in the expansion of the open pit and landfills in South Mining District [7].

LOCATION OF THE OPEN PIT AND LANDFILLS OF SOUTH MINING DISTRICT MAJDANPEK

Majdanpek is located Eastern Serbia, near the town of Bor. North of Majdanpek is the Danube River which also represents the border between Serbia and Romania. The open pit South Mining District is located on the south side of Majdanpek in Serbia and it is surrounded on all sides by hills and high waste dumps (overburden), Figure 1.

Figure 1 Disposition of facilities South Mining District - Majdanpek

DATA ON SOURCES OF EMISSION OF POLLUTANTS OF EQUIPMENT

Expanding the open pit and operation of mining machinery create dust, which, due to the terrain configuration around the open pit, is dispersed by wind currents in the urban area. The main sources of gas and dust emissions are machines that operate on technological phases of obtaining copper ore at the open pit South Mining District.

According to previous measurements at the copper open pits in RTB Bor, the possible emission of dust was forecasted in obtaining copper ore per machine and they are shown in Table 1.

Table 1 Forecasted dust emissions of equipment at the open pit South Mining District

Ord. No	Type of equipment	Concentration (mg/m^3)	
	Period	In summer	In winter
1	Truck	3.77	1.05
2	Excavator	3.92	3.14
3	Drill	5.51	4.61
4	Loader	3.40	2.27
5	Bulldozer	8.66	3.10
6	Grader	7.20	2.10

Based on the number of machines in operation and known power of mobile machines that will work at the open pit as well as the composition of outlet gases from engines, the forecast emissions of exhaust gases that occur at the open pit by operation of mobile equipment is given in Table 2.

Table 2 Forecasted gas emissions per one machine

Type of equipment	Engine power	Amount of exhaust gases	Total gas emissions (m^3/s) at their content in exhaust gas				
	kW	m^3/s	CO_2 =10%	CO =0.12	NO_4 =0.04	SO_2 =0.04	Aldehydes 0.002
Truck	875	0.6125	0.0611	0.00003	0.000245	0.000245	0.000001
Loader	783	0.548	0.055	0.000657	0.0002192	0.0002192	0.000010
Bulldozer	231	0.1615	0.016	0.00019	0.0000646	0.0000646	0.00000032
Grader	208	0.145	0.015	0.000174	0.000058	0.000058	0.0000029
Tank truck	450	0.315	0.032	0.000378	0.000126	0.000126	0.0000063

For combustion of 1 kg of oil, the amount of gas that is released during operation of internal combustion engines is between 13 and 15 m^3/kg. Concentration of gases at the open pit depends on the ratio of combustible components in the fuel, such as: carbon, hydrogen and sulfur as well as the proper chemical relations fuel-air. At the open pits in Majdanpek, the fuel D_2 is used where sulfur is from one weight percent, and it is 500 ppm of SO_2. The required amount of air for dilution the harmful components in exhaust gases of internal combustion engines depends on concentration of these components.

In liquid fuel D_2, the dominant factor which defines the required air amount for dispersion of gases from the atmosphere of the open pit is taken as SO_2 due to its MDK value that is equal to 4 ppm. For dilution $1.0m^3$ SO_2 in the atmosphere of the open pits, 125 m^3 of air is required to reduce the harmful concentration in the air to MDK value.

PROTECTIVE MEASURES OF THE TOWN ON THE DUST FROM THE OPEN PIT

The adequate protective measure is obtained by placing the PVC piping around the edges of the open pit toward the town with a device for creating a water curtain to overthrow dust. The pipeline can be connected to the system for dewatering from the open pit South Mining District.

The other measures include: the introduction of additional organizational-technical measures and strict application of the machine manufacturer's instructions for efficient suppression of gas and dust in the operation of production machines at the open pit.

To protect the atmosphere in the mine and the town, it is needed to undertake the proposed complex measures of protection at the open pit which includes: Protective measures for drilling the boreholes, Protective measures on loading, Protective measures on transport, Protective measures on disposal which will include: sprinkling of terraced plateaus at the tailings disposal site, and recultivation of open pit and landfills site according to the recultivation project

RECULTIVATION OF DEGRADED SURFACES OF TAIL LANDFILL PK JUZNI REVIR

During the expansion of the South district open pit in stages from 1 to 6, waste is excavated and landfills are formed (Figure 1).

On the north side of the open pit, Andesitski prst was formed. On east, southest Šaška landfills were formed. The Bugarski potok landfill was formed further south. Waste landfills are formed on already degraded areas and in the industrial zone. In order to save on transport costs, the waste are deposited from the final plane, resulting in high slopes of 31°.

Recultivation of degraded areas at Andesitski prst, Bugarski potok and Šaška landfill sites involves works aimed at recultivating the areas. Given that the soil of degraded areas does not contain enough nutrients for the normal development of plants, for the purpose of recultivation, an optimal approach with phases of agrotechnical, technical and biological recultivation should be used.

Data on structure and purpose of land use

The total degraded areas at the South district open pit waste landfill sites for recultivation by location are shown in table 3.

Table 3 The total degraded areas for recultivation

Landfills	Level, m	Total area , m²
Andezitski prst (AP)	500	117.389
Bugarski potok	595	352.232
Šaška landfill	580	1.197.603

According to the physical and chemical properties of the soil, the geomorphology of the waste disposal site, the exposure of the surface to the south, the climatic conditions and the natural vegetation in the environment, the biological phase of optimal recultivation comes into consideration, namely:

- The final levels of waste landfills sites - afforestation,

- Final slopes of the landfill - afforestation.

Data on the selection of cultures for recultivation

The distribution of cultures by landfill area during afforestation is given in table 4 and was carried out on the basis of microcellular conditions and research that was carried out in the period from 1988-1989 in Majdanpek at the Andezitski Prst landfill by the Institute of Forestry in Belgrade, the Technical Faculty of Bor and the Institute of Copper in Bor and based on the results achieved in the recultivation in V. Krivelj and Cerovo.

Table 4 Selection of cultures by area

Landfill site	Surface structure	Cultures	Area, m^2
Andezitski prst (AP)	Final levels	Black pine	117,389
	Final slopes	Birch tree	
Bugarski potok	Final levels	Elm	352,232
	Final slopes	Acacia	
Šaška	Final levels	Birch tree	1,197,603
	Final slopes	Acacia	

Description of methods of recultivation of degraded surfaces

The aim of the revitalization of degraded areas at the waste landfills sites in Majdanpek is to protect the environment. Degraded surfaces belong to the class of man-made soils with an insufficient share of nutrients, which is why it is necessary to apply optimal recultivation with phases of agrotechnical, technical and biological recultivation [10]. The phase of agrotechnical optimal recultivation represents the stage in which a series of measures aimed at establishing productivity on artificial formations - anthroposols - are implemented. In the case of degraded areas in Majdanpek, it is understood that the existing access roads will be equipped and the subsequent planning of the areas on the final flat level (during the final disposal process, due to the prevention of the formation of lakes on flat areas, unplanned piles of tailings are left).

2. The technical phase of optimal recultivation includes: digging, loading, transport, and unloading of soil.

3. The biological phase of optimal recultivation implies a complex of biotechnical and phytoremedial measures for the cultivation of forest crops on tailings disposal sites in order to restore the ecosystem.

CONCLUSION

The Majdanpek copper mine is an important part of the Bor mining and smelting basin system. The expansion of the South and North surface mines in Majdanpek with the application of complex protection measures enables continuity in the production of copper ore, which has a positive impact on the social structure (national and ethnic) of the population in terms of creating new jobs and keeping young people working and living in Majdanpek as and revival of villages in surrounding municipalities.

The implemented optimal type of recultivation of degraded areas combined with self-reclamation and semi-reclamation represents a permanent solution for preserving the environment of the city of Majdanpek, enabling better microclimate conditions as well as a better appearance of the environment.

ACKNOWLEDGEMENT

This work was financially supported by the Ministry of Education, Science and Technological Development of the Republic of Serbia, contract no. 451-03-47/2023-01/ 200052.

REFERENCES

1. Mikić, M., Kržanović, D., Jovanović, M. (2009) Suppression of creating and raising the dust with dumper transportation of excavation at the open pits, Innovation and development, 1, 3-14.
2. Sinha, S., Banerjee, S. (1997) Characterization of haul road dust in an Indian opencast iron mine. Atmospheric Environment, 31, 2809–2814.
3. Apostolovski, Trujić, T., Mikić, M., Tasić, V., (2014) Air quality control in the area of environmental influence, The 46th International October Conference on Mining and Metallurgy-Proceedings, Serbia, 545-549.
4. Wheeler, A.J, Williams, I., Beaumont, R.A., Manilton, RS. (2000) Characterization of particulate mattersampled during a study of children's personal exposure to airborne particulatematter in a UK urban environment. Environmental Monitoring and Assessment, 65, 69–77.
5. Zhang, R., Li, G., Fan, J., Wu D., Molina, M. (2007) Intensification of pacific storm track linked to Asian pollution. Proceedings of the National Academy of Sciences of the United States of America, 104:5295–5299.
6. Davidson, C., Phalen, R., Solomon, P. (2005) Airborne particle matter and human health: A review.Aerosol Sci Technol, 39, 737–749.
7. Molina, M., Molina, L., Zhang, R., Meads, R., Spencer, D. (1997) The reaction of $ClONO_2$ with HCl on aluminum oxide. Geophys Res Lett, 24 (13). 1619–1622.
8. Tie, X., Madronich, S., Walters, S., Zhang, R., Rasch, P., Collins, W. (2003) Effect of clouds on photolysis and oxidants in the troposphere. Journal of Geophysical Research 108, 4642–2664.
9. Mikić, M., Kržanović, D., Rajković, R. (2012) Effect of exploitation at social community, and other public facilities in zone of open pit Južni Revir in Majdanpek, Mining, Privredna Komora Srbije, 397-402.
10. Mikić, M., Rajković, R., Kržanović, D. (2012) Recultivation of degraded area at open pit Južni Revir in Majdanpek, Mining, Privredna Komora Srbije, 491-499.

XV International Mineral Processing and Recycling Conference
17-19 May 2023, Belgrade, Serbia

APPLICATION OF GEOGRIDS IN RECULTIVATION MEASURES AGAINST LAND DEGRADATION

M. Jovanović, D. Kržanović, R. Rajković, M. Mikić, M. Maksimović
Mining and Metallurgy Institute Bor, Bor, Serbia

ABSTRACT – Geogrids are most often used to strengthen and stabilize weak-bearing soil. In some cases, the material, the fraction of which is larger than the opening of the mesh, is piled on the geogrid and the material is trapped in the openings of the geogrid and a system resistant to external forces is created. Now we have geogrids made of natural (organic), sintetic and composite type of materials. Geogrids and organic geotextiles are a natural and 100% biodegradable solution to erosion control using geogrids or geotextile mats made from coconut (or jute) fibers. They are designed to hold the soil in place until vegetation is established. A geogrid or permeable geotextile provides a natural support system to the soil and vegetation.

Keywords: Geogrids, Recultivation, Organic Geomaterials, Degraded Land.

INTRODUCTION

Geogrids - Types

Geogrids are mainly made of polymer materials such as polyethylene, polyester and polypropylene and are characterized by high tensile strength. The original geogrids were made by drilling holes in a sheet of material. Today, such geogrids are made by the so-called extrusion process. Now we have geogrids made of polyester fibers coated with polyethylene. Many unbroken fibers are combined into a thread, which is then woven in longitudinal and transverse directions with a certain distance between the ribs, and the folds are additionally strengthened and then the fibers are coated.

Geogrids are most often used to strengthen and stabilize weak-bearing soil. In some cases, the material, the fraction of which is larger than the opening of the mesh, is piled on the geogrid and the material is trapped in the openings of the geogrid and a system resistant to external forces is created.

The main difference between geogrids is in the type of material they are made of. There are geogrids made of artificial or natural fibers (materials), as well as geogrids that use geocomposites.

We call geogrids made of artificial materials synthetic geogrids, and those made of natural materials organic geogrids. Due to the large number of factors that directly affect negative effects during mining or construction works, a special review should be made, not only on the application of geogrids and other types of geosynthetics, but also on the application and selection of the right (adequate) materials and technologies in that area.

A particularly suitable type of geogrid for the recultivation of land degraded by mining operations is the one made of natural materials - an organic type of geogrid [1,2,3].

corresponding author: milenko.jovanovic@irmbor.co.rs

Organic geogrids

Geogrids and geotextiles made of organic (natural) materials such as coconut or jute (Fig. 1 and Fig. 2) represent a natural and 100% biodegradable solution for erosion control using geogrids or geotextile mats made of coconut fibers. Organic geogrids have unique characteristics, they consist of biologically and chemically photo-degradable natural fibers. They are designed to hold the soil in place until vegetation is established. A geogrid or permeable geotextile provides a natural support system (improvement of characteristics) to the soil (soil, landfill...) and vegetation.

An organic geogrid has the following roles:

- To absorb the kinetic energy of erosive elements (rain, wind)
- To facilitate the penetration of rain into the ground
- To retain moisture from rain: In addition to being eco-friendly, they can absorb water about five times compared to dry weight
- Allows to avoid loss or dispersion of seeds necessary for revegetation
- Ensures root establishment of plant species
- Allows control of soil temperature by mitigating its natural oscillations: so that extreme temperatures can be mitigated and you can create a pleasant micro-climate for the growth of vegetation.
- Allows reduction of soil moisture loss.

Figure 1 Coconut Geogrid

Figure 2 Geogrid of Jute

Organic geogrids are more flexible than most types of synthetic geogrids. This allows them to easily follow the contour of the soil surface. The ability to make direct contact between the fibers and the soil and allow the bond between them to develop allows for a reduction in soil loss by 90% or more. After degradation, they do not leave any toxic material in the soil [1,3,4,5].

EXPERIMENTAL

Application of geogrids in measures of recultivation of degraded land

Natural recultivation of certain, inactive mining facilities (dumps, mines, quarries, etc.) is a very slow process, measured in time intervals of several years, while in some locations it is not possible. An adequate approach to recultivation implies the development of a professional plan (Project), based on a database.

The application of new materials and technologies makes it possible to achieve significant improvements in many areas of mining and construction in the domain of faster, safer, more efficient construction, insurance, maintenance and rehabilitation of mining and construction facilities.

In general, technical, bio-technical and biological measures should be applied within the reclamation of degraded areas.

Technical measures contribute to the improvement of the resistant and deformable characteristics of the landfill, which directly affect the increase in erosion stability of the slopes.

The substrate, the land on which the landfill is formed may have unfavorable geomechanical characteristics. Geogrids have a lower coefficient of stretch than geotextiles, they do not adapt to the terrain and loads to the same extent.

Bio-technical measures, together with technical measures, contribute to faster achievement and maintenance of permanent landfill stability.

Biological measures include the application of agricultural and forest reclamation, which contribute to the stability and maintenance of recultivated areas, but are much more significant from the aspect of area revitalization and the establishment of natural biocenoses. Horticultural species play a significant role in biological measures.

As a possible, life-saving solution in many cases, where an efficient result is sought, and on the ecological (less so on the construction side), field security plan, there is an organic approach of usable materials. By using (coconut, jute, hemp, etc.) organic type of material in the production of geogrids or geotextiles, we can solve seemingly contradictory requirements in their application.

Material of organic origin would have a positive effect on the development and preservation of vegetation and the entire ecosystem, while it would have a lesser effect on mechanical stabilization factors. In addition to the above, organic geogrids act as "mulch" and thereby improve the establishment of vegetation. After degradation, they do not leave any toxic material. In particular, it should be emphasized that many of the presented materials have a very wide application in the field of environmental protection, especially in the prevention of groundwater and surface water pollution through infiltration control, and also in the treatment and immobilization of various types of waste, especially hazardous waste [3,4,8,9].

RESULTS AND DISCUSSION

Erosion processes and their control

The occurrence of erosion processes depends on the degree of implementation of technical measures and the possibility of occurrence of unexpected excessive natural or anthropogenic processes. In terms of erosion stability, the landfill formed with the application of technical measures is a heterogeneous, conditionally consolidated environment sensitive to the origin and development of both internal and surface forms of erosion.

Figure 3 Achieving erosion stability using geosynthetics

Analysis of erosion stability should be performed taking into account: physical and mechanical characteristics of natural soil and landfill, indicators of filtration current flow, probability of high water occurrence, landfill geometry, as well as other specific indicators that can affect erosion stability.

The formation of surface forms of erosion on slopes is caused by water, which arrives on the slope: as atmospheric sediment, by the discharge of underground water on the slope, from irrigation, or their simultaneous action. Water on slopes can cause washing of soil particles, plastic flow, sliding, landslides or gully formation, which depends on the amount and energy of surface water and the physical and mechanical properties of the soil that makes up the surface of the slope.

The landfill is an environment, suitable for the creation of filtration current flows, due to the acceptance of underground water around the perimeter of the landfill from the natural soil and surface water infiltration. In the conditions of the formation of filtration current flows in different porous environments, there are changes in the speed and filtration forces, that is, the intensity of internal erosion processes.

Prevention of surface erosion is done by reducing the water reaching the slope, using a system of drainage channels with a mandatory perimeter channel and drainage or geosynthetics (Fig. 3). By using geogrids, like protection from erosion, they are placed and secured with wedges, and then covered with a substrate mixed with grass seed or weeding is done by hydroseeding.

Geomembranes produced from natural fibers of jute or hemp, consist of natural cellulose veils as a supporting layer, grass seeds and additives for accelerated growth. In

order to prevent erosion, a vegetation geomat is also used, which consists of a thin layer of non-woven geotextile that is sewn to a natural canvas composed of a mixture of grass seeds. If these measures are added to the proper selection of species for biotechnical measures, along with their proper arrangement, one can count on achieving permanent stability as a function of time [1,2,3,8,9].

CONCLUSION

Geogrids and organic geotextiles are a natural and 100% biodegradable solution to erosion control using geogrids or geotextile mats made from coconut (or jute) fibers. They are designed to hold the soil in place until vegetation is established. A geogrid or permeable geotextile provides a natural support system (improvement of characteristics) to the soil (land, landfill...) and vegetation.

The installation of these efficient systems (geogrids, geotextiles, geomembranes) in various branches of ecology and industry and their usefulness directly depends on the materials from which they are made. The application and selection of types and materials in road construction is important because the application of these materials affects savings and improvements in the area of faster, safer and more efficient road construction. It also refers to the protection and stabilization (stiffening) of the surfaces (slopes) of landfills and other mining facilities, where the choice of the type and material of the covering layer depends on the deposited material, the size and shape of the landfill itself [3,8,9].

Geomembranes produced from natural fibers of jute or hemp, consist of natural cellulose veils as a supporting layer, grass seeds and additives for accelerated growth. In order to prevent erosion, a vegetation geomat is also used, which consists of a thin layer of non-woven geotextile that is sewn to a natural canvas composed of a mixture of grass seeds. If these measures are added to the proper selection of species for biotechnical measures, along with their proper arrangement, one can count on achieving permanent stability as a function of time [5,7,8,9].

As a possible solution for savings in many cases, where an efficient result is needed, both in terms of ecology, as well as in terms of construction, safety, and security of the terrain, it represents a hybrid approach to the use of construction materials. Namely, by using (cross-hybrid) different types of materials in the production of geogrids or geotextiles, we can solve seemingly contradictory requirements in their application.

Special attention in further development should be paid to the use of new natural materials and hybrid technology of geomaterials, as products of the future [9].

ACKNOWLEDGEMENT

This work was financially supported by the Ministry of Education, Science and Technological Development of the Republic of Serbia, contract no. 451-03-47/2023-01/ 200052.

REFERENCES

1. Veinović, Ž., Kvasnička, P. (2007) Surface landfills, Internal script. Faculty of Mining, Geology and Petroleum, University of Zagreb, Zagreb.

2. Bogićević, M. Građevinarstvo.rs/ Građevinarstvo.rs/ (December 3, 2008).
3. Zidar, M. (2009) Methods of rehabilitation of landslides. Faculty of Geotechnical Engineering, University of Zagreb, Varaždin.
4. Jovanović, M. (2022) Mining 2022 - Sustainable development in mining and energy [Chamber of Commerce and Industry of Serbia]: Application of combined (hybrid) materials in geogrids.
5. SRPS EN ISO 10318:2015- Geosynthetics/ Geosynthetics - Terms and definitions (ISO 10318:2015).
6. Lenče, S. Final work (paper): Application of geosynthetics in landscape design - k 3 6.
7. Lukavečki, I. Final thesis (2010/2011): On geosynthetics and application in landfill remediation, 1821.
8. Jovanović, M. (2019) Study research II (doctoral studies): Geosynthetics - purpose and application (in mining). University of Belgrade, Technical Faculty in Bor.
9. Jovanović, M. (2019) Study research III (doctoral studies): "Organic geonetworks". University of Belgrade, Technical Faculty in Bor.

XV International Mineral Processing and Recycling Conference
17-19 May 2023, Belgrade, Serbia

APPLICATION OF SUSTAINABLE CYCLING MANAGEMENT SYSTEM IN PHYTOREMEDIATION TECHNOLOGY OF CONTAMINATED SOILS

V. Gardić[1#], R. Marković[1], Z. Stevanović[1], A. Isvoran[2], T. Marković[3]
[1] Mining and Metallurgy Institute Bor, Bor, Serbia
[2] West University of Timisoara, Department of Biology-Chemistry and Advanced Environmental Research Laboratories, Timisoara, Romania
[3] Independent research

ABSTRACT – Mining and metallurgy activities in the Bor area have a big influence on water, air and soil quality. Phytoremediation technology can solve this problem but produces hazardous biowaste. Because of that, it is necessary to develop Sustainable Cycling Management System in Phytoremediation Technology (SCMS-PT) for contaminated soils, as is presented in this paper.

Keywords: Phytoremediation Technology Sustainable Cycling Management System, Contaminated Soil.

INTRODUCTION

Mining and metallurgy activities in the Bor area have a big influence on water, air and soil quality. The main pollution in the Bor area become from mining waste that is deposed many years ago and generates acid main drainage and from ongoing mining activity, drainage water from the flotation tailings which are no longer in function. The main pollutants are heavy metals (HM), but also, because of the directly discharged of urban wastewater without treatment, organic pollutants are present [1,2]. Also, air pollution is present. High concentrations of suspended particles are sufficient to cause adverse health effects, including increased morbidity or mortality. There is only one automatic measurement station that measures PM10 in the Bor Agglomeration and there is not enough data for the PM10 assessment but according to the existing data, air quality in Bor was very poor in the time period 2006-2010, regarding levels of As in total suspended particles [3].

Phytoremediation is a remediation technology to remove pollutants from contaminated soil, water or sediments by using plants. It is eco-friendly green engineering technology. Soil contamination by various inorganic and organic compounds can be clean-up by phytoremediation. The process involves the accumulation of pollutants, including heavy metals, into the plant through its root structure from the surrounding soil, water or sediments [4-8].

The plant biomass, the product of the phytoremediation technology, contains heavy metals (HM) and present highly contaminated bio-waste and it is a difficult problem for the phytoremediation technology, because could easily become a secondary pollution

corresponding author: vojka.gardic@irmbor.co.rs

source if mishandled. The bio-waste is hazardous waste. Thus, appropriate disposal and utilization methods for such biowaste are required.

In this paper are presented solution for problem of contaminated soil in Bor area by developing the Sustainable Cycling Management System in phytoremediation technology (SCMS-PT).

MATERIAL AND METHOD

In Bor area phytoremediation technology can be applied Ex-situ and In-Situ, continually and induces to clean up contaminated area of toxic metals. We chose to based our model of SCMS on In-Situ phytoremediation technology.

Phytoremediation process

In -situ Phytoremediation process are consisting of following phases:

1. Identification of sub-area in Bor region for implementation CMS-PT
2. Chemical analysis of the contaminated soil (determination of inorganic and organic pollutants)
3. Determine the plant that already grow in investigated area and determine accumulation efficiency of all part of plats
4. Perform in-situ phytoremediation based on selected plants
5. Picking and drying the plants
6. Chemical analysis of the soil near the root after finished phytoremediation
7. Determination of co-efficient (Concentration factors) of plants.

Establishment sustainable cycle management system of contaminated soil phytoremediation process products

Sustainable cycle management system of contaminated soil phytoremediation process products from Bor area are consisting of following phases:

1. incineration,
2. leaching, and
3. solid waste stabilization after the leaching process.

RESULTS AND DISCUSSION

SCMS -PT system for investigated Bor area will give following data:

- ✓ *In-situ Phytoremediation process* followed by chemical analysis of contaminated bio waste will give data for prediction of number of phytoremediation process cycles needed for clean-up of contaminated soil in investigated Bor area based on selected plants.
- ✓ *Established sustainable cycle management system of contaminated soil phytoremediation process products will give data of the process of incineration includes investigation of calorific value of tested plant samples with aim of economical view of the selected process as well as chemical composition of ash. Beyond of mentioned parameters, follows the analyses that includes an elemental analysis of plant samples (C,*

H, N, S), technical analysis of plant samples (moisture, ash, volatile content) with aim of ecological view of selected process (CO_2 and SO_2 emission in air). Incineration ash treatment: leaching process, treatment of obtained leaching solution, treatment of solid residue after leaching (if needed). The treatment process of solid residue, includes investigation of stabilization agent and optimal ratio waste to an agent in aim to obtained new product with possibilities of civil construction usage or similar.

The proposed SCMC-PT system solves the problem of contaminated soil, but in the first step, it is very good for application because it has a big influence on decreasing the contamination spread by air. The proposed SCMC-PT system (incineration, leaching, stabilization, and usage in civil construction) has its own advantages and disadvantages. SCMC-PT system presented zero-waste process. However, there are not many studies on this aspect. Thus, it will be the future task to continue studying the technical parameters and mechanism of the combination methods.

CONCLUSION

Application of phytoremediation technology in Bor area is not enough to solve environmental problem, because of a big risk of secondary pollution from remaining hazardous biowaste.

Cycling Management System in phytoremediation technology (CMS-PT) should be investigated on smaller area and based on obtained result established Sustainable Cycling Management System in phytoremediation technology (SCMS-PT), that also should be in future studying and continuously upgrading.

Proposed SCMS-PT for Bor area consisted of: in-situ phytoremediation process, incineration, leaching process of ash from incineration, treatment of obtained leaching solution, treatment of solid residue after leaching (as zero-waste process).

ACKNOWLEDGEMENT

We acknowledge the financial support of the Project RoRS 337- ROmania Serbia NETwork for assessing and disseminating the impact of copper mining activities on water quality in the cross-border area (RoS-NET2), implemented under the Interreg-IPA Cross-border Cooperation Romania-Serbia Programme that is financed by the European Union under the Instrument for Pre-accession Assistance (IPA II) and co-financed by the partner states in the Programme.

This work was also financially supported by the Ministry of Science and Technological Development and Innovations of the Republic of Serbia, Grant No. 451-03-47/2023-01/ 200052.

REFERENCES

1. Project name: ROmania Serbia NETwork for assessing and disseminating the impact of copper mining activities on water quality in the cross-border area, Programme 2014 - 2020 Interreg IPA CBC Romania - Serbia,
https://keep.eu/projects/22351/ROmania-Serbia-NETwork-for--EN/.
2. Filimon, M.N., Popescu, R., Horhat, F.G., Voia, O.S. (2016) Environmental impact of mining activity in Bor area as indicated by the distribution of heavy metals and bacterial population dynamics in sediment, Knowledge and Management of Aquatic Ecosystems, 417, 30, DOI: 10.1051/kmae/2016017.

3. Tasić, V., Kovačević, R., Trujić, T.A., Milošević, N. (2013) Air Quality Plan for the Bor Agglomeration, Serbia, In: The 8th Conference on Sustainable Development of Energy, Water and Environment Systems – SDEWES Conference. Dubrovnik, Croatia, Volume: CD Proceedings.
4. Oh, K., Cao, T., Li, T., Cheng, H. (2014) Study on Application of Phytoremediation Technology in Management and Remediation of Contaminated Soils. Journal of Clean Energy Technologies, 2 (3), 216-220.
5. Sumiahadi, A.,Acar, R. (2018) A review of phytoremediation technology: heavy metals uptake by plants, IOP Conf. Series: Earth and Environmental Science 142, 012023, doi :10.1088/1755-1315/142/1/012023.
6. Lee, J., Kaunda, R.B., Sinkala, T., Workman, C.F., Bazilian, M.D., Clough, G. (2021) Phytoremediation and phytoextraction in Sub-Saharan Africa: Addressing economic and social challenges. Ecotoxicology and Environmental Safety 226, 112864, https://doi.org/10.1016/j.ecoenv.2021.112864.
7. Kafle, A., Timilsina, A., Gautam, A., Adhikari, K., Bhattarai, A., Aryal, N. (2022) Phytoremediation: Mechanisms, plant selection and enhancement by natural and synthetic agents. Environmental Advances 8, 100203.
8. Liu, Z., Tran, K.Q.(2021) A review on disposal and utilization of phytoremediation plants containing heavy metals. Ecotoxicology and Environmental Safety 226, 112821, https://doi.org/10.1016/j.ecoenv.2021.112821.

XV International Mineral Processing and Recycling Conference
17-19 May 2023, Belgrade, Serbia

SUSTAINABLE APPROACH TO THE LACTIC ACID PRODUCTION AND ANTIBACTERIAL USE

D. Đurđević-Milošević[1#], A. Petrović[1], J. Elez[1], G. Gagula[2], V. Kalaba[3]
[1] Institute of Chemistry, Technology and Microbiology, Belgrade, Serbia
[2] Karlovac University of Applied Science, Karlovac, Croatia
[3] PI Veterinary Institute of Republic of Srpska "Dr Vaso Butozan" Banja Luka, Banja Luka, Bosnia and Hercegovina

ABSTRACT – Food waste is a suitable substrate for the growth of microbial biomass and the controlled production of lactic acid. Lactic acid is an eco-friendly raw material used in many branches of industry. This work evaluated the bactericidal activity of lactic acid in accordance with the adopted standard EN 1276:2019. Tasted 5% (v/v) and 1% (v/v) lactic acid aqueous solutions showed differences in log reductions of Gram-negative and Gram-positive bacteria, with no influence of applied organic soiling and tested contact times. The obtained results are a contribution to the sustainable and rational application of the bactericidal activity of lactic acid.

Keywords: Bactericidal Activity, Lactic Acid, Waste

INTRODUCTION

Lactic acid is present in nature as a weak organic acid that is considered not to endanger the environment and is considered safe [1, 2]. Lactic acid can be produced by fermentation or chemical synthesis. Chemical synthesis is the production of lactic acid from non-renewable petrochemical sources via acetaldehyde and acetonitrile, and the product is a racemic mixture of DL isomers. Of the total world production of lactic acid, it is estimated that only 10% of lactic acid is produced by synthesis from lactonitrile against 90% of production from renewable sources containing fermentable carbohydrates [3]. Recently, the focus of scientists is the development of lactic acid production from food waste [4, 5]. Lactic acid has significant applications in the food, chemical, pharmaceutical, polymer, and chemical industries [6]. As a permitted food additive lactic acid complies with food standards [7]. Also is known that most organic acids have an antibacterial effect as a consequence of reducing the pH value of the environment and the cell, and increasing the accumulation of anions [8].

Lactic acid is usually used with minimally processed food, while acetic and citric are suitable for use in food preparation [9]. Regardless of the knowledge of the exact mechanism of action on microorganisms, lactic acid, among other organic acids, is recognized as a bio-preservative in naturally fermented products [10], and numerous applications of lactic acid for meat decontamination have been described [11-12]. The paper examined the bactericidal activity of lactic acid with the aim of optimizing the use

corresponding author: dragica.milosevic@ihtm.rs

of lactic acid for antimicrobial purposes. The experimental design and results are intended to provide information for lowering of overuse of lactic acid for antibacterial use.

MATERIALS AND METHODS

The quantitative suspension test based on EN 1276:2019 [13] for bactericidal activity was performed. Bactericidal activity was tested separately in simulated clean (0,3 g l^{-1} bovine albumin) and simulated dirty (3 g l^{-1} bovine albumin) condition; interfering substance bovine albumin, CAS No. 9048-46-8, HiMedia. Bactericidal test suspensions were prepared using third passages of strains grown on Tryptone soy agar (TSA, HiMedia). Strains from American Type Culture Collection (ATCC) were used: *Pseudomonas aeruginosa* ATCC 15442, *Escherichia coli* ATCC 10536, *Staphylococcus aureus* ATCC 6538, *Enterococcus hirae* ATCC 10541, and with optical density 0,6 McFarland, 0,6 McF, 0,5 McF and 2 McF respectively. Also, in addition to the listed strains obligatory according to standard [13], strain *Salmonella enterica* subsp. *enterica* serovar Enteritidis ATCC 13706 was used. The optical density of the prepared suspension was 0,5 McF. The dilutions 10^{-6} and 10^{-7} of every bacterial suspension were pure plates with TSA in duplicate to obtain the count of bacteria in a milliliter of suspension (cfu/ml). Validations suspensions were prepared separately from dilution 10^{-5} of each bacterial suspension, and in accordance with standard [13]. L(+) lactic acid, p.a. (CAS No. 79-33-4, concentration 80%, Centroprom) was used for the preparation of the water solutions with final concentrations: sample I – 6.25 % v/v lactic acid and sample II – 1.25% v/v lactic acid. Also was tested sample III – 0.001% v/v lactic acid, as a concentration that is not expected bactericidal activity. Compared to standard [13] exception was that test was not performed on the product and from the product prepared additional test concentrations. The test was performed on three samples with various concentrations of lactic acid. The dilution-neutralization method of choice was used. Neutralizer was prepared in the laboratory using the following components: L-histidine (CAS No. 9048-46-8, Merck), Saponine (CAS No. 8047-15-2, Sigma Aldrich), Tween 80, CAS No. 9005-65-6, HiMedia), Sodium thiosulphate pentahydrate (CAS 10102-17-7, Merck). Briefly, the test was run as follows. After 2 minutes 8 ml of sample was added in obtained mix of 1.0 ml microbial suspension and 1 ml interfering substance solution. After a contact time of 5 minutes, 1.0 ml of mixture is added in a mix of 8.0 ml of neutralizer and 1.0 ml of water. Neutralization is performed in order to quench the antimicrobial activity of the product. After 5 minutes of neutralization, 1.0 milliliter was transferred to a petri plate in a duplicate and pure plated. The test was performed for each microorganism Incubations of plates were during 48 h at 37±1 °C. For every test in parallel three controls were performed in accordance with standard [13]: validation A to ensure that there was no biocide activity of used water, validation B to ensure no lethal activity of neutralizer, and validation C to confirm that the tested biocidal product was neutralized. For each sample concentration and each experimental condition were calculated decimal log reduction, using the following formula:

$$lg\ R = lg\ (\frac{N}{10}) - lg\ (x_{sr} \cdot 10) \quad (1)$$

where lg R is reduction (lg cfu/ml), N – number of viable cells in suspension (cfu/ml), and X_{xr} – the average of viable microorganisms after treatment.

Tests were performed three times on freshly prepared samples I, II, and III, on a different day and with newly prepared bacterial suspensions. The requirement for bactericidal activity is at least a 5 lg reduction of strain.

RESULTS AND DISCUSSION

The performed experimental design gave the results of viable cell count in the suspensions of particular microorganisms (Figure 1) which satisfy the requirements of EN 1276 [13] for cell number in interval 1.5-5.0x10^8 cfu/ml for each strain. Performed controls (validation A, validation B, and validation C) show growth <0.5 x growth of validation suspension, and that is confirmation of the validity of performed test and results of reduction. During the test, because of adding microbial suspension and interfering substances for simulation of dirty or clean conditions, the initial concentration of lactic acid 6.25%, and 1.25% are diluted to 80%. Consequently tested concentrations of lactic acid were 5% (v/v), 1% (v/v), and an inactive concentration 0.008% (v/v).

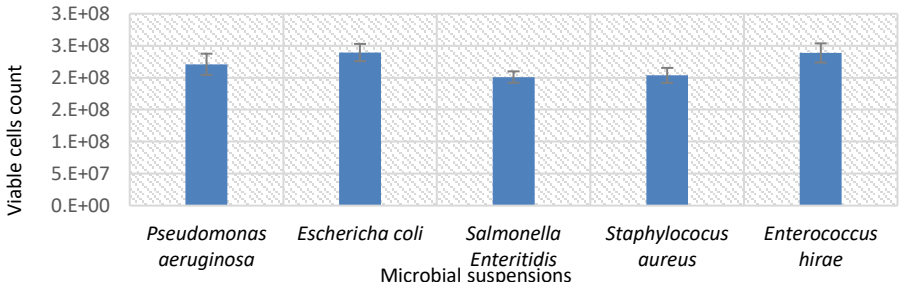

Figure 1 Viable cells count in the microbial suspensions

Taking into account the results of a viable cell count in the suspensions and the results of performed tests calculated reductions of microorganisms were presented in Table 1. The action of lactic acid in concentration 5% (v/v) and 1% (v/v) for the contact time 5 minutes was successful against *P. aeruginosa, E. coli,* and *S.* Enteritidis. The tested Gram-negative strains had log reductions of more than 5 lg. In contrary to the Gram-negative strains, log reductions of *S. aureus* and *E. hirae* were less than 5 lg and unsatisfactory. The same results were obtained in simulated dirty and clean conditions indicating that a ten times higher concentration of organic soiling (albumin bovine) did not affect the results. The paper of Neubauer et al. [14] presented testing without soiling, according to modified EN 1040, and found that condition for five minutes contact time 1% lactic acid is active against *P. aeruginosa*, but not active against *E. coli.* Lactic acid 5% showed more than 5 lg reduction against *E. coli* and *P. aeruginosa* in the same conditions without soiling which is similar to our results in conditions with organic soiling for test concentration 5% (v/v). They reported that 10% lactic acid showed 5 lg reduction of S. a*ureus*. Also was found that 5% lactic acid did not show 5 lg reduction of S. a*ureus*., which is similar to our finding, with the difference that our test was performed with organic soiling.

Table 1 Bactericidal activity of tested products for the contact time 5 minutes

Microorganism	The concentration of lactic acid in the sample (% v/v)	Tested concentration of lactic acid (% v/v)	Conditions	Reduction *X_{sr}±SD (lg cfu/ml)
Pseudomonas aeruginosa ATCC 15442	6,25	5	clean	>5,19±0,03
	6,25	5	dirty	>5,19±0,03
	1,25	1	clean	>5,19±0,03
	1,25	1	dirty	>5,19±0,03
	0,001	0,0008	clean	<3,82±0,04
	0,001	0,0008	dirty	<3,82±0,04
Escherichia coli ATCC 10536	6,25	5	clean	>5,23±0,02
	6,25	5	dirty	>5,23±0,02
	1,25	1	clean	>5,23±0,02
	1,25	1	dirty	>5,23±0,02
	0,001	0,0008	clean	<3,86±0,02
	0,001	0,0008	dirty	<3,86±0,02
Salmonella enterica subsp. *enterica* serovar Enteritidis ATCC 13706	6,25	5	clean	>5,15±0,02
	6,25	5	dirty	>5,15±0,02
	1,25	1	clean	>5,15±0,02
	1,25	1	dirty	>5,15±0,02
	0,001	0,0008	clean	<3,78±0,02
	0,001	0,0008	dirty	<3,78±0,02
Staphylococcus aureus ATCC 6538	6,25	5	clean	<3,79±0,02
	6,25	5	dirty	<3,79±0,02
	1,25	1	clean	<3,79±0,02
	1,25	1	dirty	<3,79±0,02
	0,001	0,0008	clean	<3,79±0,02
	0,001	0,0008	dirty	<3,79±0,02
Enterococcus hirae ATCC 10541	6,25	5	clean	<3,87±0,02
	6,25	5	dirty	<3,87±0,02
	1,25	1	clean	<3,87±0,02
	1,25	1	dirty	<3,87±0,02
	0,001	0,0008	clean	<3,87±0,02
	0,001	0,0008	dirty	<3,87±0,02

*X_{sr}±SD – average value ± standard deviation.

In the work of Singh et Yemmireddy [15], an examination of the effects of various environmental factors, including lactic acid, on the reduction of *Salmonella*, *E. coli* O157, *Listeria monocytogenes* cells was carried out, but the results are not comparable to ours since the log reduction was about 1 or less than 1, for all tested microorganisms.

The use of 2-5% of lactic acid solution sprayed on bovine carcasses was approved and admitted in Europe according to Commission Regulation (EU) No 101/2013 [16]. Roila et al. [17] showed a reduction of the aerobic colony count and *Enterobacteriaceae* by treating carcasses with a 2% lactic acid solution of about 1 log/25 cm^2 or less than 1 log/25 cm^2. These results also are not comparable with ours because of different experimental designs and calculations per surface. Anyway, based on our results treatment of carcasses with the lactic acid solution can not give the same results for Gram-negative and Gram-positive bacteria. In support of the use of lactic acid for disinfection in food processing and for surfaces in food plants are our findings that 1% lactic acid solution showed 5 lg reduction against pathogenic microorganism *Salmonella* Enteritidis for the contact time 5 minutes and regardless of organic load.

According to recent information, the world market for lactic acid is estimated at 2.9 trillion US dollars in 2021, and is expected to increase by 8.0% in the period 2022-2030 [18]. Taking into account these facts, the correct application and rational quantification of lactic acid due to its antibacterial properties contribute to sustainable use and give feedback for planning the production of biocides. As a result, there is also a reduction in the waste generated by the excessive use of biocides.

CONCLUSION

The action of lactic acid in concentration 5% (v/v) and 1% (v/v) for the contact time 5 minutes was successful against tested Gram-negative strain and reductions of bacteria were more than 5 lg. Contrary to the Gram-negative strain, log reductions of the Gram-positive strains *S. aureus* and *E. hirae* were less than 5 lg and unsatisfactory. No difference between results obtained in simulated dirty and clean conditions, which means that a ten times higher concentration of organic soiling did not affect the results. In support of the use of lactic acid for disinfection in food processing and for surfaces in food plants are our findings that 1% lactic acid solution showed 5 lg reduction against pathogenic microorganism *Salmonella* Enteritidis for the contact time 5 minutes and regardless of organic load. The rationale use of 1% lactic acid instead of 5% enables similar activity on Gram-negative bacteria, provides a five times less consumption of lactic acid, and lowers the generation of waste.

REFERENCES

1. Espadale, E., Pinchbeck, G., Williams, N.J., Timofte, D., McIntyre, K.M., Schmidt, V.M. (2018) Are the hands of veterinary staff a reservoir for antimicrobial-resistant bacteria? A randomized study to evaluate two hand hygiene rubs in a veterinary hospital. Microbial Drug Resistance, 24(10), 1607–1616.
2. Komesu, A., Oliveira, J. A.d., Martins, L.H.d.S, Wolf Maciel, M.R., Maciel Filho, R. (2017). Lactic acid production to purification: A review. BioResurce, 12(2), 4364-4383.
3. Datta, R., Henry, M. (2006) Lactic acid: recent advances in products, processes and technologies – a review, Journal of Chemical Technology & Biotechnology, 81(7), 1119–1129.
4. Marzo-Gago, C., Venus, J., Lopez-Gomez, J. P. (2022) Production of lactic acid from pasta wastes using a biorefinery approach. Biotechnology of Biofuels and Bioproducts, 15, 128.
5. Song, L., Yang, D., Liu, R., Liu, S., Dai, L., Dai, X. (2022) Microbial production of lactic acid from food waste: Latest advances, limits, and perspectives. Bioresource Technology. 345, 126052.
6. Kim, J., Kim, Y-M, Lebaka, V. R., Wee Y-J. (2022) Lactic Acid for Green Chemical Industry: Recent Advances in and Future Prospects for Production Technology, Recovery and Applications. Fermentation, 8(11), 609.
7. Bai, Y., Ding, X., Zhao, Q., Sun, H., Li, T., Li, Z., Wang, H., Zhang, L., Zhang, C., Xu, S. (2022) Development of an organic acid compound disinfectant to control food-borne pathogens and its application in chicken slaughterhouses. Poultry Science, 101(6), 101842.

8. Carpenter, C. E., Broadbent, J. R. (2009) External concentration of organic acid anions and pH: key independent variables for studying how organic acids inhibit growth of bacteria in mildly acidic foods. Journal of Food Science, 74(1), R12-R15.
9. Ölmez, H., Kretzschmar, U. (2009) Potential Alternative Disinfection Methods for Organic Fresh-Cut Industry for Minimizing Water Consumption and Environmental Impact. LWT – Food Science and Technology, 42(3), 686-693.
10. Ray B., Sandine W E. (1992) Acetic, propionic, and lactic acids of starter culture bacteria as biopreservatives. In: Ray B, Daeschel M, editors. Food preservatives of microbial origin. CRC Press, 103–136.
11. Smulders, F. J. M., Greer, G. G. (1998) Integrating microbial decontamination with organic acids in HACCP programmes for muscle foods: prospects and controversies. International Journal of Food Microbiology., 44(3), 149–169.
12. Sallam, K.I., Abd-Elghany, S.M., Hussein, M.A., Imre, K., Morar, A., Morshdy, A.E, Sayed-Ahmed, M. Z. (2020) Microbial decontamination of beef carcass surfaces by lactic acid, acetic acid and trisodium phospahate sprays. BioMed Reserch International, Nov 2, 2324358.
13. EN 1276:2019, Chemical disinfectants and antiseptics. Quantitative suspension test for the evaluation of bactericidal activity of chemical disinfectants and antiseptics used in food, industrial, domestic and institutional areas. Test method and requirements (phase 2, step 1).
14. Neubauer, M. P., von Nessen, K., Weiher, F. Lactic Acid. Efficient disinfecton inspired by nature. (2017) Facts. Jungbunzlauer Suisse AG. https://www.jungbunzlauer.com/fileadmin/content/_PDF/PRINT_PROJECTS/Article_facts/JBL_AR_Lactic_Acid_-_Efficient_disinfection_inspired_by_nature_2017-099.pdf (accessed 21.02.2023).
15. Singh, A., Yemmireddy, V. (2022) Pre-Growth Environmental Stresses Affect Foodborne Pathogens Response to Subsequent Chemical Treatments. Microorganisms, 10(4), 786.
16. Commission Regulation (EU) No 191/2013 of 4 February 2013 Concerning the Use of Lactic Acid to Reduce Microbiological Surface Contamination on Bovine Carcases. https://eur-lex.europa.eu/legal-content/EN/ALL/?uri=CELEX%3A32013R0101 (accessed on 21.02.2023).
17. Roila, R., Altissimi, C., Branciari, R., Primavilla, S., Valiani, A., Camibotti, F., Cardinali, L., Cioffi, A., Ranucci, D. (2022) Effects of Spray Application of Lactic Acid Solution and Aromatic Vinigar on the Microbial Loads of Wild Boar Carcasses Obtained under Optimal Harvest Conditions. Applied Sciences, 12(20), 10419.
18. Anon (2022). Lactic Acid Market Size, Share & Trends Analysis Report By Raw Material (Sugarcane, Corn, Cassava), By Application (PLA, Food & Beverages, Personal Care, Pharmaceuticals), By Region, And Segment Forecasts, 2022 – 2030. https://www.grandviewresearch.com/industry-analysis/lactic-acid-and-poly-lactic-acid-market (accessed on 21.02.2023).

XV International Mineral Processing and Recycling Conference
17-19 May 2023, Belgrade, Serbia

DIGITALIZATION OF WASTE, WAYS FOR MORE EFFICIENT WASTE MANAGEMENT

B. Cekova[1#], M. Matlievska[2], M. Marina–Puncheva[3], V. Velkoski[2], B. Kuzmanovski[1]

[1] MIT UNIVERSITY, Faculty of Environmental Resource Management, Skopje, Republic of North Macedonia

[2] MIT UNIVERSITY, Faculty of Economics, Skopje, Republic of North Macedonia

[3] MIT UNIVERSITY, Faculty of Security Sciences, Skopje, Republic of North Macedonia

ABSTRACT – Waste is any substance, matter or object from the categories of waste determined in the List of types of waste from Article 15 in the Law on Waste Management, which the creator or possessor rejects, intends to discard or is required to discard. Digitalization is transforming the 21st century, affecting every area of daily life, including the environmental technology sector. Digital technologies are expected to provide more efficient ways of managing waste. For the European economy, it will mean the return of valuable materials from the waste processing cycle, while avoiding the associated environmental and climate impacts. Advanced digitalization in waste management and treatment is currently mostly in the innovation phase. New business models are emerging, such as waste trading platforms and specific waste and data analysis software. The use of digitization technologies throughout society is largely the result of continued advances in miniaturization, increased processing power, and falling costs. Waste management is no exception and also benefits from the improvement of digital technologies. Examples of specific digital technologies that are used and expected to have a major impact in the future on the efficiency of the waste industry include robotics, the Internet of Things, cloud computing, artificial intelligence and data analysis. Here, digital tools offer the potential to improve the process by storing, processing, analyzing and optimizing the necessary information. Generally digital tools provide us with comprehensive information that is generated during the collection process, e.g. how the task execution process progresses, which can be monitored in real time.

Keywords: Waste, Environment, Waste Management, Waste Selection, Digital Technologies.

INTRODUCTION

"Waste is any substance, matter or object from the categories of waste determined in the List of types of waste from Article 15 of the Law on Waste Management, which the creator or owner rejects, intends to discard or is required to discard "Waste can be dangerous or non-hazardous [1]. Hazardous waste means any waste that contains substances that have properties such as: explosiveness, reactivity (oxidants), flammability, irritation, toxicity, or release when in contact with water, air or any acid. poisonous gases. Hazardous waste also includes non-hazardous waste that is somehow mixed with hazardous waste. The use of digitization technologies throughout society is largely the result of continued advances in miniaturization, increased processing power,

corresponding author: cekovab@yahoo.com

and falling costs. Waste management is no exception and has also benefited from the improvement of digital technologies. Examples of specific digital technologies in use and expected to have a major future impact on the efficiency of the waste industry include robotics, the Internet of Things, cloud computing, artificial intelligence and data analytics [1].

A REVOLUTION IN WASTE MANAGEMENT LOGISTICS

Digital technologies are increasingly being applied in almost all areas of waste collection. Certain aspects of billing are being transformed by advances in digitalization, especially logistics—the process of organizing, scheduling, and dispatching tasks, human resources, and vehicles. Here, digital tools offer the potential to improve the process by storing, processing, analyzing and optimizing the necessary information. Generally digital tools provide us with comprehensive information that is generated during the collection process, e.g. how the task execution process progresses, which can be monitored in real time [1,2]. As greater amounts of information are collected, so does complexity. In such cases, optimization algorithms help to find the most suitable options for allocating resources, such as manpower or vehicles. Important technologies include telematics, including routing systems, vehicle navigation and tracking software, enterprise resource planning systems, and the like. Processes that result in improvements are most evident in increased efficiency [1,2]. Another example is the so-called Internet of Things, including applications such as smart bins and robotics for semi-autonomous waste collection vehicles [2]. There remains considerable room for improving the process of waste collection in the future and for compliance with the needs of a circular economy. Another part of waste collection is the process of documentation, communication and billing. Here, the steady shift from paper-based administration systems to digital systems, as seen in other industries, will further increase the efficiency of processes and information flow. The technologies involved include digital identity tags for waste bins and containers, digital order processing, digital billing and payment, digital user interfaces for communicating with consumers and connecting public waste collection providers to other relevant government databases.If these digital technologies are applied in documentation processes, they can be used to collect waste-related data from the public. By analyzing data, turned into valuable information, they can support a circular economy by "better understanding the spatial and temporal patterns of waste generation". In addition, the potential to collect many individual data points rather than just reporting cumulative values can give local authorities additional insight [2].

DIGITALIZATION AS A TOOL TO ENCOURAGE GREEN BEHAVIOR

Pay-as-you-throw systems become successful by using digital identification and billing techniques. These systems allow for a "fair" charging scheme by allocating costs proportional to the amount of waste generated. It has been shown, however, that such schemes can have negative effects through attempts to avoid payment, such as increased illegal littering, use of public bins and "waste tourism" in neighboring regions with traditional charging schemes [1]. Digitization also enables the development of advanced "you-know-how-to-throw" schemes. In these schemes, waste management

operators use radio frequency identification (RFID) to track waste fractions at the household level. The chip tracks the waste and, once the operator has determined the quantity and quality of the separation, this information is automatically fed back to the individual or company that generated the waste. In addition, providing a tailored message according to needs - for example, an appreciation for saving waste or good separation behavior - can help attract consumers to better waste management practices, intersecting with waste prevention programs. Exchanges of environment created by increasing digitization for waste management. Greater digitization can help achieve circular economy goals throughout the entire waste management cycle, from material procurement, production and use to resource reuse. However, the digital transformation of Europe's waste management infrastructure may create several generic trade-offs. The first is energy use. Supporting digital technologies can involve significant energy demands [2]. A second concern is the material use required to produce infrastructure, computing machines, sorting robots and other elements. Finally, all infrastructure has a lifespan, after which it becomes waste. Preliminary life cycle analysis examples already show that environmental benefits can outweigh such trade-offs by a wide margin. However, more knowledge is needed to better understand this balance, illustrated in general terms, in the figure below [2].

Figure 3. Environmental effects of digitalisation in the waste sector

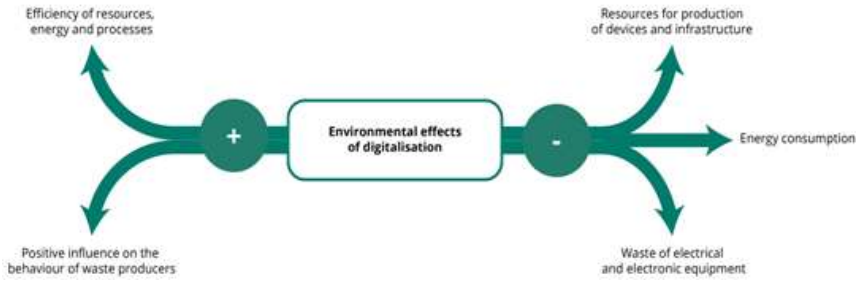

Figure 1 Effects on the environment of digitization in the waste sector

BENEFITS OF THE SMART WASTE MANAGEMENT SOLUTION

The benefits of waste management are as follows [3,4]:

▪ **Simple to implement**: Sensors are easily installed in all types of waste containers.

▪ **Complete automation of the waste collection processes**: Data on the condition of the containers and their filling, as well as the data on the collected waste are automatically downloaded and processed by the software application.

▪ **Reduction of logistics costs**: Level sensors allow direct savings (up to 40%) on fuel costs and overall operational costs for waste collection.

▪ **Possibility of introducing a new collection system**: the infrastructure in the trucks (upgraded version of the solution), enables information about the amount and location of the collected waste and the introduction of a new collection system "pay what you throw away".

▪ **Environmental protection**: By avoiding the overflow of waste from containers, the solution helps not to lose valuable material for recycling, and by optimizing routes and reducing the need for fuel, to reduce CO_2 emissions and noise [5].

RESEARCH AND RESULTS

For this purpose, research was carried out with the Selectiram initiative to set up a system for primary selection in households and ensure decent working conditions for waste collectors, their protection and education, as well as integration into a formalized waste management system. The reason why started with this kind of activity started from the root of the problem. That is exactly why, in order to protect the environment and human health, one of the ways to contribute to better waste management, to prevent its disposal, is the primary selection. Why is primary selection important? Since the process significantly contributes to the quality of urban living and reducing the total amount of waste, it brings economic and financial benefits and increases the awareness and responsibility of waste generators and service providers. Additional reasons are:

- The quality of the waste material is maintained and can then be fully used for recycling
- Through active action, the awareness and habits of citizens to preserve the environment increase
- The waste will not end up in a landfill, thus protecting the soil, water and air.

Figure 2 Primary selection

The initiative lasted from September to December 2020, during that period 2400 kilograms of plastic and 4550 kilograms of paper were collected and 46 buildings or 1750 households were covered. To hear the opinion of the tenants, about the experience they had with the initiative as part of the organizing team conducted a questionnaire answered by 140 tenants. Below is a graphic representation of the questions and answers.

When asked about the evaluation of the #selektiram initiative, it can be concluded that most of them (111 answers) evaluate it as "excellent" and 17 answers as "very good", which means that 90% of the tenants are satisfied (grade 4 and 5). Only 4.2% are dissatisfied and evaluate it with 1 or 2.

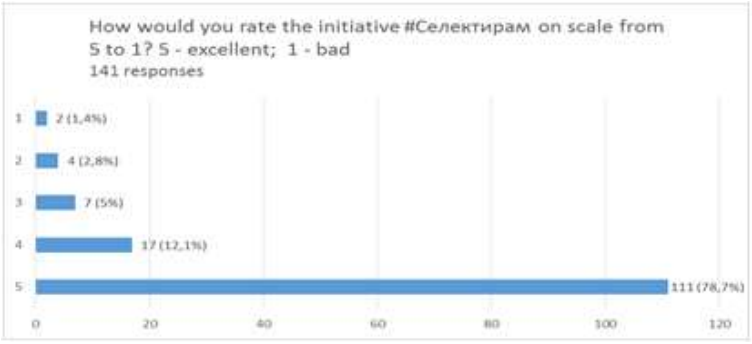

Figure 3 Graphic representation of the questions and answers - Chart 1

When asked about the motivation for selection, 92.2% answered that "They want to contribute to the community" and more than half of them (53.2%) answered that they want to be a good example for their children. 38.3% choose because they want to feel good about themselves. One third (31%) answered that the motivation to select is to help vulnerable groups.

Figure 4 Graphic representation of the questions and answers - Chart 2

78.7% answered that this initiative influenced them to be more aware of their waste habits. Only 11.3% said "No", and the remaining 10% answered that they were already aware.

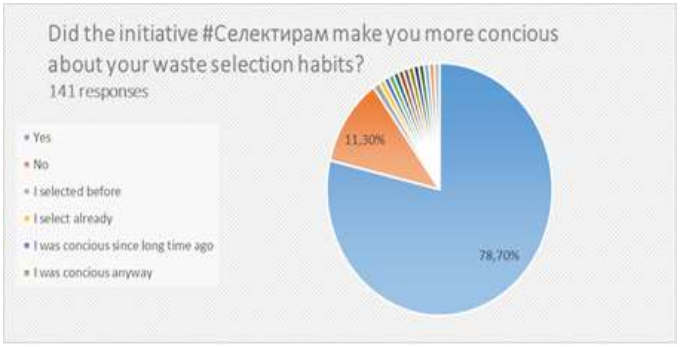

Figure 5 Graphic representation of the questions and answers - Chart 3

When asked about inviting other people to join the #Select initiative, 95% answered "Yes", that is, they would invite other people, and only 3.5% answered "No".

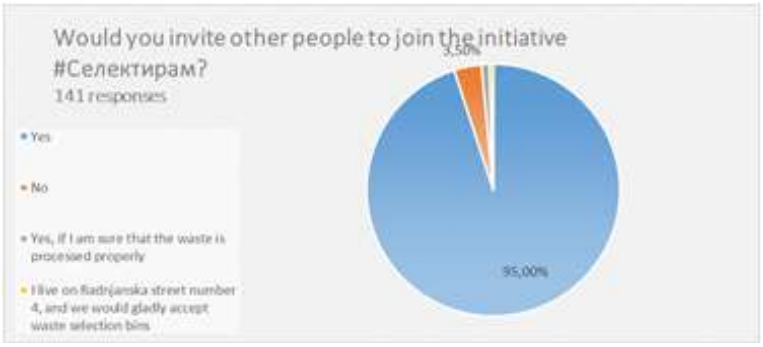

Figure 6 Graphic representation of the questions and answers - Chart 4

The last question clearly indicates the desire of the citizens to select and the need to expand this network. The analysis of citizens' opinion shows that by strengthening awareness and education, citizens can get used to selecting. In order for the selection process to take place, it is necessary to establish an appropriate infrastructure and for each concerned party to responsibly complete its part of the "contract". On the other hand, the organizer stated that although he is facing many challenges during the realization of the project, and it is not yet economically sustainable, he will continue with this initiative and will persistently search for appropriate ways to improve the service and employ collectors who will have a decent salary work.

Figure 7 Green growth

CONCLUSION

The image that we see from our environment is actually a final call for setting up a functional system for waste management. From the research we saw that less than 2% of the waste is sorted in our country, this means that the rest of the waste goes to the landfills and thus ends up in the soil, water and air and pollutes the environment. Pollution of the environment leads to many other unwanted processes, such as poisoning of animals, damage to human health, spread of diseases, etc. That circle, which brings many negative consequences, can only be prevented if the issue of waste management is one of the priority challenges that will be dealt with by the central, local authorities

and citizens. That is why we position sustainability in the creation of an infrastructural system, which needs to be put into operation as soon as possible by the authorities. But in the meantime, bearing in mind that research shows that citizens want to select and would continue to select in the future, the question remains how to implement it. Currently, the collection system depends on informal collectors and the cost of waste. That is, the background for waste treatment starts from economic benefit and existential reasons, if it is profitable, companies and informal collectors will pick it up and treat it. That leaves several potential ways to proceed with selection in order to create a sustainable model that does not depend on short-term opportunities and the selling price of waste. In order to practice primary selection, it is necessary to adopt a legal rule that citizens must select the waste.

REFERENCES

1. Kinnaman, T. C. (2009) The economics of municipal solid waste management. Waste Management 29, 2615-2617.
2. Final report of the performance audit "Efficient treatment and management of plastic waste" State Audit Office, January 2021, Skopje.
3. Koscicovski, Lj. (2017) The report of the survey of public opinion on waste sorting in households, with a special focus on waste cooking oil, http://gogreen.mk/images/pdf/selektiranje_otpad-ggskopje_izvestaj.pdf.
4. Environmental Law, Sl. Journal no. 53/2005.
5. The Law on Waste Management ("Official Gazette of the Republic of Moldova" No. 68/04, 71/04, 107/07, 102/08, 134/08, 09/11, 123/12, 147/13, 163/13, 51/15, 146/15, 156/15, 192/15, 29/16 and 63/16 and "Official Gazette of the Republic of North Macedonia" No. 31/20).

XV International Mineral Processing and Recycling Conference
May 17-19, 2023, Belgrade, Serbia

INVESTIGATION OF SLAGGING CHARACTERISTICS OF INDUSTRIAL SOLID WASTES

A. Vasileiadou[1,2#], S. Zoras[1], A. Dimoudi[1]
[1] Department of Environmental Engineering, Faculty of Engineering, Democritus University of Thrace, Xanthi, Greece
[2] Department of Mineral Resources Engineering, University of Western Macedonia, Kozani, Greece

ABSTRACT – In order to investigate slagging characteristics of olive mill solid wastes, two samples were used as fuels (EOP: Extracted olive pomace, OLS: Olive stone). The experiments of the ash characterization of samples were carried out by a scanning electron microscope equipped with an energy dispersive spectrometer. Moreover, several ash indices that were introduced by the authors of this study and other indices that exist in literature were used. The results demonstrated that ash samples rise to type C ("calcium angle" type) (high melting point temperature, and low deposits) and total quality ash index is a new useful tool for ash characterization.

Keywords: Ash, Characterization, Olive oil mill solid wastes, Slagging, Ternary diagram.

INTRODUCTION

Every year, quite large amounts of ash are produced from the burning of fossil fuels. Biomass fuels exhibit the advantage of producing much smaller amounts of ash compared to fossil fuels. In order to characterize the ash that is produced by the fuel's combustion, it is important to know not only the amount of the ash, but also the chemical composition of the ash, as some biomass fuels, when burned, produce super-alkaline ash (pH>12), reactive with high concentrations of metals and nutrients which are dangerous for the environment if disposed of for landfill or land reclamation, without any special treatment before disposal (e.g. pollution/leaching of metals with adverse effects on soil microorganisms, transport of metals from soil to plants, water, etc.)[1, 2]. Some biomass fuels, and their ashes, containing high concentrations of heavy metals that can cause serious global environmental concerns regarding water, air and soil contamination when biomass combustion is applied in large-scale installations. More specifically, ash that belong to the type 'K' and type 'CK' category can contaminate waters, soils, flora and fauna in ash disposal sites [3].

In the last decade (2010–2019), olive production in Greece was approximately 23,264,758 metric tons [4]. Olive oil production has an important role in the industry of the Mediterranean countries. Greece, in 2019, was the fifth country in olive cultivation areas (925,232 hectares) with an increase of +2.5% in the last 5 years [5], fourth in olive production (1,525,543 metric tons) and third in olive oil production after Spain and Italy

corresponding author: avasileia@env.duth.gr

[5]. Olive oil production is associated with huge amounts of mill waste[6]. The amount of waste produced depends on the technology used (2-phase, 3-phase), the cultivation conditions and the variety [7]. In Greece, in 2002, there were over 2,900 olive mills, with 80% of them using the three-phase process [8]. The three-phase process of 1,000 kg of olives with 500 kg of water produces 600 kg of pomace oil, 750 kg of wastewater and 180 kg of olive oil, while the 2-phase process of 1000 kg of olives produces 820 kg of pomace and 180 kg of olive oil [7]. In the Mediterranean, Greece, Italy and Spain are the main producers, with approximately 2 million tons of olive oil per year, i.e. 30 million m^3 of olive mill wastewater and 20 million tons of olive pomace [9].

In Greece there is no sustainable strategy for the recovery/treatment of olive mill waste. The use of these wastes as a fuel (Waste-to-Energy practice) can contribute to reduce wastes, produce energy from wastes and reduce environmental problems related to the uncontrol deposits as wastes (such as toxicity to aquatic life, toxicity to plants, groundwater pollution and soil pollution).

In this work, two solid wastes produced from olive oil industry were examined via analytical method (Scanning electron microscope and energy dispersive spectroscopy), and empirical slagging index (total Ash Quality Index, and ash Ternary plot of oxide elements in groups) in order to predict slagging tendency in combustion facilities.

EXPERIMENTAL

Two different samples were collected from olive oil mill industry located in Central Macedonia, in Greece: Extracted olive pomace - EOP, and Olive stone – OLS. The samples were air dried and dried in an oven at 80 ^oC for 24 hours. A cutting mill were used in order to ground samples to a size lower than 1 mm. Scanning electron microscope and energy dispersive spectroscopy (SEM-EDS INCA 300 were used in order to determine ash composition of the samples. For SEM observations the samples were coated with carbon (200 Å) using a vacuum evaporator (JEOL-4X). The samples were examined at least twice.

Several slagging and fouling indices, SiO_2 index, Cl index, B/A index, BAI index, Rs index, Fu index, and Sr index) as described in previous study of the authors [10], and ternary diagram, were used in this study in order to characterize the analyzed ashes resulting from combustion of olive mill solid wastes as fuels. A novel total Ash Quality Index (tAQI) was developed in previous study of authors by taking into account the Gross Calorific Value (GJ/kg), the ash content (in wt%, from the results of proximate analysis) of the samples, and the ash indices that are used in the literature (B/A, BAI, Fu etc.) [10].

RESULTS AND DISCUSSION

Figure 1 presents the results of chemical ash composition of olive oil mill solid wastes OLS and EOP in form of oxides. Silicon (Si), and Calcium (Ca) are the major ash forming elements occurring in the analyzed industry solid wastes. The results are in agreement with other studies [11, 12]. The calcareous minerals of biomass fuels contribute to the high content of calcium oxides in the ash. EOP sample revealed approximate 60 wt.% CaO whilst OLS sample revealed about 56 wt.%. These percentages are much higher than ligneous biomass. High content of calcium oxides leads to alkaline ash leading to self-desulfurization in CFB plants [13]. In addition to the qualitative analysis of the ash, it is

important to take into account the amount of ash produced by combustion of these waste as fuels. The percentage of ash produced by the combustion of these samples was examined in a previous study by the authors [14] and found to be in low levels (EOP: ash=6.4 wt.% and OLS: ash=4.6 wt.%).

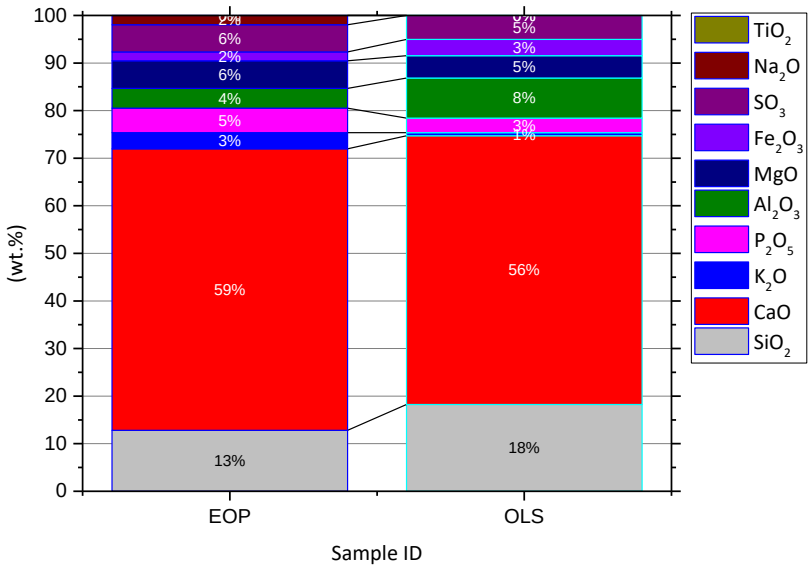

Figure 1 Chemical ash composition of the analyzed samples, in the form of oxides

SEM-EDS electron microscopy images of the analyzed ashes of industrial solid wastes is illustrated in Figure 2.

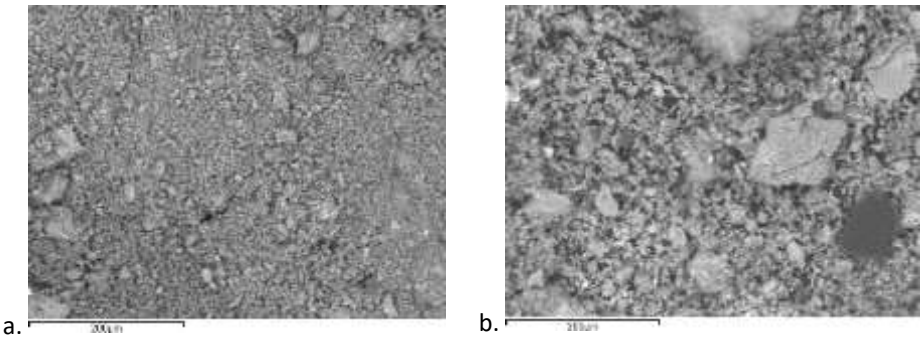

Figure 2 Results SEM spectrums: **a.** EOP, and **b.** OLS sample

Figure 3 presents the Ternary (triangular) diagram with peaks the oxides $SiO_2+Al_2O_3+Fe_2O_3+Na_2O+TiO_2$, $CaO+MgO+MnO$ and $K_2O+P_2O_5+SO_3$ of the chemical analysis of the analyzed ashes of all categories. The Ternary diagram categorizes the ash samples according to their acidity into high, medium and low, which affects the corrosion phenomena and the melting point of the ash. The analyzed ash samples (EOP, OLS)

showed low acidity. According to the diagram, four types of ash are distinguished (Type C, Type S, Type K, and Type CK), depending on the point at which the examined ash is located. Type S ("silicon angle" type) and K ("potassium" type) present high risks of deposits due to the formation of silicates and the presence of potassium. Type C ("calcium angle" type) is expected to have a high melting temperature, so low deposits due to high Ca concentrations [15]. Moreover, according to the melting temperature of biomass ash, ash can be divided into three categories [16]: DT (deformation temperature) <1100 °C, DT between 1100 and 1300 °C, and DT > 1300 °C. The analyzed ash samples (EOP, OLS) occurred in the C ash type region. In this region belong the Greek lignite sample, as resulted from previous study of authors [10]. Type CK is an intermediate type of ash between type C and type K and has a medium tendency to slag [17].

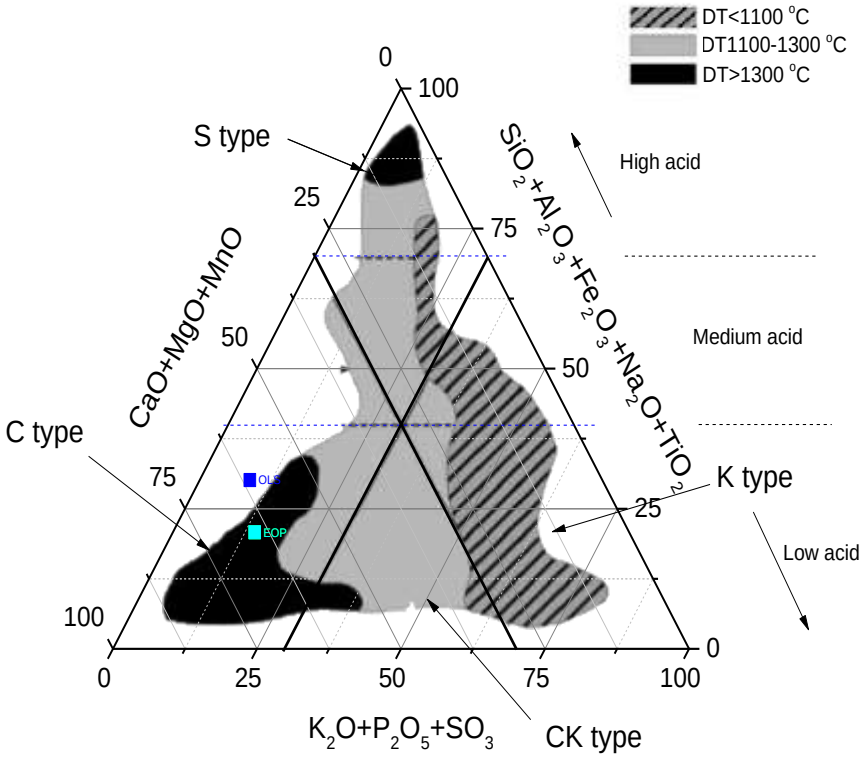

Figure 3 Chemical ash composition, in the form of oxides, of oil mill solid wastes (EOP, OLS) and Lignite sample (LIGA) as reference sample

The modified slagging and fouling indices (Cl, SiO_2, B/A, BAI, Rs, Fu and Sr index) and the total Ash Quality Index (tAQI) for the analyzed samples are presented in Table 1, and Figure 4, respectively. The tAQI was developed based on the modification available from the literature ash indices, by a novel concept, by taking into account not only the chemical ash composition but also combustion characteristics as Gross Calorific Value and ash content of the samples.

Table 1 Results of the modified slagging/fouling indices of the samples (H: High, M: Medium, L: Low tendency) [10]

Sample ID	Cl^-	Cl	SiO_2	SiO_2	B/A	B/A	BAI	BAI	Rs	Rs	Fu	Fu	Sr	Sr
EOP	0.007	L	0.41	L	14.77	H	1.13	H	0.07	M	0.78	M	0.52	H
OLS	0.003	L	0.37	L	5.3	M	11.15		0.03	L	0.03	L	0.46	H

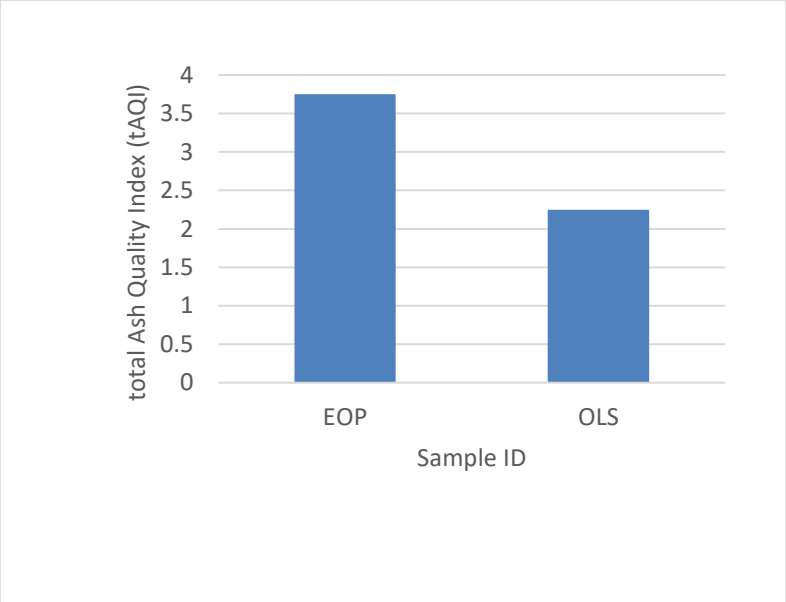

Figure 4 The total Ash Quality Index (tAQI) of the analyzed samples

CONCLUSION

In this work two solid wastes of an olive oil mill industry were studied in order to determine slagging tendency of the ashes in a combustion facility. The total Ash Quality Index can summarize in a very brief way several fuel quality characteristics (ash quality, ash quantity, gross calorific value, ash slagging and fouling indices etc.) thus, it could be a useful tool for ash characterization.

ACKNOWLEDGEMENT

This research is co-financed by Greece and the European Union (European Social Fund- ESF) through the Operational Programme «Human Resources Development, Education and Lifelong Learning» in the context of the project "Strengthening Human Resources Research Potential via Doctorate Research – 2nd Cycle" (MIS-5000432), implemented by the State Scholarships Foundation (IKY).

REFERENCES

1. Ondrasek G., Bubalo Kovačić M., Carević I., Štirmer N., Stipičević S., Udiković-Kolić N., et al. (2021) Bioashes and their potential for reuse to sustain ecosystem services and

underpin circular economy, Renewable and Sustainable Energy Reviews, 151, 111540.
2. Ondrasek G., Kranjčec F., Filipović L., Filipović V., Bubalo Kovačić M., Badovinac I.J., et al. (2021) Biomass bottom ash & dolomite similarly ameliorate an acidic low-nutrient soil, improve phytonutrition and growth, but increase Cd accumulation in radish, Science of The Total Environment, 753, 141902.
3. Vassilev S.V., Baxter D., Andersen L.K., Vassileva C.G. (2013) An overview of the composition and application of biomass ash.: Part 2. Potential utilisation, technological and ecological advantages and challenges. Fuel, 105, 19-39.
4. NationMaster-FAO (2020) Greece - Olives Production. www.nationmaster.com.
5. NationMaster-FAO (2020) Greece - Olive Oil Production. www.nationmaster.com.
6. Tsarouhas P., Achillas C., Aidonis D., Folinas D., Maslis V. (2015) Life Cycle Assessment of olive oil production in Greece. Journal of Cleaner Production, 93, 75-83.
7. Christoforou E., Fokaides P.A. (2016) A review of olive mill solid wastes to energy utilization techniques, Waste Management, 49, 46-63.
8. IMPEL. Impel olive oil project (2003) 2003/3: European Union Network for the Implementation and Enforcement of Environmental Law.
9. Khdair A., Abu-Rumman G. (2020) Sustainable Environmental Management and Valorization Options for Olive Mill Byproducts in the Middle East and North Africa (MENA) Region, Processes, 8, 671.
10. Vasileiadou A., Papadopoulou L., Zoras S., Iordanidis A. (2022) Development of a total Ash Quality Index and an Ash Quality Label: Comparative analysis of slagging/fouling potential of solid biofuels, Environmental Science and Pollution Research, 29, 42647-63.
11. Klisović D., Novoselić A., Režek Jambrak A., Brkić Bubola K. (2021) The utilisation solutions of olive mill by-products in the terms of sustainable olive oil production: a review, International Journal of Food Science & Technology, 56, 4851-60.
12. Alonso-Fariñas B., Oliva A., Rodríguez-Galán M., Esposito G., García-Martín J.F., Rodríguez-Gutiérrez G., et al. (2020) Environmental Assessment of Olive Mill Solid Waste Valorization via Anaerobic Digestion Versus Olive Pomace Oil Extraction, Processes, 8.
13. Li L., Yu C., Bai J., Wang Q., Luo Z. (2012) Heavy metal characterization of circulating fluidized bed derived biomass ash. Journal of Hazardous Materials, 233-234, 41-7.
14. Vasileiadou A., Zoras S., Iordanidis A. (2021) Bioenergy production from olive oil mill solid wastes and their blends with lignite: thermal characterization, kinetics, thermodynamic analysis, and several scenarios for sustainable practices. Biomass Conversion and Biorefinery.
15. García R., Pizarro C., Álvarez A., Lavín A.G., Bueno J.L. (2015) Study of biomass combustion wastes, Fuel, 148, 152-9.
16. Chen C.Y., Chen W.H., Hung C.H. (2021) Combustion performance and emissions from torrefied and water washed biomass using a kg-scale burner. Journal of Hazardous Materials, 402.
17. Wang Y., Tan H., Wang X., Du W., Mikulčić H., Duić N. (2017) Study on extracting available salt from straw/woody biomass ashes and predicting its slagging/fouling tendency. Journal of Cleaner Production, 155, 164-71.

XV International Mineral Processing and Recycling Conference
May 17-19, 2023, Belgrade, Serbia

MODELLING OF CO_x AND NO_x EMISSIONS FROM INDUSTRIAL SOLID WASTES COMBUSTION USING ANSYS CHEMKIN PRO

A. Vasileiadou[1,2#], S. Zoras[1], A. Dimoudi[1]
[1] Department of Environmental Engineering, Faculty of Engineering, Democritus University of Thrace, Xanthi, Greece
[2] Department of Mineral Resources Engineering, University of Western Macedonia, Kozani, Greece

ABSTRACT – In order to investigate emissions of the combustion of olive mill solid wastes as fuels (EOP: Extracted olive pomace, OLS: Olive stone) the ANSYS Chemkin PRO modelling software was used along with several analytical experimental results of the samples: energy content determination, ultimate analysis, and proximate analysis. The maximum potential emission factors were calculated using ultimate analysis. The results of modelling showed that all the maximum potential CO_2 emissions are emitted, whilst only a small portion of maximum NO emissions are emitted. The emissions expressed per produced energy were found to be more objective than emissions expressed per fuels kilogram.

Keywords: Ash, Characterization, Olive mill solid wastes, Slagging, Ternary diagram.

INTRODUCTION

In addition to laboratory and pilot tests, modelling allows for optimal techno-economic design of processes. There are different types of modelling tools from simple heat and mass balance models to advanced user level and time-consuming computational fluid dynamics (CFD) tools. In addition to CFD models, there are other modelling tools that are coupled with experimental results, such as heat and mass balance models, chemical balance models, chemical kinetics of combustion (using ideal chemical reactors) and thermodynamic models, as well as simplified CFD-type models [1].

Today's energy standards require high efficiencies and high quality with minimal combustion by-products and waste. Therefore, in recent years software programs have been developed to model the chemical process of combustion successfully predicting the combustion products [2-4]. ANSYS Chemkin Pro software is the industry leader in modelling complex chemical reaction systems, has been validated in many chemistry applications, and is widely known for its fast simulation time [5]. The ANSYS Chemkin Pro software is an evaluation product from the Chemkin II combustion kinetic code developed at the Scandia National Laboratories of the Reaction Design Company (US Company) [4]. This software allows for the simulation of complex chemical reactions for modelling in order to approach cleaner technology in the design and improvement of burners, engines, etc. [6]. Various modelling studies have been performed using ANSYS

corresponding author: avasileia@env.duth.gr

Chemkin Pro chemical combustion process modelling software [7-10].

In this work, ANSYS Chemkin software was used in order to simulate CO_x and NO emissions of the combustion of olive mill solid wastes as fuels.

EXPERIMENTAL

Two samples (extracted olive pomace, EOP, and olive stone, OLS) were collected from olive mill industry located in Katerini, in Greece. Firstly, the samples were air dried and then dried in an oven (80 ^oC for 24 hours). A cutting mill were used for grounding the samples (size: lower than 1 mm). The Gross Calorific Value of the samples was performed using an isoperibol bomb calorimeter Leco AC 500 according [11]. Ash content was determined using the Leco TGA 701 machine, according [12]. Sulfur and Nitrogen content of the samples were determined using an elemental analyzer ThermoFinnigan 1112 CHNS as described in [13]. CO_2 and NO emission factors (maximum potential emissions) were calculate using the results of ultimate analysis as described in [13]. Scanning electron microscope - energy dispersive spectroscopy (SEM-EDS JEOL JSM – 6390VL, INCA 300) was performed in order to determine ash composition of the samples. For SEM observations the samples were coated with carbon (200 Å) using a vacuum evaporator JEOL-4X as described in [14]. The samples were examined at least twice.

In this study, ANSYS Chemkin Pro software was used to perform several calculations of the combustion process. After several different tests, the optimal modelling parameters (optimal combustion temperature: 750 ^oC, excess air λ: 1.1, residence time: 4 sec, etc.) were selected. Firstly, the combustion simulation circuit was designed. For the combustion simulation, the 'Perfectly Stirred Reactor' reactor model, from the Open 0-D reactors category, was chosen, which is mainly used for the modelling of complex problems of the combustion process [4, 9]. Then, the gas phase kinetic file *'Grimech30_chem.inp'* and the thermodynamics data file *'Grimech30_thermo.dat'* were chosen and were uses as input to the software. The air flow rate, the chemical composition of the fuels (EOP and OLS), and the mass flow rate of the air and the fuel and the temperature were determined. This chemical model consists of 325 chemical reactions, 5 elements (O, H, C, N, and AR) και 53 species. The calculations were carried out with a pressure (initial gas pressure) of 1 atm and problem type 'Fix Gas Temperature', 'Steady State solver' [6]. Steady State solver methods for homogeneous 0-D systems use the TWOPNT numerical solver to determine a solution to the set of algebraic equations governing these reactant models. The numerical solver TWOPNT solves the system of algebraic equations by applying a modified Damped Newton's Method for 0-D Reactors damping algorithm to the set of nonlinear algebraic equations represented by the steady state equations [15].

The mass of air (m_a, in g) was calculated separately for each sample (and mixture), having first calculated the mass of oxygen (m_o, in g) taking into account the coefficient (coef.) of O_2 reacting with the different fuel and for a fuel mass (m_f) of 1000 g. The composition of dry air, mole fraction, which was used for the combustion modelling is N_2=0.7809, O_2=0.2094, Ar=0.0093 CO_2=0.0004. An inlet temperature of 25 ^oC was used. The emissions of carbon oxides and nitrogen oxides were studied with the ANSYS Chemkin software.

RESULTS AND DISCUSSION

Table 1 presents the energy content, the ash content and the results of ultimate analysis of the samples that were used in this study in order to model CO_2 and NO emissions of the samples using ANSYS Chemkin Pro software.

Table 1 Energy content, ash content and ultimate analysis of the samples. Oxygen was calculated by difference (O=100-C-H-N-S-ash). Lignite sample was used as a reference sample [13]

Sample ID	GCV (MJ/kg)	Ash (%)	C (%)	H (%)	N (%)	S (%)	O (%)
EOP	19.6	6.4	48.7	5.8	1.4	0.5	37.2
OLS	22.3	4.6	55.3	7.1	1.0	0.5	31.5
LIGA	12.7	38.9	35.6	3.7	0.9	1.0	19.9

The results of the modelling of the CO_2 and NO_2 emissions per kg fuel of the EOP, OLS and lignite sample are presented in Figure 1 and Figure 2. From the results it was found that OLS revealed the highest CO_2 emissions per kg fuel, followed by EOP whist lignite sample showed the lowest CO_2 emissions. However, expressing these emissions per produced energy (see Figure 2), the exact opposite result was obtained (due to the high calorific value of these fuels) with the olive mill samples showing the lowest emissions (about 91 gCO_2/MJ) and the lignite sample showing the highest emissions (about 103 gCO_2/MJ).

Regarding the NO emissions per kg of fuel, the EOP sample showed the highest emissions, slightly lower than the OLS sample and the lignite sample showed the lowest. If the NO emissions are expressed per produced energy, the evaluation order of the samples changes as the lignite sample showing the highest emissions (>0.14 gNO/MJ) and the OLS sample the lowest (<0.11 gNO/MJ), and the EOP sample showed approx. 0.12 gNO/MJ.

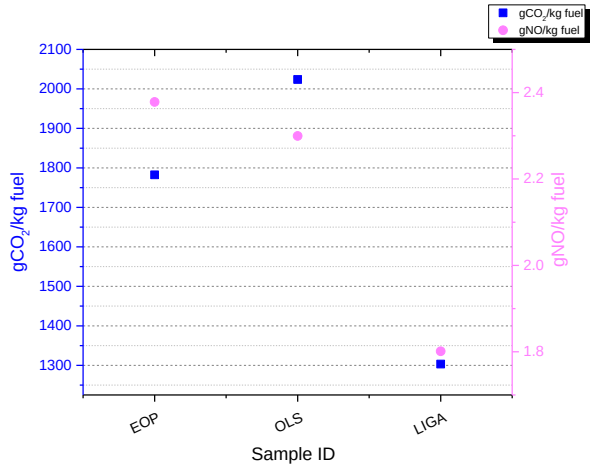

Figure 1 Modelling results of CO_2 emissions per kilograms (gCO_2/kg fuel) and NO emissions per kilograms (gNO/kg fuel) of EOP, OLS and lignite sample

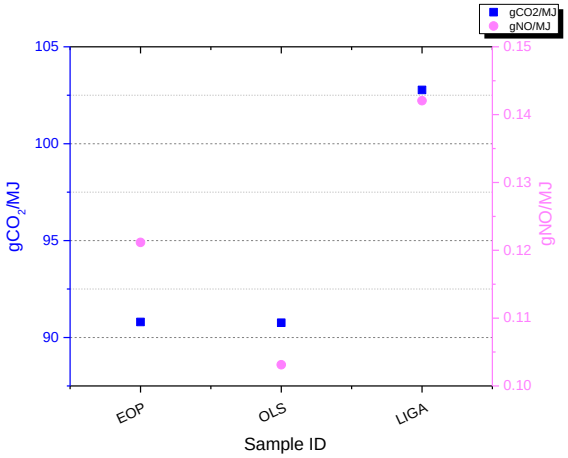

Figure 2 Modelling results of CO_2 emissions per produced Megajoule (gCO_2/MJ) and NO emissions per produced Megajoule (gNO/MJ) of EOP, OLS and lignite sample

The percentage of CO in relation to C-containing species and the percentage of NO and NO_2 in relation to N-containing species are presented in Figure 3 and 4, respectively.

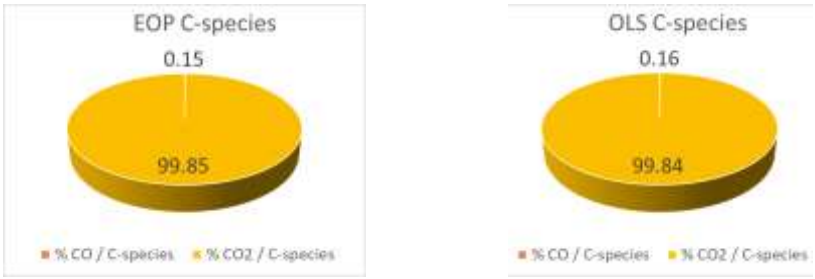

Figure 3 Percentage occupied by CO, and CO_2 emissions in relation to C-containing species

Figure 4 Percentage occupied by NO, and NO_2 emissions in relation to N-containing species

Percentage of CO_2 emissions, and NO emissions as a function of maximum theoretical emissions are illustrated in Figure 4. The CO_2 emissions of the samples consist of 99.9%

of the corresponding maximum theoretical emissions. The NO emissions of the combustion of EOP, OLS, and LIGA consist about 7.5%, 10% and 9% of the theoretical maximum emissions, respectively.

The results are in accordance with the annual report of Agios Dimitrios Power Plant of the year 2018 [16].

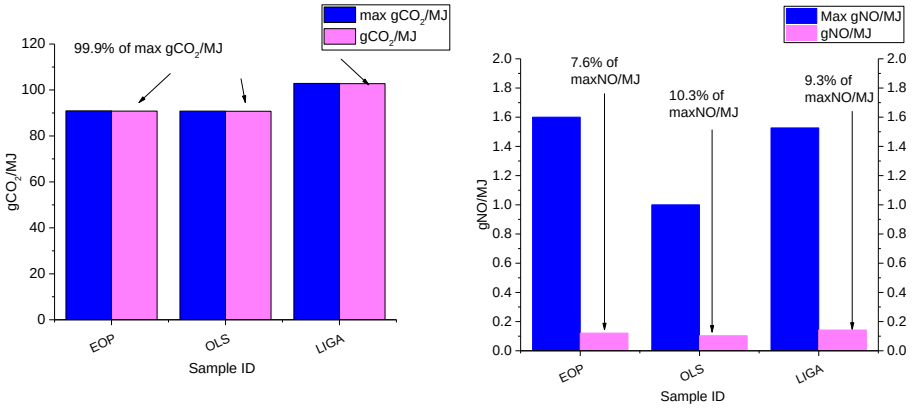

Figure 4 Percentage occupied by CO_2 emissions, and NO emissions as a function of maximum theoretical emissions

CONCLUSION

This paper presents the modelling of the combustion of two olive mill solid wastes using ANSYS Chemkin Pro software in order to stimulate CO_x and NO_x emissions produced from biomass combustion. Several properties were determined in order to be used in the modelling. The results showed that 99.9% of maximum CO_2 emissions are emitted whilst lower than 11% of the maximum NO emission are emitted. Moreover, the results showed that the emissions produced from a fuel combustion could be assessed more correctly, if they are expressed per produced energy (and not per kilogram of fuel), as each fuel has different calorific value (energy per kilogram of fuel).

ACKNOWLEDGEMENT

This research is co-financed by Greece and the European Union (European Social Fund- ESF) through the Operational Programme «Human Resources Development, Education and Lifelong Learning» in the context of the project "Strengthening Human Resources Research Potential via Doctorate Research – 2nd Cycle" (MIS-5000432), implemented by the State Scholarships Foundation (IKY).

REFERENCES

1. Loo Sv., Koppejan J. (2008) The Handbook of Biomass Combustion and Co-Firing, UK: Earthscan.
2. Roberts G.W. (2009) Chemical reactions and chemical reactors. Hoboken, NJ: John Wiley & Sons.

3. Paraschiv L.S., Serban A., Paraschiv S. (2020) Calculation of combustion air required for burning solid fuels (coal / biomass / solid waste) and analysis of flue gas composition, Energy Reports,6, 36-45.
4. Sieradzka M., Rajca P., Zajemska M., Mlonka-Mędrala A., Magdziarz A. (2020) Prediction of gaseous products from refuse derived fuel pyrolysis using chemical modelling software - Ansys Chemkin-Pro. Journal of Cleaner Production, 248, 119277.
5. ANSYS (2021) Ansys Chemkin-Pro, Chemistry Simulation Software. https://www.ansys.com/products/fluids/ansys-chemkin-pro: ansys.
6. Magdziarz A., Wilk M., Zajemska M. (2011) Modelling of pollutants concentrations from the biomass combustion process. Chemical and Process Engineering, 423-33.
7. Zhukov V.P. (2012) Verification, Validation, and Testing of Kinetic Mechanisms of Hydrogen Combustion in Fluid-Dynamic Computations. ISRN Mechanical Engineering, 475607.
8. Yan L., He B., Ma L., Pei X., Wang C., Li M., et al. (2013) Numerical study with ChemKin for hydrogasification mechanism of pulverized coal and Hg speciation transformation inside a hydrogasifier. Strojarstvo, 55, 73-85.
9. Zajemska M., Urbańczyk P., Poskart A., Urbaniak D., Radomiak H., Musiał D., et al. (2017) The impact of co-firing sunflower husk pellets with coal in a boiler on the chemical composition of flue gas. E3S Web Conf., 14, 02021.
10. Liu C., Zhao H., Yang W.Y., Qiu K.Z., Yang J.G., Geng Z.W., et al. (2018) Chemical kinetics simulation of semi-dry dechlorination in coal-fired flue gas. Journal of Zhejiang University-SCIENCE A., 19, 148-57.
11. ASTM International (2013) ASTM D5865 - 13 Standard Test Method for Gross Calorific Value of Coal and Coke. West Conshohocken, PA: ASTM International.
12. ASTM International (2015) ASTM D 7582-15 Standard Test Methods for Proximate Analysis of Coal and Coke by Macro Thermogravimetric Analysis, West Conshohocken. PA: ASTM International.
13. Vasileiadou A., Zoras S. (2021) Iordanidis A. Bioenergy production from olive oil mill solid wastes and their blends with lignite: thermal characterization, kinetics, thermodynamic analysis, and several scenarios for sustainable practices. Biomass Conversion and Biorefinery.
14. Vasileiadou A., Papadopoulou L., Zoras S., Iordanidis A. (2022) Development of a total Ash Quality Index and an Ash Quality Label: Comparative analysis of slagging/fouling potential of solid biofuels. Environmental Science and Pollution Research., 29, 42647-63.
15. ReactionDesign A. (2016) Chemkin Theory Manual 17.0, 1-412.
16. PPC (2018) Annual report of Agios Dimitrios, power plant - year 2018 Monitoring environmental operation parameters.

XV International Mineral Processing and Recycling Conference
17-19 May 2023, Belgrade, Serbia

THE USAGE AND EFFECT OF BASALT CUTTING WASTE (BCW) IN CERAMIC GLAZE COMPOSITIONS CONTANING OPAQUE AND MATT FRIT

Z. Bayer Öztürk[1], S. Kurama[2#], A. Eser[1]
[1] Hacı Bektas Veli University, Department of Metallurgy & Materials Engineering, Nevsehir, Turkey
[2] Eskisehir Teknik University, Department of Materials Science & Engineering, Eskisehir, Turkey

ABSTRACT – Basalt, a natural volcanic rock with high compressive strength and wear resistance, but during its processing leave as industrial waste. In this study evaluate the color effect of BCW obtained from a stone company in Kayseri/Turkey for the production of matt and opaque frits. Therefore, glaze mixtures were prepared with different frits and BCW at proportions of 0–20 wt.%. The glazes were applied to the engobed wall tiles and fired at 1200 °C. Increasing the proportion of stone dust in the glaze formulation resulted in the color tone change of the final surfaces from cream to yellow and brown tones.

Keywords: Basalt Stone, Glaze, Pigment, Color, Characterization.

INTRODUCTION

Industrial developments that improve people's health and living conditions also bring negative effects such as environmental pollution. The production sector of ceramic materials, which is one of the most important materials of daily living spaces, is an industry area that generally results in high amounts of waste with no recovery process after the process. With the increasing technological developments in the production of ceramic products, the need for clean raw materials is also increasing. However, supplying clean raw materials also brings air and environmental pollution depending on the energy used. In recent years, many processes, including the wars and the pandemic period, have caused difficulties in the supply of raw materials, and this has been reflected in the prices economically.

Today, suitable and economical raw material deposits limit traditional ceramic production and cause a continuous increase in production costs. For this purpose, studies on the use of waste materials have increased in recent years. To this end cullet [1-3], different industrial wastes [4,5], and also some outcrops with an acidic component such as volcanic ash and zeolite [6-8] are used. This type of igneous rocks is suitable for the ceramic industry and forms alkaline basaltic structures. Basalt is one of the most common raw materials for industrial applications and is preferred because of its durability and stain resistance. However, in the process of shaping the product of this material, which is a natural stone, waste dust, and fragments are generated. These waste powders are stored by business owners in an area that is not operational [9]. It is seen that there are

corresponding author: skurama@eskisehir.edu.tr

different studies in the literature regarding the use of basalt in the ceramic industry. Basalt, which has a fine-grained structure in different colors from gray to black, is in the group of volcanic rocks. It has a very large area (2.5 million square meters) on the earth and is a cheap and easily available raw material. It contains SiO_2 and Al_2O_3 as major oxides with about 40-55 wt.% and 10-20 wt.% SiO_2, Al_2O_3, Fe_2O_3, CaO, MgO and there are other oxides such as K_2O and TiO_2. Due to the silica content, it is primarily preferred in the production of glass ceramic materials. Basalt-based glass-ceramics exhibit good to wear, abrasion, and chemical resistance. Moreover, this material is also known to have good resistance to heat, sound, and fire insulation [10-12].

Regardless of the areas in which ceramic materials are used (whether for coating, sanitary ware, or decorative purposes), glazing is required for contributions to surface, cleaning, and visual appearance. While the glazes applied on the tile surface have some requirements according to the usage area, as much as their visual properties. Coloring of glazes, features such as glossy/matte, and surface smoothness are provided by the harmony of the colorants and additives used together with the glaze raw materials. In recent years, the use of waste materials in glaze development has attracted great attention in terms of both reducing the current cost and reducing environmental pollution. When the studies in the literature in this area are examined, it is seen that the waste materials are used in different areas as a pigment source, glaze, and additive to the body. In the field of glaze and visuality application, studies on the use of marble waste [13], borax solid waste [14], vitrified waste [15], fly ash [16], and zinc ore waste [17] are available in the literature.

In the study, the possibility of using BCW powder in ceramic tiles for glaze improvements, such as color, surface, and ripening temperature was investigated. For this aim, the basalt-cutting waste powder was added in two types of glaze compositions, and their sintering behavior and physical properties of the final product were investigated.

EXPERIMENTAL

The basalt cutting waste was taken from Emre Tas Mining (Kayseri, Turkey). The chemical analysis of BCW powder was given in Table 1. The waste powder has 49.47 wt% SiO_2, 17.24 wt% Al_2O_3, 10.26 wt% Fe_2O_3 and 10.35 wt% CaO. The phase analysis of basalt cutting waste was determined by X-ray diffractometer (XRD, Rigaku Miniflex 600) as Andesine ($Al_{0.735}Ca_{0.24}Na_{0.26}O_4Si_{1.265}$), Albite ($AlK_{0.2}Na_{0.8}O_8Si_3$), Quartz ($SiO_2$) and presented in Figure 1. The thermal behaviour of BCW was investigated by using the termogravimetric/differential thermal analysis (TGA/DTA- STA 409PG LUXX). The BCW and frits were examined through the heat microscopy (MISURA). Chemical compositions range of the different frits (opaque and matt frits) supplied from Gizem Frit are determined in Table 3. Glaze compositions containing BCW (0-5-10-15-20 wt%), dry frit (92 wt%), kaolin (8 wt%), sodium tripolyphosphate (STPP 0.2 g) and 60 cc water were prepared by wet milling using a laboratory ball mill (residue <2% at 63 μm). The glazes at 1500 g/L were applied on 5×5×5 mm the engobed tiles and fired in the laboratory kiln (at 1200 °C for 6h.). Glaze preparation process in the laboratory and waste-based glazed tiles were shown in Figure 2. The codes of glazes were presented in Table 2. Phase analysis of opaque and matt glazes prepared with BCW (0-20 wt.% waste addition) was performed

with an X-ray diffraction (XRD, Rigaku Miniflex 600). The color parameters (L*, a*, b* values) were determined by using a Minolta CM-3600d color measuring device in the color analysis of glazed samples. The development of the phases in the microstructure was determined by examining the glazed samples containing 20 wt.% BCW by scanning electron microscope (SEM, Zeiss EVO 50 EP).

Table 1 Chemical composition (wt.%) of BCW

SiO_2	Al_2O_3	Fe_2O_3	CaO	MgO	Na_2O	TiO_2	K_2O	MnO	P_2O_5	SO_3	Loss of ignition (LOI)
49.47	17.24	10.26	10.35	6.24	3.42	1.33	0.61	0.16	0.22	0.07	0.53

Table 2 Glaze mixture proportions and their codes

Glaze code	Opaque-Matt Frits (wt.%)	Kaolin (wt.%)	BCW (wt.%)
M0	92 Matt	8	0
M5	92 Matt	8	5
M10	92 Matt	8	10
M15	92 Matt	8	15
M20	92 Matt	8	20
O0	92 Opaque	8	0
O5	92 Opaque	8	5
O10	92 Opaque	8	10
O15	92 Opaque	8	15
O20	92 Opaque	8	20

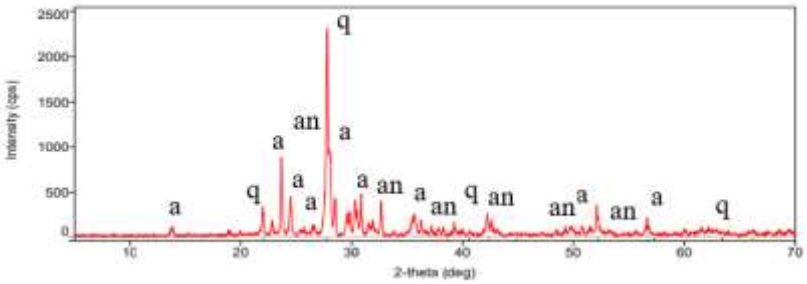

Figure 1 XRD pattern of basalt cutting waste; (**Andesine**: $Al_{0.735}Ca_{0.24}Na_{0.26}O_4Si_{1.26}$; **Anorthite**: $Al_2Ca(SiO_4)_2$; **Quartz:** SiO_2)

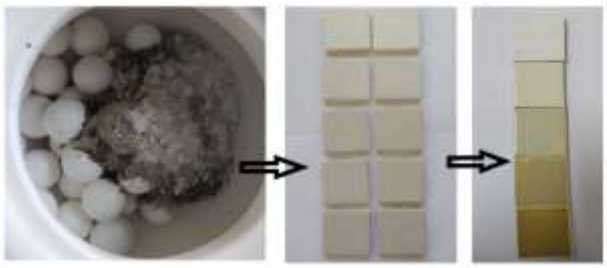

Figure 2 Ceramic glazes based basalt waste preparation process in laboratory

RESULTS AND DISCUSSION

Characterization of basalt cutting waste

The presence of significant endothermic peaks was observed in the DTA/DTG analysis of BCW in Figure 3. A distinct endotermic peaks and corresponding mass changes in the graph are as follows, respectively: 0.097 µV/mg mass loss occurred at 670.9 °C, 0.247 µV/mg mass loss at 953 °C, 0.311 µV/mg mass loss at 1036 °C and 0.413 µV/mg mass loss at 1188 °C, respectively. The phase analyses of the BCW (Fig.1) revealed the presence of large amount of feldspar (albite and andesine) and pyroxene which is probably cause the endotermic peaks [18]. In addition, no crystallization peak was detected in the DTA analysis of the BCW. This shows that BCW retains its structure when exposed to heat. The characteristic temperatures of the BCW analyzed by a heat microscopy were determined between 1166 and 1214 °C in Figure 4. Considering the sample image as 100%, the temperature at which it is subjected to a 5% dimension change accordingly is gives the sintering temperature. The softening point is the point at which the liquid phase appears on the sample surface. At sphere temperature, the sample consists entirely of the liquid phase, and the shape of the sample is controlled by surface tension. The hemisphere temperature is defined as the case where the height of the sample is half the width. The melting point is the point at which the sample drops below one-third of its original height [19-20].

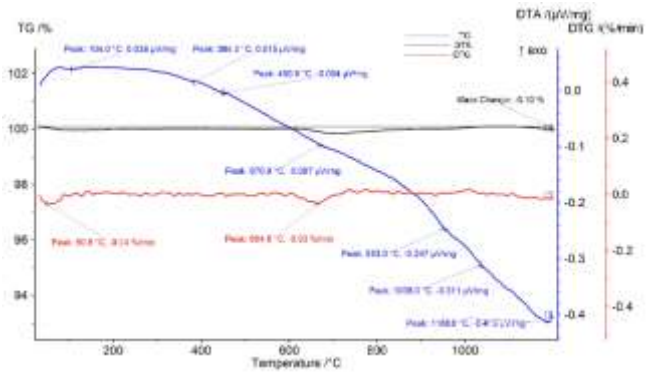

Figure 3 DTA-DTG graph of basalt cutting waste

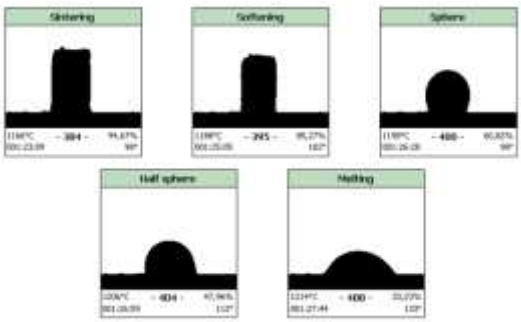

Figure 4 Heat microscopy results of basalt cutting waste

Characterization of the obtained glazes

The chemical compositions of studied frits supplied from Gizem Frit were presented in Table 3. In terms of oxides, opaque frit has higher SiO_2, B_2O_3, K_2O and ZrO_2 levels than matt frit.

Table 3 Glaze mixture proportions and their codes

Firit	SiO_2	Al_2O_3	Fe_2O_3	CaO	MgO	Na_2O	K_2O	ZnO	B_2O_3	TiO_2	ZrO_2
Matt (MT)	47-49	13-15	0.05-0.1	12-14	0.25-1	6-8	0.05-0.5	17-19	0.5-2	0.05	-
Opaque (OP)	54-57	5-7	0.05-0.1	8-10	2-4	1-3	3-5	5-7	9-11	0.05	6.8

The characteristic temperatures were determined between 740 and 1102 °C for matt frit, 840 and 1264 °C for opaque frit in Table 4.

Table 4 Typical points result of frits obtained by hot-stage microscopy (°C)

Sample	$T_{sintering}$	$T_{softening}$	T_{sphere}	$T_{hemisphere}$	$T_{melting}$
Matt (MT)	740	1082	-	1092	1102
Opaque (OP)	840	1012	1076	1202	1264

The obtained glazes based on basalt cutting waste were a light yellow-beige color and the firing colors of glazed tiles fired at 1200 °C was shown in Figure 5. Beige and yellow tones were increased depending on basalt cutting waste from 5 to 20 wt.%. The color parameters of glazed tiles were presented in Table 5. In matte and opaque glazes containing 20 wt.% BCW, L* values were measured as 58.19 and 61.73 at low values compared with the other glazes. It is seen that a* and b* values also increase with the increase of BCW. The most important factor affecting the color parameters (L*-a*-b*) is the iron oxide content (10.26 wt.%) in the BCW.

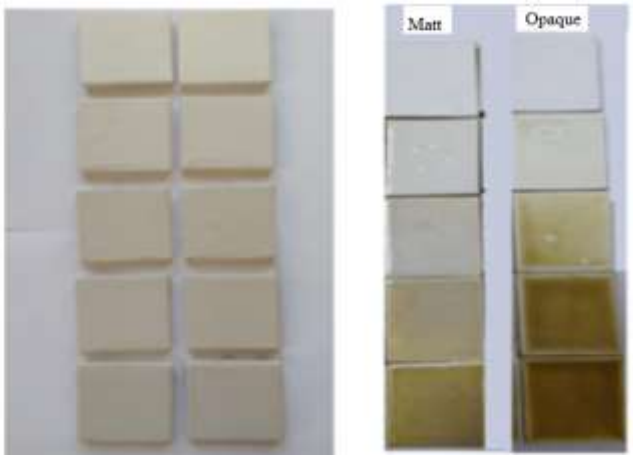

Figure 5 Difference between standard glazes and glazes based basalt cutting waste glazes

Table 5 The color parameters of glazed tiles

Sample	L*	a*	b*
M0	89.73	-0.29	2.82
M5	88.37	-1.62	10.25
M10	80.65	-1.15	22.91
M15	64.20	3.47	34.62
M20	58.19	7.96	36.78
O0	90.17	-0.52	1.69
O5	85.17	-1.22	8.74
O10	76.48	-0.16	12.44
O15	68.43	1.35	16.88
O20	61.73	3.01	25.67

The color change became evident at 20 wt.% of BCW addition. For this reason, XRD and SEM analyses were performed on standard (without BCW) and glazed samples containing 20 wt.% BCW. The phases of glazed samples were seen in Figure 6 and 7. The major crystalline phases were identified as quartz, zircon and anorthite for opaque glazes (O0-O20). The quartz, anorthite, diopside and aluminum silicate were observed in matt glazes (M0-M20). In XRD analysis, it was determined that the addition of BCW to the glazes increased the anorthite and diopsite phase intensities.

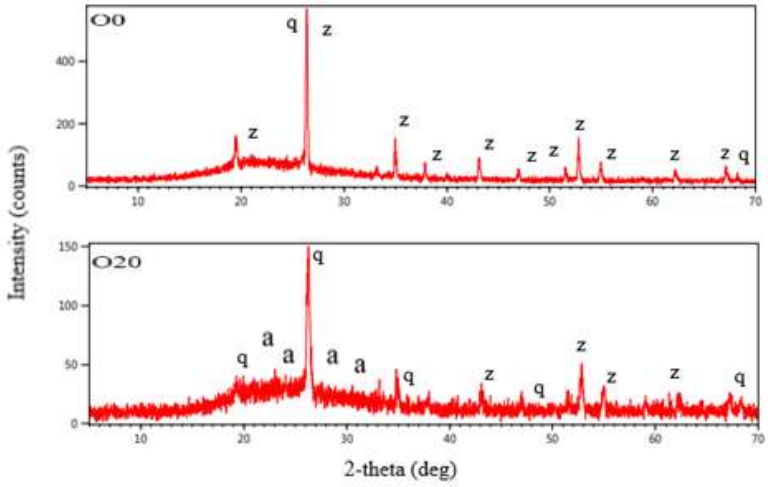

Figure 6 XRD pattern of O0(std) and O20 glazes (**q:**quartz, **z:**zircon, **a:**anorthite)

According to the SEM-EDS results of the opaque glazed tiles, while zircon crystal was contained 60.92 wt% Zr, 20.49 wt% Si, 18.59 wt% O in standard opaque glazed tiles, other zircon region for O20 sample contained 22.46 wt% O, 33.66 wt% Si, 4.85 wt% Al, 23.88 wt% Zr, 3.30 wt% Zn, 5.01 wt% Ca, 2.25 wt.% Fe, 1.26 wt.% Mg, 1.18 wt.% Na in Figure 8. It is seen that the zircon contained in the opaque frit is detected in the phase and microstructure analyses of the opaque glazed samples.

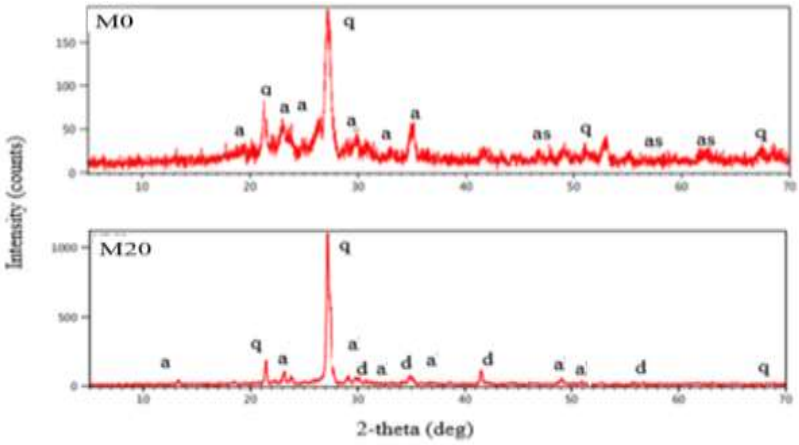

Figure 7 XRD pattern of M0 (std) and M20 glazes (q:quartz, as:aluminum silicate, a:anorthite, d:diopsite)

Anorthite containing phase region involved 47.78 wt% O, 30.46 wt% Si, 4.03 wt% Na, 10.33 wt% Al, 4.67 wt.% Ca, 0.98 wt.% K, 1.74 wt.% Zn for standard matt glazed tile in Figure 9. On the other hand, anorthite region was detected as 42.26 wt% O, 25.51 wt% Si, 6.11 wt% Al, 6.94 wt% Ca, 2.37 wt% K, 2.80 wt.% Na, 11.38 wt% Zn and 2.63 wt% Fe in M20. It is determined that the addition of BCW formed a needle-like anorthite crystal, especially in the matte-glazed sample. It has been reported in the literature that anorthite crystallizes in the glazing as a needle-like shape [21-22]. As detected in the EDS analysis, samples containing BCW in the glassy phase contain iron. This proves that there are iron oxide crystals in the glassy phase, although they cannot be detected in XRD, and color development occurs depending on iron oxide [23].

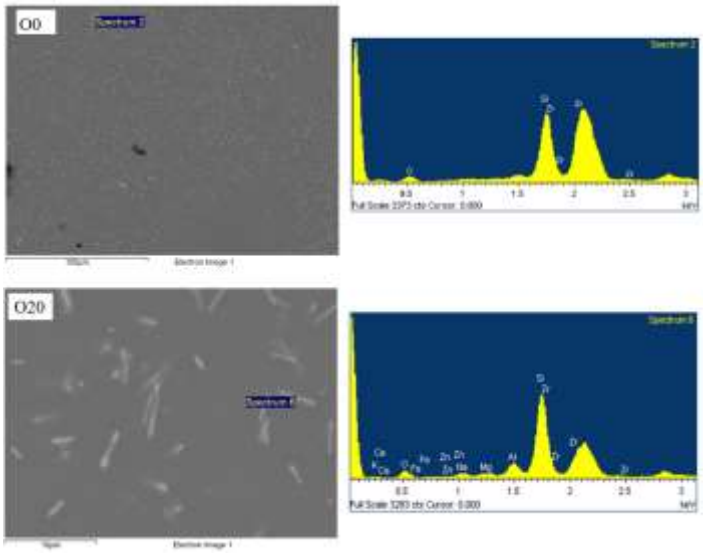

Figure 8 EDS spectra and spot analysis of glazed samples (O0 and O20)

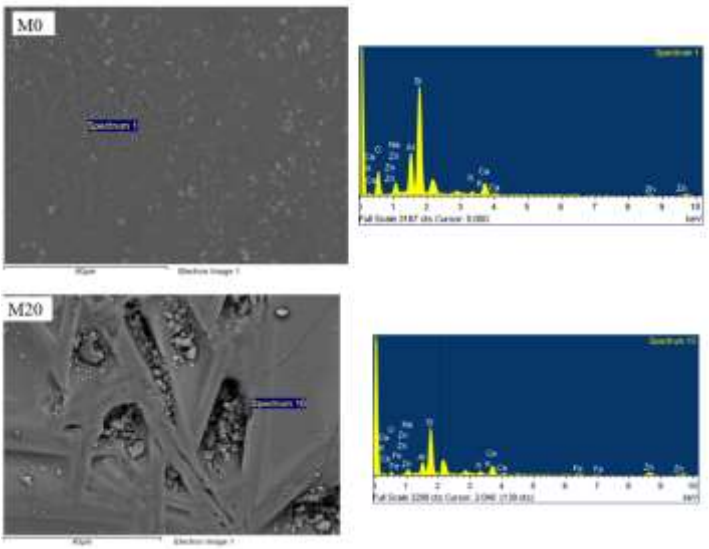

Figure 9 EDS spectra and spot analysis of glazed samples (M0 and M20)

CONCLUSION

In the study, basalt cutting waste was added in different proportions to opaque and matte glazes, the yellow and beige tonnes were observed in glazed tiles. Due to the iron oxide content of the BCW, the L* values decreased with the increasing BCW content of all glazes compared to the standard, opaque and matt glazes. The a* and b* values were increased with the increasing BCW content in glazes. When the phases formed in the glazed samples were examined, it was determined that the opaque glazed samples contained zircon and quartz as crystal phases, and anorthite crystals began to form with the addition of BCW. It was observed that anorthite and quartz as crystal phases in matte-glazed samples and anorthite peak intensity increased in samples with BCW and the diopside phase was formed. It can be concluded from the present study that BCW can be used to economically produce yellow-beige pigments for different industrial ceramic glazes depending on glaze composition.

ACKNOWLEDGEMENT

The authors would like to thank the Gizem Frit Manufacture (Sakarya/Turkey) and Emre Stone Mining Inc. (Kayseri/Turkey) for their material support. This study is supported by Scientific Research Project Programme (102 ADP-BAP) of Eskisehir Teknik University, Project No:22ADP32.

REFERENCES

1. Garbonchi, G., Dondi, M., Morandi, N., Tateo, F. (1999) Possible use of altered volcanic ash in ceramic tile production. Industrial Ceramics, 19, 67-74.
2. Matteucci, F., Dondi, M., Guarini, G. (2002) Effect of soda-lime glass on sintering and technological properties of porcelain stoneware tiles. Ceramics International, 28, 873-880.

3. Gennaro, R., Cappelletti, P., Cerri, G., Gennaro, M., Dondi, M., Guarini, G., Langella, A., Naimo, D. (2003) Influence of zeolites on the sintering and technological properties of porcelain stoneware tiles. Journal of European Ceramic Society, 23, 2237-2245.
4. Andreola, F., Barbieri, L., Corradi, A., Lancellotti, I., Manfredini, T. (2002) Utilisation of municipal incinerator grate slag for manufacturing of porcelainized stoneware tiles manufacturing. Journal of European Ceramic Society, 22,1457-1462.
5. Karamanov, A., Karamanova, E., Ferrari, A.M., Ferrante, F., Pelino, M. (2006) The effect of scrap addition on the sintering behavior of hard porcelain. Ceramics International, 32, 727-732.
6. Abadir, M.F., Sallam, E. H., Bakr, I. M. (2002) Preparation of porcelain tiles from Egyptian raw materials. Ceramics International, 28, 303-310.
7. Dana, K., Das, S., Das, S.K. (2004) Effect of substitution of fly ash for quartz in triaxial kaolin–quartz–feldspar system. Journal of European Ceramic Society, 24, 3169-3175.
8. Torres, P., Fernandes, H.R., Agathopoulos, S., Tulyaganov, D.U., Ferreira, J.M.F. (2004) Incorporation of granite cutting sludge in industrial porcelain tile formulations. Journal of European Ceramic Society, 24 3177-3185.
9. Koçyiğit, S., Cay, V.V. (2019) Investigation of mechanical and thermal behaviour of basalt cutting waste (bcw) added clay brick. European Journal of Technique (EJT), 9, 209-219.
10. Ergul, S., Ferrante, F., Pisciella, P., Karamanov, A., Pelino, M. (2009) Characterization of basaltic tuffs and their applications for the production of ceramic and glass–ceramic materials. Ceramics International, 35, 2789-2795.
11. Binici, H. (2007) Effect of crushed ceramic and basaltic pumice as fine aggregates on concrete mortars properties. Construction and Building Materials, 21, 1191-1197.
12. Ercenk, E., Guven, B., Yilmaz, S. (2018) Crystallization kinetics of machinable glass ceramics produced from volcanic basalt rock. Journal of Non-Crystalline Solids, 498, 262-271.
13. Yesilay, S., Cakı, M., Ceylantekin, R. (2017) Recycling of Afyon- Iscehisar marble waste in transparent stoneware glaze recipes. J. Aust. Ceram. Soc., 53, 475-484.
14. Karasu, B., Kaya, G., Çakir, A. (2011) Characterization of diopside-based glass-ceramic porcelain tile glazes containing borax solid wastes. J. Ceram. Process. Res., 12, 135-139.
15. Tarhan, B., Tarhan, M., Aydın, T. (2017) Reusing sanitaryware waste products in glazed porcelain tile production. Ceram. Int., 43, 3107-3112.
16. Bayer Ozturk, Z., Ay, N. (2010) The effect of ferrochromium fly ash as a pigment on wall tile glaze. Adv. Sci. Tech., 68, 213-218.
17. Bayer Ozturk, Z., Aycan, S., Bağıran, M.N., Arslan, L., Sağlar, B., Toprakçı, O. (2017) Usage of zinc ore waste in concrete structures. International Conference on Civil and Environmental Engineering Proceedings, Nevsehir/Turkey, 32-38.
18. Mahmood, A. S. (2014) Physical, structural and thermal properties of basalt-clay mixes. Tikrit Journal of Pure Science 19, 104-106.
19. Paganelli, M., Sighinolfi, D. (2008) Understanding the behaviour of glazes with the automatic heating microscope. Ceramic Forum International, 85, E63-E67.

20. Bayer Ozturk, Z. (2020) Effects of alumina and white fused alumina addition on technological properties of transparent floor tile glazes. Journal of Thermal Analysis and Calorimetry, 142, 1215-1221.
21. Tunalı, A., Selli, N.T. (2014) Effect of B_2O_3/SiO_2 ratio on transparency of anorthite based glass-ceramic glazes. Acta Physica Polonica A, 125, 511-512.
22. Tunalı, A., Özel, E., Turan, S. (2015) Production and characterization of granulated frit to achieve anorthite based glass-ceramic glaze. Journal of the European Ceramic Society, 35, 1089-1095.
23. Eren Gultekin, E. (2020) Investigation of Basalt Addition to Opaque Pottery Glaze. International Journal of Engineering Research and Development, 12, 91-97.

XV International Mineral Processing and Recycling Conference
17-19 May 2023, Belgrade, Serbia

SYNTHESIS AND CHARACTERIZATION OF POROUS CERAMICS BASED ON COPPER SLAG

D. Dinić[1#], S. Stupar[2], N. Jovanović[3], M. Tanić[4], S. Jevtić[1]
[1] University of Belgrade, Faculty of Technology and Metallurgy, Belgrade, Serbia
[2] Military Technical Institute, Belgrade, Serbia
[3] Serbia Zijin Copper doo, Bor, Serbia
[4] University of Defense, Military Academy, Belgrade, Serbia

ABSTRACT – This paper discusses usage of sacrificial templates for fabrication of porous ceramics with varying porosities. Copper slag and natural clay were used as the main raw materials, and starch as the pore former to form the desired pore structure. The raw materials were molded into green bodies and sintered at a temperature of 950°C. A qualitative analysis of the pore morphology and surface topography was conducted using optical microscopy. The obtained results indicate that an increase in starch content resulted in a rise in porosity from 26.84% to 35.93%. This method of producing porous ceramics from copper slag not only resolves problem of waste copper slag but also demonstrates its potential as a raw material in the production of porous ceramics.

Keywords: Porous ceramic, Copper slag, Clay, Starch, Sacrificial template.

INTRODUCTION

The rapid growth of the copper industry has resulted in a steady increase in the accumulation of copper slag in recent years. Copper slag (CS) is a byproduct produced during the pyrometallurgical processing of metals from copper concentrates, with the production of 1 ton of copper yielding approximately 2.2 tons of copper slag [1]. According to the Mineral Commodity Summaries 2022 of the U.S. Geological Survey, the total global production of refined copper in 2022 was approximately 26 million tons [2], which translates to a global CS accumulation of around 57 million tons in 2022.

Mining and Smelting Complex Bor is the only manufacturer of copper and precious metals in Serbia, with an annual ore production of about 2 million tons or about 30,000 tons of copper in metal [3]. Storing copper slag in heaps not only pollutes the environment but also wastes resources. Copper slag is highly heterogeneous and chemically diverse, consisting mostly of silica (SiO_2), ferrous oxide (FeO), ferric oxide (Fe_2O_3), small amounts of alumina (Al_2O_3), and calcium oxide (CaO). It also contains metal oxides, sulfides, and metallic forms such as copper (Cu), cobalt (Co), silver (Ag), nickel (Ni), zinc (Zn), lead (Pb), cadmium (Cd), and iron (Fe).

Despite this, the utilization of copper slag remains minimal. Copper slag has been employed in the production of construction materials such as cement [4], concrete [5], and structural ceramics [6].

corresponding author: denis.dinic@yahoo.com

Porous ceramics are a unique class of ceramics possessing three-dimensional (3D) network structures. These ceramics possess remarkable features, such as low density, low thermal conductivity, and exceptional resistance to high temperatures and corrosion [7]. Corrosion resistance is a crucial factor in the application of porous ceramics in corrosive environments. The two principal types of corrosion resistance that porous ceramics show are acid and alkali corrosion resistance [8].

Porous ceramics are highly desirable materials for various applications in industries such as aerospace, energy, metallurgy, military, chemical, medicine, and environmental protection due to their unique characteristics [9]. Different manufacturing techniques can be used to produce porous ceramics, including replica, sacrificial template, and direct foaming [7]. The sacrificial template technique involves preparing a biphasic composite consisting of ceramic precursors and a dispersed sacrificial material. The sacrificial material, acting as a pore former, is subsequently removed at high temperatures to create pores in the microstructure. Starch is a widely used pore former that can be applied to any material that can be dispersed in an aqueous suspension [10].

Recent studies have focused on the utilization of solid waste as raw materials in the production of porous ceramics. Examples of solid waste that have been used include waste glass [11], steel slag [12], spent automotive catalysts [13], red mud, and fly ash [14]. Copper slag, due to its similar chemical and mineral composition to the raw materials used in the preparation of porous ceramics, is also a suitable material for producing porous ceramics.

This study investigates the use of copper slag and clay to produce porous ceramics, utilizing starch as the pore former and polyvinyl alcohol (PVA) as the organic binder.

EXPERIMENTAL

Materials

The materials utilized in this experiment were copper slag natural clay, soluble starch, and PVA. The copper slag was obtained through industrial processing in the Mining and Smelting Complex located in Bor, Serbia. Figure 1 depicts a sample of CS aggregate.

Figure 1 Copper slag aggregate used in the study

The natural clay used in this experiment was obtained from deposits situated in Bogovina, Serbia. The soluble starch was acquired from Centrohem, while PVA was obtained from Sigma-Aldrich. The sulfuric acid (H_2SO_4) and sodium hydroxide (NaOH) employed for corrosion tests were obtained from Centrohem.

Sample preparation

The CS and clay were washed with distilled water and air-dried for 24 hours. The two materials were then ground for 30 minutes using a laboratory disc-mill to achieve a desirable grain size. Particles in the 1-100 μm range were separated by sieving using plastic sieve.

Following the grinding process, CS and clay were mixed with distilled water in a 1:1 ratio and stirred in a magnetic stirrer (IKA C-MAG HS 7 digital) for 10 minutes at a stirring speed of 500 rpm. Different amounts of soluble starch (5 wt.% and 10 wt.%) were added to the suspension, making two different samples. After addition of soluble starch, both samples were stirred for 5 minutes until a homogenous ceramic suspension was obtained. Subsequently, PVA (3 wt.%) was added to the suspension, and stirred at 60°C. The suspension was then placed in cylindrical moulds (25 mm diameter and 10 mm height). The green bodies were demoulded after 24 hours and dried at 80°C for 2 hours. After drying, the green bodies were sintered at 950°C for 2 hours, with a heating rate of 10°C min^{-1}. A holding time of 1 hour was observed at 400°C to burn-out the added starch and remove inherent structural water. Depending on the starch content, the porous ceramic bodies were denoted S-1 and S-2, with 5 wt.% and 10 wt.% of starch respectively.

Characterization

The microstructures were analyzed using an optical microscope (Leitz Metalloplan) equipped with a DFC295 camera and Last4.3.1 image processing software.

To determine the open porosity of the sintered samples, Archimedes' method was employed, and water was used as the medium. The open porosity of porous ceramics bodies, P_o,was calculated using Equation (1):

$$P_0 = \frac{m_2 - m_1}{m_2 - m_3} \cdot 100\ \% \quad (1)$$

where m_1 is the mass of the dried sample, m_2 is the wet weight of the sample, and m_3 is the mass of the sample when it is immersed in deionized water.

Immersion tests were used to investigate the corrosion resistance of materials. Immersion tests were carried out in 1M H_2SO_4 and 1M NaOH solutions at room temperature (25 °C) for 60 h. The percent mass loss after corrosion for 60 h were calculated according to the following Equation (2) and (3):

$$M_{ac} = \left(1 - \frac{m_{ac}}{m_{0ac}}\right) \cdot 100\ \% \quad (2)$$

$$M_{al} = \left(1 - \frac{m_{al}}{m_{0al}}\right) \cdot 100\ \% \quad (3)$$

where M_{ac} and M_{al} are the acid and alkali percent mass loss of porous ceramics, respectively; m_{ac} and m_{0ac} are the mass of samples before and after being immersed in 1M H_2SO_4 solution, while m_{al} and m_{0al} are the mass of samples before and after being immersed in 1M NaOH solution.

RESULTS AND DISCUSSION

Formation of green bodies

Figure 2a and 2b illustrates the dried green bodies that were prepared for sintering. The strength of the green bodies is a critical factor, as weak ones are susceptible to cracking during the sintering process. To address this, PVA was included as a binder. Despite this, cracking or warping was observed in all samples after drying, with sample S-2 exhibiting more significant changes.

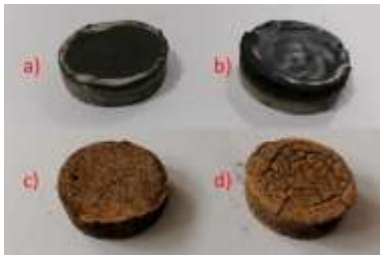

Figure 2 Samples: a) green body S-1, b) green body S-2, c) ceramic body S-1, d) ceramic body S-2

Porous ceramic characterization

Figure 2c and 2d illustrates the porous ceramics bodies. Samples evidently underwent some degree of shrinkage during the sintering process. This can be attributed to the transition of green bodies from a hydrous to an anhydrous state. Both porous ceramics bodies displayed visible cracks, which can be attributed to the nature of starch. This observation indicates that the disintegration of the sintered sample results in the emission of a high volume of steam and gases during starch burnout [15]. As can be seen in Figure 2c and 2d, many more and larger cracks appeared on the surface of sample S-2 than on sample S-1.

Figure 3 illustrates the morphology of the porous ceramics with varying starch contents. The pores were irregularly shaped, with a size of approximately 10 µm, which is comparable to studies conducted by Chen et al. using 5 wt.% and 10 wt.% starch as pore formers [8]. In sample S-2, the number of cracks on the skeleton increased, which can be attributed to the higher starch content in sample S-2. It can be assumed that the surface is rough.

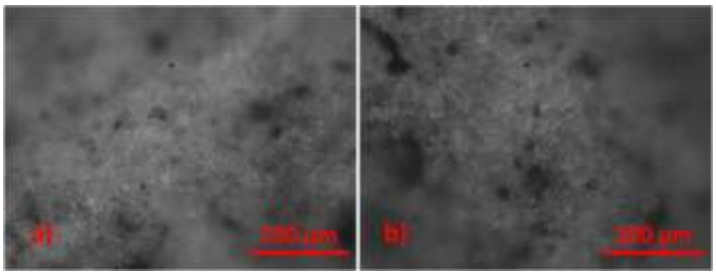

Figure 3 Microscopic images of sintered samples: a) S-1, b) S-2

Porosity and corrosion resistance

Porous ceramics are usually understood as materials having porosity over 30% [16]. The apparent porosity of the ceramic bodies increased with increasing amount of starch. Apparent porosity of 35.93% was calculated for the sample S-2, while sample S1 showed smaller value of 26.84%. Compared to a previous study of ceramics based on clay and CS (Xu et al., 2023), a higher porosity was obtained in this investigation [17]. This is understandable because a pore former was used. But, compared to a previous study of ceramics based on clay and starch, we obtained a lower porosity [18].

Porous ceramics are typically defined as materials with a porosity greater than 30% [16]. The obtained results showed that porosity of the ceramic bodies increased with an increasing amount of starch. A value of 35.93% was calculated for sample S-2, while sample S-1 had a lower value of 26.84%. Compared to the study of ceramics based on clay and chitosan (CS) conducted by Xu et al., this experiment yielded a higher porosity [17], which can be attributed to the use of a pore former. However, when compared to a previous study of ceramics based on clay and starch, our experiment resulted in a lower porosity [18]. After the immersion test in 1M H_2SO_4, the mass losses for S-1 and S-2 were 2.70% and 3.03%, respectively. After immersion in a 1M NaOH solution, the mass losses for S-1 and S-2 were 0.15% and 0.29%, respectively. The higher porosity of sample S-2 led to a higher corrosion rate, as the pores act as corrosion sites. However, these porous ceramics demonstrated better corrosion resistance under alkaline conditions. This is expected because H_2SO_4 is typically used for metal recovery from CS [19].

CONCLUSION

This study has demonstrated the possibility of utilizing sacrificial templates for the production of porous ceramics with varying porosities based on copper slag, thus enabling its reuse. In this study, starch was employed as the pore former, and it was observed that increasing the starch content correspond increased the porosity of the resulting ceramics. These results clearly indicate that copper slag possesses favorable properties for the synthesis of porous ceramics. Moreover, the results suggest a waste-to-resource strategy that can treat and reused copper slag under thermal conditions.

REFERENCES

1. Gorai, B., Jana, R.K. (2003) Premchand, Characteristics and utilisation of copper slag—a review. Resources, Conservation and Recycling, 39 (4), 299-313.
2. United States Geological Survey (USGS), (2023) Mineral commodity summaries 2023, https://doi.org/10.3133/mcs2023, (accessed 12 March 2023)
3. Ulniković, V.P., Kurilić, S.M., Staletović, N. (2020) Air Quality Benefits From Implementing Best Available Techniques in Copper Mining and Smelting Complex Bor (Serbia). Water Air Soil Pollut, 231, 160.
4. Jin, Q., Chen, L. (2022) A Review of the Influence of Copper Slag on the Properties of Cement-Based Materials. Materials, 15 (23), 8594.
5. Filipović, S., Đokić, O. A. (2021) Radević, D. Zakić, Copper Slag of Pyroxene Composition as a Partial Replacement of Natural Aggregate for Concrete Production.

Minerals, 11 (15), 1-19.
6. Lemougna, P.N., Yliniemi, J., Adesanya, E., Tanskanen, P., Kinnunen, P., Roningc, J., Illikainen, M. (2020) Reuse of copper slag in high-strength building ceramics containing spodumene tailings as fluxing agent. Minerals Engineering, 155, 106448.
7. Chen, Y., Wang, N., Ola, O., Xia, Y., Zhu, (2021) Y. Porous ceramics: Light in weight but heavy in energy and environment technologies. Materials Science and Engineering: R: Reports, 143, 100589.
8. Chen, Z., Xu, G., Cui, H., Zhang, X., Zhan, X. (2018) Preparation of porous Al_2O_3 ceramics by starch consolidation casting method. The International Journal of Applied Ceramic Technology, 15 (6) 1550-1558.
9. Wang, Y., Wang, X., Liu, C., Su, X., Yu, C., Su, Y., Qiao, L., Bai, Y. (2021) Aluminum titanate based composite porous ceramics with both high porosity and mechanical strength prepared by a special two-step sintering method. Journal of Alloys and Compounds, 853, 157193.
10. Studart, A.R., Gonzenbach, U.T., Tervoort, E., Gauckler, L.J. (2006) Processing Routes to Macroporous Ceramics: A Review. Journal of the American Ceramic Society, 89 (6), 1771-1789.
11. Xi, C., Zheng, F., Xu, J., Yang, W., Peng, Y., Li, Y., Li, P., Zhen, Q., Bashir, S., Liu, J.L. (2018) Preparation of glass-ceramic foams using extracted titanium tailing and glass waste as raw materials. Construction and Building Materials, 190, 896-909.
12. Wu, Q., Huang, Z. (2021) Preparation and performance of lightweight porous ceramics using metallurgical steel slag. Ceramics International, 47 (18), 25169-25176.
13. Ding, Y., Zhang, X., Wu, B., Liu, B., Zhang, S. (2021) Highly porous ceramics production using slags from smelting of spent automotive catalysts. Resources, Conservation and Recycling, 166, 105373.
14. Hou, L., Liu, T., Lu, A. (2017) Red mud and fly ash-based ceramic foams using starch and manganese dioxide as foaming agent. Transactions of Nonferrous Metals Society of China, 27 (3), 591-598.
15. Lyckfeldt, O., Ferreira, J.M.F. (1998) Processing of porous ceramics by 'starch consolidation'. Journal of the European Ceramic Society, 18 (2), 131-140.
16. Obada, D.O., Dodoo-Arhin, D., Dauda, M., Anafi, F.O., Ahmed, A.S., Ajayi, O.A. (2016) Potentials of fabricating porous ceramic bodies from kaolin for catalytic substrate applications. Applied Clay Science, 132-132, 194-204.
17. Xu, L., Y. Liu, Y., Chen, M., Wang, N., Chen, H., Liu, L. (2023) Production of green, low-cost and high-performance anorthite-based ceramics from reduced copper slag. Construction and Building Materials, 375, 130982.
18. Suarez, M., Bermudez, D., Peña-Rodriguez, G., Ferrer, M., Dulce-Moreno, H.J. (2020) Effect of concentration of starch in the properties morphological and structural of porous ceramic based on expansive clays. Journal of Physics: Conference Series, 1448, 012022.
19. Banza, A., Gock, E., Kongolo, K. (2002) Base metals recovery from copper smelter slag by oxidising leaching and solvent extraction. Hydrometallurgy, 67 (1-3) 63-69.

XV International Mineral Processing and Recycling Conference
17-19 May 2023, Belgrade, Serbia

ANALYSIS OF THE CHARACTERISTICS OF SLAG FROM METALLURGICAL PLANTS IN ZENICA DISPOSED OF INDUSTRIAL WASTE LANDFILL "RACA"

M. Šišić[1#], Dž. Dautbegović[1], M. Duraković[2]
[1] University of Zenica, Faculty of Mechanical Engineering, Zenica, Bosnia and Herzegovina
[2] University of Zenica, Metallurgical Institute "Kemal Kapetanović", Zenica, Bosnia and Herzegovina

ABSTRACT – Due to the appearance of an increasing amount of slag that is produced as industrial waste in the metallurgical processes of steel production, the disposal of this type of waste represents one of the biggest environmental protection challenges in Zenica. With the development of environmental awareness, increasing costs and other conditions of waste disposal, the use of slag as an industrial by-product and/or waste has become an attractive alternative to disposal. The paper describes possible methods of slag disposal, taking into account the results of research on the types, chemical and granulometric properties of slag from metallurgical plants. The focus of the research is on determining the characteristics of the slag that has already been disposed of at the "Rača" landfill in order to assess the possibility of its use, thereby freeing up space for the disposal of new amounts of industrial waste or providing conditions for repurposing the space.

Keywords: Slag, Disposal, Waste, Use.

INTRODUCTION

Industrial waste from the production facilities of "Zeljezara Zenica" and later "Arcelor Mittala" in Zenica was intensively disposed of at the "Rača" industrial waste landfill (Figure 1). Smaller amounts of industrial waste are also disposed of today. Solving the problems caused by the uncontrolled accumulation of industrial waste imposes the need for a comprehensive analysis of the amount, content and condition of the disposed materials, as well as an assessment of the real possibilities of reusing the disposed materials and/or repurposing the area of the "Rača" landfill. [1]

The basic types of industrial waste that were deposited at the "Rača" industrial landfill and that will be treated in the process of rehabilitation of this landfill are: blast furnace slag, steel slag, refractory materials, foundry sand, other waste materials from the technological process of the metallurgical complex. [2]

Previous research with the intention of defining a solution to the problem of disposal of industrial waste materials from metallurgical plants in Zenica (primarily blast furnace and steel slag) mainly related to research into the composition and the possibility of reusing these materials immediately after they were created in the plant. The analysis in this paper involves researching the composition, quantities and

corresponding author: muvedet.sisic@unze.ba

condition, as well as assumptions for the reuse of materials that have been disposed of for a long period at the "Rača" industrial waste landfill.

Figure 1 Industrial waste disposal site "Rača"

MATERIALS AND METHODS

In order to determine the amount of deposited slag at the industrial waste disposal site, a survey of its entire surface was performed using the WINGTRON aerial surveying drone and a 3D model of the landfill was created. On the basis of these data, a three-dimensional mapping of the entire area was carried out, and the micro-location arrangement and deep stocks of certain types of disposed waste materials were defined.

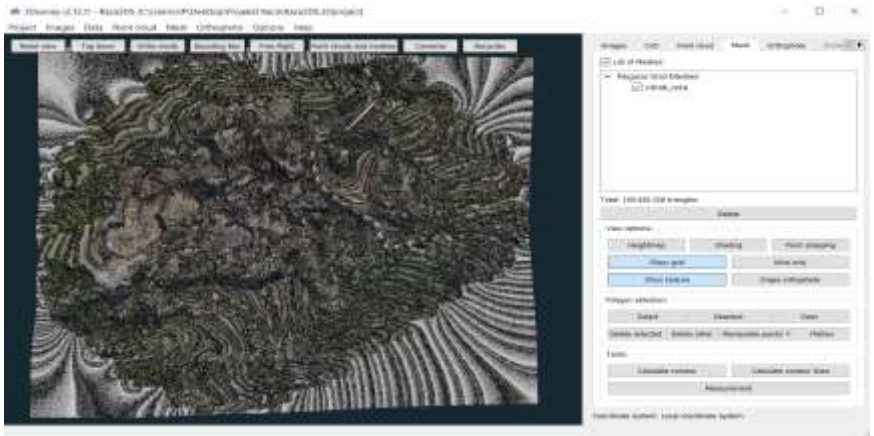

Figure 2 3D-model of the landfill site generated in the 3Dsurvey software package based on georeferenced point clouds obtained by Wingtron drone imaging

Based on the collected data and information from the phase in which the spatial coverage, mapping and 3D recording of the terrain and the current state of industrial waste disposal at the “Rača” landfill were defined, it was started to determine, i.e. the implementation of the II phase, which includes the sampling of disposed waste materials and the determination of the chemical and granulometric characteristics of the disposed materials.

For the causation procedure, it is necessary to comply with the relevant national guidelines on sampling of FBiH, as well as ISO guidelines and EU norms, as follows:

- Standard ISO/IEC 17025:2017 - General requirements for the competence of testing and calibration laboratories
- EN 14899 Waste characterization - Sampling of waste materials - Framework for preparing and implementing a sampling plan
- CEN/TR 15310 Characterization of waste - Sampling of waste materials. [2]

The material sampling methodology implies respect for the spatial and locational arrangement, the number and size of the required number of samples,
To assess the state of the sampled materials, chemical and granulometric analysis of the samples was performed using Shimadzu Analytical Methods for Atomic Absorption Spectrometry; JUS HZ1.111/87; JUS B.B8.070:1982.

RESULTS AND DISCUSSION

The results of the chemical analysis are presented in Table 1.

Table 1 Chemical analysis of slag samples

Parameter	Sample									
	1	**2**	**3**	**4**	**5**	**6**	**7**	**8**	**9**	**10**
moisture	4.23	4.23	0.06	0.09	0.67	6.9	0.46	17.89	3.49	4.22
Ash	79.51	78.15	100	99.41	98.2	84.76	98.81	79.18	79.51	78.14
Al_2O_3	6.43	5.1	10.77	9.07	9.26	4.91	10.77	14.18	6.05	8.13
Fe_2O_3	21.59	23.6	0.57	0.49	0.93	7.44	0.53	6.15	12.58	23.88
CaO	19.6	16.3	31.1	17.7	34.2	8.5	20.9	24.1	31.8	17.4
MgO	7.14	7.64	2.82	4.15	3.82	2.32	5.81	1.99	8.13	7.47
Cr_2O_3	0.035	0.041	0.006	0.004	0.006	0.01	0.004	0.012	0.032	0.045
P_2O_5	0.321	0.343	0.206	0.177	0.206	0.252	0.183	0.252	0.366	0.275
K_2O	0.36	0.35	0.09	0.088	0.93	1.08	0.79	0.19	0.12	0.45
Na_2O	0.14	0.12	0.27	0.28	0.26	0.3	0.16	0.32	0.07	0.12
SO_3	0.57	0.2	0.33	1.08	0.63	1	0.43	1.2	0.5	0.5
MnO	2.71	1.81	5.86	4	6.45	0.27	3.74	0.06	2.71	1.94
TiO_2	<0.03	<0.02	<0.01	<0.08	<0.08	0.13	0.13	0.1	<0.01	0.17
Cu	0.011	0.01	0.002	0.002	0.002	0.003	0.001	0.003	0.004	0.011
Mn	2.1	1.4	4.4	3.1	5	0.21	0.29	0.05	2.1	1.5
Ni	0.008	0.009	0.002	0.001	<0.001	0.008	<0.001	0.005	0.003	0.007
Hg	<0.0006	<0.0022	<0.0001	<0.0001	<0.0001	<0.0001	<0.0001	0.0001	0.0001	0.0022
Cr	0.024	0.028	0.004	0.003	0.004	0.007	0.003	0.008	0.022	0.031
Cd	0.0025	0.0031	0.0011	0.0003	<0.0001	0.0005	0.0005	0.0004	0.0008	0.0016
Co	0.003	0.003	0.003	0.003	0.003	0.002	0.002	0.003	0.001	0.003
Zn	0.212	0.571	0.002	0.002	0.002	0.013	0.002	0.007	0.045	0.623
As	0.0006	0.00089	0.00002	0.00002	0.00002	0.00017	0.00002	0.00093	0.00059	0.00086
Pb	0.631	0.233	0.005	0.002	0.002	0.005	0.004	0.004	0.011	0.213
$G_ž$	20.7	22.77	prirast	0.43	2.08	16.08	1.15	21.1	20.56	22.04

Chemical analysis of slag provides information on its composition, which will determine the possibility and methods of its use. For more complete information about the characteristics of the deposited slag, it is necessary to carry out a granulometric analysis. The results of granulometric analysis are shown in Table 2.

Table 2 Granulometric analysis of slag samples

Sieve (mm)	Residue on the sieve of individual samples (%)									
	1	**2**	**3**	**4**	**5**	**6**	**7**	**8**	**9**	**10**
35	-	-	-	-	-	-	-	-	6.6	-
31.5	-	-	-	-	-	-	-	-	16.39	-
25	-	-	-	-	-	-	-	-	34.43	15.95
20	-	-	-	-	-	-	-	-	62.23	-
18	-	-	-	-	-	-	-	-	66.36	38.47
10	32.41	13.62	-	-	-	-	-	-	83.52	53.91
8	41.44	21.62	-	-	-	-	-	-	87.95	60.8
6	-	-	-	-	-	-	-	-	88.87	63.78
5	-	-	-	-	-	-	-	-	91.77	-
4	60.64	42.12	-	-	-	-	-	-	92.57	-
3	-	-	-	-	3.64	3.09	0.76	-	93.41	75.6
2	73.16	60.62	14.61	24.01	21.75	6.29	14.05	-	94.57	81.6
1.4	-	-	34.2	47.21	-	-	-	-	-	-
1	83.23	74.83	55.2	65.12	67	16.36	49.95		95.8	87.97
0.71		-	76.43	79.32	-	-	-	-	-	-
0.5	90.03	84.44	89.53	88.63	93.63	32.48	79.89		96.79	92.33
0.355	-	-	94.99	93.12	-	-	-	-	-	-
0.25	93.8	91.04	97.85	96.24	98.25	54.41	90.03		97.79	95.28
0.2	-	-	98.63	97.27	-	-	-	-	-	-
0.18	-	-	98.84	97.61	-	-	-	-	-	-
0.125	96.27	95.16	99.33	98.52	99.05	74.76	94.68		98.77	97.26
0.1	-	-	99.48	98.87	-	-	-	-	-	-
0.09	-	-	99.54	99.04	-	-	-	-	-	-
0.075	-	-	99.61	99.22	-	-	-	-	-	-
0.063	98.62	98.27	99.68	99.39	99.43	87.48	97.73	0.02	99.48	98.58
- 0.063	100	100	100	100	100	100	100	99.98	100	100

Granulometric analysis of the slag samples shows that samples 1 and 2 and samples 9 and 10 have larger grains, which points to the potential need for additional processing before use. During the collection of samples at the "Rača" landfill, larger pieces were registered at some locations, which were created by dumping and compacting slag over a long period of time.

In addition, a test of water absorption, volumetric mass and coarse moisture was carried out. The results of this finding are shown in Table 3.

Table 3 Test results, water absorption, volumetric mass and gross moisture

Sample	Water absorption %	Volumetric mass kg/m^3	Gross moisture %
1	10.76	1276	2.2
2	26.67	1292	2.1
3	34.40	1248	0.9
4	40.25	1261	1.0
5	22.87	1201	1.1
6	69.56	712	1.3
7	48.57	1147	1.1
8	30.33	520	1.9
9	3.41	1386	1.4
10	15.18	1370	1.6

From Table 3, it is evident that samples 3-8 show a high ability to absorb water, which will determine their method of use. Samples 3-8 are samples with full or majority slag content from steel production plants.

In order to be able to confirm the usability of slag, like any other material, it is necessary to standardize it from the point of view of technical and environmental aspects. Most of the national standards relevant for the construction industry are harmonized according to the provisions of "EURONORMA". Therefore, everything that applies to natural aggregates also applies to slag aggregates. According to the views of the European Association of Slag Processors “EUROSLAG”, the most important standards for slag are: EN 197, EN 15176, EN 206, EN 1744-1, EN 12945, EN 12620, EN 13043, EN 13242, EN 14227, EN 13282, EN 13450. [3]

CONCLUSION

Based on the results of the analysis of the properties of the slag deposited at the "Rača" industrial waste landfill, and taking into account earlier research [4,5] and valid standards in this area, we can state and confirm the following possibilities of its use:

- Cement production (granulated slag from the blast furnace);
- Aggregate for concrete production (granulated blast from the furnace slag);
- Production of slag concrete blocks for masonry (granulated and crystalline slag from the blast furnace);
- Aggregate for the production of asphalt mixtures (granulated and crystalline slag from the blast furnace and slag from the electric furnace);
- Material for making various embankments in road construction (slag from the blast furnace);
- Material for making embankments in water management (coarse slag from the blast furnace);

- Construction of various railway embankments (coarse slag from the blast furnace);
- Covering waste in landfills (slag from steel production plants);
- In agriculture for agrotechnical measures, regulation of soil pH, Ca, Mg, etc. (slag from steel production plants);
- Sprinkling material for winter road maintenance (blast furnace slag);
- Filling for drains, (sieved slag from the electric furnace);
- Backfilling of macadam roads (blast furnace slag, steel production plant slag).

Blast furnace slag shows better properties for use in the cement industry. Coarse-grained slag and formations created by slag compaction must be crushed to the required granulation before use. Slags that show a high ability to absorb water should be planned for use, taking this specificity into account.

REFERENCE

1. Dopuna plana upravljanja otpadom,Arcelormittal Zenica, 2022.
2. Sredojević, J., Krajišnik, M. (2011) Ekološko - ekonomski efekti sanacije deponije industrijskog otpada „Rača“,Zenica.
3. Ahsun-sirovinacomerc d.o.o. Zenica (2013) Ferometalurška troska u industriji Bosne i Hercegovine.
4. Božić, B. (1973) Metalurgija gvožđa, Univerzitet u Beogradu, Beograd.
5. Sofilić, T., Mladenovič, A., Sofilić, U. (2011) Defining of EAF steel slag application possibilities in asphalt mixture production, Journal of Environmental Engineering and Landscape Management, 19 (2), 148-157.

XV International Mineral Processing and Recycling Conference
17-19 May 2023, Belgrade, Serbia

ANALYSIS OF THE IMPACT OF THE INTRODUCTION OF LARGER CONTAINERS INTO THE WASTE COLLECTION SYSTEM IN THE CITY OF ZENICA

Dz. Datubegovic#, M. Hasanbasic, M. Sisic, V.Birdahic
University of Zenica, Zenica, Bosnia and Herzegovina

ABSTRACT – ALBA Zenica d.o.o. Zenica is a municipal company, which is responsible for the municipal waste collection in the area of the city of Zenica. In the past five years, there has been a targeted replacement of containers and the transition to containers with a larger volume, in order to optimize and improve the waste collection service. The paper will present an analysis of the efficiency indicators of municipal waste collection before and after the installation of larger containers (metal bell type containers and underground containers) in the city area.

Keywords: Waste Management, Municipal Waste, Environmental Protection, Underground Container, Metal Bell Container.

GENERAL CHARACTERISTICS OF THE MUNICIPAL WASTE COLLECTION SYSTEM IN ZENICA

The city of Zenica is located in the central part of Bosnia and Herzegovina on an area of 550 km^2, and 44 km^2 is inhabited. The number of inhabitants, according to the 2013 census, is 110,663. Zenica has a moderate continental climate with an annual average precipitation of 778 mm.

ALBA Zenica d.o.o. is a utility company that provides the service of collection and transport of municipal waste from the area of the city of Zenica. Collected waste is taken to the Regional Landfill "Mošćanica", 17 kilometers from the city center, where it is disposed.

The inhabited area is connected with roads, which together with the locations of waste collection containers and the frequency of emptying, determine the type of vehicles used for waste collection, i.e. define the waste collection system.

In Zenica, waste collection containers are used that differ in volume, shape and method of emptying. For the collection of municipal waste, special vehicles are used for containers emptying and transporting waste, which can be classified into the following groups:

a) little waste trucks (6-8 m^3) for waste collecting from 120 – 240 liters bins,
b) medium waste trucks (11-17 m^3) and large waste trucks (20-22 m^3) for waste collecting from 1.100 liters containers,
c) waste trucks with grapple (24-40 m^3) for waste collecting from underground containers (3000 l) and metal bells (2500 l).

corresponding author: dautbegovic@alba.ba

For the past five years, the task of optimizing of the waste collection system from public places in the city of Zenica has been set. The goal of the optimization is to reduce the time required for emptying and taking municipal waste to the Mošćanica Regional Landfill, as well as reducing fuel consumption for carrying out this activity. Reducing the time of work on the waste collection also implies a reduction in vehicle maintenance costs.

The indicators of the provision of waste collection services in the second half of 2017 will be analyzed, compared with the indicators of municipal waste collection in the second half of 2022 year. The results will be compared with the subsequent analysis of the obtained performance indicators.

Employees and means of work engaged in the collection of municipal waste from the urban part of the city will be observed. This applies to medium and large waste trucks, which empty containers with the volume of of 1.1 m^3, and waste truck with grapple that empties containers with the volume of 2.5 m^3 and 3.0 m^3.

OBSERVED PARAMETERS OF THE WASTE COLLECTION SYSTEM

The municipal waste collection area for individual housing is located on the outskirts of urban areas or in rural, mostly hilly areas. Each user, a private house, has his own waste container and can choose its size and frequency of emptying. In this area, there are mostly narrow roads, which require the use of smaller (waste truck) vehicles.

In the urban part of the city, common containers are used, which are located in places accessible to vehicles with a larger capacity and volume of loading space.

For the purposes of the analysis of efficiency indicators in 2017 and 2022, the following will be observed:

a) urban part of the city
b) containers with the volume of 1,1 m^3, 2,5 m^3, 3,0 m^3
c) vehicles for emptying above mentioned containers.

The observed urban part of the city includes 19 local communties. The total number of housing units (apartments) that use common containers for waste collection in the aforementioned 19 local communities is 17,622, as of December 31, 2022.

In the observed area, the following waste collection containers are used for collecting waste from collective housing units (buildings and skyscrapers):

- containers with volume of 1.100 liters on wheels with lids,
- metal bells with volume of 2.500 liters with foot and manual lid opening,
- underground containers with volume of 3.000 liters with foot and manual lid opening.

The technical characteristics of the vehicles with which municipal waste is collected and transported are shown in the Table 1.

Table 1 Technical characteristics of trucks for waste collection from urban areas

reg. number	**872J250**	**J23A461**	**E92A952**	**O84K623**	**T02J557**
type	waste truck	waste truck	waste truck	waste truck	grapple
manufacturer	MERCEDES	MAN	MERCEDES	MERCEDES	MAN
tip	970.07	N18	950.60	950.62	H21
year	1999	2008	2007	2005	2007
engine volume	6374	6871	6374		10580
engine (kW)	170	206	210	205	265
axles number	2	2	3	3	3
total weight	15000	18000	26000	26000	25500
capacity	4220	6640	10960	11200	16200
additional device	waste compaction	waste compaction	waste compaction	waste compaction	puller with crane
manufacturer	Schörling	Faun	Haller	SKK	Penz Crane
volume (m^3)	12	18	21	21	32
external dimensions	L=8; B=2,3; H=3,25	L=8,5; B=2,4; H=3,45	L=10,1; B=2,3; H=4	L=9,5; B=2,5; H=3,5	L=7,7; B=2,3; H=2,7

ANALYSIS OF MUNICIPAL WASTE COLLECTION AND TRANSPORT SYSTEM INDICATORS

Operational controlling of work processes of ALBA ZenicA d.o.o. keeps data on consumption and realization parameters. The company owns an internal gas station with personalized monitoring of the fuel consumption of waste collection employees, the company also has a certified 50-ton scale for trucks, which is also equipped with a personalized electronic record. All the company's vehicles are equipped with a GPS device, which enables constant insight into the movement of vehicles, and digital records are used to analyze and improve the organization of the transport service.

For the purposes of this paper, data on work processes from 2017 and 2022 were used.

The fuel consumption per unit of time or distance is noticeably higher in vehicles intended for waste collection and transport compared to trucks for long distance transport. The difference in the consumption indicators is due to the way of driving (start-stop), the area of movement (populated places with slow traffic) as well as the fact that the extension for collecting and compacting waste with hydraulic elements driven by a hydraulic pump is connected to the engine of the truck.

When analyzing municipal waste collection activities, the working process is usually divided into:

a) **emptying containers** with waste, which means unloading them into waste truck and moving the vehicle up to 100 meters away between the containers,
b) **waste transport** from the starting station to the area with containers for emptying, transport between distant emptying areas and transport from the containers emptying area to the landfill, or municipal waste processing plant.

Since the same urban parts for waste collection are observed and analyzed, the comparison will be reduced to the observation of overall indicators by vehicles, containers, fuel and spent time.

Operational indicators of the provision of municipal waste collection services from the urban part of the city of Zenica are listed separately in the following Table 2 and Table 3.

Table 2 Data on vehicles used for the municipal waste collection from the observed urban area July 1-December 31, 2017

vehicle	label	hours (trucks)	tons collected	kilometres	fuel (lit.)	hours (people)
medium waste truck	461	1.557	3.765	14.953	9.366	4.670
	250	981	1.904	8.436	4.625	2.551
large waste truck	975/590	409	989	4.575	4.276	1.227
	952	428	1.159	5.031	3.956	1.070
truck with grapple	557	260	511	4.079	3.689	520
total	5	3.634	8.327	37.074	25.911	10.037

Table 3 Data on containers for waste collection in the period 1.7.-31.12.2017

containers	volume /m^3/	public	firms	total volume /m^3/
containers	1,1	652	239	980
underground cont	3,0	11		33
total		663	239	1.013

emptyings (weekly)	3.728	469
volume (weekly) /m^3/	4.164	516

After the introduction of a larger number of containers with a larger volume, the values of the service provision indicators changed, which can be seen in the following two Tables 4 and 5.

Table 4 Data on vehicles used for the municipal waste collection from the observed urban area July 1-December 31, 2022

vehicle	label	hours (trucks)	tons collected	kilometres	fuel (lit.)	hours (people)
medium waste truck	461	995	1.919	7.608	4.832	1.990
	250	353	682	2.631	1.407	1.060
large waste truck	623	1.097	2.148	9.904	7.044	2.369
	952	345	541	3.775	2.906	690
truck with grapple	557	950	1.749	9.209	9.495	1.901
total	5	3.741	7.040	33.127	25.684	8.011

Table 5 Data on containers for waste collection in the period 1.7.-31.12.2022

containers	volume /m^3/	public	firms	total volume /m^3/
containers	1,1	443	433	964
underground cont	3,0	47		141
metal bell	2,5	76		190
total		566	433	1.295

emptyings (weekly)	3.218	651
volume (weekly) /m^3/	4.222	716

Efficiency indicators, which were derived based on the data in Tables 2-5, are visible in Tables 6 and 7.

Table 6 Comparison of the efficiency of municipal waste collection in 2017 and 2022

	2017			2022		
vehicle	l/t	l/km	l/h	l/t	l/km	l/h
medium waste truck	2,49	0,63	6,02	2,52	0,64	4,86
	2,43	0,55	4,71	2,06	0,53	3,98
large waste truck	4,32	0,93	10,45	3,28	0,71	6,42
	3,41	0,79	9,25	5,37	0,77	8,42
truck with grapple	7,22	0,90	14,19	5,43	1,03	9,99

Table 7 Comparison of the efficiency of municipal waste collection in 2017 and 2022

	2017			2022		
vehicle	t/l	t/km	t/h	t/l	t/km	t/h
medium waste truck	0,40	0,25	2,42	0,40	0,25	1,93
	0,41	0,23	1,94	0,48	0,26	1,93
large waste truck	0,23	0,22	2,42	0,30	0,22	1,96
	0,29	0,23	2,71	0,19	0,14	1,57
truck with grapple	0,14	0,13	1,96	0,18	0,19	1,84
total	0,32	0,22	2,29	0,27	0,21	1,88

On the basis of the data presented in the tables, it is possible to gain insight into the efficiency of waste collection according to various parameters. As the basic unit in waste is the ton, the evaluation of the performance and costs of the waste management organization, in this case waste collection, is often expressed in relation to mass. In our case, we see that the parameters are worse in relation to the tone. Our analysis processed the service in a certain area and it includes the waste collection that was generated in that area during the period of service provision. The service provider cannot influence the amount of waste that will be generated in a certain space with its abilities, so the optimization of the service cannot be quantified in every review of the parameters with the previous state.

Traffic conditions also change over time, unfortunately in urban areas, as a rule, traffic slows down and the movement of larger vehicles becomes difficult, as well as difficult access to waste containers due to the growing number of vehicles in the so-called stationary traffic.

The increased vehicle fleet age and extended time of use also contribute to increased fuel consumption, which partly worsens consumption results from year to year.

CONCLUSION

By installing containers with a larger volume and a smaller opening for waste diisposal, the following was achieved:

- an increase in the volume for disposal of municipal waste on a smaller area required for placing containers compared to the previous of 1.100 liters,
- the spreading of food remains was reduced, because the lids, which close automatically, prevented the access for birds and other animals,
- it is made impossible to dispose larger pieces of waste (bulky waste) in municipal

waste containers (bulky waste is a special category of waste and is handed over to recycling yards),
- the humidity of the waste is reduced (lids prevent the influence of atmospheric precipitation),
- the spread of unpleasant odors from municipal waste containers is reduced (underground containers. are located below the surface of the earth, the waste heats up less and the production of unpleasant odors is reduced, the lid that closes on underground containers and metal bells also reduces the spread of odors),
- underground containers and metal bells prevent leakage of leachate generated in municipal waste at the location where they are placed, all leachate is in the vehicle when emptying and is taken to the landfill,
- from the operational data on the provision of the waste collection service (Table 2 and table 4), it is evident that for the increased number of users and scope of the service in the form of emptied volume per unit of time, consumption indicators have improved.

By changing the type and size of container for disposal (collection) of municipal waste, the quality of the waste collectionl service for users has been improved. The optimization made it possible to provide services to a greater number of container users in public places (containers for people in buildings and skyscrapers), as well as to an increased number of companies with a corresponding container. The volume of disposed containers has also increased, while the hygienic conditions of regular emptying of municipal waste containers have been respected.

By optimizing the organization of municipal waste collection based on new technical possibilities, better management was achieved, that is, the management sustainability was increased through:
- less environmental pollution (the negative impact of the container location, vehicles for waste collection in traffic has been reduced through reduced vehicle mileage),
- the working conditions of the employees have been improved by increasing the share of the use of hydraulic machines when emptying containers for municipal waste, as well as by reducing working time,
- operating costs in the area of municipal waste collection have been reduced by reducing fuel consumption, by reducing containers failures in the past period, i.e. the efficiency of the municipal waste collection service has increased.

REFERENCES

1. Junemann, R. (1995) Entsorgungs logistik III, Eric Schmidt Verlag GmbH & Co, Berlin.
2. Prof.Dr-Ing. B.Gallenkemper and Prof.Dr-Ing. H. Doedens (1988) Getrennte Sammlung von Wertstoffen des Hausmulls, Eric Schmidt Verlag GmbH & Co, Berlin.
3. Vogel, A. (1993) Controlling in der gewerblichen Enstorgungslogistik. Peter Lang GmbH, Frankfurt am Main.
4. Kranert, M. (2017) Einfuhrung in die Kreislaufwirtschaft. Springer Vieweg, Stuttgart.
5. Data from ALBA Zenica d.o.o. Zenica.

XV International Mineral Processing and Recycling Conference
17-19 May 2023, Belgrade, Serbia

ENVIRONMENTALLY ACCEPTABLE CEMENTS WITH THE ADDITION OF GRANULATED BLAST FURNACE SLAG

N. Bušatlić[1#], I. Bušatlić[1], A. Halilović[1], N. Merdić[2], L. Kovač[1]
[1] University of Zenica, Faculty of metallurgy and technology, Zenica, Bosnia and Herzegovina
[2] Kakanj cement factory, Kakanj, Bosnia and Herzegovina

ABSTRACT – In this paper, the possibility of producing more environmentally friendly (mixed) cements (classes CEM II/B-M (S+LL)) in the Kakanj Cement Factory was examined. The goal of producing such cements is to reduce the clinker content in the cement itself by increasing the content of granulated blast furnace slag, which would have numerous ecological advantages. Two cement samples U1 and U2 were prepared. Sample U1 consists of 65% clinker, 26% granulated blast furnace slag, 5% marly limestone and 4% gypsum. Sample U2 consists of 75% clinker, 16% granulated blast furnace slag, 5% marly limestone and 4% gypsum. Before the preparation of cement samples, the initial raw material components were characterized in terms of chemical and mineralogical composition and specific mass, while the chemical composition and physical characteristics of the prepared Portland composite (mixed) cements were determined. Detailed tests of physical-mechanical properties were performed on the prepared cement samples. The obtained results meet the requirements of EN and BAS standards. As a result of the conducted tests, it can be concluded that it is possible to produce more ecologically acceptable (mixed) cements in the Kakanj Cement Factory, and that its production would provide a number of ecological and economic benefits. For the sake of comparison with samples U1 and U2, in the paper are presented the results of the cement that is currently produced in the Kakanj cement factory.

Keywords: Portland cement, Clinker, Granulated blast furnace slag, Compressive strength, Volume Stability, Setting time.

INTRODUCTION

Today, binders are key materials in construction and the construction industry, and the Portland cement industry represents an industrial branch without which the development of human civilization cannot be imagined. Cement is one of the most popular and widely applicable construction materials [1,2].

Cement production accounts for 5% of the total CO_2 emission into the atmosphere caused by human activity. The concept of "green cement" was developed as a replacement for current cement production methods. Green cement uses less natural raw materials, energy and water and is emerging as a substitute for Portland cement. Green cement means cement that is produced with as little consumption of natural raw materials and fossil fuels as possible, and with the maximum use of technogenic waste materials as raw materials for the production of cement and alternative fuels instead of fossil fuels. Research is continuously being carried out for the development of innovative methods of green cement production in order to reduce, and even eliminate, the

corresponding author: nadira.busatlic@unze.ba

emission of gases that enhance the greenhouse effect and other toxic pollutants. In any case, for both environmental and economic reasons, we should resort to the greatest possible use of these waste materials, which has a direct consequence of less exploitation of natural raw materials. One type of such "green cement", which is much more environmentally friendly than ordinary Portland cement, is Portland-composite (mixed) cement [3,4].

Portland-composite cements with mixed additives are cements which according to EN 197-1, in addition to clinker as the main ingredient in the cement and gypsum as a binding regulator, can contain at least two other mineral additives. These additives are granulated blast furnace slag (GBFS), silica dust, pozzolans, fly ash, calcined shale and limestone. The amount of these additives in cement can be from 6 to 35 wt. % [5].

Special importance in cement production is given to the importance of reducing CO_2 emissions in the cement industry. By reducing the content of clinker and using other additives in the production of Portland composite cements, it is possible to reduce CO_2 emissions during production. Not only the environmental aspect is given as an argument for favoring the production of Portland composite cements, but also a sustainable alternative to Portland cement from a technical point of view, because certain additives in the production of Portland composite cements are much softer to grind than pure Portland cement, and thus large amounts of electricity are saved. By the way, the cement industry is one of the largest consumers of heat and electricity. The possibilities of combining several additives (fly ash, GBFS, limestone, silica dust) give Portland composite cement great advantages when using this type of cement in various areas. From a technical point of view, this implies very good development of strength, good workability of the cement composite, and especially durability, while the price of production is important for Portland composite cement manufacturers. The production of Portland composite cements has many advantages [1]:

- increasing cement production without installing new equipment,
- reduction of fuel consumption per ton of cement,
- reduction of CO_2 emissions per ton of cement,
- control of alkali silicate reactivity even with highly alkaline clinker,
- reducing the generation of furnace dust if the alkali content in the clinker is increased,
- improvement of workability due to the replacement of cement with particles of a spherical shape and a smooth surface (fly ash), whereby an additional calcium-silicate hydrate (C-S-H) gel is formed.

The greatest potential advantage of Portland composite cements for users is the achievement of outstanding cement composite properties by using these cements. The production of this type of cement offers the possibility of optimizing the ratio of the already mentioned additives, chemical composition and particle size distribution, all in order to obtain cement with the best properties for different conditions. Possible benefits for cement manufacturers include [1]:

- fly ash and granulated blast furnace slag can be chemically activated by alkalis that can come either from furnace dust or from highly alkaline clinker,
- clinker production can be fully adapted to cement additives,

- joint grinding or mixing of individual components (clinker and additives) in cement plants can contribute to more perfect mixing compared to preparation in concrete plants, therefore a more homogeneous cement composite can be created,
- particle size distribution can be adjusted to minimum standard consistency and optimal reactivity.

Cement manufacturers face various market demands for certain cement properties. Therefore, it is not enough to make a cement that will give adequate strength after 28 days, but one day strength of the cement, stability or resistance to freezing and thawing, resistance to sulfate corrosion, heat of hydration, etc. should also be considered. There is a large amount of information related to the properties of mixed cements, but some phenomena related to them have not yet been fully explained, namely:

- cement additives can have different fineness and composition from one place to another; it has not been determined how many differences can be tolerated or what changes in composition can be compensated for by adjusting the composition of the clinker,
- information on the mutual influence of additives during grinding is not yet complete,
- optimization of particle size distribution becomes more complicated as the number of individual components in cement increases;
- the question is how to obtain the desired particle size distribution in the best possible way, either by joint grinding or mixing or a combination of the two procedures [1].

The aforementioned additives enable cement manufacturers to produce high-quality cements in accordance with strictly defined environmental requirements. By producing Portland composite cement, cement manufacturers can on the one hand save part of the fuel, and on the other hand, increase cement production while maintaining the quality and properties of cement [6].

EXPERIMENTAL

The aim of this work is to examine the possibility of producing more environmentally friendly ("green") cement of the CEM II/B-M (S+LL) class at the Kakanj Cement Factory. Mixed (portland-composite) cements will be obtained by replacing part of the clinker with 26% GBFS (granulated blast furnace slag) and 5% limestone (U1), i.e. 16% GBFS and 5% limestone (U2), while the gypsum content will be the same for both samples (4%). Cement currently produced at the Kakanj Cement Factory of CEM II/B-W 42.5N class is used as a reference sample. These cements should meet the requirements of the EN 197-1 standard.

The practical work consisted of several stages: determination of the chemical and mineralogical composition and specific mass of the raw materials used in this work, mineralogical (microscopic) analysis of the clinker, preparation of mixed cement samples (mixing of the starting components and grinding to the appropriate specific surface in a laboratory ball mill), determination of the chemical composition of cement samples,

determination of the specific mass, specific surface and grinding fineness of cement samples, preparation of cement pastes, determination of the standard consistency, setting time and constant volume of cement pastes, preparation of standard prisms 40×40×160 mm from mortar with mixed cements for strength testing, aging of the prisms in water and their flexural and compressive strength testing (after 2, 7 and 28 days), collection and analysis of the obtained results.

For the experimental part of this work, the following were used: standard clinker from the Kakanj Cement Factory, marly limestone "Ribnica", granulated blast furnace slag from the "ArcelorMittal" Zenica factory and raw gypsum from the Bistrica deposit near Gornji Vakuf.

RESULTS AND DISCUSSION

Chemical, mineralogical and microscopic analysis of clinker

The results of the chemical analysis of clinker, performed on an XRF device, are given in Table 1. The mineralogical composition of clinker according to XRD analysis is given in Table 2.

Table 1 Chemical composition of clinker

Oxides	SiO_2	Al_2O_3	Fe_2O_3	CaO	MgO	SO_3	Na_2O	K_2O	Free CaO	Chlorides
wt.%	21.67	5.44	3.09	65.86	1.14	0.79	0.08	0.65	0.70	0.001

Table 2 Mineralogical composition of clinker

Minerals	C_3S	C_2S	C_3A		C_4AF	Arcanite K_2SO_4	Portlandite $Ca(OH)_2$
			Cubic	Orthorhombic			
wt. %	64	16	4.7	0.4	10.0	1.3	1.8

Chemical and mineralogical analysis of granulated blast furnace slag

In order to use granulated blast furnace slag as an ingredient in cement production, the following conditions must be met:

- at least 2/3 of the blast furnace slag particles must be in a glassy (amorphous) state,
- $(CaO+MgO+SiO_2) \geq 66.6$ wt. %
- $(CaO+MgO)/(SiO_2) > 1.0$

The specific mass of granulated blast furnace slag is 2.58 g/cm^3. The results of the chemical composition of granulated blast furnace slag are given in Table 3.

Table 3 Chemical composition of GBFS

Oxides	SiO_2	Al_2O_3	Fe_2O_3	CaO	MgO	SO_3	Na_2O	K_2O	Chlorides
wt. %	39.90	7.70	1.58	36.70	6.98	0.89	0.34	1.22	0.001

The Table 3 shows that granulated blast furnace slag meets both conditions of the EN 197-1 standard, i.e. sum $(CaO+MgO+SiO_2)=83.58 \geq 66.6$ wt.%, and the ratio

(CaO+MgO)/(SiO_2)=1.09 ≥ 1.0. The results of the mineralogical composition of GBFS are given in Table 4, from which it can be seen that the slag is dominated by the glassy (amorphous) phase with 98.2%.

Table 4 Mineralogical composition of GBFS

Minerals	Glassy phase	Mervinite(C_3MS_2)	Akermanite (C_2MS)	Quartz (SiO_2)	Calcite ($CaCO_3$)
wt. %	98.2	0.1	0.7	0.1	0.8

Marly limestone "Ribnica"

According to EN 197-1, marly limestone must meet the following conditions:
a) the content of calcium carbonate ($CaCO_3$) must be at least 75 wt. %,
b) the clay content must not exceed 1.20 g/100 g
c) the total organic carbon content (TOC) must meet one of the following criteria:
- cannot exceed 0.20 wt. % (denoted by LL),
- cannot exceed 0.50 wt. % (denoted by L)

In this work, marly limestone from the "Ribnica" deposit near Kakanj was used, the chemical composition of which is given in Table 5.

Table 5 Chemical composition of marly limestone

Oxides	$CaCO_3$	SiO_2	Al_2O_3	Fe_2O_3	CaO	MgO	SO_3	Na_2O	K_2O	TOC	Clay
wt. %	97.12	1.46	0.76	0.18	54.41	0.60	0.07	0.23	0.07	0.17	0.73(g)

Looking at the results of the chemical composition, the marly limestone that was used as a mineral additive to Portland-composite cement meets all the conditions prescribed by the EN 197-1 standard.

Chemical and mineralogical composition of gypsum

The chemical composition of gypsum from the deposit "Bistrica" near Gornji Vakuf is given in Table 6, and the mineralogical composition is given in Table 7.

Table 6 Chemical composition of gypsum

Oxides	SiO_2	Al_2O_3	Fe_2O_3	CaO	MgO	SO_3	Na_2O	K_2O
wt. %	4.10	1.27	0.40	33.23	3.12	44.09	0.14	0.53

Table 7 Mineralogical composition of gypsum

Minerals	Gypsum $CaSO_4*2H_2O$	Dolomite $CaMg(CO_3)_2$	Calcite $CaCO_3$	Quartz SiO_2	Ilite $(K,H_3O)Al_2Si_3AlO_{10}(OH)_2$
wt. %	88.3	4.7	1.8	2.2	3.0

Chemical composition of prepared cement samples

The chemical analysis of mixed cement samples is given in Table 8. The Table shows that with an increase in the content of clinker and a decrease in the content of granulated blast furnace slag, the content of CaO increases and SiO_2 decreases, while the content of

other oxides changes slightly. It can be concluded that the prepared cement samples meet EN and BAS standards in terms of chemical composition.

Table 8 Chemical composition of mixed cement samples

Sample label	SiO_2	Al_2O_3	Fe_2O_3	CaO	MgO	SO_3	Na_2O	K_2O
	wt. %							
U1	24.70	5.63	2.45	56.40	2.71	2.51	0.16	0.76
U2	22.69	5.38	2.61	59.61	2.07	2.50	0.13	0.70
CEM II/B-W 42.5N	26.84	9.58	4.64	52.02	1.63	2.82	0.17	0.87

Physical characteristics of prepared cement samples

The test results of specific mass, specific surface and residue on the 0.09 mm sieve are shown in Table 9. From the results shown in the Table 9, it can be seen that samples U1, U2 and CEM II/B-W 42.5N have similar specific mass, which slightly increases with by increasing the clinker content. The specific surface areas of the samples are approximately the same because we tried to grind all the samples equally.

Table 9 Specific mass, specific surface and residue on the 0.09 mm sieve of cement samples

Sample label	Specific mass (g/cm^3)	Specific surface (cm^2/g)	Residue on the 0.09 mm sieve (%)
U1	2.95	3970	1.8
U2	3.01	3990	1.9
CEM II/B-W 42.5N	2.99	3614	0.5

Standard consistency and setting time of samples

The test results of standard consistency, initial and final setting time, as well as volume constancy are given in table 10.

Table 10 Results of testing the initial and final setting time of samples

Sample label	Initial setting time (min)	Final setting time (min)	Standard consistency (%)	Expansion (mm)
U1	140	210	24.5	0.5
U2	170	230	24.0	0.5
CEM II/B-W 42.5N	191	242	26.4	0.5

From the results given in Table 10, it can be concluded that with a change in the content of granulated blast furnace slag in samples U1 and U2, their values for standard consistency change slightly. It is also evident from the table that samples U1, U2 have a somewhat shorter initial and final setting time compared to the reference cement CEM II/B-W 42.5N. The sample with a higher content of granulated slag (U1) has a shorter setting time. The results of the volume constancy (expansion) test show that both samples have the same result values for volume constancy, i.e. that the expansion of both samples is 0.5 mm, and considering that the EN 196-3 standard for determining

expansion allows a tolerance of ≤ 10 mm, it means that the samples meet the requirements of the standard. Also, the 0.5 mm expansion of the samples shows that there is very little free CaO and MgO in these samples, which affect the internal stresses of the cement. All tested sizes for both samples meet the standard prescribed values.

Testing of flexural and compressive strength of cement mortars

The results of flexural strength tests after 2, 7 and 28 days of hydration are given in Table 11.

Table 11 Flexural strength test results

Flexural strength (MPa)			
Sample label	Test time		
	2 days	7 days	28 days
U1	4.2	5.8	8.2
U2	5.4	6.4	8.3
CEM II/B-W 42.5N	3.2	5.5	7.9

From the results shown in Table 11, it can be seen that regardless of the different slag content, the flexural strength of both samples shows similar values after 2, 7 and 28 days. It can be concluded that after 28 days of hydration, both samples (U1 and U2) have slightly higher flexural strength values compared to the reference sample. The results of the compressive strength test after 2,7 and 28 days are given in Table 12.

Table 12 Compressive strength test results

Compressive strength (MPa)			
Sample label	Test time		
	2 days	7 days	28 days
U1	20.0	35.0	51.6
U2	26.2	40.0	58.5
CEM II/B-W 42.5N	17.7	33.4	52.3

From Table 12, which shows the values for the samples, it can be seen that the reference sample CEM II/B – W 42.5N has a lower compressive strength after 2 and 7 days compared to U1 and U2, and after 28 days it has a lower strength than U2, and the approximate compressive strength with the sample U1. It is also visible that the sample with a lower content of blast furnace slag (U2) has a higher compressive strength at every moment than sample U1, which has a higher content of blast furnace slag.

Discussion of results

Table 1 shows the chemical analysis of clinker, and Table 2 shows the mineralogical analysis of clinker determined on a diffractometer (XRD). The ratio of alite and belite is 4:1, which shows that the firing conditions were very good and that such clinker is very reactive. The content of free CaO is 0.7%, and the clinker is considered to be well fired if the content of free CaO is between 0.8-2.0%. According to EN 197-1, the content of MgO in clinker must not exceed 5 wt. %, and the chemical analysis shows that the MgO content

in the clinker is much lower than the standard prescribes. Also, the sum of alite and belite must be at least 66 wt. % of the total amount of minerals. Table 2 shows that this amount is 70 wt. %. The mass ratio of CaO/SiO_2 must not be less than 2 (for clinker from the Kakanj cement factory, this amount is 3.04, Table 1).

Table 3 shows the chemical composition of granulated blast furnace slag, and according to the EN197-1 standard, the total content of CaO, SiO_2 and MgO must be greater than 66.6%, and the granulated blast furnace slag used for these tests has the content of these components 83.58% and that the ratio $(CaO+MgO)/SiO_2$ should be greater than 1.0, and that ratio for granulated blast furnace slag is 1.09. In Table 4, a mineralogical (phase) analysis is given, from which it can be seen that the glassy phase in the slag accounts for 98.2%, and that the standard foresees a minimum of 2/3 of the glassy phase.

Table 5 shows the characteristics of the marly limestone that was used in the given tests, and it can be concluded that it fully meets the conditions given by the standards in terms of $CaCO_3$ content (97.12 wt. %), TOC content (0.17 wt. %) and clay content (0.73 wt. %).

Table 9 shows the results of the sieve analysis, more precisely the residue on the 90 μm sieve, and the results show that this value was 0.10% for both cement samples, and according to the EN 196-6 standard, the maximum allowed residue on the same sieve must is ≤ 10.0%, which means that the rest on the sieve also meets the standard. Such a small residue on the sieve is attributed to the newer generation separator used in the production of cement at the Kakanj Cement Factory.

The specific surface is determined by the Blain method. The results of these tests are given in Table 9. The results show that the specific mass of cement increases with increasing clinker content in the samples, which is logical because clinker has the highest specific mass of all the components used in the production of this cement.

Standard consistency, setting time and volume constancy are determined according to EN 196-3. The standard consistency of cement samples is very similar. The difference in the initial and final setting time between the samples is not great. The reference cement sample CEM II/B-W 42.5N used in the Kakanj Cement Factory has a longer initial and final setting time compared to the prepared samples U1 and U2.

Volume constancy (expansion) is the same for all samples and amounts to 0.5 mm (Table 10), which means that the mentioned samples do not have expansion, which meets the BAS EN 197-1 standard, and this property is one of the most important in terms of durability of cement composites. The reason for the very low expansion of these cements is that all samples have a very low content of free CaO and MgO, which affect the internal stress of the cement due to subsequent hydration.

Table 12 gives the results for the compressive strength as it is required according to the standard EN 197-1. Both samples have values of compressive strength after 2 days greater than 10 MPa and meet the requirements of the EN 197-1 standard. The samples after 28 days meet the requirements of the EN 197-1 standard in terms of compressive strengths and have values higher than 42.5 MPa. The CEM II/B-W 42.5N sample used in the Kakanj Cement Factory has lower compressive strength after 2 and 7 days. After 28 days, sample CEM II/B-W 42.5N has higher compressive strength than sample U1, and lower than sample U2.

CONCLUSION

According to the test results, the samples of more environmentally acceptable (mixed) cement meet the EN 197-1 standard in terms of physical-mechanical properties both after the initial period (2 days) and after the final period (28 days) of hydration. In general, increasing the content of mineral additives (granulated blast furnace slag) and decreasing the clinker content results in environmental and economic advantages. The production of the new class of cement U1 would reduce the production of clinker by the corresponding percentage of clinker. The Kakanj cement factory currently produces CEM II/B – W 42.5N with a clinker content of about 70%, and if U1 cement containing 65% clinker were produced, the exploitation of natural resources would be reduced, i.e. raw material for the production of clinker, and as a consequence CO_2 emission into the atmosphere would also decrease. As a final goal, financial benefits would be realized because clinker is the most expensive component in the production of cement. The test results of the new class of cement U2, due to its increased compressive strength after 28 days of hydration, meet the requirements of the EN 197-1 standard for the higher class of cement (52.5N). The Kakanj cement factory currently produces cement class CEM I 52.5N with a clinker content of 96%, and if U2 cement containing 75% clinker was produced, it would really lead to great savings, both financially and in terms of reducing CO_2 emissions into the atmosphere.

On the other hand, the use of granulated blast furnace slag would increase, and this would mean less accumulation of that material in existing landfills. The addition of marly limestone to previous cement samples contributes to the reduction of gas emissions, mostly CO_2. Since the Kakanj cement factory has a concession on the "Ribnica" quarry, there would be significant financial savings in this regard.

REFERENCES

1. Bušatlić, I., Bušatlić, N., Merdić, N., Haračić, N. (2020) Osnove hemije i tehnologije Portland cementa, Zenica.
2. Brzaković, P. (2000) Priručnik za proizvodnju i primjenu građevinskih materijala nemetaličnog porekla, Orion, Beograd.
3. Petrovski, P., Bušatlić, I. (2006) Cementi i druga neorganska mineralna veziva, Hijatus, Zenica.
4. Đureković, A. (1996) Cement, Cementni kompozit i dodaci za beton, Institut građevinarstva Hrvatske i Školska knjiga, Zagreb.
5. Evropski standard EN 197-1:2013.
6. Merdić, N. (2015) Doktorska disertacija, Razvoj nove klase portland-kompozitnih cemenata u tvornici cementa Kakanj, Zenica.

XV International Mineral Processing and Recycling Conference
17-19 May 2023, Belgrade, Serbia

VEGETABLE INDUSTRY BY-PRODUCTS AS RAW MATERIALS IN FUNCTIONAL FOOD PRODUCTION

A. Stojićević[1#], M. Antić[2], M. Purić[1]
[1] The Academy of Applied Technical Studies Belgrade - Technical College of Applied Studies Požarevac, Serbia
[2] Faculty of Agriculture, Belgrade, Serbia

ABSTRACT – Food industry generate large amounts of by-products which are environmental and economic problem. The utilization of food by-products become strong global demand especially bearing in mind they are unused source of valuable compounds (dietary fibre, proteins, pigments and phenolics). Addition of vegetable by-products to enhance functional properties of food products proved to be successful as well as partial substitution of fat or wheat fluor to developed the low-fat, gluten-free or fiber-rich food products. This paper summarized the results of the latest research in valorization of vegetable processing industry by-products with a focus on the carrot, beetroot, tomato and potato by-products.

Keywords: Food Industry, Utilization, Vegetable By-Products, Functional Ingredients.

INTRODUCTION

Food industry by-products represent severe global issue especially in developed countries. Overproduction of food, population expansion and economic growth includes a big amount of waste [1]. Some food industry sectors generate enormous amounts of residues which are an enviromental and economic problem. Food by-products are a rich source of different phytochemicals (antioxidants, dietary fibers, proteins, natural colorants, aroma compounds etc.), they are not utilized and mostly used as a cheep cattle feed and for soil fertilization. Food by-products can be used directly as food components or biomolecules are extracted, purified, concentrated and reused as functional ingredient in the food industry [2,3]. Proper use of by-products as raw materials or food additives, could generate economic gains for the industry, contribute to reducing nutritional problems, would produce beneficial health effects and would reduce the environmental implications that generate mismenagement of waste [4].

For that reason, in recent years there is a growning interest of producers and researchers to examine the possibilities of utilization of by-products which remains after industrial processing of vegetables. Vegetable by-products are considered as good sources of dietary fibre and other biologically important compounds [5]. These valuable by-products can improved nutritional, functional and technological quality of food products which are very well accepted. As vegetable by-products rich source of dietary

corresponding author: astojicevic@atssb.edu.rs

fibre, the valorization of these by-products contribute to increasing the intake of these valuable compounds. The incorporation of fibers into bakery, meat and dairy products was successful, especially at the level of 10% or less [6].

In addition, during the usage of by-products certain challenges and limitations may occure. In food processing industry, food waste require further processing before being used in food products. This transformation impies high cost in research and development [7]. As the component of interest should be extracted, the selection of appropriate extraction conditions is crucial at this stage. Elimination of toxic materials and antinutritional factor should be considered as well [3]. Also, sensory evaluation showed that higher levels of added by-products are not favorable because in some cases had negative impact on taste, texture, colour or overall acceptabillity of fortified and developed products [6,8,9].

Thus, the purpose of this paper was to sumarizing the latest results of investigation of usage vegetable industry by-products in order to obtain new or impoved food products. Special emphasis is placed to the carrot, beetroot, tomato and potato processing industry by-products.

Carrot

Carrot is traditionally used for the preparation of salads and soups, and at the industrial level, to obtain products such as juice, carrot concentrate, dry powder and canned carrots [10]. During the production of carrot juice, up to 50% of the row material mass is lost as pomace, but for economic and logistical reasons it is not subjected to futher processing [11]. Carrot pomace (CP) is rich source of fiber: 52% total dietary fiber of which insoluble dietary fiber made 42% [12]. Aside from health-promoting effects, in food matrices, dietary fibres have shown potential as fat, sugar, and flour replacer to improve textural, rheological or sensorial properties [6]. After juice producing, in CP remains up to 80% of present carotenoids [13]. Natural carotenoids are more popular as food aditives than synthetic colors due to legislative actions and consumers concerns [2,14]. Also, their intake has a multiple benefit on the human health. Improving functional characteristics of food products by addition of bioactive compounds from carrot waste was aim of several studies. Šeregelj et al. [2] examined the fortification of yogurt with 2.5 and 5.0 g/100g of encapsulated carrot waste extract. Both applied concentrations provided a part of β-carotene recommended daily intake while all physico-chemical and microbiological properties of the fortified yogurts did not change to the end of the examination period. Improving of physico-chemical properties of yogurt with addition of carrot waste extract was also confimed by Sharifi et al. [14]. In addition, carrot waste improve antioxidant properties of fortified yogurt and act as prebiotic for probiotic bacteria increasing their survival. Prebiotic capacity of CP flour was confirmed by Hernández-Alcántara et al. [12]. These authors found that apple peel flour and carrot bagasse flour promoted the growth of lactic acid bacteria while banana peel flour obtained poor results as prebiotic. CP powder was examined as a functional ingredient for a wheat rolls and biscuits [5,10]. Kohajdova et al. [5] stated that blend of flours which contained up to 3% of CP powder enable production of wheat rolls with acceptable quality while higher levels of CP powder (5% and 10%) are not preferable due to their negative impact on rheological

parameters of dough and sensory properties of wheat rolls. The replacement of durum wheat semolina with millet flour and CP powder in order to achieve better cooking qualities, color and textural properties of pasta was investigated by Gull et al. [13]. Maximum addition of CP flour was 4 g/100g on flour basis. On the other hand, higher level of substitution are nutritionally desirable but it leads to lower cooking qualities i.e cooking loss and firmness. Chepkosgei and Orina [15] investigated the replecement of wheat flour with soybean and CP flour in instant fried noodles production. Noodles made from 80% wheat flour, 15% soybean flour and 5% of CP flour has improved nutritional quality and sensory attributes. Kultys and Moczkowska-Wyrwisz [11] examined CP as a functional ingredient of pasta. Addition of 10% of CP was characterized as pasta with very good technological properties and positive consumer acceptance. Majzoobi et al. [16] investigated the effects of CP (0-30%) on quality of batter and gluten-free cakes. Result of this study indicate that addition of CP in level of 30% can promote reological, sensory and nutritional quality.

Beetroot

Beetroot is globally consumed as part of the normal diet and used to fabricate a natural food coloring agent (E162) and ready-to-drink nonalcoholic beverages [17]. After beetroot processing, large quantities of beetroot pomace (BRP) remains as a by-product. Though still rich in valuable compounds and with proven antioxidant and antipoliferative activity, BRP from the juice industry (15-30%) is disposed as feed and manure [18]. Potential of BRP utilization lays in the high dietary fiber content and sighnificant amount of antioxidants, such as nitrogenous pigments (betalains) and polyphenolics [17]. Jovanović et al. [17] developed a yogurt premix based on BRP flour. These authors patented the fermented beverage with improved functional properties where BRP flour was employed as a source of dietary fibres and carrier of lactic acid bacteria. The influence of incorporation different levels (2-10%) of BRP powder on rheological and sensory quality of wheat rolls was investigated [9].

The most acceptable baked rolls from assessors were rolls with addition of 2% of BRP powder while higher levels had a negative impact on both sensory and physical properties. The application of BRP extract or powder for improving of nutritional and technological properties of cookies and biscuits was successfull in moderate applied levels [19,20].

Abdo et al. (2021) invenstigated addition of various concentration (5-20%) of BRP powder to biscuits. It was observed that biscuits with 15% of beetroot powder exhibited a notable enhancement in the chemical and sensory parameters. Incorporation of developed beet biscuit in a daily intake by 10% showed an antianemic effect after 14 days feeding which authors attributed to the high iron content. Effects of BRP extracts (pure and microencapsulated) addition on antioxidant properties, heat damage and color of biscuits enriched with pseudocereals were examined by Hidalgo et al. (2018). The microancapsulate-enriched biscuits had the highest contents of betanin, isobetanin, total phenolics and antioxidant capacity. Substitution of wheat flour with different levels of BRP powder and CP powder in order to produce fiber rich biscuits was succesfull in terms of phisico-chemical and sensory characteristics [21].

Tomato

Million tons of tomatoes are processed yearly to produce juice, sauces, purees, ketchup, pastes and canned which generate large quantities by-products such as peels and seeds, together with small amounts of pulp [1,22]. Around 40% of fresh tomatoes produced is considered waste they do not achive the standards of commercializaiton [23]. Tomato residues are a good source of bioactive molecules, especially carotenoids, such as β-carotene and lycopene, which confers not only high nutritional value but also beneficial health properties, due to their antioxidant capacity [4]. Incorporation of tomato pomace (tomato peel and tomato seed) (TP) in formulation of extruded snack product was aim of study which was conducted by Karthika et al. [7]. Based on results obtained in this study, the best formulation of nutritious fiber enriched snack food with high desirabillity was the one consisting of 40% corn flour, 30% rice flour, 25% tomato peel and 5% tomato seed. Different level of TP (6% and 10%) were incorporated in bread to improve some technological properties [22]. It was found that the acceptabillity of bread was decreased with the increasing of TP concentration and that 6% of TP addition showed high sensory quality and acceptable physiochemical properties. Addition of tomato waste in meat products is studied as well. Savadkoohi et al. [24] examined the usage og bleached TP in beef frankfurters, beef ham and meat-free sausage products. Improvement of hardness and chewiness of sausages with addition of tomato waste was observed while there was no significant difference in the colour compared to control sample. So et al. [25] investigated the addition of dried tomato waste powder in different levels to improve the quality of frankfurter sausage made from Thai native beef. The addition of higher levels of tomato waste powder promoted the sensory properties and lycopene content but in the same lipid oxidation was increased. Tomato fiber pectin recovered from TP was applied as a potentional fiber source and fat replacer in low-fat beef burger [26]. Samples with fat replacement levels of 12.5% and 25% of tomato fiber pectin (2.5% and 5% fiber pectin addition) had the highest acceptance while all levels of tomato fiber pectin could improve the cooking properties of burger. Bread and muffin were supplemented with TP (5-50%) in order to enchance with bioactive compounds such as fibers, vitamin C, minerals and antioxidants [27]. Improvement of bread and muffin were observed in crude fiber content, vitamin C content and softer texture than control samples while sample with 35% of TP of flour weight was with acceptable sensory properties. Low calorie jams with increased content of dietary fibre made from TP were developed by Belović et al. [28]. Jam formulations were characterized by a lower total carbohydrate content and energy value. Further, developed TP jams contained 15-20 times more dietary fibre than commercial jams.

Potato

Potato manufacturing industries generate a huge volume of potato waste [23]. Such waste includes potato wastewater, pulp and peel which are mainly formed during the production of potato chips and fries. Potato peel waste is a major waste from the potato which can be used as a potential source of functional and biocative compounds including antioxidants, dietary fibre, minerals, vitamins and pigments [29]. In order to

improve certain nutritional and technological characteristics of existing products or to develop new, potato waste is successfully incorporated in some bakery and confectionary products. Based on physical and sensory acceptability, incorporation of potato pulp (200-800 g/kg of rice flour) into gluten-free biscuits was successfull [30]. Formulation of biscuit with substitution of rice flour with 600 g/kg of potato pulp was with best scores of all tested proterties. Biscuits prepared from wheat flour blends containing 5-15% of extracted fiber from potato peel were investigated by Dhingra et al. [8]. Results of this study indicated that addition of potato peel fibre above 5% led to alteration of physical and sensory charasteristics of prepared biscuits. Utilization of potato peel extract as a source of natural antioxidants for stabilization of fat in biscuits was examined [31]. Based on sensory evaluation biscuits with addition of 0.5% and 1% potato peel extract were the most acceptable. Methanolic extract revealed an excellent antioxidants activity compared to synthetic antioxidant and other extracts applied. Partial replacement (45%) of wheat flour of biscuits by potato starch recovered from fries processing effluent was study conducted by de Morais et al. [32]. Formulated biscuits have good physical and microbiological conditions and being able to be consumed for a period of 180 days. Potato peel extract was used as a natural antioxidant which prevent lipid oxidation in soybean oil [29]. In acelerated storage condition, potato peel ethanolic extract was able to limit lipid oxidation minimising peroxide and anisidine value.

CONCLUSION

Although the vegetable by-products contain valuable components which can be reintegrated into food products, the largest amounts of this valuable food industry waste still remains unused or used as cattle feed. This cheep and widely available source of fiber, natural antioxidants and colourant can be directly or in form of purified extracts added into food products to improve nutritional and technological characteristics. The results of the latest researches in the field utilization of by-products, clearly demonstrated that application of vegetable by-products can improve the quality of existing products or develop new ones. Moreover, the amount of food industry waste and its negative impact on the environment are reduced.

REFERENCES

1. Szabo, K., Mitrea, L., Călinoiu, L.F., Teleky, B.E., Martău, G.A., Plamada, D., Pascuta, M.S., Nemeş, S.A., Varvara, R.A., Vodnar, D.C. (2022) Natural Polyphenol Recovery from Apple-, Cereal-, and Tomato-Processing By-Products and Related Health-Promoting Properties. Molecules, 27 (22), 7977.
2. Šeregelj, V., Pezo, L., Šovljanski, O., Lević, S., Nedović, V., Markov, S., Tomić, A., Čanadanović-Brunet, J., Vulić, J., Šaponjac, V.T., Ćetković, G. (2021) New concept of fortified yogurt formulation with encapsulated carrot waste extract. LWT, 138, 110732.
3. Capanoglu, E., Nemli, E., Tomas-Barberan, F. (2022) Novel approaches in the valorization of agricultural wastes and their applications. Journal of Agricultural and Food Chemistry, 70 (23), 6787-6804.
4. Torres-León, C., Ramírez-Guzman, N., Londoño-Hernandez, L., Martinez-Medina, G.A., Díaz-Herrera, R., Navarro-Macias, V., Alvarez-Pérez, O.B., Picazo, B., Villarreal-Vázquez,

M., Ascacio-Valdes, J., Aguilar, C.N. (2018) Food waste and byproducts: An opportunity to minimize malnutrition and hunger in developing countries. Frontiers in sustainable food systems, 2, 52.

5. Kohajdová, Z., Karovičová, J., Jurasová, M. (2012) Influence of carrot pomace powder on the rheological characteristics of wheat flour dough and on wheat rolls quality. Acta Scientiarum Polonorum Technologia Alimentaria, 11 (4), 381-387.
6. Soleimanian, Y., Sanou, I., Turgeon, S.L., Canizares, D., Khalloufi, S. (2022) Natural plant fibers obtained from agricultural residue used as an ingredient in food matrixes or packaging materials: A review. Comprehensive Reviews in Food Science and Food Safety, 21 (1), 371-415.
7. Karthika, D.B., Kuriakose, S.P., Krishnan, A.V.C., Choudhary, P., Rawson, A. (2016) Utilization of by-product from tomato processing industry for the development of new product. Journal of Food Processing and Technology, 7, 608.
8. Dhingra, D., Michael, M., Rajput, H. (2012) Physico-chemical characteristics of dietary fibre from potato peel and its effect on organoleptic characteristics of biscuits. Journal of Agricultural Engineering, 49 (4), 25-32.
9. Kohajdová, Z., Karovičová, J., Kuchtová, V. Lauková, M. (2018) Utilisation of beetroot powder for bakery applications. Chemical Papers, 72, 1507-1515.
10. Catană, M., Catană, I., Asănică, A.C., Lazăr, M.A., Constantinescu, F. (2022) Fortification of biscuits with carrot pomace powder in order to increase the nutritional value and antioxidant capacity. Scientific Paper. Series B: Horticulture, 66 (2), 369-375.
11. Kultys, E., Moczkowska-Wyrwisz, M. (2022) Effect of using carrot pomace and beetroot-apple pomace on physicochemical and sensory properties of pasta. LWT, 168, 113858.
12. Hernández-Alcántara, A.M., Totosaus, A., Pérez-Chabela, M.L., (2016) Evaluation of agro-industrial co-products as source of bioactive compounds: fiber, antioxidants and prebiotic. Acta Universitatis Cibiniensis. Series E: Food Technology, 20 (2), 3-16.
13. Gull, A., Prasad, K., Kumar, P. (2015) Effect of millet flours and carrot pomace on cooking qualities, color and texture of developed pasta. LWT- Food Science and Technology, 63 (1), 470-474.
14. Sharifi, Z., Jebelli Javan, A., Hesarinejad, M.A, Parsaeimehr, M. (2023) Application of carrot waste extract and Lactobacillus plantarum in Alyssum homalocarpum seed gum-alginate beads to create a functional synbiotic yogurt. Chemical and Biological Technologies in Agriculture, 10 (1), 3.
15. Chepkosgei, T.M., Orina, I. (2021) Quality and sensory properties of instant fried noodles made with soybean and carrot pomace flour. African Journal of Food Science, 15 (3), 92-99.
16. Majzoobi, M., Vosooghi Poor, Z., Mesbahi, G., Jamalian, J., Farahnaky, A. (2017) Effects of carrot pomace powder and a mixture of pectin and xanthan on the quality of gluten-free batter and cakes. Journal of texture studies, 48 (6), 616-623.
17. Jovanović, M., Zlatanović, S., Micić, D., Bacić, D., Mitić-Ćulafić, D., Đuriš, M., Gorjanović, S. (2021) Functionality and palatability of yogurt produced using beetroot pomace flour granulated with lactic acid bacteria. Foods, 10 (8), 1696.
18. Vulić, J., Čanadanović-Brunet, J., Ćetković, G., Tumbas, V., Djilas, S., Četojević-Simin, D., Čanadanović, V. (2012) Antioxidant and cell growth activities of beet root pomace extracts. Journal of functional foods, 4 (3), 670-678.
19. Abdo, E.M., Shaltout, O.E.S., El-Sohaimy, S., Abdalla, A.E., Zeitoun, A.M. (2021) Effect of functional beetroot pomace biscuit on phenylhydrazine induced anemia in albino rats: Hematological and blood biochemical analysis. Journal of Functional Foods, 78, 104385.

20. Hidalgo, A., Brandolini, A., Čanadanović-Brunet, J., Ćetković, G., Šaponjac, V.T. (2018) Microencapsulates and extracts from red beetroot pomace modify antioxidant capacity, heat damage and colour of pseudocereals-enriched einkorn water biscuits. Food chemistry, 268, 40-48.
21. Parveen, H., Bajpai, A., Bhatia, S., Singh, S. (2017) Analysis of biscuits enriched with fibre by incorporating carrot and beetroot pomace powder. The Indian Journal of Nutrition and Dietetics, 54 (4), 403.
22. Nour, V., Ionica, M.E., Trandafir, I. (2015) Bread enriched in lycopene and other bioactive compounds by addition of dry tomato waste. Journal of food science and technology, 52, 8260-8267.
23. Lobo, M.G., Dorta, E. (2019) Utilization and management of horticultural waste. In: Postharvest technology of perishable horticultural commodities (Elhadi M. Yahia) Woodhead Publishing, 639-666.
24. Savadkoohi, S., Hoogenkamp, H., Shamsi, K., Farahnaky, A. (2014) Color, sensory and textural attributes of beef frankfurter, beef ham and meat-free sausage containing tomato pomace. Meat science, 97 (4), 410-418.
25. So, S., Uriyapongson, S., Uriyapongson, J. (2020) Effects of dried tomato waste powder levels on lycopene content, lipid oxidation, color, antioxidant activity, and sensory properties of frankfurter sausage made from Thai native beef. Songklanakarin Journal of Science & Technology, 42 (1).
26. Namir, M., Siliha, H., Ramadan, M. F. (2015) Fiber pectin from tomato pomace: characteristics, functional properties and application in low-fat beef burger. Journal of Food Measurement and Characterization, 9, 305-312.
27. Mehta, D., Prasad, P., Sangwan, R.S., Yadav, S.K. (2018) Tomato processing byproduct valorization in bread and muffin: Improvement in physicochemical properties and shelf life stability. Journal of food science and technology, 55 (7), 2560-2568.
28. Belović, M., Torbica, A., Pajić-Lijaković, I., Mastilović, J. (2017) Development of low calorie jams with increased content of natural dietary fibre made from tomato pomace. Food chemistry, 237, 1226-1233.
29. Amado, I.R., Franco, D., Sánchez, M., Zapata, C., Vázquez, J.A. (2014) Optimisation of antioxidant extraction from Solanum tuberosum potato peel waste by surface response methodology. Food chemistry, 165, 290-299.
30. Batista, J.R., de Morais, M.P., Caliari, M., Soares, J. (2016) Physical, microbiological and sensory quality of gluten-free biscuits prepared from rice flour and potato pulp. Journal of Food and Nutrition Research, 55 (2), 101-107.
31. Rowayshed, G., Sharaf, A.M., El-Faham, S.Y., Ashour, M., Zaky, A.A. (2015) Utilization of potato peels extract as source of phytochemicals in biscuits. Journal of Basic and Applied Research International, 8 (3), 190-201.
32. Morais, M.P.D., Caliari, M., Nabeshima, E.H., Batista, J.E.R., Campos, M.R. H., Soares Junior, M.S. (2018) Storage stability of sweet biscuit elaborated with recovered potato starch from effluent of fries industry. Food Science and Technology, 38, 216-222.

XV International Mineral Processing and Recycling Conference
17-19 May 2023, Belgrade, Serbia

CARBON NANOTUBES AS POTENTIAL MATERIAL FOR WASTEWATER TREATMENT - A REVIEW

A. Petrović[#], R. Marković, D. Božić
Mining and Metallurgy Institute Bor, Bor, Serbia

ABSTRACT – The integrity of ecosystem is significantly impacted by water quality. Scientists and researchers are always searching for innovative wastewater treatment methods. Purification of water is only one of the many scientific and technological uses of carbon nanotubes. For the elimination of different water contaminants, carbon nanotubes have proven to be an economical, efficient, and ecologically responsible alternative to current water treatment techniques. Utilizing carbon nanotubes for wastewater treatment is reviewed and evaluated in this article, along with how various carbon nanotube structures react in different ways.

Keywords: Carbon Nanotubes, Water Purification, Wastewater Treatment, Inorganic Pollutants.

INTRODUCTION

Water pollution is becoming a significant issue worldwide and a major challenge for humans and the environment as a result of industrial expansion, increasing urbanization, and climate change [1]. With the world's rapidly increasing population, the World Bank predicted that by 2030, there would be a 40% gap between forecast demand and available supply of water [2]. Purification of contaminated water (including drinking water, groundwater and surface water) demands both the improvement of existing wastewater treatment technology and the introduction of new ones. Supplying clean and safe water, particularly drinking water, has become a major concern and an important mission in developing nations [3].

A variety of water purifying methods are used to solve this problem. Carbon nanotubes (CNTs)-based water treatment technology is currently one of the prospective leaders [4].

This article offers a review of literature data on the use of carbon nanotubes for the wastewater purification process, which has been one of the most prominent and major areas for their utilization since their development and commercial use. To acquire clean water, it is important to meet the regulatory standards for the cleanliness of the water itself. That could be achieved utilizing the methods mentioned in this article. From an ecological aspect, these methods protect soil from contaminated streams and offer suitable conditions for the maintenance of plant and animals, as well as human health.

[#] corresponding author: ana.petrovic@irmbor.co.rs

NANOMATERIALS FOR WASTEWATER TREATMENT

Nanotechnology is regarded as the important technology of the twenty-first century, with industrial applications. Nanoadsorbents, nanometals, and nanomembranes provide a variety of solutions for environmental problems. It has also been demonstrated that reactive nanostructures are effective in converting harmful pollutants into non-toxic compounds [5]. Since nanomaterials come in a variety of shapes and sizes, they can be distinguish between nanoparticles, nanotubes, nanofibers, nanowires, and nanomembranes. The most fundamental classification of nanomaterials is between inorganic and organic-based nanomaterials. Carbon nanoparticles (graphene, graphene oxide, carbon nanotubes) and boron nitride or silicon nanomaterials are examples of inorganic nanomaterials. The second type of nanoparticle is one that is supported by organic chemicals or polymers. These nanoparticles have a bright future since they are widely used in the removal of organic and inorganic contaminants; nevertheless, when used in high quantities, nanomaterials may have a harmful influence on aquatic organisms [6].

CNTs for wastewater treatment

Sumio Iijima, a Japanese physicist, discovered carbon nanotubes in 1991 [7]. That is one of the carbon allotropes containing one or more graphene layers concentrically rolled, resulting in tubular shapes. CNTs are classified into three types based on the number of graphene layers: single-layered (SWCNTs), double-layered (DWCNTs), and multilayered (MWCNTs) [8].

CNTs are incredibly light and robust materials. Its width ranges from several nanometers to several tens of nanometers and their length ranges from several tens of microns to several tens of microns. The structural characteristics of SWCNT and MWCNT determine their differences in solubility and dispersion [9].

REMOVAL OF HEAVY METALS FROM WATER USING CNT

Water pollutants are divided into inorganic toxic elements, organic chemicals and microorganisms. Inorganic toxic elements include various metallic elements such as mercury, cadmium, lead, chromium and copper. So far, more than one million organic chemicals with different functional groups, properties and applications have been found, synthesized or produced. Organic pollutants mainly include pharmaceuticals, personal care products, organic dyes, pesticides, detergents and common industrial organic wastes such as phenols, halogens and aromatics [6].

Temperature is one of the factors that largely determines the rate and degree of adsorption. The removal of Cd^{2+} by MWCNTs increases with increasing temperature. With increasing temperature, the value of the Gibbs free energy change decreases, resulting in more efficient operation at higher temperature. Besides the temperature, contact time between adsorbent and adsorbate is also a parameter that has a strong influence on the adsorption of ionic metals from solution. Adsorption increases with contact time until equilibrium is reached. Equilibrium was reached within 1 hour when Pb^{2+} ions were adsorbed on the polyamine/CNT composites. Also, the composite of

magnesium oxide and CNT for Pb^{2+} removal showed that the removal is higher with longer contact time. The third key parameter affecting the adsorption capacity is the initial metal ion concentration. The increase in adsorption capacity occurs with a higher initial concentration of metal ions. To be attributed to increased mass transfer from the solution to the adsorbent surface [10].

Methods such as fluorination, cycloaddition, reactions with diazonium salts, oxidation and polymerization of free radicals are used to increase the solubility and reactivity of CNTs. MWCNTs prepared by microwave heating can remove Zn(II) ions from aqueous solution and the removal rate can reach more than 99% [11].

In Enugu, Nigeria, there is a coal mine that includes a coal washery pond. The waste water produced by this process contains hydrocarbons and toxic metals such as iron, lead, chromium, cadmium and arsenic. Relatively high densities and atomic weights of these heavy metals over time can lead to bioaccumulation, which directly causes consequences for the environment and human health. Therefore, the effect of adsorption of Fe^{3+} and Pb^{2+} from these wastewaters using MWCNTs was investigated. 200, 400, 600, 800 and 1000 mg of MWCNTs are added to 1000 ml of the wastewater sample. The removal of the highest amount of Fe^{3+} and Pb^{2+} was achieved at the dosage of 1000 mg of MWCNT. In addition, MWCNTs with the largest length (58.17 mm) and diameter (71 nm) show good Fe^{3+} removal ability, while MWCNTs with the smallest length (38.84 mm) and diameter (45 nm) remove Pb^{2+} well [12].

The removal of arsenic from water is more complicated than the removal of other heavy metals. It is known that arsenic has a rapport with various types of metal oxides with different adsorbent bases. Therefore, adsorption of arsenic ions was carried out using functionalized MWCNTs. MWCNTs were oxidized with a mixture of HNO_3 and H_2SO_4, using ultrasonic treatment for 3 hours at 40 °C. The maximum adsorption capacity of oxidized MWCNTs was 12 mg/g arsenic [13].

In one of the experiments [13], it was investigated the adsorption capacity of Pb^{2+} by CNTs acidified with HNO_3. The initial concentration of Pb^{2+} was 50 mg/L, during 6 h an adsorption capacity of 85 mg/g Pb^{2+} was achieved. If $KMnO_4$ and NaOH are added to HNO_3-treated MWCNTs at 70 °C, a maximum reaction speed of adsorption increases up to 5 min, while the adsorption capacity of these MWCNTs varied depending on the pH of the solution, increasing from 77% to 98% as the pH value moved from 2 to 4. When testing the mixture of sugar cane and MWCNT, at a temperature of 28 °C and an increase in pH value from 1 to 4.5, there was an increase in adsorption capacity as well from 23.4% to 99.8% [14]. These experiments confirmed the fact that with increasing pH value, the adsorption capacity also increases.

Synthesized zeolite carbon nanotubes represent a new adsorbent for the removal of Pb^{2+} ions, producing an adsorption capacity of 55.74 mg/g. One of the latest techniques for removing Pb^{2+} from water solutions is electrochemical adsorption. SWCNT and stainless steel mesh are used as the cathode and anode, respectively. This method achieved a maximum removal efficiency of 97.2% for initial concentrations of 20 mg/dm^3 and 99.6% for initial concentrations of 159 mg/dm^3 [15].

Group of scientists [16] made a comparation between MWCNTs functionalized by $KMnO_4$ / H_2SO_4 and MWCNTs with HNO_3 for removal of Hg^{2+} from water. Adsorption

capacity of functionalized MWCNTs showed higher value than non-functionalized MWCNTs. Sulfur-containing MWCNTs achieved a maximum adsorption capacity of 72.8 mg/g for the removal of Hg^{2+} from water with a good isotherm model, which fits the Langmire equation. Considering this fact it can be concluded that functionalized MWCNTs are better adsorbents of Hg^{2+} than non-functionalized MWCNTs.

CONCLUSION

So far, great progress has been made in the study of nanomaterials as adsorbents of heavy metals and polluting components from the aquatic environment. In this paper, emphasis is placed on carbon nanotubes, because they are adsorbents that are easy to deal with the growing challenges of environmental protection, especially water purification. CNTs offer numerous advantages over other adsorbents and possess unique properties.

Based on previous experiments, CNTs have proven to be excellent adsorbents of heavy metal ions (especially arsenic, cadmium, lead, zinc and mercury). Their efficiency depends on a number of parameters such as the initial concentration of the polluting component, the temperature at which the adsorption process takes place and the contact time between the adsorbent and the treated solution. In lakes, rivers and oceans, the application of CNTs is not a widely applied technology for water pollution control, because despite the good results of experiments at the laboratory level, the technology has not yet been fully explored. An environmental and human health risk assessment should be performed before large-scale applications, as nanomaterials might have toxic effects on aquatic organisms when applied in a large amounts.

ACKNOWLEDGEMENT

The authors are grateful for funding by the Minister of Science, Technological Development and Innovation of the Republic Serbia, the Grant No. 451-03-47/2023-01/ 200052. Also, this work was financially supported by the EU under Interreg – IPA CBC Romania-Serbia Programme and co-financed by the partner states in the Programme. Project Romania Serbia NETwork for assessing and disseminating the impact of copper mining activities on water quality in the cross-border area (RoS-NET2) eMS code RORS - 337.

REFERENCES

1. Stevanović, Z., Obradović, Lj., Marković, R., Jonović, R., Avramović, Lj., Bugarin, M., Stevanović, J. (2013) Mine Waste Water Management in the Bor Municipality in Order to Protect the Bor River Water. In: Waste Water - Treatment Technologies and Recent Analytical Developments (F. S. García Einschlag, L. Carlos), IntechOpen, London, 41-62.
2. https://www.worldbank.org/en/topic/waterresourcesmanagement, (accessed date: 03.03.2023.)
3. Reddy, K.R. (2008) Physical and Chemical Groundwater Remediation Technologies. In: Overexploitation and Contamination of Shared Groundwater Resources (C. J. G. Darnault), Springer, Berlin, 257-274.

4. Mishra, S., Sundaram, B. (2023) Efficacy and challenges of carbon nanotube in wastewater and water treatment. Environmental Nanotechnology, Monitoring & Management, 19, 100764.
5. Nasrollahzadeh, M., Sajjadi, M., Iravani, S., Varma, R.S. (2021) Green-synthesized nanocatalysts and nanomaterials for water treatment: Current challenges and future perspectives. Journal of Hazardous Materials, 401, 123401.
6. Lu, F., Astruc, D. (2020), Nanocatalysts and other nanomaterials for water remediation from organic pollutants. Coordination Chemistry Reviews, 408, 213180.
7. Iijima, S. (1991) Synthesis of Carbon Nanotubes. Nature, 354, 56-58.
8. Vedhanarayanan, B., Praveen, V.K., Das, G., Ajayaghosh, A. (2018) Hybrid materials of 1D and 2D carbon allotropes and synthetic π-systems. NPG Asia Materials, 10, 107–126.
9. Schroeder, V., Savagatrup, S., He, M., Lin, S., Swager, T.M. (2018) Carbon Nanotube Chemical Sensors. Chemical Reviews, 119 (1), 599–663.
10. Verma, B., Balomajumder, C. (2020) Surface modification of one-dimensional Carbon Nanotubes: A review for the management of heavy metals in wastewater. Environmental Technology & Innovation, 17, 100596.
11. Zhu, Y., Liu, X., Hu, Y., Wang, R., Chen, M., Wu, J., Wang, Y., Kang, S., Sun, Y., Zhu, M. (2020) Behavior, remediation effect and toxicity of nanomaterials in water environments. Environmental Research, 174, 54–60.
12. Aliyu, A., Kariim, I., Abdulkareem, S.A. (2017) Effects of aspect ratio of multi-walled carbon nanotubes on coal washery waste water treatment. Journal of Environmental Management, 202, 84e93.
13. Fiyadh, S.S., AlSaadi, M.D., Jaafar, W.Z., AlOmar, M.K., Fayaed, S.S., Mohd, N.S., Hin, L.S., El-Shafie, A. (2019) Review on heavy metal adsorption processes by carbon nanotubes. Journal of Cleaner Production, 230, 783e793.
14. Hamza, I.A., Martincigh, B.S., Ngila, J.C., Nyamori, V.O. (2013) Adsorption studies of aqueous Pb (II) onto a sugarcane bagasse/multi-walled carbon nanotube composite. Phys. Chem. Earth, Parts A/B/C 66, 157e166.
15. Liu, Y., Yan, J., Yuan, D., Li, Q., Wu, X. (2013) The study of lead removal from aqueous solution using an electrochemical method with a stainless steel net electrode coated with single wall carbon nanotubes. Chem. Eng. J., 218, 81e88.
16. Chen, P.H., Hsu, C.-F., Tsai, D.D.-W., Lu, Y.-M., Huang, W.-J. (2014) Adsorption of mercury from water by modified multi-walled carbon nanotubes: adsorption behaviour and interference resistance by coexisting anions. Environ. Technol., 35 (15), 1935e1944.

XV International Mineral Processing and Recycling Conference
17-19 May 2023, Belgrade, Serbia

REMOVAL OF METHYLENE BLUE FROM AQUEOUS SOLUTIONS USING AN IRON-RICH SOIL

M. Marić[1], A. Ivković[2], B. Ivković[3#], A. Janošević Ležaić[3], S. Uskoković-Marković[3], J. Savić[4], M. Milojević-Rakić[1], D. Bajuk-Bogdanović[1]

[1] University of Belgrade-Faculty of Physical Chemistry, 11000 Belgrade, Serbia
[2] The Academy of Applied Technical Studies Belgrade, Belgrade, Serbia
[3] University of Belgrade-Faculty of Pharmacy, 11221 Belgrade, Serbia
[4] School of Pharmacy and Physiotherapy, 11000 Belgrade, Serbia

ABSTRACT – Organic dyes from industry wastewater pollute water tables. Here proposed environmental solution relies on pristine red soil for oxidative degradation of methylene blue dye. Soil analysis comprised spectroscopic (FTIR and Raman) and microscopic (SEM/EDS) techniques, while spectrophotometry was applied for dye quantification. The dominant soil mineral is kaolinite, while Fe homogeneous distribution is witnessed in the γ-FeO(OH) form. Soil/Fenton reagent achieved substantial 93% dye removal. An optimal oxidant concentration in the Fenton system is 10 mM. We confirm the excellent performance of pristine red soil samples as naturally occurring adsorbents and catalysts in Fenton oxidation of environmental pollutants.

Keywords: Methylene Blue, Fenton Reagent, Red Soil, Dye Oxidation.

INTRODUCTION

The uncontrolled release of organic dyes from textile, plastic, printing, paper pulp, paint, and leather industries can contaminate water. Removing these pollutants from wastewater has become decisive because of their adverse effect on the environment. Among various processes available for wastewater treatment, adsorption is the most promising technique, due to its ability to remove different types of pollutants, high efficiency and minimum energy requirement. Various clays with different structures and morphology have been recognized to be effective solid adsorbents for wastewater treatment owing to their high surface area and versatile active sites [1].

In the processes of pedogenesis, primary soil particles of different sizes are created under the influence of physical-chemical and biological decay and decomposition of the parent substrate. The clay fraction (< 0.002 mm) is the most active part of the soil due to its large specific surface area, unique surface chemistry and adsorption characteristics. Clay minerals are a class of hydrated phyllosilicates which form parallel sheets of silicate tetrahedra.

The clay fraction of soil often contains non-phyllosilicate minerals, such as carbonates, feldspars, and quartz along with iron and aluminum hydroxides. The red soils in the Dinarides area are called reddish or red soil (*terra rossa*). Their red colour

corresponding author: blucic@pharmacy.bg.ac.rs

originates from the peptization of amorphous iron hydroxides, whereby crystals of goethite (α-FeO(OH)) and hematite (Fe_2O_3) are formed in the dense base of the soil.

Although many researchers have reported that Fenton-like oxidation using heterogeneous iron catalysts can efficiently degrade dyes, high manufacturing costs are problems that need to be solved [2]. The present study investigated the efficacy of terra rossa (TR), as a natural, inert, nontoxic, environmentally friendly, available, and economical adsorbent, for organic dye removal from wastewater.

EXPERIMENTAL

Terra Rossa soil (TR) is collected from the location in the northern parts of Bosnia and Herzegovina (village of Papažani in the municipality of Laktaši). The soil was sampled in the surface layers (10–20 cm in depth). The dried sample of TR was crushed in a mortar and sieved through laboratory sieves with apertures of 0.5 mm. Then, the aqueous suspension of TR was filtered through a filter paper with a pore diameter of 25 µm. The filtrate was dried at 110 °C. Finally, the soil samples were stored in a desiccator over silica gel. A Phenom ProX scanning electron microscope (Thermo Scientific) with integrated energy−dispersive X−ray spectroscopy (EDS) detector was employed to investigate the surface features and elemental composition of samples. Infrared and Raman spectroscopy were performed on the Nicolet iS20 spectrometer and DXR Raman microscope (Thermo Scientific, USA). The batch adsorption suspensions comprised 10 mg of solid adsorbent and 10 mL of 100 ppm Methylene blue (MB) (Reag. Ph. Eur., Merck) solution. The suspensions were placed in an ultrasonic bath for 10 min. 1 mL of the suspension was centrifuged for 5 min at 13400 rpm and UV–Vis spectra were recorded after 24 h equilibration time on an Evolution 220 spectrometer in a quartz cuvette with an optical path of 0.1 cm.

RESULTS AND DISCUSSION

According to the EDS analysis, the most abundant element in TR is oxygen, due to abundant silicon and aluminum oxides, while iron can be of both inorganic and organic origin. Carbon is attributed to mineral and organic components, while nitrogen is mostly ascribed to organic components. Silicon and aluminum are found in the tested soil in the approximately same amount, about 7-8 wt%, while the iron is present at about 6.6 wt%. In certain, localized recording spots, Fe occurs in a significantly higher concentration, 16.6% (Figure 1).

The FT-IR spectrum of the TR clay fraction (Figure 2a) in the high-frequency region shows four OH stretching vibrations of inner hydroxyls seen at 3700, 3670, and 3650 cm^{-1} (surface) and at 3621 cm^{-1}. These bands are characteristic of kaolinite, one of the polytypes of the kaolin minerals [$Al_2Si_2O_5(OH)_4$], common phyllosilicates. Additional bands at 3420 and 1640 cm^{-1} are assigned to clay-trapped water. In the low-frequency region, the vibrations in the TR can be seen for Si-O stretching at 1105, 1036 and 1004 cm^{-1}, Al-OH bending at 911 cm^{-1} with a shoulder at 935 cm^{-1}, Si-O at 749 and 695 cm^{-1}, Al-O-Si bending at 536 and Si-O-Si bending at 470 cm^{-1} and are all characteristic of kaolin minerals. A weak doublet at 798 and 780 cm^{-1} indicates presence of quartz [3]. Thus, FT-IR spectra show that kaolinite is one of the main constituents of the examined soil.

An important aspect is identifying the various iron species types in the natural red soil. Raman spectroscopy, due to its ability to distinguish between the multiple phases of iron oxides and oxyhydroxides, has been successfully used to identify iron oxides. Raman spectrum of TR (Figure 2b), suggests the presence of lepidocrocite, γ- FeOOH (the bands at 249, 306, 339, 388, 534, 655 and 1298 cm^{-1}) [4], which generally occurs in soils much less frequently than goethite or hematite.

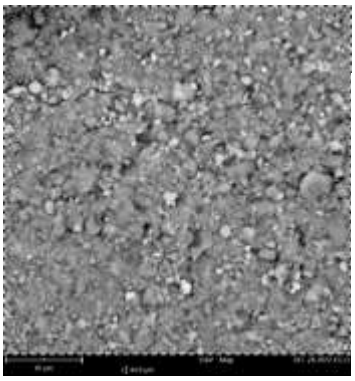

Element Symbol	Atomic Conc. %	Weight Conc.%
O	45.53	44.76
C	37.38	27.59
N	5.75	4.95
Si	4.62	7.98
Al	4.25	7.05
Fe	1.92	6.60

Figure 1 SEM-EDS micrograph (left) with elemental surface composition (right)

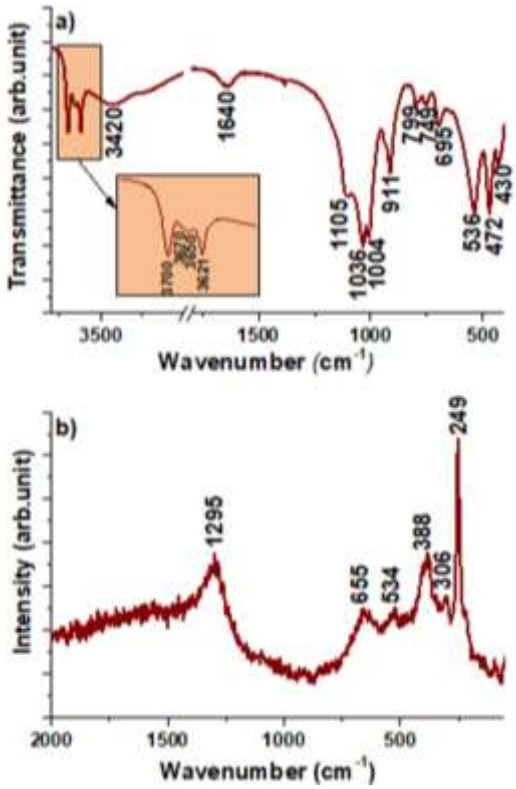

Figure 2 FTIR (a) and Raman (b) spectra of Terra Rossa soil

The UV-Vis spectrum of MB, in the region 400-800 nm, shows two characteristic absorption bands at 662 and 607 nm with their intensities dependent on the monomer/dimer ratio. For accurate quantification of MB, calibration curves are based on the integral band surface instead of the Absorbance value [1]. A minute intrinsic absorption of soil suspension is subtracted from values recorded for the MP/soil suspension.

The equilibrium adsorption quantity is 77 mg g^{-1} for TRS, significantly higher than that obtained for pure kaolin clay, 17 mg g^{-1} [1]. The higher adsorption capacity of TR is a consequence of an additional electron transfer process driven by electrostatic attraction involving the nitrogen in MB and oxygen of Fe_xO_y [5].

The Fenton reaction consists of the degradation of H_2O_2 by ferrous or ferric ions and the formation of $OH^{\bullet}$ radical, a nonspecific oxidant that can degrade pollutants efficiently. In the Fenton process, the concentration of H_2O_2 needs to be optimized to favour the maximum generation of $OH^{\bullet}$, as a concentration above the optimum, leads o the generation of other radicals like $HO_2^{\bullet}$ with lower oxidation potential [6].

The results shown in Figure 3 indicate that the optimal concentration of peroxide in the system is 10 mM, while ten times and hundred times higher concentrations do not lead to a significant increase in the MB removal efficiency.

Without the presence of TR, that concentration of H_2O_2 decolorizes only 4% of the initial concentration of MB.

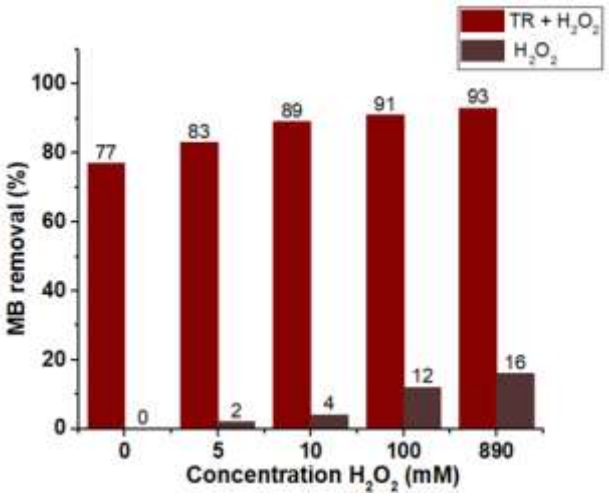

Figure 3 The efficiency of MB removal in the presence of different peroxide concentrations

CONCLUSION

Here investigated is a naturally occurring red soil sample for oxidative degradation of cationic dye, methylene blue. Physicochemical analysis of the red soil sample comprised spectroscopic (FTIR and Raman spectroscopy) and microscopic (SEM/EDS) techniques. Spectral findings reveal that the dominant mineral composition of investigated red soil sample is kaolinite, while Fe is found in the Lepidocrocite phase (γ-FeO(OH).

Microscopy confirms homogeneous surface features of high Fe-content particles. To test whether intrinsically occurring iron species in the soil can take the role of efficient catalysts in the Fenton reagent, an exemplary degradation of organic dye is investigated. First, MB dye removal is analysed with and without oxidant to resolve whether adsorption or oxidative degradation is occurring in the tested system. A significant percentage of initial dye content can be removed by adsorption (77%), while hydroxyl radical formation and dye degradation account for another 16%, giving excellent 93% removal. An experimental optimisation shows that there is an optimal oxidant concentration in the Fenton degradation system of 10 mM peroxide concentration. The presented results point to the excellent performance of pristine red soil samples as naturally occurring adsorbents and catalysts in Fenton oxidation of environmental pollutants.

ACKNOWLEDGEMENT

This research was funded by the Ministry of Science, Technological Development and Innovation (no. 451-03-47/2023-01/200146, and 451-03-47/2023-01/200161).

REFERENCES

1. Popadić, D., Gavrilov, N., Ignjatović, Lj., et al. (2022) How to Obtain Maximum Environmental Applicability from Natural Silicates. Catalysts, 12, 519.
2. Milojević, M., Dondur, V., Damjanović, Lj., et al. (2007) The Activity of Iron-Containing Zeolitic Materials for the Catalytic Oxidation in Aqueous Solutions. Mater. Sci. Forum, 555, 213–218.
3. Madejová, J., Gates, W.P., Petit, S. (2017) IR Spectra of Clay Minerals. Dev. Clay Sci., 8, 107–149.
4. Lafuente, B., Downs, R.T., Yang, H., Stone, N. (2016) The power of databases: The RRUFF project. Highlights Mineral. Crystallogr., 1–29.
5. Zhang, P., O'Connor, D., Wang, Y., et al. (2020) A green biochar/iron oxide composite for methylene blue removal. J. Hazard. Mater., 384, 121286.
6. Veetil Nidheesh, P., Gandhimathi, R., Thanga Ramesh, S. (2013) Degradation of dyes from aqueous solution by Fenton processes: a review. Env. Sci. Pollut. Res., 20, 2099-2132.

XV International Mineral Processing and Recycling Conference
17-19 May 2023, Belgrade, Serbia

BOR DISCRICT RIVERS WATERCOURSES CONTAMINATION BY Cu AND Ni IONS

R. Marković[1#], V. Gardić[1], R. Kovačević[1], Z. Stevanović[1], A. Isvoran[2], V. Marjanović[1], A. Petrović[1]

[1]Mining and Metallurgy Institute Bor, Bor, Serbia
[2]West University of Timisoara, Department of Biology-Chemistry and Advanced Environmental Research Laboratories, Timisoara, Romania

ABSTRACT – The influence of the acid mine drainage and metallurgical wastewater on Cu and Ni ions concentration on the Bor district rivers watercourses is tested in the period from September 2020 to September 2021. Four sampling campaigns are realized in this period. Sampling points are selected in relation to the impact on Bor River, Krivelj River, Bela River, Timok River and Danube River. The presence of Cu and Ni ions in metallurgical wastewater has the dominant influence on the presence of Cu and Ni ions in the Bor district river watercourses.

Keywords: Wastewater, Acid Mine Drainage, Metallurgical, Cu, Ni.

INTRODUCTION

The need for minerals and metals necessary for global development makes mining one of the most important branches of the economy. The development of mining and related industries of production leads to significant economic growth and the benefit of countries on the one hand and on the other hand to the generation of different type of wastes. Mining operations have a huge local impact on the environment and population and the common challenge of all human society is to reduce the pollution and environmental damages produced by different processes. Even if the mining activities are stopped, the accumulated waste continuously pollutes and conduct to environmental damages and health effects. In the Bor Discrict, copper mineralization is mostly porphyry type of deposits containing mainly sulphur minerals associated with pyrites that are one of the sulphuric acid generators in contact with the atmosphere. Generally, the pH drops to values below 4, which causes dissolving of the metal ions [1,2]. Also, mining wastes generated during the copper ore treatment could be divided in the next types: tailings generated during flotation processes containing a variety of metallic and non-metallic minerals, spent ores consisting of the material remaining in either dump or heap leach piles when leaching ceases, acid rain resulting from the combination of rain and SO_2 causing damage to crops, trees and buildings for many miles downwind. Furthermore, the disposal of an enormous volume of tailings dumps poses a serious risk to the surrounding environment through air pollution due to air-dried out tailings,

corresponding author: radmila.markovic@irmbor.co.rs

erosion of the tailings with the potential of valuable land degradation, and leaching of soluble inorganic potentially toxic chemical species (Cu, Ni, Pb, Zn, Cd, and Cr) occurring in a variety of minerals present in the solid wastes [3].

During the metallurgical activities, harmful and dangerous materials also are generated.

In the area of the influence of mining and metallurgy activities the wastewater are discharged into the local watercourses through the Bor and Timok rivers as a tributaries of Danube River [3].

In order to find measures and solutions for the reduction, remediation and elimination of Cu and Ni ions, it is necessary to have a true picture of the consequences of more than a century of continuous mining and metallurgical activities in the Bor District. The influence of the type of wastewater on the Cu and Ni ions concentration in the rivers downstream was analyzing in a period from September 2020 to September 2021 on fifteen sampling points that are selected in relation to the impact on Bor River, Krivelj River, Bela River, Timok River and Danube River as a target river.

EXPERIMENTAL

In this paper, aiming to assess the risk of mining activities in the vicinity of the Bor copper mine from Serbia which pollutes the surface water of Bor and Krivelj rivers with Cu and Ni ions, physico-chemical analysis of the collected samples were performed. Sampling was performed quarterly in the period September 2020 to September 2021, of the Bor River (W5), as well as from locations upstream and downstream of the Bor River (marked W1-W4, W6-W10). The sampling points that are selected for the Cu and Ni ions concentration monitoring are: W1 - Robule accumulation (AMD); W2 - Robule accumulation 1 (AMD); W3 - AMD from flotation tailing dam RTH; W4 - Metallurgical wastewater; W5 - Bor River; W6 - Krivelj River; W7 - Bela River after the confluence of Bor and Krivelj rivers; W8 - Ravna River; W9 - Bela River after flows of Ravna River; W10 - Bela River before of confluence with Timok River; W11 - Timok River before of confluence with Bela River; W12 - Timok River after confluence with Bela River (near the village Rajac); W13 - Timok River (near the village Mokranje); W14 - Timok River (near the village Bukovce); W15 - Danube River (near the village Radujevac). After confluence of Bor and Krivelj rivers downstream from the village of Slatina arises the Bela River. Ravna River which is outline of the copper mining activities inflows in Bela River, and Bela River inflows in Timok River which flows in Danube River. Bor and Krivelj rivers are polluted by the acid mine drainage originating from the active copper mining activities or from delayed mine overburden and flotation tailings. Krivelj River is polluted with the wastewater originating from the active mines (Bor pit, Veliki Krivelj, Cerovo, tailing dam in operation), as well as with the wastewater from the waste dump and flotation tailings which are not in operation during the long period (field 2 of the large flotation tailings Veliki Krivelj) [4]. The pollution of the Bor River is a consequence of the untreated municipal wastewater, metallurgical wastewater from copper metallurgical plant, wastewater from the mine tailings dump of the old Bor mine and Bor flotation tailing, as well as, from the old flotation tailings in Bor.

Sampling is realized by a hand tools, according to the sampling methods: SRPS EN ISO 5667-1; SRPS EN ISO 5667-3; SRPS ISO 5667-4; SRPS ISO 5667-6 [4].

Atomic emission spectrometer with inductively coupled plasma (ICPAES), model Spectro Arcos was used for determination the Cu and Ni ions concertation. The method of calibration curve was used. All reagents used for the Reagents of high purity grade chemicals were used for analyses. The certified reference material (CRM) and blank samples were used for quality control of chemical analysis. Measurement of the sample pH values was conducted in the field by the pH meter, model Dostmann.

RESULTS AND DISCUSSION

Results for pH values as so as the values of Cu and Ni ions concentration obtained during the measurement campaigns are discussed in this paper. Measured pH values for the water sampling points are presented in Figure 1. From Figure 1 it can be seen that the lowest pH value is registered for the sample point W4 (metallurgical wastewater) during each sampling campaign. The pH values that are in the range from 1.87 to 5.61 are lower than the allowable pH values regarding to Serbian legislation (range from 6.5 to 8.5) [5,6,7]. pH values for the sampling points W6 and W11 – W15 are in accordance with Serbian legislation.

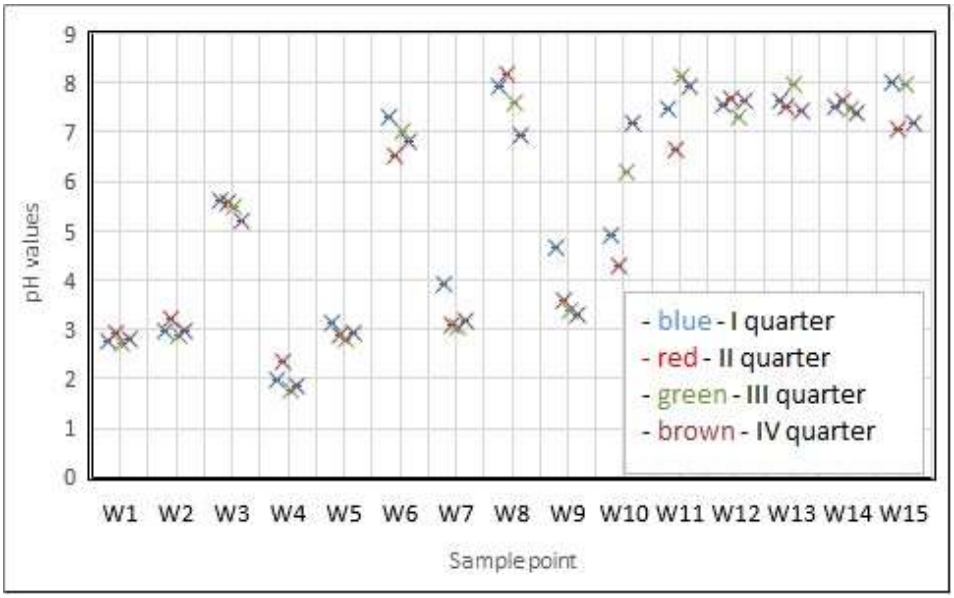

Figure 1 pH value

The pH values for the similar sample points, except for W10 - Bela River before of confluence with Timok River, were the similar for realized sampling campaigns.

The values of the Cu and Ni ions concentration in the water samples from the selected sample points are presented in Figure 2.

Cu ions maximal concentration is measured for the sampling point W4 - Metallurgical wastewater for all sampling campaigns. Having in mind that W4 – metallurgical wastewater inflows in Bor River (W5), concentration of Cu ions is also high in those samples. Cu ions are also present in AMD samples (W1, W2 and W3). Bela River (W7), a

river formed by the joining of W5 – Bor River and W6 – Krivelj River has the lower values for the Cu ions concentration. The presence of the Cu ions in the other sampling points is consequence of the inflows of W4 – metallurgical wastewater and AMD from the sampling points W1 - Robule accumulation, W2 Robule accumulation 1 and W3 - AMD from flotation tailing dam RTH. Concentration of Cu ions in metallurgical wastewater is about 300 times higher that maximal allowed concentration (MAC) according to the Serbian legislation for the IV class waters (Cu = 1 mg/l) and concentration of Cu ions in the AMD waters is maximal about 65 times higher than MAC. Similar flow rate of those wastewater confirmed that the Cu ions concentration from the metallurgical wastewater has the significant influence on the rivers downstream of the sampling points. Values for Cu concentration in W6 – Krivelj River, W8 - Ravna River and W11- Timok River upstream of the copper mining activities, are the lower than MAC value. After confluence of Bela River with Timok River, concentration of Cu ions has the lower values than MAC value for III water class of 0.5 mg/l.

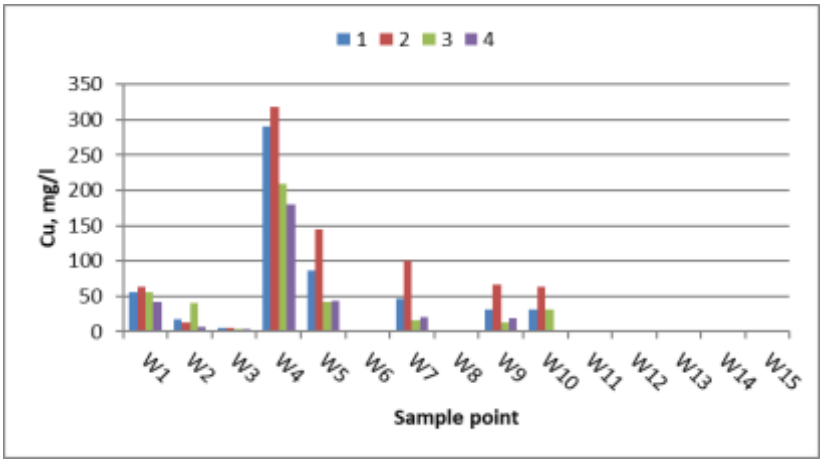

Figure 2 Cu ions concentration for different sampling quarters

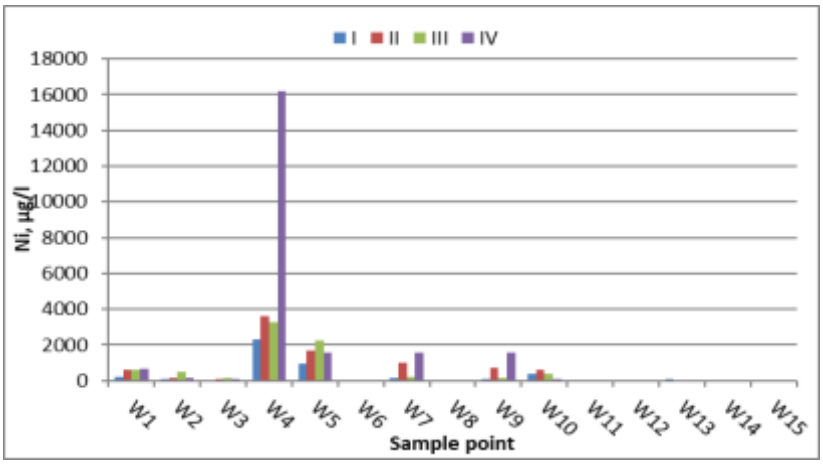

Figure 3 Ni ions concentration for different sampling quarters

Maximal value of Ni ions concentration is registered in the sample W4 - Metallurgical wastewater and this value is about 470 times higher than MAC value (Ni = 34 µg/l). Regarding the maximal concentration of Ni ions in AMD wastewater (sample W1), obtained value is about 20 times higher than MAC value for IV water class [7]. Based on the data presented in Figure 3, increased Ni ions concentration in W5 - Bor River, W7, W9 and W10 – Bela River on a different sampling points regarding to the confluence with the other rivers downstream of Bor River is consequence of the Ni ions content in metallurgical wastewater and AMD. Also, as in the case of the wastewater type influence on Cu ions concentration in the in the Bor district rivers watercourses, metallurgical wastewater has the significant influence on the value of Ni ions concentration in the rivers. After confluence of Bela River with Timok River the Ni ions concentration is reduced, but only in W15 – Danube River concentration is for realized sampling campaigns was lower than MAC value for II surface water class according to Serbian legislative.

CONCLUSION

Obtained results for Cu and Ni ions concentration in AMD and metallurgical wastewater sampling points are confirmed that values are higher than MAC values according to the Serbian legislation. Concentration of Cu ions in metallurgical wastewater is about 300 times higher than the MAC value and Ni ions concentration is higher about 470 times than the MAC. Value for Cu and Ni ions concentration in the AMD wastewater is higher for about 65 times and 20 times, respectively. Also, pH value of metallurgical wastewater sample is much lower than the pH of AMD samples. Results are confirmed that the high concentration of Cu and Ni ions in metallurgical wastewater has the main impact on Cu and Ni content in the Bor district rivers watercourses.

ACKNOWLEDGEMENT

We acknowledge the financial support of the Project RoRS 337- ROmania Serbia NETwork for assessing and disseminating the impact of copper mining activities on water quality in the cross-border area (RoS-NET2), implemented under the Interreg-IPA Cross-border Cooperation Romania-Serbia Programme that is financed by the European Union under the Instrument for Pre-accession Assistance (IPA II) and co-financed by the partner states in the Programme.

This work was also financially supported by the Ministry of Science and Technological Development and Innovations of the Republic of Serbia, Grant No. 451-03-47/2023-01/ 200052.

REFERENCES

1. Project name: ROmania Serbia NETwork for assessing and disseminating the impact of copper mining activities on water quality in the cross-border area, Programme 2014 - 2020 Interreg IPA CBC Romania - Serbia, https://keep.eu/projects/22351/ROmania-Serbia-NETwork-for--EN/
2. Štirbanović, Z., Gardić, V., Stanujkić, D., Marković, R., Sokolović, J., Stevanović, Z. (2021) Comparative MCDM Analysis for AMD Treatment Method Selection, Water Resources Management, 35 (11).

3. Stevanović, Z., Obradović, Lj., Marković, R., Jonović, R., Avramović, Lj., Bugarin, M., Stevanović, J. (2013) Chapter 2: Mine Waste Water Management in the Bor Municipality in Order to Protect the Bor River Water. In: Waste Water - Treatment Technologies and Recent Analytical Developments (F. S. García Einschlag, L. Carlos), IntechOpen, London, 41-62.
4. Marković, R., Obradović, Lj., Gardić, V., Kovačević, R., Stevanović, Z., Isvoran, A., Marinković, V. (2021) Contamination of rivers watercourses in Bor district with As and Cd ions, In: XIV International Mineral Processing and Recycling Conference. Belgrade, Serbia, Proceedings, 388-394.
5. Regulation on the categorization of watercourses ("Official Gazette of the SRS", no.3/1968) (In Serbian).
6. Regulation on Pollutant Limit Values into Surface and Groundwater and Sediment and Deadlines for their Achievement ("Official Gazette of the RS", no. 50/2012) (In Serbian).
7. Regulation on Limit Values Priority and Priority Hazardous Substances that Pollute Surface Water and Deadlines for Achieving them, ("Official Gazette RS", no. 24/2014) (In Serbian).

XV International Mineral Processing and Recycling Conference
17-19 May 2023, Belgrade, Serbia

DEVELOPING SAFE OPERATING PRACTICES (SOP) FOR POST-COMBUSTION CHAMBER IN A SPONGE IRON PLANT

P. Kekarjawlekar[1#], N. Kamal[1], K. Maniyar[1], B. Deo[1], P. Nanda[2], P. Malakar[2], R. Manchanda[2]
[1] Indian Institute of Technology Bhubaneswar, Odisha, India
[2] Tata Steel Long Products Limited Joda, Odisha, India

ABSTRACT –The exhaust gases at approximately 1000 -1173 K, laden with carried over fine unburnt coal particles and coal ash, enter the post combustion chamber (PCC) placed at the end of coal fired sponge iron rotary kiln. This waste heat in exhaust gas and that generated from combustion of CO is used for power generation. Uncontrolled combustion inside PCC, combined with dust deposition, can cause explosion. Energy balance and heat transfer calculations are done for the first time and one specific case of an explosion in the PCC is thoroughly analyzed. Safe operating practice (SOP) for the PCC is developed.

Keywords: Direct Reduced Iron, Post Combustion Chamber, Deposits, Explosion.

INTRODUCTION

The post-combustion chamber (PCC) is associated with a rotary kiln spinning at a constant RPM in the sponge iron plant. Raw materials such as coal, iron ore, and dolomite are used. Inside the rotary kiln, the iron ore is reduced into sponge iron. The coal enters the rotary kiln from both ends; one end is called the feed side and the other the injection side. Iron ore, dolomite, and coal are all fed from one end (feed side) of the rotary kiln, while only coal is fed from the other end (injection side). The PCC is attached towards the feed side of the rotary kiln. The gases enter the PCC at a high temperature of 860–880 °C combined with fine dust particles (fly ash from feed inputs) and unburned coal particles. An induced draught (ID) fan damper located on the kiln's feed side causes the gases to flow from the injection side to the feed side, maintaining the flow of gases inside the kiln.

The heavy solid particles carried with the flue gas settle in the Dust Settling Chamber (DSC), which is at the bottom of PCC. The heavy particles settled through DSC are collected and dumped with the help of Wet Scrapper. The very light dusts move along with gases and are collected at Electrostatic Precipitators (ESP), present after the PCC system. Some of the particles fuse and attach to the walls of PCC due to the high temperature of the system. These particles form of a layer of deposits along the inner wall of PCC. When these deposits grow up to a certain critical size, they tend to detach from the walls of PCC and fall into the DSC. In some cases, this falling of deposits may lead to explosive conditions.

corresponding author: 20mm02002@iitbbs.ac.in

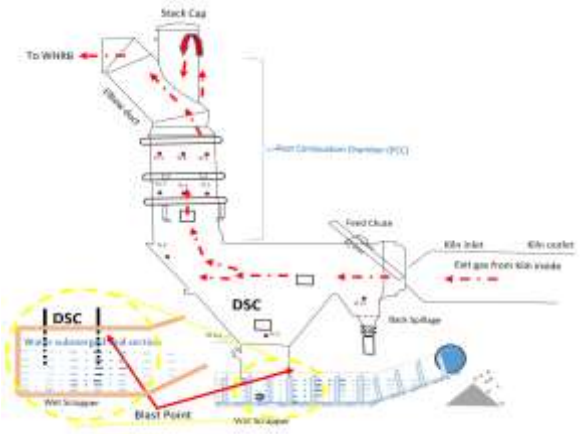

Figure 1 Schematic of PCC and DSC attached to rotary kiln

The aim of the present work is to determine the thickness of deposits by continuous monitoring of the surface temperature of the outer wall of PCC. The paper also deals with analysing a process incident (explosion) and states a potential cause of such incidents and some preventive measures.

EXPERIMENTAL: Determining Thickness of Deposits

PCC is a hollow cylindrical system made of mild steel and lined inside with a refractory material layer. The dust particles attach to the refractory and form a layer of deposits. For estimating the thickness of these deposits, by heat transfer calculations the temperature of gases flowing inside the PCC is required and these are measured with the help of thermocouples. There are 6 thermocouples present inside PCC.

Three thermocouples are present in the upper PCC region positioned 120^0 apart. The other three thermocouples are present in the lower PCC region similarly, with a phase shift of 60^0. For the analysis, the PCC is divided into six vertical sections, and each vertical section can be further divided into any even number of horizontal sections in accordance with the number of surface temperature readings taken.

The outer surface temperature of the PCC at different positions is measured with the help of thermal guns. Steady-state heat transfer is assumed. The heat flux associated is calculated by radiation and convection taking place on the outer surface of PCC by equation (1).

$$Flux = \sigma A \in \left(T_{surface}^4 - T_{ambient}^4\right) + h_{out}A\left(T_{surface} - T_{ambient}\right) \quad (1)$$

Here $\in$ is the emissivity of the outer layer of PCC, as it is made of mild steel, it is the emissivity of mild steel at that temperature [1]. A is the surface area considered. σ is the Stefan's Boltzmann constant. h_{out} is the convection heat transfer coefficient associated with gases external to the PCC system. $T_{surface}$ and $T_{ambient}$ are the surface temperature of the external surface of PCC and the temperature of surroundings associated with PCC respectively.

Heat flux is also given by equation (2), in terms of the inside and ambient temperatures of the PCC system and the resistances associated with different layers. In equation (3), $R_{conv1}, R_1, R_2, R_3, R_{conv2}, R_{rad}$ are the resistances offered to the heat flow by PCC gases, the layer of deposits, refractory layer, mild steel layer, gases in the ambient atmosphere and radiation respectively.

$$Flux = \frac{T_{in} - T_{ambient}}{R_{net}} \quad (2)$$

$$R_{net} = R_{conv1} + R_1 + R_2 + R_3 + R_{conv2} + R_{rad} \quad (3)$$

As PCC is considered to be a cylindrical system, the resistances for heat transfer calculations for conduction, convection, and radiation can be expressed in terms of the below equations.

$$R_{cond} = \left(\frac{2\pi}{\theta}\right) * \frac{1}{2\pi l K_1} * \left(ln \frac{rout}{rin}\right) \text{ for } R_1, R_2, R_3 \quad (4)$$

$$R_{conv} = \left(\frac{2\pi}{\theta}\right) * \frac{1}{2\pi r h l} \text{ for } R_{conv1}, R_{conv2} \quad (5)$$

$$R_{rad} = \frac{1}{2\pi\sigma \epsilon r l} * \left(\frac{2\pi}{\theta}\right) * \frac{1}{(T_{surf}^2 + T_{amb}^2)(T_{surf} + T_{amb})} \text{ for } R_{rad} \quad (6)$$

Here, r_{out} and r_{in} indicate the outer and inner radius of the layer considered, θ is the angle of one section considered, h, K are convection heat transfer coefficient and conduction heat transfer coefficient respectively, and l is the length of the section of PCC considered. The values of h at as a function of temperature and k of layers are found from the literature and are used for the model [2-4]. The consistent solution of equations 1 and 2 gives the thickness of deposits for that section.

SOP FOR EXPLOSION PREVENTION: The Method Followed

At the time of process incident, a blast sound was noticed from PCC Wet scrapper area. Huge quantities of dust were flying around PCC. Wet Scrapper tripped around to Zero speed. The RCC wall surrounding the Wet Scrapper cracked and bent outwards. Figure 2 shows a captured image during the time of explosion. The rotary kiln was on hold from operation during the time of explosion. Hence, the thermocouple temperatures in the Upper and Lower PCC region have fallen while the temperatures in the DSC region had increased very rapidly, as indicated in Table 1. This indicates that an exothermic reaction might have occurred. It might also indicate the falling of the deposits in the DSC area and hence the temperature around that area shot up. But the site findings suggest that there were very little traces of material found and as the damage was very severe, an exothermic reaction with an explosion might have taken place in the lower portion of DSC.

The exothermic reaction with explosive characteristics is the one in which H2 could be produced in a specific amount.

Figure 2 Photograph of the explosion on site

Table 1 Observed temperature values before, during, and after the explosion

Process parameter	Thermocouple Number	General Operational Temperature (^{0}C)	Temperature during the incident (^{0}C)	Value after the incident (^{0}C)
Upper PCC	T7002	840 – 910	470	800 – 840
Upper PCC	T7003	790 – 850	420	870 – 910
Upper PCC	T7004	870 – 940	112	890 – 930
Lower PCC	T7005	918 – 950	627	958 – 960
Lower PCC	T7006	910 – 930	604	830 – 850
Lower PCC	T7007	930 – 970	590	830 – 860
DSC	T7008	350 – 450	687	400 – 450
DSC	T7009	190 – 230	779	300 – 500

It is known that if the hydrogen content in the volume exceeds 4-6% [5] it might lead to an explosive situation. The reaction mentioned below is exothermic which also supports the fact that it could have led to rise in temperature.

$$C + 0.5\,O_2 + H_2O \rightarrow CO_2 + H_2$$

The way in which the problem has been approached is by considering the idea of the formation of air pockets in the DSC region. When the hot deposits fall from the PCC, it might lead to the formation of such air pockets in the DSC area. The deposits falling may also lead to the evaporation of water in the Wet Scrapper which makes H_2O available for the reaction. As the water evaporates, the water level in the Wet Scrapper might decrease and the gases can flow in and out of the DSC. These air pockets act as a chamber for the above-mentioned reaction. The reaction is feasible due to the high temperature in this region, and the availability of water, air, and carbon from the deposits. As the reaction proceeds, the pressure inside these air pockets increases with a subsequent increase in the percentage of H_2 in the system. When the pressure in these air pockets reaches a value that is comparable to the pressure of the flue gases outside the air

pocket, the gases tend to escape from the air pocket. Now, as the water level in the Wet Scrapper has decreased, it is an easy path for the gases to escape and when the H_2 comes out of the system it encounters the atmospheric Oxygen and an explosion occurs.

RESULTS AND DISCUSSION

The values of the deposit thickness in different sections of PCC are determined from the surface temperatures, as described above. A Graphical user Interface is developed which takes surface temperatures and thermocouple readings at different sections of the PCC as inputs and displays the corresponding thickness value as the output. Sample input and outputs are shown in Figure 3.

If the surface temperature at a position of PCC increases abruptly, it generally means that the deposits have dislodged into the DSC. If these deposits are not removed on a timely basis, it might lead to explosion conditions as explained in the above sections. The amount of material, that needs to dislodge for explosive conditions (5-6 vol% of H_2), is calculated by balancing pressure. The increased pressure inside the air pocket due to the exothermic reaction taking place is balanced with the external pressure. For this calculation the amount of carbon in the dislodged deposits is assumed to be around 1wt%. The total amount of deposits to be dislodged with hydrogen evolution is estimated.

CONCLUSION

Proper instrumentation for continuously monitoring surface temperature of PCC and DSC with a warning system for abrupt changes in the values should be included to prevent similar events in the future. Decrease in the level of water due to evaporation when hot deposits fall, leads to paving in of air to the DSC. In order to foresee this, a water level warning system is required which sounds an alarm when the water level in the Wet Scraper falls below a specified threshold.

Figure 3 GUI developed for correlating deposit thickness, inside temperatures, and surface temperatures

REFERENCES

1. Heaja, S., Bil, W., Jawdat, T., Riadh, Al. M., & Xiao-Ling, Z. (2013) Determination of Steel Emissivity for the Temperature Prediction of Structural Steel Members in Fire. Journal of Materials in Civil Engineering, 25, 167-173.
2. Samal, S., Lee, J., Jeong, D. Y., & Kim, H. (2015) Characterization of thermal conductivity of SiO2–Al2O3–Y2O3 glasses. Thermochimica Acta, 604, 1-6.
3. Peet, M. J., Hasan, H. S., & Bhadeshia, H. K. D. H. (2011) Prediction of thermal conductivity of steel. International Journal of Heat and Mass Transfer, 54, 2602-2608.
4. Vitiello, D., Nait-Ali, B., Tessier-Doyen, N., Tonnesen, T., Laím, L., Rebouillat, L., & Smith, D. S. (2021) Thermal conductivity of insulating refractory materials: Comparison of steady-state and transient measurement methods. Open Ceramics, 6, 100118.
5. Dagdougui, H., Sacile, R., Bersani, C., & Ouammi, A. (2018) Chapter 7 - Hydrogen Logistics: Safety and Risks Issues, Hydrogen Infrastructure for Energy Applications, Published by Academic Press, 127-148

XV International Mineral Processing and Recycling Conference
17-19 May 2023, Belgrade, Serbia

ARRANGEMENT OF FIELDS DEVASTATED BY CONSTRUCTION OF MAIN GAS PIPELINE

D. Milošević [#], M. Radosavljević, S. Polavder, Ž. Praštalo
Mining Institute Belgrade, Belgrade, Serbia

ABSTRACT – The construction of the main gas pipeline creates preconditions for the expansion of the gas pipeline network and enables a larger scope and a wider range of natural gas use. In the future, this will have a significant impact on raising the energy efficiency system through the construction of gas-fired thermal power plants and the expansion of the electricity system.

Keywords: Main Gas Pipeline, Section, Reclamation.

INTRODUCTION

Energy-industrial activity has the greatest impact on the degradation of space and is a technological process, which in comparison with other work certainly contributes the most to the change in appearance. Depending on the degree of disturbance and the possibility of performing the reclamation process, reclamation methods were analyzed, namely: technical, agrotechnical and biological. However, the best results in this regard are achieved by applying eurecultivation, which involves the planned application of materials according to the degree of recultivation, so that in the end of the formation of the substrate on the surface was the most suitable material. Finally, the humus layer is spread evenly over the devastated surfaces. Organizational and technological scheme of construction implies a chain-combined method of execution of works, which maximally affects the reduction of execution time and reduction of the negative impact on the working and environment.

PROJECT NOTES

The basic principles of construction of the main gas pipeline "Bulgarian border - Hungarian border" through Serbia, rely on the standards of the Russian Federation and the European Union, while respecting the principles of spatial development of Serbia and include: Respect for European standards and good practice in planning, construction and use of gas pipelines; Stability of the system, which enables long-term functioning and meeting the basic goals of its realization; Ecological reliability, which provides protection from negative impacts on the environment, nature, natural values and cultural values in the gas pipeline corridor and contact zone; Security, which with a high degree of reliability guarantees the safety of human lives and material goods from possible damage to the system; Economy, which proves that the owners and users of the transnational

[#] corresponding author: dragan.milosevic@ribeograd.ac.rs

gas pipeline system will have economic viability. The spatial plan also determines the reserved space for the corridor of the main gas pipeline, with a total width of 600 m, with previously defined belts, so that during the preparation of project documentation it is possible to translationally move the belts in relation to the gas pipeline route. The projected route of the main gas pipeline with associated facilities on the territory of the Republic of Serbia includes six sections, namely:

- Section 1: from the Bulgarian-Serbian border (around Zaječar) to Žabari, approximately 147 km long [1];
- Section 2: from Žabar to Kovin, approximately 48 km long [2];
- Section 3: from Kovin to Gospođinci, approximately 112 km long [3];
- Section 4: from Gospođinci to the Serbian-Hungarian border (near Horgoš) approximately 92 km long [4];
- Section 5: compressor station with auxiliary facilities near Velika Plana;
- Section 6: Connecting gas pipeline and measuring station (MS3), near Pančevo (processed by special planning documentation).

Figure 1 Map of the route of the main gas pipeline "Bulgarian-Hungarian border" [1]

Works on the construction of the line part of the gas pipeline are planned and performed by applying progressive technologies for accelerated line construction of the pipeline with the implementation of measures aimed at reducing the negative impact during construction activities on the environment. The technological procedure for the construction of the main gas pipeline included a number of activities: Clear the terrain in the width of the working zone 25 m to the left and 25 m to the right of the axis of the gas pipeline route; Humus removal in the width of 13 m to the left and 19 m to the right of the axis of the gas pipeline route; Laying of the main gas pipeline along the entire length of the route is planned underground. The depth of installation of the gas pipeline is in accordance with the Rulebook on conditions for unhindered and safe transport of natural gas through gas pipelines with a pressure higher than 16 bar (Official Gazette of RS no. 37/2013). He minimum depth of burial of the gas pipeline, measured from the ground level to the upper edge of the pipe, is 1 m.

After the completion of the construction of the main gas pipeline, protection belts have been defined: The belt of direct protection, the exploitation belt on both sides of the axis of the branch of the gas pipeline and the border of the construction plots of the gas pipeline facilities is 7.5 m wide; The protection belt is 50 m from the axis of the gas pipeline; Belt of wider protection, the belt of detailed elaboration is 100 m from the axis

of the corridor; Controlled construction belt, the protection belt is a belt 200 m wide from the axis of the corridor; Populated places and cities; Railway and bus stops; Bridges with a span greater than 20 m; Storage of flammable liquids with a volume of more than 1,000 m^3; Gathering places of more than 100 people.

CONSTRUCTION TECHNOLOGY

The construction of the main gas pipeline and accompanying above-ground facilities was carried out in stages and phases. Each phase of the main gas pipeline and accompanying above-ground facilities was a functional unit defined by project solutions and is in accordance with the legislation of the Republic of Serbia.

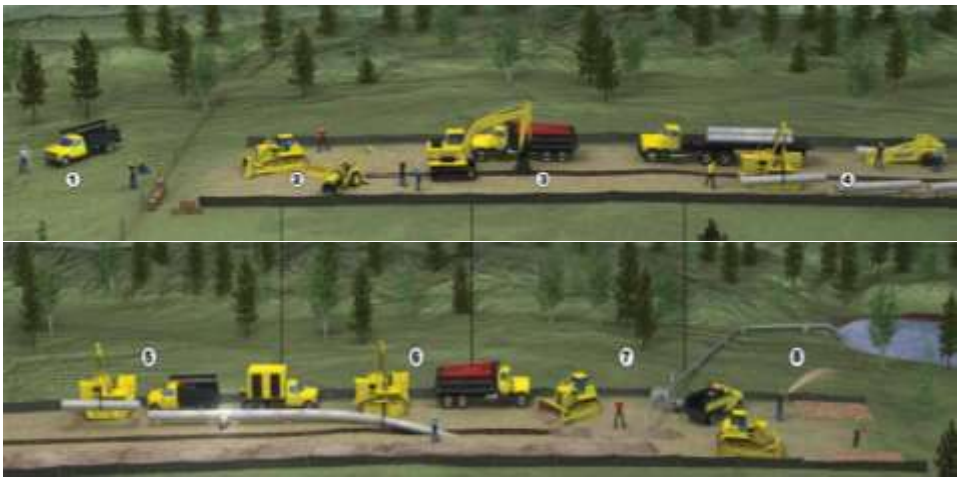

Figure 2 The concept of construction of the main gas pipeline [2]
1 – Research and design; 2 – Preparing the ground; 3 – Canal excavation; 4 – Delivery of gas pipeline elements; 5 – Pipeline connection; 6 – Installation of gas pipeline; 7 – Testing of the installed gas pipeline; 8 – Arrangement of degraded space

Pipeline level, excavation technology and pipeline laying is adapted to the terrain configuration as well as a larger number of intersections with existing installations. The pipelines were laid in an excavated trench with an earth layer. The trench was dug without excavation, with the proviso that in some parts of the route, depending on the geotechnical conditions and where the depth of burial is greater due to the terrain configuration, excavation was performed with sloping sides. The slope of the side flats is formed depending on the geomechanical properties and the category of land in which the excavation was performed. The trench was backfilled by machine, with excavated material. The route of the projected main gas pipeline along its trajectory is crossed with energy infrastructure, traffic infrastructure, telecommunication infrastructure, communal infrastructure, river and watercourse. Crossings were performed in two ways: by digging - the method of open trench and by the method of drilling. Crossings with smaller watercourses and canals were made by the open trench method. After laying the pipe in the bottom of the canal, the terrain was returned to its original condition.

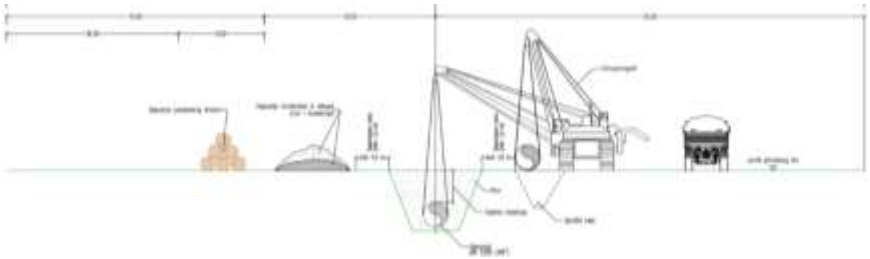

Figure 3 Scheme of organization of works - deforestation [2]

Figure 4 Construction of the gas pipeline on the route of Section 1 (location of the photo) [1]

Drilling crossings were performed by hydraulic pushing and retraction of the protective steel pipe. A gas pipeline runs through the laid protective pipe. The crossing of state and other asphalt roads with the main gas pipeline is planned to be performed by the drilling method. Crossing with larger watercourses was done by digging, drilling and microtunneling, while crossing with smaller ones was done by the method of open trench.

Figure 5 Direct pipe laying method [1]

CONCEPTUAL SOLUTION OF SPATIAL PLANNING

For a remediation to be successful, it must meet certain functional, economic and environmental criteria. Before the start of the works, a belt is determined which serves as a working area for the construction of the gas pipeline and which should be adjusted to the diameter of the gas pipeline, the type and quantity of excavation as well as the applied machines. Before laying the pipes, the terrain must be cleaned and leveled. The working zone can destroy the plants that are on the route during the works. Activities during the execution of works must not cause soil erosion, destroy young plants and cause damage to valuable tree species. Among other things, the technological procedure for the construction of the gas pipeline is defined by the conditions submitted by the competent institutions, which the Investor, Designers and Contractors must comply with. After laying and burying the gas pipeline, the working belt along the route and all neighboring areas that were used during the works must be planned. Pieces of rock, trench excavation or drilling that could not be used before and after trench backfilling

must be removed from the working area. If the pipeline is laid over lawns, gardens or access roads, the lawns must be covered with sods again, the damaged gardens should be replaced with ornamental shrubs and other vegetation, and the access roads must be restored to their previous condition. Also, the damage caused to fences, private roads and buildings must be restored and returned to their previous condition. Landscaping activities envisage measures in the field of reclamation, which include the restoration of vegetation and relief after the completion of construction works. Depending on the engineering - geological conditions on different sections of the route, measures are envisaged that will improve the characteristics of the soil. Reclamation of the main gas pipeline route is the first step in the arrangement and includes works on reshaping surfaces in order to achieve a safe shape of the final slopes as well as the necessary conditions for implementing measures to control surface and drainage water and thus form the final landscape for future purposes. Planned activities for arranging degraded areas include leveling the terrain, cutting terraces and leveling surfaces. During the construction of the main gas pipeline, the fertile layer of soil was removed, temporarily deposited and the microrelief was partially changed. The resulting changes were temporary, because after the completion of construction and reclamation, the disturbed land plots were returned to their original condition. Based on the previously described, we come to the choice of the technical solution that was applied during the construction of the main gas pipeline. After the completion of burying and installation of the gas pipeline, the deposited humus layer, using machines, bulldozers, graders and tractors with attached machines, was spread on the terrain that was cleared and on which the works on laying the gas pipeline were performed. The application of deposited humus on the route of the gas pipeline was done with a bulldozer and the leveling of unevenness and depressions with a grader. For the purpose of complete homogeneity, the reclamation layer was formed by evenly passing the tractor with the disc harrow several times in the same place, in order to remove all unevenness and larger pieces and return the soil to its original condition. Also, the project solutions envisage, and during the execution of works, the tillage was performed at the site of the humus landfill, in terms of its spreading.

Figure 6 Principle scheme of arranging the devastated space [2]

Figure 7 Work of agricultural machines on landscaping after the construction of the gas pipeline [1]

CONCLUSION

Any human intervention in a natural or disturbed ecosystem, which aims at a certain rehabilitation or the desire for qualitative and quantitative improvement, requires knowledge of that ecosystem. Detailed analysis of certain parameters related to pedological, climatic, orographic, phytocenological and other eco-conditions, is extremely important when it comes to areas where these conditions can be permanently changed. On the route for the installation of the main gas pipeline, the natural ambient conditions have been disturbed. In that sense, it was necessary to take measures so that the site affected by the activities and after the completion of works on the installation of gas pipelines and areas where temporarily deposited materials were recultivated and as much as possible returned to its previous purpose. Reclamation of a space in a narrower sense means bringing it to its original purpose and appearance (and sometimes improvement) to the greatest possible extent, by human activity of the disturbed appearance and purpose of the mentioned space. The main goal of reclamation, in addition to the general ecological effects, is primarily to bring the affected and degraded areas to a useful economic purpose. After the completion of works on the installation of the main gas pipeline, the conditions for land reclamation have been defined, as well as its future purpose, all in accordance with the legal basis. Reclamation activities include the entire route on which the installation of the main gas pipeline was performed, taking into account topographic, ambient, pedological, hydrological, technical - technological and other specifics. This means maximum rehabilitation of all areas for agricultural purposes, as well as future grassing while defining other possible solutions.

REFERENCES

1. Milošević, D. (2019) Project of technical reclamation of the line route of the main gas pipeline (Interconnector) of the Bulgarian border - Hungarian border, Book 1. Section 1 - from the Bulgarian - Serbian border (around Zaječar) to Žabari, approximately 147 km long, Mining Institute Belgrade.
2. Milošević, D. (2018) Project of technical reclamation of the line route of the main gas pipeline (Interconnector) border of Bulgaria - border of Hungary, Book 2. Section 2 - from Žabari to Kovin approximately 48 km long, Mining Institute Belgrade.
3. Praštalo, Ž. (2019) Project of technical reclamation of the line route of the main gas pipeline (Interconnector) border of Bulgaria - border of Hungary, Book 3. Section 3 - from Kovin to Gospođinci approximately 112 km long, Mining Institute Belgrade.
4. Praštalo, Ž. (2019) Project of technical reclamation of the line route of the main gas pipeline (Interconnector), Bulgarian border - Hungarian border, Book 3. Section 3 - from Gospođinci to the Serbian-Hungarian border (near Horgos), approximately 92 km long, Mining Institute Belgrade.

XV International Mineral Processing and Recycling Conference
17-19 May 2023, Belgrade, Serbia

ENVIRONMENTAL PROTECTION THROUGH THE RATIONAL USE OF SODIUM HYPOCHLORITE AS A FUNGICIDE

D. Đurđević-Milošević[1#], A. Petrović[1], J. Elez[1], V. Kalaba[2], G. Gagula[3]
[1] Institute of Chemistry, Technology and Microbiology, Belgrade, Serbia
[2] PI Veterinary Institute of Republic of Srpska "Dr Vaso Butozan" Banja Luka, Banja Luka, Bosnia and Hercegovina
[3] Karlovac University of Applied Science, Karlovac, Croatia

ABSTRACT – Disinfectants are widely used in the past few years and an unfavorable outcome is their contribution to environmental pollution. Especially, sodium hypochlorite is known to pose many toxic effects on living beings. This work investigated the fungicidal activity of sodium hypochlorite in accordance with the standard EN 1650:2019 on obligatory microorganisms *Candida albicans* ATCC 10231 and *Aspergillus brasiliensis* ATCC 16404, with some exceptions in the number of tested product concentrations. The obtained results showed some direction to the optimization of sodium hypochlorite used as fungicide with regard to the tested contact times as well as contribution to environmental protection in case of excess use of disinfectant.

Keywords: Environmental Pollution, Fungicide, Sodium Hypochlorite.

INTRODUCTION

Sodium hypochlorite (NaOCl), a chlorine-containing compound, is a strong oxidizer with potent antimicrobial activity. As a relatively inexpensive chemical, NaOCl is widely used to reduce bacterial and fungal contamination. Fukuzaki [1] listed the advantages of sodium hypochlorite solution as the ideal disinfectant and some of them are a broad antimicrobial spectrum, rapid bacterial action, solubility in water, easy to use, and action of cleaning, deodorizing and bleaching.

In medicine, NaOCl is used routinely in the treatment of burns, wounds, and ulcers. The industrial application of NaOCl is common and has wide use ranging from textile cleaning to water purification [2]. In agriculture, sodium hypochlorite is used as a potential disinfecting agent for seed surface disinfection. The seed treatment with 1% NaOCl for 5 min could be used for minimizing the incidence of seed-borne fungi and also hasten the germination of okra seeds [3]. Higher concentrations of NaOCl may have negative effects both on germination and seedling growth in some plant species [4]. In dentistry, NaOCl is considered the gold standard disinfectant in endodontic applications due to its proven antimicrobial properties against biofilms and its ability to dissolve organic material [5]. When NaOCl is added to water and wastewater, because of a reaction with biological materials, are produced a variety of organic chlorinated compounds, which are mostly lipophilic, persistent, and toxic in aquatic environments

corresponding author: dragica.milosevic@ihtm.rs

[6]. Sodium hypochlorite was extensively used in preventing coronavirus infection. The spraying of high concentrations and uncontrolled concentrations can be hazardous to human beings and have a negative environmental impact [7].

The aim of this work was to research the fungicide activity of sodium hypochlorite with the purpose to use appropriate concentration and to reduce environmental pollution as a result of an excess in use.

EXPERIMENTAL

The experimental design is based on EN 1650:2019 [8] with the exception of the number of test concentrations. Namely, fungicide activity was tested only on three target concentrations, but the concentration in the expected non-active range was not tested. Test concentrations were prepared from a commercial product labeled 10% sodium hypochlorite diluting 3.0ml, 1.5ml, or 0.7ml of the product to 100 ml with water.

Yeast test suspension was prepared using third passages of strain *Candida albicans* ATCC 10231 grown on Malt extract agar (MEA, HiMedia). Suspension of *Aspergillus brasiliensis* ATCC 16404 was prepared after growth for seven days and sporulation on MEA. From dilutions 10^{-5} and 10^{-6} of suspensions 1 ml was pour-plate in duplicate; for *Aspergillus brasilienis* 1 ml is divided into 2 plates and pour-plate in duplicate. After solidification inoculated plates were incubated at 30±1 ^{o}C for 48 h for *Candida albicans* and 72 h for *Aspergillus brasiliensis*. From dilution 10^{-4} of microbial suspensions were prepared as validation suspensions as stated in EN 1650 [8]. Validation suspensions were used for three controls of the test: validation A to ensure that there was no lethal effect of the used water, validation B to ensure no fungicidal activity of the neutralizer, and validation C to confirm that the tested product was neutralized. Tests were performed three times with different microbial suspensions on freshly prepared samples in simulated dirty conditions. The interfering substance was 3 g l^{-1} albumin bovine, CAS No. 9048-46-8, HiMedia.

The dilution-neutralization method of choice was used how is described in EN 1650 [8]. Contact times were 10 minutes and 1 minute. Neutralizer was prepared in the laboratory using the following components: L-histidine (CAS No. 9048-46-8, Merck), Saponine (CAS No. 8047-15-2, Sigma Aldrich), Tween 80, CAS No. 9005-65-6, HiMedia), Sodium thiosulphate pentahydrate (CAS 10102-17-7, Merck).

For each product concentration and each experimental condition were calculated decimal log reduction, using the following formula:

$$lg\ R = lg\ (\frac{N}{10}) - lg\ (x_{sr} \cdot 10) \quad (1)$$

where:

lg R is reduction (lg cfuml^{-1}),
N – number of strains in suspension (cfuml^{-1})
X_{xr} – an average of viable microorganisms after treatment

The reduction of microorganisms for tested time is expressed as the average and standard deviation of the tests performed on a different day.

RESULTS AND DISCUSSION

Obtained results show that the number of viable cells in the test suspension of *Candida albicans* was (2.92±0,12)x10^7 cfuml^{-1}, and in the suspension of *Aspergillus brasilienis* was (2.38±0,26)x10^7 (Figure 1). The cells number of both suspensions was between 1.5 x10^7 cfuml^{-1} and 5.0x10^7 cfuml^{-1} required by standard EN 1650 [8].

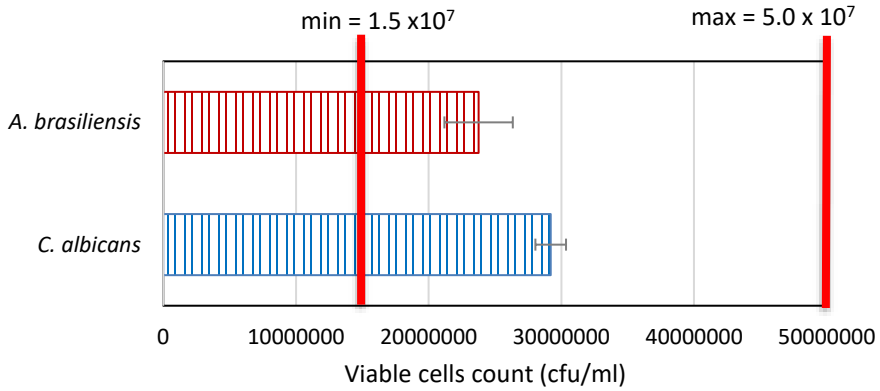

Figure 1 Viable cells count in microbial suspensions

Initial dilution of validation suspensions of *Candida albicans* and *Aspergillus brasilenisis* also were between 3.0x10^1 cfuml^{-1} and 1.6x10^2 cfuml^{-1} required by standard EN 1650 [8]. Compared to validation suspension, controls A, B, and C satisfied requirements "are equal to or greater than 0.5 times of validation suspension (initial dilution) (cfu/ml)" (Figure 2) and they confirm no lethal effect of the used water, no biocidal activity of neutralizer, and validation the tested samples were neutralized in contact times 10 minutes and 1 minute.

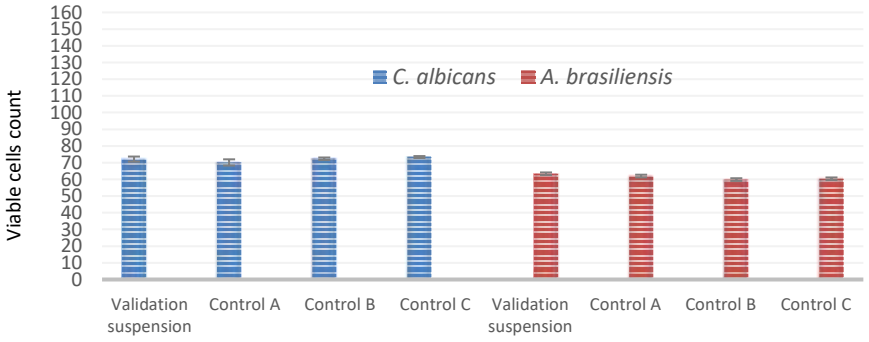

Figure 2 Validation suspensions and controls of *C. albicans* and *A. brasiliensis*

Results of NaOCl activity against *C. albicans* and *A. brasiliensis* in simulated dirty conditions are presented in Table 1. For the expression of the tested concentration of

NaOCl is taken into account concentration of the commercial product (10% NaOCl) and the tested concentration 80% due the experimental design.

Table 1 Fungicidal activity of tasted samples in dirty conditions

Microorganism	The concentration of product (% v/v)	Tested concentration of the product (% v/v)	Tested concentration of NaOCl (mg/kg)	Contact time (min)	Reduction *X_{sr}±SD (lg cfu/ml)
C. albicans ATCC 10231	3.0	2.4	2400	10	>4,31±0,02
	3.0	2.4	2400	1	>4,31±0,02
	1.5	1.2	1200	10	>4,31±0,02
	1.5	1.2	1200	1	>4,31±0,02
	0.7	0.56	560	10	<2,94±0,02
	0.7	0.56	560	1	<2,94±0,02
A. brasiliensis ATCC 16404	3.0	2.4	2400	10	>4,22±0,05
	3.0	2.4	2400	1	>4,22±0,05
	1.5	1.2	1200	10	>4,22±0,05
	1.5	1.2	1200	1	>4,22±0,05
	0.7	0.56	560	10	>4,22±0,05
	0.7	0.56	560	1	>4,22±0,05

Reduction of *C. albicans* ATCC 10231 and *A. brasiliensis* ATCC 16404 required by standard [8] is at least 4 lg. Tasted concentrations 2400mgkg^{-1} and 1200mgkg^{-1} had more than 4 lg reduction. The concentration of NaOCl 560 mgkg^{-1} showed activity against *A. brasiliensis* for contact times 10 minutes and 1 minute but did not reach 4 lg reduction against yeast *Candida albicans.* In accordance with EN 1650 [8], for yeasticidal activity is required reduction of *Candida alibican*s ATCC 10231 at least 4 lg, but for fungicidal activity is required reduction of *Candida albicans* ATC 10231 and *Aspergillus brasiliensis* ATCC 16404 at least 4 lg. It means that despite activity against A. brasiliensis, for fungicide activity is necessary activity against yeast and fungi, and in this case, it is realized with a concentration of 1200 mgkg^{-1}. Consequently, fungicidal claims and prescribed concentrations of NaOCl could be overuse of biocidal products in case of action against fungal spores.

Our results are comparable with the research Reynolds et al. [9] and the finding that the laboratory isolates of molds were reduced by >5lg after 5-minute exposures with 2.4% NaOCl. It is usually that many fungi colonize indoor environments and consequently induce adverse health symptoms including allergenic reactions. The conclusion of Reynolds et al. [9] is that a low concentration (2.4%) of NaOCl is effective at reducing mold from indoor surfaces. Based on our findings, even much lower concentrations as 0.24% or 0.12% possess fungicidal activity and the use of NaOCl in excess should be reconsidered. On one side is proper and experiments confirmed the active concentration of NaOCl, and on the other side is the proper use of labeled and recommended concentration. Both of them should be harmonized.

A study by Dindarloo et al. [10] investigated the pattern of disinfectant used during the outbreak of COVID-19. They reported that 74.2% of participants used the wrong proportion of sodium hypochlorite to make this disinfectant at home and approximately

42% experienced at least one side effect on their hands, feet, eyes, respiratory or gastrointestinal systems after sequential uses of disinfectants. Korukloglu et al. [11] found that the mold *Penicillium roqueforti* did not show any growth, even at a concentration of 0.55%, while *Aspergillus niger* was inhibited within a maximum of 3 minutes. They also found differences between the tested yeasts. Namely, *Kloeckera apiculata* was the most sensitive yeast and did not show growth after treatment 12 minutes and a concentration 0.5% NaOCl. *Sacharomyces cerevisiae* was the most resistant yeast ever at a disinfectant concentration of 2%. Sauer et Burroughs [12] for the purpose of determining the fungicidal activity of NaOCl on the presence of internal fungi in grain, treated the wheat kernels with NaOCl and plated them on agar. Results showed that spores *Aspergillus* spp. were inactivated by 1-5% solution of NaOCl. Mattei et al. [13] tested eighteen *Aspergillus* genus fungal isolates obtained from veterinary hospital surfaces against sodium hypochlorite. Minimum Inhibiting concentration and minimum fungicidal concentration capable of inhibiting 50% and 90% of the isolates were determined. The minimum inhibitory concentration 50% of sodium hypochlorite was 55 $\mu l ml^{-1}$ and for a concentration 90% was >160 $\mu l ml^{-1}$. The minimum fungicidal concentration 50% of sodium hypochlorite was 72.9 $\mu l/ml$ and for 90% was >160 $\mu l ml^{-1}$.

Various experimental designs obtain an active concentration of NaOCl against yeasts and molds but target concentrations were higher than those tested in our design with no attention to excess use. Chung et al. [14] reported that except for intentional exposures such as attempts of suicide, exposures to high concentrations of hypochlorite were mostly accidental, but reports of the health impact of long-term occupational or environmental exposure to low concentrations were rare. Anyway, the overused NaOCl as a residue in wastewater will find its own way to the surface waters. Information that residual chlorine content increased up to 0.4 $mg l^{-1}$ in Wuhan lakes during the early months of COVID-19 (Chu et al., 2021) [15] is very worrying and required optimization and rational use of NaOCl and other chlorine-based products.

CONCLUSION

Sodium hypochlorite (NaOCl), a chlorine-containing compound has potent antimicrobial activity and wide use in the domestic, industrial, public, and medicinal areas. Our results showed that concentration NaOCl 560 $mg kg^{-1}$ is active against *A. brasiliensis* for contact times 10 minutes and 1 minute but did not reach 4 lg reduction against yeast *Candida albicans.* In this case and in accordance with EN 1650 fungicidal activity can be claimed only on higher concentrations where is also activity against *C. albicans*. Consequently, fungicidal claims and prescribed concentrations of NaOCl could be overuse of biocidal products in case of action against fungal spores. The optimization of the use of biocidal products is necessary for the reduction of environmental pollution and the presence of harmful residuals.

REFERENCES

1. Fukuzaki, S. (2005) Mechanisms of Actions of Sodium hypochlorite in Cleaning and Disinfection Processes. Biocontrol Science, 11(4), 147-157.
2. Peck, B., Workeneh, B., Kadikoy, H., Patel, S.J. Abdellatif, A. (2011) Spectrum of

sodium hypochlorite toxicity in mal-also a concern for nephrologists. NDT Plus. 4 (4): 231-235.
3. Abduhu, M., Khan, A. A., Mian, I. H., Mian, M. A. K., Alam, M. Z. (2018) Effect of seed treatment with sodium hypochlorite and hot water on seed-borne fungi and germination of okra seed. Annals of Bangladesh Agriculture, 22(2): 41-50.
4. Sen, M. K., Jamal, A.H.M., Nasrin, S. (2013) Sterilization factors affect seed germination and proliferation of Achyranthes aspera cultured in-vitro. Envrionmental and Experimental Biology, 11: 119-123.
5. Zehnder R. (2006) Root canal irrigants. Journal of endodontics, 32(5), 389-398.
6. Salinoja-Salonen, M. S, Jokela, J.K. (1991) Measurement of organic halogen compounds in urine as an indicator of exposure. Scandinavian Journal of Work, Environment and Health, 17(1), 75-8
7. Bhat, s. A, Sher, F., Kumar, R., Karahmet, Haq, S. A. U., Zafar, A., Lima, E. C. (2022) Environmental and health impacts of spraying COVID-19 disinfectants with associated challenges. Environmental Science and Pollution Research, 29, 85648-85657.
8. EN 1650:2019, Chemical disinfectants and antiseptics. Quantitative suspension test for the evaluation of fungicidal or yeasticidal activity of chemical disinfectants and antiseptics used in food, industrial, domestic and institutional areas. Test method and requirements (phase 2, step 1).
9. Reynolds, K. A., Boone, S., Bright, K. R., Gerba, C. P. (2012) Occurrence of household mold and efficacy of sodium hypochlorite disinfectant. Journal of occupational and environmental hygiene, 9(11), 663-669.
10. Dindarloo, K. Aghamolaei, T., Ghanbarnejad, A., Turki, H. Hoseinvandtabar, S. Pasalari, H., Pasalari, H., Ghaffari, H. R. (2020) Pattern of disinfectants use and their adverse effects on the consumers after COVID-19 outbreak. Journal of envrionmental health science and engineering, 18(2), 1301-1310.
11. Korkukluoglu, M., Sahan, Y., Yigit, A. (2006) The fungicidal efficacy of various commercial disinfectants used in the food industry. Annals of Microbiology, 56(4), 325-330.
12. Sauer, D. B., Burroughs, R. (1986) Disinfection of Seed Surfaces with Sodium Hypochlorite. Phytopathology, 76(7), 745-749.
13. Mattei, A. S., Madrid, I. M. Santin, R, Schuch, L.F.D. (2013) In vitro activity of disinfectants against Aspergillus spp. Brazilian Journal of Microbiology, 44(2), 481-484.
14. Chung, I, Ryu, H., Yoon, S-Y, Ha. J.C. (2022) Health effects of sodium hypochlorite: review of published case reports. Environmental Analysis Health and Toxicology, 37(1), e2022006.
15. Chu, W, Fang, C., Deng, Y, Xu, Z. (2021) Intensified disinfection amid COVID-19 pandemic poses potential risks to water quality and safety. Environmental Science and Technology, 55(7), 4084-4086.

XV International Mineral Processing and Recycling Conference
17-19 May 2023, Belgrade, Serbia

CASE STUDY OF ENERGY SAVING IN A PUBLIC SCHOOL THROUGH THE INSTALLATION OF A PHOTOVOLTAIC SYSTEM ON THE ROOF

G. Kyparissis[1#], A. Goulkoudis[2], G. Papadimas[1], E. Tasiopoulos[1], A. Vasileiadou[1,2]

[1] University of Thessaly, Facility of Technology, Department of Energy Systems, 41500 Larissa, Larisa, Greece

[2] Democritus University of Thrace, Faculty of Engineering, Department of Environmental Engineering, 67100 Xanthi, Greece

ABSTRACT – The purpose of this paper is to find alternative ways to upgrade public school buildings in order to consume smaller amount of energy. Under this scope, a case study of installing a photovoltaic system on the roof of the school building of the Argyropoulio Junior High School of Larisa was conducted. The energy needs of the building were examined, and the optimal photovoltaic system (type, location, dimensions etc.) was chosen. Furthermore, a techno-economical study was performed. The results of the study showed that such interventions could save high amounts of energy, if implemented in the school units of the country.

Keywords: Energy Saving, School Building, Public Buildings, Photovoltaic System.

INTRODUCTION

The phenomenon of climate change as well as the energy dependence on third countries and the improvement of energy security, led the European Union to look for ways to save energy and to establish rules regarding the construction of new buildings as well as the upgrading of the existing building stock of all its member countries. In September 2022, the European Parliament set a target for all its member states to have reduced energy consumption by 2030 by at least 40% in final energy consumption and by 42.5% in primary energy consumption [1]. A key sector with great energy saving potential is public buildings. A proposed intervention is the placement of photovoltaic systems on the roofs of these buildings. This aims at the production of electricity with the initial purpose of self-production and partial coverage of basic energy needs and in combination with additional future interventions to convert into zero consumption buildings.

In Greece but also at a European level, according to the Renewable Energy Resources Centre (hereinafter CRES) the building sector is responsible for approximately 40% of the total final energy consumption. This is due to the high cost of energy but also the heavy burden of the atmosphere with pollutants, mainly carbon dioxide (CO_2), which causes the greenhouse effect. According to a related report by the Bank of Greece [2], the energy demand of buildings as a direct function of the climate of each region is

corresponding author: gkyparissis@uth.gr

inextricably linked to climate change. In Europe, the latest figures show that wholesale electricity prices rose in the first quarter of 2022 by 411% in Spain and Portugal, by 343% in Greece, by 336% in France and by 318% in Italy compared to those from a year ago [2].

The Ministry of the Environment created an application (publicenergysavings.gov.gr) to monitor the implementation of actions regarding to the electricity consumption related to buildings of the wider public sector infrastructure (school buildings included), to achieve the target of 10% savings in consumption, holding 2019 as the year of reference [3].

Greece harmonized with Directive 91/2002/EC in 2008 with the issuance of Law 3661/2008 (Government Gazette A' 89) "Measures to reduce the Energy Consumption of Buildings and other provisions" [4].

The new European directive 31/2010/EC came to amend the directive 91/2002/EC and our country harmonized with the law 4122/2013 (Government Gazette A'42), and then the relevant TCG guidelines were amended with the ministerial decision number 2618/23-10-2014 (Government Gazette B΄2945) on the subject of "Approval and implementation of the Technical Chamber of Greece Guidelines for the Energy Performance of Buildings". Their last edition was published in the year 2017 and is valid until today [6].

The ELOT EN ISO 13790 standard defines the methodology for calculating the energy efficiency of buildings, in conjunction with other European standards that are related to energy [6].

In Greece for the first quarter of 2022, the Independent Power Transmission Operator (PTO) data shows that natural gas and lignite underpin renewables and large hydroelectric projects in power generation [7]. Cumulatively in the first two months of the year, natural gas (3,050 GWh) marginally regains the lead over renewable energy sources (mainly wind and solar energy, 2,936 GWh) in Greece's interconnected grid [7].

As for photovoltaics, according to the Association of Photovoltaic Companies (hereinafter HELAPCO), in 2021 in Greece they produced 5.26 TWh (billion kilowatt hours) or otherwise 9.2% of the country's electricity demand, i.e., approximately as much as lignite production, preventing the release of 3.7 million tons of CO_2 in the atmosphere from the substitution of fossil fuels [8].

In 2020, according to the official data published by HELAPCO, the new installed capacity reached 913 MW_p and the new installed capacity of interconnected photovoltaics reached 459 MW_p [9]. The total installed capacity of photovoltaics up to 2020 reached 3742 MW_p while the total installed capacity of interconnected photovoltaics reached 3288 MW_p [9].

In 2021, more megawatts (Mwp) in photovoltaics were installed in Greece than any other technology, 838 MW_p in new capacity of interconnected photovoltaicstons, bringing the total power to 4,126 MW_p [8].

The Energy Classification of Buildings (2008) is carried out with the issuance of the Energy Performance Certificate (EPC) in accordance with REPB [5]. The EPC shows the energy rating of the building, its general data, the calculated annual total primary energy consumption of the reference building and the building under review.

Buildings that are not used as residences in Greece, reports CRES [10], constitute approximately 5% of all buildings and represent 26% of the total area of the building

stock. The energy-standard air-conditioned office building consumes approximately 138 kWh/m^2/year (final consumption, of which 35 kWh/m^2/year for air conditioning and 85 kWh/m^2/year for heating). The average consumption of non-air-conditioned office buildings is around 75 kWh/m^2/year (57 kWh/m^2/year for heating) [10].

The state, with the support of the European Union, finances subsidized programs such as "Exoikonomo", the "ELECTRA" program as well as investment programs through National Strategic Reference Framework for the Regions and the Municipalities that subsidize the energy upgrade of public buildings, schools and sports facilities.

A solution that offers immediate results with the cost of its implementation being manageable, is the installation of a photovoltaic system (PV) on the roof of the building.

The main scope of this work is to contribute to energy saving in public schools via installation of the photovoltaic system on the roof of the school building at the Argyropoulio High School of Larisa, for the self-production of electricity. This aims at the saving of energy and, by extension, the saving of important financial resources so that they can be channeled in the future towards strengthening and upgrading the educational needs of the school.

MATERIAL AND METHODS

In this work, a case study regarding the installation of the photovoltaic system on the roof of the school building of the Argyropoulio, Larisa Junior High school for the production of electricity using the net metering method, with a total installed power of 4.95 kWp will be presented. Finally, a technical and financial study will be offered.

The school unit was built in 1998 in the local community of Argyropoulio, in the Municipality of Tyrnavos in the Regional Unit of Larissa, with a total area of 1800 m^2, 8 classrooms, and some other auxiliary rooms and teachers' offices. At the time the building was constructed, the 1998 building Thermal Insulation Regulation was in force, so the building has been thermally insulated but it is not energy efficient.

For the dimensioning of the PV system, electricity bills of the building were collected from the years 2020 to 2022, holding the data of the school year 2021-2022 as a base, due to pandemic reasons. The average consumption of the building needs is 5500 kWh per year.

Description of the system – Dimensioning

The PV system will consist of 9 monocrystalline silicon PV panels with a nominal power of 550 W, which will be installed in the south side of the building's roof and will occupy a space of 23 m^2. The PV panels will be connected in series of two strings. The first will include the five PV panels and the second the remaining four PV panels, which will be placed on fixed supports with special supports for tiled roofs and oriented with a deviation from the south corresponding to the building, and on a slope similar to that of the roof. The array of PV panels is connected to and supplies a three-phase voltage inverter, which converts the direct voltage at the output of the array into an alternating voltage.

The electrical installation concerns direct current (DC) wiring, i.e., the cables that will connect the PV panels, the strings to the inverter and the alternating current (AC) wiring

for the connections of inverter with the panel of the PV system and the self-production meter.

Finally, grounding with a conductor will be installed in the system, which will equally connect all the metal bases of the PV panels and will end up in three copper electrodes placed inside the ground while forming the grounding triangle.

Below are some details of the wiring:

String 1 (string 1) - 5 PV panels

- MPP voltage (maximum power point) at 70°C -> 179.50 V
- Open circuit voltage at -10°C -> 272.53V
- MPP voltage at 0°C -> 226.56 V
- Short circuit current at 25°C -> 13.98 A
- MPP power at 25°C ->2.75 kW_p

String 2 (string 2) - 4 PV panels

- MPP voltage (maximum power point) at 70°C -> 143.60 V
- Open circuit voltage at -10°C -> 218.02 V
- MPP voltage at 0°C -> 118.25V
- Short circuit current at 25°C -> 13.98 A
- MPP power at 25°C ->2.20 kW_p.

RESULTS AND DISCUSSION

Estimated output of the proposed PV system – Cost

The estimated annual energy production for the area of the Larissa Regional Unit is 1500 kWh per installed KW_p. PV panel manufacturers assume that each panel has a 2% drop in efficiency for its first year of operation (final efficiency is 98%). For each subsequent year -over the total of 24 years- the drop in efficiency is 0, 55%/year, so the total return is about 84.8%. An average annual estimate of the drop in efficiency of PV panels can be 0.55%.

Table 1 shows the production data of the PV system, starting with 7277 kWh and reaching 169906 kWh for a 25-year production. The annual output of the PV system is greater than the annual consumption of 5500 kWh calculated from the total bills of the electricity company.

Table 1 Estimated efficiency of PV system

General description			
1	Rated power	4.95	kW_p
2	Estimated annual energy production	1500	kWh/kW_p
3	Annual productivity decline	0.55	%
4	Annual energy production (first year)	7277	kWh
5	Energy production in 25 years	169906	kWh

Indicatively, the cost of the proposed PV system with PV panels and European-made inverter, roof support system, electrical panels, cables and other accessories, reaches

8,000.00 euros. Adding the cost of connecting to the Electricity Distribution network (HEDNO) for three-phase supply – 400,00 euros - and the cost of purchasing and certifying the meter of electricity produced – 850,00 euros - the total cost amounts to 9,250.00 euros.

In this time, the electricity price is fluctuating. From August 2022, all electricity companies are required to announce the price per kWh that they will charge consumers each month [11]. From January to September of 2022, it was 0.2305 euros/kWh, so the calculations will be made with this value [11].

The total annual cost of electricity supply for this consumption is 1,267.75 euros. The school unit will use funds from the subsidized programs of the NSRF of Regions, since its legal nature does not allow it to borrow from a financial institution, and the investment amount is not considered prohibitive. Also, for the calculation of the investment, the electricity price should be assumed to remain constant for the next years, so the payback period of the investment is calculated to be 7.29 years. Since the price of electricity has been increasing in recent years, there is a chance that the payback period will be much shorter than the calculated one.

The last few years, the upgrading electricity energy cost combined with the underfunding of the Greek Public Schools, resulted to a constantly reducing ability of covering the schools' expenses. Thus, the whole operation of a school unit could be negatively affected. Under these circumstances, each school unit could try to find its own ways to reduce its maintenance costs by saving energy. The installation of a photovoltaic system on the roof of a school building is a solution that works immediately and reduces the cost from the moment it starts to operate. This system is also environmentally favorable because it reduces carbon emissions once it is installed.

The case study that is presented in this study shows that it is profitable and allows the school unit to invest the gained profit in other ways that will help the improvement of its operation as well as making a statement on behalf of the school regarding its environmental behavior, giving an impeccable example to its students. They have the chance to learn about renewable energy and how important it is to our daily life. They can learn about the upkeep, monitoring, and operation of the system in a realistic way. The findings of the study thus not only show the financial and environmental advantages of solar power but also point out its potential to advance sustainability teaching and awareness in educational institutions.

CONCLUSION

A vital component of sustainable living and environmental preservation is energy conservation. Using energy-efficient techniques and technologies has become crucial due to growing worries about climate change and global warming.

The results of this study showed that the installation of a photovoltaic system on the roof of Argyropoulio Junior High School could be a profitable investment as it can upgrade the school, preparing it for a future shell and E/M systems upgrade, with the goal of making the building a self-contained, environmentally friendly power plant with a low energy footprint and lower operating costs.

The inclusion of renewable energy sources in public buildings is an important step in the energy upgrade of the country's building stock, since it reduces the operating costs

of buildings and creates an urban and peri-urban environment friendly to the actual environment, in an effort to deal with climate change, which is increasingly affecting the daily life of citizens.

REFERENCES

1. European Parliament (2022) Energy saving: EU action to reduce energy consumption, https://www.europarl.europa.eu/news/en/headlines/society/20221128STO58002/energy-saving-eu-action-to-reduce-energy-consumption, (accessed at 13/01/2023).
2. Bank of Greece (2022) Greek energy market report, https://www.haee.gr/publications/haee-publications/greek-energy-market-report/greek-energy-market-report-2022/, (accessed at 15/01/2023).
3. Ministry of the Environment (n.d.). Public Energy Savings, https://publicenergysavings.gov.gr/, (accessed at 03/01/2023).
4. Government Gazette (2008) Measures to reduce the Energy Consumption of Buildings and other provisions, https://ypen.gov.gr/wp-content/uploads/2020/11/KYA_D6_B_14826_17_06_2008_FEK_B1122.pdf, (accessed at 18/01/2023).
5. Government Gazette (2010) Approval and implementation of the TCG Technical Guidelines Energy Performance of Buildings, https://edu.klimaka.gr/arxeio/nomothesia-fek/fek-1387-2010-anatheseis-mathimata-eidikis-agwghs-klimaka.pdf, (accessed at 15/01/2023).
6. Technical Chamber of Greece (2017) Detailed national parameter specifications for the calculation of the energy performance of buildings and the issuance of the energy performance certificate, http://portal.tee.gr/portal/page/portal/SCIENTIFIC_WORK/GR_ENERGEIAS/kenak/files/TOTEE_20701-1_2017_TEE_1st_Edition.pdf, (accessed at 02/02/2023).
7. Power Transmission Operator (2022) Financial Report, https://www.dei.gr/el/dei-omilos/ependytikes-sxeseis/enimerosi-ependyton/oikonomikes-ektheseis-ana-etos/oikonomikes-ektheseis-2022/, (accessed at 02/02/2023).
8. Association of Photovoltaic Companies (2021) 2021 Report, https://helapco.gr/reports/, (accessed at 05/02/2023).
9. Association of Photovoltaic Companies (2020) 2020 Report, https://helapco.gr/reports/, (accessed at 05/02/2023).
10. Renewable Energy Sources Centre (2022) Buildings: Energy inspection, http://www.cres.gr/services/istos.chtm?prnbr=24782&locale=el, (accessed at 14/01/2023).
11. Eurostat (2022) Electricity prices components for consumers - annual data (from 2007 onwards), https://ec.europa.eu/eurostat/web/products-datasets/-/nrg_pc_204_c, (accessed at 12/01/2023).

XV International Mineral Processing and Recycling Conference
17-19 May 2023, Belgrade, Serbia

THE ARSENIC SORPTION CAPACITY OF DIFFERENT SERBIAN SOILS

D. Topalović#, J. Marković, M. Jović, S. Dragović, I. Smičiklas
University of Belgrade, VINČA Institute of Nuclear Sciences - National Institute of the Republic of Serbia, Belgrade, Serbia

ABSTRACT – Arsenic (As) added to the soil by various industrial activities, landfills, and agricultural pesticide use poses a significant threat to the environment and biota. The As-binding capacity of soil organic and inorganic constituents governs this element's fate, mobility, and bioavailability. To improve the understanding of As sorption by soils in Serbia, eight selected samples were artificially contaminated with increasing As concentrations. Significant variations in maximum sorption capacities demonstrated their strong dependence on soil properties. The association between maximum As sorption capacities and Mn, Fe, and Al concentrations in the soil samples was revealed.

Keywords: Arsenic, Sorption capacity, Soil pollution, Soil properties.

INTRODUCTION

Long-term exposure to inorganic arsenic (As) through contaminated drinking-water and food causes a range of adverse health effects, including developmental disorders, diabetes, pulmonary and cardiovascular disease, and cancer [1]. Arsenic is a metalloid that tends to appear in anionic forms. Arsenates ($H_2AsO_4^-$ and $HAsO_4^{2-}$) are more common than arsenites in the normal range of pH-Eh conditions of the soil [2]. The background levels of As in various soil groups range from <0.1 to 67 mg/kg, with the overall mean value of 6.83 mg/kg [3]. While the natural As concentrations in soil are based on the lithology of the parent rocks, its concentrations can be significantly increased in the top soils, by dry and wet deposition from mining and smelting activities, burning of fossil fuels, incineration of wastes, cement production, application of As-contained fertilizers and pesticides, and disposal of sludges containing As [4].

In Serbia, As emission is substantial due to As presence in fuels and the composition of raw materials used in the production of glass, iron, and steel [5]. According to the Serbian Regulation on the limit values of polluting, harmful and dangerous substances in the soil [6], the maximum limit value for As of 29 mg/kg indicates a disturbed ecological balance and imposes additional tests of that soil, while 55 mg/kg is a limit above which the remediation measures are needed. The screening of 32 selected industrial sites in Serbia, presumed to be contaminated, disclosed As concentrations above limit values and even above remediation values at several locations, including factory of wagons and metal industry in Kraljevo, metal Industry in Kragujevac, mining and foundry basin in Bor, leather-textile combine in Zaječar, non-ferrous metallurgy in Šabac, non-ferrous metal factory in Prokuplje, [7]. The toxicity of As depends on the concentration of soluble As

corresponding author: dusan.topalovic@vin.bg.ac.rs

forms which are highly dependent on soil properties [3].

The aim of this study was to improve the understanding of As sorption in Serbian soils by determining the As sorption capacities of different soil types and examining the association between As sorption parameters and soil properties.

EXPERIMENTAL

Soil samples (s1-s8) with contrasting agrochemical properties collected (0-25 cm) from different locations in Serbia were previously characterized [8,9]. Additionally, the As content in native soils was determined following the microwave-assisted digestion of the samples in 9 mL HNO_3 and 3 mL HCl. The sorption isotherms of As were established via batch experiments. Solutions with different As concentration levels (10^{-4}-10^{-2} mol/L), prepared from $Na_2HAsO_4x7H_2O$ salt and deionized water, were mixed with each soil sample at a soil/solution ratio of 1g/20 mL. The suspensions were agitated for 2 months to ensure equilibrium conditions. The aqueous phase was separated by centrifugation, and the supernatant was filtered using the syringe microfilters (<0.45 µm). The As concentrations were measured by inductively coupled plasma mass spectrometer - ICP-MS (model iCAP Q, Thermo Scientific). The amounts of As sorbed by the soil samples were calculated based on the difference between the initial and equilibrium concentrations. Statistical analysis of experimental data was performed using MINITAB software.

RESULTS AND DISCUSSION

Figure 1 displays the isotherms of As sorption by eight selected soil samples. The Q_e (mmol/g) and C_e (mmol/L) denote equilibrium As concentrations in the solid and liquid phase. The high affinity of the soil at low sorbate concentrations and the subsequent decrease in affinity with progressive coverage of the active centers generally explain the curvature of the obtained typical L-shaped isotherms [10]. Besides, substantial variations in sorption capacities were observed by comparing different soil types.

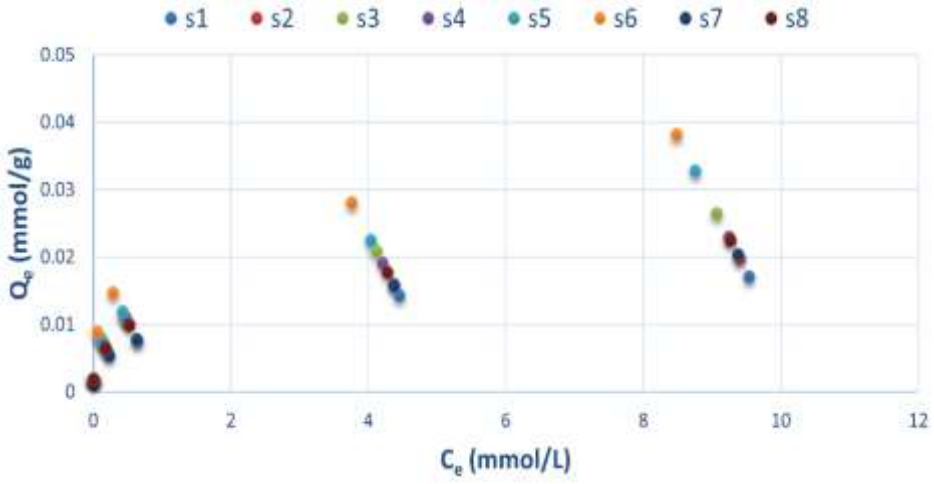

Figure 1 Sorption isotherms of As on different soil types

The experimental data were fitted by the two most used isotherms models, Langmuir (Eq. 1) and Freundlich (Eq. 2):

$$\frac{C_e}{Q_e} = \frac{1}{Q_{max}K_L} + \frac{1}{Q_{max}C_e} \quad (1)$$

$$logQ_e = \log K_F + \frac{1}{n} logC_e \quad (2)$$

The Q_{max} is the maximum sorption capacity of the soil, K_L (L/mmol) is the Langmuir constant, while the K_F (mmol/g)/(mmol/L)$^{1/n}$ and *1/n* represent the Freundlich empirical constants related to the sorption capacity and affinity.

Both models were applicable for the description of As sorption (Figure 2, a and b), but based on the coefficients of determination (Table 1), the Freundlich equation ($0.984<R^2<0.999$) fitted the data better than the Langmuir ($0.961<R^2<0.992$). This might be influenced by the fact that the condition of homogeneity of the surface sorption sites, presumed by the Langmuir model, is not met. Soils with relatively low content of organic matter, dissolved organic matter, and extractable P, are particularly expected to have both the high-energy and low-energy sites available for As sorption [11].

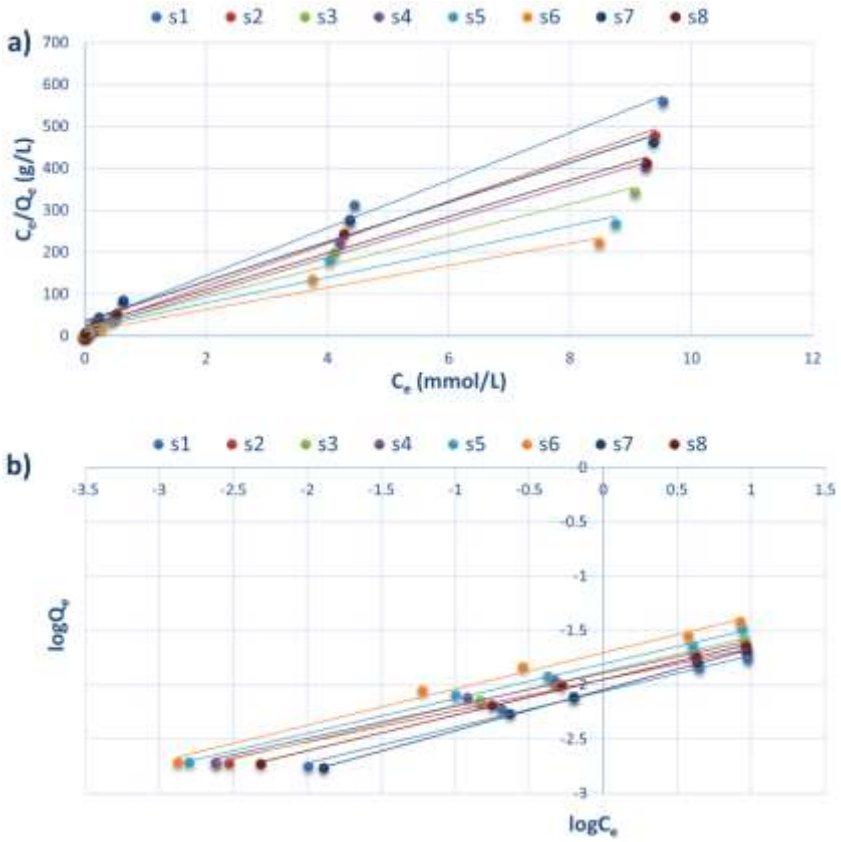

Figure 2 Linear fitting of experimental data using a) Langmuir and b) Freundlich model

Table 1 Sorption parameters of As calculated using Langmuir and Freundlich equations

Soil sample		Langmuir model		Freundlich model		
	Q_{max} (mmol/g)	K_L (L/mmol)	R^2	*1/n*	K_F (mmol/g)/(mmol/L)$^{1/n}$	R^2
s1	0.017	1.897	0.991	0.330	0.009	0.990
s2	0.019	2.781	0.989	0.287	0.011	0.984
s3	0.027	1.929	0.986	0.320	0.013	0.999
s4	0.023	2.788	0.961	0.300	0.013	0.990
s5	0.033	1.716	0.992	0.320	0.016	0.997
s6	0.038	2.489	0.977	0.333	0.020	0.989
s7	0.021	1.298	0.982	0.376	0.009	0.999
s8	0.023	1.887	0.985	0.330	0.011	0.997

Even though evidence on the As sorption mechanism cannot be derived from applied mathematical models, comparing the calculated maximum sorption capacities for different soils is beneficial. The Q_{max} values for As varied between 0.017 and 0.038 mmol/g (Table 1), which corresponds with the 1723-2846 mg/kg range.

The selected properties of investigated soils are summarized in Table 2. The relationships between soil attributes and As sorption parameters was assessed by the linear correlation analysis. Both the Q_{max} and K_F were found to be significantly ($p<0.05$) and positively correlated only with the pseudo total content of Mn in the soil (R 0.73 and 0.72, respectively).

Table 2 Descriptive statistics of soil properties [8,9]

Variable	Mean	SE Mean	StDev	Minimum	Maximum	Range
$CaCO_3$ (%)	2.90	1.85	5.24	0.00	11.70	11.70
pH_{H2O}	7.05	0.32	0.91	5.50	8.00	2.50
CEC (cmol/kg)	32.03	3.05	8.62	22.50	47.80	25.30
TOC (%)	2.28	0.49	1.30	0.82	4.75	3.93
P_2O_5 (mg/100g)	9.69	3.59	10.16	0.01	30.00	29.99
K_2O (mg/100g)	28.19	4.10	11.60	8.80	43.00	34.20
Al (mg/kg)	1728	96.9	274.2	1413	2214	801.0
Fe (mg/kg)	15508	1885	5332	11448	24354	12906
Mn (mg/kg)	1086	276	779	216	2408	2192
As (mg/kg)	10.90	1.32	3.74	4.90	16.20	11.30

Furthermore, the cluster analysis of soil variables and calculated parameters of As sorption capacity was performed by the complete-linkage method in order to group the entire set of variables into clusters according to their similarity. Dendrogram presented in Figure 3 indicated the highest similarity between As sorption capacity (Q_{max} and K_F) and the content of Fe in the soil. While the contents of Al and Mn were also associated with As sorption, other soil variables (pH_{H2O}, cation exchange capacity (CEC), content of carbonates, total organic matter (TOC), available P and K, and background As concentration in the soil), were less important.

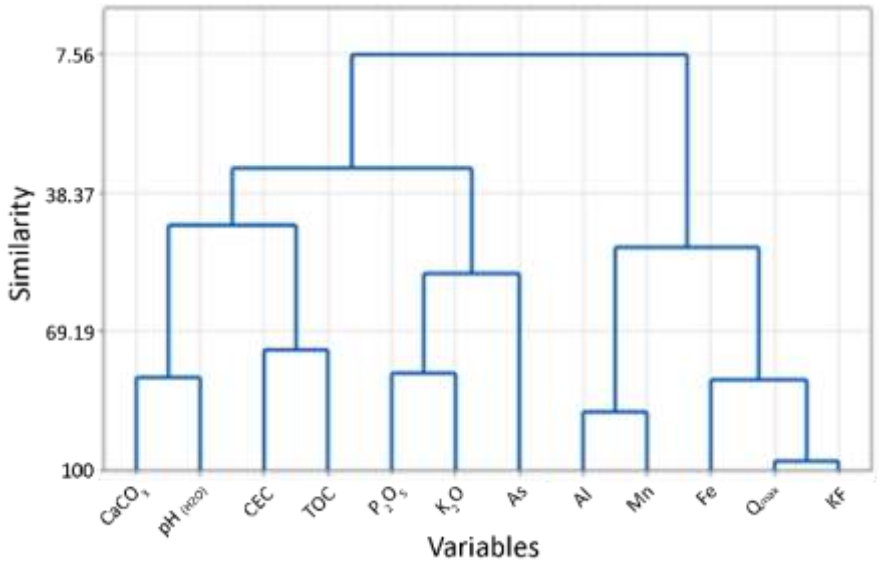

Figure 3 Dendrogram of cluster analysis of soil variables and As sorption parameters

Both arsenates and arsenites are assumed to be primarily chemisorbed at reactive sites of variable charge soil minerals (e.g., metal oxides), and the role of Fe and Al contents in reducing As mobility was previously stressed [3]. The study of As sorption by different Chinese soils also emphasized the importance of citrate-dithionite extractable Fe content [12]. For comparison, the maximum capacity of As sorption reached up to 3580 mg/kg in Oxisols from Brazil, rich in Fe and Al oxide minerals [13]. Moreover, the As toxicity of the soil leachate evaluated by bioassays showed a significant decrease in the iron-rich soil and an increase in calcareous soils [2]. The results from this study confirm that the most significant role of Fe-compounds in the binding of As can be identified considering the set of soil samples with a wide range of all essential agrochemical properties.

CONCLUSION

The understanding of As sorption by the soil matrix is crucial for predicting the environmental behavior of this pollutant, but also in the decision-making process regarding the most effective remediation technologies. The results of this study demonstrate a high variability in As sorption capacity influenced by the properties of Serbian soils. Higher Fe, as well as Mn and Al content in the soil, was associated with a higher ability to retain As and reduce its migration. However, the potential for releasing sorbed As into the soil solution may rise with fluctuations in soil conditions, such as pH, Eh, the amount of dissolved organic matter, or competing species.

ACKNOWLEDGEMENT

This work was supported by the Ministry of Science, Technological Development, and Innovation of the Republic of Serbia (Contract No. 451-03-47/2023-01/200017).

REFERENCES

1. World Health Organization (2022) Arsenic, https://www.who.int/news-room/fact-sheets/detail/arsenic (accessed date: 25.01.2023).
2. Romero-Freire, A., Sierra-Aragón, M., Ortiz-Bernad, Martín-Peinado, J.F. (2014) Toxicity of arsenic in relation to soil properties: implications to regulatory purposes. Journal of Soils and Sediments, 14, 968–979.
3. Kabata-Pendias, A. (2011) Trace elements in soils and plants. 4th Edition, CRC Press, Boca Raton.
4. Nriagu, J.O., Bhattacharya, P., Mukherjee, A.B., Bundschuh, J., Zevenhoven, R., Loeppert, R.H. (2007) Arsenic in soil and groundwater: an overview. Trace Metals and other Contaminants in the Environment, 9, 3-60.
5. SEPA (2022) Izveštaj o stanju životne sredine u Republici Srbiji za 2021. godinu, http://www.sepa.gov.rs/download/IZVESTAJ_2021.pdf (accessed date: 25.01.2023).
6. "Sl. glasnik RS", br. 30/2018 i 64/2019. Uredba o graničnim vrednostima zagađujućih, štetnih i opasnih materija u zemljištu, https://www.paragraf.rs/propisi/uredba-granicnim-vrednostima-zagadjujucih-stetnih-opasnih-materija-zemljistu.html (accessed date: 25.01.2023)
7. SEPA (2018) Towards soil decontamination in the Republic of Serbia, http://www.sepa.gov.rs/download/zemljiste/TowardsSoilDecontamination.pdf (accessed date: 25.01.2023).
8. Dimović, S., Smičiklas, I., Šljivić-Ivanović, M., Dojčinović, B. (2013) Speciation of ^{90}Sr and other metal cations in artificially contaminated soils: the influence of bone sorbent addition. Journal of Soils and Sediments, 13, 383–393.
9. Marković, J., Jović, M., Smičiklas, I., Pezo, L., Šljivić-Ivanović, M., Onjia, A., Popović, A. (2016) Chemical speciation of metals in unpolluted soils of different types: correlation with soil characteristics and an ANN modelling approach. Journal of Geochemical Exploration, 165, 71–80.
10. Sparks, L.D. (2003) Sorption phenomena on soils. In: Environmental soil chemistry (D.L. Sparks), 2nd Edition, Academic Press, Oxford, 133-186.
11. Jiang, W., Zhang, S., Shan, X.Q., Feng, M., Zhu, Y.G., McLaren, R.G. (2005) Adsorption of arsenate on soils. Part 1: Laboratory batch experiments using 16 Chinese soils with different physiochemical properties. Environmental Pollution, 138(2), 278-284.
12. Jiang, W., Zhang, S., Shan, X.Q., Feng, M., Zhu, Y.G., McLaren, R.G. (2005) Adsorption of arsenate on soils. Part 2: modeling the relationship between adsorption capacity and soil physiochemical properties using 16 Chinese soils. Environmental Pollution, 138(2), 285-289.
13. Fontes, M.P.F., Almeida, C.C., Dias, A.C., Caires, S.M., Rosa, G.F. (2019) Arsenic in soils: natural concentration and adsorption by oxisols developed from different lithologies. Journal of Agricultural Science, 11(6), 260-268.

XV International Mineral Processing and Recycling Conference
17-19 May 2023, Belgrade, Serbia

USING SHERPA TOOL FOR ASSESSMENT OF EUROPEAN WATERBORNE TRANSPORT SECTOR IMPACT ON AIR QUALITY

F. Popescu[1#], M. Zot[1], E. A. Laza[2]
[1] University Politehnica Timisoara, Timisoara, Romania
[2] National Institute of Research and Development for Machines and Installations Designed for Agriculture and Food Industry, INMA – Timisoara Branch, Timisoara, Romania

ABSTRACT – At European level SHERPA (Screening for High Emission Reduction Potential on Air) screening tool was developed by EU Joint Research Centre (JRC) to assist decision factors in evaluating the potential of air quality improvements resulting from localized emission reduction measures. In the paper, a discussion on quantifying emissions and an analysis of European waterborne transport sector is done with an assessment of most polluted areas and eventual potential on reducing emissions generated by waterborne transport.

Keywords: Sherpa, Air quality, Waterborne Transport Emissions.

INTRODUCTION

Waterborne transport can contribute to pollution in Europe through various emissions, including greenhouse gases, nitrogen oxides, sulfur oxides, particulate matter, and other harmful substances. These emissions can have negative impacts on air quality, human health, and the environment.

One of the main sources of emissions from waterborne transport in Europe is the use of fossil fuels in ships. Most ships use heavy fuel oil, which is high in sulfur content and can lead to the release of SOx, NOx and PM. Other sources of emissions from waterborne transport include ballast water discharge, anti-fouling paints, and accidental spills of oil and chemicals. These can have negative impacts on marine ecosystems and biodiversity, as well as human health in coastal and riverside communities.

To address these issues, the European Union has implemented various policies and regulations aimed at reducing emissions from waterborne transport. These include the Sulphur Directive (Directive 2012/33/EU), which limits the sulfur content in fuels used by ships operating in EU waters, and the Marine Strategy Framework Directive, which aims to protect and restore the marine environment through various measures, including reducing emissions from ships. [1] To address the issue of inland waterborne transport pollution in Europe, the EU has introduced several policies and measures. The most notable of these policies is the Inland Waterway Vessel (IWV) certification system, which sets emission standards for NOx and PM emissions from inland waterway vessels. The EU has also established the Blue Corridors project, which aims to promote the use of LNG

corresponding author: Francisc.popescu@upt.ro

and other alternative fuels in inland waterway transport.

In 2020, the MARPOL Convention members decided under IMO 2020 regulation notes the reduction of the Sulphur content of fuel oil used for ships from 3.5 % to a maximum of 0.5 % by mass [2]. A significant reduction of Sulphur oxide emissions from waterborne transport is expected in future years, at European level. Due to high transport load capacities the waterway vessels are considered environmental friendly ways of transport, when focus is on CO_2 emissions. However, as the main enforcements on limiting emissions levels only started in early 1990's, with limits for NOx and PM emissions, most of the marine and inland vessels in operation today are free of emission control. This is mostly due to high life span of engines designed for marine and inland water transport and is expected that vessel fleet renewal with new diesel engines will not happen before 2040. [3]

Methodology

The evaluation of the impact of emissions generated by marine and inland vessels is usually done using chemical transport models that include in their core pollutants transports, pollutants diffusion and pollutants atmospheric reactions. However, because these models require significant computing power they are applied on localized, limited areas, from 50 to 500 km in diameter.

The "Screening for High Emission Reduction Potentials for Air quality" tool (SHERPA) was been developed by the Joint Research Centre specifically to avoid this limitations and to run on regular computing systems while covering entire European continent. This screening tool simulates a chemical transport model, based on statistical data obtained from regulatory bodies of European countries and provides a fast response time for any given air pollutants dispersion [4].

SHERPA is based on source-receptor interaction and it was developed for the analysis of potential air quality improvements resulting from decision making stakeholders emission reduction measures. It is based on a simplified version of a chemistry transport model and provides estimates of concentration levels of precursor pollutants, NOx, NMVOC, PPM, SO2 and NH3, from a single or a group of activity sectors over a domain [5]. The SHERPA tool has 3 independent modules: source allocation, governance and scenario analysis, each focusing on a specific approach on air quality issues.

The main equation implemented in SHERPA is based on cell by cell approach, with a cell spatial resolution of 7x7 km^2 with EU available data on emissions and source-receptor models and emission reduction scenarios. The links between emission $\Delta E_{j,k}$ and concentration ΔC_i are computed cell by cell:

$$\Delta C_i = \sum_j^{Nprec} \sum_k^{Ncell} a^1_{i,j,k} \Delta E_{j,k} \quad (1)$$

This has the main benefit given by its spatial flexibility due to the fact that coefficients $a_{i,j,k}$ are approximated by a distance function:

$$a_{i,j,k} = \propto_{i,j} (1 - d_{i,k})^{-\omega^{i,j}} \quad (2)$$

Where *i* is the grid cell in which the concentration is estimated and *di,k* is the distance between cells *i* and *k* [6]

In SHERPA the areas of interest are defined on the European Nomenclature of territorial units for statistics (NUTS) and Gridded Nomenclature For Reporting (GNFR). In this study we used all European territory and focused on GNFR7, G_Shipping, national navigation including inland waterways sector.

RESULTS AND DISCUSSION

The SHERPA approach is based on GWR (Geographically Weighted Regression) and local modelling approaches, methodologies who uses bell-shaped kernel functions to determine weighted regressions of input versus output variables. [7, 8, 9]

In the scenario assumed in this study we focused mainly on NMVOC, SO2, NOx and PPM emissions generated from marine and inland shipping sector with inclusion of EMEP total emissions per sector (GNFR 7), countries (EU28 and outside) and applying automated SHERPA gridding methodologies, for the year 2022.

The results obtained are presented in figure 1 to 4.

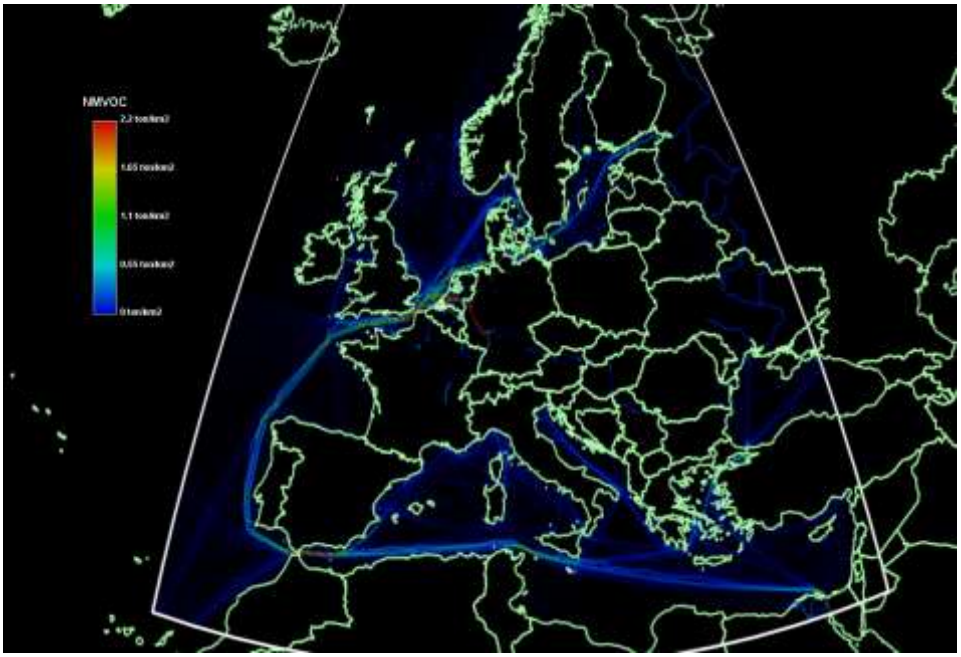

Figure 1 Europe-region level, NMVOC annual average concentration, exclusively GNFR7 water shipping navigation transport sector.

In figures 1 to 4 the relative impact of maritime and inland transport sector and facilities in Europe (EU28 and outside countries) on air quality is given as result of SHERPA modelling tool output, as pollutant concentration in ton/km^2. Figure 1 shows the results obtained for NMVOC emissions, reaching 2.2 ton/km^2 in intense maritime traffic coastal areas in North-West and South Europe.

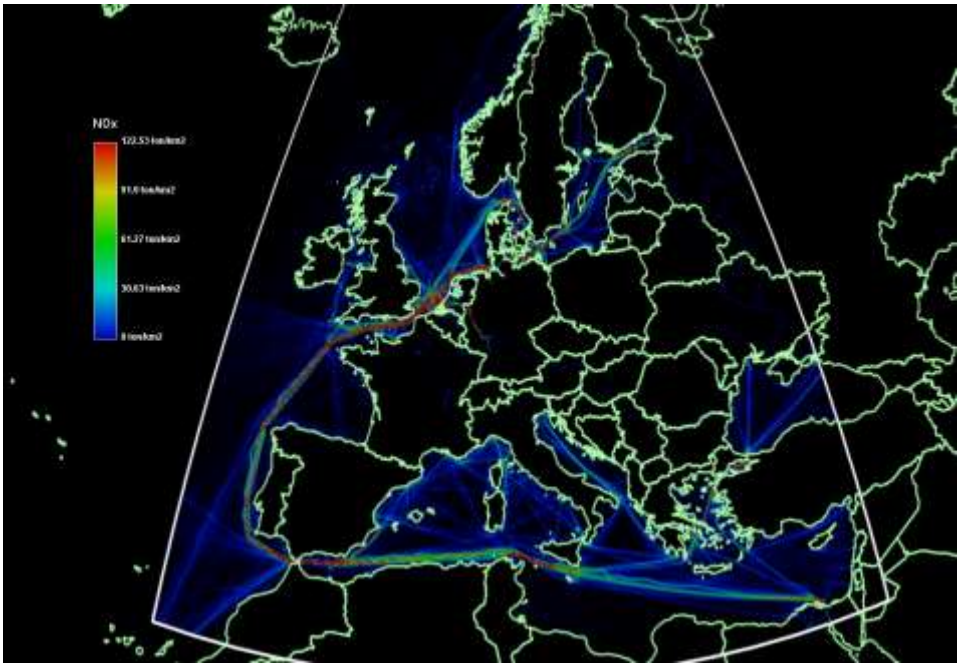

Figure 2 Europe-region level, NOx annual average concentration, exclusively GNFR7 water shipping navigation transport sector.

Figure 3 Europe-region level, PPM annual average concentration, exclusively GNFR7 water shipping navigation transport sector.

Figure 4 Europe-region level, SO_2 annual average concentration, exclusively GNFR7 water shipping navigation transport sector.

Figure 2, 3 and 4 shows the results obtained for NOx, PPM and SO_2 emissions, reaching 122 ton/km^2 for NOx, 5 ton/km^2 for PPM and 14 ton/km^2 for SO_2, all occurring in the intense maritime traffic coastal areas in North-West and South Europe.

CONCLUSION

Based on a study conducted by International Maritime Organization (IMO) in 2018, the overall contribution of water shipping to global anthropogenic GHG emissions was about 3% in 2018 [10] and considering this low contribution the maritime and inland water transport can be considered the most efficient method of international transportation of goods. However, even if the maritime transport sector has a low CO2 contribution than others, in terms of SO_2 and NOx emissions is relevant, with about 13% quota for SO_2 and 15% for NOx global emissions [10]. This data shows that naval shipping, especially on inland waters constitute a major source of local pollution, inland and on coastal areas.

Also, a research study conducted in France (2015-2016), [3] with direct measurements of emissions onboard of different types of marine and inland vessels, a pusher tug vessel produces up to 2 times higher emissions of NOx, CO and particulate matter than Euro V road trucks for 1 ton of goods transported. Similar results were found in this research, for example by running SHERPA for GNFR6 sector (Road transport) we found that emissions from road transport in Europe reached maximum of 44 ton/km^2 in comparison to 122 ton/km^2 for water transport and SO_2 of 1.3 ton/km^2 in comparison to 14 ton/km^2. At the same time the NMVOC emissions generated by road transport, 67 ton/km^2, are much higher than 2.2 ton/km^2 found for water transport.

In the recent years the European Union focused on reducing or eliminating the GHG emissions from all sectors, with an emphasis on energy and transport sectors. This study is intended to show that SHERPA tool can help researches and EU decision makers to implement more pin-point strategies in reducing pollution and GHG in geographical areas where it most frequently occurs.

ACKNOWLEDGEMENT

This research was partially supported by the cross-border cooperation project AEPS (http://aeps.upt.ro) "Academic Environmental Protection Studies on surface water quality in significant cross-border nature reservations Djerdap/Iron Gate national park and Carska Bara special nature reserve, with population awareness raising workshops", RORS-462, project funded by the INTERREG IPA-CBC Romania-Serbia Programme.

REFERENCES

1. E.U. (2012) Directive 2012/33/EU of the European Parliament and of the Council, amending Council Directive 1999/32/EC as regards the Sulphur content of marine fuels, 2012/33/EU, https://eur-lex.europa.eu/, (10.04.2023)
2. I.M.O (2020) Amendments to MARPOL annex VI, regulations for the prevention of air pollution from ships, MEPC 73/19/Add.1, Annex 1, page 2, https://www.imo.org/en/OurWork/Environment/ (10.04.2023)
3. Pillot, D., Guiot, B., Cotties, P.L., Perret, P., Tassel, P. (2016) Exhaust emissions from in-service inland waterways vessels, Journal of Earth Sciences and Geotechnical Engineering, 6(4), 205-225
4. Thunis, P., Degraeuwe, B., Pisoni, E., Ferrari, F., Clappier, A. (2016) On the Design and Assessment of Regional Air Quality Plans: The SHERPA Approach, Journal of Environmental Management 183(Pt 3) 952-958
5. Popescu, F., Vujic, B., Cioabla, A.E., Mrceta, U., Dungan, L., Trif-Tordai, G., Laza A. (2020) Using SHERPA screening tool for design and assessment of local and regional air quality management, Journal of Physics: Conference Series, 1781, 012055
6. Albrecht, D., Mara, T.A., Pisoni, E., Rosati, R., Tarantola, S. (2018) Sensitivity Analysis of the SHERPA Air Quality Model, EUR 29122 EN, Publications Office of the European Union, Luxembourg, doi:10.2760/78023, JRC110322
7. Wolf, L.J., Oshan, T.M., Fotheringham, A.S., (2018) Single and multiscale models of process spatial heterogeneity. Geographical Analysis, 50, 223–246.
8. Lloyd, C., (2010) Local Models for Spatial Analysis. CRC Press, Boca Raton. https://doi.org/10.1201/EBK1439829196
9. Belis, C.A., Pisoni, E., Degraeuwe, B., Peduzzi, E., Thunis, P., Monforti-Ferrario, F., Guizzardi, D. (2019) Urban pollution in the Danube and Western Balkans regions: The impact of major PM2.5 sources. Environment International, 133 (A), 105158
10. I.M.O. (2020) International Maritime Organization. Fourth Greenhouse Gas Study 2020, https://www.imo.org/en/OurWork/Environment/Pages/Fourth-IMO-Greenhouse-Gas-Study-2020.aspx (10.04.2022)

XV International Mineral Processing and Recycling Conference
17-19 May 2023, Belgrade, Serbia

THE IMPACT OF EXPLOITATION OF PRIMARY AND ALTERNATIVE ENERGY SOURCES ON THE ENVIRONMENT

A. Stojić[1#], D. Tanikić[1], E. Požega[2]
[1] University of Belgrade, Technical Faculty in Bor, Bor, Serbia
[2] Mining and Metallurgy Institute, Bor, Serbia

ABSTRACT – Primary sources of energy are the foundation of all industrial processes, and their exploitation is crucial for the functioning and maintenance of the modern world. However, the majority of primary energy sources come from non-renewable sources, such as coal, oil, and gas, whose exploitation can have negative consequences for the environment. This paper will investigate how the exploitation of primary energy sources affects the environment and which are the negative consequences for the air, water, soil, and animal life. Additionally, measures that can be taken to reduce the impact of primary energy source exploitation on the environment will be presented, and alternatives that can be used as a replacement for traditional energy sources will be considered. The aim of this paper is to assess the impact of the exploitation of primary energy sources on the environment, in order to gain a better understanding of the importance of sustainable development and environmental protection for the future.

Keywords: Energy, Environment, Exploitation, Sustainability, Modern World.

INTRODUCTION

During industrialization and with the increase in population on Earth, as well as the increase in transportation, the demand for energy has also increased. This has led to an increased use of fossil fuels, and the world economy currently relies on them. Energy and environmental problems are closely related, since it is nearly impossible to produce, transport, or consume energy without significant environmental impact.

The environmental problems directly related to energy production and consumption include air pollution, climate change, water pollution, thermal pollution, and solid waste disposal. The emission of air pollutants from fossil fuel combustion is the major cause of urban air pollution. Fossil fuels burning is also the main contributor to the emission of greenhouse gases. Diverse water pollution problems are associated with energy usage. One of the main problems are oil spills. In all petroleum-handling operations, there is a finite probability of spilling oil either on the earth or in a body of water. Coal mining can also pollute water.

Changes in groundwater flow produced by mining operations often bring otherwise unpolluted waters into contact with certain mineral materials which are leached from the soil and produce an acid mine drainage. Solid waste is also a by-product of some forms of energy usage. Coal mining requires the removal of large quantities of earth as well as coal.

corresponding author: astojic@tfbor.bg.ac.rs

PRIMARY AND ALTERNATIVE SOURCES OF ENERGY

Scientists define energy as the ability to do work. People use energy to walk and ride a bicycle, to move cars along roads and boats through water, to cook food on stoves, to make ice in freezers, to light our homes and offices, to manufacture products, and to send astronauts into space… [1] Energy can be converted from one form to another. For example, the food you we eat contains chemical energy, and our body stores this energy until we use it as kinetic energy during work or play. The stored chemical energy in coal or natural gases and the kinetic energy of water flowing in rivers can be converted to electrical energy, which can be converted into the light and heat. There are many different sources of energy, but they can all be divided into two categories. Renewable energy sources and nonrenewable energy sources. Renewable and nonrenewable energy sources can be used as primary energy sources to produce useful energy such as heat, or they can be used to produce secondary energy sources such as electricity and hydrogen. Energy transition from one fuel source to another are accompanied with each phase of economic development. The current energy mix is dominated by fossil fuels (coal, oil, and natural gas). However, the beginning of a new energy era in the twenty-first century is already in progress as there is a noticeable transition of energy sources away from fossil fuels towards renewable energy. The major factors driving this transition include but are not limited to environmental concerns on climate change, limited nature of fossil fuel and supplies, prices, and advancement in technology. Society will sooner or later adopt renewable energy since fossil fuels have limited supply and are only formed over a long period of geological time. [1] Fossil fuel reserves may be extended by developing new methods and technologies for extraction, but the need to decrease the negative effects of fossil fuel on climate change is a more immediate problem than the depletion of fossil fuel. However, it has been argued that renewable energy (i.e., solar power, hydro power etc.) is fairly developed majorly because the most of its application is in areas of electricity generation. Although renewable energy is a cleaner form of energy, the dark sides of renewable energy sources have not received considerable attention yet. This study analyses the negative impacts of the exploitation of renewable energy sources on the environment, society and the global economy.

Alternative energy sources have become a popular topic of discussion in recent times, as the world looks for ways to reduce its carbon footprint and combat climate change. The use of solar, wind, and hydropower is on the rise, with many countries investing heavily in renewable energy infrastructure. These sources of energy are not only environmentally friendly but also have the potential to provide a sustainable source of energy for the future. However, their implementation also presents challenges such as high upfront costs, intermittency, and limited scalability. Despite these challenges, the growing demand for renewable energy makes it clear that alternative energy sources will play a significant role in the energy mix of the future. The benefits of alternative energy sources go beyond environmental considerations. They can also lead to energy independence, job creation, and economic development in local communities. In addition, the use of alternative energy sources can reduce the dependence on finite resources and volatile global energy markets.

IMPACT OF PRIMARY AND ALTERNATIVE ENERGY SOURCES EXPLOITATION ON THE ENVIRONMENT

The exploitation of primary energy sources, including fossil fuels, hydroelectric power, nuclear energy, and others, has a significant impact on the environment. The process of energy exploitation and production often leads to air, water, and soil pollution, which can have harmful consequences for human health and animal species.[2] For example, burning of fossil fuels such as coal, oil, and gas releases large amounts of carbon dioxide into the atmosphere, which can lead to global warming and climate change. Nuclear energy exploitation can also have dangerous consequences for the environment, such as possible nuclear accidents and nuclear waste that can be harmful to humans and animals. Hydroelectric power can have a significant impact on ecosystems, including changes to river flows and the impact on animal species that live in those river systems. The installation of hydroelectric power can also have a serious impact on the environment, including the destruction of animal habitats and migration routes. In this sense, there is a growing need to switch to renewable energy sources, such as solar energy, wind energy, and geothermal energy. However, although these energy sources are clean and renewable, their exploitation can have negative consequences on the environment, including the impact on wildlife, the local economy, and communities living near these energy sources. Therefore, it is important to consider the impact of primary energy source exploitation on the environment and to develop sustainable ways of energy production and use that minimizes their impact on the environment.

The dark sides of renewable energy refer to the negative impacts from the exploitation of renewable energy sources. These negative impacts can be broadly categorized into environmental and socio-economic impacts. In order to harness energy from renewable energy sources, a lot of metals and materials are required. A car battery weighs about 1,000 pounds. Fabricating one requires digging up, moving and processing about 500,000 pounds of raw materials. [2] All the mineral products and metals needed to make wind turbines and solar panels rely on mining and these mining activities, from the processing stage to the finishing of the final products, are powered by fuels derived from crude oil. To meet the goals to go “green” may likely cause a rare earth emergency as increase in demand for green energy requires a corresponding increase in mining for rare solid minerals. These minerals are used for the manufacturing of components required for wind turbines, solar panels, batteries, etc. Most of these minerals are harmful and may cause respiratory problems and irritation when contacted, ingested or inhaled. A spike in demand for metals could drain the planet’s reserves. About 60% of cobalt comes from the Democratic Republic of Congo, whose which has been charged for using child labour in unsafe mines. The production level of lithium and nickel would increase to about 280% and 136% respectively if renewable energy was to contribute 100% of the energy mix [2]. Recycling is recommended but also expensive. Recycled cobalt cost 5 times more than newly mined cobalt. In 2019, two dams collapsed in Vale’s Brumadinho mine, Brazil, killing 247 workers and local residents, with 23 still missing. This increase in the exploitation of rare solid minerals and the accidents that occur therefrom are directly or indirectly linked to the drive to increase renewable energy utilization.

Huge wastes are left during decommissioning of renewable energy plants. The average lifespan of a wind turbine is 20 to 25 years. Researchers estimate the U.S. will

have more than 720,000 tons of blade material to dispose of over the next 20 years. Solar panels generally last about 20-30 years. When solar panels are damaged due to storms or hurricanes, they leave a large amount of waste. There will be an estimated 60 million tons of cumulative solar photovoltaic waste by 2050. Added to the waste footprint left on the environment are issues of noise pollution, aesthetic and visual impact, air and water quality reduction and natural resource depletion which renewable energy mix share in common with the fossil fuel family. [2]

Raw materials for wind and solar energy equipment are mined in more than 60 countries. Mineral's extraction already exact significant cost on people and the environment, fueling conflict and human rights violations, massive water pollution, and wildlife and forest destruction. Wind farms kill birds and bats, and affect fishing activities when they are built offshore, while solar power plants ignite birds killing about 1,000 birds per year [3]. According to office of Energy Efficiency and Renewable Energy, a US Department of Energy Agency, wind energy can have adverse environmental impacts, including the potential to reduce, fragment or degrade habitat for wildlife, fish, and plants [4]. Land use estimate for solar plants is averagely 3.5 to 10 acres per megawatt for utility-scale PV systems, while the estimate is between 4 and 16.5 acres per megawatt for Concentrated Solar Plant (CSP). A report published by Union of Concerned Scientists in the United States, on the Environmental Impact of Solar Power shows that CSP plants that use wet-recirculating technology with cooling towers withdraw between 600 and 650 gallons of water per megawatt-hour of electricity produced [5]. Hydro energy sources cause environmental and social threats such as damage to wildlife habitat and water quality, obstruction of fish migration pathways and cause limitations to the recreational benefits of rivers. Dams constructed for hydro energy can also create division between nations, an example being the current tension between Egypt and Ethiopia regarding the dam constructed by Ethiopia on the Nile river for generation of electricity.

Time is not on the side of fossil industries and this represents a significant threat to the global economy. The city of Berkeley, California, U.S. has banned new natural gas hookups in new buildings, and there are dozens of other cities exploring similar prohibitions. There would be a big challenge if financial institutions stop funding fossil fuel companies or projects. According to John Fullerton in his article "Big Choice", some of the wealthiest companies and some countries with the biggest sovereign wealth funds in the world have huge fossil fuel assets on their balance sheets [4]. A shift from these fossil assets would imply at least 20 trillion dollars in stranded assets which would trigger a financial collapse. Such financial collapse would be greater than the 2008 financial collapse caused by the stranding of 2.7 trillion USD mortgage assets. If this occurs, it will possibly lead to the complete loss of the oil, gas and coal industries, power producers, insurance companies and banks that hold loans for these industries.

The dark sides of renewable energy utilization come with significant cost implications. For instance, as stated above, windmills and photovoltaic (PV) installations result in huge wastes during decommissioning, at the end of their useful life. There are significant costs associated with managing the resultant wastes, either through recycling or complete disposal. The economic impacts arising from the damage to the ecosystem (fish, birds, bats, impact on land and water, etc.) are huge if reversible, and may sometimes be

irreversible. The depletion of the rare solid minerals exerts pressures on other sectors of the economy that compete for these minerals. In terms of human health, coming in contact with some of these minerals and the collapse of renewable energy facilities are hazards that could lead to illness, accidents and/or deaths, with significant cost implications.

MEASURES TO REDUCE THE NEGATIVE IMPACT OF PRIMARY AND ALTERNATIVE ENERGY SOURCES EXPLOITATION ON THE ENVINROMENT

There are several measures that can be taken to reduce the negative impact of primary energy source exploitation on the environment. [5] One of the most effective measures is to shift towards renewable energy sources such as solar, wind, and geothermal power. This will not only reduce the emissions of greenhouse gases but also reduce the dependence on non-renewable sources of energy. Another measure is to improve energy efficiency by using energy-saving technologies and practices. This includes using energy-efficient appliances, buildings, and transportation systems, as well as implementing energy management systems in industries and businesses. Regulations and policies can also play a crucial role in reducing the negative impact of primary energy source exploitation on the environment. Governments can implement measures such as carbon taxes and emissions trading schemes, as well as regulations to limit the environmental impact of industries and energy producers. Finally, public awareness and education are essential in reducing the negative impact of primary energy source exploitation on the environment. By promoting sustainable lifestyles and educating the public on the importance of reducing energy consumption, we can collectively contribute to reducing the environmental impact of primary energy source exploitation.

CONCLUSION

Renewable energy has the potential to minimize the overall impact that the energy industry has on the environment, especially its contribution to climate change. However, the renewable energy industry causes reasonable negative impacts on people and the environment. Such impacts, arising from the activities in the industry, have significant financial implications. The technology to harness energy from renewable sources have only been well developed for the electricity market. There is currently a strong drive to increase renewable energy electricity generation capacity and to expand the scope beyond electricity generation. Such increase in capacity and increase in scope will place an increasing demand for rare solid minerals and invariably impact negatively on the environment, society and affect the economics of production. Mitigating these impacts will require a proper plan and policy to control supply, regulate decommissioning and encourage recycling of renewable energy products which may also affect the cost of supply in the long run.

ACKNOWLEDGEMENT

"The research presented in this paper was done with the financial support of the Ministry of Education, Science and Technological Development of the Republic of Serbia, within the funding of

the scientific research work at the University of Belgrade, Technical Faculty in Bor, according to the contract with registration number 451-03-47/2023-01/200131".

REFERENCES

1. Timmons, D., Harris, J.M., Roach, B. (2014) The Economics of Renewable Energy. Tufts University. Global Development and Environment Institute.
2. IEA (2010) Renewable Energy Essentials: Hydropower. International Energy Agency.
3. IEA (2012) Technology Roadmap: Bioenergy for Heat and Power. Paris: International Energy Agency.
4. Easton, J. (2019) Report: Clean Energy Must Not Rely on Dirty Mining. Retrieved from Earthworks: https://www.earthworks.org/media-releases/report-clean-energy-must-not-rely-on-dirty-mining/.
5. Jenkins, J. (2019) The Dark Side of Renewable Energy. Pikes Peak Environmental Forum.

XV International Mineral Processing and Recycling Conference
17-19 May 2023, Belgrade, Serbia

MOBILE PHONES – A VALUABLE COMPONENT OF E-WASTE STREAM

A. Radojević[#], S. Šerbula, T. Kalinović, J. Milosavljević, J. Kalinović
University of Belgrade Technical faculty in Bor, Bor, Serbia

ABSTRACT – As the fastest growing stream of waste, electric and electronic waste (e-waste) became one of the top priorities in the waste management policies in recent years. Since discarded mobile phones contain valuable metals such as gold, silver, platinum group of metals, copper, and nickel, as well as harmful ones, like lead and cadmium, the recycling should be considered both from the ecological and economical point of view. Metals in mobile phones are concentrated in printed circuit boards, as well as in batteries. Different technologies are being developed for the recovery of metals, plastic, and other components of the mobile phones.

Keywords: E-waste, Mobile Phones, Recycling, Environment Protection.

INTRODUCTION

The waste management data are critical in the process of creating policies for the treatment and disposal of all kinds of waste. Understanding the quality and quantity of generated waste, especially with the rapid urbanization and population growth, allow selection of a suitable management method. During 2016 more than 2 billion tonnes of municipal solid waste was generated in the world, on average 0.74 kg/person/day. The waste generation rates vary widely from 0.11 kg/person/day in Sub Saharan Africa to 4.54 kg/person/day in North America. In Serbia, the generation rate was at the world´s average, amounting to 0.72 kg/person/day. There is generally a positive correlation between the municipal waste generation rate and income level. The high-income countries (the gross national income – GNI, around US$12,500), account for 16% of the world's population and generate about 34% of the world's waste (683 million tonnes) [1]. Global consumption of materials such as biomass, fossil fuels, metals and minerals are expected to double in the next 40 years, while annual waste generation is projected to increase by 70% by 2050 [2], reaching 3.4 billion tonnes in 2050 [1].

Modern life is defined by various electronic devices and electrical equipment, from washing machines to smartphones. However, relatively short time of usage of some of the household appliances and portable devices, which cannot be easily reused, repaired, or recycled, is responsible for making it the fastest growing waste stream increasing at 3–5% per year in the European Union (EU). Electrical and electronic equipment type of waste is called WEEE or simply e-waste. The problem of fast-growing quantities of e-waste was recognized more than two decades ago, and the EU has made many improvements in waste management and legislative since the 1970s. The WEEE Directive 2002/96/EC was replaced with the Directive 2012/19/EU with the aim to

[#] corresponding author: aradojevic@tfbor.bg.ac.rs

prevent and reduce the negative environmental effects resulting from the resource use, generation, and management of e-waste through sustainable production and consumption, by supporting reuse, recycling, and other forms of recovery of such type of waste [2–4].

The generation of e-waste is strongly associated with the economic development, just like the generation of municipal waste. The high-income countries are generating 5 times the volume of e-waste generated by lower middle-income countries (the GNI US$1,026–4,035), that is 0.05 kg/capita/day compared to less than 0.01 kg/capita/day, respectively (on average 0.02 kg/capita/day). The share of recyclable materials from waste (paper, cardboard, plastic, metal, and glass), is also increasing with the economic development, ranging from 16% in low-income countries (US$1,025 GNI) to about 50% in high-income countries [1].

Considering all the categories of e-waste, smartphones are the most abundant electronic devices. As a result of the rapid technology development which simultaneously affects the improvement in the performances and the drop of prices, consumers replace their mobile phones more frequently [5]. The time of use of mobile phones is one of the shortest for all electronic devices, and lately it is getting shorter. Mobile phones are replaced after 3 years on average in developing countries, or in less than 2 years in developed countries [6]. However, compared to other electrical and electronic equipment, smartphones are more likely to be disposed of even if they are still in function, due to the reasons such as fashion trends and product obsolescence [7].

Discarded mobile phones should be considered from the ecological as well as from the economical point of view. They contain many harmful substances, such as Pb, Cd, and other chemicals with high potential to severely pollute the environment, and pose harm to the human health if not handled properly. On the other hand, many valuable materials such as Au, Ag, Cu, Ni, etc. can be recycled [5].

RESULTS AND DISCUSSION

In 2015, the European Commission started implementation of a new Circular Economy Action Plan (CEAP), with one of its priorities focused on the reduction of e-waste. In a circular economy, products, and the materials they contain are highly valued, unlike in traditional, linear economic model which is based on pattern “take-make-consume-throw away”. The CEAP is aimed to reduce the waste to minimum through reusing, repairing, refurbishing, and recycling of products. Benefits from implementation of the CEAP are numerous: reduced pressure on the environment, enhanced security of supply of raw materials, increased competitiveness, innovation, and opening new jobs. Between 2012 and 2018 the number of jobs linked to the circular economy in the EU grew by 5% reaching around 4 million jobs. One of the most effective environmental strategies of the CEAP approach is increasing product lifespan. For example, by repairing broken e-products, materials are kept longer in use. At the same time, by slowing down the production and consumption cycle, waste generation is prevented, as well as emissions from the production and transport are reduced, and energy is saved. Additionally, the measures such as introduction of a common charger for mobile phones/tablets are very simple to implement and yet could

have big impact on the sum of e-waste generation worldwide [3,4]. The economic value of electronic products is lost when fully or partially functional products are discarded mainly because they are not reparable, the battery cannot be replaced, or the software is no longer supported. It should be noted that two types of lifespan exist. The "technical" lifespan refers to the products' technical abilities, while "social" lifespan is linked to the products' flexibility concerning social changes, changes in life situations, and changes in personal taste. Both aspects are a part of the sum quality of the product [7].

During 2012, out of 9 million tonnes of electrical and electronic products distributed on the EU market, 3.5 million tonnes were collected, of which 2.5 million tonnes were recycled or reused [3]. Large household appliances, such as washing machines and electric stoves, were the most collected ones, making 52.7% of all the collected e-waste. This is followed by consumer equipment (e.g. video cameras) with 14.6%, computer equipment (laptops, printers) with 14.1%, and small household appliances (vacuum cleaners, toasters) with 10.1% of the share. Other categories of electrical and electronic equipment make 8.4% of all the collected e-waste [8]. According to some estimation, an increase of 16–28% of e-waste for the EU region is going to happen every 5 years [6]. Due to the complexity of e-waste streams, the collected data need to be treated with caution, but still, represent a good reflection of the current situation in the EU [3].

During 2019, over 1.5 billion mobile phones were sold worldwide. The data from 2021 showed that China had the highest number of mobile phone users – 912 million. Although up to 80% of the materials in phones can be reused or recycled, the recycling rate of used phones in China is only 2%, and most of the phones end up with municipal waste or just "hibernate" [9]. Zhang *et al.* [5] showed that, approximately half of the respondents keep their last obsolete mobile phone at home because of stored personal information. 25% of respondents recycled their mobile phones through formal recycling channels. Also, recycling of packaging of mobile phones is important because it might also harm the environment since it contains plastic [9].

Laitala *et al.* [7] showed that among electric appliances included in the survey conducted in Norway, mobile phones were most frequently malfunctioning (28%), followed by dishwashers and laundry washing machines (12%), while 10% or less referred to malfunctioned refrigerators, freezers, and stoves. Out of all broken mobile phones, 55% were not repaired, for 19% the repairment failed, and only 16% of mobile phones were successfully repaired. The price and the availability of repair services, especially for mobile phones, are a crucial part of the circular economy. By increasing phone lifespan, better resource utilisation and less waste generation is obtained [7].

By the recycling technologies, materials are recovered and extraction of natural resources is avoided. Although recycling rate is globally low, amounting to 13.5%, it varies among countries with different income level. For example, in low-income countries the dominant disposal method is open damp with 93% of the total share, while recycling rate is less than 4%. On the other hand, in high-income countries, open dumps account only for 3% compared to recycling with 29% of the share. In Europe and Central Asia, the data showed similar share of unspecified landfilling and recycling (20.1% and 20%, respectively), with open dump (25.6%) as the preferred method. The

data about Serbia (upper middle-income country, US$4,036–12,475 GNI), showed enormous gap between unspecified landfilling (73.9%) and recycling (0.8%) [1]. The average recycling rate of e-waste in the EU region is about 40% with some differences, for example, during 2016, the recycling rate of e-waste in Croatia was 81.3%, while in Malta was 20.8% [8].

Mobile phone producers, such as Apple [10], Huawei [11], and Samsung [12], and producers of other electronic devices [13,14] have already launched recycling programs, as measure for fulfilling an environmental corporate social responsibility. However, an effective recycling program of mobile phones must overcome the key barriers to consumers' participation, such as the lack of economic incentives and the inconvenience of return processes [9].

The precious metals (e.g. Au, Ag, and Pd) are widely used as contact materials or plating layers due to their electric conductivity and chemical stability. Moreover, e-waste contains about 10 times more precious metals than the corresponding natural minerals, providing a strong incentive for recycling it [15]. According to the data, 1 t of waste mobile phones contains 347 g of Au on average [16], while about 100 kg of Cu can be recovered from 1 t of used mobile phones [17], thus the recovery of materials has significant financial benefit other than environmental.

The typical recycling process of smartphones and tablets (Fig. 1) consists of separate processing of printed circuit boards and batteries [18]. Batteries incorporated in all kinds of e-waste should be collected, removed (manually, mechanically, chemically or in other way of handling) [4], and subjected to the recycling requirements of the Battery Directive 2006/66/EC.

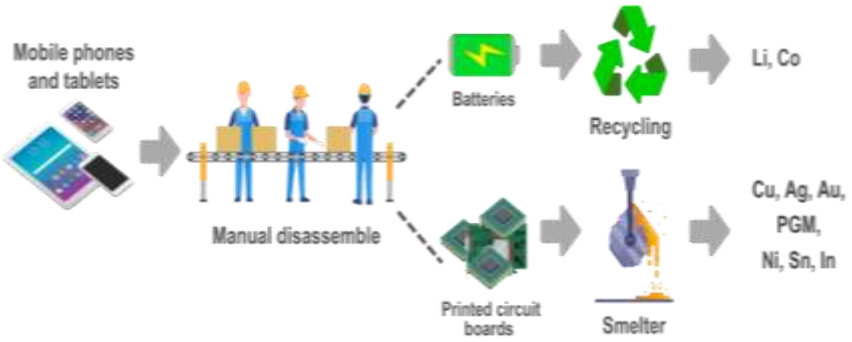

Figure 1 The end-of-life processes for smartphones and tablets (adopted from Schischke *et al.* [18])

However, recycling activities also have negative impact on the environment. Sugiyama *et al.* [17] estimated environmental impact of transportation and activities related to recycling of end-of-life mobile phones in Japan. According to simple mathematical model based on the total CO_2 emissions, a shipping transportation length has a biggest influence on environmental impact. Although shipping contributes only about 16% to the total fuel consumption of all traffic related sources, these emissions significantly contribute to emissions of pollutants from all transport modes, e.g. shipping emits approximately 1,200 times more particulate matter than aviation [19].

Printed circuit boards in mobile phones

Most of the printed circuit boards (PCBs), which are an essential subset of mobile phones, are incinerated or landfilled, causing pollution due to the emission of toxic compounds such as metals, dioxins, furans, polyhalogenated organic pollutants (POPs) and polycyclic aromatic hydrocarbons (PAHs). Heavy metals such as Pb, Cd, and Hg can leach on landfill sites, while gaseous compounds diffuse in the air. Within PCBs, Cu and Ni are the most abundant metals (Fig. 2), with 13–26 times higher content compared to natural resources, while the most valuable metal is Au, with almost 100 times higher concentration compared to ores. However, the main problem of metal recovery process is much lower concentration of Au compared to the base metals. The first step in recovering metals from PCBs is often selective dissolution of base metals in order to concentrate Au in a solid residue for subsequent recovery. The leaching of base metals is mostly carried out with strong acids (sulfuric, nitric or hydrochloric acid, or *aqua regia*) with adequate oxidant (H_2O_2, Cl_2, O_2, or even bacteria), since the metals are present in PCBs in their elemental forms [20]. Knowing the negative effects of strong acids, eco-friendly processes, compared to conventional methods, have been developed for recovery of base and other metals. Rao *et al.* [20] optimized the selective leaching process of Cu and Ni at lower temperatures (30 °C), in which energy consumption and effluent generation is reduced. However, under these conditions, Au cannot be dissolved. Yet, formed gold-rich residue (Fig. 2) is easy to manipulate with and could be subsequently used for the obtaining gold by hydrometallurgy.

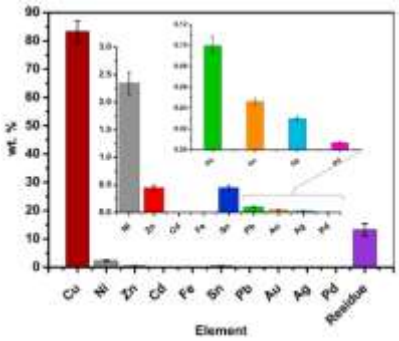

Figure 2 Composition (wt. %) of PCBs separated from mobile phones [20]

Batteries in mobile phones

The lead-acid, nickel-cadmium (Ni-Cd), nickel-metal hydride (Ni-MH), and Li-ion technologies are the most important battery systems used in electronic equipment today. The Ni-MH system was developed in 1989 for the replacement of portable Ni-Cd batteries, due to the toxic properties of Cd. Hence the newer batteries are based on the metals which have lower impact on the environment compared to Cd [21]. Lithium-ion batteries (LIBs) represent one of the biggest growth areas of the 21st Century since Li is preferred material among all metals because of the lightest, highest electrochemical potential, and the highest energy density. Spent LIBs usually contain 5–20% Co, 5–7% Li, 5–10% Ni and other metals (Cu, Mn, Al, Fe, etc.), 15% organic compounds, and

7% polymer separators. The composition differs depending on the producer and the type of the battery [22]. LIBs from mobile phones, other than plastics, contain about 15% Cu, 13% Al, 7.6% Fe, and 3% Ni, which all have high economic value. The total income of recycling of 1 tonne of LIBs could be more than US$3,200. Mobile phone batteries, have an average life span of 3 years, compared to batteries for electric vehicles, which have eight-year warranty, thus the recycling cycle of phone batteries is more than 2.5 times faster [23]. Recycling of spent batteries can be divided into three main processes: pre-treatment, metal extraction, and end-product preparation. Metal-extraction processes play the most important role in the entire recovery process and involve one of pyro-, hydro- or bio-metallurgical methods [21,22]. For example, Mennik *et al.* [23] showed that combination of flotation and magnetic separation could be a feasible technology with the recovery rate of 99% of metals and plastics from spent LIBs. However, hydrometallurgical methods have superiority because of industrial applicability, eco-friendly nature, high recovery rates and additional equipment is not required. The disadvantage of this method is the requirement of reagents such as strong acids used for leaching [22].

CONCLUSION

The environmental problems need to be resolved through sustainable resource management and circular economy in order to achieve zero-waste goal. As a fastest-growing stream of the e-waste, mobile phones, need to be properly managed and recycled due to the high content of hazardous components. The ecological benefit is equal to the economical, since two main components of the phones, printed circuit boards and batteries, contain valuable metals such as copper, nickel, gold, platinum group of metals, lead, cadmium, aluminium, etc. Importantly, the ongoing research studies are focused on the development of environmentally friendly recycling approach with the maximum recycling rate and minimum operating costs.

ACKNOWLEDGEMENT

The authors are grateful to the Ministry of Education, Technological development, and Innovations of the Republic of Serbia for financial support, within the funding of the scientific research at the University of Belgrade, Technical Faculty in Bor (No. 451-03-47/2023-01/200131). Our thanks go to Prof. Mara Ž. Manzalović from the University of Belgrade, Technical Faculty in Bor, for providing language assistance.

REFERENCES

1. Kaza, S., Yao, L, Bhada-Tata, P., Van Woerden, F. (2018) What a Waste 2.0 – A Global Snapshot of Solid Waste Management to 2050. The World Bank Group.
2. Circular Economy Action Plan for a cleaner and more competitive Europe, EU, 2020.
3. Bourguignon, D. (2018) Circular economy package four legislative proposals on waste, European Parliamentary Research Service. European Union.
4. European Commission (2014) Frequently Asked Questions on Directive 2012/19/EU on Waste Electrical and Electronic Equipment (WEEE).

5. Zhang, L., Ran, W., Jiang, S., Wu, H., Yuan, Z. (2021) Understanding consumers' behavior intention of recycling mobile phone through formal channels in China: The effect of privacy concern. Resources, Environment and Sustainability, 5, 100027.
6. Soo, V.K., Doolan, M. (2014) Recycling Mobile Phone Impact on Life Cycle Assessment. Procedia CIRP 15, 263-271.
7. Laitala, K., Klepp, I.G., Haugrønning *et al.* (2021) Increasing repair of household appliances, mobile phones and clothing: Experiences from consumers and the repair industry. Journal of Cleaner Production, 282, 125349.
8. E-waste in the EU: facts and figures (infographic), European Parliament www.europarl.europa.eu/news/en/headlines/society/20201208STO93325/e-waste-in-the-eu-facts-and-figures-infographic (accessed on March 7, 2023).
9. Hu, Y., Frank, B., Lu, Z. (2022) Market success through recycling programs: Strategic options, consumer reactions, and contingency factors. Journal of Cleaner Production, 353, 131003.
10. apple.com/recycling/nationalservices/ (accessed on March 7, 2023).
11. consumer.huawei.com/en/support/recycling/ (accessed on March 7, 2023).
12. samsung.com/us/aboutsamsung/sustainability/environment/responsible-recycling/ (accessed on March 7, 2023).
13. lgrecyclingprogram.com/ (accessed on March 7, 2023).
14. mi.com/in/service/support/ewastetakeback.html (accessed on March 7, 2023).
15. Wang, R., Zhang, C., Zhao, Y. *et al*. (2021) Recycling gold from printed circuit boards gold-plated layer of waste mobile phones in "mild aqua regia" system. Journal of Cleaner Production, 278, 123597.
16. Navazo, J.M.V., Mendez, G.V., Peiro, L.T. (2014) Material flow analysis and energy requirements of mobile phone material recovery processes. International Journal of Life Cycle Assessment, 19, 567-579.
17. Sugiyama, K., Honma, O., Mishima, N. (2016) Quantitative Analysis of Material Flow of Used Mobile Phones in Japan. Procedia CIRP, 40, 79-84.
18. Schischke, K., Berwald, A., Dimitrova, G. *et al.* (2022) Durability, reparability and recyclability: Applying material efficiency standards EN 4555x to mobile phones and tablet computers. Procedia CIRP, 105, 619-624.
19. Eyring, V., Kohler, H.W., van Aardenne, J., Lauer, A. (2005) Emissions from international shipping. Journal of Geophysical Research, 110, D17305.
20. Rao, M.D., Singh, K.K., Morrison, C.A., Love, J.B. (2021) Optimization of process parameters for the selective leaching of copper, nickel and isolation of gold from obsolete mobile phone PCBs. Cleaner Engineering and Technology, 4, 100180.
21. Santos, V.E.O., Celante, V.G., Lelis, M.F.F., Freitas M.B.J.G. (2012) Chemical and electrochemical recycling of the nickel, cobalt, zinc and manganese from the positives electrodes of spent Ni-MH batteries from mobile phones. Journal of Power Sources, 218, 435-444.
22. Kaya, M. (2022) State-of-the-art lithium-ion battery recycling technologies. Circular Economy, 1 (2), 100015.
23. Mennik, F., Dinç, N.I., Burat, F. (2023) Selective recovery of metals from spent mobile phone lithium-ion batteries through froth flotation followed by magnetic separation procedure. Results in Engineering, 17, 100868.

XV International Mineral Processing and Recycling Conference
17-19 May 2023, Belgrade, Serbia

APPLICATION OF COAL COMBUSTION BYPRODUCTS IN SELF-COMPACTING CONCRETE: INFLUENCE ON FLOWABILITY

K. Janković[1#], M. Stojanović[1], D. Bojović[1], A. Terzić[1], S. Stanković[2]

[1] Institute for Materials Testing, Belgrade, Serbia

[2] Vinča Institute of Nuclear Sciences, University of Belgrade, National Institute of the Republic of Serbia

ABSTRACT – Compared to traditional concrete, self-compacting concrete (SCC) demonstrates greater flowability, which is achieved by including an extra high percentage of ultra-fine particles. As a result, the required high paste content is obtained while the cement content is strictly limited. The coal combustion byproduct (fly ash) is one of the most efficient SCC fillers because it extends the lifecycle of SCC by improving its microstructural properties, strength, and durability. In this study, the amounts of fly ash in SCC compositions varied. The changes in physical and mechanical characteristics of fresh SCC samples related to variations in the water/binder ratio were monitored.

Keywords: Recycling; Mineral fillers; Industrial waste; Construction materials; Sustainability.

INTRODUCTION

Coal combustion residuals (fly and bottom ash), commonly known as coal ash, are created when the coal is burned in power plants to produce electricity. Fly ash is a fine, powdery raw material (collected from filters) consisting of mostly spherical, hollow particles. Bottom ash is a granular, incombustible by-product collected from the furnace bottom. Bottom ash is predominantly sand-sized (50-90% passing a 4.75 mm sieve, with a mean particle diameter typically ranging from 19 to 38.1 mm). The size of fly ash particles ranges from 0.5 to 300 µm. Coal ashes appear in different colors. Their characteristics depend on the type of coal, the geo-location of the deposit, as well as the furnace construction and combustion procedure used in the power plant [1-4]. The average coal ash phase composition is 60-85% amorphous solid matter, 10-30% crystalline components, and up to 5% unburned carbon. Fly ash is classified into two types: C-class ash with up to 10% CaO and F-class ash with 15-40% CaO. F-class fly ash is highly pozzolanic. Bottom ash comprises approximately 2–18% CaO, which makes it less pozzolanic.

Self-compacting concrete (SCC) has increased flowability in comparison with conventionally vibrated concrete. This characteristic is achieved through the incorporation of high amounts of extra-fine particles (mineral fillers) in its composition [5]. The goal is to limit the share of cement while reaching the required high paste content. Regarding fillers employed in SCC, fly ash is one of the most frequent used due

corresponding author: ksenija.jankovic@institutims.rs

to its availability and low cost. The type of raw componential materials and their mix-proportions, as well as the type and particle size of filler, casting, manufacturing, and curing conditions of SCC, significantly influence the properties of concrete it its fresh and hardened state. The influence that fly ash makes on the properties of cementitious materials is described as a combination of a plasticizing effect (due to its spherical shape and small particle size), a microaggregate effect (due to its filler ability), and an activation effect (due to its pozzolanic capacity). The combination of those effects makes noticeable changes in the behavior of fresh concrete but also influences the solidified concrete microstructure and its properties. Namely, the filler modifies hydration rate and microstructure formation. This leads to the change in properties of hardened SCC (mechanical strengths, Young modulus, water absorption, permeability, etc.) [6-8].

The problem of disposing of this industrial waste is typically solved by the construction of planned landfills. However, landfills occupy large areas, and disposal of waste is always complicated and expensive. By using industrial by-products and waste materials, such as fly ash, in the design of concrete, the problem of their disposal is solved, i.e., instead of creating new landfills, new ecological materials are being produced [9, 10]. This paper describes the manufacturing technology and properties of self-compacting concrete in its fresh state, with mix design based on alternating water/cement ratios and quantities of fly ash as filler. The goal of this research is to increase the fly ash content in SCC. This method compiles the circular economy principles regarding concrete production and the employment of technogenic and waste resources in their composition.

EXPERIMENTAL

Self-compacting concrete (SCC) was prepared using Portland cement CEM I 42.5R (Chemical composition of cement is provided in Table 1.). Two mineral additives were used as fillers to provide high quantity of fine particles. Limestone filler was used in the mix-design of the reference concrete. Fly ash was employed in the experimental SCC samples. Chemical analyses of mineral fillers are also provided in Table 1. The chemical analyses were conducted by EDXRF method on a Spectro Xepos system (Spectro XRF Analyzer Pro, Xepos C Software) equipped with a 50 W and 60 V X-ray tube with a binary Co/Pd alloy thick target anode. The excitation mode of the X-ray tube was combined polarized/direct excitation. The characteristic radiation emitted by the elements present in the sample was detected by a silicon drift detector with Peltier cooler system.

The grain-size distribution for fly ash was: d_{50}=0.2 mm (0.8%); d_{50}=0.09 mm (3.5%); d_{50}=0.063 mm (8.6%); d_{50}=0.043 mm (16.6%). Limestone filler had the following granulometry: d_{50}=0.2 mm (6.3%); d_{50}=0.09 mm (25.1%); d_{50}=0.063 mm (29.3%); d_{50}=0.043 mm (39.7%). Natural separated aggregate with 0/4, 4/8, and 8/16 mm fractions was used in the mix-design of SCC-s. The percentage shares of aggregate per fractions were: 0/4 mm – 45 %, 4/8 mm – 20 %, and 8/16 mm – 35 %. The grain-size analysis of the aggregate mixture is illustrated in Figure 1.

Four mix-designs of three-fraction self-compacting concretes were prepared for this experiment (Table 2). Besides the previously mentioned cement (CEM I 42.5R), mineral additives (limestone and fly ash), and naturally separated aggregate (0/4, 4/8, and 8/16 mm fractions), a superplasticizer was employed as an admixture, as well as tap water.

Fresh concrete was designed to meet the minimum requirements for the properties of self-compacting concrete, according to the EN 206 standard [11]. Reference concrete (RC1) was prepared using limestone as filler. The rest of the concrete mixtures (SCC2-SCC4) were designed using fly ash as filler. A superplasticizer was employed in all concrete mixtures. The main criterion for the design of the reference concrete was to achieve SF1 slump-flow class, which normally refers to a 55 to 65 cm spreading diameter of fresh mixture. Concrete SCC2 was designed to reach the same slump-flow class. However, in the case of SCC2 concrete, a 0.5 water/cement ratio was employed due to variations in the properties of limestone and fly ash. The reference concrete was made with w/c=0.45. Two remaining mixtures, SCC3 and SCC4, had 0.55 and 0.60 w/c ratios, respectively.

Table 1 Chemical compositions of componential materials

Oxide, %	SiO_2	Al_2O_3	Fe_2O_3	CaO	MgO	Na_2O	K_2O
Cement	18.95	4.57	2.33	63.52	1.71	0.25	0.74
Fly ash	55.57	25.59	5.41	4.75	2.89	0.44	2.89
Limestone	1.05	0.41	0.06	54.65	0.78	0.02	0.05
	SO_3	P_2O_5	Mn_2O_3	TiO_2	Cl^-	Cr_2O_3	LoI*
Cement	3.31	0.12	0.06	0.19	0.04	0.03	4.18
Fly ash	1.55	0.84	0.05	0.06	-	0.03	2.02
Limestone	0.02	0.01	-	0.01	-	0.3	42.94

*Loss on ignition at 1000°C

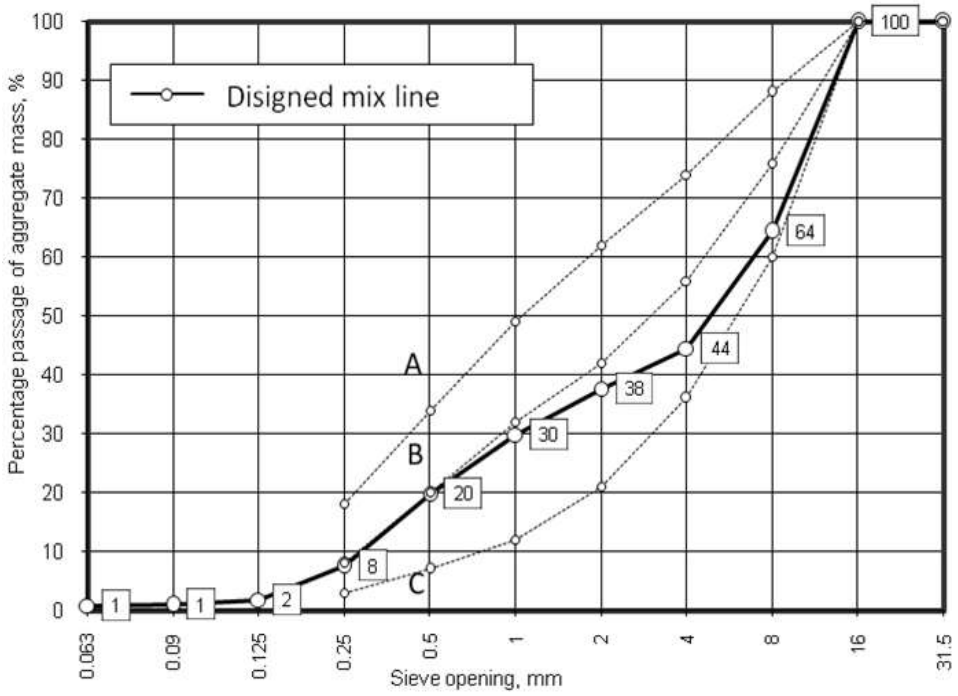

Figure 1 Grading curve of aggregate mixture for SCC samples

Table 2 Self-compacting concretes compositions

	Share of the componential material, kg/m^3					
Sample	Cement	Lime	Fly ash	Aggregate	Water	Admixture
RC1	400	100	0	1680	180	6.0
SCC2	400	0	100	1635	200	6.0
SCC3	400	0	100	1570	220	6.0
SCC4	400	0	100	1500	240	6.0

RESULTS AND DISCUSSION

The tests on fresh concrete were conveyed for the following properties: density, fluidity - slump flow test according to EN 12350-8, viscosity – T500 test according to EN 12350-8, V funnel test according to EN 12350-9, and the ability of the passage between the reinforcement – L box test according to EN 12350-10 (illustrated in Figure 2). The test results obtained for the SCC concretes in the fresh state are shown in Table 3.

Figure 2 Testing of fresh concrete properties

Table 3 Test results for concrete in the fresh state

Concrete	Density, kg/m^3	Slump-flow, cm	T500, s	L–box, H1/H2	V-funnel, s
RC1	2356	62	6	0.83	9
SCC2	2341	58	11	0.78	11
SCC3	2296	68	6	0.86	6
SCC4	2243	73	4	0.90	4

The slump-flow test, which is considered as the most important characteristic of SCC, was used for controlling the mixture's flowability. The spreading measures of the reference RC1 concrete as well as the SCC2 concrete, which were both designed to achieve the same SF1 class, varied from 580 to 620 mm. The SCC3 and SCC4 mixtures with fly ash addition were classified as SF2 flowability classes due to the inevitable increase in water/cement ratio due to the fly ash presence.

V-funnel is an experimental test used in the determination of the viscosity of a mixture. Reference RC1 concrete, as well as the SCC2 concrete sample, corresponded to the VF2 class (the established range for this class is 9–25 seconds). Measured passing time was under 9 seconds, which categorized SCC3 and SCC4 concrete mixtures in the VF1 class of viscosity, even though these mixtures exhibited a higher w/c ratio. Segregation and accumulation of water at the surface were not noticed in any of the investigated fresh concrete mixtures.

The T500 property is defined as the time needed for the fresh concrete slump to reach the spread diameter of 500 mm. This fresh concrete's characteristic is usually measured during the slump-flow test. It represents a specific assessment of the mixture's viscosity. Namely, the recommended T500 interval for class SF2 is accounted for a value between 3.5 and 6.0 s. The T500 values for concrete mixtures SCC3 and SCC4 fit into the mentioned time interval. The flow of the reference concrete mixture (RC1) and the SCC2 mixture exhibited a "slower" flow. Measured intervals that were longer than 2 s placed all tested mixtures in the VS2 viscosity class.

The L-box test is the third key property of SCC, i.e., it is the the ability of mixture to pass between reinforcing bars without blocking them. Mixtures RC1, SCC3, and SCC4 met the criterion for the height ratio of the concrete mixture at the ends of the L-box, which has to be at least 0.8. The mentioned mixtures also met the requirements for testing their flow through three reinforcing bars, which is an important requirement for densely reinforced structures. Thereby, RC1, SCC3, and SCC4 concretes belong to the same class - PL2. The test results were in the range of 0.83 to 0.90. The measured values increased with the increase in the w/c ratio. The biggest variation in height measured at the opposite ends of the L box was noticed for the SCC2 mixture. This mixture also exhibited the lowest w/c ratio of all concretes with fly ash addition. The given outcome was expected due to the minimal spreading of the SCC2 mixture. With a test result of 0.78, SCC2 concrete did not satisfy the requirements of PL2 class. Blocking of the passage between reinforcement bars by aggregate grains was not recorded in any of the conducted experiments.

It was observed that SCC mixtures with fly ash exhibited lower densities in comparison with the reference concrete. For the same level of consistency, a higher amount of water was needed for the preparation of the SCC mixture with fly ash. Increasing the w/c ratio induced more favorable properties of self-compacting concrete in its fresh state.

CONCLUSION

Fly ash, an industrial byproduct, was successfully employed in the design of three self-compacting concretes. A comparison between performances of standard self-compacting concrete with limestone filler (RC1) and experimental self-compacting concretes with varying amounts of fly ash (SCC2, SCC3, and SCC4) was carried out. The following conclusions were reached:

- The spreading of reference RC1 concrete and experimental SCC2 concrete, designed to achieve SF1 class, varied from 580 to 620 mm. SCC3 and SCC4 mixtures had higher w/c ratios, and as such, they were categorized in the SF2 flowability class.

- RC1 and SCC2 concretes corresponded to the VF2 viscosity class. SCC3 and SCC4 concrete were classified into the VF1 class of viscosity even though they had a higher w/c ratio. Segregation and accumulation of water at the surface were not noticed in any of the prepared concrete mixtures.
- According to T500 values, all concrete mixtures belong to the VS2 class.
- RC1, SCC3, and SCC4 concrete belong to the same class - PL2, since all mixtures met the criterion regarding the height ratio of the mixture at the ends of the L-box. The mixture with the smallest w/c ratio, i.e., the SCC2 mixture, had the greatest variation in heights measured at opposite ends of the L box.

ACKNOWLEDGEMENT

This investigation is financially supported by Ministry of Education, Science and Technological Development of the Republic of Serbia (contract no.: 451-03-9/2021-14/ 200012) and 2021-2023 bilateral cooperation project between Turkey and Serbia: "Tailor made self-compacting heavyweight concrete with waste materials". This support is gratefully acknowledged.

REFERENCES

1. Chindaprasirt, P. (2009) Comparative study on the characteristics of fly ash and bottom ash geopolymers, Waste Management 29, 539-54.
2. Zhou, X. (2020), Micromorphology and microstructure of coal fly ash and furnace bottom slag-based light-weight geopolymer, Construction and Budling Materials doi: 10.1016/j.conbuildmat.2020.118168.
3. Lee, B. (2020) Evaluation of time to shrinkage-induced crack initiation in OPC and slag cement matrices incorporating circulating fluidized bed combustion bottom ash, Construction and Budling Materials doi: 10.1016/j.conbuildmat.2020.119507
4. Lee, S. (2003) Effect of particle size distribution of fly ash-cement system on the fluidity of cement pastes, Cement and Concrete Research 33, 763-768.
5. Nguyen, H. (2018) Effects of sulfate rich solid waste activator on engineering properties and durability of modified high volume fly ash cement-based SCC, Journal of Building Engineering 20, 123-129.
6. Barluenga, G. (2018) Effect of full-scale pumping at early age and on hardened microstructure and properties of SCC with fly ash in hot-dry curing conditions, Construction and Budling Materials 191, 128-1138.
7. Shi, C. (2015), A review on mixture design methods for self-compacting concrete, Construction and Budling Materials 84, 387–398.
8. Domone, P.L. (2007) A review of the hardened mechanical properties of self-compacting concrete, Cement and Concrete Composites 29, 1–12.
9. Zhang, Z., Qian, S., Ma, H., (2014) Investigating mechanical properties and self-healing behavior of micro-cracked ECC with different volume of fly ash, Construction and Building Materials 52, 17-23.
10. EFNARC, ERMCO, EFCA, CEMBUREAU, bibm: The European Guidelines for SCC:Specification, Production and Use; May 2005.
11. EN 206: 2013 + A2:2021 – Concrete. Specification, performance, production and conformity.

XV International Mineral Processing and Recycling Conference
17-19 May 2023, Belgrade, Serbia

IMPACT OF STUDENT MIGRATIONS ON SUSTAINABLE AND TECHNOLOGICAL DEVELOPMENTS OF THE REPUBLIC OF SERBIA

D. Radosavljević[1#], A. Jelić[2], M. Stamenović[2]
[1] Faculty of Technology and Metallurgy, University in Belgrade, Belgrade, Serbia
[2] The Academy of Applied Technical Studies Belgrade, Belgrade, Serbia

ABSTRACT – The third and fourth scientific and technological revolutions resulted in significant changes in the workforce's professional structure and mobility. As an integral aspect of the globalization of education, the Bologna Declaration impacted the increased mobility of the highly educated professional workforce. Labor migration has long been a distinguishing element of Serbia's economic structure, and it's an issue that elicits a lot of emotion but hardly any statistics when it comes up in public discourse. The research focuses on the role, importance, and implications of continuous education and skilled labor mobility for the Republic of Serbia's economic development. A special focus will be placed on the motives, and factors that contribute to human capital migrations and brain drain in the Republic of Serbia.

Keywords: Education, Professional Harmonization, Mobility, Brain Drain, Serbia.

INTRODUCTION

Looking back on previous industrial revolutions, the first started in the late 18th century with the use of steam and water, resulting in the transition from manual to machine production; the second started in the late 19th century with the use of electricity, enabling mass production; and the third started in the 1970s with the use of electronics and internet technology, resulting in automated production. Today, we are in the midst of the fourth industrial revolution, which has applications in a variety of fields. When adapting to the new developments, the identification of changes on a national and international level begins, and innovation and technological growth become more entangled with politics and the market than they have ever been before [1-3]. In addition, a new degree of organization and control has been developed over the whole value chain of the product life cycle as well as individual requirements (Vaidya et al., 2018). Companies use intelligent features to all internal systems to create the necessary flexibility and capacity in order to meet the expectations of consumers and employees. Procedures that are simple and boring are automated, while others grow more complicated and interrelated. As a result, the profile of accessible human capital's abilities are evolving, whether it's personal or interpersonal competencies, the capacity to put a theory or concept into reality, or professional competencies. On the other side, it has been acknowledged that individuals must be motivated to share information, particularly through technology [4].

Typically, brain drain is researched in the context of population emigration or cultural

corresponding author: darko@tmf.bg.ac.rs

movement [5]. The phrase "brain drain" refers to the phenomena of people with high levels of skills, credentials, and competencies leaving their home nation and emigrating. Problems associated with the brain drain process have become a stumbling obstacle in constructing local-national scientific-technological development capacities in many new fields of study since developing nations began to build sophisticated scientific and technical institutions. In addition to political, material, and economic concerns, scientists' migration is influenced by sociological issues relating to the social organization of research and technology [6,7].

A considerable number of health experts, scientists, engineers, information technology professionals, and vocational employees are departing the region. Depending on the percentage of persons departing and the projected cost of their education, the Organization for Economic Co-operation and Development (OECD) forecasted in 2010 that Serbia would lose around $ 9 billion as a direct result of brain drain in the scientific, technology, and innovation industries. The fact that immigrants in the technology industry often receive a higher income than the general population [8]. Workforce migration and brain drain are two long-standing features of Serbia's economy and society, and themes that frequently dominate public discourse. The paper's focus is on the study of brain drain in Serbia, including statistics, motivations, and variables that contribute to the problem, as well as the effects.

What drives people to migrate?

While explaining the motives of migrations, it is of great importance to answer several questions that would give a better perspective. Is it for employment, schooling, resettlement, or anything else why they are migrating? Do they live abroad for the majority of their lives, never coming home, or do they travel between their countries of origin and destination on a regular basis? Is there evidence that the departure of high-skilled migrants is growing disproportionate in comparison to their percentage of the Serbian labor market? [11] The individual's mindset, the nation's socioeconomic status, and the worldwide position of the country of origin and the country of movement are all variables that contribute to the emergence of migration. Poor employment and an unpleasant economic situation in one's own country, better salaries and working conditions overseas, professional growth, and a better quality of life are just a few of the reasons people migrate.

Students and highly educated people form a distinct group who cite the political context, which includes the degree of democratization, the level of economic development related to living standards and the working environment, the social climate, which includes the recognition of knowledge and skills, and the position of science or level of development, institutional support, and financial transfer, as well as institutional support and financial transfer [12]. Because of the self-selective character of migration, emigrants from Serbia are not only younger and more educated but also more proactive and career-oriented, contributing significantly to Serbia's shortage of human capital. It is difficult to conduct an accurate examination of the impacts of migration of highly educated persons due to a lack of data, particularly in developing countries such as Serbia. The United States, Canada, Austria, the United Kingdom, and Germany are undoubtedly popular locations for migrating scientists and engineers [13-15].

The Government of the Republic of Serbia established the Strategy for the Growth of Education through 2020 in 2012, with the goal of minimizing emigration of highly educated persons by improving the coverage, quality, importance, and effectiveness of the education system in the development of Serbia. Mobility, according to the Strategy, is an essential aspect of higher education since it adds to the quality of education, lecturers' capacity to find better jobs, and students' ability to find better jobs. Internationalization of student activities was prioritized through collaborative programs, international joint projects, and lecturer, student, and researcher mobility. Three cycles of higher education are envisaged, in the structure of student programs and programs for obtaining desired levels with foreign universities, and linking higher education institutions with the role of students, through financing mobility, greater access to infrastructure, recognition of results, and support during studies and arrival of foreign students. The expenditures of earning a foreign language diploma are kept to a bare minimum. The Government of the Republic of Serbia established the "The Power of Knowledge" Strategy of Scientific and Technological Growth for the period 2021-2025 in February 2021, emphasizing the importance of knowledge and science as a foundation for future economic and educational development. It refers to investing in infrastructure and boosting the scientific-research community and young scientists in order to recognize them at the regional and European levels and help them solve problems on their own [16]. In principle, the newly adopted approach appears to be promising, and we will see its consequences in the near future provided it is well implemented.

The findings of the investigation on the reasons, work, and statistics of IAESTE on international student exchange in the professional practice of the University of Belgrade from 2000 to 2020, as well as the consequences on the Republic of Serbia, are described in the remainder of the article.

Research results

According to the most recent IAESTE data on foreign student exchanges for professional practice at the University of Belgrade, between 400 and 500 budget students apply each year. Students in their fourth year of undergraduate studies and first year of master's studies at technical or natural faculties who know a foreign language, have a good average, and are under the age of 28 can apply for an exchange system to receive internships for their faculty for 6 to 18 months [17,18]. One of the main reasons for applying is because as many as 47.9% of students had never visited outside of Serbia. During their internship, the majority of them (51%) get the option to go to a European Union country, while the percentage of students who travel to Africa is the lowest among the other locations. Furthermore, 45% of our graduates, postgraduates, and doctorate students have a grade of 9 or 10, and 99% of them have not renewed their academic year.

A high number of students were interested at a period from 2000 to 2010 when student exchange and these sorts of student internships in our region began to take on more serious meanings, and the need for networking was undoubtedly aided by Serbia's poor political and economical condition. In the specified time period, the maximum number of students was 193, while the lowest number was 101 in 2004. The number of students participating in professional practice through the same curriculum rose in the

following years, from 2011 to 2020, as indicated in Table 1.

Table 1 Data from the IAESTE on international student exchange in professional practice at the University of Belgrade from 2011 to 2020 [19]

Faculties of the University of Belgrade	**2011**	**2012**	**2013**	**2014**	**2015**	**2016**	**2017**	**2018**	**2019**	**2020**
Faculty of Architecture	42	38	40	38	37	37	43	45	40	41
Faculty of Biology	4	11	10	7	8	3	7	3	4	4
Faculty of Electrical Engineering	26	29	32	33	37	29	34	32	21	22
Faculty of Physical Chemistry	3	3	4	1	4	5	7	7	3	2
Faculty of Pharmacy	-	-	-	-	2	6	3	2	3	2
Faculty of Physics	7	6	5	1	1	1	3	2	3	1
Faculty of Organizational Sciences	6	7	7	8	9	2	4	7	4	1
School of Civil Engineering	7	14	9	6	8	9	15	12	5	3
Faculty of Chemistry	1	2	3	1	3	2	4	7	3	1
Faculty of Mechanical Engineering	5	9	7	6	7	9	17	14	10	6
Faculty of Mathematics	5	5	2	2	3	3	3	2	2	1
Faculty of Agriculture	2	4	3	0	2	0	2	2	3	2
Faculty of Mining and Geology	2	3	1	3	5	4	7	7	8	1
Faculty of Transport and Traffic Engineering	7	5	1	1	1	1	2	7	2	3
Faculty of Forestry	3	2	4	1	2	6	5	2	2	3
Faculty of Technology and Metallurgy	20	24	27	30	32	32	29	39	37	20

The shown results indicate the highest level of student interest in a program abroad occurred in 2018 when 185 students from Serbia had the chance to experience the

advantages of knowledge networking and more modern technologies. By default, the year in which students showed the least interest was 2020 when 112 students participated in professional internships overseas. This is the smallest number, but when we consider that this year was the year of a pandemic caused by a new virus that was completely unknown at the time, this number is meaningful and demonstrates students' unwavering desire and need to broaden their network of activities, knowledge, and skill areas.

Finally, taking into consideration the statistics, the total number of students who participated in the exchange is 3165. The students of the Faculty of Architecture and Technology and the Faculty of Metallurgy, with 800 and 532 students respectively, were undoubtedly the most interested. As previously indicated, one student from Serbia shall come to Serbia from the nation where the Serbian student would be studying, making this program really an "exchange" program. The acquired statistics, on the other hand, indicate that there is a discrepancy between these figures. Thus, the total number of international students in Serbia between 2000 and 2020 was 2423. When compared to the number of students from Serbia, this statistic is much higher. The most significant drop in foreign students occurred in 2020, when a total of 47 students arrived in Serbia for internships, as projected. Other resources indicate that most of the foreign students that come to Serbia come from Libya (35.8 percent by the data obtained in 2016) [20]. However, these data are not related to the data obtained by the IAESTE program. Data on the brain drain, which mostly affects young students and scientists who make up Serbia's intellectual diaspora, is based on a number of unreliable and sometimes inconsistent sources. As a result, obtaining information on which of the students named in the preceding table returned to Serbia and which used the professional practice opportunity to defend final or master's theses or doctorates, is extremely difficult. With the option of offering incomes or scholarships, as well as pre-arranged employment of young people who are only going to practice, it is simple to infer that only a tiny percentage of students will return, with the reasons being largely sentimental [21,22].

Modern equipment, testing facilities, materials, as well as workplace safety, are frequently listed as important aspects of working overseas. To reach the circumstances given in the industrialized countries of the globe, significant investment in education and scientific advancement is required. Our young scientists have a distinct edge in terms of innovation, especially when considering the restricted resources available to achieve outstanding scientific outcomes. When big discoveries and good results are made using low budget resources, our young scientists quickly convert their inventiveness to automated research methods that provide far more findings in a shorter amount of time and, as a consequence, are more useful in the scientific world hold a prominent position [23].

According to the Statistical Office of the Republic of Serbia, the research and development industry received 8.6% more budget funding in 2020 than it did in 2019. To truly witness the impacts, substantially more investment in education and science is unquestionably required. Until then, we will face the issue of young people who are well educated, full of passion, eagerness, and a desire to study and produce meaningful achievements while still living well.

CONCLUSION

The region's emigration statistics are unquestionably concerning. Previously, there has been a concern of national education systems' knowledge and skill bases being disrupted. These once-dangerous situations have now become a grim reality. Owing to the inability of obtaining new information and skills, a big percentage of our students move overseas for professional internships and training and stay abroad due to chances offered in advance, such as promised jobs by firms and companies that support them with scholarships. Due to the departure of young and capable individuals from the business and public sectors, as well as financial instability, student mobility has a detrimental impact on democracy in the nation. History has proven that the inability of a majority of the population with a lower educational profile to change and advance leads to authoritarianism.

Recognizing a problem is the first step towards fixing it. After many years of denial, the fact of a brain drain problem in the Republic of Serbia is finally being acknowledged, and measures and plans to address it has been presented. However, it is vital to pose a question about the factors that led to young highly skilled persons leaving to work in other countries. Poor quality of life and low employee rates are undoubtedly the most important causes, and they should be addressed first. Better communication between the school and work sectors is one of the most important reforms. Returning to Serbia after graduating from a foreign university might be difficult as well. As a result, legal restrictions must be changed to allow for speedier diploma recognition and the return of the young population to work in their home country. Of doubt, today's world necessitates global networking in order to develop and share information, but in order to increase the intensity of knowledge exchange, professionals with high scientific titles should not be engaged in positions in Serbian higher education institutions. All of the aforementioned issues have developed as a result of the country's desire for transformation. True, there is a lot of brain drain in Serbia, and in order to stop it or at least slow it down, we need to focus on improving the economic status, jobs, and practices of young people who would have the opportunity to put their knowledge into practice with acceptable working circumstances. It is feasible to assure the creation of a stable country in the long term by recruiting and maintaining young highly educated individuals, students, who would, thanks to all of their talents, equal the developed countries outside. However, this will need huge expenditures, which the government is not yet prepared to do for the sake of the country's prosperity, and the funds available are insufficient to at least reduce the brain drain from Serbia.

REFERENCES

1. Toni, M., et al. (2021) Industry 4.0 an empirical analysis of users' intention in the automotive sector. International Journal of Quality and Service Sciences, 13 (4), 563-584.
2. Gajdzik, B., Wolniak, R. (2021) Digitalisation and innovation in the steel industry in poland—selected tools of ict in an analysis of statistical data and a case study. Energies, 14.
3. Gajdzik, B., Grabowska, S., Saniuk, S. (2021) A theoretical framework for industry 4.0

and its implementation with selected practical schedules. Energies, 14.
4. Fihel, A., Kaczmarczyk, P., Sylicz, A., Wolfeil, N. Labour Mobility - Background Analyses - Brain drain, brain gain and brain waste.
5. Gibson, J., McKenzie, D. (2011) Eight Questions about Brain Drain. (The World Bank, 2011). doi:10.1596/1813-9450-5668.
6. Docquier, F. (2014) The brain drain from developing countries. IZA World of Labor doi:10.15185/izawol.31.
7. Johnson, N. (2008) Analysis and Assessment of the "Brain Drain" Phenomenon and its Effects on Caribbean Countries. Florida Atlantic Comparative Studies Journal vol. 11.
8. Kutlača, Đ. (2010) Strengthening the Capacities and Infrastructure of Innovation in Serbia. OECD Headquarters.
9. Mishra, P. (2007) Emigration and Brain Drain: Evidence from the Caribbean. The B.E. Journal of Economic Analysis & Policy, 7.
10. Rasevic, M. (2016) Migration and Development in Serbia. International Organization for Migration (IOM).
11. Arandarenko, M. (2021) How migration, human capital and the labour market interact in Serbia.
12. Pavlov, T. (2011) The motivation for migration of highly qualified people in Serbia.
13. Mcgill, J. (2013) International Student Migration: Outcomes and Implications. Journal of International Students, 3 (2), 167–181.
14. Riaño, Y., Piguet, E. International Student Migration - Geography - Oxford Bibliographies.
15. King, R., Ruiz-Gelices, E. (2003) International student migration and the European "Year Abroad": Effects on European identity and subsequent migration behaviour. International Journal of Population Geography, 9, 229–252.
16. Council for Cooperation of Science and Economy. Published Strategy of Scientific and Technological Development of the Republic of Serbia for the period from 2021 to 2025 "The power of knowledge." The Official Gazette of the Republic of Serbia No. 10/2021.
17. IAESTE history. iaeste.org/history.
18. IAESTE Srbija. IAESTE Srbija Konkurs. Konkurs.
19. IAESTE Srbija (2021) Статистички подаци IAESTE о међународној размени студената на стручној пракси за Универзитет у Београду у периоду од 2000. до 2010. године.
20. Migration Profile of The Republic of Serbia for 2016 Migration Profile of The Republic of Serbia for 2016 Republic of Serbia The Government of The Republic of Serbia.
21. Docquier, F., Rapoport, H. (2011) A Service of zbw Standard-Nutzungsbedingungen. http://hdl.handle.net/10419/96079.
22. Docquier, F., Lohest, O., Marfouk, A. (2007) Brain drain in developing countries. World Bank Economic Review 21, 193–218.
23. Truscott, M.H. The Brain Drain of Scientists, Engineers, and Physicians From the Developing Countries to the United States. https://digitalcommons.lsu.edu/gradschool_disstheses.

XV International Mineral Processing and Recycling Conference
17-19 May 2023, Belgrade, Serbia

DEVELOPMENT OF EDUCATION FOR SUSTAINABLE DEVELOPMENT AND MANAGEMENT OF RECYCLABLE WASTE IN THE REPUBLIC OF SERBIA

D. Radosavljević[1#], A. Jelić[2], M. Stamenović[2]
[1] Faculty of Technology and Metallurgy, University in Belgrade, Belgrade, Serbia
[2] The Academy of Applied Technical Studies Belgrade, Belgrade, Serbia

ABSTRACT – Education for sustainable development and the management of recyclable waste, represent major concerns for 21st-century civilization. If future generations are to live in a sustainable society, humans must adapt their lifestyles from a different perspective. Only by incorporating sustainable development policies into politics, business, and education will green growth be realized. By minimizing hazardous wastes and environmental degradation, as well as protecting ecosystems and biodiversity, can we secure the biosphere's long-term preservation and avert irreparable global devastation. The paper discusses the indisputable importance of recycling in reaching the objectives of sustainable development.

Keywords: Sustainable Development, Recyclable Waste, Management, Policy, Serbia.

INTRODUCTION

Overproduction and excessive consumption have detrimental environmental consequences. Furthermore, the climate problem has put our world in grave danger. Every day, carbon emissions hurt the environment. Our every day and industrialized practices are wreaking havoc on our world [1]. The intensive expansion of the world's population, as well as the rapid depletion of accessible natural raw resources and the buildup of pollutants, all threaten to signal the onset of a human-environmental disaster. Only by minimizing hazardous wastes and environmental degradation, as well as protecting ecosystems and biodiversity, can we secure the biosphere's long-term preservation and avert irreparable global devastation. Considering the indisputable importance of recycling, however, the fact that national rates are so low and insufficient is troubling.

Large amounts of waste are generated as a result of human manufacturing and consumption. Waste may be both a valuable asset and a burden for the environment. This means that inefficient waste management wastes a number of useful resources and might cause human health and environmental issues. When waste management fails, it may lead to difficulties with health and sanitation, as well as contamination of the surface and groundwater resources. Sustainable waste management is thus a crucial component of eco cycle activities. Education for sustainable development has been highlighted as a key method for changing society, but education for sustainability can only succeed if students' perspectives move in that direction. Graduate students must grasp that in a society where cultural, financial, and ecological systems are perfectly integrated for the

corresponding author: darko@tmf.bg.ac.rs

collective gain of everyone is a sustainable society feasible [2].

The Republic of Serbia has begun to integrate information on sustainable development and waste management, and the purpose of this article is the impact of integration, its underlying elements and aims, and, finally, the degree it has achieved in the Republic of Serbia and its system of education.

EDUCATION FOR SUSTAINABLE DEVELOPMENT

Education for Sustainable Development (ESD) was defined by UNESCO in 2014 as a concept that allows every human being to acquire the information, skills, attitudes, and values required to design a sustainable future [3]. Sustainable development was defined by the United Nations as development that satisfies current demands without jeopardizing future generations' capacity to achieve their own [4]. It is based on a balance of three basic factors in order to accomplish sustainable development: economic expansion, social integration, and nature conservation. These factors are intertwined, and they are all necessary for people's and society's well-being while all parties are required to contribute to the realization of the new agenda, including authorities, civil institutions, the corporate sector, among others.

Sustainable development is achieved by making and executing decisions that guarantee that environmental protection and economic development goals are aligned. The amount and method in which a country uses its natural resources in the pursuit of sustainable development are determined by its governing legislation, which includes environmental education as a key component. Most people link the term "sustainable development" with environmental preservation, social development planning, and environmental, economic, and political challenges. The notion of sustainable development denotes a new development paradigm, as well as a new social development strategy and philosophy. Ecology is frequently confused with environmental protection in this context. It's critical to understand the differences between these two notions, as well as their relationship to the concept of sustainable development. Environmental protection is simply one element of ecology, which is the study of the interrelationships between living beings and the surrounding world. The issues that come with the danger to the environment add to the notion of sustainable development's relevance [5,6].

As a result, the global community is now committed to sustainable development based on environmental principles, which incorporates wise natural resource management, biodiversity conservation, and natural self-reproduction, logical and reasonable utilization and conservation of energy and materials, particularly non-renewable, recycling, and so-called clean technologies, and environmental protection measures, all to meet the demands of growing regions of the world [7,8].

Environmentally, the quality of life for all generations is attained by attempting to balance what we take from nature with what we give back to it. Mankind needs a global morality based on which the meaning of nature may be disclosed and a unique vision of the world can be developed in which man and nature can live in harmony. Science, culture, and education all contribute to the creation of that worldview. Since individuals seek a different approach to the adoption and application of information, skills, and behaviors of individuals and communities, all based on new values, education for

sustainable development necessitates dramatic changes in the cultural and educational realm. The implementation of sustainable development in everyday life will be possible only when people's awareness and sense of responsibility grow, i.e. when they acquire new knowledge and skills about how to place that paradigm into practice, hence why the system of upbringing and education bears such a large role in achieving that goal. In other words, universities and the academic profession have a significant problem in providing education for sustainable development.

RECYCLING IN THE FUNCTION OF SUSTAINABLE DEVELOPMENT

The circular economy, low waste, and zero waste are examples of concepts that arose from the necessity to develop a concept of sustainability, and they have begun to appear in our society as well. Recycling, as one of the waste management options, must be integrated into a system that follows the principles of sustainable development in order to offer circumstances for healthy living for both ourselves and future generations. Recycling is the process of converting waste materials into new ones. It cleans up our neighborhood and the environment, as well as makes nature and man healthier. The trend of using waste as energy has already been conquered, according to the VI International MITECO Forum, which was held in 2020. Now that garbage is being turned into a new product, we must look for new and novel energy sources, including solar and step energy, which can be converted into power [9].

Humans must discover ways to raise revenue while maintaining the natural systems from which mankind exists in order to go forward on a sustainable development path. This means that dramatic changes in our communities and economy, as well as in the methods we produce and consume, are required. Simultaneously, it necessitates a transformation in all areas, including the environment, energy, agriculture and fisheries, transportation, and building. It also necessitates global action since weak governance in one nation may have far-reaching implications. Policymakers must clearly identify action limitations and provide appropriate relief, but in the end, the type of planet future generations inherit is determined by the actions of every individual in every country.

ESD AND RECYCLABLE WASTE IN THE REPUBLIC OF SERBIA

The fact that waste recycling is the most significant problem in the globe, but also in Serbia, especially in recent years, says a lot about how vital it is. More and more effort is being put forward to create a simple system that is accessible to individuals and contains all packing in one location. Serbian people are becoming more aware of the necessity of recycling, but more work has to be done to maintain that knowledge. As it was previously stated, it is critical to concentrate on educating individuals about their contribution to sustainable development and recycling system i.e. to educate them about the difference between waste sorting that residents perform at home and primary selection, vs recycling, which is a secondary process of processing such sorted waste.

The Eco-package initiative began as a worldwide Eco-school program in 2013/2014, with the goal of educating customers on proper disposal of used Tetra Pak packaging and raising awareness of the need of having a responsible attitude toward the environment. Eco-package is a hands-on activity in which students make genuine little pieces of art out

of recycled Tetra Pak packaging and compete in a creative competition for substantial prizes. The old Tetra Pak packaging is given a new function and becomes a reusable item thanks to creative competition. The process of recycling used Tetra Pak packaging in a palper machine was explained in a fun and innovative way during educational seminars organized in a significant number of schools in Serbia until 2019 [10]. Various procedures are necessary to minimize waste quantities and regulate waste streams according to the hierarchy for various treatment processes. The aim is to improve waste material recovery. When opposed to the usage of fresh raw materials, recycled raw materials save energy, and material recycling frequently results in fewer emissions than alternative treatment techniques [11].

The five-year Development Partnership Framework (2016-2020) between the Government of the Republic of Serbia and the United Nations team includes environmental preservation as one of its pillars. One of the initiatives is to increase recycling capacity through the production of technical documentation, as well as to build and equip a recycling facility in Novi Pazar and afterward in Nova Varoš [12].

As a partner, the Association of Citizens PLANT began implementing the project "Environmental education - a bridge for sustainable development of the cross-border area" from the beginning of 2020. The Directorate of Vitosha Nature Park from Sofia, Bulgaria, is the project's lead partner, while "Open Door" from Pernik, Bulgaria, is the project's other partner. The main objectives of the project are to build capacity and provide opportunities for environmental education in the cross-border region, to promote environmental awareness, responsible behavior, and eventual action through education and building environmental links, and to change young people's perceptions of the environment [13]. Within the project, the Manual for Environmental Education was prepared [14].

According to a poll done by the Consumer Center of Serbia (CEPS) in 2020, the majority of respondents have a favorable attitude toward recycling, with as many as 85 percent seeing the deposit system as a decent approach to encourage recycling [15]. Despite the fact that there is some public awareness and that illegal landfills are cleaned every year, the number of illegal landfills is not diminishing, and waste remains visible everywhere. The Waste Management Strategy, which expired in 2019, laid the groundwork for the formation and development of an integrated waste management system in our country [16]. According to the most recent information, the Government of Serbia has approved the Waste Management Program in the Republic of Serbia for the years 2022-2031 in order to align the waste management system with the European Union's aims and acquis communautaire [17]. The previous Strategy's goals have not been fully realized, particularly in terms of structured waste collection, primary waste separation and recycling, infrastructure construction and the elimination of waste disposal in unsanitary landfills and dumps, economic instruments, and the establishment of a sustainable waste management financing system. Only bigger cities in Serbia have designated recycling garbage bins, and there aren't enough of them.

Ninety percent of Serbia's garbage is disposed of at Vinca's dump, where informal collectors sort out what may be recycled. Serbia's landfills are growing by the day, and recycling plants are importing PET material to recycle. Utility companies only get a little portion of the revenue. Despite the fact that primary separation is mandated by law,

separate waste collection does not operate in practice in Serbia. The Program's purpose is to decrease the waste environmental effect and raise the efficiency of its use based on the principles of the circular economy after examining the present status and potential in the field of waste management. In addition to limiting harmful effects on the environment, the Waste Management Program for the period 2022-2031 should enable the fulfillment of preconditions for the use of waste in a circular economy, the development of which goals and measures are specified in a unique program. The notion of reimbursement for waste collection and disposal services, as well as the development of incentives for reuse and recycling, should be implemented. The idea "Pay as much as you throw away," which allows families and legal entities to determine the amount they will pay for municipal waste services, is a new addition to the Program. They can seek a cheaper waste cost if they segregate garbage at the point of origin, compost it, process it, or use it in other ways.

CONCLUSION

Can we, as individuals, impact the overall climate on this subject at the global level? While there is no simple answer to this question because the system's sustainability varies depending on the whole system, not just its components, such as the government and all of its establishments, the economic system, various associations, and participants, it is certain that innumerable movements and initiatives for environmental protection have brought this issue to the public's attention. Serbia has a strong starting point, with up to 20% renewable energy sources, which many other nations lack, thus there is no question Serbia can achieve much more. Serbia's renewable energy sources might be increased by 40%, according to estimates.

In the Republic of Serbia, the state has a role in the implementation of the European Green Agreement. Green transformation is a thorough, sophisticated, and demanding process that necessitates governmental involvement and commitment, as well as major investments and efforts, particularly in light of the current circumstances, and action on this subject is unavoidable.

However, the only thing we can conclude in the end is that in a country where the issue of sanitary landfills, raw material recycling, and obtaining sustainable solutions, the road to change is long and winding, and residents are frequently forced to fend for themselves. The necessity for answers and united action, on the other hand, is becoming increasingly obvious from the voices of ordinary residents who are determined about dealing with it. Even though the obligation for adopting green policies resides with the government in nations where the need for such policies is acknowledged, it is very unusual for this to happen under the pressure of society and civic activities.

REFERENCES

1. Nadoveza, B., Pešić, H. (2020) Sustainable development: Production force of modern society. Održivi razvoj, 2, 31-40. https://doi.org/10.5937/odrraz2001031n.
2. Segovia, V.M. (2010) Transforming Mindsets Through Education for Sustainable Development. In: International Encyclopedia of Education, Elsevier, pp. 746-752. https://doi.org/10.1016/B978-0-08-044894-7.00224-4.

3. UNESCO, (2014) Education for Sustainable Development.
4. The United Nations, The Sustainable Development Agenda. Sustainable Development Goals.
5. Klauer, B. (1999) Defining and achieving sustainable development. International Journal of Sustainable Development & World Ecology, 6, 114-121. https://doi.org/10.1080/13504509909470000.
6. Shao, G., Li, F., Tang, L. (2011) Multidisciplinary perspectives on sustainable development. International Journal of Sustainable Development & World Ecology, 18, 187-189. https://doi.org/10.1080/13504509.2011.572304.
7. Omer, A.M. (2008) Energy, environment and sustainable development. Renewable and Sustainable Energy Reviews, 12, 2265–2300. https://doi.org/10.1016/j.rser.2007.05.001.
8. Voon, Y., Yvonne, T. Green marketing Intervention Strategies and Sustainable Development: A Conceptual Paper kinoti mary Green marketing Intervention Strategies and Sustainable Development: A Conceptual Paper.
9. Reciklaza.biz (2020) Okončan VI međunarodni MITECO Forum.
10. http://ambassadors-env.com/, Eko-paket.
11. WasteManagement.
12. UNDP_SRB_DPF_ENG_30_May_2017_FINAL_SIGNED.
13. PROJEKAT: CB007.2.32.151 „EKOLOŠKA OBRAZOVANJE – MOST ZA ODRŽIVI RAZVOJ PREKOGRANIČNOG REGIONA“, Nvoplant.Rs. (2020).
14. ИнтеррегИПА (2020) Програм прекограничне сарадње Бугарска-Србија, Приручник за еколошко образовање, Удружење грађана ПЛАНТ.
15. C. potrošača S. (CEPS) Anokić, M. Održivi razvoj: Depozitni sistem kao mehanizam za povećanje nivoa reciklaže u Srbiji, Www.Instore.Rs/.
16. „Службени гласник РС“ (2010) СТРАТЕГИЈА управљања отпадом за период 2010–2019. године, број 29 од 2. маја 2010.
17. ПРОГРАМ управљања отпадом у Републици Србији за период 2022–2031. године.

XV International Mineral Processing and Recycling Conference
17-19 May 2023, Belgrade, Serbia

SUSTAINABLE RECOVERY OF INDIAN PLACER MINERALS-THEIR DISTRIBUTION AND MINERAL ASSEMBLAGES

D. Singh[#]
CMD, IREL (India) Limited, Mumbai

ABSTRACT – Mining and mineral beneficiation through responsible and scientific mining, processing guided by sustainable resource development, best practices of environmental management and recycling of mineral-based products are the requirement of a sustainable heavy mineral mining industry. Extraction of heavy minerals from off shore and inland placer deposits using state of the art technology for dredging operation and high efficient mineral processing equipment can reduce the heavy minerals in the reject tailings to less than 1%.Due to the critical nature and huge demand of the titanium, zirconium and rare earths in nuclear, space and defence sector, IREL is practicing key metrics for environmental sustainability in mining related to efficiencies in resource consumption, minimizing land disturbance, pollution reduction, closure and reclamation of exhausted mine lands for habitat development.

Keywords: Heavy Mineral, Titanium, Zirconium, Rare Earths, Sustainable Mining, IREL.

INTRODUCTION

Indian subcontinent has been endowed with vast placer resources of various minerals. Placer minerals by nature are highly resistant to weathering and are located along the coastal lines of the eastern and the western parts of India. Placer deposits are formed because of the weathering of source rocks and mechanical concentration of heavy minerals takes place due to the action of running water, wind, waves and shore currents. They occur in beaches, rivers, dunes and offshore areas because of their high specific gravity. The sands are sediments of hindered land rock types brought by rivers into the sea. The hinterland geology along the coast is mainly dominated by the rocks of the Charnockite, Migmatite and Khondalite Group. The formation of these placer deposits takes place with combined effect of various parameters viz. provenance geomorphology, tropical climate, drainage pattern, wind action aided by coastal waves and currents. Figure 1 shows Indian beach placer deposits containing heavy minerals belonging to the Tertiary and Quaternary age and are located all along the eastern and the western coastline of India [1].

GEOLOGY

Mining of the placer deposits and quantity of mineral production from Indian beach placer deposits is significant. Indian beach placer sand deposits are, in general, ilmenite-rich. However, some concentrations are dominated by pyriboles with amphiboles with hornblended composition. Garnets are mostly of almandine and pyrope type.

[#] corresponding author: cmd@irel.co.in

Subordinate heavy minerals are sillimanite, zircon and rutile. Characteristic morphology, mineralogy and chemistry of amphibole, garnet and ilmenite together indicate that the placer sands are derived from the amphibolites, granite gneisses and basic igneous rocks. The zircon and monazite mostly occur as accessory mineral in the granitic, metaluminous to paraluminous granitoid rocks and in politic schists and gneisses albeit rarely in sedimentary rocks. The inherited geological history such as crystallization of igneous rocks, provenance ages of detritals, age of medium to high grade metamorphism are well understood by studying the heavy minerals like zircon and monazite.

The process of occurrence of heavy mineral deposit are due to a number of factors such as constant wave action which moves sand from off shore to shore. Because of the density and size difference, the sand and heavy minerals are segregated from each other and heavy mineral rich deposits are also formed due to the sorting of the lighter sand. Geomorphology and drifting phenomena of the coastline has profound influence on the heavy mineral sand deposit and its distribution. Weathering of heavy mineral occurs only when deposition occurs in coastal plain and are influenced by ground water, humic acid and intrabasinal fluids. [2].

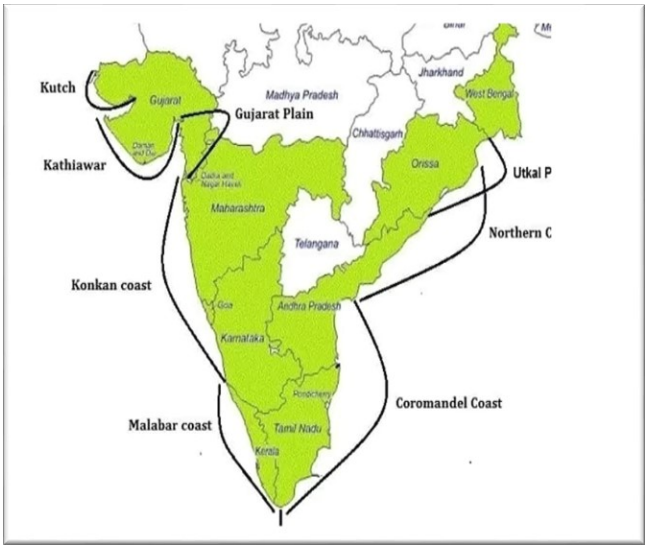

Figure 1 The Indian beach placer deposits all along the eastern and the western coastline

MINERAL RESERVES

The occurrence of the mineral deposits in India can be broadly divided into four zones, such as, i) Eastern Zone: Covering States of Orissa and Andhra Pradesh, ii) Tamil Nadu Zone (iii) Kerala Zone and iv) Others: Covering small deposits also occurring in the coastal Maharashtra and inland placers in Bihar and West Bengal. The Heavy mineral content in Indian deposits by and large ranges between 10-50%. Within this, the ilmenite content (which is the dominant constituent) varies from zone to zone [3]. Table 1 shows

the beach sand mineral reserves of India.

Table 1 Indian reserves of beach sand minerals [11]

Minerals	Indian Reserves in million tones
Ilmenite	629
Sillimanite	70.2
Garnet	56.16
Zircon	33.71
Rutile	33.95
Monazite	13.07
Total	1,065

RESOURCES

Ilmenite and rutile along with other heavy minerals are important constituents of beach sand deposits found right from Moti Daman-Umbrat coast (Gujarat) in the west to Odisha coast in the east. These minerals are concentrated in five well defined zones, (1) Over a stretch of 22 km between Neendakara and Kayamkulam, Kollam district, Kerala (known as 'Chavara' deposit after the main mining centre), (2) Over a stretch of 6 km from the mouth of Valliyar river to Colachal, Manavalakurichi and little beyond in Kanyakumari district, Tamil Nadu (known as MK deposit), (3) On Chatrapur coast stretching for 18 km between Rushikulya river mouth and Gopalpur lighthouse with an average width of 1.4 km in Ganjamdistrict, Odisha (known as 'OSCOM' deposit, (4) Brahmagiri deposit stretches for 30 km from Giralanala to Bhabunia villages with anaverage width of 1.91 km in Puri district, Odisha, (5) Bhavanapadu coast between Nilarevu and Sandipeta with 25 km length and 700 m average width in Srikakulam district, Andhra Pradesh. The state wise resources of three economic important heavy minerals such as Ilmenite, Rutile and Zircon (in million tones) are given in Table 2. [3]

Table 2 State wise distribution of three economic important heavy minerals

State Resources*	Ilmenite	Rutile	Zircon
Andhra Pradesh	163.05	10.25	11.94
Bihar/Jharkhand	0.73	10.25	11.94
Gujarat	2.77	0.02	0.01
Kerala	145.70	8.41	7.83
Maharashtra	3.74	0.01	
Odisha	96.44	4.47	3.25
Tamil Nadu	179.02	8.00	10.20
West Bengal	2.05	0.19	0.39

Indian Placers Minerals

In India, major beach sand deposits are found in the states of Tamilnadu, Kerala, Odishaand Andhra Pradesh. Ilmenite-rich major beach and dune sand deposits occur in the coastal stretches of Kerala (Chavara), Tamilnadu (Manavalakurichi, Midalam, Vayakallur), Andhra Pradesh (Kakinada, Pentakota, Bhimunipatnam, Konada

Kandivalasa-Mukumpeta-Bendicreek-Donkuru), Orissa (Sanaeka-sangi-Gopalpur, Chatrapur, Bajarkot, Satpara and Puri) and Maharashtra (Kalbadevi, Newre and Malgund). Rich concentration of almandine-rich garnet (upto 31% in the raw sand) is observed in the 68 km beach stretch of Navaladi-Periathalai, South of Tiruchendur in Tamilnadu. The red Teri inland sands occurring in the coastal plains of southern Tamilnadu contain HMs upto 10% and occupy vast tracts with large tonnage of heavy minerals. The southern Kerala forms ilmenite-sillimanite province containing essentially of these minerals with zircon whereas the northern Kerala is pyriboles-ilmenite province of essentially pyriboles and seconded by ilmenite. Charnockites and khondalites contribute for ilmenite-sillimanite province whereas horn blendebiotite gneisses and retrograded rocks for pyriboles-ilmenite province. The geomorphic features of the south Kerala are excellent favouring the formations of placers and the localisation is mainly by long-shore drifts. In addition to the major deposit of Chavara, many other deposits/occurrences have been identified by the exploration work of AMD. The deposits/occurrences to the south and in the northern contiguity of Chavara, are ilmenite-rich with prevalent leucoxenisation. Viable mineralisation is recorded in lake bed sediments and also in sea bed sediments off the Chavara coast. The deposits/occurrences in the northern Kerala at Azhikode-Chavakkad, Chavakkad-Ponnaniand, Valarpattnam-Azhikode are pyribole-predominant, ilmenite-depleted and, hence, not of economic interest concurrently [4]. The provenance rocks for heavy mineral deposits of Andhra Pradesh are mainlythe Khondalite– harnockite Supergroup, with lesser proportion of granite-gneisses and sedimentsin the coastal plains. Of the Khondalite-Charnockite provenance, the relative proportion ofthese two varies in different areas, which is reflectedin the relatively higher proportion of garnet andsillimanite in the northern deposits like Srikurmam and Kakinada, and more of pyriboles in the sourthern ones like Nizampatnam [5]. Based on the variations in geology and geomorphology, the coast has been sub-divided into north, central and south segments. Beach and dune sands in the northern segment extend for 352 km and are best developed in the embayment headland combination that has abetted and helped in the formation of placer deposits. Central khondalite zone and eastern migmatitic zone of the Eastern Ghat Mobile Belt and coastal Gondwanas are the important litho-units in this segment. Important deposits identified are Bhavanapadu, Kalingapatnam and Srikurmam of high-tonnage and Donkuru-Barua, Koyyam, Bhimilipatnam and Pentakota of medium-tonnage. Geologically, western charnockitic zone dominates over central khondalite zone, Rajahmundry sandstone and Deccan Traps. Ilmenite, pyriboles and magnetite dominate in THM of around 10 to 15%. The segment hosts at least two known heavy mineral deposits, viz., Kakinada and Nizampatnam, of medium-grade and large-tonnage.

The coastal deposits of Odisha along the eastern part of the Indian Peninsula are known for the high abundance of heavy minerals. The Eastern Ghat Province consists of the majority of charnockite-migmatitezone [6] and mostly comprises assemblages of basic and massif-type anorthosites, garnetiferous gneiss, enderbitic granulites, khondalite gneiss and granite-charnockite complexes [7, 8, 9]. The beach area of Odisha is bordered by the Singhbhum shear zone to the north, the Bay of Bengal to the east, the EGMB to the west and the Markandi canal to the southwest. The composition of the

placers along the study area is primarily controlled by the detritus from the proximal hinterland rock type(s). Figure 2 shows the geology and drainage pattern responsible for heavy mineral resource of India [10].

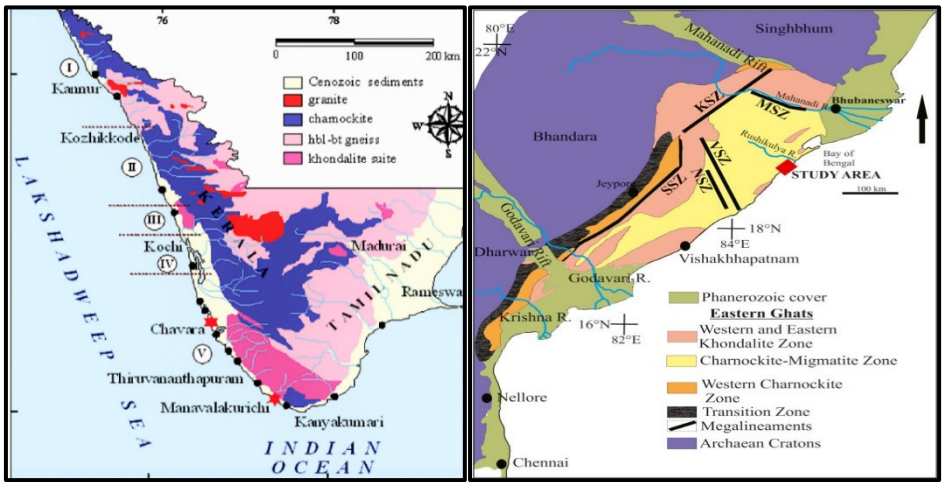

Figure 2 Geology and drainage pattern responsible for heavy mineral resource of India

Physical and Chemical properties of beach sand minerals

The physical and chemical properties of Indian beach sand minerals are well characterized and plays a vital role for physical separation from each other. Based on their characteristic properties, gravity concentration, electro static separation, magnetic separation, and froth floatation equipment are used to produce the minerals. Table 3 provides a glimpse of physical and chemical properties of minerals.

Processing

Heavy minerals naturally occur in relatively small concentrations, so that specialized preparation systems equipped with spiral separators, electrostatic separators and magnetic separators are required for concentration and separation. Separation of the valuable heavy minerals from the primary ore is carried out in two stages: (a) wet concentration, utilizing sizing and gravity differentiation between heavy minerals, clay and quartz, and (b) dry separation, exploiting the magnetic and electrostatic properties of the minerals based on the physical properties of the heavy minerals as mentioned in Table 3. Froth floatation process is used for separation of sillimanite. A schematic diagram of the flow sheet used for heavy mineral separation is given in Figure 3.

Sustainability in heavy mineral processing

Heavy mineral sands are valuable and important source of titanium, zirconium, rare earths. Due to very low concentration and limited resource, mining and mineral beneficiation activities are crucial and challenging. The lowest cut off grades of heavy mineral as total heavy minerals from the feed raw sand is less than 1% of heavy minerals.

Table 3 Composition and properties of beach sand minerals

Mineral	Composition	Properties
Ilmenite, (50-60% TiO_2)	Oxides of Iron and Titanium,Sp.Gravity:4.2-4.6	Magnetic & Conducting
Lecoxene, (79-82% TiO_2)		Medium Magnetic & Conducting
Rutile, (>92% TiO_2)		Non Magnetic & Conducting
Zircon, (62-64%)	Zirconium silicate, Sp.Gravity: 4.7	Non Magnetic & Non Conducting
Monazite (58% RE_2O_3, 9%ThO_2, & 27% P_2O_5)	Phosphates of Rare Earths & Thorium, Sp.Gravity: 5.2	Low Magnetic & Non Conducting
Sillimanite, (56-58% Al_2O_3)	Aluminium Silicate,Sp.Gravity:3.2	Non Magnetic & Conducting
Garnet (43% FeO, 21% Al_2O_3, & 36% SiO_2)	Iron Aluminium silicate, Sp.Gravity: 4.1	Medium Magnetic & Non Conducting

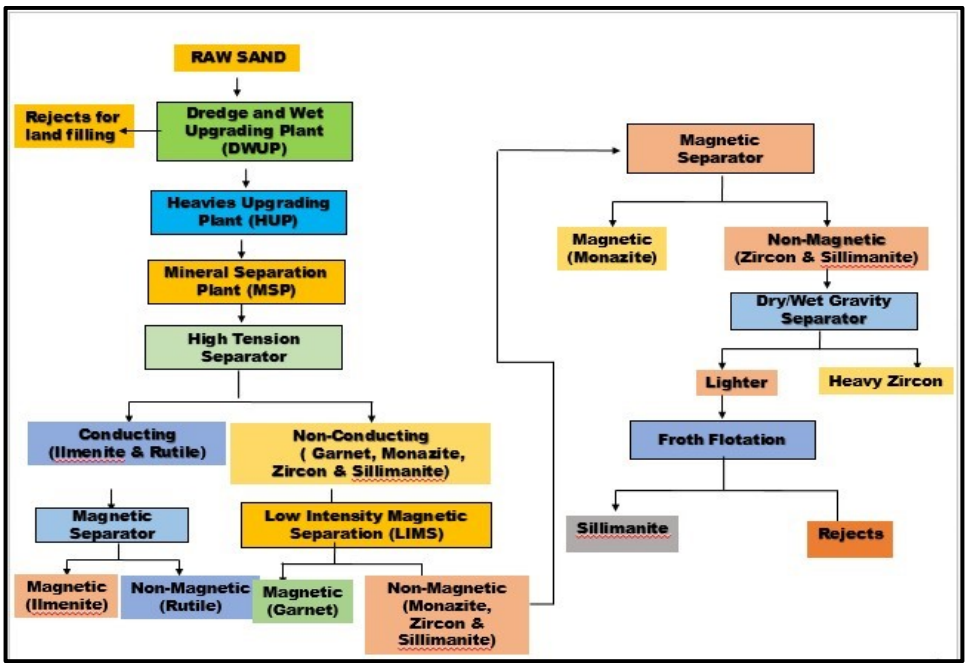

Figure 3 Process flow sheet from mining to mineral beneficiation

The heavy mineral mining and beneficiation sector has played an important role in Indian economy and human development. Sustainable development of mineral resources seeks to attain a balance between economic development, environmental protection, community benefits, and government responsibilities. IREL has realized the

importance of sustainable mining and mineral beneficiation through responsible mining and processing guided by sustainable resource development, best practices in environmental management and recycling of mineral-based products. Precise separation of desired substances with minimum energy consumption has become the requirement for implementation for extraction of few important minerals from beach sand heavy mineral deposits and also occupies an extremely important position in industry. Physical separation has become the mainstay of industrial minerals processing and have been used in mineral industry for centuries to separate valuable minerals from gangues by exploiting the differences in their physical characteristics, such as specific gravity, magnetic susceptibility and/or electrical conductivity. They have several advantages over other mineral processing techniques due to their high efficiency, low capital and operating costs, no addition of chemicals and consequently, less environmental hazard. They are applied to ores from mines and tailings or at the recycling stage for scavenging the desired elements.

The innovations in mineral separation engineering are now implemented for improvement of conventional separating technologies with reduced energy consumption and improved precision in separating operations, such as the extraction of desired materials or the removal of unwanted substances from mixtures consisting of diverse substances in a mixed state. In order to solve various important social and industrial issues in which separation is crucial, innovation has been the main stay for IREL for separation of target substances by means of engineering methods while returning to the basic scientific principles that governs the separation processes.

Properties and uses of individual minerals

Almost all rutile and ilmenite is processed into non-toxic white titanium dioxide pigment for use in the manufacture of paints, plastics, paper, ink, rubber, textiles, cosmetics, leather and ceramics. Titanium dioxide pigment has excellent brightness and high opacity for good hiding power (e.g. in paint for covering undercoats) and has replaced lead carbonate pigments. Nanocrystalline anatase titania becomes increasingly important because of its potential application in catalysis/photocatalysis, coating for self-cleaning surfaces, ceramic membranes and sensors.

Rutile is also used to produce light, strong, corrosion-resistant titanium metal for use in aircraft, spacecraft, motor vehicles, desalination plants and surgical implants. It is used also in fibreglass, chemicals and as a coating on welding rods. Ilmenite is used as a fluxing agent in blast furnace feeds and as a sand-blasting abrasive.

Zircon is used in foundry sand moulds and zircon sand or powder is used for glazes on pottery and other ceramic surfaces as well as in the production of various refractory metals. Heat-resistant zirconia is used in a fused form to line ladles holding molten steel, in molten metal moulds and as small beads for abrasives. Zircon is the major source of zirconium, a corrosion-resistant metal that is used in nuclear reactors and chemical processing equipment. Research and development continues into the use of zirconium ceramics to improve diesel engines and in the metal extrusion industry where heat resistance and strength are required. It is also used for catalytic converter purposes.

Monazite is a major source of certain rare earth elements and thorium. Rare earth elements are used in high-strength permanent magnets, catalysts, ceramics and colour

television tubes. Thorium is used in incandescent gas mantles and as fuel for a few nuclear reactors.

The industrial uses of natural garnets originate from the latter's properties of hardness, chemical inertness, recyclability and cleavage / fracture-pattern. They are used as excellent abrasives for applications such as: sand or air blasting, assisted water-jet cutting of metals, blast-cleaning and in sand paper manufacturing. There are also additional industrial applications of natural garnets, including conditioning of Al and other soft metals for use in air-crafts and ships, deburring welds, grinding and polishing optical / optometric lenses, production of high-quality scratch-free semi-conductor materials, finishing of hard rubber, plastic and wood products, making of non-skid paints and coatings, cleaning of drill pipes and well casings, filtration medium for water, construction tiles / bricks and many such uses

Sillimanite as a natural and untreated mineral is a very important raw material for high alumina refractories which are extensively used in Iron and steel, Petrochemical, Electrical, Cement, Zinc and Glass industries. About 95% of the sillimanite minerals produced are used as raw material for the refractory industry in the manufacturing of non-basic, high-alumina refractories. The refractory characteristics of these minerals is related to their ability to form the refractory mullite phase which combines high strength with resistance to physical and chemical corrosion at high temperatures. Mullite is therefore an essential component of refractories forming the inner lining of furnaces and high-temperature containers widely used in the manufacturing of metals, glass, ceramics and cement. The major end use of sillimanite minerals is in the iron and steel industries which consume 60% or more of the mullite refractories. They are used in critical areas of furnaces, steel degassing chambers, soaking pits and many types of auxiliary pouring and handling equipment. The second most important application is as furnace linings in the non-ferrous metallurgical and glass industries as well as in ceramic and cement kilns. Other uses, minor in volume terms, include foundry-mould facings, combustion chamber linings, burner bodies, pyrometer tubes and welding rod coatings. Some amounts of the produced sillimanite minerals (c.5%) have non-refractory uses. Raw and calcinated minerals are utilised in the manufacture of high-tension insulators and other electrical ceramics, ceramic tile body components, sanitary ware, ceramic honeycombs, blown aluminium-silicate high-temperature insulation, brake linings, glass melt additives, spinnablemullitefibres, grinding media and extrusion dies. Sillimanite minerals are also locally used to produce Si-Al alloys, metallic fibres and selected aluminium oxides. High-purity and fine grained (< 200 mesh). Kyanite is preferentially used by ceramic manufacturers of wall tile and sanitary porcelain to offset shrinkage and cracking after firing.

CONCLUSION

India hosts few largest and richest shore line deposit containing heavy minerals. The mining industry itself and government bodies have long recognized the importance of environmental and social aspects of mining. Incorporation of environmental and social aspects into beach sand mining projects from planning through operations to closure would reduce the doubt of environmental sustainability. Better co-ordination between industrialist, academics and Research and Development institutions is highly desirable

for exchanging the information needed for the growth of this industries.

ACKNOWLEDGEMENT

The author would like to thank IREL(India) Limited for providing the support to carry out research work. He also expresses his sincere thanks to all staff members of his organization. There are no separate funds provided for carrying out this research work.

REFERENCES

1. Ali, M.A. (1989). Studies on the beach placers of Ratnagiridistrict, Maharastra, India. Explor. Research Atomic Minerals, 2, 167-175.
2. Van Gosen, S.B., Fey, D.L., Shah, A.K., Verplanck, P.L., Hoefen, T.M. (2014) Deposit model for heavy-mineral sands in coastal environments. U.S. Geological Survey Scientific Investigations Report 2010-5070-L, 51.
3. Indian Minerals Yearbook 2019, (Part-III: Mineral Reviews), 58th Edition, Government of India,Ministry of Mines, Indian Bureau of Mines, Nagpur, India.
4. Krishnan, S., Viswanathan, G., Balachandran, K. (2001), Heavy mineral sand deposits of Kerala. Exploration and Research for Atomic Minerals, 13, 111-146.
5. Setty, B.K., Raju, R.D. (1988) Magnetite content as a basis to estimate other major heavy mineral content in the sand deposit along the Nizampatnam coast, Guntur district, Andhra Pradesh. Journal of the Geological Society of India, 31 (5), 491-494.
6. Ramakrishnan, M., Nanda, J.K., Augustine, P.F. (1998) Geological Evolution of the Proterozoic Eastern Ghats Mobile Belt. Geological Survey of India Special Publication, 44, 1-21.
7. Sengupta, P., Sen, J., Dasgupta, S., Raith, M., Bhui, U.K., Ehl, J. (1999) Ultra-high Temperature Metamorphism of Metapelitic Granulites from Kondapalle, Eastern Ghats Belt: Implications for the Indo-Antarctic Correlation. Journal of Petrology, 40 (7), 1065-1087.
8. Dasgupta, S., Sengupta, P. (2003) Indo-Antarctic Correlation: A Perspective from the Eastern Ghats Granulite Belt, India. In: Yoshida, M., Windley, B.F. and Dasgupta, S., Eds., Proterozoic East Gondwana: Supercontinent Assembly and Breakup, Geological Society, London, Special Publications 206, 131-143.
9. Dobmeier, C.J., Raith, M.M. (2003) Crustal architecture and evolution of the Eastern Ghats Belt and adjacent regions of India. In: Yoshida, M., Windley, B.F., and Dasgupta, S. (Eds.) Proterozoic East Gondwana: Supercontinent Assembly and Breakup. Geological Society, London, Special Publications, 206, 145-168.
10. Kumar, G.R.R., Sreejith, C. (2010) Relationship between heavy mineral placer deposits and hinterland rocks of southern Kerala: A new approach for source-to-sink link from the chemistry of garnets. Indian Journal of Geo-Marine Sciences, 39 (4), 562-571.
11. Minor Minerals, Indian Minerals Yearbook 2020 (Part- III: Mineral Reviews), 59th Edition, Government of India Ministry of Mines Indian Bureau of Mines, Nagpur, India.

ABSTRACTS

XV International Mineral Processing and Recycling Conference
17-19 May 2023, Belgrade, Serbia

SIMULATION OF HYDRODYNAMIC CAVITATION-ASSISTED BIODIESEL PRODUCTION FROM WASTE COOKING OIL USING ASPEN PLUS

M.B. Tasić[1], I.J. Stojković[2], V. Pavićević[3], V.B. Veljković[1,4]
[1] University of Niš, Faculty of Technology, Leskovac, Serbia
[2] University of Belgrade, Faculty of Technology and Metallurgy, Innovation Centre, Belgrade, Serbia
[3] University of Belgrade, Faculty of Technology and Metallurgy, Belgrade, Serbia
[4] The Serbian Academy of Sciences and Arts, Belgrade, Serbia

ABSTRACT – To reduce production costs, industries gradually lean towards process intensification techniques, like technologies based on hydrodynamic cavitation, due to their cost-effectiveness, minimizing the use of toxic solvents, and the ability to obtain superior products compared to conventional methods. Although hydrodynamic cavitation technology has been applied in commercial biodiesel production, there is a lack of material and energy balance information for further economic and environmental impacts analysis of this process. This study developed a simulation-based model using Aspen plus v.8.6 to compare material flow and energy consumption through a biodiesel production process based on hydrodynamic cavitation technology. The plant produces 127 t/day of biodiesel from waste cooking oil. The final biodiesel product meets the quality standard EN14214 specification. Unpurified glycerol as a by-product was handed over to an authorized operator for further care, while process streams enthalpies (8.8 MJ/kg) could be recycled in the process. The heat released from the hydrodynamic cavitation reactor's diesel engine powered the processing plant, so the model did not need an external heat source.

Keywords: Biodiesel, Hydrodynamic Cavitation, Simulation, Waste cooking oil.

corresponding author: marijat14@yahoo.com

XV International Mineral Processing and Recycling Conference
17-19 May 2023, Belgrade, Serbia

RECOVERY OF METALS FROM INDUSTRIAL EFFLUENTS USING AN IONIC LIQUID-BASED STRATEGY

A. Jocić#, S. Marić, A. Dimitrijević
University of Belgrade, VINČA Institute of Nuclear Sciences - National Institute of the Republic of Serbia, Belgrade, Serbia

ABSTRACT – This work addresses the treatment of industrial effluents containing a high concentration of various metals. The discharge of large amounts of metal-contaminated wastewater represents a huge problem from an environmental and economic perspective. The main goal of our work is to test an innovative ionic liquid-based strategy as an extraction platform for valuable metals from wastewater. Phosphonium-based ionic liquids were designed with appropriate anions intending to obtain the highest efficiency for the metals dominated in industrial effluents. Proposed integrated platform will pave the way for further investigation on a larger scale.

Keywords: Ionic Liquid, Wastewater, Extraction.

corresponding author: ana.jocic@vin.bg.ac.rs

XV International Mineral Processing and Recycling Conference
17-19 May 2023, Belgrade, Serbia

IONIC LIQUID-BASED TECHNOLOGY FOR METAL RECOVERY FROM ELECTRONIC WASTE

S. Marić[#], A. Jocić, A. Dimitrijević
University of Belgrade, VINČA Institute of Nuclear Sciences - National Institute of the Republic of Serbia, Belgrade, Serbia

ABSTRACT – Recycling metals from electronic waste is an important subject not only for environmental protection but also for the recovery of valuable materials. The main goal was to test an innovative technology that involves new solvents, ionic liquids, and an aqueous biphasic system as an extraction platform for metal valorization from PCB. Ionic liquids are considered green solvents due to their many unique features (non-volatility, non-flammability, etc.). Selected ionic liquids have salicylate-based anion known as a complexing agent that forms stable complexes with different metals. Various extraction parameters were assessed to test the feasibility of the proposed technology.

Keywords: Ionic Liquid, Electronic Waste, Extraction, Aqueous Biphasic System.

[#] corresponding author: sladjana.maric@vin.bg.ac.rs

XV International Mineral Processing and Recycling Conference
17-19 May 2023, Belgrade, Serbia

CURRENT STATE OF THE QUALITY OF THE LUG RIVER IN THE MUNICIPALITY OF MLADENOVAC

J. Vučićević[1], S. Čupić[2], M. Jauković[3], V. Đurđević[3], M. Stamenović[3], A. Božić[3], A. Janićijević[3]

[1] SuperLab, Belgrade, Serbia

[2] Vinča Nuclear Research Institute, Belgrade, Serbia

[3] The Academy of Applied Technical Studies Belgrade, Belgrade, Serbia

ABSTRACT – This study examined the physico-chemical properties of water samples taken from two locations on the Lug River in the municipality of Mladenovac in March 2023. The tests included determining the levels of nitrates, nitrites, phosphorus, ammonia, BOD5, COD, as well as the content of metals such as Zn, Ni, Cu, Cr, Fe, Cd, Pb, Mn, and Mg. Given that Mladenovac was once an industrial center, and all of its industries are now inactive, and production has ceased, the current contamination of the watercourse is exclusively caused by anthropogenic factors and the neglect of the local population. Since the sampling location is exposed to the aforementioned pollution factors, and the testing was not conducted for an extended period, this study's results show that the water quality exceeds the limits of Class IV.

Keywords: Contamination, Physico-Chemical Properties, Water Quality.

corresponding author: ajanicijevic@atssb.edu.rs

XV International Mineral Processing and Recycling Conference
17-19 May 2023, Belgrade, Serbia

THE ENERGY CRISIS AND THE EXPLOITATION OF MINERAL RESOURCES IN THE LIGHT OF INCREASING LOADS IN SPACE

D. Žnidarič
Civil initiative for the Eco-social Society and Development of Zasavje, Trbovlje, Slovenija

ABSTRACT –In the last twenty years, mining has represented an industry with a distinctly negative environmental image in the developed world. Inadequate technological systems. The lack of awareness of the consequences of activities in place and especially the visible and felt consequences of the use of coal, due to emissions of pollutants, have caused a situation where many countries have decided to limit or close down mining activities. The current energy crisis has made coal mining relevant again. Germany and other European countries extended the operation of the coal industry, others from the former Eastern bloc abandoned the idea of closing. Author therefore describes in the article the concept of ecological modernization in the context of greater energy self-sufficiency. It reduces the political dependence caused by the import of energy products, and at the same time offers some thoughts on the re-exploitation of mineral wealth in a more human, nature and people-friendly way. Through the concept of greater ecological justice, he describes what should be done in the area, that the inhabitants of the potential mining areas would accept the industry and there would be no conflicts between different interests in the area.

Keywords: Negative Environmental Image, Ecological Modernization, Coal Industry, Political Dependence, Mining.

corresponding author: davorinznidaric@gmail.com

XV International Mineral Processing and Recycling Conference
17-19 May 2023, Belgrade, Serbia

A NEW GLOBAL CHALLENGES AND REGULATION FOR SUSTAINABLE SPATIAL DEVELOPMENT OF MINING

S. Zeković[#]
Institute of Architecture and Urban& Spatial Planning of Serbia, Belgrade

ABSTRACT – The paper provides an insight into the new global challenges, including environmental regulation, in the development of mining and their possible consequences on the sustainable spatial development, on the example of Bor basin. Challenges in further mining development are intensified by the global economic crisis, the energy crisis, climate change and local contextual conditions. The identification of main challenges is undertaken through a combination of the preliminary approach to a comprehensive development framework and an integrated assessment. The paper indicates that the key challenges of spatial development in mining areas must be integrated into corporate plans, public policies and spatial plans.

Keywords: Global Challenges, Environmental Regulations, Environment, Sustainability and Governance, Spatial Development and Social Licenses.

[#] corresponding author: slavka@iaus.ac.rs

XV International Mineral Processing and Recycling Conference
17-19 May 2023, Belgrade, Serbia

HYDROTHERMAL TREATMENT OF BAUXITE RESIDUE FOR IRON RECOVERY ENHANCEMENT BY MAGNETIC SEPARATION

P.M. Angelopoulos[#], P. Oustadakis, G. Anastassakis, M. Georgiou, N. Kountouris
National Technical University of Athens, Greece

ABSTRACT – Bauxite residue (BS) is the major by-product of the Bayer process for the aluminum production. About 150 million tones is the global annual production of BR, while due to the high alkalinity and fineness the material is accumulated causing deposition problems of potential environmental risk. Typically, BR composition: 10-20% Al_2O_3, 30-60% Fe_2O_3, 3-50% SiO_2, 2-10% Na_2O, 2-8% CaO, > 25% TiO_2[1]. Particularly important is BR content in REE and CRMs including Nd (110 ppm), La (150 ppm), Y (120 ppm), Ds (20 ppm). Additionally, BR is rich in scandium (Sc). BR contains ~120 ppm Sc per ton of dry BR (0.02% Sc_2O_3). In the frame, the REEScue project concept (https:/reescue.com/) and the proposed technical solutions are based on the smart combination of physical and hydrometallurgical processes that will enable the recovery of valuable marketable products and the drastic reduction of the quantity of BR to be disposed.[1]

Keywords: Bauxite residue, Magnetic separation, Hydrothermal treatment, Magnetite, Hematite.

[#] corresponding author: nkountouris@metal.ntua.gr

XV International Mineral Processing and Recycling Conference
17-19 May 2023, Belgrade, Serbia

TEXTURAL MINERALOGICAL UNDERSTANDING OF MAGNETITE LIBERATION CONTAINING COPPER INCLUSIONS

O. Ayoglu[1#], M. Sinche-Gonzalez[1], M. Moilanen[1,2]
[1] Oulu Mining School, University of Oulu, Oulu, Finland
[2] Centre for Material Analysis, University of Oulu, Oulu, Finland

ABSTRACT – This research investigated developing a textural and mineralogical understanding of magnetite liberation and determining the compositional heterogeneities and the inclusions within the different magnetite-bearing orebodies that might affect the quality of the magnetite concentrate. Core samples of a new greenfield project were investigated. Optical microscopy, electron probe microanalysis, and scanning electron microscope analysis were applied as research methods. Magnetite grain sizes varied from 5 µm to up to 1.4 mm in Zone 1 and from 10 to 200 µm in Zone 2. The mineralogical characterization study showed various textural associations of chalcopyrite, pyrite, pyrrhotite, amphibole and apatite with magnetite. The chemical composition characterization studies showed a high amount of V_2O_3 and TiO_2 in ilmenomagnetite formation and the occurrence of rare earth elements (REEs) such as Yttrium, Dysprosium, and Erbium in a REE-phosphate mineral.

Keywords: Magnetite, Fe-oxide ores, Kiruna, Ore Characterization.

[#] corresponding author: olcay.ayoglu@oulu.fi

XV International Mineral Processing and Recycling Conference
17-19 May 2023, Belgrade, Serbia

MASTER IN MINERAL PROCESING (EMJM-PROMISE) IN THE CONTEXT OF DEMAND OF CRITICAL MATERIALS AND ENERGY TRANSITION

M. Sinche-Gonzalez[#]
Oulu Mining School, University of Oulu, Oulu, Finland

ABSTRACT – The Erasmus Mundus Joint Master in Sustainable Mineral and Metal Processing Engineering (EMJM-PROMISE) is being established due to the awareness of increasing demands in the quantity and diversity of minerals, metals, and materials as we move towards renewable energy, electromobility, digital communication and other clean-energy technologies. The aim is the preparation of highly skilled mineral processing engineers-postgraduates and future leaders to support the sector into a sustainable future. PROMISE is the consortium involving the cooperation between four leading universities in mineral processing and mining engineering, University of Oulu from Finland, University of Zagreb from Croatia, Montanuniversität Leoben from Austria, and Universidad Federico Santa Maria from Chile.

Keywords: Mineral processing, Education, Master, Cooperation.

[#] corresponding author: maria.sinchegonzalez@oulu.fi

AUTHORS ARE RESPONSIBLE FOR THE CONTENT AND LANGUAGE OF THEIR PAPERS

ADVERTISING MATERIALS

The **Department for Mineral and Recycling Technologies** was founded at the Technical Faculty in Bor in 1962 under the name Department for Mineral Processing. The department was established in order to educate experts needed by RTB BOR and other mining companies in the country. In addition to the existing profile: Mining Engineer for Mineral Processing, in 2002, a new profile: Mining Engineer for Recycling Technologies and Sustainable Development, was introduced and the Department changed the name to the Department for Mineral and Recycling Technologies.

Since the existence of the Department 237 students have graduated, 22 have completed MA, 31 have obtained master's degree, and 14 students have defended their doctoral dissertations. All these students are esteemed experts who are professionally engaged with companies and scientific institutions in Serbia and abroad.

The Department for Mineral and Recycling Technologies is a part of Mining Engineering study program, which is one of four study programs at the Technical Faculty in Bor – University of Belgrade. The Department currently employs 12 teachers and associates: 4 full professors, 2 associate professors, 1 assistant professor, 4 assistants, and 1 teaching associate, as well as one laboratory assistant. In addition to qualified employees, the Department has classrooms equipped with modern computer equipment and teaching aids, and laboratories where classes and scientific research are conducted in the fields of mineral processing, recycling technologies and sustainable development.

There are three levels of study: undergraduate, master's, and doctoral studies with modern programs accredited in 2020. The undergraduate and master academic studies offer a choice between two modules: Mineral Processing and Recycling Technologies and Sustainable Development. However, doctoral studies are the same for the entire Mining Engineering study program where students choose subjects from the field they want to expert. Classes are interactive with students' active participation and are organized in classrooms and laboratories at the Technical Faculty in Bor. Practical education is also organized in the form of visits to the institutions and companies in the field of study.

The experimental work is performed at the laboratories at the Department which are equipped for testing and characterization, comminution and classification, physical and special methods for concentration, flotation, and chemical methods for concentration, and in laboratory designated for the teaching staff (postgraduate studies).

The laboratories have been significantly equipped recently with modern measuring devices with funds provided through the Interreg-IPA CBC international project involving cross-border cooperation between Serbia and Romania (2019-2021) and projects of the Ministry of Education, Science and Technological Development of the Republic of Serbia.

The teaching staff and associates at the Department for Mineral and Recycling Technologies are involved in scientific research through the publication of articles in leading international and national scientific journals and international and national conference proceedings, as well as through their engagement in a large number of projects, studies, technical validation, and auditing. The members of the Department are also authors of a number of textbooks, books, and monographs.

Two scientific journals are published by the Technical Faculty in Bor: **Journal of Mining and Metallurgy – Section A: Mining** and **Recycling and Sustainable Development** that include some members of the Department in their editorial boards.

www.rsd.tfbor.bg.ac.rs

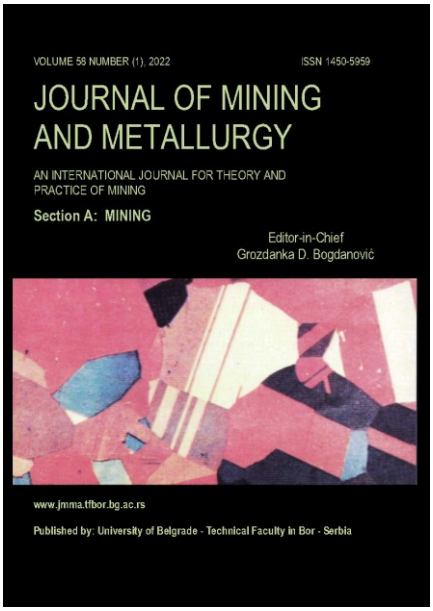

www.jmma.tfbor.bg.ac.rs

The Recycling and Sustainable Development journal was established in 2008 and at first it was published in Serbian. Due to the change of the editorial board, name, and journal's policy, the articles have been published in English since 2011. The original scientific and review articles are published in journal in the field of: generation and characterization, recycling and reuse, treatment (mechanical, biological, chemical, thermal, and other), landfill disposal (including design, monitoring, and remediation of old sites), environmental engineering, material flow analysis, and waste and resource management and related areas. According to the journal's categorization for 2021, it is classified in category M51 (leading journal of national importance) in the field of materials and chemical technologies and in the fields of regulation, protection and use of water, land and air, and category M52 (prominent national journal) in the field of energetics, mining and energy efficiency.

The Journal of Mining and Metallurgy has had a publishing tradition since 1965, and since 1997, the journal has been published as an international journal under its current name in English, in two sections - Section A: Mining and Section B: Metallurgy. Original scientific and review articles in the fields of geology, mineralogy, mining, environmental protection and related fields are published in Section A: Mining. The journal has been categorized as a national journal of international importance (M24) in the field of energetics, mining and energy efficiency since 2021.

Throughout its 60-year history, the members of the Department have been active in organizing a large number of conferences, such as the October Conference on Mining and Metallurgy, Ecological Truth, and the Serbian Symposium on Mineral Processing. The Department traditionally organizes an international conference called: International Mineral Processing and Recycling Conference, where experts in the field of Mineral Processing and Recycling

Technologies and related areas have the opportunity to present the results of their research, exchange experiences and discuss current issues, trends and the latest scientific achievements. The first scientific conference of national importance with international participation called the Symposium “Recycling Technologies and Sustainable Development” was organized in 2006. Since 2015, the symposium has grown into an international one and is held under the name International Symposium on Recycling Technologies and Sustainable Development.

Following the modern trends in the field of processing of both primary mineral raw materials and various types of waste, the topics of the symposium are expanding, therefore, this scientific-professional gathering has been organized under the new name, International Mineral Processing and Recycling Conference, since 2019.

The members of the Department for Mineral and Recycling Technologies are active participants in the management of the Technical Faculty in Bor through engagement in a large number of committees and professional bodies.

Čukaru Peki - the first green mine in Serbia

The company Serbia Zijin Mining is the owner of the copper and gold ore deposit in Bor and the first green mine in Serbia - Čukaru Peki, which moved the boundaries in Serbian mining in terms of technologies and standards applied in the ore mining process.

Čukaru Peki Mineral processing plant

The basis of green mining was established by the construction of plants that use the most modern technology and apply the highest European and world standards.

The company has a unique work system and has introduced new, modern methods of ore mining. Since the ore body is deeply positioned, the method of opening with ventilation shafts and declines was adopted. The mine has a Lower Zone, where exploration works are ongoing, and an Upper Zone, where exploitation is carried out.

Čukaru Peki decline

The ore deposit is divided into three mining areas, and the method of excavation in horizontal bands from the bottom up and the method of sub-excavation of chambers with subsequent filling was adopted. The process of thickening the tailings, which is later used for filling in underground corridors, is carried out in the unique Back filling station plant, the only one of its kind in Serbia. Apart from the excavation method, there is a unique ventilation and drainage system in the mine. The mine has an organized traffic network with light signaling, mobile signal and 4G network, as well as fixed telephony, which enables smooth communication, and for security reasons, the system is covered by video surveillance, which monitors the mining of ore, its transport and the development of traffic.

Mill and conveyor belt in MPP

The world's leading technology and high-efficiency equipment are integrated into the production process. In the mineral processing plant, the internationally advanced "SAB" process and the flotation system developed by the company itself are used for crushing and grinding. In the production process, only electricity is used and no harmful gases are emitted into the atmosphere. During the construction of the plant, a closed circular drainage system was constructed, which returns the technical water back to production, without releasing it into nature.

The entire work procedure is carried out in accordance with the laws, national regulations and technical standards of the Republic of Serbia, and includes compliance with international regulations in the field of environmental protection.

By choosing the most innovative technological solutions, the most important foundations of green mining were laid, which, along with safety and protection at work, emphasize an ecologically sustainable production process that strives for zero pollution. From the very beginning of work, the mine has been successively carrying out reclamation and greening procedures, and the plan is to introduce renewable energy sources, which are one of the priorities of this ecologically oriented company, dedicated to environmental protection, but also to the development of the local community and the employment of young people and professional people, including numerous engineers who graduated from the Technical Faculty in Bor.

The motto of the company Serbia Zijin Mining, aimed at the welfare of local communities, citizens, society and the state, is "Mining for a better society". As a leader in innovation in terms of technology, whose function is to preserve and improve the environment, the company Serbia Zijin Mining strives wholeheartedly to contribute to the development of mining in Serbia by moving the framework in the work of the mining industry, and to place the Čukaru Peki mine in the first place among the most successful European and world copper and gold producers.

SERBIA ZIJIN COPPER DOO

Serbia Zijin Copper DOO is the company operating in the **Zijin Mining Group.**

It was founded on December 18th, 2018, on the day when Zijin signed the closing documents with the Government of the Republic of Serbia, i.e., the Contract on taking over 63% of the ownership in RTB Bor. In that way, Zijin became the holder of 63 % of the share in the capital of the Company from Serbia. Zijin's first Company in Serbia, and in the Balkans, is called Serbia Zijin Copper DOO and is the only producer of copper and precious metals (gold and silver) in Serbia. All products are the stock exchange products and the quality, demand, sales prices and trading terms are regulated by the rules prescribed by the world's non-ferrous metal stock exchanges.

The Company owns four copper mines ("Veliki Krivelj", "Novo Cerovo", "Jama" and Copper Mine Majdanpek), the Limestone Mine and the Smelter.

Because it is one of the largest companies in Serbia, which is a pillar of development of Bor and Majdanpek, the Company is recognized as a serious legal entity, with promising capabilities and the responsibility to contribute to strengthening the iron friendship between China and Serbia and as such symbolizes the wonderful friendship between the people of two countries that share good and bad and help each other.

In 2022, the Company produced 93,600 tons of mineral copper and 2,675 kilograms of mineral gold, and completed an output value of about $1.06 billion. During the four years since Zijin has taken over, the Company has paid a total of $348 million in taxes and made a total social contribution of $607 million.

By 2025, after the completion of all technological transformation projects, the Company is expected to have an annual production capacity of 180,000 tons of cathode copper and an annual production capacity of 3-5 tons of gold.

The company, as a joint investment of Zijin Mining Group and the Republic of Serbia, will cooperate with all stakeholders to ensure a healthy and quality way of doing business within the legal framework, and complete all technical upgrade and expansion projects.

Production program

Our main activity is the exploitation and processing of copper ore, production of cathode copper, gold, silver, sulfuric acid, copper II sulphate – pentahidrate, selenium, platinum and palladium. The basis of green mining was established by the construction of plants that use the most modern technology and apply the highest European and world standards.

OUR MISSION

In 2022, Zijin Mining Group proposed a new development goal, to build a "green, high-tech, superior and international Mining Group". Adhering to this goal, the Company

has been promoting the construction of ESG system in an all-round way, tried very hard to become a benchmark enterprise in Europe in ecological protection, production safety, legal compliance, corporate governance, social responsibility, labor human rights and other aspects.

By developing a sustainable and green mining, we hope to create development opportunities for as many people as possible and achieve coordinated development between enterprises, employees and society.

Social Responsibility

In Serbia Zijin Copper, we are committed to the responsible management of our mines. Our priority is to maintain harmonious relations with the local community, while reducing the impact on the environment. By supporting our commitment to responsibility, we protect our license to operate so that we can continue to create wealth for our employees, our host community and shareholders. Therefore, responsible mining is a business imperative and the foundation of Serbia Zijin Copper business operations.

We focus on the development of the communities and give priority to supporting the development of infrastructure, medical, education, culture and sports in Bor and Majdanpek. Over the past four years, nearly US $4 million has been donated in related fields.

In recognition of the Company's contribution to economic development and green transformation of mines, on December 9, 2022, Serbian Chamber of Commerce (PKS) awarded the "Outstanding Business Achievement Award 2022" to the Company.

Health&Safety

Serbia Zijin Copper is committed to building a safety culture to achieve a zero incident in the working environment. The safety of our people is a priority that can never be compromised and we believe that accidents at work can be prevented.

Safety is the bottom line of the Company's development. In the past four years, the safety awareness of the Company's employees had been significantly improved. In 2022, the number of recorded injury incidents of the Company decreased by 34% compared to 2021 and decreased by 37% compared to 2020, and 28,867 people had received safety education and training.

Environment

Serbia Zijin Copper is committed to reducing the unfavorable environmental impact in order to preserve the valuable resources and keep the work permit. Through innovative technology and education, we save the energy and protect the environment.

We invest in research and development of various technologies and apply standardized management procedures.

The Company adopts industry-leading standards to protect the ecological environment. By the end of 2022, the Company had invested $197 million in ecological protection. The comprehensive wastewater reuse rate of the Company reached 92.5%, which was the leading level in the mining industry. In the past four years, the Company had completed a total green area of 2.31 million square meters. Thanks to continued investment in ecology field, our mines and cities have been becoming greener and more beautiful.

ANALYSIS
LABORATORY EQUIPMENT

Since it was founded in 1996, **Analysis d.o.o.** offers high-quality instruments and reliable solutions for your laboratory.

The primary activities of **Analysis d.o.o.** are wholesale, maintenance and servicing of analytical, process, and general laboratory equipment, along with training users and providing application support for successful and high-quality work on the instrument.

The sales assortment includes equipment applied in the pharmaceutical industry, environmental sciences, food and drink production, and other industries, as well as science, forensics and medicine – whether it is used for analysis, research, quality control or process monitoring.

Analysis d.o.o. collaborates with world leaders in laboratory equipment manufacturing, in order to fulfill the needs of our users and establish long-term collaboration to the pleasure of both parties.

ARL PERFORM'X Sequential XRF Spectrometer

thermo scientific
Authorized Distributor

ARL Niton XL5 handheld XRF analyzer

ICP-OES iCAP PRO XP

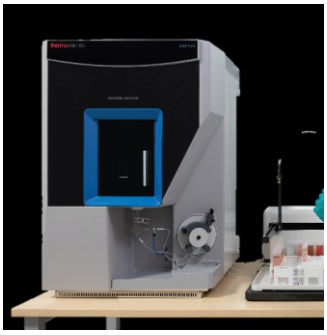

ICP-MS iCAP RQ

www.analysis.rs

tozero

tozero is a Munich-based startup co-founded by **Dr. Ksenija Milicevic Neumann** and **Sarah Fleischer**. The company's mission is to establish Europe's leading lithium-ion battery recycling plant, focused on recovering critical materials such as lithium, nickel, cobalt, manganese and graphite in a sustainable way.

By reintroducing these materials into the supply chain, tozero aims to support the creation of new batteries while promoting a circular economy. To achieve their ambitious goals, tozero is investing in advanced technologies and processes that enable efficient and cost-effective recovery of valuable materials from battery waste.

tozero is focused on developing a proprietary lithium-ion battery recycling process to recycle battery waste for the EV Industry and recover the critical materials. These materials include lithium, nickel, cobalt, and graphite, which are in high demand for the production of new batteries. By reintroducing these materials back into the supply chain, tozero is reducing the dependence on mining and promoting a circular economy.

At tozero, the focus is on innovation, efficiency, and sustainability. The recycling process is designed to recover as much material as possible from battery waste, with minimal environmental impact.

In addition, the process is cost-effective, making it an attractive solution for battery waste management.

To learn more, visit their website at www.tozero.solutions.

The company **Monicom** from Nis has been successfully operating and growing since 1991 and today it represents one of the more successful private companies in Serbia that is the leader in the business areas it is involved in. During nearly 30 years of existence, Monicom has grown from a small enterprise to a successful business group with over 600 employees and production facilities positioned throughout southern Serbia.

The business portfolio consisting of the energy and trade sectors.


EMJM PROMISE
EMJM-PROMISE
Erasmus Mundus Joint Master in Sustainable Mineral and Metal Processing Engineering
EMJM PROMISE is suited for graduates in mineral processing, metallurgical and chemical engineering, mining engineers, geological engineers, raw materials engineers, materials and rock waste treatment engineering, or related engineering, with minimum BSc degree at the moment of application.
OULU MINING SCHOOL
UNIVERSITY OF OULU
MONTAN UNIVERSITÄT LEOBEN
University of Zagreb
Faculty of Mining, Geology and Petroleum Engineering
UNIVERSIDAD TECNICA FEDERICO SANTA MARIA
Finland
Austria
Croatia
Chile
Application and Scholarships open each year
Oct 1st to Dec 31st 2023, 2024
Apply online!
www.master-promise.eu
Co-funded by the European Union

The **Erasmus Mundus Joint Master in Sustainable Mineral and Metal Processing Engineering (EMJM-PROMISE)** is being established due to the awareness of increasing demands in the quantity and diversity of minerals, metals, and materials as we move towards renewable energy, electromobility, digital communication and other clean-energy technologies. The aim is the preparation of highly skilled mineral processing engineers-postgraduates and future leaders to support the sector into a sustainable future.

PROMISE is the consortium involving the cooperation between four leading universities in mineral processing and mining engineering, University of Oulu from Finland, University of Zagreb from Croatia, Montanuniversität Leoben from Austria, and Universidad Federico Santa Maria from Chile.

The website is www.master-promise.eu

ISBN-978-86-6305-133-1